Carlos García-Legaz Martínez
Francisco Valero Rodríguez

Editors

ADVERSE WEATHER IN SPAIN

Under the sponsorship of

CONSORCIO DE COMPENSACIÓN • DE SEGUROS •

ADVERSE WEATHER IN SPAIN

Editors

Carlos García-Legaz Martínez
Francisco Valero Rodríguez

ISBN: 978-84-96709-43-0
Printed by Service Point

Published by:

AMV EDICIONES

A. MADRID VICENTE, EDICIONES
Calle Almansa, 94, 28040-Madrid (España)
Phone: + 34 915336926 Fax: + 34 915530286
e mail: amadrid@amvediciones.com
Internet: www.amvediciones.com

Photograph of the book cover:
José A. Quirantes

Whatsoever the LORD pleased,
that did he in heaven, and in earth,
in the seas, and all deep places.

He causeth the vapors to ascend from the ends of the earth,
he maketh lightnings for the rain,
he bringeth the wind out of his treasuries."

(Psalms, 135, 6-7)

In memory of Professors Francisco Morán and Joaquín Catalá, Meteorologists and *Catedráticos* of Atmosphere Physics in Complutense University of Madrid, our masters.

Francisco Valero Carlos García-Legaz

ADVERSE WEATHER IN SPAIN

CONTENTS

PRESENTATION

Climatic projections carried out for decades provide estimations of a potential climate change towards a greater probability of occurrence of extreme weather events such as waves of heat, drought, tropical cyclones and intense precipitation with consequent floods, severe thunderstorms with associated tornadoes or destructive wind gusts. These adverse weather events have serious socio-economic consequences because they constitute a source of considerable human and economic losses. Natural disasters seem to be more and more frequent as it can be deduced from the economic damage amounts. This increase in the frequency of severe phenomena is the result of set of factors acting jointly, the geographic concentration of goods and people living in the risk zones, deficiencies in environmental management and, of course, the consequences of climate change.

The natural disaster more common in Spain is flooding, which is determined by a extreme weather situation coupled with the geographical relief and human's bad actions in relation with the use of the territory. If the claims paid by the Spanish Insurance Compensation Consortium in the period 1987-2006 are used as a reference, the 93.5% of the compensation paid due to natural disasters were owed to flooding. Taking into account the data updated until 2001 that included extraordinary cyclonic storms, the 68% were due to floods, another 17% would be due to storms, leaving only 15% due to several natural factors such as earthquakes and falling meteorites. Therefore, it is essential to advance in scientific knowledge and technological development on the extreme weather phenomena in order to achieve a more accurate prediction.

I have the pleasure to introduce this book, which includes the most up-to-date information on extreme weather events in Spain. The experience and prestige of authors, experts from universities, research centers, Spanish Insurance Compensation Consortium and the Spanish Meteorological Agency, guarantee the scientific quality of the book which I have the great honour of presenting and I hope that readers will find out interesting contributions on the adverse meteorological phenomena that occur in our country.

Daniel Cano Villaverde

President, Agencia Estatal de Meteorología

FOREWORD

Within the scope of the extraordinary risk insurance coverage, the Consorcio de Compensación de Seguros (CCS) has the mission of indemnifying damage to persons and assets arising as a result of the occurrence of certain natural phenomena or violent acts whenever these are covered by an insurance policy.

Among the natural perils covered by the CCS, those which have historically caused most damage qualifying for indemnity are, as one might expect, those associated with the weather, namely flooding from torrential rain and atypical cyclonic storms, which basically includes strong winds and tornadoes. Thus in the 1987-2012 period the damages paid out by the CCS as a result of flooding totalled 4.3 billion euros (69% of total indemnification), while pay-outs arising from atypical cyclonic storms came to 989 million euros (16% of the overall amount).

This original and essential mission of providing indemnification was over time complemented with a role related to prevention, as is laid down in the CCS Legal Statutes. The policy of the CCS as regards this particular function has always focussed on one vital and basic facet of the natural catastrophe risk management: awareness of them. This is why in this area the CCS promotes research and disseminates the findings. To this end, the CCS sponsors and supports, in collaboration with other institutions, the realisation of studies and the organisation of talks, courses, conferences and seminars, as well as the publication of material to be circulated free among those concerned. This kind of involvement by the CCS in the preventive aspect is faithfully reflected in the entity's strategy planning via successive Three-Year Action Programmes.

The collaboration of the CCS in this new publication in support of the initiative by the Spanish Committee on the World Climate Research Programme is an opportunity which has been presented to us to carry on working on the exercise of the policy of promoting awareness of natural perils, in this case adverse weather phenomena. The subjects broached in this book and the high professional and academic level of its authors, whose efforts should be recognised and the work of its publishers praised, will ensure that this publication will set a new milestone for this line of action which the CCS has marked out in the field of prevention.

Consorcio de Compensación de Seguros

PREFACE

The WCRP International Programme (*World Climate Research Programme*) (www.wcrp-climate.org) was created in 1980 under the auspices of the World Meteorological Organisation (WMO) and of the International Council for Science (ICSU). Since 1993 it has also been sponsored by the Intergovernmental Oceanographic Commission (IOC) belonging to UNESCO. The WCRP's two main objectives involve determining to what degree climate can be predicted and to what extent human activity can influence it.

The *Spanish Committee of the World Climate Research Programme* depends institutionally upon the Secretariat of State for Research, Development and Innovation of the Ministry of Economy and Competitiveness and since 2010 it avails of the physical support of the Spanish Climatology Association (AEC) (www.aeclim.org). The Spanish Committee comprises Javier Martín-Vide, as Chairperson, Mª José Estrela as secretary and Joaquín Meliá, Francisco Valero, José Mª Cuadrat, José Antonio Guijarro, Carlos García-Legaz and Pablo Fernández de Arróyabe as committee members.

The Spanish Committee promotes dissemination of the WCRP's aims and objectives among Spain's climatology community and those associated with it and is also the official interlocutor with the international programme. It avails of grant ACI-COM-2011-1070, "Activities of the Spanish Committee of the WCRP", of the ministerial programme ACI-COMITÉS Sub-programme for promotion of international scientific cooperation for the biennial 2012-2013. Precisely, the activities to be developed within the framework of this grant included conducting a study on drought in Spain aimed at informing of the special characteristics and unique features of this phenomenon in our country. The financial aid by the Insurance Compensation Consortium and the institutional guarantee by the Spanish Meteorology Agency (AEMET), to whom the Committee wishes to express its gratitude, have enabled the initial objective to be extended to include practically all climatic risks affecting the country. Thus, the present research constitutes a substantial and notable complete contribution to our knowledge of climate-related risks in Spain. The English language version of the study should enable wide-scale international dissemination, in accordance with the aims of the financial aid provided by the Ministry, which supports the Committee.

The authors involved in the project are a guarantee of the quality of its content. A total of 23 chapters prepared by 56 authors, renowned in our country and abroad, have made high-impact contributions in the themes addressed. Francisco Valero and Carlos García-Legaz, Committee members, coordinated the project dynamically and efficiently, a fact that honours the Committee as a whole. Most significantly, the results of the study will be highly useful with regard to managing risks and reducing the damage and human victims they cause in Spain.

Javier Martín-Vide

Chairperson of the Spanish Committee of the WCRP

EXPLANATION OF THE WORK

As the Chairman of the Spanish Committee of the World Climate Research Programme, Professor Martin Vide, so rightly states in the preface that precedes these lines, this book has its origin in an initiative arisen within the aforementioned Committee that asked us, as members of the same, to complete the development of the full publication in quality of editors. Extremely honored by this charge we proceeded to tackle the task starting with the choice of the name of the book and the selection of the topics and authors.

We are fully aware of the lack of literature in Spanish about the global consideration of weather phenomenology of what has come to be called adverse. Even though there are articles about many of the aspects here treated in specializing journals, certainly almost all of them in the English language.

Thus, one of the primary goals that we have tried it has been to cover the gap mentioned to put at the service of the scientific and professional community, as well as to that of the governmental entities involved in protecting lives and goods. The outcome achieved has been a compilation and updating of the knowledge gained un the development of these phenomena of such an important impact on society.

Precisely the work sees the light a short time after the meeting of the 2013 World Meteorological Day, the year in which the WMO has commemorated the 50th anniversary of the creation of the World Weather Watch (WWW) having the motto chosen for the mentioned celebration "*Watching the weather to protect life and property*". In this way, we are able to say, even at the expense of abusing the journalistic cliché that the appearance of the publication is of a "highly topical".

We cannot fail to reflect that the development of the work has represented without any doubt a worthy effort, mainly of the authors of the articles, that have due deliver the originals in a very short time, which, despite being recognized specialists, clearly entails an added difficulty attributable to the intense dedication to the teaching and research tasks of virtually all of them. As editors we wish to express our gratitude, in addition to highlighting his selfless and generous contribution.

We must also emphasize that the collective work has been able to see the light thanks to the essential support provided by two affectionate institutions for us by clear reasons: the Spanish Meteorological Agency (AEMET) and the Insurance Compensation Consortium (CCS). Both entities have contributed not only with the participation of prominent authors as experts, but also with the strong backing of the first and with the funding of the publication by the CCS, on the grounds that it is of full interest to the committed that Spanish society has entrusted them.

Once this preliminary statement has been made we pass to expose the objectives aiming to the publication, as well as to describe the content of the different chapters globally.

The global climate is changing. In the course of the last century there has been a warming in all the continents with a mean increase of temperature of 0,6 ± 0,2 °C, corresponding more accused changes to medium and high latitudes in the northern hemisphere. In recent decades it seems obvious that global warming is partially attributable to human activities, a fact that has been termed anthropogenic environmental change. It is very likely that climate change will be accompanied by an increase in the frequency and intensity of extreme weather events, that is, that the variability of climate occurs both in the form of gradual evolution and through atmospheric incidents of high impact.

Although there is no clear and universally accepted definition, it is usually considered adverse weather phenomenon to any event that has its genesis within the atmosphere and causes damage to people and goods that the society is unable to avoid. Europe has experienced in the past 30 years an unprecedented increase in this kind of phenomena. Known are the waves of heat that took place in France, Italy, Spain and Portugal a decade or so ago. We are also aware of the manifestations of cold waves that caused severe health problems in northern Europe and Russia. We are also conscious of how massive floods have produced enormous damage in the United Kingdom, Germany and Italy in recent years. Taking the current climatic predictions as a starting point, it is glimpsed that in the coming years we will have to cope with an increased number of extreme weather events and it is very likely to reach even greater intensity. In this regard, it is essential to address the appropriate actions aimed at protecting the population and the affected regions.

This book constitutes a nationwide meeting platform of researchers who analyze the effects of the changing climate on the adverse weather phenomena and the impact they can have on the future. In general, the findings of the articles follows that very localized phenomena, such as individual storms, are extremely difficult to predict, while projections of the number of days where conditions are appropriate for the formation of these violent processes can be achieved.

We hope that the results of this work will help to raise awareness about the climate change, and thereby to promote long term actions to cope with severe weather conditions, such as the development of this kind of emergency response plans. In this sense, it seems to be detected that the areas placed in the proximity of the main sources of moisture, especially those of the Mediterranean coast, show the most significant increases both in the frequency of the so called atypical cyclonic storms and in the potential and number of the thunderstorms, all this due to greater virulence and intensity of the cyclogenetic processes, that associated to the odd characteristics and structure of the territory can cause disastrous effects.

Although the immediate is to observe the global warming in terms of increase in temperature, one may say emphatically that the effects go far beyond and are deeper. Of the works gathered in this book can be inferred in some way that the global warming would result in severe events more common than they are today-

A substantial part of the results that are included in the work include the comparison of past environmental conditions with the current with the object of attempting to

determine whether effects on the genesis of adverse phenomena can be inferred or not. Likewise, it becomes evident that the pairing of the high-resolution regional models with global climate models gets greater depth in the results. Regional models divide the domain into a grid of cells spaced just a few kilometers apart and provide information about the conditions that occur in each cell. This adds detailed information to the data of the global models. For this reason, the next step, always unfinished, is to use higher-resolution models that explicitly allow us to study certain adverse phenomena as individual severe storms or tornadoes, solving some of the limitations of current research.

The size and scope of extreme events such as droughts or hurricanes is not limited to cause damage to the landscape, but that affects substantially to the economy of the citizens causing a general loss of quality of life and altering the environment and wildlife in a way that is extremely costly for many different reasons. In summary, the disasters associated with an increase in adverse weather conditions give rise to enormous costs that pose a considerable burden on public funds and private capital.

For all these reasons, the book explores our current understanding of severe weather by conducting a thorough study of the atmospheric phenomena that, directly or indirectly, produce damage in Spain. The work is therefore structured in four generic paragraphs referred to in the index.

The first section look towards the clearly and manifestly atmospheric phenomena, both for those presenting an exclusively meteorological character (thunderstorms, heavy rainfall, extreme wind, …) and others in that the adversity obeys to multiple complex causes. In either case, the atmospheric disturbance is conceived as a primary factor or trigger (landslides, floods, …). This first paragraph contains seventeen chapters, which refer to multiple phenomena, from the Mediterranean cyclones to the forest fires.

The second section includes a content more framed in climatological studies that in the actual weather, though, without a doubt, all of the referred chapters relates in a very straightforward way with adverse weather phenomenology.

Section III refers to the analysis of the weather conditions related to the human health. Although not strictly constitutes an adverse meteorological phenomenon, it has the peculiarity of presenting an interest and a clear convergence with the targets claimed by the book.

Finally, the work concludes with the section IV, which deals with an integrating aspect of all the studied phenomena related to the coverage in our country by the CCS of adverse weather risks.

The pool of experts that they have contributed to the achievement of the book per se guarantee a high academic level, being composed mostly of accredited researchers of matter belonging to the spanish university, with the additional participation of the reputed experts in the field from the AEMET and the CCS. Their scientific high levels have not prevented them to develop understandable contributions to a broad number of potential readers without loss of rigor that necessarily must possess all scientific articles. We are in a position to affirm that

this objective, by no means easy to reach, has been fully achieved.

Finally, we would like to warmly thank AMV editions for the excellent typographic quality of the work that we present as well as for having carried it out at our request within a period of time extremely brief.

Francisco Valero Rodríquez

Carlos García-Legaz Martínez

Madrid, 10 May 2013

I. ADVERSE PHENOMENA

A) PURELY ATMOSPHERICS

CHAPTER 1

THE MEDITERRANEAN CYCLONES AND THEIR IMPACTS IN SPAIN

Agustín JANSÀ CLAR

PhD (Physics), Spanish State meteorologist (retired)
agustí.jansa@gmail.com

ABSTRACT

The Mediterranean region is an area with high frequency of cyclones, many of them native in the same region. The frequency is especially important if small and weak cyclones are also included. In the first part of this chapter the Mediterranean cyclones are characterised, taking into account the frequency, location, typology, thickness and intensity, with especial attention to the Spanish zone or near it. The second part is devoted to review possible impacts of the cyclones on Spain, with especial attention to high impact weather, namely heavy rain or strong wind. The chapter ends with some brief conclusions. Although the most intense cyclones almost always produce high impact, some of the most critical impacts, like some of the heavy rain events, are not proportional to the intensity of the cyclones, but sometimes are associated even to weak cyclones.

Key words: Cyclones, depressions, Mediterranean, high impact weather, heavy rain, strong wind.

1. MEDITERRANEAN CYCLONES: FREQUENCY, CHARACTERIZATION, TYPOLOGY

Let us to clarify that in this chapter the term cyclone is used as equivalent to centre of cyclonic circulation, depression or low pressure centre, independently of the intensity, size or thickness of the concerned disturbances.

1.1 Frequency

A first question to be raised is if there are many of few cyclones formed or appeared in the Mediterranean. This first question has no an absolute answer, because the frequency depends on how the cyclones are defined, the detection technique or the type of analysis that is used.

When subjective or handmade analyses are used, a cyclone is usually defined as a low pressure zone where a closed isobar can be drawn. The number of cyclones so defined is a function of the scale of the used map and of the isobar spacing. A large scale map with large isobar spacing provides less detail and permits to detect fewer cyclones than a small scale map with smaller isobar spacing.

Petterssen (1956) is a classical study, based on subjective analyses and referred to the Northern Hemisphere. The detail of the maps is poor and so the number of detected cyclones is small, but it is remarkable that the Western Mediterranean appears as the most cyclogenetic region of the Hemisphere, in winter.

Radinovic and Lalic (1959) counted 40 (synoptic scale) cyclones per year in an area covering the most of the Western Mediterranean. Most of them (74%) were formed in situ and some of them lasted more than one day in the area. Radinovic (1965) refined the counting by using more detailed maps and shifted the area to the East, centring it in the old Yugoslavia; 116 cyclonic presences per year were found with four maps per day (note than the same cyclone can be counted two or more times in successive maps).

The Figures published in the classical work of the British Meteorological Office (H.M.S.O., 1962) are quite consistent with the former Figures: the book indicates the presence of 60 cyclones per year in the Western Mediterranean, 51 in the Central basin and 28 in the Eastern one, as well as 14 cyclones in Northern Africa. More details and references to statistical studies can be found in Radinovic (1987).

Still within the subjective method and the handmade analyses, Figures of cyclonic presence become multiplied if the space-time scale is refined. Radinovic (1978), by using maps of 1:5000000 scale and an isobar spacing of 2 hPa, with analyses every three hours, found 2000 cyclonic centres per year in a quite reduced area. With the same map scale and isobar spacing, but with only two maps per day and in a different area, the Iberian-Mediterranean zone, Genovés and Jansà (1989) found 511 cyclonic centres in one year, including as cyclones even some configurations without a closed isobar.

Moving from handmade to objective analyses (based on weather prediction numerical models) ambiguity is not overcome. The number of cyclones found in each analysis depends on the objective detection method that is established, as well as on the requirements that are considered and on the analysis resolution.

Alpert *et al.* (1990) performed the first study of frequency and characterisation of the Mediterranean cyclones with an objective base. In principle, any minimum in the 1000 hPa geopotential field was accepted as a cyclone, however weak it was. In spite of the low resolution of the analyses (equivalent to 2,5º X 2,5º lat-lon, that is, a grid size of around 250 km) a large number of cyclonic centres was detected, 14 per analysis, although the area analysed was very large, much more than the pure Mediterranean. When a minimum pressure gradient around the centre is required (0.5 hPa / 500 km) the number of cyclonic centres is reduced, mainly in summer, by night.

Although in many later studies minima of pressure or geopotential are associated to cyclones (Trigo *et al.*, 1999; Maheras *et al.*, 2001; Picornell *et al.*, 2001 or Campins *et al.*, 2011), in some other cases (Flocas *et al.*, 2001, following Sinclair, 1997) the cyclones are defined as maxima of vorticity (or cyclonic circulation). The analysis resolution, including a possible smoothing, and the definition of additional requirements affect very much the number of cyclones or cyclonic centres that are detected.

In Picornell *et al.* (2001), with reference to the Western Mediterranean only, objective analyses of the HIRLAM system, with resolution of 0.5º X 0.5º lat-lon, grid size around 50 km, were used. This resolution was much higher than the one used in Alpert *et al.* (1990), so much more cyclones per unit of area would be expected, but a relatively hard restriction was imposed: pressure gradients of at least 0.5 hPa /100 km, at least in six directions around the centre. In these conditions, with four analyses per day, something more than 2000 cyclonic centres are detected in the Western Mediterranean. This is equivalent to around 1000 individual cyclones per year, with a mean lifetime of the individual cyclones of around 12 hours. These Figures are quite consistent with the ones obtained when using mesoscale subjective analyses (Radinovic, 1978; Genovés and Jansà, 1989; Campins *et al.,* 2000).

Smoothing the fields before performing the detection and description of cyclones was considered convenient for a number of studies performed in the MEDEX framework (http://medex.aemet.uib.es), in order to make the fields more tractable. A Cressman filter of 200 km was used to do it (Cressman, 1959). But the smoothing has an important effect on the cyclone counting. Gil *et al.* (2003; see Figure 1) have found 2910 cyclonic centres per year in the Western Mediterranean, when using operational European Centre for Medium Range Weather Forecasting (ECMWF) analyses, with four analyses per day. This is a consistent result with former accountings coming from detailed analyses. But if the ECMWFC fields are smoothed with a Cressman filter the number of cyclonic centres goes dramatically down, with 437 centres per year. It is supposed than only small and weak cyclones are eliminated by smoothing.

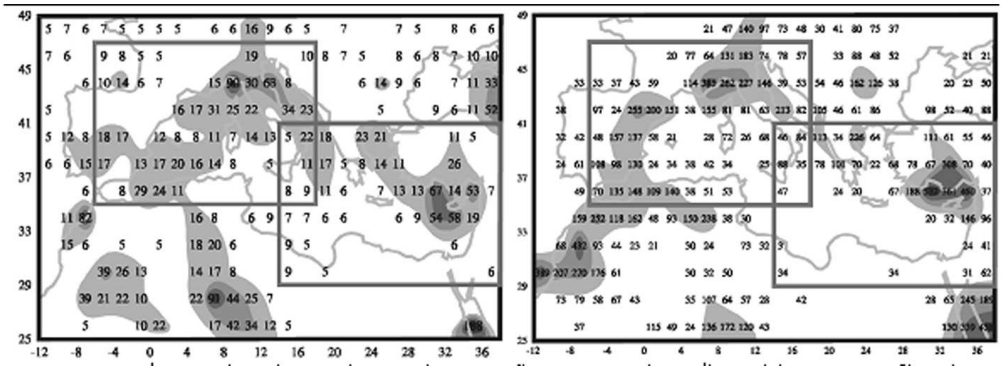

Figure 1. Number of cyclones detected per year, from ECMWF analyses, filtered (left) and non-filtered (right). (From Gil *et al.*, 2003).

In Campins *et. al.* (2011), a large area is considered, including the whole Mediterranean region and the surrounding zone. Even when the analyses resolution is low (grid size of 125 km: ERA-40 reanalyses, Uppala *et al.*, 2004) and the fields are smoothed by filtering, the total number of cyclonic centres is still important, 1800 centres per year, equivalent to around 800 individual cyclones per year, with a lifetime of a little more than 12 hours.

In summary, according to the resolution, scale or detail of the analyses of departure and depending on the restrictions that are included in the cyclone definition, in the whole Mediterranean, even the Western basin, tens, hundreds or even thousands of cyclone appearances or cyclonic centres can be detected. Clearly not all the detectable cyclones are equal, neither in structure nor in origin, intensity or size.

1.2 Characterization and typology

When all the detectable Mediterranean cyclones are considered, up to thousands in one year, it is not expected that all of them are typical extra-tropical cyclones, with upward motion and general bad weather within them. On the contrary, the most of the Mediterranean cyclones are small and weak shallow pressure disturbances, without vertical development.

In Figure 1 and in the several climatological studies already cited, the high concentration of cyclonic centres in certain areas calls the attention. It is also remarkable that the disappearance of cyclonic centres by smoothing is especially important in some specific areas. All this suggests that the geographic factors (orography and sea-land distribution) play an important role on the genesis and maintenance of the Mediterranean cyclonic centres.

In fact, the geographic singularity of the Mediterranean region – a closed sea, surrounded by high mountains – is probably the key of the high concentration of cyclonic centres in the region in general and in some areas of the region in particular.

Specifying, the area of the Gulf of Genoa, towards the south of the Alps, is the zone with the highest concentration of cyclones and cyclogenesis, at least when smoothed or low resolution maps are used. The Hemispheric maximum detected by Petterssen (1956) is associated to disturbances of this zone. This zone continues being a zone with relative high cyclonic concentration when fully detailed maps are used.

The concentration of cyclonic disturbances in the zone of Genoa and surroundings is so high (particularly when thinking on relatively large cyclones) than the concepts of Mediterranean cyclone and Genoa or Alpine cyclones have been taken as almost equivalent. The orographic factor has repeatedly been evidenced for this type of cyclones. Classical studies in this sense are Radinovic (1965) and Buzzi and Tibaldi (1978). Radinovic (1987) considers that the inclusion of a type C (orographic) cyclone, together with the cyclone types A and B of Petterssen and Smebye (1971) is necessary in the Mediterranean. The orographic factor is outstanding for the Genoa cyclones, but a key role of fronts and upper air disturbances is not excluded, particularly for the Genoa cyclones that become more than small scale disturbances.

When the capacity of detection is increased, a second maximum of frequency appears, with a magnitude that is even comparable to the one of the maximum of Genoa. This second maximum is around Cyprus, in the Eastern Mediterranean. Although some powerful cyclones can be found in the Cyprus area, Alpert *et al.* (1990) remark that this maximum is more frequent on summer and at night, associated to a relatively warm sea. Many of these cyclones disappear when the maps are smoothed, as can be seen in Figure 1. It can be inferred than many of these depressions are mild and with a thermal character. In fact, thermal singularities, particularly warm singularities, appear as the second cause of cyclonic presence in the Mediterranean, together with the orography.

In the closest to Spain part of the Western Mediterranean zone, leaving the Genoa zone apart, important maxima of frequency are observed, particularly when unsmoothed and detailed maps are used. For example, in the south of the Pyrenees there is a singular maximum (see Figure 1, right, according Gil *et al.,* 2002, as well as Genovés and Jansà, 1989; Campins *et al.*, 2000; Picornell *et al.*, 2001). The inner Iberian Peninsula and the maritime zone between the Iberian Peninsula and the African coast (Algeria, Alborán, Palos) are other significant accumulations of cyclonic centres. The Balearic Sea, the Spanish Eastern and the Catalan coasts and the gulf of Lyon present a lesser, but not negligible, frequency of depressions.

The most of the cyclonic disturbances located in the south of the Pyrenees are of the orographic type, shallow and sufficiently unimportant to disappear if the smoothing is applied or the resolution is decreased. This type of disturbance, that is associated to northern flow across the Pyrenees, is a lee orographic low, and corresponds to the negative part of the orographic "dipole" of pressure that is associated to the global mountain range drag; but also the thermal component is important, with cold air in the windward side and warm air in the lee (Bessemoulin *et al.*, 1993).

Apart of the Pyrenean disturbances, many other small scale Mediterranean depressions are also lee orographic lows, including many of the depressions in the maritime zone of Algeria-Alborán-Palos. Also many of the depressions located in the Spanish Eastern or Catalan coasts are lee orographic lows, at least in their initial phase (Genovés *et al.*, 1997; Campins *et al.*, 2000). But it is also possible than in many of the Algeria-Alborán-Palos lows the thermal factor (a warm nucleus, formed by warm advection or sea-land contrast) is determinant or important.

With rare exceptions, almost all of the low centres located in the inner Iberian Peninsula have a thermal (warm) character. Their great seasonality, with a maximum of frequency on summer, particularly early in the afternoon, corroborates it (Hoinka and Castro, 2003; Campins *et al.*, 2000; Picornell *et al.*, 2001; Campins *et al.*, 2006a; Campins *et al.*, 2011).

1.3 Thickness and intensity

A simple way to discriminate between cyclonic centres, trying to identify typical extra-tropical cyclones, is looking to their thickness. A typical extra-tropical cyclone, associated to upwards motion and "bad weather", is expected to be deep, with a large vertical thickness, with the cyclonic circulation reaching the limits of the tropopause.

In the work done in the MEDEX framework, oriented to construct cyclone catalogues (http://medex.aemet.uib.es), the vertical structure of the detected cyclonic centres was included. When a cyclonic centre was detected at surface, its possible presence (and description) was considered at progressively higher levels. The last level at which a minimum of geopotential or a maximum of vorticity was found, defined the vertical thickness of the cyclonic centre. By this way, we define shallow cyclones (detected up to 850 hPa, but not at higher levels), deep cyclones (those reaching up to 300 hPa) and intermediate cyclones (the rest).

Even if only the cyclones detectable by smoothed analyses are considered, that is, once the most weak and small cyclones are removed by smoothing, still many of the remaining cyclones are shallow, specifically 51% of all the cyclones, according Campins *et al.* (2006a), or 42%, according Campins *et al.* (2011).

Following Campins *et al.* (2011), many of the shallow centres are thermal or orographical-thermal centres, as suggested by their seasonality, with a much higher percentage in summer (62% of all the centres) than in winter (26%), while the percentage of deep cyclones higher in winter (55%) than in summer (21%).

With regard to the thickness, the differences between geographical areas are remarkable. The Genoa centres are shallow in only a 27% of the cases and they are deep in a 55%. On the contrary, the inner Iberian Peninsula centres are shallow in a 59% of the cases and deep in only a 27%; the Algeria-Alborán-Palos cyclones are shallow in a 52% of the cases and deep in a 33%. (Campins *et al.*, 2011).

When only cyclones with a lifetime of more than 6 hours are considered, an important detail (Campins *et al.,* 2011) is that the percentage of deep centres increases with the maturity of the cyclone: it is less in the initial phase than in the mature phase. This corroborates the idea that some (at least) of the more significant Mediterranean cyclones are the result of a coupling between a small scale shallow germ (an orographical or thermal low) and a large scale upper air disturbance. The peculiar geography of the Mediterranean region would permit the generation of a lot of cyclonic germs; only few of them would become well developed cyclones (Genovés and Jansà, 1991; Jansà, 1997). Apart of it, in some of the most developed cyclones a contribution of the diabatic factors, like the latent heat release, is also important (Homar *et al.*, 2002, or Genovés and Jansà, 2003, for example).

Thinking in the cyclones themselves and on their impacts, the intensity or intrinsic importance of the cyclones can be an outstanding magnitude. There are several ways to define the intensity or the intrinsic importance of a cyclone, like the central pressure or the pressure gradient, the pressure Laplacian or the vorticity around the centre. To construct cyclone catalogues in the MEDEX framework (http://medex.aemet.uib.es) the Sinclair (1997) option was adopted, taking the total geostrophic circulation (GC) as the cyclone intensity or intrinsic importance of the cyclone. GC is the vorticity integrated to the whole cyclonic domain, that is, to all the area with positive vorticity or cyclonic circulation. To equal size the cyclone with higher vorticity (o pressure gradient) is more intense. But to equal vorticity the larger cyclones will be considered more intense (or important). A practical unit for GC is 1 GCU = 10^7 m^2 s^{-1}.

The classification of the cyclones in weak, moderate or intense attending to GC value is certainly subjective, but it seems reasonable to define as weak the cyclones with GC less than 2 GCU and as intense those with GC of 6 GCU or more (Picornell *et al.*, 2001). In Campins *et al.* (2006a), Campins *et al.* (2011) or Homar *et al.* (2007) the qualification of intense is reserved for the cyclones with 7 GCU or more.

Many weak cyclones are detected when unsmoothed analyses with relatively high resolution are used. In Picornell *et al.* (2001) 53% of all the cyclones are weak. With the same resolution, but after smoothing, the frequency of weak cyclones decreases to 16% (Campins *et al.*, 2006a), and it becomes only 8% if also the resolution is reduced (Campins *et al.*, 2011). As expected, many of the weakest cyclones disappear when the resolution is reduced and the fields are smoothed by filtering them.

Intense cyclones are always scarce, in particular only 6,3% of all the cyclones in Campins *et al.* (2011); when only considering intense cyclones with a lifetime of at least 24 hours, the approximate number in the whole Mediterranean is 30 per year (Homar *et al.*, 2007). Their geographical distribution can be seen in Figure 2.

F

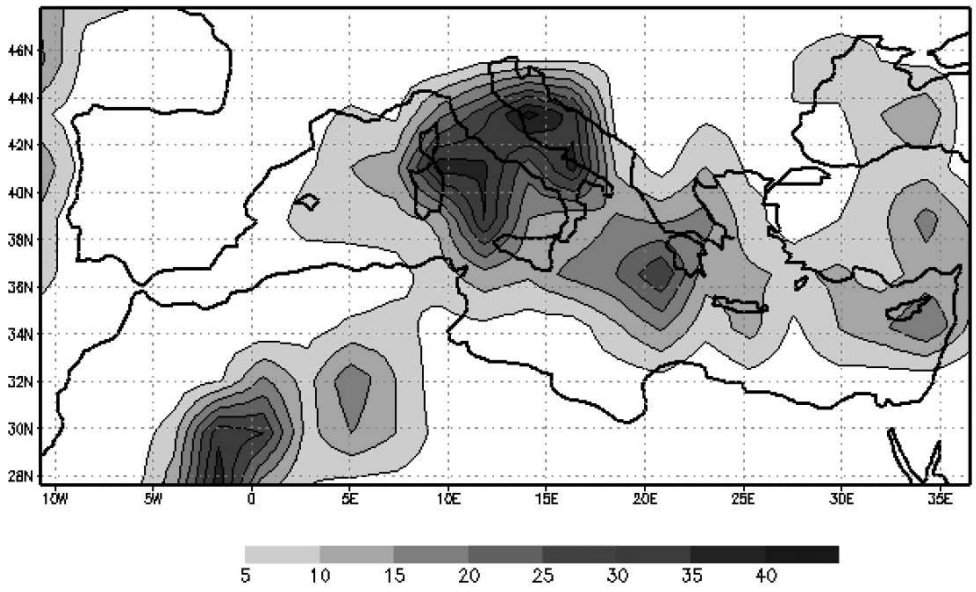

igure 2. Distribution of intense cyclones with lifetime of at least 24 hours. The number of cyclones during the 1957-2002 period, ERA-40, is represented in 2,25º X 2,25º lat/lon boxes. (From Homar *et al.*, 2007).

The process of maturation of the cyclones, usually with pressure dropping and size increasing, requires time and space, therefore the intense cyclones (high GC) tend to appear separated to the generation zones, towards the open seas. By this way the cyclones born in Genoa provide the most important maxima of frequency of intense cyclones, but these maxima are shift downstream of the generation zone, towards the Tyrrhenian Sea and the Adriatic Sea (Figure 2).

According to fig. 2, in inner Africa there is another important maximum, but this one is explained for the large extension of many thermal and lee lows there generated. Secondary maxima can be observed in the Central and Eastern Mediterranean. In the most western part of the Mediterranean, the area closest to the Iberian Peninsula, the frequency of intense cyclones looks low, although a secondary maximum towards the Balearics can be guessed. In fact in the zone close to Spain (Balearic Sea and surrounding) around three intense and durable cyclones per year can appear in average (Homar *et al.*, 2007).

Looking to cyclones with exceptional intensity, their fully maritime character is stressed, with a preferred location in open zones (Genovés *et al.*, 2006). From ERA-40 smoothed analyses, the six most intense cyclones observed during the 1957-2002 period have been centred in the Tyrrhenian or in the Central Mediterranean. The seventh most intense cyclone (with more than 12 GCU) was centred in the Balearics in its most mature moment.

This part can be ended by saying that, in general, shallow cyclones are smaller and weaker than deep cyclones, although there are exceptions (Campins *et al.*, 2006a).

2. IMPACTS

In the Spanish area influenced by the Mediterranean, high social impact weather events, like heavy rain or strong wind, are not rare. A ten year sample of this kind of events can be seen in the MEDEX data base (http://medex.aemet.uib.es). The presentation of a climatology of high impact weather events in the zone is not the objective of this chapter. What is intended is to link them with the Mediterranean cyclones. It can be anticipated that there is no a pure and universal proportionality between cyclone intensity and violence of the associated phenomena, although it seems obvious that the most intense cyclones have to have significant effects.

2.1 Impact of the intense cyclones

In the intense extra-tropical cyclones there is combination between strong divergence in upper air levels and strong convergence in the low levels, leading to a vigorous upwards motion, associated to important rainfall. On the other hand, very low pressure in the centre, associated to strong pressure gradient, implies strong wind. Therefore intense and deep extra-tropical cyclones produce significant combined storms, with strong wind and heavy rain.

The Mediterranean storm of 10-11 November 2001 is a paradigmatic case. It is associated with the seventh most intense cyclone in the Mediterranean, during the whole ERA-40 period (1957-2002) and it is the most intense of all the Mediterranean cyclones observed near Spain in this period (Genovés *et al.*, 2006). Rainfall was very heavy in Algiers, where flooding produced hundreds of deaths (Hamadache *et al.*, 2003); also in Mallorca more than 250 mm of precipitation were registered. In fact the heavy rainfall is a consequence, but also a factor of the big cyclone development (Genovés y Jansà, 2003). Winds on land overpassed 150 km/h. Extreme winds affected a large maritime zone, producing very rouge seas. Some wave analyses indicated up to eleven meters of significant wave high. In the Balearic Islands, the combination between strong wind and heavy rain caused the uprooting

of hundreds of thousands of trees. This storm was generated in northern Africa and progressed over the Mediterranean. An analogue evolution occurred with the storm of 22 December 1979, also very intense, with a GC something less than the November 2001 storm, but also above 12 UCG.

Although the wind and rain combined storms associated to Mediterranean intense cyclones are not frequent in the vicinity of Spain and tend to have a maritime character (see Figure 2), they can affect some Spanish areas, like the Balearics, Catalonia ot the Valencia Community, several times per year, at least their coastal zones.

The cyclone intensity defined by the GC perhaps is not always the best magnitude to measure the potential damage of a cyclonic disturbance. The central pressure can be an alternative indicator. For instance, cyclones with a central pressure of less than 990 hPa can be considered important. When using ERA-40 smoothed analyses, 37 of these cases appear in the most western Mediterranean area, in the period 1957-2002, the most of them centred on the sea (http://medex.aemet.uib.es). A high impact of these cyclones on Spanish areas can be expected. In particular, the cyclone with the lowest central pressure among the former series of very low pressure cyclones corresponds to the case of 1 December 1959, with a central pressure of 975 hPa. The prestigious newspaper "La Vanguardia" from Barcelona, on 2 December devoted the following words to this cyclone: "Furious rain, wind and show storm on the night from Monday to Tuesday. There are important damages in the whole country as a consequence of the hurricane, which in some places reached 140 km/h". The second cyclone in the lowest pressure ranking was the one of 30 January 1986, with a central pressure of 980 hPa and producing a paralyzing snowfall in Catalonia (Jansà y Vázquez, 1991). The two cyclones cited just above presented high GC, particularly the first, (11.51 GCU and 7.78 GCU, respectively), but these GC are not the maximal values. On the contrary, the big storm of November 2001, with the highest GC in the most western Mediterranean, has a non-extreme central pressure, with a 993.6 hPa value. The December 1979 storm was one the highest GC cyclone and also one with the lowest central pressure, with 985 hPa.

The low resolution analyses (including here those with 50 km of grid size), particularly if they are smoothed by filtering, tend to overestimate the central pressure values, especially when the size of the cyclones is small. The "medicanes" (to which a specific chapter of this book is devoted) are a particular case. For example, the medicane that passed across Mallorca on 12 September 1996, with a central pressure of around 992 hPa (Gili *et al.*, 1997), was detected by the smoothed ERA-40 and HIRLAM-INM analyses (http://medex-aemet-uib.es), but with central pressures of only 1002 and 1000 hPa, respectively. Apart from the medicanes, there are other small and intense Mediterranean cyclones; in 2010, for instance, three cases with less than 990 hPa were observed near the Balearics, producing heavy rain and/or strong wind. Little is known about the frequency or distribution of the small intense cyclones, but the present analyses, with resolutions on only few kilometres and improved technique, will provide rich information soon. In any case, it can be supposed that the medicanes and the other small intense cyclones increase the incidence of combined storms with respect to what the former paragraphs say.

2.2 Cyclones and heavy rain

Several mechanisms can produce heavy rain, which are not necessarily excluding, from intense isolated thunderstorm, associated to large instability, to large mesoscale convective systems, anchored by appropriate upper and lower levels circulations (Doswell, 1982; Doswell *et al.*, 1996; Rivera and Riosalido, 1986; Riosalido, 1997; Romero *et al.*, 2000; etc.). An interesting ingredient for the rain totals a large amount of precipitation in a relatively short time is a sustained warm and wet low level flow, producing destabilisation and feeding the rainfall. The Mediterranean air-mass, relatively warm and humid, particularly in autumn, can provide the matter for this flow. The presence of a depression in the zone can organise and start the feeding flow. The combination with a convergence at the end of the warm and wet current, below cold air, complete a conceptual model that can in principle be descriptive of many cases of Mediterranean heavy rain (Figure 3, Jansà, 1997).

This conceptual model is easy to be identified in many particular cases of convective system or heavy rain in the whole Western Mediterranean (Jansà *et al.*, 1991; Jansà *et al.,* 1996).

Jansà *et al.* (2001) have attempted a systematic and statistical checking of the above conceptual model. Taking 60 mm/day as a threshold for heavy rain, all the cases observed during the 1992-1996 period, in a wide part of the Western Mediterranean have been analysed. The whole Spanish Mediterranean coast (divided in provinces and islands) is covered by the study. The period is not very large, but the number of cases is above 30 in Girona, Barcelona, Valencia, Alicante and Mallorca. A data base of cyclones is explored looking for a cyclone in the vicinity of the heavy rain area. The cyclone data base is mixed, mostly coming from handmade high resolution analyses and part coming from objective direct HIRLAM-INM analyses, without smoothing. The result is that there is a cyclone, simultaneous to the heavy rain event, centred at 600 km or less of the heavy rain area, in a 94-100% of the cases, except in Andalusia, where the percentage decreases to 69% (Málaga). The high percentages found in the most of the territory could not be demonstrative of a direct relationship, but they could be result of chance, because the used cyclone data base contains a lot of cyclones, not excluding small and weak cyclones. But two factors point to a true relationship between cyclone and heavy rain. First, the location of the simultaneous cyclone is not random, but it is consistent with the conceptual model before described: for Catalonia, the Valencia Community and Murcia and the Balearics, the cyclonic centre is located towards the south of the heavy rain area, forcing towards it an easterly warm and wet Mediterranean inflow. Second, if a random sample of days is used, instead of heavy rain days, the percentage of close cyclone decreases from near 100% to only 60-70% (Andalusia excluded).

It can be added here that not all the cyclones associated no heavy rain are necessarily intense cyclones (Jansà *et al.*, 2001). In fact, when the fields are smoothed (by filtering), which eliminates the weakest and smallest cyclones, the percentage of simultaneity between heavy rain a a close cyclone decreases significantly. Apart from Andalusia, the percentage goes from near 100% to around 70%. Furthermore the decreasing is not the same in the whole territory. The greatest reduction occurs in the Valencia Community and Murcia, where the percentage of simultaneity goes from 99% to 57% (Campins *et al.*, 2002). The

smallest decline is in the Balearics, where the frequency of simultaneity between heavy rain and cyclone in the vicinity remains at 86% even alter smoothing the fields (Campins *et al.*, 2006b). In the Balearics case the cyclonic centres tend to be very close to the heavy rain area; furthermore the proportion of deep cyclones is significantly larger for the cyclones associated to heavy rain than for the ensemble of cyclones near to the Balearics (Campins *et al.*, 2006b). Catalonia is in an intermediate position and the percentage of simultaneity of heavy rain a close cyclone decreases from 95% to 78% when the fields are smoothing, that is, after eliminating the weakest and smallest cyclones (Campins *et al.*, 2007).

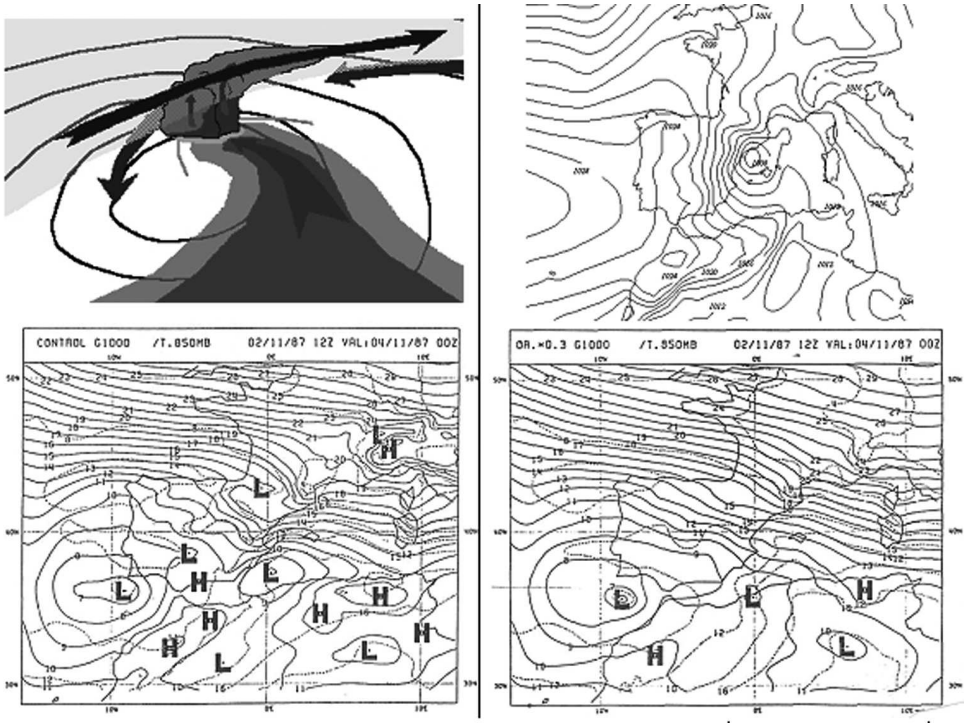

Figure 3. Up: Conceptual model of heavy rain organised by cyclone (left) (Jansà, 1997). Sea level pressure on 10 June 2000, at 06 UTC, with floods in Montserrat, Catalonia (right) (http://medex.aemet.uib.es). Down: Rainfall record in southern Valencia, with more than 800 mm in 24 h, 3-4 November 1987. Numerical experiment: the control run (left) exhibits a cyclonic centre in Palos-Alborán-Algeria that creates and orients a well defined flow towards to heavy rain area; when the orography is lowered (to only 30%) the cyclone almost disappears and the Mediterranean flow losses organisation (right) (Jansà *et al.*, 1991).

In summary, the heavy rain events in the Balearics are almost always simultaneous to a close cyclonic presence, very close in fact, and this cyclone is rarely weak and shallow. The majority of the heavy rain events in Catalonia are associated to cyclones centred by the Balearics Sea, which are usually moderate. There is a

significant part of cases in which a weak cyclonic centre appears as the simultaneous ccylone, but the connection could not be real. On the contrary, in some cases there is a connection with a distant cyclone, which provides a vigorous flow against the Pyrenees (Campins *et al.*, 2007). In the regions of Valencia and Murcia, where the events of heavy rain have the highest frequency in the Spanish Mediterranean zone, almost all the heavy rain events are simultaneous with a close cyclonic presence, with the centre located in the Algerian-Alborán-Palos maritime zone, but the range of intensity of the involved cyclone is wide. Many of these cyclones are weak and shallow and are therefore they are missed with the smoothing (filtering) of the fields, but they exist and can be enough efficient to organise a warm-wet feeding flow, according to the conceptual model above described (Figure 3).

2.3 Cyclones and strong winds

The existence of strong winds within an intense cyclone, with strong pressure gradient, does not need demonstration. By this way, some of the windstorms in the Mediterranean and its coastal areas can be associated to close cyclones with high GC. But, looking to Spain, we know that this kind of cyclones is not frequent in the most western Mediterranean, so the frequency of windstorms by this mechanism could not be very high. Also close cyclones with very low central pressure, even with non-high GC (due to their small size) can be associated to windstorms; but also these cyclones are not very frequent in the Spanish Mediterranean area.

Nevertheless, in the Spanish Mediterranean area, at least in some of its zones, the incidence of strong winds is quite important and frequent. There is no doubt that the Mistral-Tramontane wind system is the most important in the whole Mediterranean, causing frequent maritime storms in zones close to Spain and including some terrestrial areas, like the north-eastern part of Catalonia and of the Balearics (H.M.S.O., 1962; Jansà, 1987; Campins *et al.*, 1995). In some points of these areas (like the Capdepera lighthouse or Begur Cape) over passing 100 km/h, even 130 km/h is not rare. Strong Tramontane is not always simultaneous in NE-Catalonia and NE-Balearics; in fact, it is more frequent in Catalonia than in the Balearics. About the Cierzo in the Ebro valley, this is a quite frequent strong wind too, frequently associated to the Mistral-Tramontane system (Riosalido *et al.,* 1986; Jansà, 1997). Other strong winds, particularly some strong westerly and easterly winds, can affect many other points of the Spanish Mediterranean area, but they are much more occasional.

With regard to the Balearics Islands, the strong wind events (with gusts of 25 m/s in general or 33 m/s in the most windy places) can be associated to cyclones in the 98% of the cases, although they are mostly quite distant cyclones, up to 1500 km, frequently located in the Genoa-Tyrrhenian-Adriatic zone, in coincidence with the zone where the intense cyclones are more frequent (Figure 2). In spite of it, cyclones close to the Balearics, within a radius of 600 km, can be found in 34% of the strong wind cases. The most of the cases associated to strong wind in the Balearics are quite intense (with GC around 7 GCU) and deep (Campins *et al.,* 2006b).

In Catalonia, the simultaneity between strong wind and cyclone can be established in a 64% of the cases. Then the cyclone centre uses to be located towards the south of Catalonia (Balearic sea) or towards Genoa and vicinity (Campins *et al.,* 2007). There are many cases of strong Tramontane that are simultaneous in Catalonia and the Balearics and that are linked to intense cyclones in the Genoa-Tyrrhenian-Adriactic zone, but there are also cases in which the strong Tramontane wind is quite local in Catalonia, without connection with an important cyclone centre. In both types of cases, the general air flow blows from the north, across the Pyrenees, then forming an orographic pressure dipole (Bessemoulin *et al.*, 1993). In both cases, the strong pressure gradient associated to the positive (anticyclonic) component of this dipole provides local acceleration of the wind in the eastern edge of the Pyrenees (Campins *et al.,* 1995; Campins *et al.,* 1997). On the other hand, the negative component of the same dipole, which is displayed by the frequent small scale depressions in the south of the Pyrenees (Figure 1), provides local acceleration for the Cierzo wind (Riosalido *et al.,* 1986).

Small orographic and coastal small depressions can provide pressure gradient increasing and local acceleration, like in some Westerlies in the Gulf of Valencia and the Balearics (Jansà, 1997), although sometimes the main engine of a strong Mediterranean wind is a distant cyclone, located out of the Mediterranean, far from the strong wind zone (Nissen *et al.*, 2010).

3. CONCLUSIONS

In the Mediterranean, even in the Spanish Mediterranean or in the part of the Mediterranean closest to Spain, a high number of cyclones, or cyclonic centres, is found, particularly if weak, small and shallow cyclones are included (most of them orographic or thermal). Only a small percentage of the Mediterranean cyclones are intense and can produce important combined impacts in the same area where they are located. In particular, there are very few intense cyclones in the most western Mediterranean zone, so the frequency of strong combined storms of rain and wind of this type is low in the Spanish Mediterranean area, although some of them can be very important.

By contrast, the intense Mediterranean cyclones are concentrated in the Genoa-Tyrrhenian-Adriatic zone, from where they have an important distant effect in the Spanish territories, contributing to the high incidence of strong Tramontane and Cierzo winds.

Weak or moderate cyclones do not produce marked impacts in general, but in some circumstances they become a key factor in triggering heavy rain events, through the organisation of a feeding inflow. In fact, the most of the heavy rain events in the Spanish Mediterranean are linked to Mediterranean cyclones, which do not need to be intense, frequently being moderate or weak. The relative percentage of weak cyclones that are associated to heavy rain, in front of moderate or intense cyclones, is important for the Valencia Community and Murcia, and not so much for Catalonia and especially for the Balearics, where few cyclones related to heavy rain are weak.

ACKNOWLEDGEMENTS

This chapter presents some results of the work made by a lot of scientists, in particular by the members of the group of AEMET in the Balearics Islands dedicated to the Mediterranean Meteorology, especially Ana Genovés, Joan Campins and María Ángeles Picornell. This work has been made in the frame of several international projects, as WMO-MCP, PYREX, MAP and MEDEX, above all.

REFERENCES

Alpert, P.; Neeman, B. U. y Shay-El, Y. (1990). Climatological analysis of Mediterranean cyclones using ECMWF data. *Tellus*, 42A, 65-77.

Bessemoulin, P.; Bougeault, P.; Genovés, A.; Jansà, A. y Puech, D. (1993). Mountain Pressure Drag during PYREX. *Beitr. Phys. Atmosph.*, 66, 305-325.

Buzzi, A. y Tibaldi, S. (1978). Cyclogenesis in the lee of the Alps: a case study. *Quart. J. R. Met. Soc.,* 104, 271-287.

Campins, J.; Jansà, A.; Benech, B.; Koffi, E. y Bessemoulin, P. (1995). PYREX Observation and Model Diagnosis of the Tramontane Wind. *Meteorol. Atmos. Phys.,* 56, 209-228.

Campins, J.; Calvo, J. y Jansà, A. (1997). The Tramontane Wind: Dynamic Diagnosis and HIRLAM Simulations. *INM/WMO International Symposium on Cyclones and Hazardous Weather in the Mediterranean.* Universitat de les Illes Balears y Ministerio de Medio Ambiente. ISBN-84-7632-329-8, 503-508.

Campins, J; Genovés, A.; Jansà, A.; Guijarro, J.A. y C. Ramis (2000). A catalogue and a classification of surface cyclones for the Western Mediterranean. *Int. J. Climatol.,* 20, 969-984.

Campins, J.; Jansà, A.; Genovés, A. y Picornell, M.A. (2002). Heavy rain and cyclones in the Western Mediterránean. *EGS 2002 General Assembly, Nize.* (Presentación sin publicar).

Campins, J.; Jansà, A. y A. Genovés (2006a). Three-dimensional structure of Western Mediterranean cyclones. *Int. J. Climatol.,* 26, 323-343.

Campins, J.; Jansà, A. y Genovés, A. (2006b). Heavy rain and strong wind events and cyclones in the Balearics. *Advances in Geosciences,* 7, 73-77.

Campins, J.; Aran, M.; Genovés, A. y Jansà, A. (2007). High impact weather and cyclone simultaneity in Catalonia. *Advances in Geosciences,* 12, 115-120.

Campins. J.; Genovés, A.; Picornell, M.A. y Jansà, A. (2011). Climatology of Mediterranean cyclones using ERA-40 dataset. *Int. J. Climatol.,* 31(11), 1596-1614.

Cressman, G. (1959). An operational objective analysis system. *Mon. Wea. Rev.,* 87(10), 367-374.

Doswell, C.A. (1982). *The operational meteorology of convective weather, Vol I, Operational mesoanalysis*. NOAA Tech. Mem. NWS NSSFC-5, 157

Doswell, C.A.; Brooks, H.E. y Maddox, R.A. (1996). Flash Flood Forecasting: An Ingredients-Based Methodology. *Weather and Forecasting,* 11, 560-581.

Flocas, H.A.; Maheras, P.; Karakostas, T.S.; Patrikas, I. y Anagnostopoulou, C. (2001). A 40-year climatological study of relative vorticity distribution over the Mediterranean. *Int. J. Climatol.,* 21, 1759-1778.

Genovés, A. y Jansà, A. (1989). Statistical Approach to Mesoscale Non-Alpine West Mediterranean Cyclogenesis. *WMO/TD* No. 298, 77-85.

Genovés, A. y Jansà, A. (1991). The use of potential vorticity maps in monitoring shallow and deep cyclones in the Western Mediterranean. *WMO/TD* No. 420, 55-65.

Genovés, A.; Jansà, A. y Estarellas, C. (1997). First evalutation of orographic factor in Western Mediterranean cyclones. *INM/WMO International Symposium on Cyclones and Hazardous Weather in the Mediterranean.* Universitat de les Illes Balears y Ministerio de Medio Ambiente. ISBN-84-7632-329-8, 273-282.

Genovés, A. y Jansà, A. (2003). Diabatic processes contribution to the November 2001 storm. *Proceedings of the 4th EGS Plinius Conference held at Mallorca, Spain, October 2002.* Universitat de les Illes Balears. CD-ROM, ISBN-84-7632-792-7.

Genovés, A. ; Campins, J. y Jansà, A. (2006). Intense storms in the Mediterranean: a first description from the ERA-40 perspective. *Advances in Geosciences,* 7, 163-168.

Gil, V.E.; Genovés, A.; Picornell, M.A. y Jansà, A (2003). Automated database of cyclones from the ECMWF model: preliminary comparison between West and East Mediterranean basins. *Proceedings of the 4th EGS Plinius Conference held at Mallorca, Spain, October 2002.* Universitat de les Illes Balears. CD-ROM, ISBN-84-7632-792-7.

Gili, M.; Jansà, A.; Riesco, J. y García-Moya, J.A. (1997). Quasi-tropical cyclone on 12th September in the Balearics. *INM/WMO International Symposium on Cyclones and Hazardous Weather in the Mediterranean.* Universitat de les Illes Balears y Ministerio de Medio Ambiente. ISBN-84-7632-329-8, 143-150.

H.M.S.O. (1962). *Weather in the Mediterranean*. *Volume 1. General Meteorology*. Meteorological Office, London, 362

Hamadache, B.; Terchi, A. y Brachemi, O. (2003). Study of the meteorological situation which affected the west and the center of Algeria in general and Bab-el-Oued in particular on the 10th November 2001. *Proceedings of the 4th EGS Plinius Conference held at Mallorca, Spain, October 2002.* Universitat de les Illes Balears. CD-ROM, ISBN-84-7632-792-7.

Hoinka, K. y Castro, M. (2003). The Iberian thermal low. *Quart. J. R. Met. Soc.*, 129, 1491-1511.

Homar, V. ; Ramis, C. y Alonso, S. (2002). A deep cyclone of African origin over the Western Mediterranean: diagnosis and numerical simulation. *Ann. Geophys.,* 20, 93-106.

Homar, V.; Jansà, A.; Campins, J.; Genovés, A. y Ramis, C. (2007). *Nat. Hazards Earth Syst. Sci.,* 7, 445-454.

Jansà, A. (1987). Distribution of the Mistral. A satellite observation. *Meteorol. Atmos. Phys.,* 36, 201-214.

Jansà, A. y Vázquez, L. (1991). Situación meteorológica del 30 de enero de 1986. *Segundo Simposio Nacional de Predicción, Madrid 20-22 Noviembre 1990.* Instituto Nacional de Meteorología, Madrid, 19-27.

Jansà, A.; García-Moya, J.A. y Rodríguez, E. (1991). Numerical experiments on heavy rain and Mediterranean cyclones. *WMO/TD No. 420,* 37-47

Jansà, A.; Genovés, A.; Riosalido, R. y Carretero, O. (1996). Mesoscale cyclones vs heavy rain and MCS in the Western Mediterranean. *MAP Newsletter,* 5, 24-25.

Jansà, A. (1997). A general view about Mediterranean meteorology: cyclones and hazardous weather. *INM/WMO International Symposium on Cyclones and Hazardous Weather in the Mediterranean.* Universitat de les Illes Balears y Ministerio de Medio Ambiente. ISBN-84-7632-329-8, 33-42.

Jansà, A.; Genovés, A.; Picornell, M.A.; Campins, J.; Riosalido, R. y Carretero, O. (2001). Western Mediterranean cyclones and heavy rain. Part 2: Statistical approach. *Meteorol. Appl.,* 8, 43-56.

Jansà, A.; Campins, J.; Picornell, M.A. y Guijarro, J.A. (2011). Intense small cyclonic vortices in the Mediterranean. *13th Plinius Conference on Mediterranean storms.* (Presentación sin publicar).

Maheras, P.; Flocas, H.A.; Patrikas, I. y Anganostopouolou, C. (2001). A 40 year objective climatology of surface cyclones in the Mediterranean region: spatial and temporal distribution. *Int. J. Climatol.,* 21, 109-130.

Nissen, K.M.; Leckebusch, G.C.; Pinto, J.G.; Renggli, D.; Ulbrich, S. y Ulbrich, U. (2010). Cyclones causing wind storms in the Mediterranean: characteristics, trends and links to large-scale patterns. *Nat. Hazards Earth Syst. Sci.,* 10, 1379-1391.

Petterssen, S. (1956). *Weather Analysis and Forecasting. Volume 1. Motion and motion systems.* Mc Graw Hill, New York. 428

Petterssen, S. y Smebye, S.J. (1971). On the development of extratropical cyclones. *Quart. J. R. Met. Soc.,* 97, 457-482.

Radinovic, D. y Lalic, D. (1959). *Cyclonic activity in the West Mediterranean*. Memories 7, Federal Hydromet. Institute, Belgrade, 57

Radinovic, D. (1965). Cyclonic activity in Yugoslavia and surrounding areas. *Arch. Met. Geoph. Bioklim.,* A 14, 392-408.

Radinovic, D. (1978). Numerical model requeriments for the Mediterranean area. *Riv. Met. Aer.,* 38, 191-205.

Radinovic, D. (1987). *Mediterranean cyclones and their influence on the weather and climate*. WMO PSMP Rep. Series, no. 24, Geneva, 131

Riosalido, R.; Vázquez, L.; Gordo, A. y Jansà, A. (1986). Cierzo: Northwesterly wind along the Ebro Valley as a meso-scale effect induce don the lee of the Pyrenees mountain range: a case study during ALPEX Special Observing Period. *Scientific Results of the Alpine Experiment (ALPEX), Vol. 2.* WMO/TD – No. 108, 565-575.

Riosalido, R. (1997). Mesoscale convective systems in the Western Mediterranean, a satellite view. *INM/WMO International Symposium on Cyclones and Hazardous Weather in the Mediterranean.* Universitat de les Illes Balears y Ministerio de Medio Ambiente. ISBN-84-7632-329-8, 353-359.

Rivera, A. y Riosalido, R. (1986). Mediterranean convective systems as viewed by Meteosat. A case study. *6th Meteosat Scientific Users Meeting, Amsterdam 25-27 November 1986,* EUMETSAT, 101-104

Romero, R.; Doswell, C.A. y Ramis, C. (2000). Mesoscale Numerical Study of Two Cases of Long-Lived Quasi-Stationary Convective System over Eastern Spain. *Mon. Wea. Rev.,* 128, 3731-3751.

Sinclair, M.R. (1997). Objective identification of cyclones and their circulation intensity, and climatology. *Weather and Forecasting,* 12, 595-612.

Trigo, I.R.; Davies, T.D. y Bigg, G.R. (1999). Objective climatology of cyclones in the Mediterranean region. *Journal of Climate.* 12, 1685-1696.

Uppala, S.; Kallberg, P.; Hernández, A.; Saarinen, S.; Fiorino, M.; Li, X.; Onogi, K.; Sokka, N.; Andrae, U. y Bechtold, V.D.C. (2004). ERA-40: ECMWF 45-year reanalysis of the global atmosphere and surface conditions 1957-2002. *ECMWF Newsletter,* 101, 2-21.

CHAPTER 2

MEDICANES: QUASI-TROPICAL MESOSCALE CYCLONES IN THE MEDITERRANEAN

Climent RAMIS[1], María TOUS[1], Víctor HOMAR[1],
Romualdo ROMERO[1], Sergio ALONSO[1,2]

[1]*Departamento de Física. Universitat de les Illes Balears.*
[2]*Departamento de Investigación del Cambio Global. IMEDEA. UIB-CSIC.*
cramis@uib.es, maria.tous@uib.es, victor.homar@uib.es,
romu.romero@uib.es, sergio.alonso@uib.es

ABSTRACT

Certain mesoscale cyclones (diameter up to 300 km) that form over the Mediterranean have been called *medicanes*. The cloud structures associated with these depressions, including a cloud-free eye, resemble a tropical cyclone in satellite images. They have been observed in the western and central but scarcely in the east. They develop embedded in mature larger scale cyclones that cause cold air intrusions over the . A cold core cut off low with remarkable potential vorticity characterizes the higher levels. Numerical simulations of various episodes have shown the importance of sensible and latent heat surface fluxes but not of the topography on the path and intensification of *medicanes.* The latent heat release in convective clouds that accompany these cyclones proves to be a decisive factor for its development, as well as the high levels cyclonic disturbance during its genesis phase.

Key words: *medicane*, Mediterranean, cyclone, mesoscale.

INTRODUCTION

Satellite images, especially from Meteosat, have evidenced the occasional formation of cloud systems over the largely resembling, except for its size, tropical cyclones. Indeed, these systems are nearly axi-symmetric and possess convective cloud bands wrapped around a cloud-free central eye (see Figure 1).

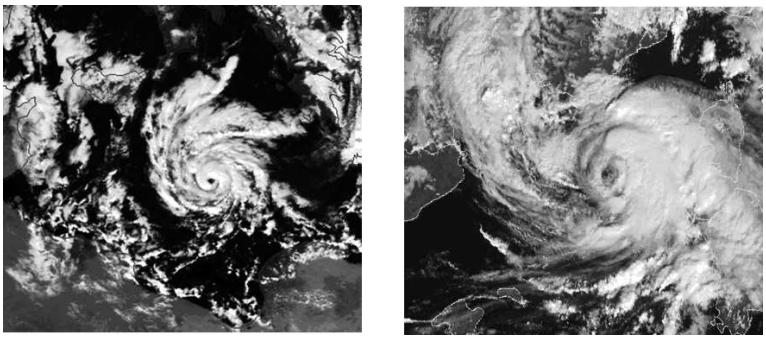

Figure 1. VIS images from Meteosat. a) 16 January 1995 at 13:00 UTC; b) 8 November 2011 at 10:00 UTC (source EUMETSAT).

When the size of these cloud clusters is small, on the order of in diameter, (Jansà, 2003), the atmospheric disturbances causing them have been called *MEDICANES* (MEDIterranean+hurriCANES; Emanuel, 2005). The cloudy structure of *medicanes* is very similar to that of polar lows that develop at high latitudes, especially off the Atlantic coast of the ; some authors even consider *medicanes* as polar lows forming at lower latitudes owing to the similarity of the physical mechanisms involved in their genesis and development (Bussinger and Reed, 1989).

Medicanes are nearly circular mesoscale cyclones that exhibit a great pressure gradient. This feature is well manifested by the shape of the barogram (Figure 2) and the translational speed registered for some of the cases. The storms generally produce heavy rainfalls and the associated winds can reach great intensities, in some cases close to the speeds produced by tropical cyclones. In the event that these cyclones approach the continental coast or move over an island, hazardous meteorological phenomena might be produced, causing great material losses and even personal injury. As an example, the *medicane* that formed on 1 October 1986 near the Algerian coast evolved northwards and crossed the during the night. The associated strong winds (higher than 50 kt) inflicted important damages to boats moored in the where a nautical exhibition was taking place. Estimated damage surpassed 5 M€. More recently, another *medicane* formed on 8 November 2011 between Mallorca and (Figure 1b). That one was named '*tropical storm 01M*' by NOAA. Its central pressure was estimated at 991 hPa and associated winds on the order of 45 kt could be inferred. It moved northwards and affected southern and north , where rainfalls in excess of in 24 h and 11 fatalities were produced. Further information on this case can be found at

http://oiswww.eumetsat.org/WEBOPS/iotm/iotm/20111108_tropstorm/20111108_tropstorm.html

From the pioneering work of Pettersen in 1956, the Mediterranean sea is well known as one of the most cyclogenetic zones worldwide. The Gulf of Genoa is particularly prone to the development of low-pressure systems when a primary cyclone evolves over Europe towards the east and the associated cold front enters over the Mediterranean and is distorted by the Alps and Pyrenees (Buzzi and Tibaldi, 1978).

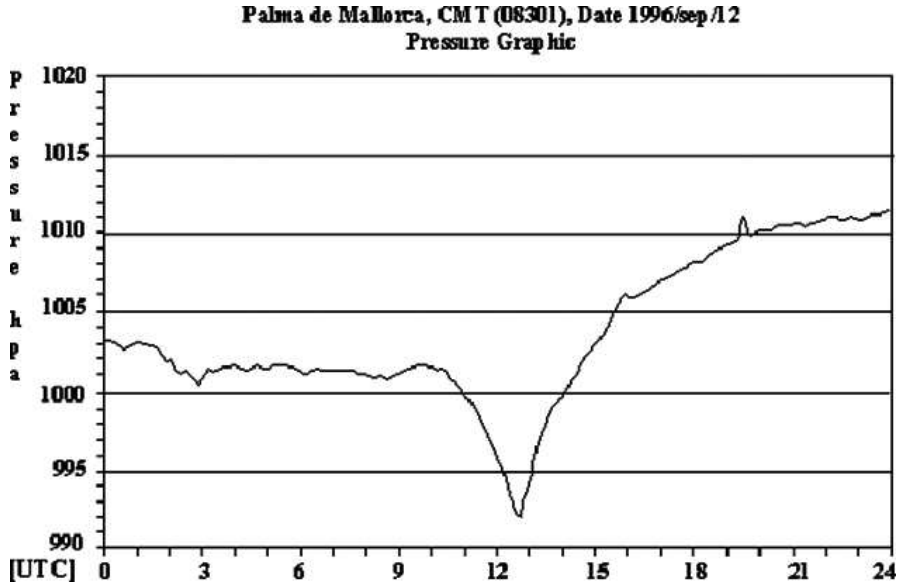

Figure 2. Barogram at Palma de Mallorca on 16 September 1996 (source AEMET).

The so developed cyclones very often give place to northerly windstorms in the Gulf of Lyon extending southwards even as far as Tunisia. On some occasions strong cold air advections reach the and interact with the Saharan warm air, producing a baroclinic zone along which the pre-existing desert cyclone deepens. As this depression develops and moves northwards over the , it experiences an additional intensification and a reinforcement of the associated winds. Some examples of this kind of developments are the 19-22 December 1979 (Homar *et al.,* 2002) and 10-12 November 2001 (Ramis *et al.,* 2003) cyclones. Both storms were highly damaging and also produced numerous fatalities, especially in .

It is possible to detect Mediterranean depressions that cover the full spectrum of sizes, from synoptic scale cyclones to *medicanes* or even smaller disturbances. This chapter will deal only with the type of cyclones described above as *medicanes* and which preserve the indicated cloud structure for a relatively long period. A few studies have investigated the environments in which these cyclones develop (Rasmussen and Zick, 1987; Pytharoulis *et al*., 2000; Tous and Romero, 2011; Tous and Romero, 2013) while other works have analysed, by means of numerical simulations, the most influential factors on the development and trajectory of some *medicanes* (e.g. Homar *et al.,* 2003; Tous *et al.,* 2013). The most relevant aspects obtained from both approaches are presented in the following sections.

2. CLIMATOLOGY OF MEDICANES

Objective methods aimed at cyclone detection and characterization of the thermal structure, e.g. Picornell *et al.* (2001), cannot be applied to *medicanes* using standard objective analyses and reanalyses (e.g. ERA40). The resolution of these

products impedes the characterization of these cyclones. As alternative, Tous and Romero (2011) followed the visual inspection of Meteosat IR images, once assembled at 30 min intervals in the form of movies. They considered the period from February 1982 to December 2005 and looked for cloud structures fulfilling the conditions: maximum diameter of , radial symmetry, presence of a cloud-free eye, evidence of convective clouds and lifespan longer than 6 h.

Inspection of satellite movies along with consideration of some bibliographical references of studied cases resulted in the identification of 12 cases strictly satisfying the above criteria. Figure 3 shows the spatial localization of these cyclones. It can be observed that *medicanes* have occurred in both the western and central . Half of them, 6 cases, have been observed in winter (DJF), 3 cases in autumn (SON), 3 cases in spring (MAM) and none during summer. The events list should be completed with the recent cases of 22 March 2007, 18 October 2007 and 8 November 2011, all of them over the western Mediterrane

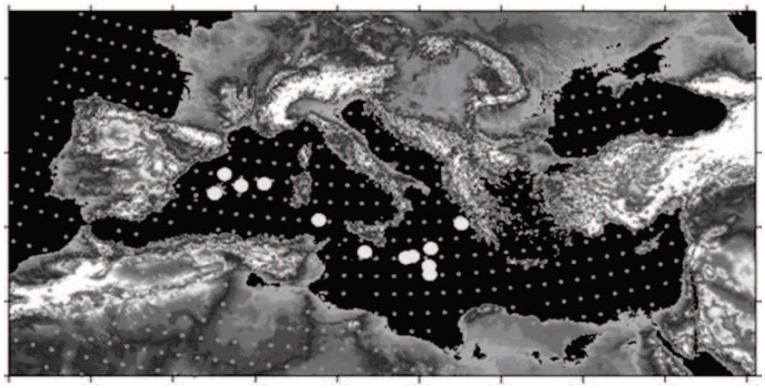

Figure 3. Geographical distribution of detected medicanes (from Tous and Romero, 2011).

3. METEOROLOGICAL ENVIRONMENTS

From the studies undertaken by Pytharoulis *et al.* (2000) and Homar *et al.* (2003), among others, it is deduced that *medicanes* develop in the core of cyclonic environments, characterized by a depression and a well marked cold front at surface and a prominent trough of cut-off cyclone at higher levels. These disturbances aloft have a cold character and possess high values of Potential Vorticity (PV) (Figure 4). This synoptic situation favours the intrusion of cold air over the . It was also observed that the *medicane* develops during the mature or final phase of the baroclinic cyclone.

It seems clear that the formation and subsequent development of the *medicane* requires some kind of seed as well as small scale mechanisms responsible for its deepening. The development of such a mesoscale cyclone by means of baroclinic instability alone would require very large wind shear and weak static stability, at

least at low levels. Thus, it is more logical to attribute this development to small-scale mechanisms such as the latent heat release in the convective systems occurring around the nucleus of the cyclone and to an intense evaporation from the sea that would permit the maintenance of the convection during a prolonged period of time. Though at larger scale, these are the mechanisms that concur during the development of tropical cyclones.

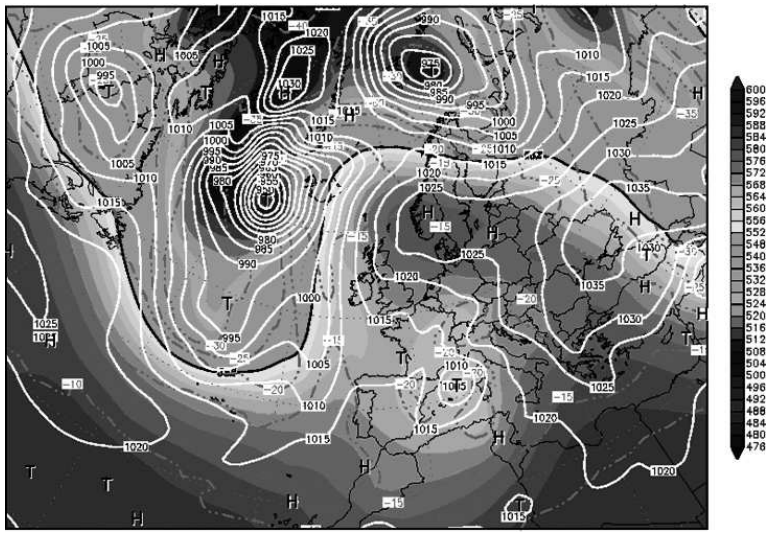

Figure 4. GFS analysis from 8 November 2011 at 00:00 UTC. White contours are isobars at surface (hPa), shading represents the isohypses at 500 hPa (damgp) according to the grey scale and dashed lines are isotherms (ºC) at 500 hPa.

Using the ERA40 reanalyses, Tous and Romero (2013) calculated, for the Mediterranean environments observed on the days of *medicane* development, values of several parameters that have shown its utility in characterizing the environments leading to tropical cyclones. Justification of this approach lies on the structural resemblance, although at different spatial scale, of *medicanes* and tropical cyclones. Calculated parameters were: AVOR85 (absolute vorticity at 850 hPa; high values of vorticity favour development), RH600 (relative humidity at 600 hPa; high values of humidity at mid-tropospheric levels reduce the likelihood of strong downdrafts in the convective clouds), SST (sea surface temperature; high values compared to the overlying air favours evaporation), and VSHEAR8525 (wind shear between 850 and 250 hPa; low shear values across the troposphere favour the development). Another factor, related with the sensible and latent heat fluxes, is the local tendency of equivalent potential temperature at surface level (DIAB1000). Taking into account the temporal and spatial discretization of the used data, this can be written as:

$$DIAB1000 = \frac{\theta_e(t+dt) - \theta_e(t-dt)}{2dt} - Adv\theta_e(t)$$

where $Adv\theta_e(t)$ (equivalent potential temperature advection) is calculated at the given time *t* by means of spatial finite differences and *dt* is the time interval between analyses.

The 'air-sea interaction' theory developed by Emanuel (1986) for tropical cyclones demonstrates that these disturbances can be idealized as a thermodynamic Carnot cycle, where the heat input occurs largely in the form of latent heat of evaporation acquired from the sea surface by the inward airflow. The application of this model in equilibrium conditions allows to estimate the maximum wind speed of the storm that the environment can support (Bister and Emanuel, 1998; 2002):

$$MAXWS \approx \sqrt{\frac{C_k}{C_D}\frac{T_s - T_0}{T_0}(k_0^* - k)}$$

where T_S is SST, T_0 is the temperature at the top of convective clouds, k is the specific enthalpy of the air near the surface, k_0^* is the specific enthalpy of the air in contact with the sea, assumed to be saturated at sea surface temperature, and C_D and C_k are the dimensionless transfer coefficients of momentum and enthalpy.

Emanuel (2003) proposed an empirical genesis index for tropical cyclones (GENPDF) that combines the indicated parameters in the following expression:

$$GENPDF = \left|10^5 AVOR85\right|^{\frac{3}{2}}\left(\frac{RH600}{50}\right)^3\left(\frac{MAXWS}{70}\right)^3(1+0.1VSHEAR8525)^{-2}$$

Tous and Romero (2013) calculated the mean value of that index over a square of 600x600 km^2 centred at the point where each of the *medicanes* of the database was detected, focusing on the cyclone maturity time. For this calculation, the closest available time of the analysis (00, 06, 12 or 18 UTC) was used. As an additional index, the maximum value found inside the considered geographical squared region, GENPDFmax, was also considered. In its original formulation, the GENPDF index was adjusted as the number of tropical cyclones observed per decade in a square of 2.5º x 2.5º. Owing to the few cases of observed *medicanes* and, therefore, to the lack of a wider climatology, the GENPDF parameter lacks true dimensions in this study and is merely used in qualitative terms, as a possible indicator of the environments leading to *medicanes*.

Table 1 shows the calculated values of the above parameters for the cases of *medicane* and for the bulk of intense cyclones extracted from the MEDEX database (Campins *et al.,* 2006):

Observe from the table that sensible and latent surface heat fluxes are always directed upwards in the case of *medicanes*, that sea surface temperature was never below 15 ºC, and that MAXWS acquires always high values in the case of *medicanes* and also that GENPDF and GENPDFmax are much higher for *medicanes* than for intense cyclones. By tracking in time the GENPDFmax index during the life cycle o

	MEDEX 5%	MEDEX 95%	MEDIC min	MEDIC max
AVOR850 (10^{-5} s^{-1})	10.2	18.8	9.6	17.7
DIAB1000 (ºC/12h)	-5.9	6.4	0.2	7.7
RH600 (%)	30.8	89.9	49.2	80.9
SST (ºC)	7.9	19.0	15.0	23.2
VSHEAR8525 (m s^{-1})	7.3	42.3	4.7	29.0
MAXWS (m s^{-1})	0.3	49.1	31.6	49.5
GENPDF	0.0	16.8	0.9	36.6
GENPDFmax	0.0	61.5	3.8	329.5

Table 1. Values of the parameters for MEDEX intense cyclones (percentiles 5% and 95%) and for medicanes (minimum and maximum) (from Tous and Romero, 2013).

medicanes, it is observed that this parameter exhibits a rapid increase during the formation phase of the cyclone, reaching the maximum values near the mature state. Finally, it was shown that some environments presenting high values of GENPDF did not lead to the formation of *medicanes*, and thus such ingredient must be considered a necessary but not sufficient condition for the genesis of these cyclones, suggesting the relevance of other smaller scale factors for the genesis of the phenomenon. See for more details Tous and Romero (2013).

4. INFLUENCE OF SURFACE FLOWS ON THE PATH AND INTENSITY

Current mesoscale numerical models make use of advanced parameterizations of physical phenomena allowing the study of the influence of physical factors that are considered important in the development of small-scale circulations. Numerical simulations will then determine whether *medicanes* follow a common pattern regarding energy flows from the sea. Specifically, we can quantitatively assess the effects of these flows on the path and intensification of the *medicanes*, besides discerning whether they are a necessary condition for their genesis and further development.

By using the 12 *medicanes* identified and highlighted in Figure 3, Tous *et al*. (2013) show a study of these characteristics. Initially, they performed control simulations to ascertain the model capacity to simulate with good approximation the observed *medicanes*. Only if the model is able to reproduce satisfactorily the physical processes involved in the system, the derived experiments and conclusions will be representative of the real system. Subsequent simulations were conducted with sensible and latent heat fluxes

removed. The comparison of the results allows to retrieve quantitative information about the influence of these factors.

The model used by Tous *et al*. (2013) was the NCAR/Penn State University MM5V3 (Dudhia, 1993). The integration domain consists of 196 x 196 points with a grid size of 7.5 km in the zonal and meridional directions, and was centered over the point of maximum development of the *medicane* being studied in each case. In the vertical, 31 σ levels were considered with higher resolution in the low troposphere. Each simulation ran for 48 hours beginning 24 hours prior to the time of maximum development of the cyclone. The Kain-Fritsch (1990) scheme was used for the convective parameterization, the Reisner scheme for the microphysics and the MRF for the boundary layer processes. The initial and boundary conditions (time-varying) were taken from the ECMWF analysis.

Only one out of the 12 control simulations did not develop a *medicane* or any similar structure. In two of them, despite generating a small cyclone, it was very short-lived, much shorter than actually observed. The remaining 9 cases simulated a small cyclone with warm core and a life cycle similar to the observed. The model thus shows ability to simulate this type of disturbances. Figure 5 shows the results of two simulations. The small cyclones (they meet the aforementioned definition of a *medicane* on satellite images) are clearly depicted, with a strong pressure gradient, a great symmetry and a warm core at 700 hPa.

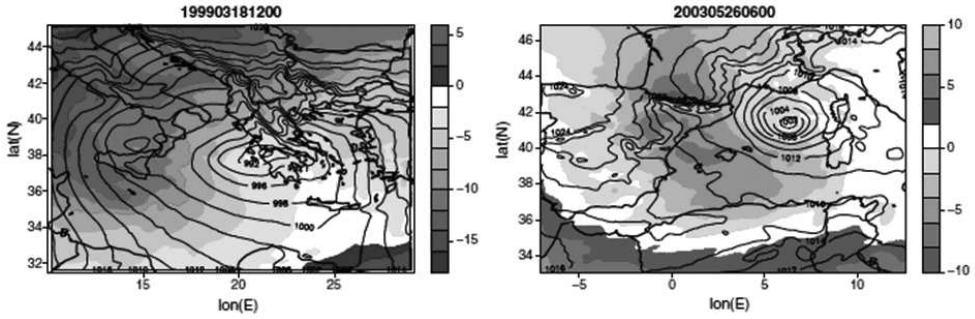

Figure 5. Control simulation of 2 *medicanes* (the date and time (UTC) is indicated on top of each panel). The isobars (hPa) are indicated with continuous lines. Temperature (ºC) at 700 hPa is shown with shaded greys according to the scale (from Tous *et al.,* 2013).

Considering only the 9 cases well reproduced by the model, both in its spatial structure and life cycle, Tous *et al.* (2013) analyzed, by comparing control simulations with those in which sensible and latent heat fluxes are removed, the influence of these fluxes on the cyclone's path, travel speed and life-time. Results indicate that three groups of *medicanes* can be considered depending on the impact of such changes: in the first group, comprising three events, a significant deviation

from the path between the two simulations is found; the second group, which includes four events, also shows some deviation between the trajectories but much lower than the previous group; and finally the third group, comprising the remaining two cases, shows remarkable overlapping between the paths in the control and modified simulations. Figure 6 shows the trajectories for a case in each group, as well as the spatial distribution of sensible and latent heat flux

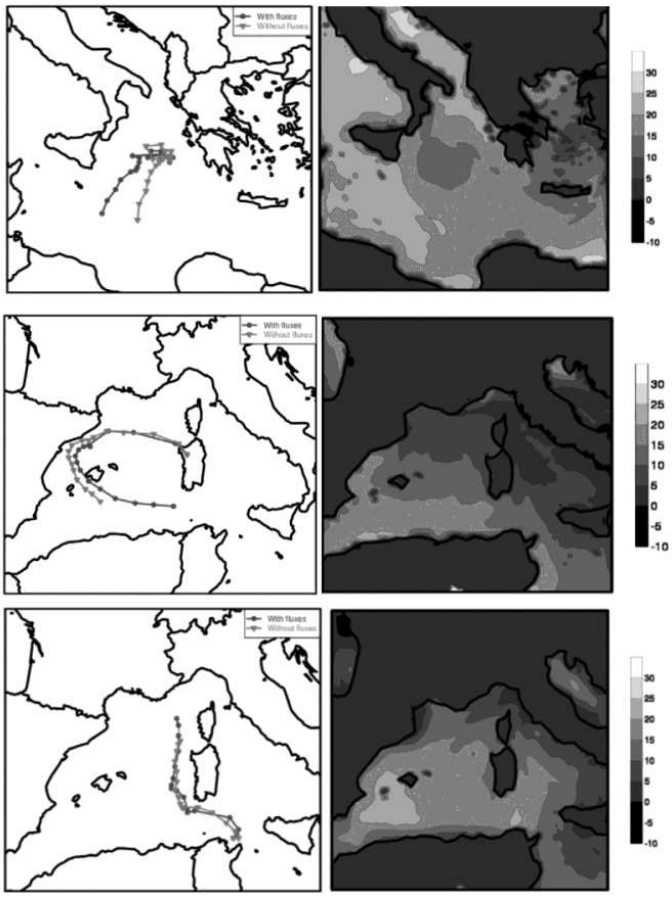

Figure 6. Simulated trajectories and spatial distribution of sensible and latent heat fluxes (10^3 J/kg according to the scale of grey shadings) of an event of the first group (upper row), second group (central row) and third group (lower row) (from Tous *et al.,* 2013).

Using the same 9 cases, Tous *et al.* (2013) analyze the influence of the fluxes on the intensification of the *medicanes* by comparing the evolution of the pressure at the center of the cyclone in the control and modified simulations. In general, the influence of these flows is noticeable; in all cases the control simulation shows lower values of sea level pressure at the center of the cyclone than the simulation with no surface fluxes, that is, these fluxes favor the intensification of *medicanes*. They

have also identified three groups with different behaviors. The first group, which is analogous to the previous first group in the trajectory analysis, shows a strong influence of surface fluxes, with differences in depth at the end of the simulation that reach the 20 hPa. In the second group, which coincides with the second group of trajectories, the pressure difference increases with time but does not reach values as high as in the first group. Finally, the third group shows a behavior in which the influence of the fluxes does not appear to be crucial for the evolution of *medicane*.

The explanation for the different behavior of the *medicanes* in each group can be found in terms of the values and spatial distribution of the surface fluxes and the spatial distribution of precipitable water (PW, not shown), which always takes higher values in the control simulations than in the experiments without fluxes, especially in the first group. In this group, the cyclone moves (steered by the upper levels dynamics) towards areas with high values of surface fluxes, especially of latent heat flux. The associated strong winds favor the evaporation, and the large amount of precipitable water contained in the atmosphere above the area of the incipient cyclone cause the developed convection to release large amounts of heat, which causes a strong intensification of the *medicane*. For the second group, surface fluxes are smaller than for the first group and quite uniform along the path of the incipient *medicane*. The evaporation and precipitable water are also smaller in this group. That is indeed the main cause for the convection to be less intense, as the warming by latent heat release is lower and therefore the cyclone does not develop as deeply. Finally, the last group is characterized by showing high values of heat fluxes in areas away from the trajectory of the cyclone; the values of the fluxes in the *medicane* area are lower than the two preceding groups and fairly uniform.

These results reveal the strong influence surface fluxes have on the path and intensification of *medicanes*. However, other factors may also be relevant and make the dynamics of these small cyclones different from that of tropical cyclones. For example, high-level disturbances, always present in such weather conditions. The following section presents a study of their influence.

5. INFLUENCE OF DYNAMICAL FACTORS ON THE DEVELOPMENT AND INTENSIFICATION

An important case of a *medicane* affecting the Balearic Islands, where strong winds were registered, occurred on 12 September 1996. The barogram of the day from Palma de Mallorca is plotted in Figure 2. During the previous day, intermittent severe weather occurred over the western Mediterranean: very heavy rainfall over the coast of Valencia and six tornadoes on the Balearic Islands. For a description of this event see Homar *et al.* (2001).

The influence of the mid and upper tropospheric levels disturbance on the *medicane* development was studied by Homar *et al.* (2003) by means of numerical simulations. Initially, the structure of the disturbance in terms of PV was identified. The influence of the isolated vorticity structure is analyzed by obtaining the balanced geopotential, wind and temperature fields associated with the original PV structure and those balance fields associated with a weakened PV structure. To do so, a PV inversion technique, developed by Davis and Emanuel (1991), is used. The resulting

fields are used as initial conditions of the respective numerical simulations. Additionally, also by means of numerical simulations, the influence on the development of the *medicane* of the regional orography, evaporation from the sea, surface sensible heat flux, latent heat release in convective clouds, as well as the interaction between some of these factors was investigated using a methodology developed by Stein and Alpert (1993).

The meteorological setting in which the *medicane* formed is shown in Figure 7

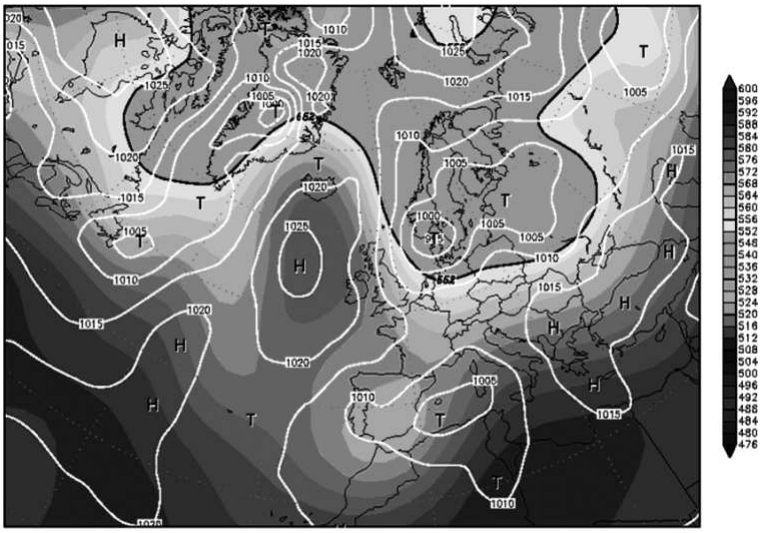

Figure 7. NCEP reanalisis of 12 September 1996 at 00:00 UTC. The contours show isobars (hPa) at surface. The grey shading depicts isohypses at 500 hPa (damgp) following the scale.

At synoptic scale it matches the situation described above: a cyclone over the western Mediterranean with no remarkable barometric gradient and a depression at mid and upper tropospheric levels, which is isolated from the zonal circulation of higher latitudes.

The numerical model used by Homar *et al.* (2003) was the non-hydrostatic version MM5V2 (Dudhia 1993) developed by NCAR/Penn State University. The initial and boundary conditions were obtained from the NCEP analysis, available at 00:00 and 12:00 UTC. The simulations start on September 11 at 12:00 UTC and extend for 36 hours. They used a configuration with two-way nested domains. The lower resolution domain had a grid size of 60 km with a total of 82 x 82 grid points covering much of Europe, North Africa and parts of the Atlantic Ocean. The higher resolution domain was 109 x 109 grid points with 20 km grid size, covering the western Mediterranean, the Iberian Peninsula and much of France. In the vertical, 32 σ levels were used, with higher resolution near the ground. We used the convective parameterization of Kain and Fritsch (1990) in both domains. The microphysical processes were parameterized using the Tao and Simpson (1993) scheme and for the boundary layer a modified version of Hong and Pan (1996) was

activated. The sea surface temperature, from the NCEP analysis, remained constant during the 36 hours of simulation.

The control experiment reproduces with sufficient approximation the evolution of the *medicane* but the simulated trajectory is shifted about 100 km southward of the *medicane* path inferred from satellite imagery (Figure 8). Also the pressure at the cyclone center fails to be as low as the one registered by the Palma de Mallorca barogram (Figure 2)**Figure 8. Isobars (hPa) at sea level on 12 September 1996 at 06:00 UTC for the**

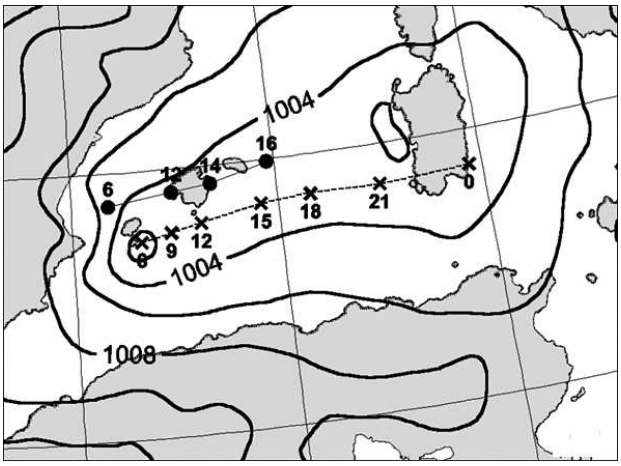

control experiment. Crosses indicate the position of the simulated *medicane* at the indicated time. Dots depict the position of the *medicane* as inferred from satellite images (from Homar *et al.*, 2003).

Figure 9 shows the results of various simulations on 12 September 1996 at 12:00 UTC. Notice how the control experiment (Figure 9a) reproduces the small-scale cyclone (150-200 km diameter) with a strong barometric gradient. It also shows an important convective precipitation area to the west of the cyclone.

The experiment with flattened orography (Figure 9b) shows the formation of the cyclone approximately at the same position as in the control experiment and a similar precipitation field. Notably, the terrain, so important and fundamental to the development of some cyclones in the Mediterranean, plays a negligible role in this case, and even more, the no-orography simulation developed a deeper cyclone than the control experiment. The critical importance of the latent heat release, mainly in the convective clouds surrounding the center of the cyclone, is clearly revealed in the experiment in which this heat source is removed. Figure 9c shows that in this case the model does not develop the small cyclone although the primary cyclone still forms and the latent heat release is of much smaller (if any) importance. The lack of water vapor feeding the convection is also a decisive factor in the development of the *medicane*. Figure 9d shows how the cyclone is not formed if no evaporation from the sea is allowed in the numerical experiment, besides the reduction in precipitation compared to the full experiment with active evaporation. We observe the formation of a trough to the south of the Balearic Islands, but once

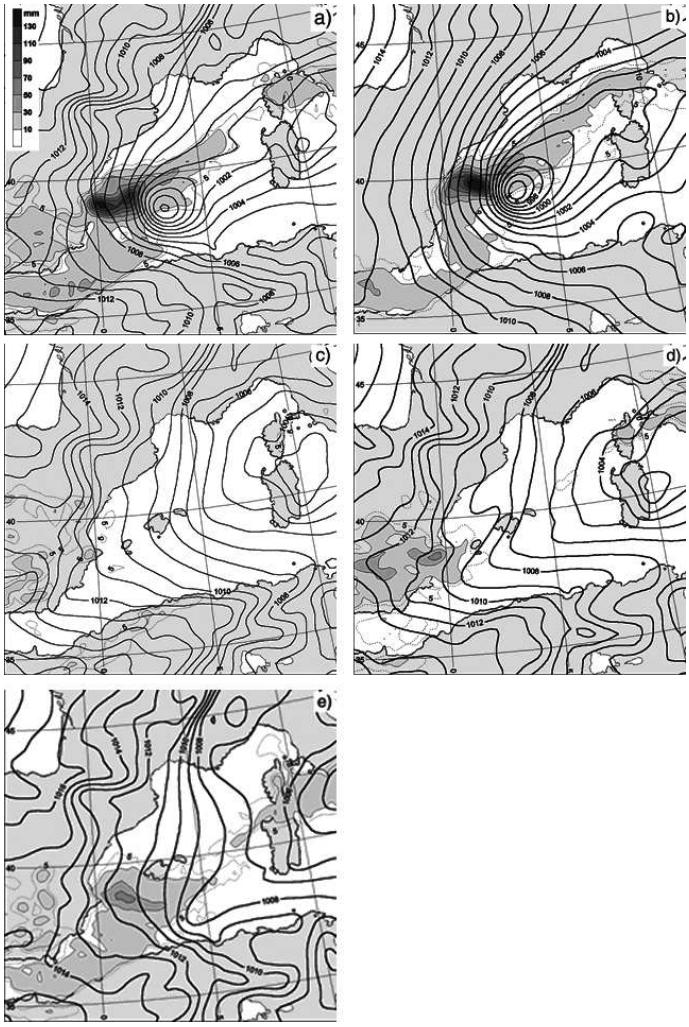

Figure 9. Sea level pressure (hPa, solid line) and accumulated precipitation (mm, ashed line and shaded areas) valid on 12 September 1996 at 12:00 UTC for: a) control experiment, b) no orography experiment, c) no latent heat release experiment, d) no evaporation experiment and e) experiment with weakened upper-level forcing (from Homar *et al.,* 2003).

the water vapor initially present in the simulation is fully used, the latent heat release cannot continue and thus the deepening of the low also stops. Although it has been shown that water-related processes (evaporation and latent heat release from condensation) are essential in the formation and development of the *medicane,* the high levels dynamic forcing is also relevant (being a distinctive feature with respect to tropical cyclones). As previously mentioned, all cases show a cold low at high levels (500, 300 hPa), which is associated with an important positive PV anomaly. Weakening the potential vorticity

anomaly and inverting this field to get the geopotential, wind and temperature, by means of the aforementioned method, results in a weaker upper-level trough and a reduced steering dynamical forcing to the lower levels. Figure 9e shows the result of the simulation initialized using the geopotential, wind and temperature fields derived from the inversion of the weakened PV field. The result shows how the *medicane* does not develop in this case, producing only a trough to the southeast of the Balearic Islands. In short, the high levels forcing is an important factor in the development of these small sized cyclones, as also shown by Nordeng and Røsting (2011) for a case of a remarkable polar low.

The role of the sensible heat flux between atmosphere and ocean in the development of the cyclone, while notable, is not as important as the evaporation from the sea. In the experiment in which this heat flux is removed (not shown), the position of the cyclone is approximately the same as in the control experiment but the pressure at the center is higher.

Once the importance of the evaporation and the upper levels forcing on the development of the *medicane* was proven, the factors separation technique of Stein and Alpert (1993) was used to analyze the isolated effects of these two factors and their synergism throughout the lifetime of the cyclone. The effect of the evaporation (E_{LGF}), PV anomaly (E_{PV}) and their interaction (E_{INT}) were obtained from the following expressions:

$$E_{LGF} = F_{10} - F_{00}$$
$$E_{PV} = F_{01} - F_{00}$$
$$E_{INT} = F_{11} - (F_{10} + F_{01}) + F_{00}$$

where F_{11} represents the control experiment, F_{00} indicates an experiment with the evaporation and upper-level forcing (partially) suppressed, F_{01} an experiment without evaporation and F_{10} the experiment with weakened upper-level dynamical forcing.

Figure 10 shows the quantitative importance of these factors on the pressure at the center of the cyclone during the simulated period. The effect of the evaporation is kept virtually constant throughout the life of the cyclone while the effect of the upper levels forcing is very important during the genesis stages of the cyclone but decreases with time. The interaction between the two factors follows the opposite evolution of the dynamical forcing. Initially this effect is almost negligible but then it grows quickly and for more than half the cyclone's lifetime, it turns to be the most determinant factor among the three. If we analyze the spatial distribution of the importance of these factors as well as their synergism at certain stages of the life cycle of the *medicane*, the evolution previously discussed becomes evident. Thus, the spatial distribution at 12:00 UTC on 12 September shows that the effect of the synergism between the two factors is located and centered on the cyclone and, therefore, it emerges as the main responsible for its deepening or maintenance.

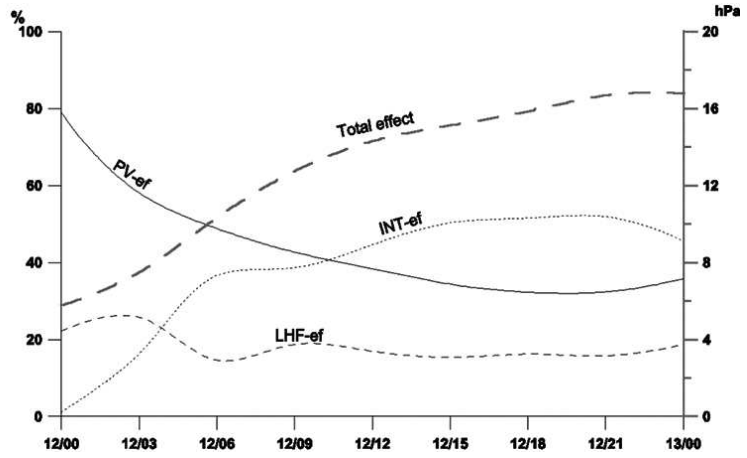

Figure 10. Effects of the evaporation, Potential vorticity and their synergism on the sea-level pressure at the center of the cyclone on 12 September 1996 (from Homar *et al.*, 2003).

6. FINAL THOUGHTS

The mesoscale cyclones called *medicanes* that develop in the Mediterranean, although rare, represent an adverse meteorological phenomenon due to their associated winds and rains but also for the damage they cause. The environments that favour their genesis have been identified and we defined a set of necessary but not sufficient conditions for its genesis, such as a relatively high sea surface temperature with respect to the air mass above. Further work is needed in order to clarify which necessary conditions become indeed collectively sufficient. The identification of a seed (initial vorticity center) from which the medicane eventually grows is a task to be addressed in the future. Numerical simulations have allowed, besides showing the paramount role of sensible and latent heat fluxes from the sea, beginning to put together a conceptual framework aimed at describing how these cyclones grow and evolve, with the evaporation that feeds the convection and the consequent focused release of significant quantities of latent heat, as important agents in the intensification of the *medicane*. Moreover, we have also shown the importance of the upper-level disturbances in the development of the cyclone, especially during the first stages, although this finding needs confirmation by studying other cases observed. The detailed and solid knowledge regarding the physical processes involved in *medicanes*, and their accurate prediction in a timely manner are both crucial challenges that, again, the always interesting Mediterranean weather is unfolding ahead of us.

AKNOWLEDGEMENTS

This work has been partially supported by projects CGL2008-01271/CLI (MEDICANES), CGL2011-24458 (PREDIMED) and the grant FPI BES-2009-022616

of the Ministerio de Ciencia e Innovación and Ministerio de Educación y Ciencia. It has also received support from grant 7/2011 of the Govern de les Illes Balears and ERDF EU funds.

REFERENCES

Businger, S. and Reed, R. J. (1989). Cyclogenesis in cold air masses, *Wea. and Forecasting*, 4, 133–156.

Bister, M. and Emanuel, K. (1998). Dissipative heating and hurricane intensity, *Meteorol. Atmos. Phys.,* 50, 233–240.

Bister, M. and Emanuel, K. (2002). Low frequency variability of tropical cyclone potential intensity, 2, climatology for 1982–1995, *J. Geophys. Res.,* 107, 4621, DOI: 10.1029/2001JD000780.

Buzzi, A. and Tibaldi, S. (1978). Cyclogenesis in the lee of the Alps: A case study, *Q. J. R. Meteorol. Soc.,* 104, 271-287.

Campins, J., Jansà, A. and Genovés, A. (2006). Three-dimensional structure of Western Mediterranean cyclones, *Intern. J. Climatol.,* 26, 323–343, DOI:10.1002/joc.1275.

Davis, C. A. and Emanuel, K. (1991). Potential vorticity diagnosis of cyclogenesis, *Mon. Weather Rev*., 119, 1929-1953.

Dudhia, J. (1993). A nonhydrostatic version of the Penn State/NCAR mesoscale model: validation tests and simulation of an Atlantic cyclone and cold front, *Mon. Weather Rev.,* 121, 1493–1513.

Emanuel, K. (1986). An air–sea interaction theory for tropical cyclones. Part I: steady-state maintenance, *J. Atmos. Sci.,* 43, 585–604.

Emanue,l K. (2003). Tropical ciclones, *The Annual Review of Earth and Planetary Sciences*, 31, 75–104.

Emanuel, K. (2005). Genesis and maintenance of Mediterranean hurricanes, *Adv. Geosci*., 2, 217–220.

Homar, V., Gayà, M. and Ramis, C. (2001). A synoptic and mesoscale diagnosis of a tornado outbreak in the Balearic Islands, *Atmos. Res*., 56, 31-55.

Homar, V., Ramis C. and Alonso S. (2002). A deep cyclone of african origin over the western Mediterranean: diagnosis and numerical simulation, *Ann. Geophysicae,* 20, 93-106.

Homar, V., Romero, R., Stensrud, D. J., Ramis, C. and Alonso, S. (2003). Numerical diagnosis of a small, quasi-tropical cyclone over the western Mediterranean: dynamical vs boundary conditions, *Q. J. R. Meteorol. Soc.,* 129, 1469-1490.

Hong, S. Y. and Pan, H. L. (1996). Nonlocal boundary layer vertical diffusion in a medium range forecast model, *Mon. Weather Rev*., 124, 2322-2339.

Jansà, A. (2003). Miniciclons a la Mediterrània, *IX Jornades de Meteorologia Eduard Fontserè*, Associació Catalana de Meteorologia (ACAM), Barcelona, 75–85.

Kain, J. S. and Fritsch, J. M. (1990). A one-dimensional entraining/detrainig plume model and its application in convective parametrization, *J. Atmos. Sci.,* 47, 2784–2802.

Nordeng, T. E. and Rosting, B. (2011). A polar low named Vera: the use of potential vorticity diagnosis to assess its development, *Q. J. R. Meteorol. Soc*., DOI:10.1002/qj.886

Petterssen, S. (1956). *Weather analysis and forecasting* (vol.1). McGraw-Hill Company, New York, USA

Picornell, M., Jansà, A., Genovés, A. and Campins, J. (2001). Automated database of mesocyclones from the Hirlam(INM)-0.5 analyses in the western Mediterranean, *Int. J. Climatol*., 21, 335–354.

Pytharoulis, I., Craig, G. and Ballard, S. (2000). The hurricane-like Mediterranean cyclone of January 1995, *Meteorol. Appl.,* 7, 261–279.

Ramis, C., Alonso, S., Romero, R. and Homar, V. (2003). Análisis preliminar del temporal del 10 al 12 de Noviembre de 2001 en Baleares*, Proceedings de la III Asamblea Hispano-Portuguesa de Geodesia y Geofísica*, Valencia (Spain), 867-869.

Rasmussen, E. and Zick, C. (1987). A subsynoptic vortex over the Mediterranean Sea with some resemblance to polar lows., *Tellus*, 39, 408–425.

Stein, U. and Alpert, P. (1993). Factor separation in numerical simulations, *J. Atmos. Sci*., 50, 2107–2115.

Tao, W. and Simpson, J. (1993). Goddard cumulus ensemble model. Part I: Model description, *Terrestr. Atmos. Ocean Sci*., 4, 35-72.

Tous, M. and Romero, R. (2011). Medicanes: cataloguing criteria and exploration of meteorological environments, *Tethys*, 8, 53-61

Tous, M. and Romero, R. (2013). Meteorological environments associated with medicane development, *Int. J. Climatol.,* 33, 1-14. DOI:10.1002/joc.3428

Tous, M., Romero, R. and Ramis, C. (2013). Surface heat fluxes influence on medicane trajectories and intensification, *Atmos. Res.,* 123, 400-411 DOI:10.1016/j.atmosres.2012.05.022.

CHAPTER 3

ATLANTIC EXPLOSIVE CYCLOGENESIS

Francisco MARTÍN LEÓN

Spanish State Meteorological Agency (AEMET)
fmartinl@aemet.es

ABSTRACT

This paper shows a brief review of the explosive cyclogenesis concept, one of the most violent processes known at the mid-latitudes synoptic scale. A surface low pressure system may suffer an extremely deepening evolution, mainly over the open ocean areas and notably in the North Atlantic. The deepening process of the low depression is extremely rapid, fast and violent, with a restructuring and reorganization of pressure, wind, and air mass fields. The result is the generation of a surface storm with associated severe weather, generating hurricane force wind gusts, intense and heavy rainfall, extreme ocean waves, bad maritime conditions, etc. Special attention and studies, from operational and research perspectives, are associated with explosive situations occurring close to land and populated areas due to its high social impact. Spain can be affected by these processes. The last part of the study will focus on Spanish cases of explosive cyclogenesis.

Key words: cyclogenesis, meteorological "bombs" weather, hurricane force wind, storm, extratropical cyclone, severe sea weather.

1. INTRODUCTION

At mid latitudes, the deepening processes of low pressure systems or extratropical cyclones are one of the critical elements that define the weather on land, sea and in the troposphere. These processes of low deepening usually occur in a timescale of days, continuously and in a "benign" way, but sometimes they occur so suddenly and explosively, in such a way that the surface low develops and deepens in just 24-48 hours, resulting in a process of explosive cyclogenesis. In these conditions the surface weather is very hazardous in the affected areas. Fortunately, many of them develop over open sea zones - large oceans such as the Pacific and Atlantic - , but other developments may do so in areas close to land, islands and coasts, and even affecting vast inland areas at continental level. Sometimes the direct effects of far away deep storms are felt at long distances: in the cold season Galician

coasts, at the northwest of the Iberian Peninsula, have been affected by ocean waves of 5-7 m in height, generated by intense and explosive storms originating far away in the middle of the North Atlantic, NA. The direct effects on land and oceans may be devastating due to the extreme winds and gusts, intense rainfall, bad weather conditions in maritime areas, etc. If they develop near the coast then they may generate storms tides and coastal flooding by combining several factors very actively. Its effects on surface tend to be accompanied by severe alterations of land, maritime and air transports, power outages, flooding, landslides, and even deaths. Warnings and the appropriate mitigations must be taken. Several countries may be affected by these explosive cyclogenesis in the NA. Many western European countries are affected every year, such as Iceland, Norway, Ireland, United Kingdom, Netherlands, France and occasionally Spain. Some Atlantic explosive storms may move towards other inland countries of Europe.

Operational prediction and monitoring of these hazardous situations are fundamental to mitigate their adverse impacts. The use of numerical prediction models and satellite data are fundamental tools for forecasting and monitoring those events, in a few days in advanced and real time, and so to warn the civil authorities and the public, in general.

2. PROCESSES AND METEOROLOGICAL PRECURSORS

Cyclogenesis means basically, creation or genesis of a cyclone (or depression, or storm, if it refers to middle or extratropical latitudes). Cyclones (it is the generic term referring to hurricanes, typhoons, storms, polar low, medicanes, etc.) are systems of low pressure where the wind rotates counterclockwise in the Northern Hemisphere, NH, (the rotation is opposite in the Southern Hemisphere, SH).

All the depressions, storms or cyclones suffer, in some way, a cyclogenesis process for their generation development, deepening and maintenance. The whole processes may all be basically explained by the baroclinic theory. Developments and deepening processes in mid latitudes are basically due to the horizontal and vertical thermal contrasts. In its initial state a surface low pressure area forms (the precursor low pressure system) with a waveform thermal structure appearing with the characteristic cold and warm frontal systems. The system is amplified over time and finally closes in on itself in the characteristic way. The minimum of pressure at surface level deepens during the first part of its life cycle. Positive interaction with an upper-middle level trough, jet stream, jet streak - i.e., at 300 hPa - generates conditions for a deepening - cyclogenesis - of the surface low. The interaction between the systems or precursors is made more efficiently and positively if the synoptic environment has low atmospheric stability.

In this paper, other types of cyclogenesis associated with tropical cyclones, Mediterranean lows, orographic-land cyclogenesis, etc. are not discussed, since their genesis and development are relatively different, however they do share common elements.

3. THE EXPLOSIVE CYCLOGENESIS

As its name suggests, it is basically a cyclogenesis but happening suddenly and violently. In other words, the surface low may evolve and deepen in a very short period of time, becoming a very adverse storm in a few hours. The meteorological "bomb" is the general term used technically to call these depressions deepening very quickly. This term and the explosive cyclogenesis have become very popular among the general public and the media.

Basically, the definition of meteorological bomb, cyclone or explosive storm is that surface low whose minimum of pressure falls 24 hPa in 24 hrs or less. This definition tends to refer to high latitudes, around 55 ° - 60 °, since the cyclogenetic processes are influenced by the rotation of the Earth. The explosive cyclogenesis happens in the extratropical areas of the Atlantic and the Pacific oceans, where interactions between upper-middle levels systems and low level cyclonic structures are more efficient than other places in the world.

The explosive cyclogenesis were characterized by Sanders and Gyakum (1980), SG80 hereafter, such as those where the drops of pressure on surface, in a period of 24 hours (Δp), following this criterium:

$$\Delta p \geq 24 \text{ hPa } (\sin \Theta / \sin 60^{o}) \quad 60^{o} \text{ as a reference}$$

where Θ represents the average latitude of the centre of the low during that specific period. Many studies and papers have analyzed the dynamic and physical mechanisms underlying and controlling this type of development. In spite of its level of uncertainty, the numerical weather prediction models, NWP, provide very valuable information about explosive cyclogenesis. Its predictions have improved considerably in particular since satellite data have been used in the initialization process of NWP. Some case studies have been conducted in Spain, as a country affected by explosive cyclogenesis. Some examples will be shortly reviewed at the end of the work.

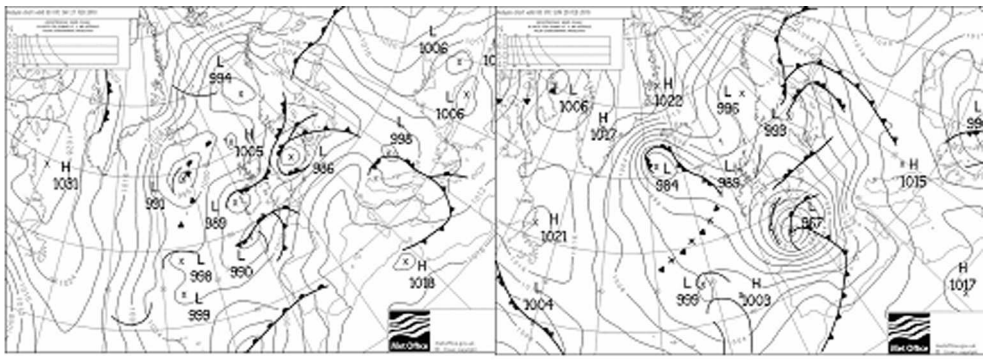

***Fi*gure 1. Conventional front and surface analyses from Met Office: Left) 27th at 00 UTC, Xynthia locates at southwest of the Iberian Peninsula, and Right) 28 th at 00 UTC, with Xynthia in the north of the Iberian Peninsula in February 2010. Source: Met Office.**

For the Spanish latitudes, 35° - 45° N, the definition to classify a cyclogenesis as explosive is one that undergoes falls of pressure of the order of 18 - 20 hPa in 24 h or submultiples, e.g., 9-10 hPa at 12 h.

An example of explosive cyclogenesis occurred in the case of Xynthia , a named storm, affecting Spain and other European countries at the end of February 2010. See Figures 1 and 2 for basic evolution, and technical details further on in the discussion.

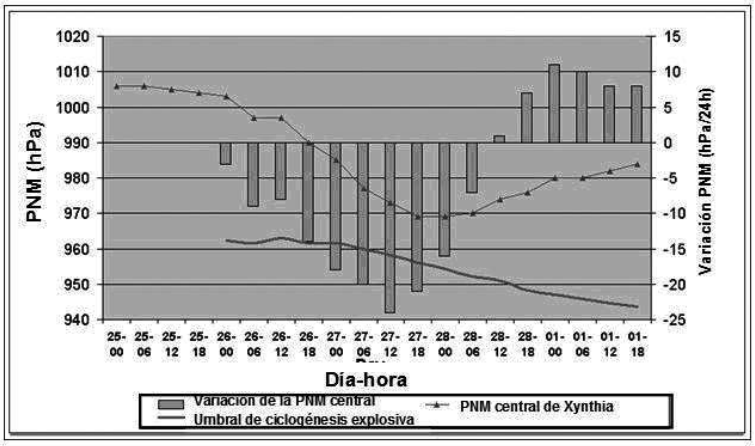

Figure 2. Xynthia's central mean sea level pressure between 25th February at 00:00 UTC and 1st March at 18 UTC (red triangles in hPa) and respective 24 hours variation between 26th February at 00:00 UTC and 1st March at 18:00 UTC (blue bars in hPa/24h) according to ECMWF analysis. The explosive cyclogenesis threshold (in magenta) according to Sanders and Gyakum (1980) is plotted for comparison during the deepening phase. Source and credit: www.eumetrain.org

Meteorological processes and synoptic framework

The meteorological conditions behind the developments and the rapid deepening of these extra-tropical lows are explained by the baroclinic theory and the sea-atmosphere energy exchange processes. In all cases studied, the importance of the upper-middle level trough is critical. It appears in the phase of rapid development, being studied by several authors (Bosart, 1981; Bosart and Lin, 1984; Uccellini *et al*., 1985). The diagnosis of Uccellini *et al*. (1985) showed that rapid cyclogenesis was defined by the arrival of upper airmass of stratospheric origin with high potential vorticity, PV, associated with an upper level, short-wave trough. An important aspect of their work is that the collapse of the tropopause is formed and evolved separately from the surface low, still present 12-24 h before the cyclogenetic development.

Additionally, several authors have emphasized the importance of the strong sensible heat flow processes and latent heat exchanges over the ocean (Bosart and Lin, 1984), the existence of deep convection in the vicinity of the surface low (Bosart 1981) and release of latent heat by condensation (Reed and Albright, 1986; Reed

et al., 1988). Special areas of strong thermal contrasts and gradients are the maritime zones such as the Gulf Stream in the NA and Kuroshivo Stream in Japan, NP, where the explosive developments occur.

Another additional factor, that is common to many cases of explosive cyclogenesis is the presence of a pre-existing cyclonic structure at low levels, which begins to deepen rapidly in response to the approximation of an upper level vorticity maximum, a jet stream, a jet streak or a trough, (Gyakum *et al*. 1992).

The existence of low values of static stability can be a key factor according to some of the research carried out (Reed and Albright, 1986; Rogers and Bosart, 1991), because the motive for growth of baroclinic waves increases when static stability is reduced (according to the cuasigeostrofic theory, less stability benefits more intense and localized synoptic forcing).

Although there are considerable variations from case to case, accumulated evidence in recent decades suggest that the explosive cyclogenesis are the result of baroclinic instability, which are modulated by factors related to diabatic (land-sea heat exchange) and frontogenetic (maximum wind) processes.

From a historical point of view, the basic ideas of the modern theory of the cyclogenesis, established by the works of Charney (1947), Eady (1949), Sutcliffe (1947) and Petterssen (1956). Charney (1947) and Eady (1949), revolutionized the theories of the instability and development to establish that cyclogenesis is the result of the amplification of infinitesimal disturbances in a baroclinic atmosphere. Petterssen (1956) showed that development at low levels occurs when and where an area of positive vorticity advection, in the upper level trough, moves over areas of warm advection in the lower troposphere.

Later, the cyclogenesis theory was formulated within the framework of the cuasigeostrofic theory, making use of the known tendency of the geopotencial equation.

During recent years, especially after the excellent work of Hoskins *et al*. (1985), which gave great impetus to concepts originally introduced in the 1950s, the ideas and concepts based on the isentropic potential vorticity have been widely used, as potential vorticity is preserved in an inviscid adiabatic flow and it can be used as an excellent tracer of air masses to describe the evolution of flows on a large scale in a clear and precise manner. In short, cyclogenesis processes are associated with various factors, many of them are linked to surface, upper levels and the interaction of the atmosphere - ocean. They are as follows:

- *Baroclinicity:*

  Strong horizontal and vertical atmospheric gradients of temperature, areas where the temperature gradients in the oceans are intense or the thermal contracts between land-sea are strong at low levels.

  Intense thermal wind. In the area of interest, a strong variation of the wind with height: speed and direction must exist.

  Ascending and descending currents coupled with intense forcing: warm temperature advection in low levels over the western part of the incipient low, and cold advection at the rear part. Positive/negative vorticity advection

in connection with the positive/negative temperature advection areas.

- *Surface sensible heat flows,* which reduce stability.
- *Flows of surface latent heat* that serve as fuel in the explosive process.

4. SOME OTHER GENERAL CONSIDERATIONS

Early studies and related climatologies of explosive cyclogenesis show the processes were eminently maritime phenomena during the cold months in the NH, occurring in areas of enhanced baroclinicity (areas of strong contrasts and gradients of temperature in the surface (SG80; Roebber,1984; Sanders, 1986; Gyakum *et al*., 1989). The climatological studies about intense storms and cyclogenesis have improved over times, thanks to satellite data, new reanalysis surface and height available from numerical prediction models (40-yr European Centre for Medium-Range Weather Forecasts (ECMWF) Re-Analysis (ERA-40), NCEP and NCEP2, 25-yr Japanese Reanalysis (JRA-25), ERA-Interim, etc.), which, at the same time, improves the procedures for the identification and storm and tropical cyclone trackings (Allen *et al*., 2010).

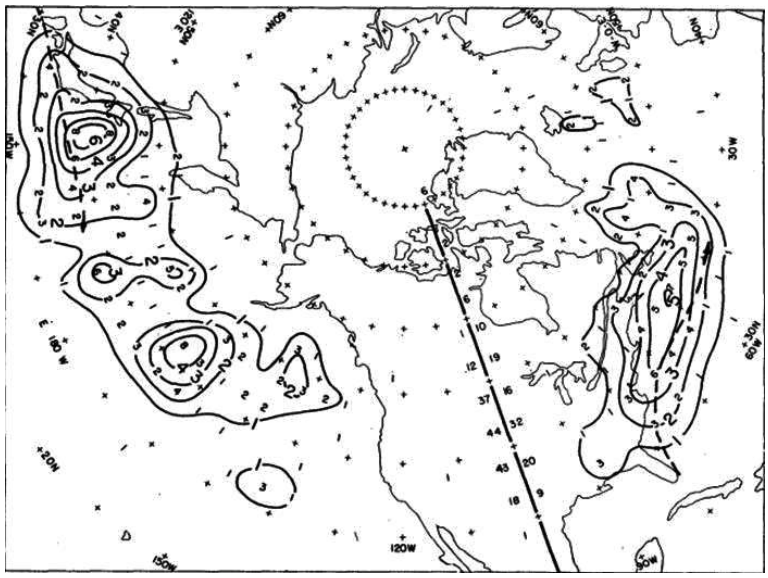

Figure 3. Distribution of explosive storms or bombs, analyzed by SG80. This map shows the relative frequencies of bombs for three cold seasons in boxes of 5 ° x 5 °. The dashed lines represent the winter average position of the ocean currents of the Gulf Stream in the NA and the Kuroshivo in the NP. The thick line on the United States., 90 ° W, has two columns with values of standard frequencies of storms by southern belts of 5 °, NP, to the left, and NA, to the right. There have been more detailed, extensive periods and recent studies (see for example, Allen *et al*. 2010), but the basic results and finds are already collected from the SG80 paper.

In all studies, those storms exceeding the index of the explosive cyclogenesis deepening rate or thresholds are taken into account.

Unfortunately it is not possible to enter into details in the different studies in the NH, and in particular, the NA. Figure 3 shows results of SG80, for historical reasons and perspective.

The number of explosive storms and cyclogenesis are greater in the NP, than in the NA, according to SG80. The monthly maximum of bombs for both oceans occurs in the cold period of the NH: the months of NDJF. The authors analyzed 109 and 154 explosive storms in the NA and NP, respectively.

Special attention has been paid recently to the bomb climatology and explosive cyclogenesis in the NH and SH. Special attention has been paid to the latest realistic data reanalysis, tracking techniques and the definition of weather bombs, etc. The idea is to provide some indications of the impact of global warming of the planet about the future evolution of the triggering processes of explosive cyclogenesis and new affected areas.

5. EXPLOSIVE CYCLOGENESIS AFFECTING SPAIN

Subsequently some of the most important and recent explosive cyclogenesis that have occurred close to Spain will be examined. Many of storms have been sponsored and named by the Institute of Meteorology of the Freie Universität Berlin. The names are not official and they are not recognized by WMO (World Meteorological Organization) and European National Weather Services, although popularly their names remain in the memory of many persons and the medi

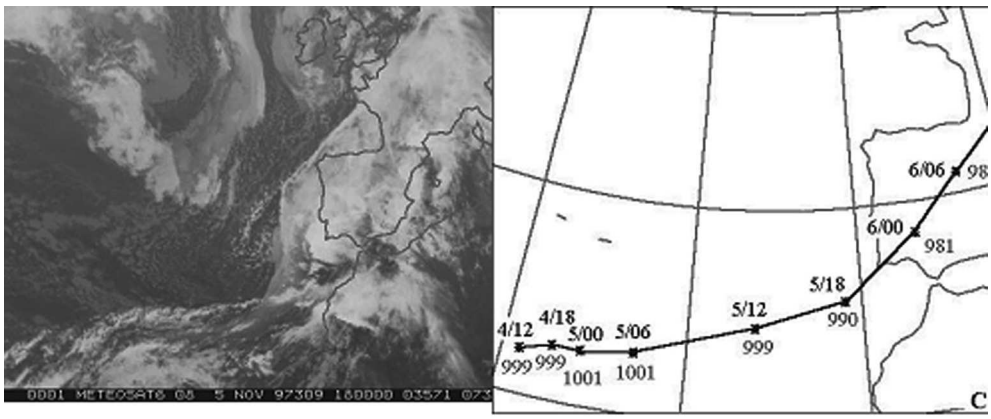

Figure 4. Explosive Cyclogenesis of Badajoz: Left) IR image on 5th November 1997 at 18 UTC. A Mesoscale Convective System, MCS, was embedded within the frontal system. The prefrontal area of the cold front was a warm and a wet air mass and it had subtropical origin. Right) Path of the low center and minimum of pressure value by day and time. Source: INM-AEMET.

5.1 Badajoz's explosive cyclogenesis: 5-6 November 1997

Historically, one of the first explosive cyclogenesis analyzed at the former INM, today AEMET, using modern day meteorological concepts, was the "Explosive cyclogenesis of Badajoz". Throughout 5th and 6 th November 1997 a deep and intense extratropical cyclone swept over the complete Iberian Peninsula from southwest to northeast, Figure 4. The low pressure center moved from the Gulf of Cádiz to France. On its trajectory, the storm produced large amounts of damage and twenty fatalities, most of them on the outskirts of the city of Badajoz. The main causes of the deaths were the river floods caused by the intense and persistent rainfall that the storm that had been associated with. The violence of the episode was reflected not only by the collected amounts of rain, but also by the intensity of the surface wind, which in some points came to exceed 100 km/h. The storm, in its maturity, reached the weather category of meteorological "bomb".

More recently, other explosive bombs have affected Spain:

5.2 Klaus: January 23-25th, 2009

From 23rd-25th January 2009, a deep and intense extratropical cyclone affected the Iberian Peninsula as it swept it from west to east. The center of the surface low moved from the Azores area to the North of Italy, sweeping and affecting mainly the northern parts of the Peninsula. Klaus produced much damage and loss of human life. The causes were the intense winds and the extreme wind gusts that had been associated with the storm, see Figure 5.

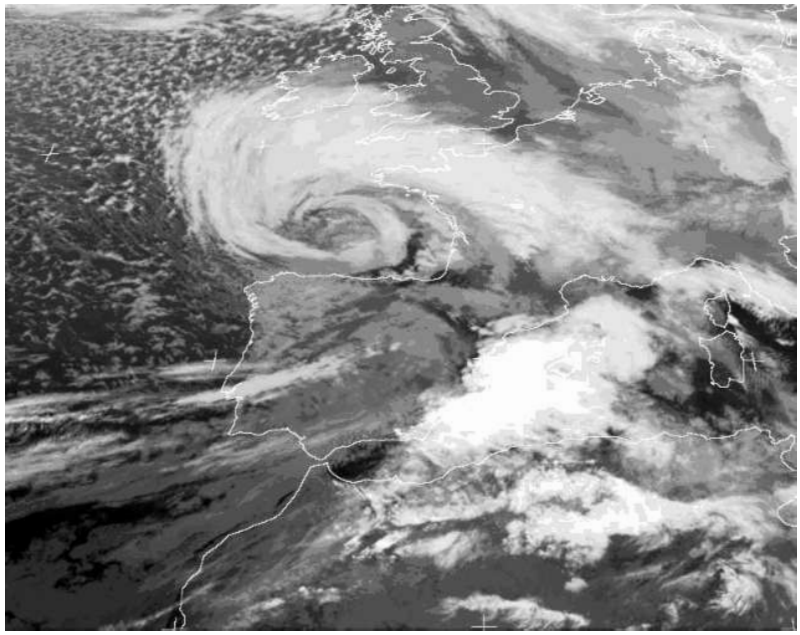

Figure 5. Infrared image, IR, from the Meteosat satellite on 24 January 2009 at 00 UTC, showing Klaus in the North of the Iberian Peninsula. Source: EUMETSAT.

Klaus had following pressure drops, according to the surface analysis of the different models:

- HIRLAM model: 1000 hPa-964 hPa, 36 hPa/24 h
- ECMWF high resolution model: 1002 hPa-968 hPa, 34 hPa/24 h
- Surface analysis of Met Office: 1001 hPa-963 hPa, 38 hPa/24 h

In Spain, Klaus caused nine deaths and many injuries by hurricane force winds, together with Figures from France and Portugal, it left 26 dead and many injuries. One of the most important effects was the collapse of a sports centre in Sant Boi de Llobregat (only 10 km from Barcelona city), which killed 4 children. The Klaus gusts surpassed 200 km/h. In Spain other important wind gusts were measured:

- Cerezo de Arriba, Segovia, 1880 m, 23/01/2009: 198 km/h.
- Machichaco-Faro Vizcaya, 93m, 24/01/2009: 193 km/h.
- Cabo Peñas (automatic station) Asturias, 100m, 24/01/2009: 166 km/h.
- Cabo Vilán, A Coruña, 50m, 23/01/2009: 145 km/h.

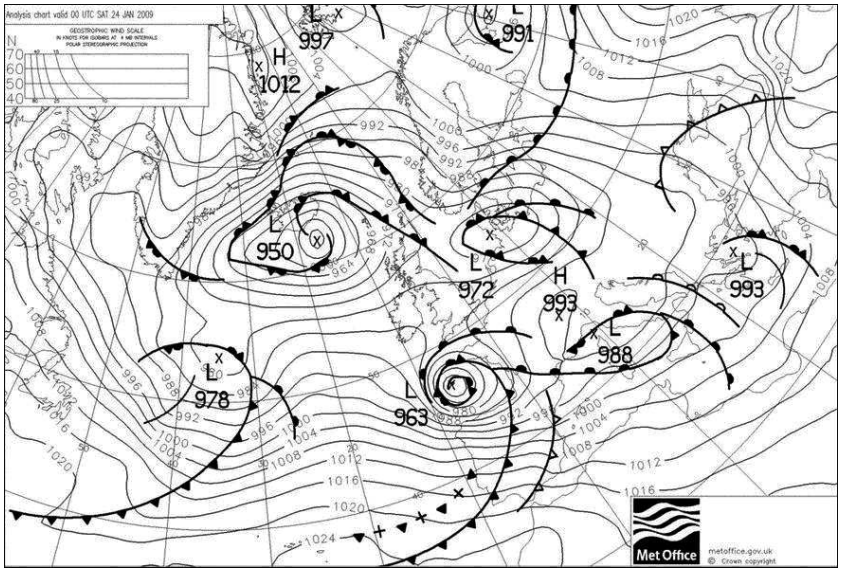

Figure 6. Surface analysis, as Figure 1, of 24 January 2009 at 00 UTC. Source: Met Office.

5.3 Xynthia: 27 February - 1 March 2010

The Xynthia storm was generated with another explosive cyclogenesis causing gale-force winds in the Basque country, with a maximum gust of 128 km/h at Vitoria-Foronda. Wind gusts of 136 km/h at Pedrosillo Castillejo (Salamanca), 142 km/h at Cervera de Pisuerga (Palencia), 144 km/h at Medina de Pomar (Burgos) and 167 km/h in Cerezo de Arriba - La Pinilla (Segovia). Before reaching the

Peninsula, Xynthia generated strong winds in the Canary Islands. Wind gusts of more than 130 km/h were recorded in wide areas of Gran Canaria, El Hierro, Tenerife, and La Palma. Three people died in Spain. See Figures 8 and 9.

Figure 7. Warnings issued by AEMET on 24 January 2009. Most of them were due to winds and gusts. Source: AEMET.

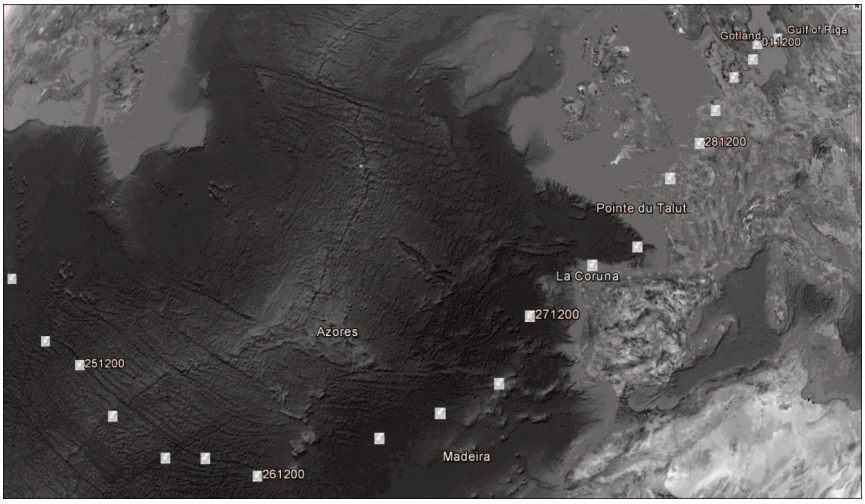

Figure 8. Trajectory of the center of Xynthia from 25th February 2010 at 00: 00 UTC to 1st March 2010 at 18:00 UTC, according to the analysis of the ECMWF model, each 6 h. Source: Eumetrain.

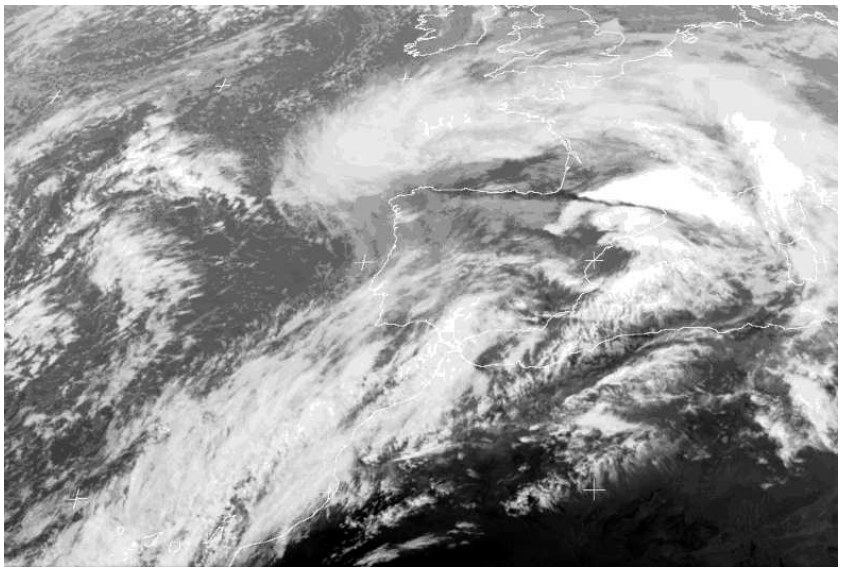

Figure 9. Infrared image, IR, of Xynthia on 27 February 2010 at 18 UTC to the west of Galicia. Source: EUMETSAT.

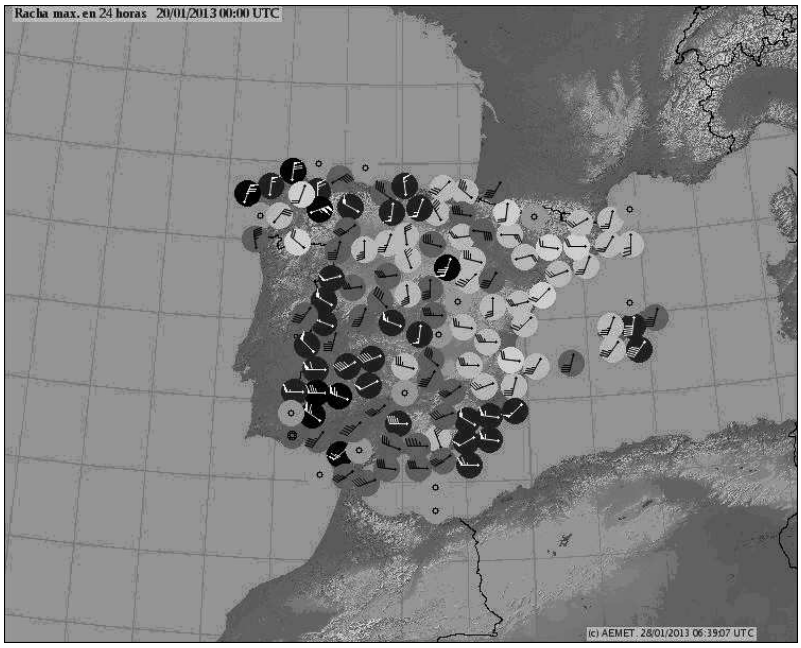

Figure 10. Maximum wind gusts in 24 h on 19 January 2013, in knots, accordiAEMET meteorological data network, represented by wind barb icons (50 kt flag, long segment 10 kt and 5 kt for short segment). The most affected areas were the west and southeast of the Iberian Peninsula. Source: AEME

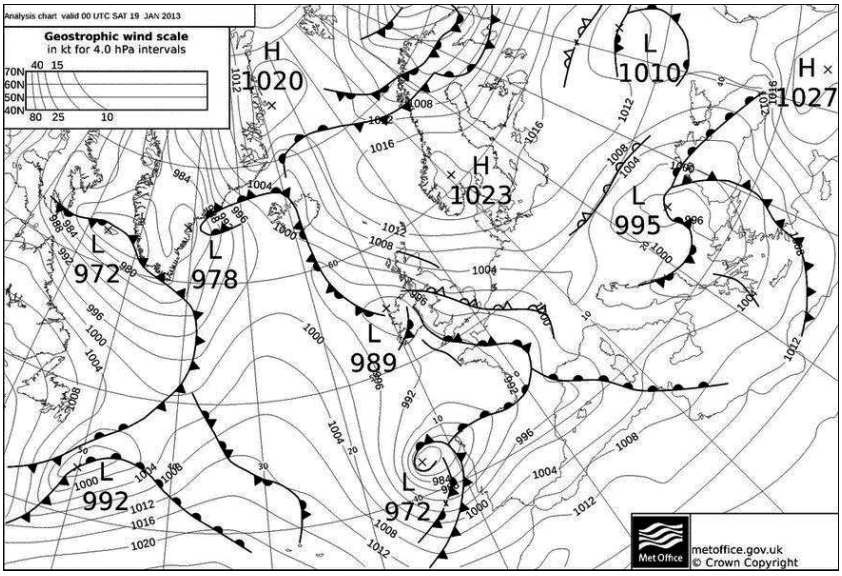

Figure 11. Conventional fronts and surface analysis of 19 January 2013 at 00 UTC with Gong to the West of the Iberian Peninsula with a minimum pressure of 972 hPa. Source: Met Offic

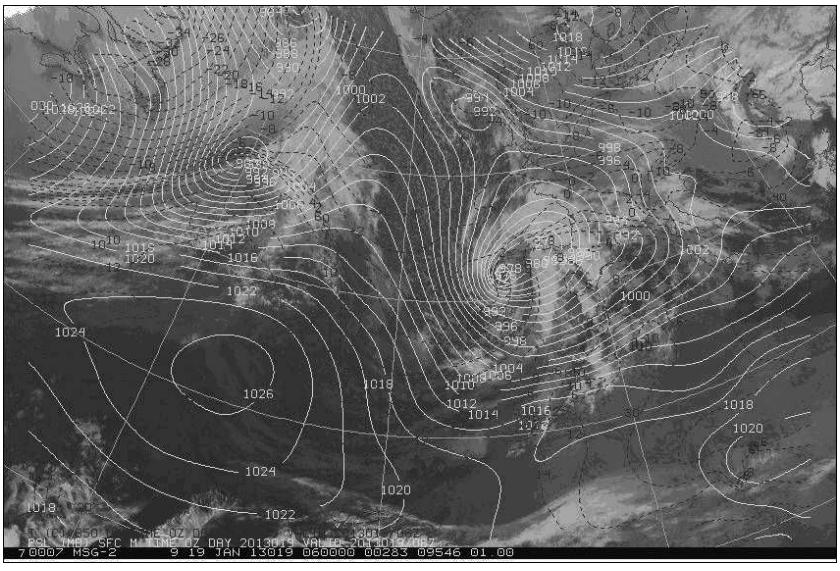

Figure 12. IR image on 19 January 2013 at 06 UTC, with surface pressure analysis, in hPa and continue lines, and the 850 hPa temperature, in °C and dashed black line. Source: AEMET.

Xynthia not only affected Spain. It moved and deepened into Western Europe persisting until March 1st, 2012, Figure 8. In France the storm left 51 people dead and 12 missing. In Germany Xynthia killed 6 people and one for every country wherever it went: Portugal, Belgium and England. In addition, Xynthia's winds provoked a powerful tidal storm surge with waves of 7.5 m. French barriers against tides proved futile at some places along the French Atlantic coast. Many of the dead were killed by these storm surge floods.

5.4 Gong: January 19-20, 2013

The Gong storm left 4 dead in Spain: 2 in Cartagena, one in Alicante and one in Badajoz. Much property was damaged by wind, storm, surges, rain floods and snow melt floods (in previous days there had been important and historical snowfalls in the Pyrenees), with many problems in road transportation, some airports were closed and setbacks in maritime traffic. See Figures 10, 11 and 12.

Winds and gusts were the protagonists of this deep storm. As an example, the map below shows the maximum gusts map for 24 h period on January 19th:

6. CONCLUSIONS

Extratropical cyclones, which have undergone a process of explosive cyclogenesis, are extremely hazardous weather systems. They evolve in open sea waters in the Atlantic and Pacific oceans. In the North Atlantic, they more often develop in the cold season, preferably in the winter months. Occasionally some of them affect the Western Europe zones, causing serious material damage and loss of life. Spanish areas are affected by this type of cyclogenesis and cyclone: directly and occasionally. Other indirect effects appear as consequences of the sea weather conditions when significant ocean waves reach the Spanish coasts from explosive cyclones far away off the Spanish coasts.

Its severe impact is very significant because they affect and sweep large and extensive areas, often being accompanied by strong winds, gusts, storm tides, intense rainfall, etc. Local effects can be amplified and modulated by the local topography: lee-side effects, channeled winds, etc. The disorders caused by these storms in day to day life are dangerous and considerable and they must be considered as generating widely hazardous weather conditions.

REFERENCES

Allen, John T., Alexandre B. Pezza, Mitchell T. Black (2010). Explosive Cyclogenesis: A Global Climatology Comparing Multiple Reanalyses. *J. Climate*, 23, 6468–6484. doi: http://dx.doi.org/10.1175/2010JCLI3437.1

Bosart, L. F. (1981). The President's Day Snowstorm of 18-19 February 1979: A subsynoptic-scale event. *Mon. Wea. Rev.*, 109, 1542 – 1566.

Bosart, L. F. and S. C. Lin. (1984). A diagnostic analysis of the Presidents' Day Storm of February 1979. *Mon. Wea. Rev.*, 112, 2148-2177.

Gyakum, J, R. (1991). Meteorological precursors to the explosive intensification of the QE II storm. *Mon. Wea. Rev.*, 119, 1105-1131.

Gyakum, J. R., P. J. Roebber and T. A. Bullock (1992). The role of antecedent surface vorticity development as a conditioning process in explosive cyclone intensification. *Mon. Wea. Rev.*, 120, 1465-1489.

Hoskins, B. J., M. E. McIntyre, and A. W. Robertson (1985). On the use and significance of isentropic potential vorticity maps. *Quart. J. Roy.Meteor. Soc.*, 111, 877-946.

Reed, R. J. and M. D. Albright, (1986). A case study of explosive cyclogenesis in the eastern Pacific. *Mon. Wea. Rev.*, 114, 2297-2319.

Reed, R. J., A. J. Simmons, M. D. Albright and P. Undén, (1988). The role of latent heat release in explosive cyclogenesis: three examples based on ECMWF operational forecast. *Wea. and Forecasting*, 3, 217-229.

Roebber, P.J., (1984). Statistical analysis and updated climatology of explosive cyclones. *Mon. Wea. Rev.*, 112, 1577-1589.

Rogers, E. and L.F. Bosart, (1986). An investigation of explosively deepening oceanic cyclones. *Mon. Wea. Rev.*, 114, 702-718.

Rogers, E. and L. F: Bosart, (1991*).* A diagnostic study of two intense oceanic cyclones. *Mon. Wea. Rev.*, 119, 965-996.

Sanders, F. and J. R. Gyakum, (1980). Synoptic-dynamic climatology of the "Bomb". *Mon. Wea. Rev.*, 108, 1589-1606.

Sanders, F. (1986). Explosive cyclogenesis in the west-central North Atlantic ocean, 1981-1984. Part I: composite structure and mean behaviour. *Mon. Wea. Rev.*, 114,1781-1794.

Uccellini, L. W., P.J. Kocin, R. A. Petersen, C. H. Wash and K.F. Brill, (1984). The Presidents ' Day cyclone of 18-19 February 1979: synoptic overview and analysis of the subtropical jet streak influencing the pre-cyclogenetic period*. Mon. Wea. Rev.*, 112, 31-55.

Uccellini, L. W., D. Keyser, K. F. Brill and C. H. Wash, (1986). The Presidents' Day Cyclone of 18-19 February 1979: Influence of upstream trough amplification and associated tropopause folding on rapid cyclogenesis. *Mon. Wea Rev.*, 114, 1019 – 1027.

En la red (consultadas el 27 de febrero de 2013):

- Ciclogénesis del 5-6 de noviembre de 1997 (8,96 MB): Publicación interna de AEMET. Módulo Tempoweb del antiguo INM.

- Agencia Estatal de Meteorología, 2009: Análisis preliminar de la situación del 22-25 de enero de 2009. Un caso de ciclogénesis explosiva extraordinaria. AEMET, http://www.aemet.es/es/infodestacada/webmaster/Nota2225enero.

- Wikipedia:

  http://en.wikipedia.org/wiki/Cyclone_Klaus

  http://en.wikipedia.org/wiki/Cyclone_Xynthia

http://www.tiempo.com/ram/9622/ciclognesis-explosiva-el-cicln-extratropical-xynthia-25-28-de-febrero-de-2010/

- Eumetrain: http://www.eumetrain.org/data/2/227/print.htm

CHAPTER 4

TORNADOES IN SPAIN: CHARACTERISTICS AND IMPACT

Miquel GAYÀ

Catalan Association of Meteorology
fiblo.miquel@gmail.com

ABSTRACT

Tornadoes reported in recent years in Spain will help us to know some of its features. In the first sections, the genesis of tornadoes and how to perform field studies or surveys allow us to recognize the type of weather phenomena affecting any region. The database developed by the author offers the ability to recognize what areas and the seasons of the year these phenomena can affect the country's geography. Finally, it is shown some implications that these events have had on the population and the importance of such work has for society.

Key words: tornado, vorticity, Fujita scale, destructive effects.

1. INTRODUCTION

Tornadoes can occur, in general, in any region of the world except the polar regions. In Spain tornadoes have occurred at all ages but only in the past twenty years it has been known that they are much more common than previously thought.

The new media, specially the Internet, have allowed the news about this phenomenon spread outside official channels or other streams. The images that were taken, both of the phenomenon and the effects produced on the goods, have confirmed cases that once were only considered as "hurricane winds".

The development of a database on tornadoes and other adverse wind-related phenomena, where deep convection had always been present, was initiated by the author in the late 80's. This database has allowed once extended to earlier times, to confirm that tornadoes have been present in the Spanish territory since a long time ago.

Today, the desire to know a geography that minimizes risk of the effects produced by tornadoes, has favoured a growing interest in this type of rare phenomena.

In this document, we present the major characteristics of recent tornadoes in Spain and where its impact has been more frequent.

2. DEFINITIONS

A tornado is a vortex extending from the land's surface (or marine) to the base of a cloud that is associated with deep moist convection and which, moreover, is so intense that can damage one or more parts of its path.

This definition excludes the vortexes that do not reach the earth's surface (*tuba*) and those where the surface convection is present and it is caused by ground's warming and there is not sufficient moisture to develop any kind of cloud (cumulus or cumulonimbus). It also excludes other vortexes where the cloudy link or its ability to cause damage doesn't exist.

This clear definition of tornado was offered by Doswell (2001). However, there are other definitions that have produced considerable confusion. We won't offer all definitions we can read in any meteorological dictionary except one that we think is very important for the economical consequences derived from it. The BOE (Official Spanish State Bulletin) of February 24, 2004 presented the conditions for which a claim could be "*consorciable*" due to the wind. One of these conditions was the presence of a tornado, whatever its speed, and when synoptic wind or other thunderstorm wind, if exceeded the 135 km/h (nowadays 120 km/h). The tornado defined by the BOE has this description: *Extra-tropical storms of cyclonic origin that generate twisting storms produced by violent storms that have a cloudy column form of a small diameter projected from a base of a cumulonimbus down to the ground.*

One consequence of this definition of the BOE was a significant increase in requests for sinister claims attributed to a tornado. If causing damage could be attributed to a tornado, despite its top speed being relatively low (e.g., 90 km/h), the disaster was consorciable and indemnities were paid by the Consorcio de Compensación de Seguros (Insurance Compensation Consortium).

3. GENESIS OF TORNADOES

Many of the conditions that are required for the formation of a tornado are well known. Still, the level of knowledge does not allow us yet to know in advance when and where there will be a violent vortex.

The vorticity required for the generation of a tornado may come from different sources:

A stormy cloud that is capable of generating a meso-cyclone, or a supercell, that has in its interior a moving structure that has magnitude order higher than the own tornado. The meso-cyclone, with dimensions between about 5 and 20 kilometers in diameter, may manifest at the ground and can be narrowed due to the strong rise of the air. The maintenance of angular momentum causes the speed of the narrower tube to reach higher speeds and eventually become visible and form the *tuba* or the incipient tornado.

The conditions for maintaining this mechanism are not the most common in a storm, quite the contrary, supercell storms are rare and only a small portion of these

generate a tornado. But this structure is undoubtedly the one that generates the strongest and most violent tornadoes.

Also, the horizontal rotation can be generated by a wind shear located at the lower levels of the atmosphere. In an unstable environment, horizontal vortexes can tilt as air rises in the ascending zone and the vertical vorticity may increase when the vortex becomes more narrow.

The horizontal vorticity produced by shear can be induced not only by storm own environment.

Vertical vorticity is also generated when a cold pool is formed in the area where rain reaching land evaporates. This remarkable front has a strong temperature gradient that, in turn, generates baroclinic vorticity and if is advected to the climbing area, vorticity tilt going up, leaning up to be vertical.

Finally, in a surface convergence or shear, with some instability, vortices are generated when starting the formation of clouds. If condensation is strong enough, the ascent of the air may also increase initial vorticity, more particularly when the air tube is tapered upward. If the vortex acquires remarkable speed, condensation will appear visible and the *tuba* or funnel cloud.

The latter process is relatively simple and does not require the cloud reaches a high thick and it is what is commonly favors the appearance of waterspouts. When these conditions are on firm ground, the tornadoes that are generated are often weak or, quite possibly, moderate.

In Anglo-Saxon literature, tornadoes generated in this way are often called, unfortunately, landspout.

We see, therefore, that most complex forms of storms organization involve throughout the lower troposphere. These storms are precisely those that can generate violent tornadoes and high land paths. By contrast, initial convergence that could generate a violent vortex will be much more ephemeral and will disintegrate, as of this convergence displacement reaches a different soil (e.g. from the sea). The same happens with terrestrial tornadoes with a path over complex terrain.

4. SURVEY STUDIES

Unless we had photographic or reliable testimony, the type and distribution of damage can facilitate the identification of the phenomenon that has occurred. It is not always easy to distinguish between tornado and other convective burst where the wind of convective origin was the protagonist.

Overall, the debris distribution will be convergent when a tornado acts, and will be divergent when a downburst is present. In a tornado, the amplitude of the path is shorter than the path length. By contrast, the distribution of a downburst damage has usually the same order of magnitude.

However, when the damage is scarce or when structures and/or vegetation are sufficiently strong, the debris distribution cannot help us to differentiate between one phenomenon or another.

The study performed by Bech *et al.* (2007) presented the distributions of the wind in a convective downburst and in an idealized tornado, with two fundamental variables **G** Max. = **V**rotational /**V**traslational and **Alfa**: angle between the radial and tangential velocity. Figure 1 presents an example of distribution of the wind to predominantly tangential angle and a rotation speed four times higher than translationa

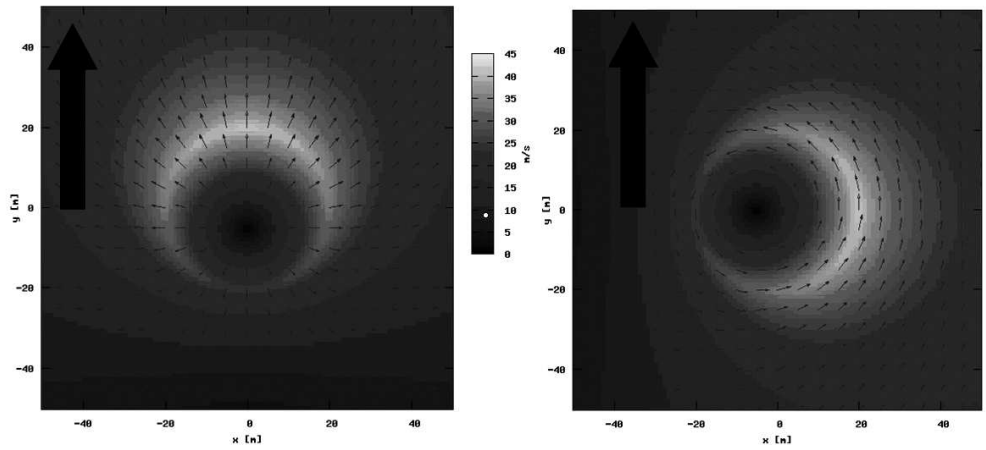

Figure 1. Wind distribution in a convective downburst and tornado with translational motion.

For a tornado or a weak convective burst, only the brightest part of the spectrum of speeds would be willing to make damage visible in a homogeneous and regularly planted vegetation. In actual cases, these plantations (such as a corn field) are not common, so that the vectors labeled S-SSE-SSW consecutive can not easily noted. A tornado or convective downburst knock down a few trees could not differentiate into survey study if we have no other evidence.

The real tornado wind is far from laminar and vertical and horizontal velocity can be of the same order of magnitude. Therefore, the speed measurements is a very complex task.

The wind speed can be measured by remote sensing equipment or static. But in most cases these instruments are not in the path of a tornado or are severely affected by their action. Another way to get speed in a tornado is through photogrammetry. The technique involves some consecutive frames recognize and track details thereof. By knowing the distances from the camera to the object and the dimensions of the tornado can be ascertained by the immediate environment of the lag, the calculation of the vertical and Side Discharge speed can be inferred with a certain degree of accuracy. This technique was used by Golden and Purcell (1977) and was tested with video images in the Tornado of Espluga de Francolí in 1994 by Gayà and Redaño (1995). Figure 2 shows four frames strongly distorted in order to identify elements that appear in them and those who perform the calculations to determine the speed of the tornado at the level where they appear.

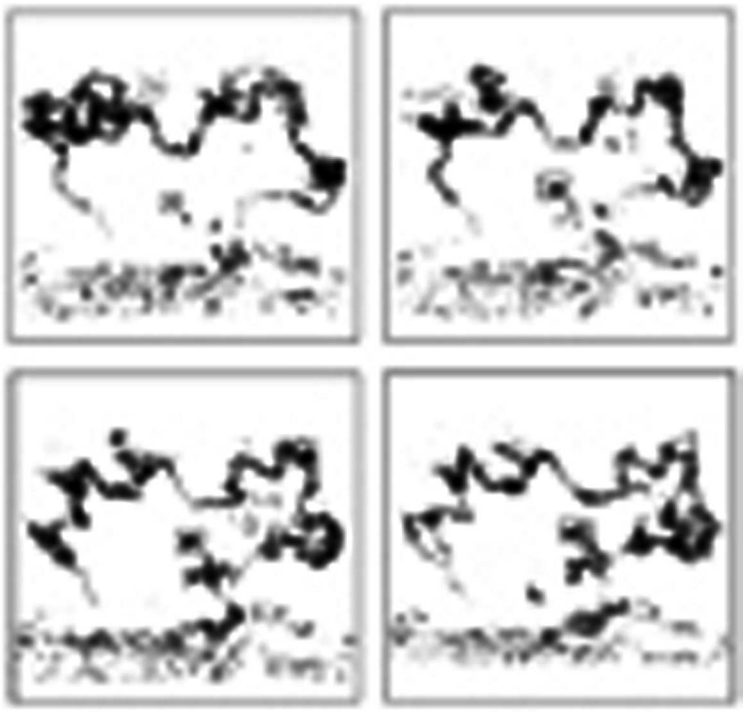

Figure 2. Frames of Espluga de Francolí Tornado, which identify elements of the periphery to calculate speed

The most accurate technique for measuring the speed of a tornado, and also the most expensive, is to use a mobile Doppler radar. This technique allows us to determine the speed of objects that have caught the tornado and circulating not only on the periphery and visible region, but also those who are close to its axis.

Unfortunately, the use of this type of radar in Spain has not been used in any occasion.

To evaluate the speed of tornadoes, Fujita (1971) developed a scale that relates wind velocity to damage.

Clearly this is not reproducible scale anywhere because the removed items are not homogeneous in all countries. Despite these incongruences, F Fujita scale was widely used in tornadic events worldwide. Recently, an Enhanced Fujita scale (EF) has been developed with more breakdown thresholds of many structural details and more tree species. For more information on the EF scale is recommended reading articles from McDonald *et al*. (2004) and NOAA (2004). This form of "forensic" study allowed to have a pretty good idea about the speed that the tornado reached.

Observation of the tornado trajectory from the an aircraft or helicopter allows us to distinguish the complexity of motion and force that the tornado had.

Figure 3 shows clearly the convergence of the wind vector and the twister path

oscillations. This type of study is useful for moderate or strong tornadoes, where the damage are important and very visible, but not for the weak. In any case, the field survey from the air should always be complemented by the study "on site".

Figure 3. Distribution of wind in a tornado that was able to knock down a pine forest in Mallorca in 1996 (Photo and © M. Gayà).

5. CLIMATOLOGY OF TORNADOES IN SPAIN

To have a climatology of meteorological variables is recommend a minimum of 30 years. For rare phenomena such as the tornadoes are, the observation period should be longer. In this sense, Schaefer *et al.* (1993) found that in the United States, to tornadoes with F2 intensity or greater, the stability period occurred after 35 years.

In the climatology of tornadoes in Spain presented here, we considered the period 1981-2012 (32 years) with all the tornadoes and possible tornadoes which we have notice, regardless of their speed. Clearly, F0 tornadoes and possible tornadoes make climatology unstable, especially in the early years of the considered period. However, it is required more contrasted information that is today available to get an idea of which areas are most likely to have a tornado.

5.1 Monthly and annual distributions of tornados during the past years

The tornado records in Spain in recent years has a very significant increase to get some stabilization in the most recent period. This is undoubtedly due to the fact the database starting in the late 80's, when we start watching and "capture" of this rare phenomenon. But also because the great increase in communications between the society and the media that publish the news. Internet is undoubtedly one of

the most efficient information exchangers. But not the only one. The traditional media have incorporated information from anonymous citizens who have put forth many of the cases we now recognize as true.

Figure 4 shows the annual distribution of tornadoes highly probable or certain (in gray) and possible tornadoes (in black). There is a progressive increase in the total number of cases to peak by 2010, with a total of 43 records.

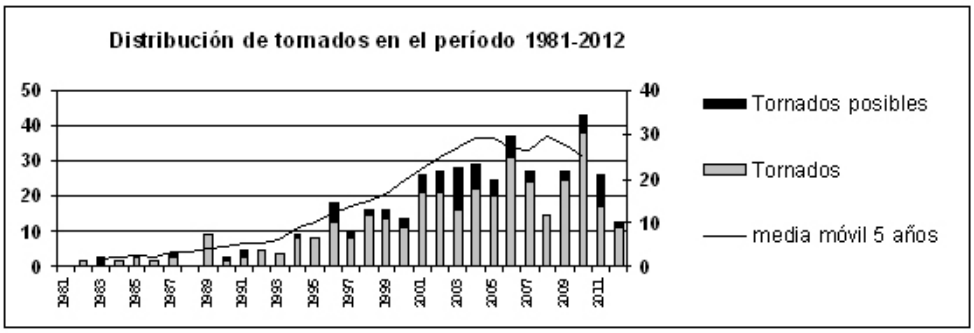

Figure 4. Annual distribution of tornadoes in Spain.

The solid line graph of Figure 4, with the scale to the right of the graph, indicates the mobile five years average of all cases (possible tornadoes and certain tornadoes) assigned to central year. It is shown that the number tends to stabilize since 2001 with variations according rare phenomena.

In the initial period of the series, it seems clear that the number of cases is well below the number of cases that occurred in reality. It is also very likely that in the end of the set period, the records underestimate the actual number of cases, however we think that this difference between the two values has been declining over the total period considere

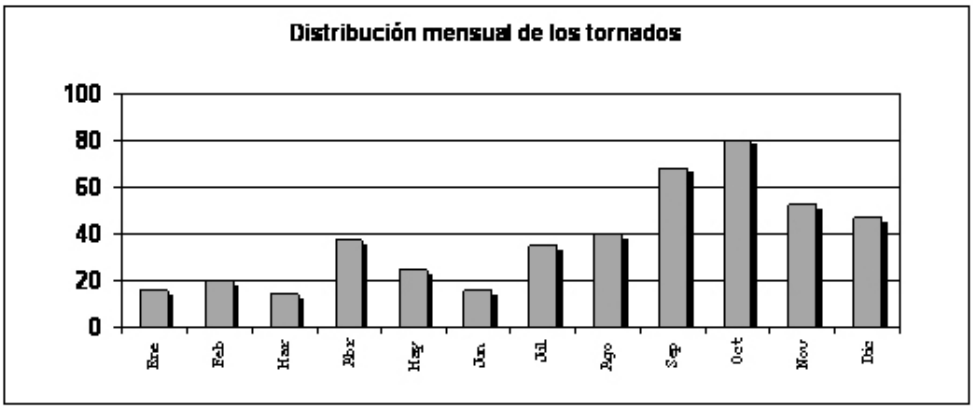

Figure 5. Monthly distribution of all tornadoes.

As regards the monthly distribution (see Figure 5), the selected sample has a maximum outstanding from late summer to November. However, this distribution is not similar if we focus our attention on the different climatic regions of the State. As it was shown by Gayà (2011), there was a high frequency of tornadoes to the Mediterranean during this time of year, and the weight of the Atlantic storms became more relevant in winter time, although a number of tornadoes is lower.

5.2 Geography of tornadoes

The values of the variables involved in the presence or absence of tornadoes are not homogeneously distributed over the Iberian Peninsula and islands. Just as it happens in other countries, like the U.S., the geography of risk of tornadoes has some preferred climatic regions.

The warm Mediterranean Sea in late summer and autumn brings many of the ingredients needed to develop convection. Only the upper atmosphere ingredients are required to provide and to facilitate the release of energy. Similarly, other Atlantic regions climatic factors contribute to the development of thunderstorms in other seasons, when the Atlantic storms descend latitude.

In recent years there have performed some tornado climatologies in Spain that have covered different periods and regions. Gayà *et al.* (2001) for the Balearic Islands, Gayà (2005) for Spain, Gayà (2011) for Spain and for a much longer period. These climatological approaches suffer from limited data for rare phenomena, especially in the ancient times, but also for the most recent. It is noteworthy that some "possible" cases may have suffered an alteration of this condition if more information was later provided. It is for that reason that some nuances of these tornado climatologies are not coincident.

Figure 6. Geographical distribution of Spanish tornadoes (except Canary Islands).

With the current database, the distribution of tornadoes (possible and verified) on the Spanish territory, except the Canary Islands, is shown in Figure 6. The image is set with every tornado considering only the starting point of its path. For those tornadoes which we have no knowledge of this run way, it is assigned to the most significant city that appeared in the chronicles.

It follows from this Figure that the tornadoes have a more noticeable presence in the coastal provinces of Catalonia and the Balearic Islands and in the southern provinces of Cádiz and Málaga. But also manifested regularly in the Atlantic provinces and in Cáceres, Galicia, and Valencia.

On the contrary, Figure 6 reveals the scarcity of these phenomena in the provinces of Cuenca and northern peninsular, both in the Cantabric provinces, from Lugo to the Basque Country and in much of Castilla and León. Despite the presence of tornadoes in these areas is not null.

A significant detail is reflected in the geographical distribution of tornadoes: the proximity of the sea. It is certainly important to note that the database consider "tornado" a waterspout that has reached the coast, although the land path was well below the marine one. Some of these features were highlighted in the study by Gayà *et al.* (2011) which indicates that most tornadoes in Catalonia the path orientation has a marked component from the S and SE, prevailing direction of the breeze on the Catalan coast, while most tornadoes in the northern hemisphere are in SW.

5.3 The maximum speed in tornadoes

Most tornadoes which we have maximum speed assignments are weak and only a small portion are moderate. Violent tornadoes have not been recorded in this period. Because this assignment Fujita scale could not be attributed to each tornado, 301 cases have only the variable speed on the total of 457 tornadoes. Figure 7 shows the percentages in each category of the Fujita scale.

This result is similar to the American tornadoes in the United States, where about 95% of tornadoes are below EF3. However, the most striking difference is in violent tornadoes during this period: this kind of tornadoes were nonexistent in Spain, and they reached 5% in the U.S. where only 0.1% was EF5 (see e.g. NOAA (2012)) .

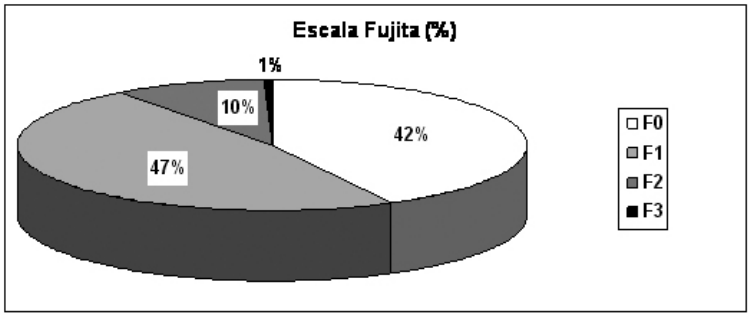

Figure 7. Percentage of tornadoes in each category of the Fujita scale.

Although violent tornadoes have been null in the period 1981-2012, there were cases that could achieve these speeds in the past centuries. So, Gayà (2011) notes that the tornado of Cádiz of 1671 could reach these values and, on the other hand, as it was indicated by Dessens and Snow (1993) violent tornadoes have been recorded in the databases of nearby countries such as France.

5. 4. Path length of the Spanish tornadoes

The path lenght run by the tornadoes is one of the variables of the database. However, this information is sufficiently accurate only in cases where some type of survey has been performed. Therefore, the distance traveled by tornadoes is scarcely known. Only 206 cases have this information.

Figure 8 shows the percentages of cases for different path length intervals. 32 tornadoes had a path exceeding 0, 2 km. These cases are mostly waterspouts reaching the costal shore and immediately disappeared. By contrast, only 13 tornadoes came to have a travel exceeding 10 kilometers. Without doubt, the longest path was recorded in Castilla and León around the towns of Vitigudino, Peralejos de Abajo, Peralejos de Arriba, Villar de Peralonso, Ledesma, and Zamayón (Salamanca) in 2010 and, interestingly, it was a weak tornad

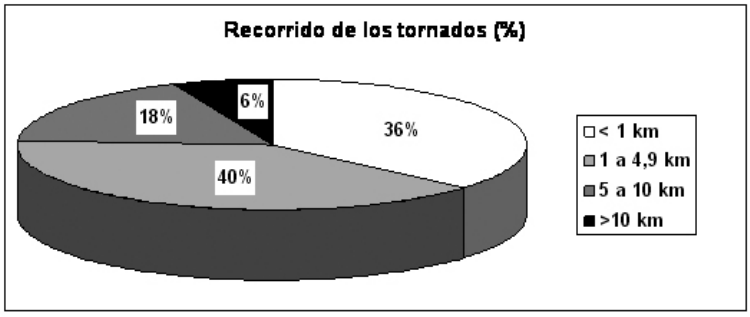

Figure 8. Average of path length of all tornadoes.

However, if we consider the double values, intensity (Fujita) and length, it is noted that significant tornadoes (F2 or more) had a travel longer than the weak tornadoes.The strong tornadoes (F2 and F3) had an average path of 7.7 kilometers. By contrast, the weak tornadoes path was significantly shorter, 2.9 kilometers. Considering all twisters (even ignoring its maximum speed), the average length of their paths was 3.6 km. The average path length of significant tornadoes we have indicated is similar to that was found in France (8.5 km) by Dessens and Snow (1993). But it is much lower for weak tornadoes. No doubt this is because we have taken into account the waterspouts that were destroyed just to reach the coast.

6. SOCIAL IMPACTS

The news of an tornadic event reaches the media when the tornado has been very harmful to people or property. In the recent times, some photographies and comments also appear on press although it was harmless.

Some of the most strong tornadoes have not appeared on the media because the tornado have had a very limited social impact. These cases that were worth F3 in the Fujita scale occurred in uninhabited places and only their forests were witnesses of its destructive violence. Ciutadella de Menorca and San Leonardo (Soria) are the municipalities that hosted these cases. However, some strong tornadoes, though inferior to the aforementioned intensity, were widely reported in the press because all towns affected and the material damage was really substantial. These relevant tornadic events have had a first-rate media coverage. We refer to the cases of the days when there were several tornadoes (outbreaks) in the Balearic Islands in 1996 and 2007, and also in the province of Barcelona in 2005, and the tornado of Málaga in 2009.

The most significant Spanish tornadoes in history occurred centuries ago and had a great social impact. The tornado of Cádiz of 1671 is undoubtedly the most remarkable and there is enough information to think it reached level 4 of the Fujita scale. It can be considered one of the deadliest tornadoes in the world. So, Gayà (2011) collected information from XVII Century in which it is stated that more than 600 people died in a city that then was one of the largest ports in the world.

A more recent tornado, the tornado of Madrid of 1886, also was an event that caused many deaths. According to Gayà (2007), the tornado caused 47 fatalities, mostly humble. The press at the time gathered many details of the event for several years, but finally, the tornado was "hidden" many years under the word "cyclone".

The recent tornadoes have not been as destructive as those quoted above. Despite which also caused some fatalities. Damages have been very important in tornadoes quoted earlier in Balearic Islands, Barcelona and Málaga.

To find out the total cost that has meant returning to the previous situation is practically impossible. Many structures were not restored and many others that were returned to their previous state had costs that were paid by their owners without being counted. The insurance policies did not cover all the damage that, for the most part, were made by the Insurance Compensation Consortium. To get a sense of these losses it can be say that the squall that hit Majorca in 2007, and several tornadoes included, had a cost to the Consortium of over 45 million euros. The tornado of Málaga of 2009 and the outbreak of Barcelona in 2005, more than 9 million euros.

7. CONCLUSIONS

Although the global climatologies do not collect information about tornadoes in Spain, these occur relatively frequently. Intensity values and paths are similar to those in other countries, although most often moves to last summer and autumn against what happens in other countries, like the United States, which occur more frequently in spring.

It is noted that this phenomenon did not have the attention it deserved in some Institutions. So, the information is limited to the years before the start of the database that the author began in the late 80's and after, till nowadays.

Also, attending to the impact that such events can cause, it is essential that the survey studies were normalized for the entire country in order to allow a higher climatic knowledge. In a society that builds large works or develops transport that

can be very vulnerable to tornadoes, it seems that studies of this phenomenon could be developed with greater intention. This would encourage a more adequate infrastructure and a system of public warnings to prevent to all people that could be affected.

REFERENCES

Bech J., Gayà M., Aran M., Figuerola F., Amaro J. y Arús J. (2009): Tornado damage analysis of a forest area using site survey observations, radar data and a simple analytical vortex model. *Atmospheric Research* , 93, 118–130.

Dessens J. and Snow J. (1993): Comparative description of tornadoes in France and the United States. The Tornado: Its Structure, Dynamics, Prediction and Hazards*. Geophys. Monogr.*, nº 79. Amer. Geophys. Union, 427-434.

Doswell III, C. (versión de 2001): What's a tornado. On-Line in april 2013: http://www.cimms.ou.edu/~doswell/a_tornado/atornado.html

Gayà M. y Redaño À. (1995): El Tornado de L'Espluga de Francolí. Medidas de campo y tratamiento de imágenes digitalizadas. *Proceedings del IV Simposio Nacional de Predicción. Memorial "Alfonso Ascaso".* Madrid, Abril 1996, 345-350.

Gayà (2005): Tornados en España (1987-2005): distribución temporal y espacial. *Revista de Climatología,* 5, 9-17. On-Line in April 2013: http://webs.ono.com/reclim2/reclim05b.pdf

Gayà, M. (2007). The 1886 tornado of Madrid. *Atmos. Res.,* 83, 201–210.

Gayà (2011): Tornadoes and severe storms in Spain. *Atmospheric Research,* 100, 334–343.

Gayà M., Llasat M.C. y Arús J., (2011): Tornadoes and waterspouts in Catalonia (1950–2009)

Nat. Hazards Earth Syst. Sci., 11, 1875-1883.

Gayà M. (2011): Tornadoes and severe storms in Spain. *Atmos. Res.* 100, 334–343

Golden J. H. y Purcell D. (1977): Photogrammetric velocities for the Great Bend, Kansas, tornado of 30 August 1974: accelerations and asymetries*. Monthly Weather Review*, 105, 485-492.

McDonald J. R., Forbes G. S. y Marshall T. P. (2004): The Enhanced Fujita (EF) Scale. On-Line in decembre 2012: https://ams.confex.com/ams/pdfpapers/81090.pdf

NOAA (2004): A Recommendation for an Enahanced Fujita Scale (EF-Scale). On-Line in april 2013: http://www.spc.noaa.gov/faq/tornado/ef-ttu.pdf

NOAA (2012): U.S. Tornado Climatology. On-Line in april 2013: http://www.ncdc.noaa.gov/oa/climate/severeweather/tornadoes.html

Shaefer J.T., Livingstone R., Ostby F.P, y Leftwich W. (1993): The Stability of Climatological Tornado Data. The Tornado: Its Structure, Dynamics, Prediction and Hazards*. Geophys. Monogr.*, nº 79. Amer. Geophys. Union, 459-466.

CHAPTER 5

DEVELOPMENT OF A TECHNIQUE FOR THE DELIMITATION OF AREAS UNDER HIGH MAXIMUM WIND GUST IN EXTREME WIND SITUATIONS

José Antonio LÓPEZ DÍAZ [1], Macarena RODRIGO FERNÁNDEZ [2]

[1]*Spanish State Meteorological Agency (AEMET)*
[2]*Consorcio de Compensación de Seguros/AEMET*
jlopezd@aemet.es, ccseguros@aemet.es

ABSTRACT

Extreme wind is one of the climatic risks that strike our country. The Consorcio de Compensación de Seguros is the national body that covers risk against unusual winds, defined as those with wind gusts exceeding 120 km/h. AEMET is responsible for the estimation of the area under this risk. To this end a geostatistical technique, the universal krigging, is applied. It is based on the observations of maximum wind gust and draws also on physiographic variables and HIRLAM forecasting model fields. This contribution contains a summary of the situations that give rise to extreme winds in Spain, as well as a description of a modification of the AEMET estimation technique for the estimate of areas under extreme winds that significantly improves the bias.

Key words: extreme wind, areal estimation, universal krigging, maximum wind-gust.

1. EXTREME WIND SITUATIONS IN SPAIN

The description of situations capable of producing strong winds in our country is not an easy task, owing to its situation in the middle latitudes zone, flanked by an ocean to the west and the Mediterranean to the east, and with a complex orography. Broadly speaking there are on the one hand the mid-latitudes storms coming from the Atlantic that hit our country from time to time, as they do to other European countries bordering the Atlantic, although more frequently owing to their greater latitude; on the other hand the Mediterranean sea, with its great heat content after the hot summer typical of the Mediterranean climate, spawns clyclogenesis and other mesoscale phenomena, complicated by the orography, that can entail severe weather. Lastly the Canary Islands can be reached by tropical storms with the potential for producing very strong winds.

In this part we go through the situations at the synoptic scale that are more likely to produce extreme winds, leaving for the second part those situations belonging to the more reduced mesoscale.

1.1 Strong wind situations in our latitudes

A comprehensive classification of the synoptic scale situations more likely producing extreme winds in our territory was proposed by J. Olcina and J. Miró (2002). These authors distinguish the following generic types of strong wing situations:

- Oceanic energetic lows with frontal structure:
  - Big pressure centre with secondary centres and relatively zonal circulation.
  - Cluster of active lows strung along a westerly quasi-zonal circulation, with strong upper-level jet stream.
  - Tropical cyclone transformed into an energetic Atlantic low with frontal structure.
  - Detached cold low in low zonal index situations inside a westerly mid-latitude circulation that fosters the formation of superficial active lows of small diameter. The Cantabric "galernas" belong here.
- Cyclogenetic developments. Very frequent in the western Mediterrenean basin owing to this sea being closed and hot. The more important are the Genoa low, the Argel low and the Catalan-Balearic low.
- Anticyclonic situations with strong horizontal pressure gradient, at the southern flank of blocking highs over the Continent or potent thermal anticyclones. Levante storms are a sub-type.

The oceanic lows belong to the Atlantic lows that affect all Europe. These lows extract their energy from the contrast between the subtropical and tropical air mass over the Atlantic. Since this contrast is at a maximum in winter it is in this season that these lows are more intense. Other factors at play are latitudinal temperature contrasts, intense jet streams (with diffluence at their exit region) and an unusually warm or cold air mass. These factors are related to the NAO (North Atlantic Oscillation) which reflects the variation in position and intensity of the two dominant pressure centres in the Atlantic: the Icelandic low and the Azores high. Big pressure differences between these pressure centres tend to favour the formation of these oceanic lows. In Spain this influence is felt especially in the SW lows (in the Gulf of Cádiz).

Cyclogenesis is the development or establishment of a cyclonic circulation in the atmosphere associated with a low. In our latitudes explosive cyclogenesis implies a decrease in pressure at the centre of the low above 18-20 hPa/24 h. The two main types are the Atlantic and Mediterranean cyclogenesis, the latter with the sub-types Catalan-Balearic, Argel and Genoa Gulf. In the latter an important role is played by the gulf effect due to the warm sea that produces a positive trend in the cyclonic circulation (vorticity) of baroclinic origin.

In addition to this genetic classification of the situations likely to produce

extraordinary winds, we can make a regional classification by looking at the areas with extreme wind. According to this criterion, the same authors offer the following summary:

- According to the littoral area we may distinguish:
  - Westerly component in Galicia
  - NW in the Cantabric coastal area
  - Easterly in the Mediterranean coast
  - SW in the Andalusian coast
- North-westerly storms on northern Galicia and Cantabric coastal area:
  - Deep lows from the Atlantic. We may distinguish: Atlantic lows, when the centre of the low lies over the maritime district of Gran Sol; British lows having their centre over the British Isles; Cantabric lows in front of the Asturias or Cantabria coast. These are more frequent between November and February.
  - Intense zonal circulations that cause strong westerly winds. These are not limited to the N but can extend over all the Iberian and Balearic regions, with particular incidence over areas with special orographic configurations that channel the wind ("ventanías").
- South-westerly wind storms related to Atlantic lows over the Cádiz Gulf, with third quadrant winds. They tend to be associated with upper-level cold lows over the same synoptic space. More frequent in November-December.
- Gales, squall lines of various durations. They happen especially in the Ebro valley including the coastal Catalan areas near the river mouth, Ampurdán region, NE area of Catalonia, more western Coruña capes, Tarifa and areas next to the Gibraltar Strait, highest summits of the bigger mountain ranges. These winds have usually a local character.

1.2 Mesoscale patterns that can produce extreme wind in Spain

The complex orography of our country, together with its position close to an important caloric reservoir in fall and winter, i.e. the Mediterranean Sea, favour the occurrence of subsynoptic mesoscale extreme winds. This scale comprises the meso-γ (2-20 km, with phenomena such as the single-cell convection, orographic winds), meso-β (20-200 km, sea breezes and lake effect winds) and meso-α (200-2000 km, includes squall lines and mesoscale convective systems).

1.2a *Non-tornadic winds that cause damage*

Dangerous straight-line winds linked to convective phenomena are related almost always with precipitation cooled outflows (by evaporation, melting or sublimation). Only in exceptional cases inflow super-cell updrafts can produce damage. This exception apart, the damaging winds associated with outflows can come either from meso-γ downdrafts, called downbursts, that impinge on the surface and have divergent trajectories, or from cool pools of air of meso-β scale that bring about

intense horizontal gradients that can produce strong winds. This type of event usually appears through accumulation of several storm outflows; vortices in the outflow boundary can contribute to the strong winds.

A downburst ("reventón") is defined as a strong downdraft that gives rise to destructive winds when hitting the ground, accompanied by an intense storm. Downbursts must have less than 10 km of horizontal width. When this is less than 4 km we call them microbursts. They can be wet or dry, according to whether the precipitation reaches the ground. Downbursts are associated with relative surface highs, which is needed to horizontally deflect the descending air. Their forcing is essentially thermodynamic through negative buoyancy in the downdraft, due to evaporative cooling or hydrometeor cooling. Both processes increase the density of air relative to its environment. Evaporation is favoured by a dry boundary layer near the surface.

Some times strong winds are linked to squall lines with little convective instability but with strong synoptic pressure gradients. In these cases the surface strong winds are produced by entrainment of upper-level strong winds by the downdraft.

The *derechos* are linked to long duration deep convection. The extreme winds that they entail can arise through any of the preceding mechanisms. The term *derecho* includes any family of downburst cluster coming from a mesoscale convective extra tropical system, and can produce very damaging straight-line winds over areas several hundred of kilometres long and more than hundred kilometres wide.

Lastly we must mention the slope winds which have an orographic character, not necessarily associated to convective phenomena, instead they are due to leeside accelerations. With adequate conditions of air flow, atmospheric stability and topography they can locally reach high speeds and cause important damage.

1.2b *Tornadic winds*

This class includes strong winds with a rotational component. A tornado is a violently rotating column of air that hangs from a cumulonimbus cloud, usually visible as a funnel cloud. In order for a vortex to be considered a tornado it must touch the ground as well the cloud base. A waterspout is a tornado over water. They are smaller and weaker than terrestrial tornados.

Most tornados have winds of less than 200 km/h speed and have less than 800 m diameter. These are the ones that occur in our country. Tornados are favoured by conditional instability stratification (i.e. instability after saturation), as well as low level high shear and humidity. They are more frequent towards the end of spring and beginning of fall, but can appear also in summer. Tornados can form from super-cells, but they are also linked to less intense convection. Other phenomena similar to tornados, but usually not producing such intense winds are:

- A gustnado occurs along the gust front of a storm and is visible through material lifted from the ground. Typically its diameter lies between a few meters and several tens of meters, rising from the surface without touching the cloud.

- Dustclouds are vortices that develop in the lower atmosphere without connection to a convective cloud, visible by the lifted dust, sand and debris. Their origin is

usually thermal owing to the strong heating of the surface, without low clouds or with low-rising clouds.

- Funnel-clouds are funnel or cone-shaped downward extensions of a convective cloud, caused by a rapidly swirling motion that does not reach the ground.

2. DESCRIPTION OF SOME EXTREME WIND SITUATIONS

This section contains a somewhat detailed analysis of some specific situations that led to very intense winds. They typify some of the situations discussed above.

2.1 Atlantic low (5-6 Nov 1997)

On 5-6 November of 1997 a deep extratropical low, coming from the Atlantic, swept the Iberian Peninsula from SW to NE. The low centre crossed from the Cadiz Gulf to the SE of France. It caused widespread material damage and more than 20 fatal casualties, most of them near the city of Badajoz, owing the floods.

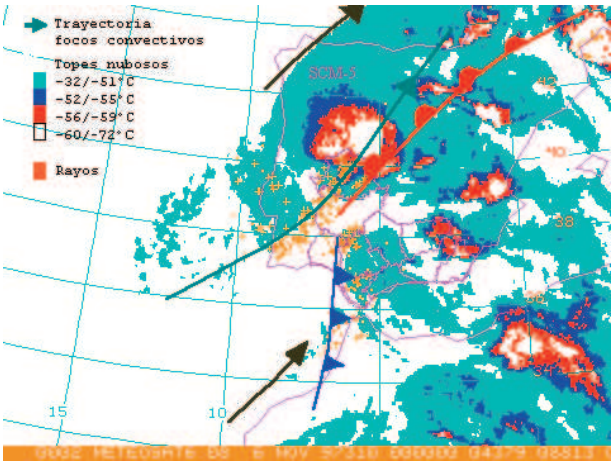

Figure 1. Mesoscale analysis on the 6/11 at 00:00 UTC (source AEMET).

Strong winds accompanied this deep low. The wind gale struck the SW of the Peninsula from late on the 5th to early on the 6th causing a lot of damage to infrastructure and crops. Catalonia suffered also harm. Normality returned in the morning as the gale moved over to the east.

2.1a *Mesoscale analysis*

Unstable subtropical air south of the Azores fostered the development of several convective nuclei, some of whom grew to mesoscale convective systems. This complex moved eastwards so that the convective nuclei reached the Peninsula with convective activity still in development (Figure 1).

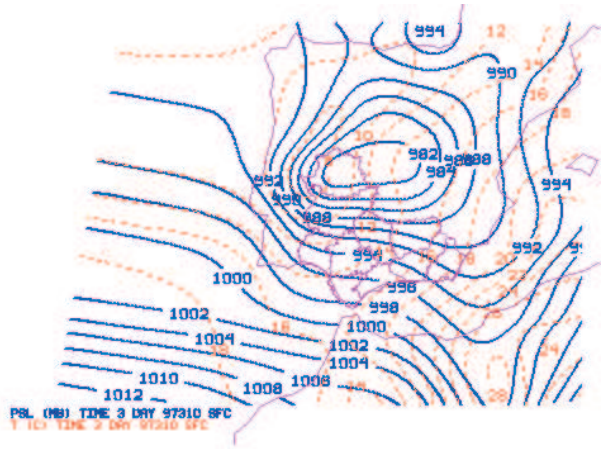

Figure 2. Surface pressure on the 6/11 at 03:00 UTC (source AEMET).

2.1b *Surface analysis*

A strong barometric gradient produced average winds in excess of 20 kts over the lower Guadalquivir area on the 6th at 00 hour (Figure 2). At that moment the front lay over the boundary between Huelva and Portugal. The low-level jet was located over Andalusia, which made for very gusty wind. Wind gusts over 100 km/h were recorded at many places seriously affecting the SW of the Peninsula. After three hours, on 6th at 03 h, the wind over 20 kts was scarce. In the following hours the strong winds shifted to the Mediterranean area.

2.2 Cantabric "galerna"

A "galerna" is a sudden and violent storm with strong wind gusts from W to NW that usually hits the Cantabric Sea and coasts, generally in spring and fall. They appear in warm and placid days when a cold front causes a swift change in the direction and force of the wind, which can reach 100 km/h. The sky turns darker, temperatures sink even by 10 ºC, and pressure plummets. Conditions at sea turn rough or very rough and short intense showers complete the picture.

There are two types of "galerna": the common "galerna" and frontal "galerna". The common "galerna" is more frequent in summer. The synoptic pattern favourable for its occurrence has weak cyclonic flow or weak baric gradient over the Cantabric Sea. Its greatest risk lies in the swift worsening of conditions at sea, but the winds are not too intense.

Quite in contrast the frontal "galerna" is capable of producing very strong winds. It is linked to the passage of a cold front characterised by the presence of a front aloft ahead of the surface front. The synoptic pattern is defined by a relatively thin and deep trough to the W of the Peninsula, with marked front flow from the S/SW that crosses the surface front. On the surface there is a low over the N of the Peninsula with associated cold low that crosses the Cantabric mountain range eastwards causing the changes in wind direction, temperature, pressure and humidity typical of a cold active front.

There are also mesoscale factors at play: the orographic effect of the Cantabric range on the south-westerly flow before the front passage, with the appearance of an orographic dipole; the foehn effect heats and dries the air on the leeside of the mountain range. Owing to these synoptic and mesoscale conditions one can expect a greater pressure and temperature gradient between the air mass before and after the front. This makes the wind, pressure, temperature and humidity changes more marked in the frontal "galerna" than in other cold fronts.

An example of frontal "galerna" that caused important damage in Santander city happened on the 3rd of October 2006 (Figure 3). The maximum wind gust recorded at Parayas airport, near the city, was 118 km/h, and at Santander observatory it was 161 km/h. The latter measurement, however, was carried out with an anemometer at 22 m above the ground (instead of the standard 10 m), so it was necessary to apply a reduction of around 10%.

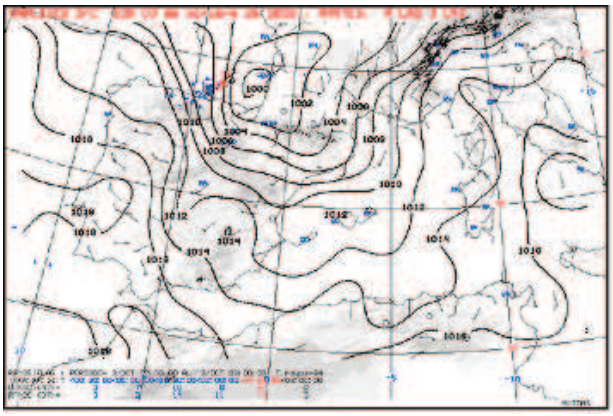

Figure 3. Surface analysis with 2 hPa isobar spacing of 3/10/2006 at 03:00 UTC (source AEMET).

2.3 Mesoscale convective system (4 Oct 2007)

Mesoscale convective systems MCS are convective structures with a higher degree of organization than the single-cell or multi-cell storms. A number of storms tend to array themselves along a line, summing their efforts, so to speak, to form a linear storm system under a higher cloud cover. The areas affected by the MCS are wide and their impact widespread owing to their greater duration and extension. In their mature phase an area of continuous and stratiform rain can be observed that can embed storms, and another area, more or less linearly shaped, with stormy foci of great intensity and potentially severe. When the MCS reaches enormous sizes they are called Mesoscale Convective Complexes.

An instance of MCS occurred on the 4th of October 2007 over Mallorca, Figure 4. This situation produced recorded wind gusts of 109 km/h at Porto Pí (Palma de Mallorca) and 107 km/h at Pollensa harbour. But from the analysis of the damage

it can be concluded that at least one tornado appeared, with winds around 160 km/h, as well as many areas affected by micro-bursts or gust vortices with winds in excess of 120 km/h.

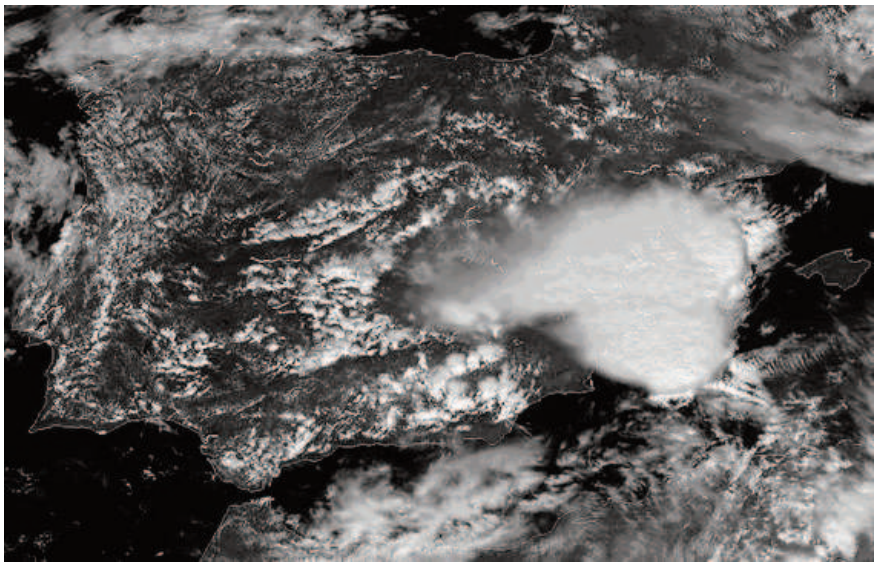

Figure 4. Visible channel high resolution image of the MSG satellite at 12:00 UTC of 4/10/2007. Note the MCS to the east of Murcia coast against the small storms to the north of Granada and Almería. Source: EUMETSAT.

2.4 Delta storm (28-29 Nov 2005)

Delta was a storm of non-tropical origin, arising from a wide low pressure area to the SW of the Azores on the 19th of November. On the 22nd it had acquired characteristics of a tropical cyclone. After a zigzagging trajectory on the 18th it had extra-tropical low status lying close to the Canary Islands towards the west and getting stronger while moving towards the baroclinic zone associated to a European trough with vertical shear and cold air entrainment.

Table 1 shows that winds during the Delta storm reached very high intensity. The 248 km/h measurement at Izaña observatory on the 28th is the record of the data series since its inception in 1938. In order to appreciate its importance, the following higher value is 216 km/h recorded in 1947.

These strong wind gusts can be explained by the presence of intense flows that surmount an orographic obstacle from upper levels and then descend experiencing adiabatic heating owing to compression (downslope windstorm). The extreme winds come about when strong winds combine with important orographic obstacles in stable environments with basically a conversion between potential and kinetic energy of the flow.

MAX GUST (KM/H)	DAY	OBSERVATORY	PROVINCE
248	28	IZAÑA	SANTA CRUZ
160	29	IZAÑA	SANTA CRUZ
152	28	LA PALMA/AIRPORT	SANTA CRUZ
147	28	TENERIFE/LOS RODEOS	SANTA CRUZ
136	28	HIERRO/AIRPORT	SANTA CRUZ
134	28	TENERIFE/SUR	SANTA CRUZ
132	29	LANZAROTE/AIRPORT	LAS PALMAS
130	29	TEGUISE (FAMARA)	LAS PALMAS
126	28	LA OLIVA	LAS PALMAS
120	29	FUERTEVENTURA/AIRPORT	LAS PALMAS

Table 1. Maximum wind gusts over 120 km/h during the delta storm in the climatological database of AEMET.

The thermodynamical diagnosis showed that above lay a layer with indifferent stability (900 hPa level), then a more stable layer and above this a quasi thermal inversion that acted as a lid of stability for the incident flow on the obstacle. It is the flow blowing above this the one that after surmounting the obstacle descends on the lee side generating an orographic wave that depending on its Froude number can be transmitted vertically, either upwards or downwards. The presence of a meso-low on the lee of the island (Figure 5), caused by the obstruction of the low-level flow on the windward side, favours that the descending wave may reach levels close to the sea and accelerate due to conversion from potential to kinetic energy. This explains the occurrence of very strong winds on the leeside of the islands.

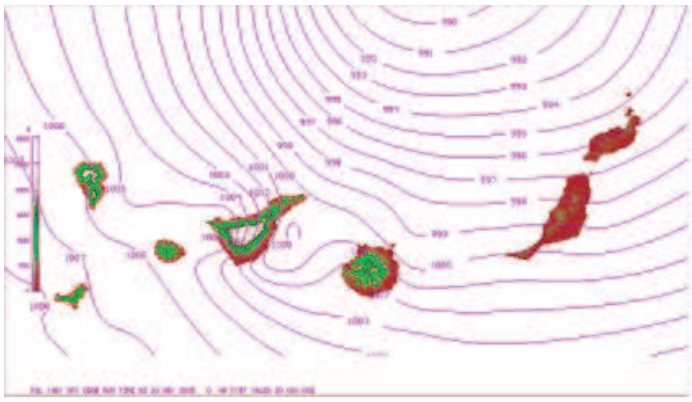

Figure 5. Sea level reduced pressure (hPa) from the analysis of ECMWF on 29/11/ 2005 at 00 UTC. Colours according to orography with scale on the left (source AEMET).

2.5 Explosive cyclogenesis (18-20 Jan 2013)

Cyclogeneses are dealt with extensively in another contribution to this book by F. Martín León, so here only an outline of two quite recent examples will be given.

DAY	STATION	PROVINCE	MAX GUST
18	LA COVATILLA, SKI RESORT	SALAMANCA	136
18	VALDEZCARAY	LA RIOJA	126
19	FISTERRA	A CORUÑA	149
19	LA COVATILLA, SKI RESORT	SALAMANCA	138
19	JEREZ DE LOS CABALLEROS	BADAJOZ	138
19	JAÉN	JAÉN	134
19	CABO VILÁN	A CORUÑA	132
19	MINAS DE ALMADÉN	CIUDAD R.	129
19	VALDEZCARAY	LA RIOJA	128
19	ALBORÁN ISLA	ALMERÍA	127
19	ESTACA DE BARES	A CORUÑA	126
20	MOSQUERUELA, DEPOSITO	TERUEL	128
20	ESTACA DE BARES	A CORUÑA	126

Table 2 . Maximum wind gusts over 125 km/h on 18-20 January 2013 in the climatological database of AEMET.

The explosive cyclogenesis Gong of 18/01/2013 evolved from a surface low that intensified swiftly helped by the strong upper level divergence at the left exit region of a marked jet stream. This deep low turned into a wind storm in the Mediterranean area by the 23rd, an example of Mediterranean cyclogenesis. The surface low in this case was the result of the strong westerly winds from Gong that after crossing the Peninsula mountain ranges suffered an increase in cyclonic circulation.

DAY	STATION	PROVINCE	MAX.GUST
22	LA COVATILLA, SKI RESORT	SALAMANCA	136
22	SIERRA DE ALFABIA	BALEARES	130
24	MACHICHACO, FARO	BIZKAIA	140
24	LÁUJAR DE ANDARAX	ALMERÍA	127
24	PUERTO DE SAN ISIDRO	LEÓN	126
24	CASTELL DEL FERRO	GRANADA	126

Table 3. As in Table 2, but for 22-24 January 2013.

This can be explained by the fact that before the range the zonal wind has a positive absolute vorticity (sum of relative and the planetary vorticities, the latter equal to the Coriolis parameter). When the column of air rises, it gets thinner and by angular momentum conservation it acquires a lesser absolute vorticity, which requires southward displacement and anticyclonic relative vorticity. The process goes in reverse in the descent, the column contracts, absolute vorticity grows with attendant cyclonic relative vorticity.

Table 2 shows that the highest values of wind gust in Gong occurred mainly in the western half of the Peninsula.

In the ensuing Mediterranean cyclogenesis (Table 3) the strongest wind gusts were recorded in the Balearic Islands, Almería and Granada, although at other more westerly points the strong winds persisted.

3. TECHNIQUES FOR THE ESTIMATE OF AREAS UNDER MAXIMUM WIND GUST

The Consorcio de Compensación de Seguros is the Spanish body that covers the risk against extraordinary winds, defined by the Reglamento del Seguro de Riesgos Extraordinarios as the wind that produces gusts in excess of 120 km/h. The precise delimitation of areas satisfying that condition carries considerable difficulties in our country, owing to the paucity of wind observations and the complex orography.

Under a collaboration agreement between AEMET and the Consorcio de Compensación de Seguros, AEMET has to make the technical reports that specity the geographic regions affected by the extreme wind when this falls under the coverage of the Consorcio.

3.1 Description of the technique used at AEMET

In order to estimate the areas where the 3-second wind gust has been over 120 km/h a geostatistical interpolation technique has been developed at AEMET. This technique is a kind of krigging, which is a geostatistical technique based on considering the observations as a realization of a theoretical random field. Stationarity is assumed, i.e., invariance of second-order moments against displacements. This allows the characterization of the second- order moments by a single (spatial) argument function, that in the case of krigging is the semivariogram (similar to the covariance but without centering). The krigging postulates an estimator for the field at an arbitrary point as a linear combination of the observations in the rest of points suitably weighted. To determine the weights two conditions are imposed on the estimator: unbiasedness (i.e. its mathematical expectation has to coincide with mathematical expectation of the estimator) and that its variance be minimized.

There are several kinds of krigging according to the additional hypotheses that are admitted. The universal krigging postulates a linear model for the trend, so that the mathematical expectation of the random field at an arbitrary point is expressed as a linear combination of the values at the point of several deterministic functions. This allows the inclusion of smooth variation effects in the geostatical interpolation.

Specifically, at AEMET the auxiliary deterministic functions used in the universal krigging are: terrain elevation, distance to the shore and the output of the numerical model HIRLAM for maximum wind gust in the analysis for the period under study. The structure of the semivariogram is specified without nugget effect, so than the krigging is an exact interpolator, i.e., in the points with observation the estimated and the observed value are the same. This is important since for the Consorcio it is compulsory to respect the observed values due to their legal binding value.

3.2 Development of an improvement in the operational technique

The idea of developing a modification of the operational technique described above came as a consequence of verification studies. These showed that in the range of maximum wind gust speeds above 80 km/h, which have more interest in finding the area with wind gust over 120 km/h, there was an important negative bias in the estimation with the universal krigging. For a set of ten strong wind situations that were studied the mean bias in the verification amounted to -14 km/h (see Table 4, 2nd col.). In all situations the mean bias (in each situation 20% of the observations were chosen randomly to verify) turned out to be negative. This negative bias can be explained as a result of the fact that the krigging, as mentioned

MEAN BIAS (Km/h)		VALIDATIONS (W_{GUST} >= 80)		VALIDATIONS (ALL W_{GUST})	
		OP.	PROX.	OP.	PROX.
ACS (date)	20100113-15	7.3	0.3	1.0	10.6
	20100227-28	4.3	0.8	0.5	9.7
	20111023-27	17.5	6.3	1.2	10.5
	20111112-14	13.4	6.0	0.9	12.4
	20111215-17	7.9	0.4	0.7	11.6
	20120105-08	20.4	7.5	0.1	11.0
	20120202-05	21.8	11.1	0.1	13.6
	20120206-08	12.9	6.3	0.8	11.0
	20120415-17	17.1	7.3	0.8	14.7
	20120423-26	15.3	9.1	0.2	6.8
MEAN		-14 Km/h	-5 Km/h		

Table 4. Mean biases for the estimation of max wind gust with the operational method (op) and the new method (prox) for 10 strong wind situations (dates in 1st col). cols. 2 - 3 biases for validation ≥ 80 km/h, cols. 4-5 biases for validation with all observations.

before, gives a globally unbiased estimator. So over a restricted range of observations, as every technique similar to linear regression, the estimator tends to the mean. As the range of observations chosen was above the mean it is to be expected a negative bias in the estimation.

It was tried then to apply the same universal krigging technique but using only the observation in the high range, over 80 km/h. In the provinces where this did not guarantee at least 3 observations more observations from the ones with greater wind gust were drawn until each province had at least 3 observations.

This ensures good spatial coverage. In this way, as was to be expected, the bias was much reduced in the same verification over the high range, with mean values on the order of 2 km/h.

But the problem now is that the interpolated field overestimated a lot over the rest of the observations range. So it was tried to combine both interpolations, the operational and the one restricted to more than 80 km/h. Noting by *COMBI.PROX* the new combined method, and by *SEL80/3* the interpolation with observations more than 80 km/h basically, the combination was made according to:

$$COMBI.PROX(\vec{p}) = F_m(\vec{p}) \times OP(\vec{p}) + (1 - F_m(\vec{p})) \times SEL80/3(\vec{p})$$

where $\vec{p}$ is an arbitrary point and F_m is a mixing factor between 0 and 1. This was obtained from another positive F'_m alter the monotone transformation:

$$0 \le F_m(\vec{p}) = \frac{F_m'(\vec{p})}{1 + F_m'(\vec{p})} \le 1$$

In order to determine F'_m it was specified that it had to be the more greater the farther away the problem point $\vec{\rho}$ lay from observations used by the *SEL80/3* method, so that the operational estimate should weight more, and vice versa. Furthermore since there are significant observation density differences among different regions, it was considered convenient to include a scale factor that accounted for this local density of observations. The formula used was:

$$F_m'(\vec{p}) = \sum_{i \in NO\,80/3} \left(\frac{dist(\vec{p}, \vec{s})}{F_{sc}(\vec{p})} \right)^{-expo}$$

where the summation extends to all stations not used by the *SEL80/3*. The scale factor has dimensions km, as *dist*, so that F_m is adimensional. The exponent – *expo* was chosen equal to -2, and the scale factor $F_{SC}(\vec{p})$ was defined by:

$$F_{sc}(\vec{p}) = \min\left[F_{scMax}, cc \Big/ \sqrt{\rho_{local}(\vec{p})} \right]$$

Its maximum value has a predefined value, with *cc* a constant to specify. The local density of observations $\rho_{k\,cal}(\vec{p})$ is determined over a circle of radius 100 km. This way under the hypothesis of uniform observation density around an arbitrary point ρ, a uniform dilation of rate *r* around ρ leaves $F'_m(\vec{p})$ unchanged (if F_{scMax} is not reached), since distances get multiplied by *r* and the local density by r^{-2}. The value of the adimensional constant *cc* was specified according to the condition that F_{SC} be 1.5 km when inside a 100 km-radius circle there are 100 observations (cc = 84.6 x10-3).

The 3rd column of Table 4 shows that the average bias for the combined method over the 10 strong wind situations analysed, verifying over observations above 80

km/h, decreased to -5 km/h, a reduction of nearly 2/3. On the other hand the last two columns display the result for validation over the whole range of observations. We can see that the operative technique, that in theory is unbiased over this range, has very little biase

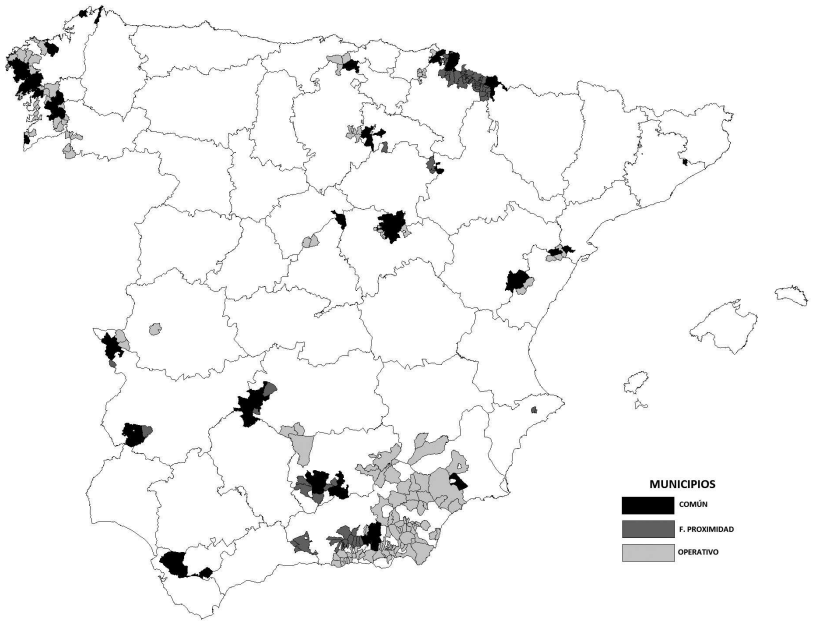

Figure 6. Municipalities with maximum wind gust over 120 km/h in the situation of 18 January 2013 for the operational, combined and both methods.

The 3rd column of Table 4 shows that the average bias for the combined method over the 10 strong wind situations analysed, verifying over observations above 80 km/h, decreased to -5 km/h, a reduction of nearly 2/3. On the other hand the last two columns display the result for validation over the whole range of observations. We can see that the operative technique, that in theory is unbiased over this range, has very little biases.

Figure 6 contains the municipalities with wind gust over 120 km/h as determined by the operational method, the new one and by both methods, for the situation of 18 January 2013. The new method increases the area especially over the eastern Pyrenees and another area close to the Penibética mountains (though here the operational method extends more over lower areas), both areas characterised by complex orography.

REFERENCES

Arteche García, J. L. (2008). 'La Galerna del Cantábrico', *Revista de la AME*, Boletín nº 22.

Cressie, N. (1993). *Statistics for spatial data*, Wiley Interscience.

Donald Ahrens, C. y Samson, P., (2011). *Extreme Weather & Climate*, Cengage Learning.

Markowski, P. and Richardson, Y., (2010). *Mesoscale meteorology in Midlatitudes*, Blackwell.

Martín León, F. (coord.), (2005). *Estudio de la tormenta tropical "Delta" y su transición extratropical: Efectos meteorológicos en Canarias.* Nota Técnica del INM. On-line: www.aemet.es/es/conocermas/estudios.

Martín León, F. Los Sistemas Convectivos de Mesoescala y "la gota fría". *Revista RAM* (en Internet).

Martín León, F. Ingredientes en las ciclogénesis explosivas: el caso de Gong. *Revista RAM* (en Internet).

Olcina Cantos, J., Miró, J. (2002). "Temporales de viento fuerte en latitudes medias y altas", en Ayala-Carcedo, F. J., Olcina Cantos, J. (coordinadores). *Riesgos Naturales*, Ariel Ciencia.

Riosalido Alonso, R. (coord.). *Ciclogénesis del 5-6 de noviembre de 1997*, Biblioteca Módulos Tempo, AEMET. On-line: www.aemet.es/es/conocermas/varios.

CHAPTER 6

AN ANALOG MODEL FOR ESTIMATING STRONG WINDS

F. VALERO[1], C. GARCÍA-LEGAZ[2], Á. PASCUAL[1], M. L. MARTÍN[3]

[1]Universidad Complutense de Madrid. [2]Agencia Estatal de Meteorología (AEMET). [3]EU Informática. Universidad de Valladolid.
valero@fis.ucm.es

ABSTRACT

The purpose of this work is to show relationships between wind and large-scale atmospheric fields, with special emphasis on extreme situation results. These connections are obtained by using different methods and procedures such as wind cumulative probability functions and composite maps. The analyses showed different mean atmospheric situations associated with the different wind patterns, in which strong atmospheric gradients can be related to moderate to strong wind in Spain. Additionally, mean wind and gust estimates have been analyzed. These estimations have been obtained by means of a downscaling analog model. The model is used to find similar atmospheric patterns, and from them wind fields were estimated. Deterministic and probabilistic results show that gust behaviour is quite better approximated than mean wind speed, in general. The model presents some underestimation except for strong winds, where the model show a similar appraisal in mean wind speeds and gusts. Moreover, the model shows better probabilistic wind results over the Spanish northern area, highlighting that the atmospheric situations coming from the Atlantic Ocean are better recovered to predict mean wind and gusts in the Northern Peninsula.

Key words: extreme winds, gusts, analogs, probabilistic results.

1. INTRODUCTION

Wind storms are one of the most costly natural hazards in Europe (Swiss_Re, 2000). They can cause severe damage and therefore lead to major economic losses. A rise in storm-related monetary losses for Europe in the course of the 20th century has been observed by Barredo (2010), explained principally by changes in economic and demographic conditions, with much of the recent infrastructure in various parts

of the world increasingly constructed in zones at risk from severe weather (Swiss Re, 2000). Furthermore, studies show that losses related to European wind storm events are likely to increase in the 21st century as a result of greenhouse-gas warming (e.g., Schwierz *et al.,* 2010).

European windstorms are triggered by extratropical cyclones rooted in the transition zone between subtropical and polar climate zones. They are mid-latitude weather systems that derive their energy from horizontal temperature contrast between cold, polar air masses and warm, subtropical air masses (Malmquist, 1999). The temperature contrasts between these air masses are greater during winter, and so is the frequency and intensity of European windstorms. Maximum wind speeds can reach 140–200 km/h and, in extreme cases, up to 250 km/h in exposed coastal locations. Wind fields may span up to 2000 km (Munich Re, 2008) and thus affect several countries.

Here, relationships between wind and large-scale atmospheric fields are shown, with special emphasis on results involving extreme situations. These connections are attained by using different methods and procedures, such us cumulative probability curves and composite maps. Composites have already been used by the authors in several studies in order to analyse different fields, obtaining relationships between them, so that maximum and minimum intensity phases of a field can be related to the other one (Valero *et al.,* 2004; Martín *et al.,* 2011a; Martín *et al.,* 2011b). Additionally, extreme wind speed and wind gust estimations in Spain by means of ANPAF model (ANalog PAttern Finder) applied to large-scale atmospheric data are gained. To do this, a principal component analysis is previously applied to the regional variables in order to extract their most remarkable atmospheric circulation patterns in order to reduce the dimensionality of the large-scale atmospheric data. Multivariate techniques have been successfully used by the authors (Morata *et al.,* 2008; Valero *et al.,* 2009; Martín *et al.,* 2011a; Martín *et al.,* 2011b) in other studies to gain a better insight into the seasonal interactions between large-scale circulation anomalies and regional variable fluctuations to provide evidence of the influence of several North Atlantic teleconnection patterns of low-frequency on the variability of the regional variables in the Western Mediterranean area as well.

2. CONNECTIONS BETWEEN EXTREME WIND SPEEDS AND LARGE SCALE ATMOSPHERIC PATTERNS

In order to analyse the relationships between wind speeds and large-scale atmospheric fields and to extract information about extreme situations it is very important to select the appropriate datasets. In this work, in order to characterize the atmospheric circulation, 1000 hPa daily geopotential heights at 12:00 UTC (Z1000) for 36 winters from 1971 to 2007 covering from 51.5º W to 15.5º E and 20º to 60º N have been used. Concerning the wind speed, firstly daily mean wind speed (MWS) data for 21 stations distributed over Spain (Figure 1) during the winter (D-J-F) season from 1970 to 2002 have been considered. These wind data come from in-situ measurements of the station network of the Spanish Meteorological Service (Agencia Estatal de Meteorología, AEMET).

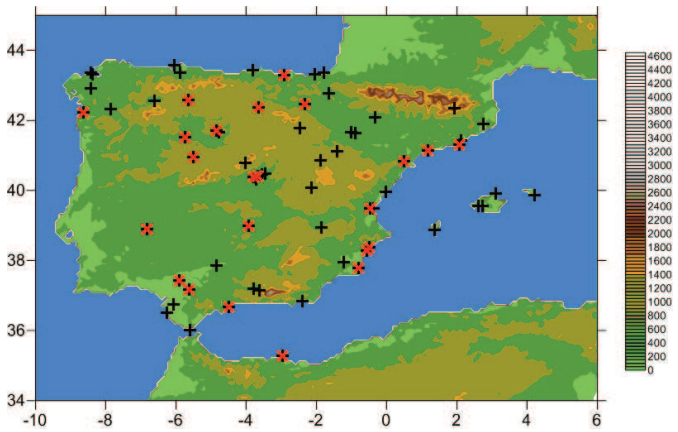

Figure 1. The Iberian Peninsula with its orography detailed with the mean wind speed stations in red crosses and the wind gust stations in black crosses.

Previously to pick up information about extreme winds a Principal Component Analysis (PCA) is applied to the MWS and Z1000 fields in order to know its general behaviour and to extract the most significant patterns from the original data (Preisendorfer 1988). The PCs are proposed to adequately represent the original dataset variation without loss of significant information. Five leading modes for both datasets have been selected (not all shown). They account for more than 66% and 77% of the total variability for MWS and Z1000, respectively.

2.1 Large scale atmospheric patterns - wind speed statistical mode relationships

For reasons of brevity only the first mode is shown. In Figure 2a, the eigenvector or spatial pattern of the retained MWS PCs is shown which helps highlighting diverse areas of different wind behaviour over Spain. The leading wind PC pattern (Figure 2a) accounts for the most important percentage of variance in the original data (37.9%). In Figure 2a the spatial pattern shows homogeneous wind behaviour in inner Iberia, and also underlines the area to the North Iberian Plateau with high correlation values. This conduct in the wind field could be related to the predominant westerly circulation regime (Poniente) in the Iberian Peninsula. The time variability of the spatial pattern above described is depicted showing the evolution of its PC time series obtained by applying the PCA over the MWS data in wintertime (Figure 2b). Significant trends are not found after applying a Mann-Kendall test and a spectral analysis of the PC time series. As stated previously, the first spatial pattern of Figure 2a showed homogeneous wind pattern over Iberia, underlying areas corresponding to the North Iberian Plateau. This behaviour can also be represented in the corresponding time series (Figure 2b) with mostly positive and high score values over the selected period (1970-2002).

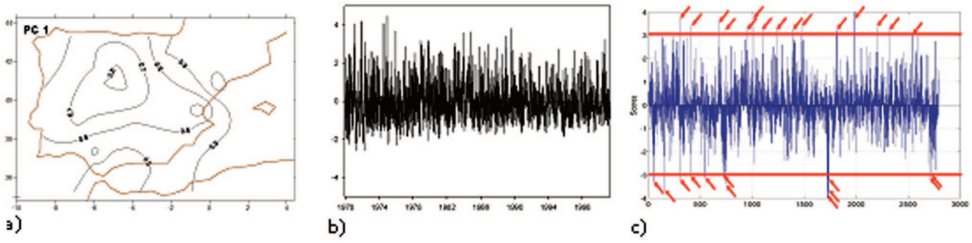

Figure 2. (a) Spatial patterns of the first PC of wind speed. The positive (negative) correlations are solid (dashed). (b) Time series of the first PC of the wind speed. Units are in standard deviations in the y-axis and the x-axis corresponds to the time period. (c) Illustration of picked up dates from the PC time series. Red rows indicate both the 5% high positive and negative scores used to build the composite maps.

However, the derived modes are statistically obtained. To analyze the extreme situations is needed to find connections between wind speed and the atmospheric field. Thus, to examine the real atmospheric circulation features associated with the winter wind speed patterns a set of positive and negative composite plots (of Z1000 and MWS) was constructed from the dates associated with 5 and 95 percentiles of the scores of the time series obtained of the PCA (Figure 2c). The composite maps represent configurations of the variable which are comparable to observations. Composites are defined here as the averaged ensemble of sets of maps of the large-scale atmospheric variable and the wind speeds (Pascual *et al.,* 2013). Physical distinctive features in the composite plots is achieved through obtaining additional information to the statistical meaning of the derived spatial modes. Here, the anomaly composites of large-scale atmospheric variables have been built for those weather configurations associated with the highest and lowest PC scores of the wind speed. This way, the composites represent the atmospheric state associated with particular extreme wind characteristics. Positive (negative) composites are constructed directly from a number of configurations with high (low) scores of the PC time series because they indicate situations in which the corresponding PC mode is dominant in its positive (negative) phase. The selected number of configurations represents 5% of the total number of cases in the dataset.

Figure 3 shows the anomaly composites for Z1000 displaying the positive and negative composite plots conditioned by the 5% highest and lowest PC scores of the MWS. Subsequently, mean maps of Z1000 anomalies are drawn up from these days, and highlight the mean atmospheric state conditioned by predominant oscillation of the selected wind speed PC mode. Additionally, maps of MWS, also corresponding to those days, are picked up to illustrate the behaviour of the wind speed field over Spain in such atmospheric situations. Thus, the Z1000 anomaly composites associated to the first wind speed PC (Figure 3a, b first positive and negative composites) highlight two different mean atmospheric situations associated with the wind behaviour. Thus, in the first positive anomaly composite (Figure 3a), a strong gradient of Z1000 is observed over the Iberian Peninsula, underlying strong winds over Iberia as it can be noted in Figure 3c with wind speeds exceeding 8 ms^{-1} (30 kmh^{-1}) in daily average. In

contrast to this atmospheric situation, the first negative composite (Figure 3b) displays high anomaly pressure over Iberia with little gradient over it and a nucleus over northern France. This situation is indicative of low wind speed over most of the area (Figure 3d).

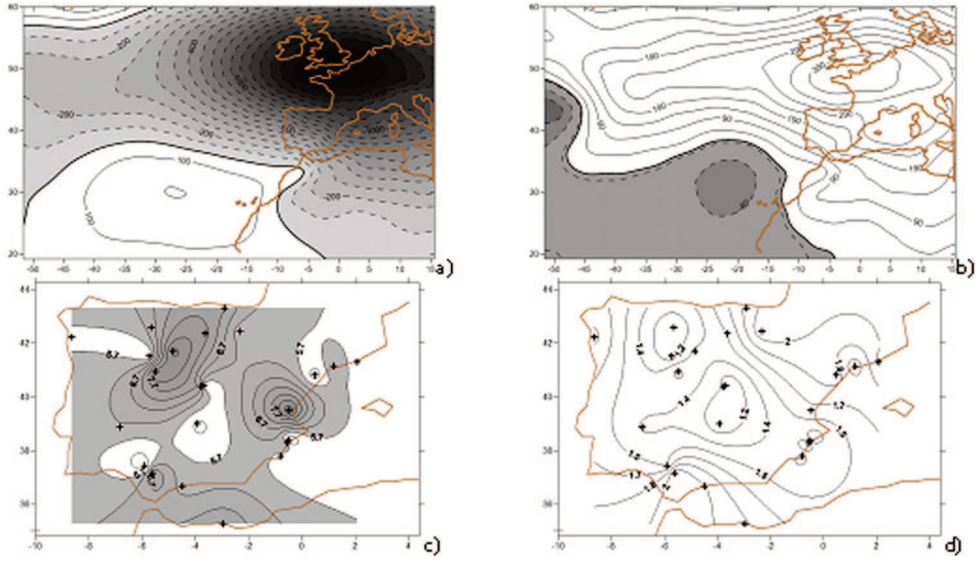

Figure 3. Composite maps of the Z1000 (gpm) conditioned by the highest and lowest scores of the first wind speed PC: (a) positive composite; (b) negative composite. Composite maps of wind (ms^{-1}): (c) positive composite and (d) negative composite with shaded areas highlighting mean wind speed higher than 5 ms^{-1}. Crosses indicate the wind stations.

2.2 Wind speed cumulated probability -large scale atmospheric statistical mode relationships

The relationships between MWS and large-scale atmospheric circulation are studied by means of wind speed cumulated probabilities associated with statistical modes of Z1000. To do this, the interactions between the PCs of Z1000 (only shown some results) and the observational local MWS are provided and analyzed. Thus, plots with cumulated probability values of wind speed associated with the highest and lowest scores of the Z1000 PC (not all shown) are described. These plots provide a fair idea about the observational wind frequency distributions conditioned by the different strong scores of the PC Z1000 time series.

In order to have an idea about the wind speed cumulated frequencies these are derived associated to dominant positive and negative scores of the Z1000 PCs. To do this, higher and lower Z1000 scores were selected and subsequently their associated dates. Thus, at every station, the MWS is picked up for such days and depicted the associated cumulative probabilities from 0 to 100%. Here only the

Madrid station results are shown (Figures 4a, b). Once the PCA has been applied to the Z1000 field, the five leading Z1000 PCs, explaining 77% of the total variability, are retained. In general, it is remarkable in Figure 4a the quite high mean wind speeds associated with the Z1000 PC3. The third most significant PC pattern obtained for the Z1000 field (Figure 5a) consists of a configuration of positive (negative) correlation values centered over the North Atlantic area (western Mediterranean). This distribution of isolines implies that northern (southern, in its negative phase) winds are mainly affecting Iberia. Such configuration is associated with dynamically coherent and characterized by intrusions of cold (warm, in its negative phase) air masses over Iberia. This third Z1000 mode has the strongest influence over the observational wind speeds in throughout Spain, with daily MWS of up to 10 ms^{-1} in Madrid station (Figure 4a) and of almost 14 ms^{-1} (50 kmh^{-1}) in Melilla and Valencia (not shown) which reflects strong winds over such areas.

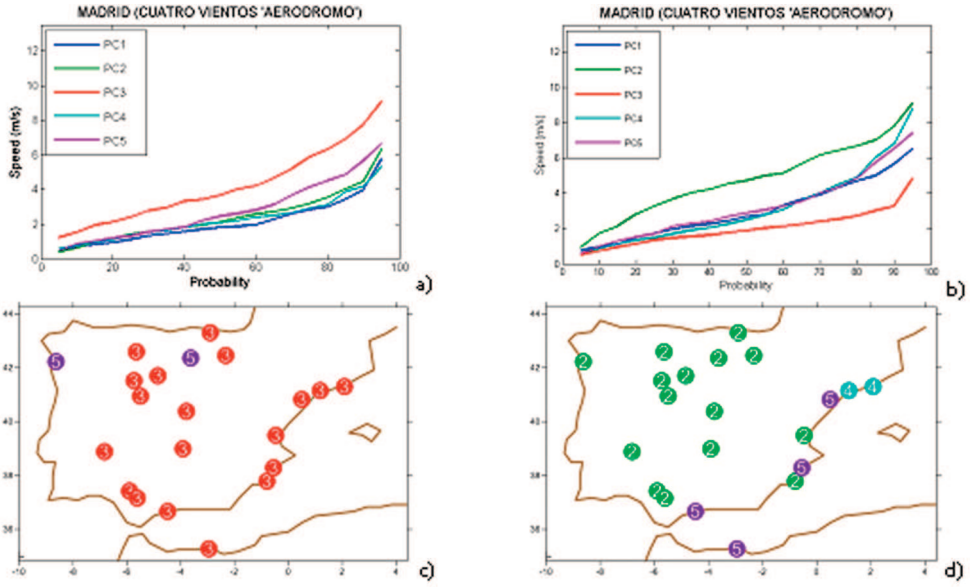

Figure 4. Wind speed cumulated frequencies associated with the strong (a) positive and (b) negative scores of the Z1000 principal components for the Madrid station. Dominant PCs (in numbers) over stations obtained from the higher area values of the wind speed cumulated frequency curves for (c) positive and (d) negative PC scores.

Figures 4c-d display the results of the cumulative probabilities (in terms of the curve area values) for all used stations over Iberia. These maps show the leading PC in the wind speed pattern. Thus, for the high positive scores of the Z1000, higher values of the probability curve areas correspond to the third PC (Figure 4c). As noted above, this dominant mode showed a configuration characterized by intrusions of cold (warm, in its negative phase) air masses over Iberia. On the contrary, Figure 4d shows the results of the dominant PCs associated with the largest area under the probability curves derived from the strong negative scores

of the PCs. As a result, the second PC of Z1000 (Figure 5b) is the leading mode for the negative PC scores (see also Figure 4b). Such PC make it possible to underline the fact that when high positive correlation values are located over western Britain Isles and the negative ones do it over southern Atlantic Ocean, the "Spanish" wind speed principally tends to deploy a homogeneous arrangement except for some stations in the eastern Iberian Peninsula. It can be noted the nearly dominance of the PC5 in most of the Spanish Mediterranean coast stations. This PC5 (Figure 5c) presents, in its positive phase, a spatial pattern similar to the second mode except for the centre of negative anomalies which is located in between two strong nuclei of positive ones. The isolines are longitudinally extended which embodies strong southern (northern, in its negative phase) air advection over Iberia. In its negative phase, this situation resembles an omega blocking situation (Bluestein, 1993). This persistent and particular configuration reflects a blocking pattern named 'Omega block' with a meridionally-oriented high sandwiched in between two lows (Bluestein 1993). At upper level, this kind of configuration can usually be characterised by a stationary ridge standing to the esat of the Atlantic Ocean and by a main trough situated over the western Mediterranean zone which promotes longitudinal incursions of maritime cold air which comes from high latitudes and flows into the Western Mediterranean area after rotating around a cut-off low nearby the Iberian Peninsula. In the region of the blocking, the weather remains essentially unchanged, as any transient weather disturbances are forced to circumvent the block. Once established, major blocking situations tend to persist for at least a week and appear to represent some quasi-equilibrium state of the atmosphere. Therefore, the PC5 configuration presents a isoline-correlation gradient and shows changes in the isoline signs. Such situation promotes advection of southern (northern) air masses over the Spanish Mediterranean coast.

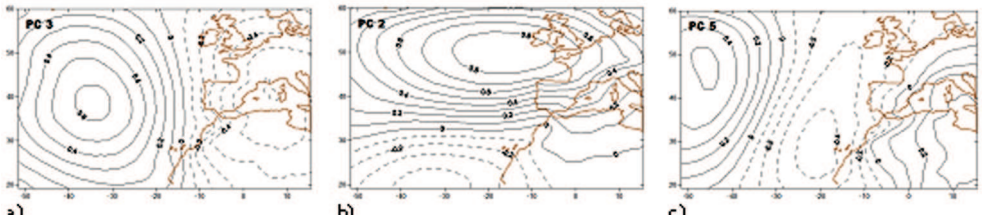

Figure 5: Spatial patterns of the obtained modes corresponding to Z1000: (a) third PC; (b) second PC and (c) fifth PC. The positive (negative) correlations are solid (dashed).

3. EXTREME WIND SPEED AND WIND GUST ESTIMATES

In this section some techniques for estimating and forecasting wind speeds will be reviewed, with special emphasis in extreme winds. The improvement of meteorological forecasts of wind has been progressing by means of dynamic limited area modelling or by ensemble prediction systems, among other methodologies (Hamill *et al.,* 2000; Pinson and Hagedorn, 2012). However, this methodology bears high computational costs. In order to overcome this problem, the constructed analogue method in a framework of temporal prediction can be used (Lorenz, 1969;

Herrera *et al.,* 2011). In this section wind speed and wind gust estimates in Spain, with special emphasis in extreme values, are obtained using the analog methodology applied to the Z1000 data base. To do this, two data sets are additionally considered: the daily MWS data above described, and daily wind gust (WGU) data over Spain, both datasets during all the year distributed in the four seasons: winter (DJF), autumn (SON), spring (MAM) and summer (JJA). The WGU data used in this paper consist of 73 time series of daily gusts in Spain (Figure 1). Taking into account the observational data quality and the methodology employed in this contribution, the three datasets finally cover the common period from 1971 to 2002.

The ANPAF downscaling analog model is used to obtain daily MWS and daily WGU over Spain (Pascual *et al.,* 2012). The idea is based on the comparison between the field of an input variable and the other input variable to determine the greatest similarity between them. Here the Z1000 data are used both as input or historical reference field with which to be compared. Because of the great amount in the freedom degrees of any large-scale atmospheric field it turns out to be necessary to use long datasets, meaning a disadvantage of the methodology. However, if the high number of freedom degrees are considered as associated noise, then the inherent noise in the data can be reduced by a previous smoothing process. Thus, a PCA is previously applied to the Z1000 data base, the obtained PCs being the historical reference field. On the other hand, several distances based on Euclidean distance functions, have been defined and validated. The search of analogue patterns is based on finding a time that minimizes such distances in the PCA space.

Following this procedure, the methodology based on analogies has been applied to the Z1000 field in order to find several analogues to a particular Z1000 input pattern taking into account the above described distances. The ANPAF method used here can be mainly illustrated in the diagram of Figure 6. In this Figure an input field score of the Z1000, $\bar{s}_t$, is compared with the different scores (s_{tk} and s'_{tk}) of the several obtained PCs of the Z1000 field by using the distance functions (d_t and d'_t) in order to find the most similar scores throughout the historic scores time record. The procedure is crossvalidated by finding different analogues for a Z1000 input day and repeating the process for all the historic time record. Finally, a set of Z1000 analogues is obtained with the distance d'_t (Pascual *et al.,* 2012). Once the closest scores have been obtained throughout the time, their corresponding concomitant dates present associated wind and gust data that finally allow us that an estimated winds and gust can be obtained. The estimates can be made by using different criterions: a single analogue, average analogues, neural networks (Zorita and von Storch, 1999; Cofiño, 2004; Gutiérrez *et al.,* 2004). Here, the mean winds and gust obtained from the analog method have been estimated by using arithmetical means of several analogues. The tests cases have been analysed by taking into account both deterministic and probabilistic tools to assess the accuracy and skill of the wind estimates.

From the ANPAF model similar atmospheric situations were isolated and from them, a number of different wind fields (MWS and MGU) subsequently obtained and averaged to characterize and provide both estimated Spanish wind fields. In order to assess the accuracy and skill of the wind estimations these fields have been

analyzed by means of both deterministic and probabilistic tools. Deterministic reault poins to a resonable method skillful in estimating the MWS and the WGU fields in Spain. Concerning some probabilistic tools, rank histograms, reliability curves and skill scores have been used assessing the model skill in estimating wind data. In order to give an idea about the WGU values in Spain, Figure 7 displays the WGU values computed taking into account several thresholds corresponding with the values of the standard deviation, σ, of the original data. For values exceeding 2σ, all stations showed higher wind speeds than 58 kmh^{-1}, which corresponds to strong winds, reaching some stations values greater than 80 kmh^{-1}, which corresponds to very strong winds.

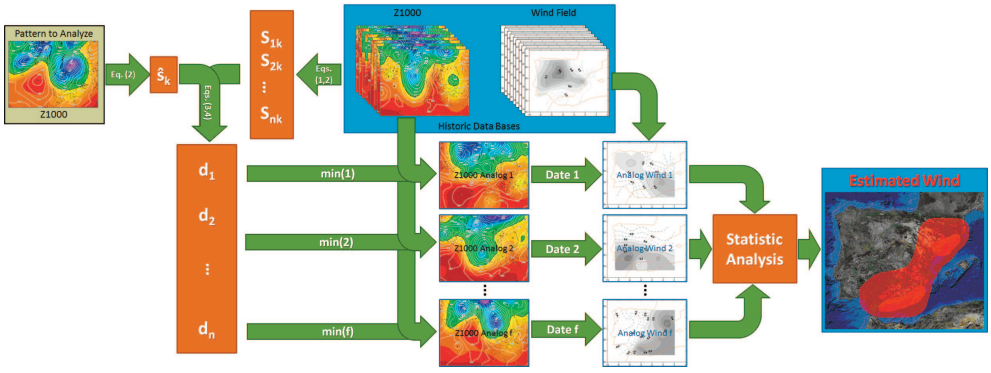

Figure 6. Illustration of the ANPAF analog method.

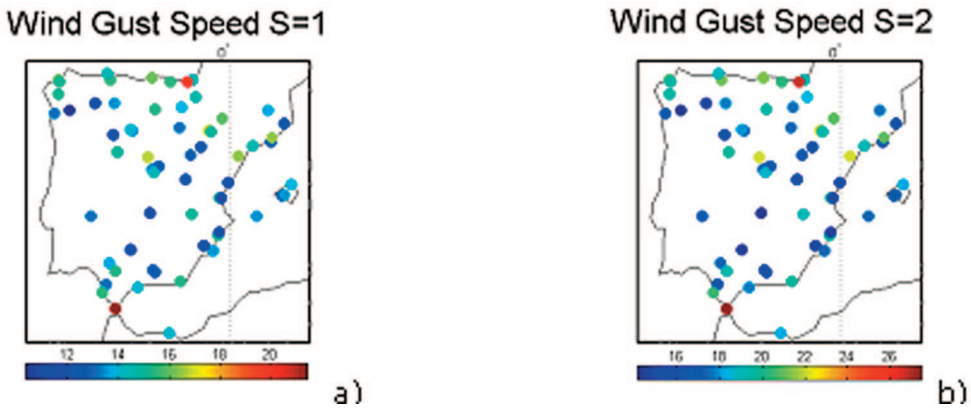

Figue 7. WGU values (ms^{-1}) for different thresholds: (a) σ = 1, (b) σ = 2.

Deterministic results are calculated for both wind variables (Table 1). Biases for MWS and WGU between the averaged wind obtained from the analog method and the observational wind fields present small values. Moreover, the absolute relative biases present values around 1.66% and 1.81% for WGU and MWS, respectively, indicating that the estimated analog wind reproduces pretty well the observed winds. The values point to significant relationships in which the input and the output

data are strongly related. Therefore, the input in the model (Z1000) involves enough information in the output (Z1000) fields, and consequently in the wind. Although the rmse values are in general small, the results of MWS and WGU are not comparable between them because of the different range of variability of each variable. On the other hand, the moderately high values of correlation highlight the relationships between the input and the output fields, thereby emphasizing a degree of skill of the method in estimating the MWS and the WGU at Spain.

	bias	**rmse**	**r**
MWS	-0.10	1,43	0.60
WGU	-0.20	3.01	0.71

Table 1. Spatial averaged bias (ms^{-1}), rmse (ms^{-1}) and correlation obtained from the estimated wind versus the observational data.

From the deterministic point of view, different statistical tools have been used to compare the results of the MWS and the WGU. On the other hand, the probabilistic performance of wind estimates can be evaluated following the difference between a forecast probability distribution and the observed probability distribution. Thus, several probabilistic verification results are also shown in addition to the deterministic verification: rank histograms, reliability curves and skill scores have been used assessing the model skill in estimating wind data.

For the MWS rank histogram (not shown) large spread has been observed, which allows to highlight the presence of several observations located between the extremes of the analog estimates. The MWS Talagrand also shows an asymmetric shape, pointing out some underprediction of the MWS values. The WGU rank histogram has shown flatter distribution than the MSW one, illustrating a general pretty better behaviour. The reliability curves have been computed taking into account several thresholds corresponding with the values of the standard deviation, σ_t of the original data, both MWS and WGU. For all the thresholds (Figure 8) the reliability curves deviate in general from the best line, the model forecast probability being smaller than observed frequency. This situation indicates an underestimation of the observational wind frequencies in both variables. Again, the WGU performance is quite better than the MWS one. It is worth noting the resemblance of the underestimation of the probabilistic values in all reliability diagrams for all thresholds. It points out that the ANPAF model reasonably matches the observational and forecast data.

Additionally, and in accordance with Brier (1950), the Brier Score (BS) and the Brier Skill Score (BSS) are here used and derived with respect to the climatological probability for different thresholds. The BS shows that the goodness of the model performance as measured by this score is very similar to the different thresholds. The BSS proves that the model generates forecasts with better skill than the climatology. The lower the Brier Score the better forecast; so, as much as the BSS tends to the unity, better is the model skill. The BSS is typically defined as the relative probability score compared with the probability score of a reference

forecast. In order to assess the accuracy and skill of all obtained wind estimates from the analogue model, the BSS has been also derived herein for values of the standard deviation of the original data, both MWS and WGU. Thus, not only the model mean skill is analysed, but the estimated tails are also evaluated. The BS of reference, BS_{ref}, used herein corresponds to the climatological value. The BS_{ref} has been obtained using the observational climatological frequencies taking into account such thresholds. The areal averaged BSSs for all selected thresholds show values greater than zero and indicate that the forecasts improve the model. The BSSs for several σs show an asymmetric shape (Figure 9), the best results being associated with the value of $\sigma = 0.5$ in both cases, although the WGU result is better than the MWS one. The analogs obtained from the ANPAF model shows the best results for σ values ranging between 0.5 and 1.5. For extreme values, associated with the BSS ≈ 0.12 for $\sigma \geq 2$, a gust range of 16 - 26 ms^{-1} is recorded, with very strong winds spreading over the Ebro Valley and the Gibraltar Strait ($\approx$ 93 kmh^{-1}). It is worth noting that MWS and WGU extreme values show similar behaviour.

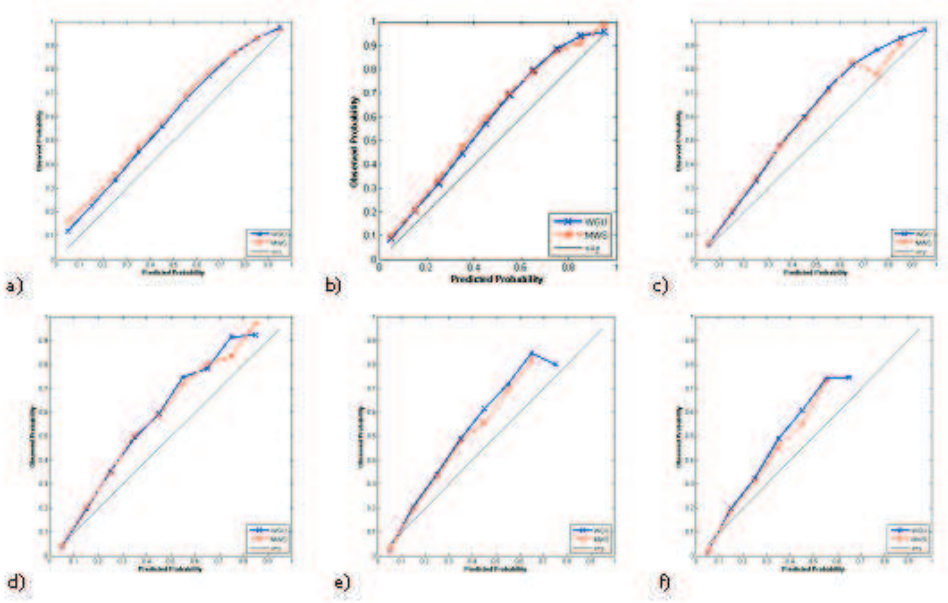

Figure 8. Reliability diagrams of MWS (red dashed line) and WGU (blue continuous line) derived for different thresholds: (a) $\sigma = 0$, (b) $\sigma = 0.5$, (c) $\sigma = 1.0$, (d) $\sigma = 1.5$, (e) $\sigma = 2.0$ and (f) $\sigma = 2.5$.

The BSSs for MWS and WGU are also derived for mean values (Figure 13) and for $\sigma = 0.5$ (not shown) in each Spanish station. The BSS spatial distribution is shown more clearly in the WGU case than in the MWS one for both thresholds, since the WGU database includes more stations than the MWS dataset. The MWS BSS results (Figure 10a) are again worse than the corresponding WGU ones (Figure 10b) in the whole domain. For both thresholds, the BSS spatial distribution presents the

best values (≈ 0.25) over Northern Iberia (Figure 10b), while the rest of stations show small values. It means that the atmospheric situations coming from the Atlantic Ocean are better to predict mean wind and gusts in the Northern Peninsula. It is worth also to note high WGU BSS values located over the Gibraltar Strait and along the Ebro Valley zones, although smaller ones in the MWS case. On the contrary, poorer BSS estimates and thereby poorer prognosis are expected to be mainly located on northern Catalonia for both σ = 0.5 values and for the mean values.

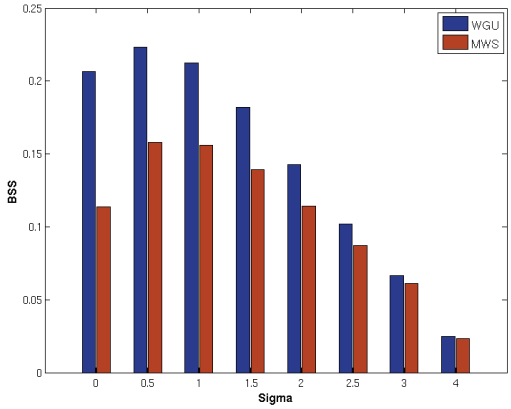

Figure 9. Illustration of BSS values for different values of σ: red bars (MWS) and blue bars (WGU).

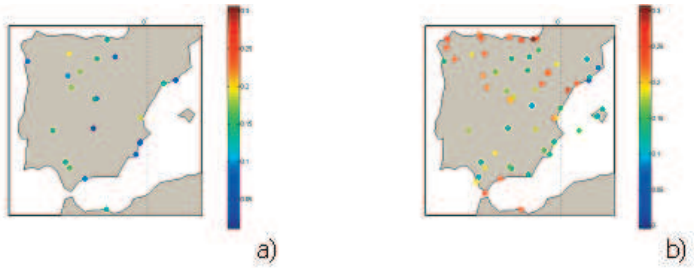

Figure 10. Spatial distributions of BSS for σ = 0 of: (a) MWS and (b) WGU stations shown in Figure 1.

4. CONCLUSIONS

The linkage between observed wind speed in Spain and surface circulation patterns has been examined with special emphasis in extreme winds. The analysis, based on composite maps built from extreme data of PC modes of the large-scale atmospheric field, has shown different mean atmospheric situations associated with wind patterns and with strong gradients of Z1000 are related to moderate to strong wind in Spain.

The analyses have revealed a strong influence of the pressure centers over the Atlantic Ocean in the Spanish wind speed field and also allowed to identify a number

of atmospheric circulation patterns that govern the wind speed variability at Spain. The PCA and the associated analyses based on composites and wind speed cumulated probabilities together with their under curve area values have shown that the atmospheric dynamics in the North Atlantic is responsible for much of the Spanish wind speed variability. The variation of intensity and/or position of pressure centres, within a climate change scenario, could possibly change the relative frequency of the large-scale atmospheric patterns or form new ones, changing the present wind regime.

Additionally, it has been revised the process to estimate wind fields based on finding analogs. The ANPAF model is used to find similar atmospheric patterns, and from them to obtain wind fields. In order to assess the accuracy and skill of the wind estimates these fields have been analyzed by means of both deterministic and probabilistic tools. The significantly close relationships between the input and the output data, and hence with the wind are shown by bias and correlation estimators. Reliability curves indicate some underestimation in the model results of the observational wind frequencies in both variables. The WGU behaviour is quite better than the MWS one, in general. It is worth noting the resemblance of the underestimation of the probabilistic values in all reliability diagrams for all thresholds except for the small probabilistic values for $\sigma \geq 1$ (gusts greater than 80 kmh^{-1}, which corresponds to very strong winds). For extreme wind values MWS and WGU show similar behaviour, and gusts of up to 26 ms^{-1} are recorded corresponding to BSS $\approx$ 0.12 for $\sigma \geq 2$. It is noticeable very strong winds over the Ebro Valley and the Gibraltar Strait ($\approx$ 93 kmh^{-1}). Moreover, the BSSs for MWS and WGU are also derived for mean values in each Spanish station, the MWS BSS results being again worse than the corresponding WGU ones in Spain. The BSS spatial distribution presents the best values (» 0.25) over the northern area, emphasizing that the atmospheric situations coming from the Atlantic Ocean are better to predict mean wind and gusts in the Northern Peninsula.

It may be concluded that the process to find analogs and the subsequent application of the ANPAF analog model has been revealed as a good technique to find similar atmospheric patterns, and from them to estimate wind fields.

ACKNOWLEDGEMENTS

This work has been partially supported by the research projects AYA2011-29967-C05-02, UE Safewind G.A. No. 21374, VA025A10-2 and CGL2011-25327. The authors wish to thank the Spanish Meteorological Agency (AEMET: Agencia Estatal de Meteorología) for providing the Spanish wind datasets and the European Centre for Weather Medium Forecast (ECWMF) for providing the ERA40 data.

REFERENCES

Barredo, J. I. (2010): No upward trend in normalised windstorm losses in Europe: 1970–2008. *Natural Hazards of Earth System Sciences*, 10, 97–104.

Bluestein HB. (1993). Synoptic Dynamic Meteorology in Midlatitudes (II). Observations and Theory of Weather Systems. Oxford University Press, 594 pp.

Brier, G.W. (1950). Verification of forecasts expressed in terms of probabilities. *Monthly Weather Review* , 78, 1-3.

Cofiño, A. S. (2004). Técnicas estadisticas y neuronales de agrupamiento adaptativo para la predicción probabilística de fenómenos meteorológicos locales. Aplicación en el corto plazo y en la predicción estacional. Tesis doctoral, Universidad de Cantabria.

Gutiérrez, J. M., Cano, R. Cofiño, A.S., Rodríguez, M.A. (2004). Clustering methods for statistical downscaling in short-range weather forecast. *Monthly Weather Review*, 132, 2169-2183.

Hamill, T., Snyder, C., Morss, R. (2000). A comparison of probabilistic forecasts from bred, singular-vector, and perturbed observation ensembles. *Monthly Weather Review*, 128, 1835-1851.

Herrera, S., Pazo, S., J. Fernández, Rodríguez, MA. (2011). The role of large-scale spatial patterns in the chaotic amplification of perturbations in a Lorenz'96 model. *Tellus* A, 63, 978-990.

Lorenz, E. N. (1969). Atmospheric predictability as revealed by naturally accourring analogues. *Journal of Atmospheric Science*, 26, 636-646.

Malmquist, D. L. (1999). European Windstorms and the North Atlantic Oscillation: Impacts, Characteristics, and Predictability – A Position Paper based on the proceedings of the Risk Prediction Initiative. Workshop on European Winter Storms and the North Atlantic Oscillation, Risk Prediction Initiative, Hamilton, Bermuda, RPI Series No. 2, 21 pp.

Martín M.L., Valero F., Morata A., Luna M.Y., Pascual Á., Santos-Muñoz D. (2011a). Springtime coupled modes of regional wind in the Iberian Peninsula and large-scale variability patterns. *International Journal of Climatology*, 31, 880-895.

Martín M. L., Valero F., Pascual Á., Morata A., and Luna M. Y. (2011b). Springtime connections between the large-scale sea level pressure field and gust wind speed over Iberia. *Natural Hazards of Earth System Sciences*, 11, 191-203.

Morata A., Martín ML, Sotillo M, Valero F, Luna MY. (2008). Iberian autumn precipitation characterization through observed, simulated and reanalysed data. *Advances of Geosciences,* 16, 49-54. www.adv-geosci.net/16/49/2008/.

Munich Re (2008): *Special feature issue – Risk factor of air*. Munich Re, Munich, Losses and loss prevention, 1/2008, 57 pp.

Pascual, A., Valero, F., Martín, M.L., Morata, A., Luna, M.Y. (2012). Probabilistic and deterministic results of the ANPAF analog model for Spanish wind field estimations. *Atmospheric Research*, 108, 39-56.

Pascual, A., Martín, M.L., Valero, F., Luna, M.Y., Morata, A., (2013). Wintertime connections between extreme wind patterns in Spain and large-scale geopotential height field. *Atmospheric Research*, 122, 213–228.

Pinson, P., Hagedorn, R. 2012. Verification of the ECMWF ensemble forecasts of wind speed against observations. Meteorological Applications, Published online in Wiley Online Library (wileyonlinelibrary.com) DOI: 10.1002/met.1339.

Preisendorfer RW. (1998). Principal Component Analysis in Meteorology and Oceanography. Elsevier Science Publishers BV: Amsterdam, 425 pp.

Schwierz C, Köllner-Heck, P., Zenklusen, E., Bresch, D.N., Vidale, P-L., Wild, M., Schär, C. (2010). Modelling European winter wind storm losses in current and future climate. *Climatic Change*, 101, 485–514.

Swiss_Re (2000): http://www.swissre.com/about_us/art_architecture/Swiss_Re_Next.html.

Valero F, Luna MY, Martín ML, Morata A, González-Rouco F. (2004). Coupled modes of large-scale climatic variables and regional precipitation in the Western Mediterranean in autumn. *Climate Dynamics*, 22, 307-323.

Valero F, Martín ML, Sotillo MG, Morata A, Luna MY. (2009). Characterization of the autumn Iberian precipitation from long-term data sets: comparison between observed and hindcasted data. *International Journal of Climatology*, 29, 527-541.

Zorita, E.Y., von Storch, H. (1999). The analog method as a simple statistical downscaling technique: Comparison with more complicated methods. *Journal of Climate*, 12, 2474-2489.

CHAPTER 7

METEOROLOGICAL RISK FACTORS AND TORRENTIAL PRECIPITATION IN THE SPANISH MEDITERRANEAN COAST

María José ESTRELA NAVARRO[1], Francisco PASTOR GUZMÁN[2],
Igor GÓMEZ DOMÉNECH[2]

[1.] *Laboratorio de Meteorología-Climatología, Unidad Mixta CEAM-UVEG, Facultad de Geografía, Universitat de Valencia, Valencia, España*
[2.] *Laboratorio de Meteorología-Climatología, Unidad Mixta CEAM-UVEG, Fundación Centro de Estudios Ambientales del Mediterráneo, Paterna, Valencia, España*
maria.jose.estrela@uv.es, paco@ceam.es, igodo1978@yahoo.es

ABSTRACT

Torrential rains are a significant phenomenon on the Mediterranean coast of the Iberian Peninsula, and specifically in the Valencia Region; having relevant effects on the territory, the population, and human activity in general. A sound analysis of the factors conducive to these precipitation events is thus essential for a better design of prediction mechanisms which, although not capable of preventing these phenomena, help in palliating their catastrophic consequences. This work aims at examining the factors involved in the genesis of intense precipitation in the Valencia Region through the analysis of spatial distribution, atmospheric configuration, and sea surface temperature (SST), the key factor in the development of these intense rain events.

Key words: torrential precipitation, sea surface temperature, meteorological risk, meteorological model, orography.

1. INTRODUCTION

The morphology of the western Mediterranean is that of a semi-enclosed basin in which a central sea is almost completely surrounded by coastal mountain ranges. This morphology results in very specific meteorological phenomena. The key feature of the prevailing Mediterranean climate, especially during the summer, is the presence of internal atmospheric circulations connected to coastal breezes which, at the regional level, favour recirculation or nearly enclosed circulation of the Mediterranean air mass.

One of the most significant results of this process is the irregular and often torrential precipitation regime. Dry periods may easily be followed by catastrophic floods or fairly regular humid cycles. In general, annual precipitation regimes comprise a relatively dry winter, a generally humid spring, a very dry summer with isolated, irregular and dispersed rainstorms, and a humid autumn with a high probability of localised torrential precipitation resulting in floods or in the overflowing of water courses (Jansá Guardiola, 1966).

Precipitation regimes in different areas of the western Mediterranean, although part of the same rainfall framework, have very different origins and must be distinguished in terms of their atmospheric triggers. In contrast to Atlantic continental Europe, affected by the general atmospheric circulation and characterised by the successive arrival of areas of low pressure from the west, the Mediterranean basin shows unique meso-meteorological processes resulting in a variety of specific precipitation regimes. With this particularity in mind, the analysis of rainfall regimes must be studies not only on the basis of periodicity and quantity, but also of meteorological causes. In the specific case of the Valencia region (Figure 1A), four key meteorological events must be considered (Millán *et al.* 2005):

a) Advections from the west: transit of areas of low pressure and cloud fronts from the Atlantic. These often result in weak or moderate precipitation.

b) Continental advections: long distance motion of an air mass over the European continent. These normally result in dry conditions with little or no precipitation.

c) Convective events: lack of well-defined pressure systems in combination with, but not necessarily or exclusively, high altitude stability. This possibility includes western Mediterranean basin internal circulation and the formation of coastal breezes.

d) Marine advections: long distance motion of an air mass along the Mediterranean. These often result in torrential precipitation in the coastal areas.

The last two synoptic sets are the most typically Mediterranean and are associated with characteristically western Mediterranean phenomena. This work will fundamentally focus on the characterisation and analysis of a specific kind of precipitation: torrential rains caused by marine advections. In some cases, mesoscale convective systems can also be the cause of intense precipitation in the western Mediterranean. These will not be considered here, however, because no convective event causing precipitations of over 125 mm in six or more of the observatories under consideration has been recorded to date, as is the case with the other 31 events examined in this paper. It is therefore unexceptional for most of the hydrological resources available in the region of Valencia to be of a torrential origin.

Torrential precipitation is one of the most significant climatic features in the region of Valencia, and represents one of the most relevant natural risks in the area.

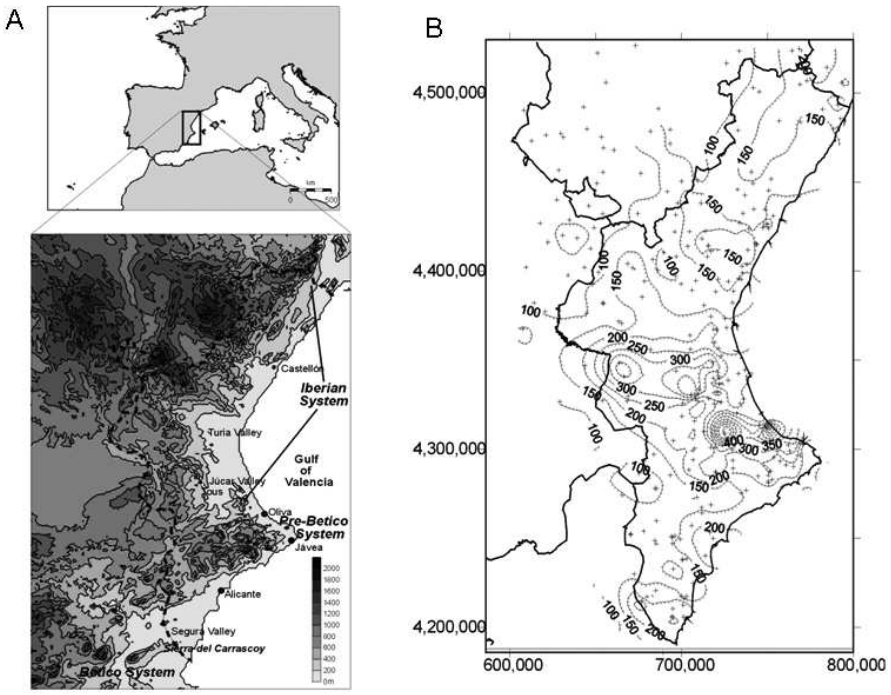

Figure 1. A: Location of the Valencia region in Europe and orography. B: Map of absolute daily maximum precipitation values (mm). Period 1971-2000.

The damage caused by this phenomenon is considerable and recurrent, mostly occurring through the overflow of the main watercourses and the flooding of the associated alluvial plains and through the sudden deluging of Mediterranean *ramblas*, which are completely dry during most of the year as a consequence of the prevailing semi-arid conditions. These situations are exacerbated by the intensive occupation of high inundation risk areas.

Precipitation in the region tends to concentrate around a specific time of the year, and it is therefore not strange that, given the torrential nature of said precipitation, most of the annual totals are recorded over a reduced number of days (for example, the 817 mm collected in the observatory of Oliva over a period of 24 hours, in 1987, against an annual total of 1325 mm) (Elías, 1979). Similarly the spatial distribution of this precipitation is not homogeneous. It is well known that torrential precipitation has a markedly coastal distribution and is directly connected with orography and the presence of mountain ranges near the coast.

The aim of this work is to show the factors, mechanisms and scenarios at play in the torrential precipitation that occurs on the eastern coast of the Iberian Peninsula (Valencia region), examining the spatial distribution, the atmospheric conditions and the SST, the key factor in the development of these phenomena. The paper ends with the analysis of the role played by orography in these events.

2. SPATIAL DISTRIBUTION OF INTENSE PRECIPITATIONS

The analysis has taken into account events of intense precipitation (threshold of 125 mm or more in a single day) occurring between 1971 and 2000 (Estrela *et al.,* 2002). For a given event to be labelled as significant in the analysis this minimum must have been recorded in at least six observatories; otherwise, the high precipitation level is regarded as strictly local, and its causes as different from the typically Mediterranean cyclogenetic phenomena which concern us here.

The examination of the daily data series collected by AEMET observatories in the Valencia region and nearby regions (497 observatories in total) has yielded a total of 899 cases of precipitation above the threshold, clustered in 177 days.

A map with the absolute maximum precipitations for one-day periods is shown in Figure 1 B. The maximum in the north is 313 mm, and in the south it is 316 mm. The humid central region includes several zones above the 300 mm threshold, including two local maximums of 790 mm and 817 mm. This zone shows high levels of torrentiality, and is in fact one of the areas with the highest incidence of torrential rainfall patterns in the whole of the western Mediterranean; other than Valencia, the 800 mm threshold is only reached in Liguria (Guigo, 1973, cit. en Pérez Cueva *et al.*, 1983), where the 900 mm threshold was broken in Bolzaneta, near Genoa. The 817 mm entry was recorded in November 3rd 1987 in Oliva (southern coast of the Gulf of Valencia), and is not an isolated case: in October 2nd 1957, 878 mm were recorded in Jávea. Within our target period, 24 entries over 350 mm and 80 over 250 mm have been attested.

It can therefore be easily appreciated that the distribution of intense precipitation is far from homogeneous in the territory of Valencia, and that the most significant feature is the existence of an area showing extreme levels of torrential nature of rainfall in the southern shore of the Gulf of Valencia. This area shows the highest torrentiality rate for 24h periods for the whole of the Iberian Peninsula (Elías Castillo *et al.*, 1979), with recurrence levels of over 300 mm for a return period of 30 years (Gumbel method for the calculation of probable maximums). The northern and southern sectors also show relatively high torrential nature of rainfall rates, with recurrence levels of around 175 mm for the same return period.

The high torrential nature of rainfall in these areas may be connected, among other elements, with orographic factors: the disposition of mountain ranges, such as the easternmost ridges of the Prebético System, the mountain ranges (SSW-NNE) across the northern region of the Valencia region and the eastern most ranges of the Bético System (Sierra de la Carrasca), favour the ascent of humid fluxes in the east-northeast.

The most intense precipitation events here analysed are connected with Mediterranean cyclogenetic phenomena on the eastern coast. Incidentally, these events are the main source of hydric resources in all areas under consideration. The localised nature of these precipitations is strongly conditioned by orography, particularly basins and valleys open to the NE. They also show a heavy tendency to be stronger on the coastline, becoming progressively weaker as they advance

inland. They are particularly significant in the humid zone covering the south of the province of Valencia and the north of the province of Alicante, and in the arid region in the far south of the Valencia region. Often, in these cases – particularly in the latter –torrential precipitation is the only source of hydric resources.

3. ATMOSPHERIC CIRCULATION AND INTENSE PRECIPITATIONS

The most common synoptic surface condition associated with intense precipitation is the presence of a high pressure zone over Central Europe, pushing a long-distance air flow upon the Mediterranean. Along with this major action focus we may find two variables: most frequently, the presence of a system of low pressure in northern Africa/the south-western Mediterranean; or, the formation of a zone of intense low pressure over the Canaries/Gulf of Cadiz, associated with a high altitude pocket of cold air or cold dro Figure 2 shows these two synoptic surface settings.

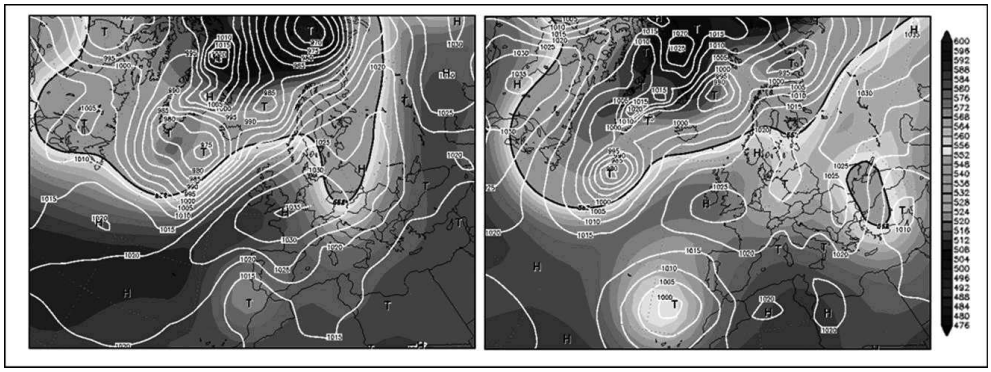

Figure 2. Surface synoptical situations relating to torrential rains in the Valencia region. October 1994 event (left) and November 1987 event (right).
Source: Reanalysis NCEP (Wetterzentrale).

In order for west-bound surface advections to occur, the normal atmospheric pressure distribution patterns in northern Hemisphere medium latitudes must be inverted; this pattern normally features low pressure to the north of the subtropical anticyclonic centres (Azores High). Therefore, the formation of high pressure areas over the north of the Iberian Peninsula and low pressures over the south is always connected with conditions that alter the normal circulation pattern. This results in the formation of large oscillations of local fluxes in high tropospheric regions (N-S circulations) and the division of jet streams in the higher levels of the troposphere.

Particularly intense precipitation in the Valencia region is associated with conditions of low zonal index (also called blocks). Blocks are so-called because they are pressure distribution patterns which remain relatively static for several days; this sharply contrasts with conditions of high zonal index, in which short oscillations

progress rapidly along the general zonal flow.

Following Bluestein (1993) the cyclonic end of oscillations in blocks is related to significant cyclogenetic processes and, for example in the Mediterranean basin, to extreme meteorological phenomena. These circulation systems are gigantic N-S energy and heat exchange mechanisms which transform potential energy associated with temperature gradients into kinetic energy, and thus play a relevant role in the redistribution of heat between mid and high latitudes worldwide (Bluestein, 1993). This sort of circulation pattern is not only responsible for Mediterranean cyclogeneses but also causes the sort of circulation resulting in extreme cold waves through the irruption of continental Arctic air masses, pushed by Siberian high pressures, and central Mediterranean depressions.

The high altitude settings in association with intense precipitation in the Valencia region can be divided into four groups:

1. Displacement of blocks.
2. Oscillation of zonal flow.
3. Inverted displacement in high altitude.
4. Weak high altitude circulation.

From the seasonal point of view, the synoptic analysis shows a certain gradation of high altitude conditions between autumn and winter. In this regard, in late summer and early autumn the events pertaining to the fourth group are particularly frequent; weak circulation at high altitude notably increases the relative significance of sea temperature and, therefore, of the contrast between SST and the temperature of air masses in interaction with it. As autumn progresses the other three groups become more likely, although we believe that inverted displacement in high altitude requires the irruption of cold air masses, more frequent in late autumn and winter (Estrela *et al.,* 2002).

4. SEA SURFACE TEMPERATURE AND ITS RELATIONSHIP WITH INTENSE PRECIPITATION

As previously stated, the advection of west-bound cold air masses upon the Mediterranean, pushed by a high pressure system over Central Europe, is one of the most significant factors in the genesis of intense precipitation phenomena in the Valencia region. This is due to the possible conditions of instability resulting from the interaction of the cold air mass with the warmer sea. This largely rests on the thermic difference and the exchange of heat between the cold air mass and the warm water mass, which is the determining factor regarding the amount of humidity that the air mass is capable of absorbing. In this regard, the sea temperature is the key factor. A second step is the displacement of the air mass towards the west, where the raised orography may trigger precipitation.

In order to evaluate the role played by the SST, 32 intense precipitation events were examined on the basis of satellite images provided by NOAA. These were processed with an algorithm developed by Bádenas *et al*. (1997), capable of calculating the

SST with an error margin of under 0.5ºC. Our methodology involved the analysis of the SST of several days before and after the event for the detection of changes in sea temperature. The analysis of images and of air mass trajectories indicated that sea temperature dropped by between 3 and 5º C after torrential precipitation events. We may assume that these drops in the SST were due to heat and humidity exchange phenomena between the atmosphere and the sea resulting in a change of the characteristics of the air mass (cooling through evaporation) during its trajectory through the Mediterranean (Estrela *et al.,* 2002), and also due to precipitation over the sea. This therefore suggested that the sea could act as a source of humidity and energy, facilitating the recharge and destabilisation of the air mass through the exchange of humidity, latent heat, and sensible heat. Although the decrease in the SST could be partially due to precipitation over the sea, the drop detected in areas where no precipitation had been observed reinforces the hypothesis that the temperature drop is mostly due to the transfer of heat between the sea and the air mass upon it. Other authors have already suggested a relationship between the SST and intense precipitations in the east of the Iberian Peninsula (Barbero, 2004), or have described some of the factors conducive to intense precipitation in the Valencia region (Riesco and Alcover, 2001); for example, the difference between the SST and the air mass at 850 hPa (Riesco *et al.,* 2003).

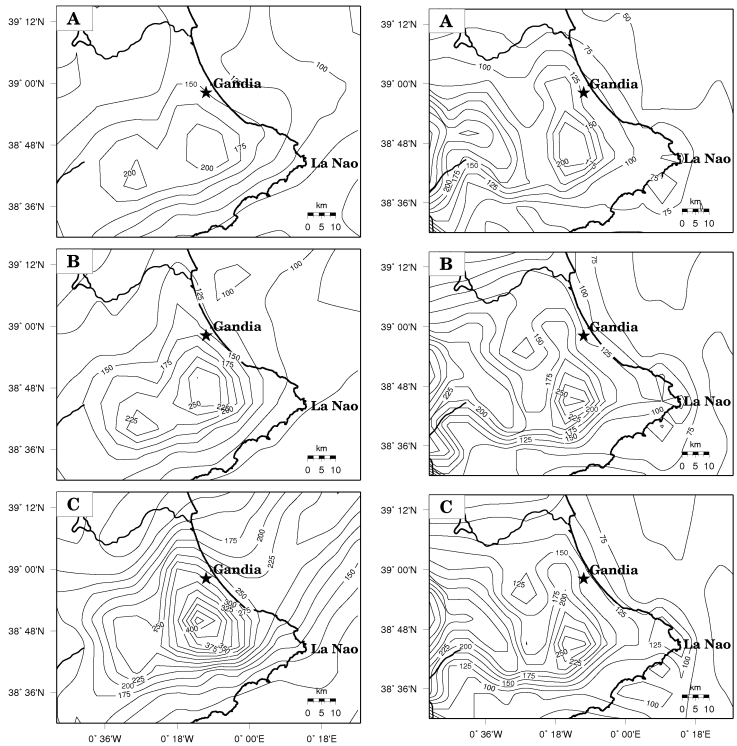

Figure 3. Total precipitation calculated by RAMS for the September 1989 event (left) and September-October 1986 event (right): (a) control, (b) ISLSCP- International Satellite Land Surface Climatology Project (monthly climatic averages of SST), and (c) satellite simulations (NOAA).

On the other hand, the numeric modelling of torrential precipitation events in the Valencia region has shown the enormous influence of SST on these events and has permitted the identification of areas in the western Mediterranean that act as sources of humidity (Duffourg *et al.,* 2011) and instability for the air mass running along it, resulting in torrential precipitation in the Valencia region (Pastor *et al.,* 2001; Fernández *et al.,* 1995, 1997; Pastor, 2012).

This section includes the results obtained from the application of the RAMS (Regional Atmospheric Modelling System) model to two episodes of intense precipitation (September 1986 and September 1989). The results have confirmed the crucial role played by SST on the development of these events (Figure 3). In fact, concordance between modelled results and recorded data – both regarding maximum precipitation and spatial distribution – was higher when the SST data used were those provided by NOAA satellite and referring to the days prior to the events, which were closer to the real data. On the other hand, the results of the simulation using SST monthly climatological averages were far less precise, again both regarding distribution and maximum precipitation. However, the total amount of rainfall calculated through the application of the RAMS model, which also incorporated data from the days of the events, was still less precise than direct observation in the observatories (Figure 3).

Another conclusion resulting from the modelling of these events is that, despite the good results obtained regarding spatial distribution, a bias towards the focalisation of precipitation into the mountain ranges has been observed. We suggest that this could be due to an excessive impact of the orographic factor on the model in its current configuration, overstressing the role played by the orographic triggers. In the area under study there are several mountain ranges between 400 and 700 m.a.s.l. near the coast. Some, less than 15 km from the coast, rise by as much as 1500 m. They must therefore be taken into account for their effect on the vertical displacement of humid air masses reaching to the coast.

5. THE OROGRAPHY AND ITS IMPACT ON INTENSE PRECIPITATION

The effect of orography in heavy rains episodes in the western Mediterranean basin, has previously been investigated in several studies by Romero *et al*. (1997), Horvath *et al*. (2006), Federico *et al*. (2008), and Miglietta and Regano (2008). In order to evaluate the role of orography in the Valencia Region, a numerical modeling of one of the latest heavy rainfall events was carried out using the RAMS model. This event took place on 11th and 12th 2007 (Pastor *et al.,* 2010) and caused huge economic losses, damage to infrastructure and human casualties. Two different simulations of the event were performed to assess the impact of orography in the development of the precipitation pattern. The first is the control run, where the orography is maintained for all simulation domains, while in the second one, this parameter is removed within the area where the highest precipitation values were recorded.

The results of this work allowed to highlight the importance of orography as a triggering mechanism. . Figure 4a shows a vertical motion in the first orographic barrier near the coast at 00 UTC on October 12th. 6 hours later, RAMS reproduces a stronger upward motion above the first significant elevations (located at about

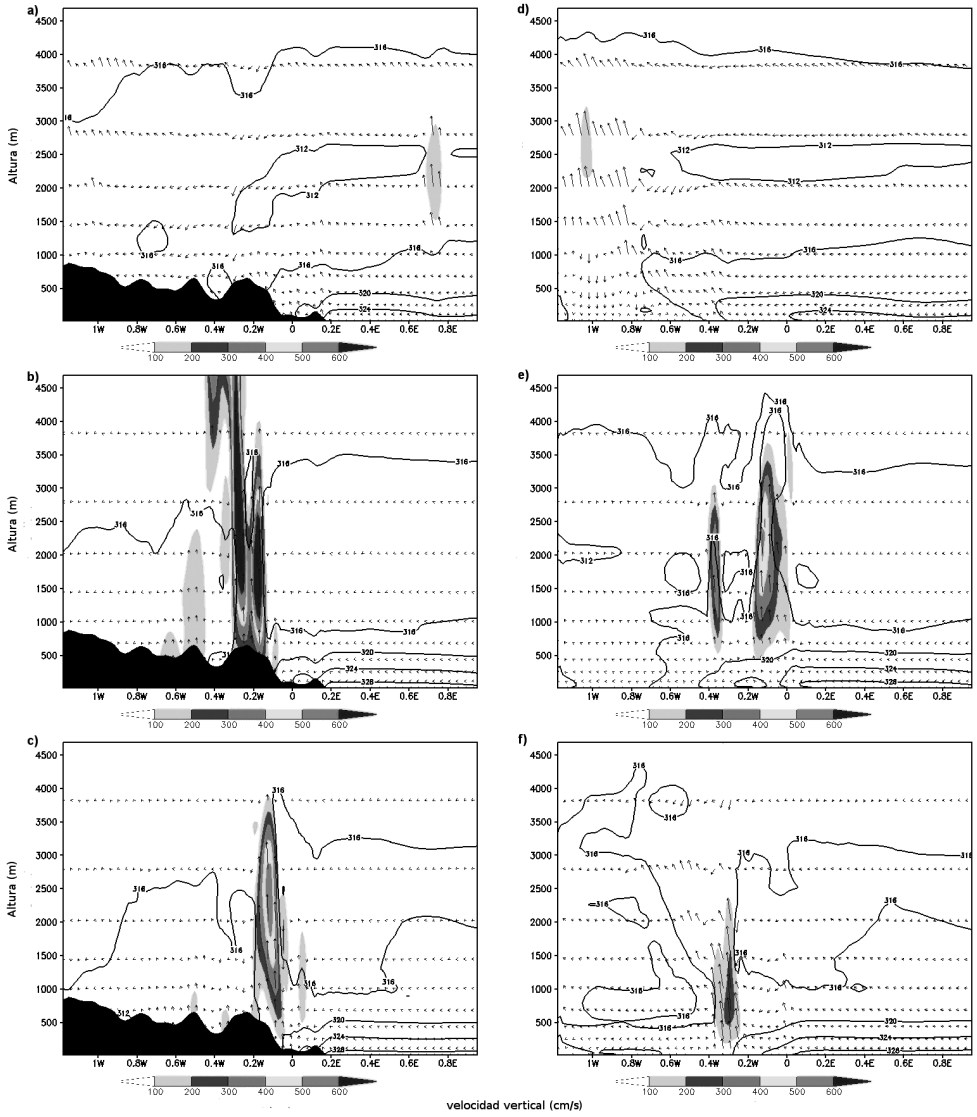

Figure 4. Vertical cross section at 38.8º N RAMS equivalent potential temperature (K), vertical velocity (cm/s) and wind vector for CTRL simulation on: (a) 00:00 UTC 12 October, (b) 06:00 UTC 12 October and (c) 12:00 UTC 12 October 2007, and simulation without orography at (d) 00:00 UTC 12 October, (e) 06:00 UTC 12 October and (f) 12:00 UTC 12 October 2007.

700 m). This circulation is related to orographic triggering. We see that at 12 UTC on October 12th still holds this updraft, although with a decreased intensity. In the same Figure, it is also shown how the persistence of the advection of moist air from

the sea in addition to the vertical motion observed, favors the onset and persistence of heavy rains over this area. When orography is removed from the simulation, we can see that the updraft at 06 UTC is located just above the rain area (Figure 4e).

This vertical motion is clearly weaker than that in the control run and remains slightly displaced eastward. At 12 UTC on October 12th, the vertical velocity decreases and continues below the values estimated in the control run.

6. CONCLUSIONS

The conclusions that we may extract from this study are several. The spatial analysis of the 31 intense precipitation events (occurring between 1971 and 2000) confirms that the Gulf of Valencia is the area in which intense precipitation events occur most frequently within the Valencia region, and is one of the most prone to this sort of phenomenon in the western Mediterranean basin. Additionally, the easternmost tip of the Pre-betico system (north of the province of Alicante and south of the province of Valencia) also features as one of the main focus for intense precipitation, mostly due to topographic factors (optimum exposition and raising orography) and to oriented moisture fluxes.

Intense precipitation events can be easily identified synoptically. In the occurrence of these events the typical surface pattern includes a strong high pressure system over Europe and either a system of relative low pressures in northern Africa or a secondary depression over the Gulf of Cadiz-Canaries. In high tropospheric levels, however, the situation can be much more variable and must not be regarded as a necessary causal factor. Thus, situations in which high tropospheric conditions have no effect may occur, while on other occasions they may exercise a strong influence (for example, in the sort of event known as a 'cold drop'). The effect of these configurations, on the other hand, varies depending on the season. In fact, the most significant factor in the generation of intense precipitation is not the strength of high altitude circulation, but SST and the thermic contrasts between this and west-bound air masses.

Regarding the relationship between the temperature of the Mediterranean sea and the generation of intense precipitation, we must stress the high concentration of events in late summer and autumn, when two basic factors for the genesis of this sort of event often appear in combination:

- Displacement of high pressure systems to Central Europe resulting in strong west-bound advections;
- Comparatively high SST with regard to yearly averages (resulting in a sharp contrast with the temperature of the air masses travelling throughout the Mediterranean).

Even regarding essentially coastal precipitation, a progression throughout the autumn-winter season can be appreciated. Thus, coastal precipitation is more common in early autumn, when the thermic contrast is particularly sharp and the advection is almost guaranteed even without the altitude factor. As the autumn progresses, the chances of high altitude troughs grow, causing an increase in pre-coastal and interior precipitations.

The trajectories associated with torrential precipitation events always traverse those areas with a higher SST for that time of the year in the western Mediterranean (Algerian coast, Balearic and Tyrrhenian Seas, and the Gulf of Tunis).

Previous results, especially those referring to the key role played by SST in the occurrence of intense precipitation events, have been confirmed by the simulations resulting from the application of the RAMS model. A higher correspondence between the simulation and real observed data – both regarding maximum precipitation and spatial distribution – was achieved when the data referring to SST on the days prior to the events from the NOAA satellite images were used. In addition, the numerical modelling has helped to identify those areas which contribute the most to the humidity input conducive to the destabilisation of the air masses running across the Mediterranean. Regarding the Valencia region, these areas are in the southern half of the western Mediterranean, especially the area between the Valencian coast and the Balearic Islands.

Sensitivity tests carried out with the RAMS model have allowed us to investigate the influence of orography on the triggering and development of intense precipitation.

The simulation has shown how orography favours the important ascent of air masses near to the coast and to areas of intense precipitation. This vertical motion is considerably reduced in the simulation when the orographic factor is removed. Additionally, the suppression of this factor also results in the displacement of intense precipitation areas towards the east. In terms of accumulated precipitation, the removing of orographic factors also causes the model to fail to reproduce some areas of intense precipitation which are otherwise generated. Moreover, the bulk of the precipitation is displaced towards the interior of the Valencia region.

The results have clearly shown that orography is a key factor in the development and distribution of intense precipitation events, acting as a triggering mechanism for the convection process.

REFERENCES

Bádenas, C., Caselles, V., Estrela, M. J., and Marchuet, R., 1997. Some improvements on the processes to obtain accurate maps of sea surface temperature from AVHRR raw data transmitted in real time. Part. 1. HRPT images. *International Journal of Remote Sensing*, 18, 1743-1767.

Barbero, J., Muñoz, J. y Rodrigo, F., (2004). Estudio sobre la relación entre precipitaciones mensuales en el levante español y temperaturas de la superficie del mar en el mediterráneo occidental. En El Clima, entre el Mar y la Montaña (editado por J. García, C. Diego, P. Fernández, C. Garmendia y D. Rasilla), Serie A, n 4, 205–212. *Asociación Española de Climatología*.

Bluestein, H.B., (1993): Synoptic-Dynamic Meteorology in Midlatitudes. Volume II: Observations and theory of weather systems. *Oxford University Press*. 594 pp.

Elías, F. y Ruiz, L., 1979. Precipitaciones Máximas en España. ICONA.

Estrela, M. J., Millán, M. M., Peñarrocha, D., and Pastor, F., 2002. De la gota fría al frente de retroceso. Las precipitaciones intensas en la Comunidad Valenciana. Colección Interciencias, 17. Centro Francisco Tomás y Valiente-Fundación Centro de Estudios Ambientales del Mediterráneo - CEAM. Valencia, España, 260 pp.

Estrela, M. J., Pastor, F., and Millán, M. M., 2002. Air mass change along trajectories in the western Mediterranean basin in the torrential rains events in the Valencia Region. In: Proceedings of the 4th EGS Pinius Conference held at Mallorca, Spain. October.

Duffourg, F. and Ducrocq, V. (2011) Origin of the moisture feeding the Heavy Precipitating Systems over Southeastern France, *Natural Hazards and Earth System Science,* 11 (4), 1163-1178

Federico, S., Avolio, E., Bellecci, C., Lavagnini, A., Colacino, M., y Walko, R. L., 2008. Numerical analysis of an intense rainstorm occurred in southern Italy, *Natural Hazards and Earth System Sciences* 8, 19–35, doi:10.5194/nhess-8-19-2008.

Fernández, C., Gaertner, M., Gallardo, C. y Castro, M. Simulation of a long-lived meso-β scale convective system over the mediterranean coast of Spain. Part i: Numerical predictability. Meteorology and Atmospheric Physics, 56, 157–179, 1995.

Fernández, C., Gaertner, M., Gallardo, C. y Castro (1997). M. Simulation of a long-lived meso-β scale convective system over the mediterranean coast of Spain. Part ii: Sensitivity to external forcings. *Meteorology and Atmospheric Physics*, 62, 179–200, 1997.

Guigo, M., (1973): Pluie et crue des 7 et 8 octubre 1970 dans la region genoise, *Mediterranée*, 1, 55-80.

Horvath, K., Fita, L., Romero, R., Ivancan-Picek, B. and Stiperski, I. (2006). Cyclogenesis in the lee of the Atlas Mountains. A factor separation numerical study, *Advances in Geosciences* 7, 327–331, doi:10.5194/adgeo-7-327-2006.

Miglietta, M. M. y Regano, A., (2008): An observational and numerical study of a flash-flood event over south-eastern Italy, *Natural Hazards and Earth Systems Sciences* 8, 1417–1430, doi:10.5194/nhess-8-1417-2008.

Millán, M. M., Estrela, M. J., and Miró, J. (2005). Rainfall components: variability and spatial distribution in a mediterranean area (Valencia region). *Journal of Climate*, 18: 2682-2705.

Pastor, F., Estrela, M. J., Peñarrocha, D., and Millán, M. M. (2001). Torrential rains on the Spanish Mediterranean Coast: Modeling the effects of the sea surface temperature. Journal of Applied Meteorology, 40: 1180-1195.

Pastor, F. (2012). Ciclogénesis intensas en la cuenca occidental del Mediterráneo y temperatura superficial del mar: Modelización y evaluación de las áreas de recarga. Tesis doctoral.

Pérez Cueva, A., Armengot, R. (1983): El temporal de octubre de 1982. En La riada del Júcar (Octubre 1982). Cuadernos de Geografía, 61-86. Universitat de València.

Riesco, J., Alcover, V. (2001). Algunas consideraciones sobre lluvias intensas en el mediterráneo occidental: Revisión de un episodio en la comunidad valenciana. En V Simposio Nacional de Predicción.

Riesco, J., Alcover, V. (2003). Predicción de precipitaciones intensas de origen marítimo mediterráneo en la Comunidad Valenciana y Región de Murcia. Ministerio de Medio Ambiente. Instituto Nacional de Meteorología Centro de Publicaciones Secretaría General Técnica Ministerio de Medio Ambiente.

Romero, R., Ramis, C., and Alonso, S. (1997). Numerical simulation of an extreme rainfall event in Catalonia: Role of orography and evaporation from the sea, *Quarterly Journal of the Royal Meteorological Society* 123, 537–559.

CHAPTER 8

OBSERVATION, ANALYSIS, AND FORECASTING OF HAIL STORMS

José Luis SÁNCHEZ[1], Andrés MERINO[1], Laura LÓPEZ[1], Eduardo GARCÍA-ORTEGA[1], Estíbaliz GASCÓN[1], Sergio FERNÁNDEZ [1], José Luis MARCOS[1]

[1]*Group for Atmospheric Physics. Institute of Environmental Studies,*
jl.sanchez@unielon.es, amers@unileon.es, llopc@unileon.es
eduardo.garcia@unileon.es, egass@unileon.es, sferg@unileon.es, jlmarm@unileon.es

ABSTRACT

The meteorological risks are those which tend to produce-year after year—increasing economic losses. One of the recommended solutions to minimize the risk of consequences of the severe atmospheric conditions consists in improving the observation and the quality of meteorological forecasts.

Diminishing the uncertainty of meteorological forecasts, especially in the short term can become helpful in severe risk management, which allows the improvement of the "prevention culture", one as such, is an especially difficult task because, when accurate results are achieved, a certain degree of "invisibility" is present.

In this paper we address different aspects for understanding the formation of hail and severe storms, improve observing systems and tools that help establish a better decision making.

Key words: hail, hailpads, meteorological radar, MSG, mesoscale modeliing.

1. INTRODUCTION

The observations, analysis, and forecasting of severe convective phenomena present important challenges. Improving knowledge about these phenomena is of great interest to reducing the risks that they create. In , hail precipitation is one of the phenomena that is most frequently associated with severe convection. In the Iberian Peninsula, the damages caused by hail are superior to those in the rest of Europe, and in the Ebro Valley, they represent a 10% loss in agricultural production (Ceperuelo, 2008).

The detection and documentation of hail fall is especially difficult because of its small spatial and temporal scale. Currently, there are various systems for the detection of these phenomena, although all of them present uncertainty. On one hand, direct methods can be used to detect its presence on the ground—for example, by observing damages to crops or making use of hailpad networks—and other, remote observations, which are more indirect, and based on remote sensing tools.

Historically, meteorological radar has been the most widely used tool for identifying phenomena associated with severe convection. Some algorithms have been developed to use radar to identify hail storms. However, given the spatial limitation and the elevated cost that these systems present, it seems reasonable to develop new tools that present greater spatial coverage and accessibility. In this sense, geostationary meteorological satellites, such as the MSG, have wide spatial coverage and high temporal and spatial resolution, and as such, are a good tool for detecting and following convection in general, and particularly for severe convection. The microphysical properties of cloud tops, inferred using reflectancies and irradiances in different wavelengths, provide information about the processes that take place within convective clouds. Thus, it is possible to find algorithms to identify cumulonimbus clouds and hailfall events.

Improving convection forecasting, specifically for hail storms, is a complicated task. In the last few years, the evolution of numerical models has allowed for continuous improvements in meteorological forecasts in diverse fields: precipitation, wind, temperature, humidity, cloud coverage, etc. However, hail precipitation has not been included in the majority of numerical models. Why? The problem that comes up when making a forecast is analogous to the problem of its identification: the small spatial and temporal scales in which they develop.

Currently, the absence of forecasts using numerical models has been substituted for the development of algorithms using parameters for dynamic and thermodynamic instability obtained using radiosondes. The main inconvenience of these methods is that they do not allow us to make a forecast about the location of hail fall. Additionally, the spatial and temporal representativeness of radiosondes is quite limited. Another method that was done was the use of radiosondes forecasted by the numerical models for the prediction of risk and severity of hail. Although these tools suppose a considerable advance in numerical prediction, the results are questionable.

It seems reasonable to assume that the improvement in forecasting occurs when developing a methodology that allows us to characterize convective hail precipitation on different scales. Firstly, by finding synoptic scale models and then selecting the mesoscale configurations and prediction parameters of hail.

2. SEVERE CONVECTION

In meteorology, the term "convection" refers to the transfer of heat and humidity through the vertical flow component associated with floatability. Convection transports heat and water vapor from low layers to the upper troposphere. Doswell et al. (1996) and Doswell (2001) affirmed that for floatability in the troposphere

not to be null, the simultaneous presence of the following ingredients is necessary: conditional instability, humidity in low layers, and the existence of mechanisms for the transfer of air parcels toward the free convection level (FLC).

One of the first projects in which atmospheric convection was studied was the Thunderstorm project (Byers and Brahan, 1949), where the cycle of a convective cloud was defined for the first time, and a storm cell was defined as a basic organization of storms, a term that continues to be used today. The organization of storm cells is related to the intensity of severe weather that originates. Habitually, different types of cell organization are distinguished:

- Linear. This is the most frequent convection organization, commonly known as a squall line. The onset mechanism of these types of structures can be a front, a line of instability, gravity waves, etc.

- Convective mesoscale systems. This term was developed by Maddox (1980) using criteria related to infrared satellite images. Its formation occurs because of the union of anvils of numerous isolated cells.

- Supercells. A supercell is a convective storm with a mesocyclone circulation (Browning, 1964). Many of the severe meteorological phenomena are produced by supercells, such as severe hail fall, tornadoes, or strong winds.

Furthermore, the type of convection that gives way to storms is known as Deep Moist Convection (DMC). This term was adopted by Bluestein (1993) to define the convective clouds that cover a substantial part of the troposphere. Throughout this paper, we use the term "deep convection". In order for this type of convection to be produced, the following two ingredients are fundamental: atmospheric instability and sufficient humidity flow.

The study of convection, specifically deep convection, is of utmost importance because of its capacity to generate adverse phenomena: hail, tornadoes, intense precipitation, and strong winds. Thorough knowledge of these phenomena can help to mitigate the risk that it presents to society and the atmosphere. Nevertheless, deep convection is not only associated with adverse phenomena; it also presents beneficial aspects, being the main mechanism of generating precipitation in many regions.

Finally, we are going to refer to the term "severe" as that which introduces the fact that convection causes relevant damages. However, there is no universally accepted definition for the term "severe convection." Convection is considered to be severe when "intense and strong" precipitation is produced (with or without hail and strong winds; Doswell, 1985). However, the term "severe" requires the definition of thresholds. In the United States, severe convection is defined as that which comes accompanied by one of the following phenomena: hail greater than or equal to 2 cm, wind with velocity of 25 m s^{-1} or higher, or formation of tornadoes. However, this definition of thresholds is often questioned. For example, important hail accumulation having a diameter about 1 cm but accompanied by strong winds, can cause damages, and, according to the previous definition, is not considered to be severe.

As previously shown, in the United States, hail is considered severe when the stones reach at least 2 cm in diameter. However, there are other classifications of hail that

use multiple categories. One of the first classifications was introduced in 1986 by the Tornado and Storm Research Organization (TORRO), for Great Britain and Ireland, developing a scale of intensity of hail storms at 11 levels (Webb *et al.,* 1986). This classification is done according to the damage that hail causes in crops and materials. Later, this classification was slightly revised by Sioutas et al. (2009), manifesting the need to adapt it to other regions according to the materials and types of construction used.

Another classification for hail that uses 6 empirical categories, based on damages to crops, was developed in France (Dessens *et al.,* 2007). In this case, its application was easier and more acceptable for cases of hail storms that are "typically" Mediterranean.

3. FORMATION OF HAIL STONES

In order for a hail stone to form, there are exactly two stages: that in which an embryo is formed, and a second in which the embryo grows and acquires a *large* size, that is, in which a hail stone forms. In storms, we distinguish between two regions: the EFR (Embryo Formation Region) and the HGZ (Hail Growth Zone).

Hail Embryos

This is understood to be the smallest unit that can be identified in the interior of a hail stone. They normally have a size of up to approximately 5 mm in diameter and they are necessary for hail stones to form. The embryos are generated in two different ways:

- From freezing cloud drops that have grown because of collision-coalescenceprocesses (it is necessary to consider that a million cloud droplets form a drop of about 2 mm in diameter) or,
- From a freezing cloud droplet that gives way to a small ice crystal that grows and collects supercooled liquid water that consists of a *graupel* (granulated snow, somewhat compact, with a density of the order or 0.5 a 0.8 g cm^{-3}).

There are some results that indicate that storms with a warm base have a tendency to form embryos of frozen drops and those that are colder usually follow the second option (Knight *et al.,* 1982).

The embryos have a density of between 0.5 and 0.9 g cm^{-3} –less than the graupel and greater than those that prevent frozen drops—and appear in the EFR in concentrations to the order of 10^3 a 10^4 m^{-3}. The velocity of the fall of the embryos with densities to the order of 0.5 g cm^{-3} is low, to the order of 1 to 2 m s^{-1}, and somewhat greater when the density increases. In both cases, the growth process of a hail embryo needs about 20 or 30 minutes to form a hailstone 5 mm in size.

Hail embryos cannot form in storm regions where there are strong ascending currents (of 15 m s^{-1}), and since the velocity is a soft fall (to the order of 1 m s^{-1}), we suppose that its vertical displacement would have an elevated velocity (in our example, 14 m s^{-1}). Since they need about 20 minutes to grow, if they were carried to the regions where the vertical current is strong, they would end up being placed

in the anvil of the storm (in our case, they cover about 20 km), and as a result, the area is completely isolated from the EFR and HGZ.

The results found up to now show that the EFR is situated in the outside flanks of the main storm structure, in the area called feeder cells, that are normally located to the right (Northern Hemisphere) or the left (Southern Hemisphere) (Browning *et al.,* 1976). With the passage of time, some of these embryos can be injected into the ascending current, beginning a rapid growth and reaching concentrations to the order of 0.1 to 1 m^{-3}.

Hail stones

We are going to assume that we have a population of embryos. It is -calculated that between 5 and 10% of the embryos are displaced from the EFR to the HGZ. Upon arriving to the HGZ, the embryos grow fundamentally because of the supercooled LWC provided that is found along the way. The equation for the growth of a hail stone is as follows:

$$dD/dt = V_t \times LWC_{eff} \times \rho_W / 2\rho_i \quad (1)$$

with D being the diameter of the hail stone, V_t the terminal velocity, LWC_{eff} the determined content of effective liquid water, ρ_w the liquid water density and ρ_i the ice density. With Equation 1, we can get an embryo of 0.5 cm to grow to 3 cm in only 20 minutes when the atmosphere is 2.5 g m^{-3}. If the atmosphere is 5 g m^{-3}, the time is reduced to half.

As we can see, the factors of terminal velocity and liquid water content are essential to explain the sizes of the hail stones formed.

The growth of these hail stones follows two paths and can be visualized, approximately, to analyzing a hail stone. Thus, in Figure 1, we can see that there is a relatively transparent area around the embryo. This indicates that the hail grew in an area collecting a great quantity of supercooled water that was not able to freeze quickly. It is necessary to consider that the supercooled water mass incorporated should freeze and, as such, yield 80 cal g^{-1}, a quantity that should be liberated. Taking the caloric capacity into account, only a part of the supercooled water mass incorporated into the stone is frozen, and the other part is adhered to its surface, at 0ºC, transferring heat to the air and freezing more slowly. In this time, the air bubbles start to get eliminated, and the water that freezes is relatively transparent. This process is called "humid". The liquid water that remains adhered to the hail stone forms a film that waits to be frozen, which can be shed and then go on form new hail embryos.

The growth of a hail stone can also be produced in a region of the storm where the LWC is low, and all of the growth is "dry", since as the supercooled drops are incorporated, they are frozen. In this case, the aspect of the incorporated layers takes is more "milky" since the air bubbles get trapped.

Again, if we are in a region in which the LWC is high, new stones form, and the process continues.

The succession of layers in a hail stone indicate the processes that it has undergone, that is, the regions that it has crossed, abandoning the idea that it went around the interior of the storm, rising and falling.

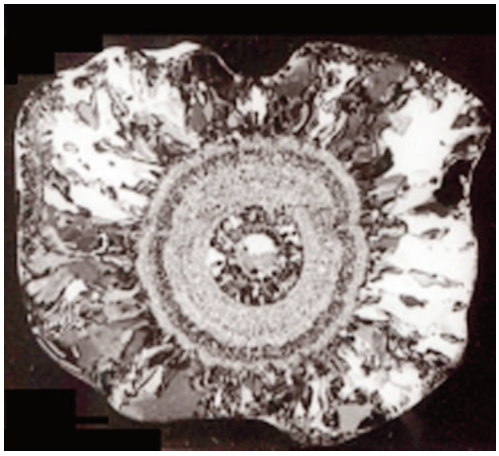

Figure 1. Cross-section of hail.

4. GROUND-LEVEL OBSERVATIONS: SIZE DISTRIBUTIONS OF HAIL

The size distributions of hail are an important part of the research projects that focus on severe convection. Also, it is convenient, not only to know the parameters that are characteristic of each area, but also to be able to establish the corresponding comparisons.

In this section, a summary of some of the results found in the analysis of the distribution of the size of hail impact registered in the hailpads in eight hailpad networks installed in Argentina, Spain, and France are presented (Sánchez *et al.,* 2009a).

Initially, it is assumed that the spectrum of hail size adjusts itself to an *exponential distribution*. Thus, it is possible to calculate the parameters of the distributions of all of the hailpad data obtained in the two Spanish networks, the three French ones, and the three Argentina ones.

Later, it is convenient to linearize the exponential distribution. In order to do so, the logarithms for frequencies of each size are used, and the *least square method* is used to calculate the parameters Ordinate at the origin and slope. From the inverse of the latter, the *average characteristic diameter* of the distribution is found.

The fit for the distribution of hail size registered in the eight networks has been done by adjusting to the exponential functions that are statistically significant. However, the parameters characteristic of the model fitting are different for each area. Thus, when comparing the results, it can be observed that the French networks present *slope* values that are greater than in the Spanish networks, as well as being greater than the Argentina ones, varying between a minimum of 2.19 cm^{-1} in the central oasis of Mendoza, and up to a maximum of 3.47 cm^{-1} in the Mediterranean area of France. As such, the lower *average diameters* of around 8 mm are found in France, and the largest ones are in Argentina, exceeding 9 mm, while in Spain, they are in the middle. These differences could be due to the proportion of *supercells* to the total number of hail cells in each of these areas.

When graphically analyzing the linearized exponential distributions, we find, in some cases, two possible "regions" in the distribution. To prove this fact, a technique known as *regression by parts* was applied. This technique allows us to find a diameter for hail that separates these different distributions. The threshold diameter is known as the *breakpoint,* and is found in four of the five networks analyzed in Spain and Argentina, with these being statistically significant. The *breakpoints* found vary between 2 cm in the central oasis and 3.7 cm in the northeast oasis. In Figure 2, we show an example of this *breakpoint*.

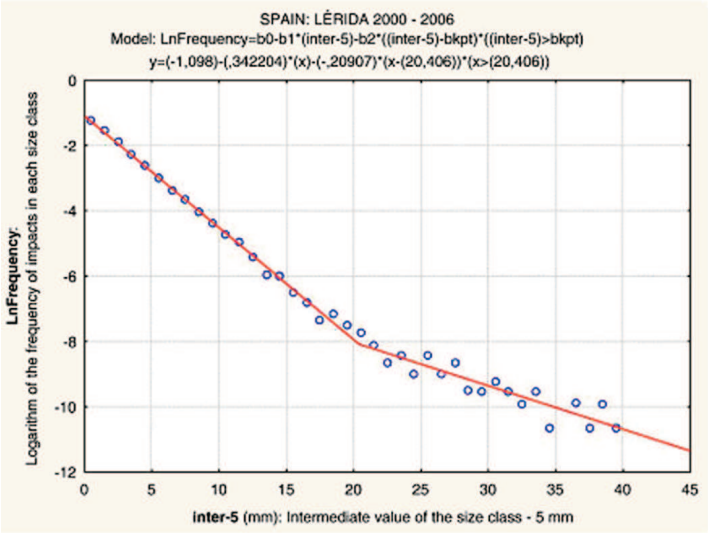

Figure 2. Model fit for the bimodal distribution of hail size.

The fact that this spectrum of hail size is bimodal indicates a different behavior in the small and large hail stones. In fact, it can be observed that the marks registered in the hailpads, 60% of the large stones (2 cm), adjust to an elliptical surface. As such, the results indicate that it can be viable that this rupture point marks the difference between two growth processes for different hail.

In the first term, the small hail grows by conventional means, collecting supercooled water (either by the *humid process* or the *dry process*) until it reaches a certain size. In the second part, the process is different, and the hail can reach large diameters, due to the amalgam or union of various small hail stones, adhering because of the presence of supercooled water, which acts as a kind of glue.

The rarity of large hail does not allow us to have access to a large sample size, and as such, it is early to confirm these physical interpretations. The progressive incorporation of these data will serve to advance our knowledge of the mechanisms of hail formation.

5. IDENTIFICATION OF HAIL STORMS USING METEOROLOGICAL RADAR

The use of conventional meteorological radar is relatively generalized in the world. This has motivated the development of diverse algorithms constructed using radar variables (Waldvogel *et al.,* 1979; Greene and Clark, 1972; Billet *et al.,* 1997; Witt *et al.,* 1998). However, the fact that many of these algorithms were constructed from X-band radar and are used for images obtained by other radar, such as C- and S-band radar, is conspicuous.

Using an ample and reliable database for hail events, López and Sánchez (2009) constructed a tool for the detection of storms with and without hail. There are some statistical techniques, using ground truth data (hail /no-hail on the ground) that allow us to classify radar variables that allow us to identify cells with and without hail with less uncertainty.

López and Sánchez (2009) made use of two mathematical methods known as logistic regression and linear discriminant analysis in order to identify, using C-band radar, the cells with and without hail. The two methods share a number of radar variables: *VIL,* or vertical integrated liquid, maximum reflectivity, and the variations of maximum reflectivity, or *ddBZ_max / dt*. Additionally, the discriminant model used makes use of the height of the storm ceiling, the highest part, and the storm tilt parameter.

Once these discriminant and logistic model parameters were found, they were evaluated with another independent data sample. The results were evaluated through the *precision* indices. Table 1 shows the values found.

Currently, the algorithms are used operatively once they are implemented in the software for the C-band radar data that the Group for Atmospheric Physics has access to.

In Figure 3 an example identifying hail cells can be seen making use of the algorithms.

Table 1. Precision indices found in the evaluation of discriminant and logistic models.

Precision index	Index	Discriminant Model	Logistic Model
False Alarm Rate	FAR	0.151	0.124
Probability of Detection	POD	0.849	0.868
Frequency of null event	FON	0.864	0.889
Probability of false detection	POFD	0.135	0.110
Proportion of failure rate	DFR	0.135	0.117
Frecuency of null events	FOCN	0.864	0.882
Critical Success Index	CSI	0.773	0.737
Heidke Index (HSS)	HSS	0.713	0.758

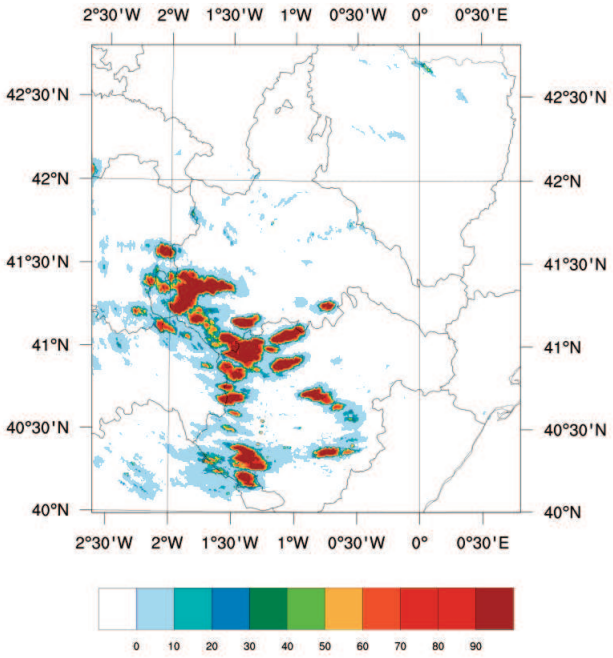

Figure 3. Hail cell identified making use of the algorithm and the probability (see the scale).

6. IDENTIFICATION OF HAIL STORMS VIA MSG

As we mentioned in the introduction, meteorological geostationary satellites—known as MSG—are a good tool for detecting and following convection in general, and particularly severe convection.

In order to do so, it is necessary to make use of microphysical cloud properties. Thus, these properties should be established using reflectancies and irradiances in different wavelengths. Merino (2013) recently applied different methodologies to detect convective clouds and establish their severity.

Merino *et al.,* (2013) developed some algorithms to identify cumulonimbus clouds and hail fall. The creation of these algorithms was carried out using a binary logistic regression model, combining data from different Meteosat Second Generation (MSG) satellite channels. First, the methodology developed allows for a convective mask to be established, with the objective of discriminating the cumulonimbus clouds from other cloud structures. This was done after identifying episodes with different types of cloud structures with Red-Green-Blue compositions. Brightness temperatures were extracted from these episodes, along with albedos from the MSG channels, and a logistic model was constructed. In this case, a consideration was made for the fact that cumulonimbus clouds are different from the rest of cloud formations because of their large liquid water content, cloud tops formed by ice particles, and high optical thickness. These characteristics are reflected in the channels used for their identification: water vapor, thermal infrared, and near infrared, respectively.

Later, following a similar methodology, an algorithm to identify hail within the cumulonimbus was developed. In this case, different parts of the cumulonimbus were identified, including the hail fall area, using data provided by meteorological radar. The regions with hail fall within a cumulonimbus were characterized by the presence of clouds that exceed the tropopause, high concentrations of water vapor in the high troposphere, and the updrafts. These characteristics are reflected in the channels selected for the identification of hail fall: visible, water vapor, and near infrared, respectively.

It is necessary to point out the importance that the filter of the cumulonimbus clouds has for the convective mask, since the hail algorithm is very sensible to the reflectancies in the near infrared channel. Thus, the reflectancies in this channel increase as the size of the ice crystals in the cloud tops decrease. However, the cloud tops formed by particles of liquid water also have high reflectancies in this region of the spectrum, and can be erroneously classified as hail. For this reason, these types of structures should be filtered previously by the convective mask.

The consecutive application of the two algorithms was validated by a database of independent events, giving way to a probability of detection of 76.9% and a false alarm rate of 16.7%. With these results, this tool can be used to follow hail events in real time, and it also has a great applicability in the register of hail storms in regions where radar measurements cannot be used.

In the Figure 4 some hailstorms detected by means of the algorithm developed can be seen.

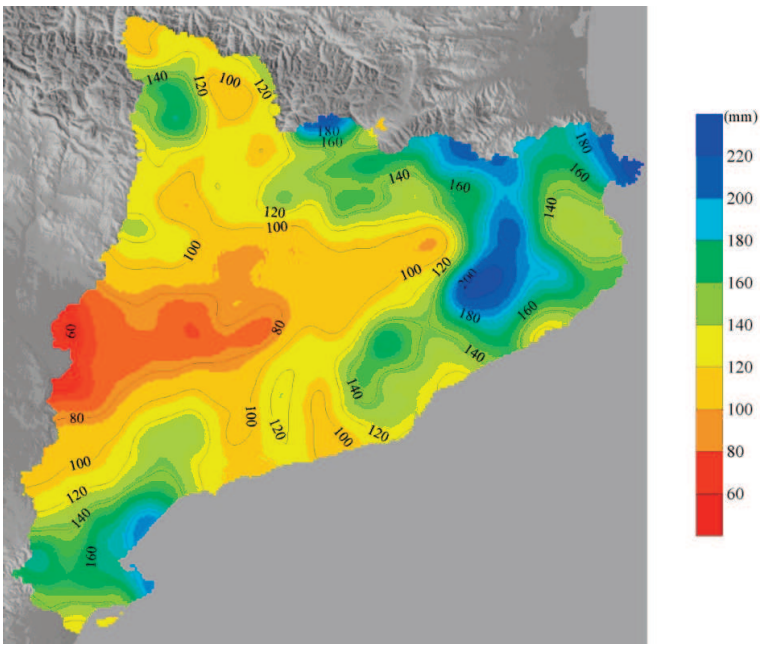

Figure 4. Hailstorm was identified by means of the tool developed by GFA making use of the MSG images. The scale of probability is shown.

7. EVALUATION OF THERMODYNAMIC INDICES AND THEIR USE FOR FORECASTING STORMS WITH OR WITHOUT HAIL

When dealing with the difficulties that the numerical models present when establishing a forecast of the appearance of hail storms, traditionally, diverse thermodynamic parameters and atmospheric stability indices have been used, obtained with radiosounding data. Many of these indices have been developed for a specific area and then later evaluated.

Sánchez *et al.,* (2009) analyzed the capacity of a series of indices to characterize preconvective conditions in diverse regions: León (Spain), Zaragoza (Spain), Bordeaux (France), and Mendoza (Argentina). In all of these areas, a reliable database of events with and without hail at the ground level was available.

First, statistical models that were determined to be discriminant for each area were used. In other words, a database for hail/no-hail or storms/no-storms was established, and diverse stability indices were calculated (Sánchez *et al.,* 2009b, López *et al.,* 2009). When comparing the results obtained by the different models constructed for each of the four study areas, it was proven that it is not possible to establish a general "rule". That is, while some could be good "predictors" in some areas, in others, it was not the case. All of this takes into account that the indices, in and of themselves, are not sufficient to detect the onset mechanism with precision.

In general, the Showalter Index can be considered to be a good indicator of static instability and, to characterize the flow of humidity, the use of temperature at dew point is very good at the level of 850 hPa. However, it is recommendable to introduce other variables, such as minimum temperature the night before, the CCL, etc.

Despite the difficulties, in the study areas, the probability of storm detection (the index known as POD), showed results to the order of 0.75, and false alarms were 0.28 in the FAR index (Sánchez *et al.,* 2009b).

In the future, it can be interesting to incorporate this analysis and the results obtained into the prediction fields and mesoscale numerical models.

8. FORECASTING STORMS WITH OR WITHOUT HAIL USING NUMERICAL SIMULATION MODELS

Numerical simulation using multidimensional models has helped to improve the knowledge of hail growth mechanisms by developing conceptual growth models (Farley, 1987). Brooks *et al.* (1992) discussed the difficulties associated with the assimilation of data for 3D models, which should be overcome before the operative use of these models. Another approximation has been the use of one-dimensional models, such as the HAILCAST model, developed by Brimelow *et al.* (2002) for forecasting hail size in Canada. This tool is very useful for determining the risk of hail fall on a large scale, but it has a high false alarm rate and it is difficult to estimate a detailed spatial distribution.

The recognition of atmospheric and climatological models, persistence, and geomorphological characteristics continues to be the fundamental axis in the process of forecasting hail storms.

The results provided by numerical models stop being precise when determining the regions that will be affected by hail precipitation. For this reason, the study of the synoptic environment and mesoscale factors responsible for the onset of convection and parameters for indicating severity continue to be one of the best tools to help with forecasting.

Obtaining synoptic scale configurations favorable to the appearance of convective storms allows us to characterize convective environments and establish relationships between the different scales. In other words, when classifying these situations, configuration groups are established (more precisely, clusters). The GAP has developed diverse papers oriented toward the characterization of these types of environments (García-Ortega *et al.,* 2007; 2011; López *et al.,* 2009; Sánchez *et al.,* 2009a; 2009b; 2012). In the case of the Mid-Ebro Valley, they were defined by García-Ortega *et al.* (2011). In this paper, we show that extratropical cyclones play an important part when generating conditions favorable to deep convection. In all of the environments described by García-Ortega *et al.* (2011), the study area is affected by the presence of a low or trough that contributes to the formation of an environment favorable to the development of convection. Nevertheless, the position of the perturbations does not explain the distribution of small-scale convective precipitation, and as such, it is necessary to analyze mesoscale factors.

It is usually wise, given the scale on which storms with and without hail is produced, to continue to determine the deviations that days with severe hail present on a synoptic scale as compared to those presented by average clusters found in the classification (García Ortega *et al.,* 2012). From these results, one can begin to do a mesoscale analysis to determine the factors that play a part in the onset of convection.

The use of mesoscale numerical models, such as the MM5 or the WRF, can be used to analyze mesoscale situations. Once these factors are identified, they can be useful for forecasting hail storms in an area. Perhaps, as a previous requisite, before performing the tasks of identifying the mesoscale factors that intervene in situations that produce hail precipitation, it is convenient to prove if numerical model simulations are capable of predicting convective precipitation fields. This requires executing different simulations with diverse parameterization schemes. The evaluation of these types of precipitation field events allows us to select a better combination of schemes to use.

When studying the onset of mesoscale convection, at least in our experience in the Mid-Ebro Valley, the variables that best explain the onset of severe convection are the following: the flow divergence of water vapor between 700-1000 hPa, the convective instability index between 700-900 hPa, and the flow and humidity at 850 hPa. Nevertheless, the weight that each variable has in the onset of convection is related to the synoptic environment (Merino *et al.,* 2013).

As of today, to establish a forecast of hail precipitation in an area, the most reasonable thing to do is perfect a series of tools that allow, among other things, to help to make decisions. These tools, when developed, should evaluate the following: (1) different stability indices, (2) give a good classification of the synoptic scale environment (clusters), (3) establish the mesoscale factors that provoke onset

mechanisms, and (4) a good prediction model for precipitation, of the convective type, expected in an area. These four tools help to make decisions with relatively good guarantees.

ACKNOWLEDGMENTS

This work was made in the frame of Projects: Granímetro (CGL2010-15930), Micrometeo (IPT-310000-2010-022) Junta de Castilla y León (LE220A11-2 y LE176/A11-2) Gobierno Regional de Aragón y Confederación Hidrográfica del Ebro.

REFERENCES

Billet, J., De Lisi, M., Smith, B.G., Gates, C., (1997). Use of regression techniques to predict hail size and the probability of large hail. *Wea. Forecasting*, 12, 154-164.

Brimelow, J. C., Reuter G. W., Poolman E. P., (2002). Modeling maximum hail size in Alberta thunderstorms. *Wea. Forecast*., 17, 1048-1062.

Browning, K.A., (1964). Airflow and precipitation trajectories within severe local storms which travel to the right of the winds. *J. Atmos. Sci*., 21, 634-639.

Browning, K.A., Fankhauser, J.C., Chalon, J.P., Eccles, P.J., Strauch, R.C., Merrem, F.H., Musil, D.J., May, E.L., Sand, W.R., (1976). Structure of an evolving hailstorm. Part V: Synthesis and implications for hail growth and hail suppression. *Mon. Wea. Rev*., 104, 603-610.

Bluestein, H.B., (1993). Synoptic-dynamic meteorology in midlatitudes. Volume II: observations and theory of weather systems. Synoptic-dynamic meteorology in midlatitudes. Vol. II: observations and theory of weather systems. Oxford University Press. 594 pp.

Byers H. R., Braham JR., R.R., (1949). The Thunderstorm. U. S. Government Printing Office, Washington D. C. 287pp.

Ceperuelo M., (2008). Identificación y cuantificación del granizo y predicción de los parámetros radar. Tesis doctoral Universitat de Barcelona. 232 pp.

Dessens, J., Berthet, C., Sánchez, J.L., (2007). A point hailfall classification based on hailpad measurements: The ANELFA scale. *Atmos. Res*., 83, 132-139.

Doswell III, C.A., Brooks, H. E., Maddox, R. A., (1996). Flash flood forecast: An ingredients-based methodology. *Wea. Forecasting*, 11, 560-557.

Doswell III, C.A., (1985). The operational meteorology of convective weather. Vol. 2: Storm scale analysis. NOAA Tech. Memo. 240 pp.

Doswell III, C.A., (2001). Severe Convective Storms-An Overview. *Meteor. Monogr*., 28, 1-26.

Farley, R.D., (1987). Numerical modeling of hailstorms and hailstone growth. part III: Simulation of an Alberta hailstorm - natural and seeded cases. *J. Climate Appl. Meteor*., 26, 789-812.

García-Ortega, E., Fita, L., Romero, R., López, L., Ramis, C., Sánchez, J.L., (2007). Numerical simulation and sensitivity study of a severe hailstorm in northeast Spain. *Atmos. Res.*, 83, 225-241.

García-Ortega, E., López, L., Sánchez, J. L., (2011). Atmospheric patterns associated with hailstorm days in the Ebro Valley, Spain. *Atmos. Res.*, 100, 401-427.

García-Ortega E., A. Merino, López, L., Sánchez, J.L., (2012). Role of mesoscale factors at the onset of deep convection on hailstorm days and their relation to the synoptic patterns. *Atmos. Res.*, 114-115, 91-106.

Greene, D.R., Clark, R.A., (1972). Vertically integrated liquid water-A new analysis tool. *Mon. Wea. Rev.*, 100, 548-552.

Knight, C.A., Smith, P., Wade, C., (1982). Storm types and some radar reflectivity characteristics. Hailstorms of the Central High Plains 1, 81-93.

López, L., García-Ortega, E., Sánchez, J. L., (2007). A short-term forecast model for hail. *Atmos. Res.*, 83, 176-184.

López, L., Sánchez, J.L., (2009). Discriminant methods for radar detection of hail. *Atmos. Res.*, 93, 358-368.

Merino A., (2013). Análisis, identificación y predicción de episodios de precipitación con granizo en la Península Ibérica. Tesis doctoral.

Merino, A., García-Ortega, E., López, L., Sánchez, J.L., Guerrero-Higueras, A.M., (2013). Synoptic environment, mesoscale conFigurations and forecast parameters for hailstorms in Southwestern Europe. *Atmospheric Research*, 122, 183-198.

Sánchez, J.L., Gil-Robles, B., Dessens, J., Martín, E., López, L., Marcos, J.L., Berthet, C., Fernández, J.T., García-Ortega, E., (2009b). Characterization of hailstone size spectra in hailpad networks in France, Spain, and Argentina. *Atmos. Res.*, 93, 641-654.

Sánchez, J.L., Marcos, J.L., Dessens, J., López, L, Bustos C., García-Ortega E., (2009ª). Assessing sounding-derived parameters as storm predictors in different latitudes. *Atmos. Res.*, 93, 446-456.

Sánchez, J.L., López, L., García-Ortega, E., Gil, B., (2012). Nowcasting of kinetic energy of hail precipitation using radar. *Atmos. Res*. Article in Press.

Sioutas, M., Meaden, T., Webb, J.D.C., (2009). Hail frequency, distribution and intensity in Northern Greece. *Atmos. Res.*, 93, 526-533.

Waldvogel, A., Federer, B., Grimm, P., (1979). Criteria for detection of hail cells. *J. Appl. Meteor*. 18, 1521-1525.

Webb, J.D.C., Elsom, D.M., Meaden, G.T., (1986). The TORRO hailstorm intensity scale. *J. Meteor.*, 11, 337-339.

Witt, A., Eilts, M.D., Stumpf, G.J., Johnson, J.T., Mitchell, E.D., Thomas, K.W., (1998). An enhanced hail detection algorithm for the WSR-88D. *Wea. Forecasting*, 13, 286-303.

CHAPTER 9

EXTREME RAINFALL RATES AND PROBABLE MAXIMUM PRECIPITATION

Jerónimo LORENTE CASTELLÓ[1], M. Carmen CASAS CASTILLO[2], Raúl RODRÍGUEZ SOLA [2] , Ángel REDAÑO XIPELL[1]

[1]Dept. D'Astronomia I Meteorologia. Facultat de Física, Universitat de Barcelona
[2]Departament de Física i Enginyeria Nuclear. EPSEVG, Universitat Politècnica de Catalunya • BarcelonaTech
jlorentec@ub.edu m.carmen.casas@upc.edu raul.rodriguez@upc.edu angel@am.ub.es

ABSTRACT

One of the most important climatic features that characterize a territory is its pluviometric regime and, in particular, the extreme rainfall rates produced in the area. Their knowledge is essential for planning hydraulic works and for designing rainwater drainage systems and flood prevention. In addition, the behavior of this variable can be very useful for the evaluation of possible effects of the climatic change. In this chapter we summarize the methodology used in the calculation of the frequencies associated to maximum precipitations expected in an area according to rainfall duration. Results about the probable maximum precipitation in 24 hours for the 145 pluviometric stations of Catalonia are also shown. The obtained spatial distribution shows rainfall amounts in the range 200-550 mm, in a good concordance with the annual average distribution but with some exceptions caused probably by the different meteorological scales involved in each case.

Key words: Probable maximum precipitation, spatial rainfall distribution, IDF curves.

1. INTRODUCTION

The pluviometric regime is one of the most important climatic features that characterize a place or territory and among the many factors that define it stand out for their interest in the meteorological, hydrological and civil engineering, extreme rainfall intensities, their durations and the frequency with which they occur. Their knowledge is essential for planning hydraulic works, roads, sewage systems and for designing rainwater drainage systems in large installations and buildings in general, optimization of water resources in river basins and flood prevention. In addition, the behavior of this variable can be useful both for the detection of climate change and the assessment of their potential impact on a territory.

The behavior of the rain intensity averaged over time intervals of 24 hours or more is often studied from data provided by manual gauges (INM 1999; Lana *et al.,* 1995). However, when it requires a finer knowledge of this variable we must use the data provided by rainfall rate gauges capable of recording its evolution during the course of the shower. In both cases the procedure is to determine the maximum expected precipitation amounts at selected time intervals for different return periods considered from the data sets provided by the meteorological observatories. If we need information in areas without data this information, usually available locally at each measuring point, has to be added territorially and interpolated or extrapolated.

From the point of view of water management, a specific application of these maximum expected precipitation maps is its usefulness in carrying out the prevention and management of the river flooding. Another example of its application can be found in waste management. In this case, to have a reliable and updated collection of maximum precipitation climate data let us to improve the design of the different treatment facilities, design properly waste disposal, and calculate and verify the sizing of pluvial networks.

Sometimes, for the design of certain hydraulic structures, one requires to know the amount of precipitation which cannot be exceeded for a given duration. In this sense, the probable maximum precipitation (PMP) is defined as the amount of precipitation theoretically higher physically possible over a region (Hansen *et al.,* 1982). Although initially the PMP is defined himself as maximum precipitation amount for a given duration, area and time of year which not can be exceeded (Wang, 1984), it was subsequently found that sometimes, the amounts of recorded precipitation had passed the PMP estimated previously. This clearly indicated that these amounts calculated as PMP could not be considered as zero risk (Koutsoyiannis, 1999).

This work presents the methodology currently used to calculate the frequencies of the maximum expected rainfall in an area depending on its duration and the results of its application to Catalonia.

2. INTENSITY-DURATION-FREQUENCY CURVES

From data provided by current gauges can calculate the maximum precipitation time intervals between 5 minutes and 24 hours. The relationship between the calculated rainfall intensities, its duration and frequency of occurrence is what is known as curves of Intensity-Duration-Frequency, or briefly IDF curves.

To calculate them we must first obtain the maximum precipitation series for each term and determine the theoretical statistical functions that best fit each of the experimental series. For example, in the case of Barcelona, from the database generated by digitizing the stripe charts recorded by the intensity pluviograph Jardí installed in the Fabra Observatory between 1927 and 1992 (Burgueño *et al.*, 1994), we have calculated the maximum rainfall amounts recorded at different durations from 5 minutes to 24 hours. For complete data sets, the best fit was obtained by the Gamma distribution, a function used extensively in engineering applications, limited to positive values and right asymmetry, whose density function is:

$$f(x) = \frac{\lambda(\lambda x)^{k-1}}{\Gamma(k)} e^{-\lambda x} \qquad para\ x \geq 0 \tag{1}$$

where λ and k are the scale parameter and shape of the distribution.

From these functions the values of precipitation for different return periods can be obtained using the relationship between the frequency F and the return period given by equation:

$$F = 1 - \frac{N/T}{D} \tag{2}$$

where N is the number of available years, 66 in our case, and D the number of values in the sample. The intensity values for each time (t) and the return period (T), ie, the points I (t, T), are represented in Figure 1.

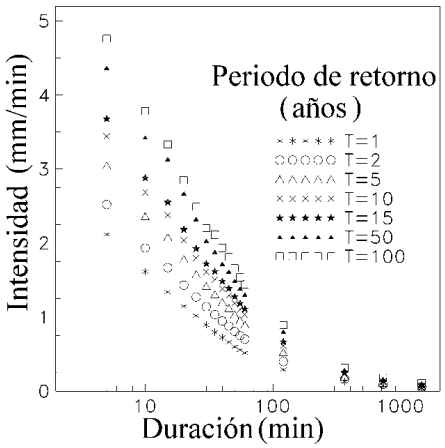

Figure 1. Rainfall rate for each duration and return period considered (Casas *et al.*, 2004).

The general equation obtained for the Intensity-Duration-Frequency curves for Barcelona:

$$I(t,T) = \frac{19 \log T + 23}{(13+t)^{0.87}} \tag{3}$$

where I is the rainfall rate expressed in mm/min t is the rainfall duration in minutes and T is the return period T in years.

Figure 2 shows the IDF curves for the return periods of 1, 2, 5, 10, 15, 50 and 100 years.

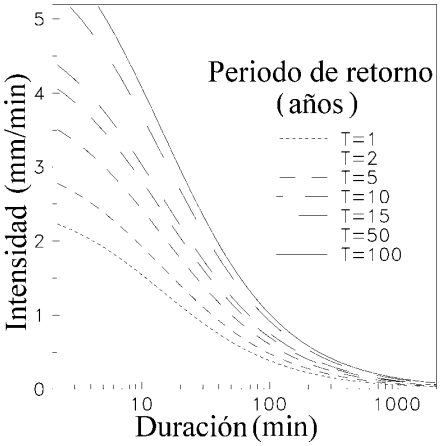

Figure 2. IDF curves for Barcelona of return periods of 1, 2, 5, 10, 50 and 100 years (Casas *et al.*, 2004).

3. SPATIAL ANALYSIS OF EXTREME DAILY RAINFALL

The knowledge of the maximum daily rainfall in an area for different return periods is necessary in many applications. This analysis is normally carried out from datasets of rain gauges installed in the area. One of the methods traditionally used for these calculations is the use of distribution functions to fit analytic functions to the annual series of maximum daily rainfall, allowing then assign a frequency or recurrence period to each value the maximum daily precipitation in one place. When the objective is to determine the maximum daily rainfall that can fall anywhere in the region under study with an established frequency, one typically resorts to the scalar analysis of the amounts calculated from data sets available in the rainfall stations. This approach, although common, has some drawbacks that can cause large uncertainties in the results and even notable errors.

The main cause of the inherent difficulty in calculating maximum precipitation in a given region lies in the nature of weather events that produce them. In general, the cloud systems that cause high intensity rains pertain to microscale or mesoscale α and the higher rainfall areas, within these organizations, are still smaller extension. This means that when in an observatory daily rainfall is recorded with large return period due to an extreme weather event, it is unlikely to be repeated in other observatories of mesoscale network and occurs much less if the density of stations corresponds to the synoptic scale or macroscale.

The high-resolution spatial analysis of extreme daily rainfall in Catalonia has been carried out from the series of annual maximum values of precipitation in 24 hours recorded in 145 rainfall stations that the Spanish Meteorological Agency (AEMET) has in this region (INM, 1999). The annual series of maximum daily rainfall selected have different lengths and correspond to the 1911-2001 period (Figure 3).

Since the approximate area of Catalonia is about 32 000 km2 and the number of rain gauges of the network is N=145, the average distance between the rainfall stations is found to be about 15 km approximately. Some of the series of annual maximum precipitation available have a relatively short length (15-20 years), and in some cases there has been the presence of extraordinary extreme cases (outliers) Hershfield (1961a and b), WMO (1986), Nobilis *et al.* (1991)).

For these occasional showers, the traditional method of setting the Gumbel function can assign to some values of precipitation return periods much smaller than it really would apply if the sample cover a greater number of years. To minimize this effect, we have estimated the Gumbel distribution parameters using the method of moments L (Hosking, 1990; Hosking and Wallis, 1997), which are linear combinations of the weighted probability moments.

To calculate these maximum daily rainfall amounts, firstly we have determined the monthly precipitation corresponding to the rainiest month at every grid point using the multiple regression obtained by Ninyerola *et al.* (2000) and they have been normalized from the relationship between these quantities and those registered in 24 hours.

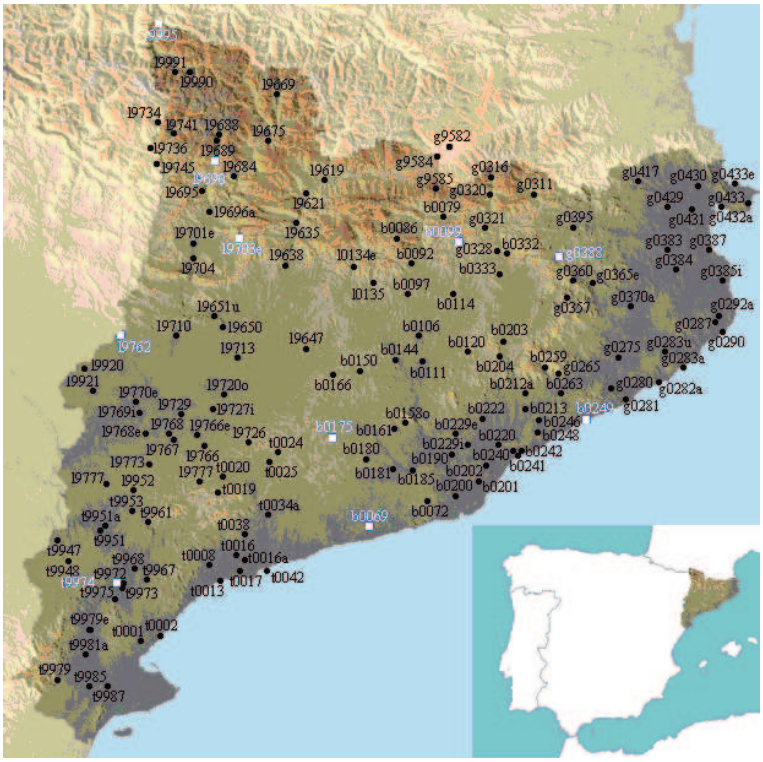

Figure 3. Rain gauges in Catalonia whose series have been analyzed. In white the stations used to test the analysis (Casas *et al.*, 2008).

Figure 4 shows the analysis obtained from the maximum rainfall in 24 hours 25 years return period for Catalonia (Casas *et al.,* 2007). Results show roughly the areas where you can expect a maximum of extreme daily rainfall are located in the eastern half of Catalonia, in the higher areas of the Pyrenees and the southern third, while the areas where we can expect the lowest extreme daily rainfall coincide largely with the central depression, extending from its western end to the highlands of Lluçanès and Plana de Vic.

In the eastern half of Catalonia the maximum values draw a line that follows the Sierra Prelitoral from Montserrat and Sant Llorenç de Munt to the Montseny and Guilleries and extending in a northerly direction along the transverse ridge until the Eastern Pyrenees, from where it continues west to the sector and eastward Moixeró by Alberas to the sea. The places where you can expect maximum values of extreme daily rainfall are Guilleries and Cape Creus (with values greater than 180 mm for a return period of 10 years), but also Though also there are prominent the values obtained in the zone between the headwaters of the rivers Ter and Muga.

In the Pyrenees highlight other areas where we can expect maximum daily rainfall important, coincident with higher altitudes. In the southern third of Catalonia is also obtained an area of maximum for extreme daily rainfall around Prelitoral hills, from the mountains of Prades to Montsià, where highlight a band oriented from west to east in which the maximum are more important.

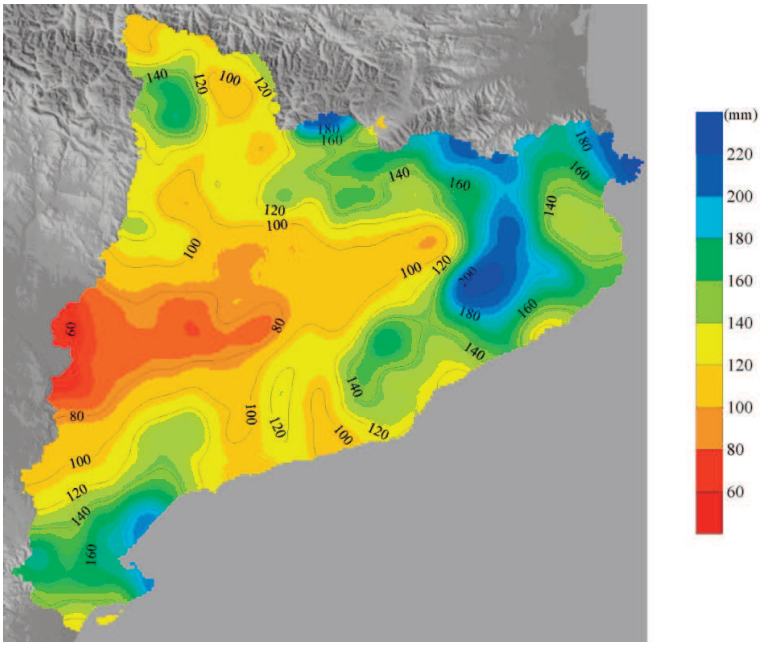

Figure 4. Maximum precipitation in 24 hours for return period of 25 years. *(Casas et al., 2007).*

4. CALCULATION OF THE PROBABLE MAXIMUM PRECIPITATION

The probable maximum precipitation (PMP) is defined as the greatest amount of precipitation meteorologically possible for a given length on a given storm area at a particular geographical location and the time of year, regardless of climate trends Long term (WMO, 1986). In hydrology PMP and their spatial and temporal distributions are used to calculate the probable maximum flood (PMF) which is one of the conceptual flood situations used in the design of hydrological structures for maximum reliability and safety.

Prior to the 50s, the concept of a potential upper limit of precipitation was known as maximum possible precipitation (MPP). The name was changed to PMP, reflecting the uncertainty involved in the estimation of maximum precipitation (Wang, 1984). Quoting Benson (1973): "*The concept of "maximum probable" began as "maximum possible" because it was considered that maximum limits exist for all the elements that act together to produce rainfall, and that these limits could be defined by a study of the natural process. This was found to be impossible to accomplish - basically because nature is not constrained to limits".* Procedures for determining the PMP are recognized as inaccurate, the results are estimates and a risk statement has to be assigned to them. The PMP concept "in no way implies actually zero risk" (Koutsoyiannis, 1999). The National Research Council (NRC, 1994) has estimated the return period of the PMP in U.S. between 105 and 109 years. Koutsoyiannis (1999) developed a method for assigning a return period PMP values obtained using the statistical of frequency factor method (Hershfield, 1961, 1965).

To estimate the PMP in a place, a variety of procedures depending on the situation of the basin have been proposed, the availability of data and other considerations (e.g. Wiesner, 1970; Schreiner and Reidel, 1978; WMO, 1986; Collier and Hardaker, 1996). Most of them are based on meteorological analysis while some are based on statistical analysis. PMP estimation techniques were listed by Wiesner (1970) as follows: [1] the storm model, [2] the maximization and transposition of real storms, [3] the use of precipitation data, their maximized duration and area from storms; [4] the use of empirical formulas determined from maximum precipitation data, duration and area, or theory, [5] the use of empirical relationships between variables in specific locations (only if detailed data are available), [6] statistical analysis of extreme rainfall. These methods are not entirely independent. Probably the easiest way to estimate a theoretical upper limit of precipitation in a basin for a given duration is the use of empirical formulas (methods [4] and [5]) to represent maximum values of local or global precipitation. Methods [2] and [3] involve the classification of storms by calculating their efficiency which is defined as the ratio between the maximum observed rainfall to the amount of precipitable water in the air column during the storm (NERC , 1975).

Among the statistical methods to estimate the PMP [6], the most commonly used is the method of Hershfield (1961b, 1965) which is based on the frequency analysis of the annual maximum rainfall data registered at the site of interest. The Hershfield technique for estimating the PMP is based on Chow's general frequency equation Chow (1951):

$$PMP = \bar{x}_n + k_m \sigma_n \quad (4)$$

$$k_m = \frac{x_M - \bar{x}_{n-1}}{\sigma_{n-1}} \quad (5)$$

where x_M , $\bar{x}_n$ and σ_n are the maximum value, the mean and the standard deviation respectively for a series of n annual maximum of a given duration, and are the mean and standard deviation in said series but excluding the maximum of these each and km is a frequency factor. To evaluate this factor, initially Hershfield (1961) analyzed 2645 stations (90% of them in USA) finding a value of 15 for km which he recommended for PMP estimation using Equation (3). Later, Hershfield (1965) found that the value of 15 was too high for rainy areas and too low to the arid, whereas it is too high for rain durations shorter than 24 hours. Thus, he constructed an empirical nomograph (WMO, 1986) with km varying between 5 km and 20 depending on the rainfall duration and the mean $\bar{x}_n$.

The methods discussed for PMP estimation can be used both for individual basins and larger regions covering several basins of different sizes. In the latter case, the estimates are known as widespread or regional estimates (WMO, 1986).

This section presents the results of the calculation of the PMP for Catalonia. As noted in the previous section, there are values of maximum precipitation in 24 hours and return periods from 2 to 500 years for 145 rainfall stations in Catalonia (Figure 3), calculated from their series of annual maximum daily precipitation. Following the technique of Hershfield, the statistical parameters $\bar{x}_n$, $\bar{x}_{n-1}$, σ_n y σ_{n-1} (means and standard deviations) involved in equations (4) and (5), and the coefficient of variation CV = σ_n / $\bar{x}_n$, have been calculated for all series.

Figure 5 shows the dependence between the average value of the series of annual maximum 24-hour precipitation and frequency factors km observed for each of them. As recommended by WMO (WMO, 1986), to estimate appropriate values of the PMP is desirable to draw an enveloping curve that fits all cases, including the most extreme. The usual technique is to select the highest values of the sample and adjust to a curve. This process can be applied to the sample frequency factors km calculated for a given duration (Dhar *et al.*, 1981, Rakhecha *et al.,* 1992). The same Figure shows, jointly with the points (k_m, $\bar{x}_n$), the enveloping curve representing the dependence between both variables.

In order to estimate the PMP for each station, the frequency factor k_m has been used that bound associated with average precipitation in 24 hours $\bar{x}_n$ of each station. These values are in all cases higher than the original k_m observed . With these theoretical values of km that give the enveloping curve for each station, the mean $\bar{x}_n$ and the standard deviation σ_n the PMP was calculated using equation (4).

Similarly to how we proceeded in section 3 the spatial analysis of PMP in 24 hours in Catalonia has been performed (Casas *et al.,* 2008) using the method of Cressman (Cressman, 1959; Thiébaux and Pedder, 1987) in order to obtain a high spatial resolution of 1km × 1km. As a first approximation to the PMP at all points of a network of 1km × 1km covering Catalonia, we will take the 24-hour precipitation

with a return period of 100 000 years which is obtained at each point from the work of Ninyerola *et al .* (2000) and IDF curves obtained in paragraph 2 (Casas *et al.,* 2004). These values are taken as the initial field of Cressman's objective analysis, which will be modified with each iteration until to achieve convergence to the data.

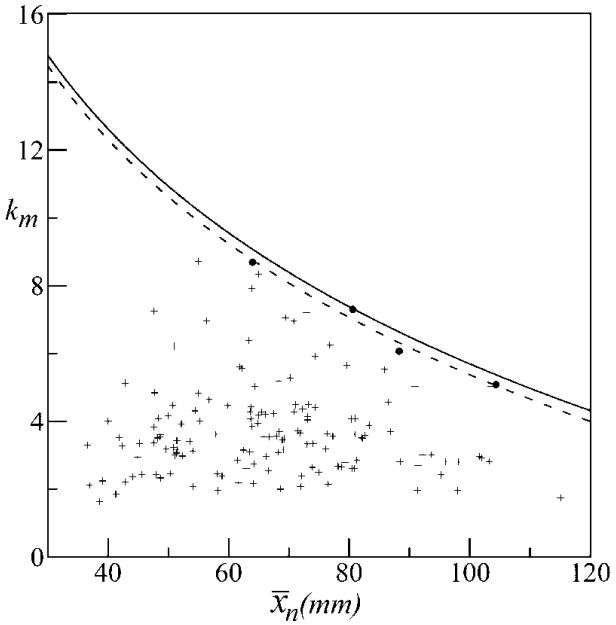

Figure 5. Enveloping frequency factor curve for Catalonia, fitted to the four upper (x_n , k_m) points (thick dots). Dashed line fitted curve for the 4 extreme cases of the sample (Casas *et al.*, 2008).

The result of the analysis of the PMP at 24 hours for Catalonia, after the filtering process to remove structures having a wavelength which cannot be resolved by the density of the network is presented in Figure 6.

The PMP in 24 hours for Catalonia ranges from values less than 200 mm to values exceeding 550 mm, with a relative difference between the maximum and minimum over 150%. Higher values are expected in the eastern half of Catalonia, in the higher areas of the Pyrenees and the southern third, while the lowest were found on the Central Depression, from its western end to the Plana de Vic The higher values of the PMP in the eastern half of Catalonia are the areas of Guilleries and Cape Creus. In the Pyrenees the most notable area with high values of the PMP is the north of Cerdanya, among Perafita and Puigpedrós peaks. In the southern third of Catalonia, there is an area of high PMP around the Gulf of Sant Jordi. The main minimum of PMP are distributed in close agreement with the driest areas of Catalonia.

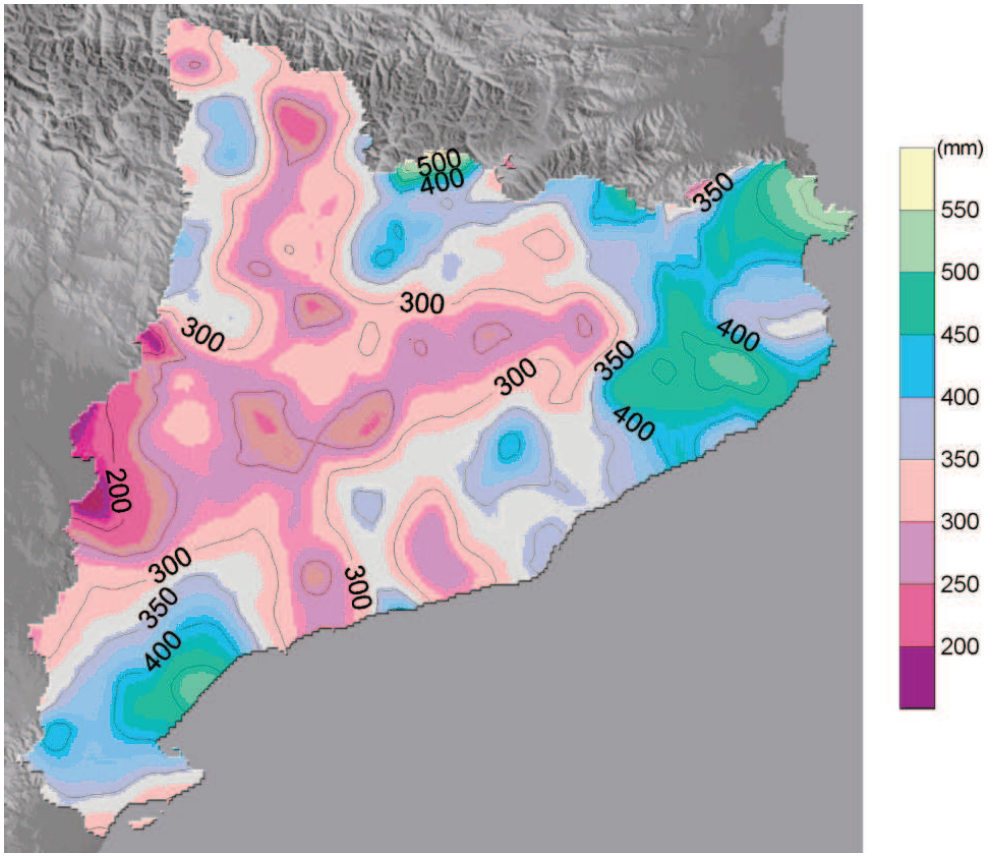

Figure 6. Probable Maximum Precipitation in 24 hours for Catalonia (Casas *et al.*, 2008).

5. CONCLUSIONS

From the records of Jardí's pluviograph of Fabra Observatory, between 1927 and 1992, we calculated the amount of maximum rainfall for durations from 5 minutes to 30 hours and also we have investigated the relationship between the maximum intensities of precipitation, duration and frequency, resulting in a revision of IDF curves for the city of Barcelona and its generalized equation $I(t,T) = \frac{19 \log T + 23}{(13+t)^{0.87}}$

(rainfall rate in mm / min, duration t in minutes and return period T in years).

For the series analyzed the calculation of the parameters of the Gumbel's extreme values distribution by the L moments method proposed by Hosking (1990), provides a more stable and realistic value of daily maximum precipitation for high return periods than when computed under the traditional procedure. With this method, the values of rainfall in 24 hours extraordinarily high registered in some observatories (La Pobla de Lillet,

b0079, Cadaqués, g0433; Vimbodí "Riudabella" t0019; Bohí "Central", l9741) do not influence significantly in the fit to the Gumbel distribution function. This has contributed to obtain, for example, over 30% difference between the amounts of rain in 24 hours, for return periods exceeding 50 years, calculated in this work and those obtained by other authors in some areas of Catalonia (INM, 1999, Lana *et al.,* 1995). The values obtained in our case are significantly lower than those that have been calculated using the traditional method of fit to Gumbel function from the mean and standard deviation of the data series. The calculated maximum rainfall amounts are more approximate the actual values because they have no so large dependence with the absolute maximum of the series, i.e., if these data are dispensed the results obtained in this study suffer a lower variation than the estimated values applying the traditional technique.

The method applied to analyze the spatial distribution of extreme rainfall in Catalonia has provided a high spatial resolution (1 km x 1 km) through the joint use of an initial field of rain calculated from the multiple regression equation obtained by Ninyerola *et al. (*2000) and Cressman analysis algorithm (Thiébaux and Pedder, 1987). Using this initial field, which has a good correlation with the variable analyzed, the analysis improves resolution especially in the mountain areas of the Pyrenees and Sierra Transversal where the station density is not sufficient to adequately represent large variations associated with the irregularity of the terrain (Willmott and Robeson, 1995). Furthermore, the analysis allows to assign to each km^2 a numerical value calculated objectively by a mathematical algorithm, which significantly improves the approximate estimates that can be made from a map analyzed manually.

Using the statistical method of estimation, we calculated the Probable Maximum Precipitation (PMP) in 24 hours for 145 rainfall stations in Catalonia, from his series of annual maximum rainfall in 24 hours. It has obtained the equation that determines the maximum frequency factor k_m depending on rainfall in 24 hours : ($\bar{x}_n$: $k_m = -7.56 \ln \bar{x}_n + 40.5$ ($\bar{x}_n$ in mm), as a calculated enveloping curve from the fit to the four points corresponding to the highest recorded extreme (Puigcerdà, La Pobla de Lillet, Capdella and Cadaqués). Over 90% of the calculated values of the PMP in 24 hours have some return periods between 104 and 108 years, almost coinciding with the range established by the NRC (1994) for the PMP.

With the iterative application of a numerical analysis filter obtained by the Cressman method we have achieved to eliminate the structures of wavelength less than the average distance between the rainfall stations used, thereby adjusting to the density variability of the network observation. The technique maintains, however, the information provided by the use of an initial field of high resolution. Furthermore, the use of this filter ensures that the spatial resolution is homogeneous analysis thus avoiding that depends upon the density of the network of observation in each area and could result in false interpretations of the actual spatial variability of the analyzed variable, improving the result obtained when a method of automatic plotting isolines is applied directly.

From the calculated values of the PMP in 24 hours was performed by applying spatial analysis algorithm Cressman (Thiébaux and Pedder, 1987) to an initial field of precipitation in 24 hours with return period of 100 000 years in all points of a grid of 1 km of arm containing Catalonia. The spatial distribution obtained for the

PMP in 24 hours has amounts ranging from values below 200 mm and others exceeding 550 mm and a relative difference between the maximum and minimum over 150%. Also, just as with the maximum precipitation maps, the spatial distribution obtained shows good agreement with that of the average annual rainfall in Catalonia, with some exceptions attributable to the different meteorological scales involved in each case in our region. So while synoptic-scale organizations have a major influence on the distribution of annual precipitation, the local and mesoscale factors most affect the map of the PMP in 24 hours.

REFERENCES

Benson, M.A. (1973). Thoughts on the design of design floods. In Floods and Droughts. Proceedings of the 2nd International Symposium in Hydrology, September 1972, Fort Collins: Colorado, pp. 27-33: Water Resources Publications, Fort Collins.

Burgueño, A., Codina, B., Redaño, A., Lorente, J. (1994). Basic Statistical Characteristics of Hourly Rainfall Amounts in Barcelona. Theoretical and Applied Climatology, 49, 175-181.

Casas, M.C., Codina, B., Redaño, A., Lorente, J. (2004). A methodology to classify extreme rainfall events in the western Mediterranean area. Theoretical and Applied Climatology, 77(3-4), 139-150.

Casas, M.C., Herrero, M., Ninyerola, M., Pons, X., Rodríguez, R., Rius, A., Redaño, A. (2007). Analysis and objective mapping of extreme daily rainfall in Catalonia. Int. Jour. Climat., 27(3), 399-409.

Casas, M.C., Rodríguez, R., Nieto, R., Redaño, A. (2008). The estimation of probable maximum precipitation: the case of Catalonia. Trends and directions in climate research. Annals of the New York Academy of Sciences, 1146, 291–302.

Chow, V.T. (1951). A general formula for hydrologic frequency analysis. Transactions American Geophysical Union, 32, 231-237.

Collier, C.G., Hardaker, P.J. (1996). Estimating probable maximum precipitation using a storm model approach. Journal of Hydrology, 183, 277-306.

Cressman, G.P. (1959). An operational objective analysis system. Monthly Weather Review. 87, 367- 374.

Dhar, O.N., Kulkarni, A.K., Rakhecha, P.R. 1981. Probable maximum point rainfall estimation for the southern half of the Indian peninsula. Proceedings of the Indian Academy of Sciences: Earth and Planetary Sciences, 90 A, 1: 39-46.

Hansen, E.M., Schreiner, L.C., Miller, J.F. (1982). Application of Probable Maximum Precipitation Estimates - United States East of the 105th Meridian. Hydrometeorological Report No. 52, (HMR-52), National Oceanic and Atmospheric Administration, National Weather Service: Silver Springs, MD, 168 pp.

Hershfield, D.M. (1961a). Rainfall frequency atlas of the United States for durations from 30 minutes to 24 hours and return periods from 1 to 100 years. Weather Bureau Technical Paper 40, U.S. Weather Bureau: Washington, D.C., 115 pp.

Hershfield, D.M. (1961b). Estimating the probable maximum precipitation. Proceedings American Society of Civil Engineers, Journal Hydraulics Division, 87(HY5), 99-106.

Hershfield, D.M. (1965). Method for estimating probable maximum precipitation. Journal American Waterworks Association, 57, 965-972.

Hosking, J.R.M. (1990). L-moments: analysis and estimation of distributions using linear combinations of order statistics. Journal of the Royal Statistical Society, Series B, 52, 105-124.

Hosking, J.R.M, Wallis, J.R. (1997). Regional frequency analysis: an approach based on L-moments. Cambridge University Press, 224 pp.

Instituto Nacional de Meteorología, (1999). Las precipitaciones máximas en 24 horas y sus períodos de retorno en España. Un estudio por regiones. Volumen 5. Cataluña. 148 pp.

Koutsoyiannis, D. (1999). A probabilistic view of Hershfield's method for estimating probable maximum precipitation. Water Resources Research, 35(4), 1313-1322.

Lana, X.; Fernandez Mills, G.; Burgueño, A. (1995). Daily precipitation maxima in Catalonia (North-East Spain): Expected values and their spatial distribution. International Journal of Climatology, 15, 341-354.

National Research Council, (1994). Estimating bounds on extreme precipitation events. National Academy Press: Washington, D.C.

Natural Environment Research Council, (1975). Flood Studies Report, I, Hydrologic Studies, p. 51. Whitefriars Press Ltd.: London.

Ninyerola, M; Pons, X.; Roure, J.M. (2000). A Methodological Approach of Climatological Modeling of Air-Temperature and Precipitation Through Gis Techniques. International Journal of Climatology, 20(14), 1823-1841.

Nobilis, F., Haiden, T., Kerschbaum, M. (1991). Statistical considerations concerning Probable Maximum Precipitation (PMP) in the Alpine Country of Austria. Theoretical and Applied Climatology, 44, 89-94.

Rakhecha, P.R., Deshpande, N.R., Soman, M.K. (1992). Probable Maximum Precipitation for a 2-Day Duration over the Indian Peninsula. Theoretical and Applied Climatology, 45, 277-283.

Schreiner, L.C., Reidel, J.T. (1978). Probable maximum precipitation estimates. United States east of 105th meridian, Hydrometeorological Report 51, U. S. National Weather Service: Washington D.C.

Thiébaux, H.J., Pedder, M.A. (1987). Spatial Objective Analysis: with applications in atmospheric science. Academic Press: London.

Wang, B-H. M. (1984). Estimation of probable maximum precipitation: case studies. Journal of Hydraulic Engineering, 110(10), 1457-1472.

Wiesner, C. (1970). Hydrometeorology. Chapman and Hall: London. 232 pp.

Willmott, C.J., Robeson, S.M. (1995). Climatologically Aided Interpolation (CAI) of Terrestrial Air Temperature. Int. J. Climatol., 15, 221-229.

WMO. (1986). Manual for estimation of probable maximum precipitation. Operational hydrology, Report.1, WMO-No.332, 269 pp.

CHAPTER 10

DAILY CONCENTRATION OF PRECIPITATION IN PENINSULAR SPAIN. A MAP OF TORRENTIAL RAINFALL RISK

Javier MARTÍN-VIDE

Universidad de Barcelona
jmartinvide@ub.edu

ABSTRACT

We present the index of daily concentration of precipitation (CI) (Martín-Vide, 2004), similar to Gini's but which makes use of exponential curves of the y=axebx type, and we review the values found for Peninsular Spain, particularly for the 1951-2010 period. The highest values, corresponding to a high percentage weight of the rainiest days within the annual total, are to be found on the eastern façade, from the mouth of the river Ebro to the north of the province of Alicante, in some places close to 0.70, this area presenting the most intense rainfall in Spain. The eastern façade of the Iberian Peninsula, along with the south of France, presents Europe's highest concentration of precipitation.

Key words: concentration index, daily concentration, precipitation, Spain.

1. INTRODUCTION

As is known, much of Spain presents a Mediterranean climate, with numerous varieties, from the coastal ones to the continental influence of the Meseta or the Ebro Valley or the arid southeast, among others. Excluded from the classification as Mediterranean climate is a zone to the north which includes much of Galicia, Asturias, Cantabria, the Basque coastal provinces and the western and central Pyrenees as far as the Arán Valley (Martín Vide and Olcina, 2001). This climatic boundary is also a geographical one, and clearly comprises the Cantabrian Mountains and to the west and east the León Mountains and the Pyrenees, respectively. Some problems arise on attempting to represent this boundary with climatic indices. For a start, the annual pluviometric total is of no use because, considering that the Mediterranean climate is quite dry compared with that of the Iberian Peninsula's northern zone, which is of the mid-latitude oceanic type, there

are numerous sectors within the broad scope of the Mediterranean climate presenting a mean annual rainfall similar to that of the north of Spain. Thus, the southern slopes of the Central Mountains in the central and western sectors, as in the north of Cáceres, the Grazalema Mountains in Cádiz, as well as other areas, present an annual rainfall rate hgher than one thousand, or even two thousand millimetres and they are therefore some of Spain's rainiest environments. But even in the lowlands, like in the south of the province of Valencia, mean annual precipitation can exceed 800 mm and should therefore be assigned to the rainy type in the basic division of the Iberian Peninsula into three classifications: rainy, dry and semiarid. All of these environments are clearly Mediterranean from the perspective of ecology, landscape, culture, etc., although the altitude factor adds an orographic component to the precipitation, or the orientation of the coast favours the pluviometric resolution of the wet flows. Mediterranean climate and pluviometry cannot be defined by a mere pluviometric total. What, then, is the best criterion to define Mediterranean pluviometry or climate within the Iberian scope? Undoubtedly, it is interannual pluviometric variability expressed by means of the coefficient of variation of annual rainfall (CV). A CV of 20%, or very slightly higher, demarcates without exceptions the boundary between the Mediterranean and mid-latitude oceanic climates on the Iberian Peninsula (Martín-Vide, 2011). Mediterranean Peninsular Spain exceeds 20% of interannual pluviometric variability. That is to say, Mediterranean precipitation and climate in general are characterised, in all places, by a sharp contrast between the annual totals, with clearly dry ones and some markedly rainy.

On the Iberian Peninsula, interannual pluviometric variability increases from north to south, in accordance with the strengthening of Mediterraneity or of subtropicality towards the south. In the same direction, too, there is an increase in the mean length of the sequences or dry spells, another variable that somewhat distinguishes the Mediterranean climates from the mid-latitude maritime ones. Thus, the CV maps and those representing the mean length of the dry sequences show isopleths or zonal areas with increasing values from north to south. This pattern can be seen in other Mediterranean-climate regions of the world (California, Chile's Central Region, South Africa's southernmost area and two sectors in southern Australia). All these regions, framed within just over 30º and a little over 40º latitude, are located to the west of the continents or face westwards, with the ocean on this route. The only exceptions are, precisely, the eastern façades of the peninsulas of the Mediterranean basin, such as the Iberian eastern slope, in which the closest sea is to the east. This purely geographical fact gives rise to certain unique pluviometric features on the Iberian Peninsula, among which we can highlight a high degree of torrentiality.

2. DAILY CONCENTRATION OF PRECIPITATION: CONCEPT AND CALCULATION PROCEDURE

In practically all climates the distribution of frequencies of daily amounts of precipitation shows a high percentage thereof in the lower classes and few in the upper ones. That is to say, there are many rainy days with small amounts and a few with high values. In this sense, it is known that the distribution of frequencies of daily amounts of precipitation can be adjusted by means of negative exponential curves (Brooks and Carruthers, 1953). In order to evaluate the relative contribution of the rainiest days, Martín-Vide (2004) proposed an index of daily concentration of

precipitation (*Concentration Index*, CI), similar to Gini's index, applied to what is known in Statistics as Lorenz curves. To this end, the daily precipitation amounts are classified into classes of length of , starting with [0.1-0.9], in increasing order, [1.0-1.9], [2.0-2.9], etc. The resulting histogram of distribution of frequencies clearly shows a negative exponential form. One now proceeds in the manner summarised in table which the example of is presented (1951-2010 period). The first column contains the above mentioned classes, or their upper limits, up to the one containing the highest recorded daily rainfall amount, and the second one contains the midpoints of the classes. The third column, n_i , indicates the absolute frequencies of each class and the fourth one, Σn_i , the accumulated absolute frequencies, this final value being the total number of days of precipitation of the whole study period. The values of the fifth column, P_i are obtained by multiplying, class by class, those of the second column by those of the third one, thus providing the total amount of rainfall contributed by each class (approximately, given that each value has been substituted by the midpoint of the class). The sixth column, ΣP_i , contains the values accumulated from the previous column, the value of the last class being the total amount of rainfall recorded during the study period. Lastly, the seventh and eighth columns indicate the percentages of the values of the fourth and sixth columns, in relation to the values of their last rows, respectively, Σn_i (%) = X and ΣP_i (%) = Y. Thus, in the 60 years of the period analysed in , there have been 3,651 days of rain (those with a negligible amount or less than are excluded) which represent –values of the last row of the fourth and sixth columns or of the third and fifth columns of the row sum-. We recorded 1,380 days with an amount ranging from 0.1 to inclusive, which represented , which means that 37.8% of the rainy days only accounted for 3,% of the total amount. The days with a quantity less than accounted for over half the total, 52.8%, providing only 7.4% of the total accumulated. The rainiest day received an amount of between 270.0 and 270.9 mm.

Representation of the values of the final columns (X, Y) gives rise to a polygonal line with a positive exponential appearance, known as a concentration curve or Lorenz curve. It can be used to calculate Gini's index (GI). Figure 1 shows two concentration curves, or Lorenz curves, with appreciably different Gini's indices.

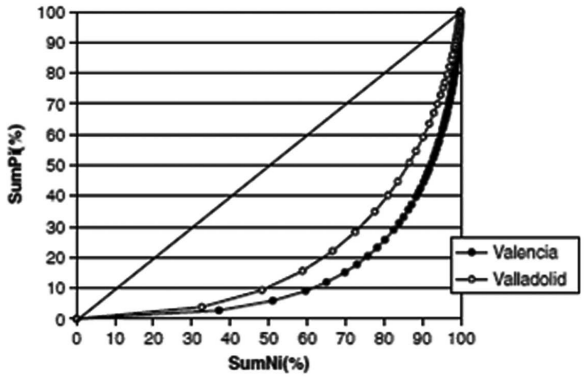

Figure 1. Concentration curves, or Lorenz curves, for Valencia and Valladolid, for the 1951-1990 period. The biggest separation of the equidistribution line for Valencia shows a higher degree of daily rainfall concentration than in Valladolid. (Source: Martín-Vide (2004)).

Table 1. Example of the previous calculations used to obtain the concentration index, CI (and Gini's index, GI). The case of Alicante for the 1951-2010 period (Source: Benhamrouche and Martín-Vide (2012)).

Upper lim.	*ma*	*ni*	*Σ ni*	*Pi*	*Σ Pi*	*Σni(%)=X*	*ΣPi (%)=Y*
0.9	0.5	1,380	1,380	690	690	37.80	3.38
1.9	1.5	547	1,927	820.5	1,510.5	52.78	7.41
2.9	2.5	318	2,245	795	2,305.5	61.49	11.31
3.9	3.5	239	2,484	836.5	3,142	68.04	15.41
4.9	4.5	151	2,635	679.5	3,821.5	72.17	18.74
5.9	5.5	136	2,771	748	4,569.5	75.90	22.41
6.9	6.5	101	2,872	656.5	5,226	78.66	25.63
7.9	7.5	85	2,957	637.5	5,863.5	80.99	28.75
8.9	8.5	92	3,049	782	6,645.5	83.51	32.59
9.9	9.5	63	3,112	598.5	7,244	85.24	35.52
10.9	10.5	50	3,162	525	7,769	86.61	38.10
11.9	11.5	41	3,203	471.5	8,240.5	87.73	40.41
12.9	12.5	43	3,246	537.5	8,778	88.91	43.05
13.9	13.5	32	3,278	432	9,210	89.78	45.17
14.9	14.5	25	3,303	362.5	9,572.5	90.47	46.94
15.9	15.5	27	3,330	418.5	9,991	91.21	49.00
16.9	16.5	26	3,356	429	10,420	91.92	51.10
17.9	17.5	22	3,378	385	10,805	92.52	52.99
18.9	18.5	23	3,401	425.5	11,230.5	93.15	55.07
19.9	19.5	22	3,423	429	11,659.5	93.76	57.18
20.9	20.5	12	3,435	246	11,905.5	94.08	58.38
21.9	21.5	10	3,445	215	12,120.5	94.36	59.44
22.9	22.5	17	3,462	382.5	12,503	94.82	61.31
23.9	23.5	11	3,473	258.5	12,761.5	95.12	62.58
24.9	24.5	15	3,488	367.5	13,129	95.54	64.38
25.9	25.5	11	3,499	280.5	13,409.5	95.84	65.76
26.9	26.5	12	3,511	318	13,727.5	96.17	67.32
27.9	27.5	13	3,524	357.5	14,085	96.52	69.07
28.9	28.5	6	3,530	171	14,256	96.69	69.91
29.9	29.5	6	3,536	177	14,433	96.85	70.78
30.9	30.5	4	3,540	122	14,555	96.96	71.38
31.9	31.5	7	3,547	220.5	14,775.5	97.15	72.46
32.9	32.5	9	3,556	292.5	15,068	97.40	73.89
33.9	33.5	5	3,561	167.5	15,235.5	97.53	74.7
34.9	34.5	4	3,565	138	15,373.5	97.64	75.39
35.9	35.5	6	3,571	213	15,586.5	97.81	76.44

Upper lim.	*ma*	*ni*	*Σ ni*	*Pi*	*Σ Pi*	*Σni(%)=X*	*ΣPi (%)=Y*
36.9	36.5	5	3,576	182.5	15,769	97.95	77.33
37.9	37.5	4	3,580	150	15,919	98.06	78.07
38.9	38.5	3	3,583	115.5	16,034.5	98.14	78.63
39.9	39.5	5	3,588	197.5	16,232	98.27	79.60
40.9	40.5	6	3,594	243	16,475	98.44	80.79
42.9	42.5	6	3,600	255	16,730	98.60	82.04
43.9	43.5	1	3,601	43.5	16,773.5	98.63	82.26
44.9	44.5	3	3,604	133.5	16,907	98.71	82.91
45.9	45.5	3	3,607	136.5	17,043.5	98.79	83.58
46.9	46.5	3	3,610	139.5	17,183	98.88	84.27
47.9	47.5	2	3,612	95	17,278	98.93	84.73
49.9	49.5	1	3,613	49.5	17,327.5	98.96	84.97
51.9	51.5	1	3,614	51.5	17,379	98.99	85.23
52.9	52.5	3	3,617	157.5	17,536.5	99.07	86.00
53.9	53.5	2	3,619	107	17,643.5	99.12	86.52
54.9	54.5	4	3,623	218	17,861.5	99.23	87.59
55.9	55.5	2	3,625	111	17972.5	99.29	88.14
56.9	56.5	1	3,626	56.5	18,029	99.32	88.41
58.9	58.5	1	3,627	58.5	18,087.5	99.34	88.70
59.9	59.5	3	3,630	178.5	18,266	99.42	89.58
61.9	61.5	2	3,632	123	18,389	99.48	90.18
63.9	63.5	1	3,633	63.5	18,452.5	99.51	90.4
65.9	65.5	2	3,635	131	18,583.5	99.56	91.13
67.9	67.5	1	3,636	67.5	18,651	99.59	91.46
68.9	68.5	1	3,637	68.5	18,719.5	99.62	91.80
75.9	75.5	2	3,639	151	18,870.5	99.67	92.54
79.9	79.5	1	3,640	79.5	18,950	99.70	92.93
85.9	85.5	1	3,641	85.5	19,035.5	99.73	93.35
90.9	90.5	3	3,644	271.5	19,307	99.81	94.68
99.9	99.5	1	3,645	99.5	19,406.5	99.84	95.1
109.9	109.5	1	3,646	109.5	19,516	99.86	95.71
119.9	119.5	1	3,647	119.5	19,635.5	9 9.89	96.29
131.9	131.5	1	3,648	131.5	19,767	99.92	96.94
133.9	133.5	1	3,649	133.5	19,900.5	99.95	97.5
220.9	220.5	1	3,650	220.5	20,121	99.97	98.67
270.9	270.5	1	3,651	270.5	20,391.5	100.00	100.00
Sum		***3651***		***20,391.5***			

However, the previous method can be perfected by adjusting the empirical distribution of the precipitation percentages provided by the corresponding percentages of the number of days of rain by means of exponential curves of the $Y=axe^{bx}$ type (Guilló and Puigcerver, 1970). Thus, an index similar to Gini's can be defined on the exponential curve. The concentration index (*Concentration Index,* CI) is defined as the quotient between the area (S) demarcated by the equidistribution line, the exponential fit curve and x=100, and the area of the triangle defined by the equidistribution line, the abscises axis and x=100, which is 5,000,

$$CI = S/5{,}000$$

With ideal extreme values of 0 (all the daily amounts equal) and 1 (one single day of precipitation). It should be noted that the higher the value of CI, the greater the weight of a small amount of very rain days in the pluviometric total.

The constants a and b of the exponential curve are determined by means of squared minimums in the following manner:

$$\ln a = \frac{\sum X_i^2 \sum \ln Y_i + \sum X_i \sum X_i \ln X_i - \sum X_i^2 \sum \ln X_i - \sum X_i \sum X_i \ln Y_i}{N \sum X_i^2 - \left(\sum X_i\right)^2}$$

$$b = \frac{N \sum X_i \ln Y_i + \sum X_i \sum \ln X_i - N \sum X_i \ln X_i - \sum X_i \sum \ln Y_i}{N \sum X_i^2 - \left(\sum X_i\right)^2}$$

It should be mentioned that the CI is highly sensitive to data quality. If in an observatory, the smallest amounts, several tenths of a mm (excluding negligible values) have not been considered or recorded, or if the amounts of two consecutive days have been combined, the CI value obtained will be anomalous, generally lower than what would correspond if all the daily data had been considered. In this case we have to do without the observatory. In order to "save" observatories, one can analyse the daily concentration with classes of 5 mm or of 10 mm. With the aforementioned calculation procedure, daily concentration indices can be found with the use of exponential curves of the same type and classes of 5 mm, which can be called CI5, and of 10 mm, CI10. Gini's indices can also be calculated using the empirical values (X, Y) of classes of 5 mm, which can be termed GI5, and of 10 mm, GI10. The values of GI5, GI10 and GI, hereinafter GI1, will verify GI1 > GI5 > GI10, because with classes of 5 mm we convert into linear sections of the exponential polygonals of the analysis with 1 mm classes. The same occurs when we employ 10 mm classes in relation to the 5 and 1 mm ones. Likewise, CI1 > CI5 > CI10 must generally be fulfilled (CI1 being the previously defined CI).

The observatories analysed present very high and significant (and naturally positive) values of Pearson's correlation coefficient between CI1, and CI5 and CI10 (0.98 and 0.95, respectively) and an almost perfect correlation with GI1 (0.998). On the contrary, the correlations of CI1, with GI5 and GI10 are modest (0.59 and 0.40,

respectively). Consequently, it is perfectly correct to use concentration indices CI5, CI10 and GI1 as alternatives to CI1. In the cases of CI5 and CI10 the values are naturally lower but the spatial patterns must be very similar to those of CI1 and GI1.

The methodology described herein in relation to the CI or CI1 has been applied, following the article by Martín-Vide (2004), in different countries and regions, as well as throughout the Iberian Peninsula (Sánchez Lorenzo and Martín-Vide, 2006), in Iran (Alijani *et al.,* 2008), in the Pearly River Basin in China (Zhang *et al.,* 2009), on the Malaysian Peninsula (Suhaila and Jemain, 2012), etc., and the results thereof enable daily concentration of precipitation in Spain to be suitably addressed and appraised.

3.VALUES OF DAILY PRECIPITATION CONCENTRATION AND ITS SPATIAL PATTERNS IN PENINSULAR SPAIN

To analyse the concentration of daily rainfall in peninsula Spain we selected 32 first class meteorological stations belonging to the AEMET network and presenting high-quality daily records with a reasonable coverage of the territory. The values of the concentration index CI and of the other correlated indices for the 1951-2010 period are presented in Table 2.

Table 2. Values of the indices CI1, CI5, CI10 and GI1 from 32 meteorological stations in peninsular Spain for the 1951-2010 period (Source: Benhamrouche and Martín-Vide (2012)).

Meteor.stations	*CI=CI1*	*CI5*	*CI10*	*GI1*
Albacete	0.60	0.54	0.50	0.61
Alicante	0.68	0.62	0.58	0.69
Almería	0.63	0.57	0.51	0.64
Ávila	0.59	0.52	0.48	0.60
Barcelona	0.65	0.60	0.55	0.66
Burgos	0.59	0.52	0.47	0.59
Cáceres	0.58	0.53	0.48	0.58
Ciudad Real	0.57	0.51	0.48	0.57
Córdoba	0.59	0.54	0.51	0.59
Cuenca	0.57	0.51	0.46	0.57
Gerona	0.63	0.59	0.55	0.64
Gijón	0.60	0.54	0.50	0.60
Granada	0.57	0.51	0.47	0.57
Huelva	0.60	0.55	0.51	0.60
Huesca	0.60	0.54	0.50	0.61
La Coruña	0.57	0.51	0.47	0.57
León	0.57	0.51	0.48	0.58

Meteor.stations	*CI=CI1*	*CI5*	*CI10*	*GI1*
Logroño	0.60	0.54	0.49	0.61
Madrid	0.60	0.52	0.47	0.60
Murcia	0.67	0.61	0.56	0.68
Orense	0.57	0.52	0.47	0.58
Pamplona	0.59	0.54	0.50	0.60
Salamanca	0.57	0.51	0.47	0.58
San Fernando	0.60	0.55	0.51	0.61
San Sebastián	0.60	0.54	0.50	0.60
Sevilla	0.59	0.55	0.50	0.59
Soria	0.57	0.51	0.46	0.58
Tortosa	0.69	0.64	0.59	0.70
Valencia	0.69	0.65	0.60	0.70
Valladolid	0.59	0.52	0.47	0.59
Vigo	0.59	0.54	0.51	0.58
Zaragoza	0.62	0.56	0.52	0.63

The highest CI values for the 1951-2010 period are those for Valencia and Tortosa (0.69), followed by Alicante (0.68) and Murcia (0.67), and therefore the centre of the eastern façade of the Iberian Peninsula, from the mouth of the river Ebro to the north of the province of Alicante, is the area presenting the highest daily concentrations, a fact already determined in the work of Martín-Vide (2004) for the 1951-1990 period, and of Sánchez Lorenzo and Martín-Vide (2006). The lowest values, 0.57, are found in parts of the northern Meseta (Salamanca and Soria), the southern Meseta (Cuenca and Ciudad Real), the 'hoya' of Granada and the northwest (La Coruña, Orense and León). As a reference, and only approximately, a CI of 0.61 tends to be the equivalent of 25% of the rainiest days providing 70% of the annual total, this percentage increasing to 75% for a CI of 0.67, and to 80% for a CI of 0.70.

Figure 2 shows the CI map corresponding to the 1951-1990 period, where one can clearly see a concentration of isopleths with a high gradient, individualising the eastern façade of the Iberian Peninsula and where daily concentration is high, albeit moderate in the rest of the country. Isopleth 0.70 appears because in this period Valencia reaches this value, and isopleth 0.71 is insinuated at the boundary between the provinces of Valencia and Alicante. The initial study by Martín-Vide (1987) highlights the vicinity of Cape Nao or, more accurately, the section between the south of the province of Valencia and the north of Alicante as the sector likely presenting the highest daily rainfall concentration on Spain's Mediterranean coast, which would coincide with the area of highest daily and hourly pluviometric intensities in the country (Elías Castillo and Ruiz Bertrán, 1979). As is known, the highest values for daily precipitation in Spain are in Oliva (Valencia), with 817 mm,

on November 3rd 1987, a fact that is now considered as dubious by the AEMET, although in nearby Gandía (Valencia) there is evidence that rainfall exceeded 700 mm, reaching one thousand in 36 hours during the same episode (In one record of the National Meteorological Service, the forerunner of the AEMET, corresponding to Jávea, very close to the aforementioned cape, a value of 871 mm was recorded in October 1957, this datum never being officially recognised).

At the other extreme, in Figure 2 isopleth 0.55 appears in Orense, because this observatory presented this CI value during the 1951-1990 period, whereas the former isopleth, along with isoplete 0.54, in Malaga are mere a graphic artefact resulting from the cartographic programme used.

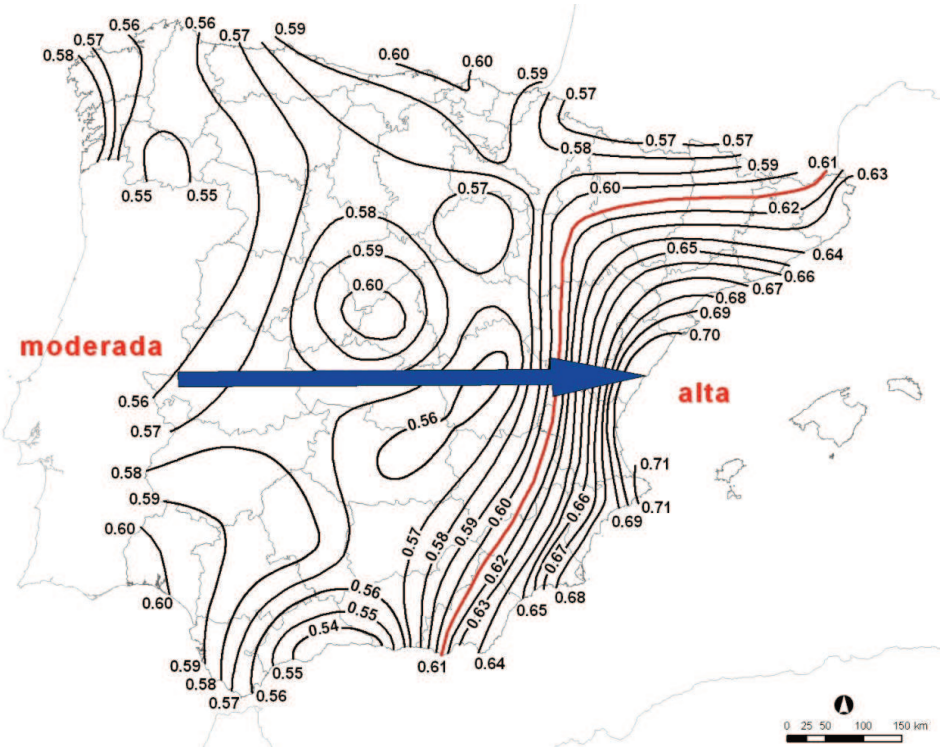

Figure 2. Isopleths of the CI in Peninsula Spain, from 32 observatories, for the 1951-1990 period. (Source: Martín-Vide (2004)).

The CI map implies a non-zonal pluviometric regionalisation of the Iberian Peninsula, with isopleths presenting a meridian arrangement in the east, opposite to the zonal basic regionalizations of other pluviometric indices such as interannual pluviomentric variability, expressed with the variation coefficient, or the duration of spells of consecutive dry days. In these cases –as has been pointed out- the fundamental spatial pattern is an increase in values from the north to the south of the Iberian Peninsula, in accordance with the increase in Mediterraneity or subtropicality of the climate (Martín Vide, 2011). On the contrary, the spatial pattern

of daily concentration is quite different, reflecting the influence of the Mediterranean Basin, which shows an increase from west to east.

The indices of daily concentration of precipitation do not express the same as the variable daily intensity of precipitation or even less as the hourly, minute or instantaneous intensity, quotients between amount and period of time of the record (dP/dt for the instantaneous intensity). The concentration indices appraise, in some manner, the imbalance between the contribution of many daily small amounts of rainfall and the contribution of the few higher distribution values. Thus, they likely reflect aspects of rainfall torrentiality not directly linked to the magnitude of the amounts, but rather, for instance, to the erosive capacity of the precipitation. This does not only depend upon certain high pluviometric records, but also upon the type of environment, with greater or lesser degrees of aridity, finally resulting from the set of pluviometric records. As complementary texts regarding the significance of daily precipitation in the case of Spain or its regions, the reader can consult the works of Gallego *et al.* (2006), Beguería *et al*. (2009), Burgueño *et al*. (2010), Rodrigo (2010) and González-Hidalgo *et al*. (2011), among others.

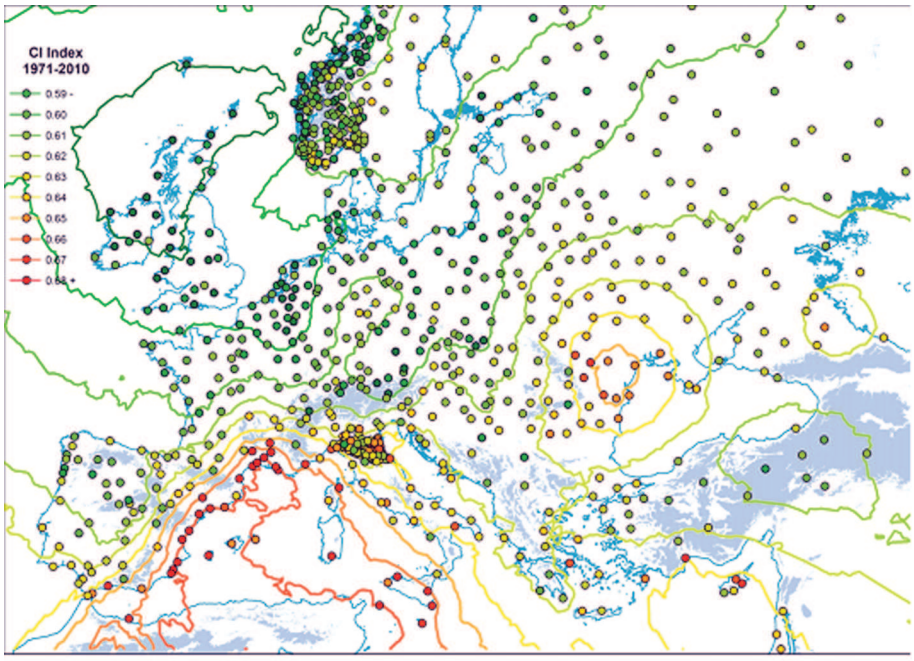

Figure 3. Values of the CI for Europe, from 530 observatories, for the 1971-2010 period. (Source: Cortesi *et al*., 2012)).

4. VALUES OF DAILY PRECIPITATION CONCENTRATION IN SPAIN IN RELATION TO THAT OF OTHER REGIONS

Research into daily precipitation concentration conducted with the same

methodology in recent years in other countries and territories enable us to start appraising whether the CI values found for the eastern façade of the Iberian Peninsula are truly high. The most valuable reference study is related to Europe (Cortesi *et al.*, 2012) and analysed 530 series of daily data for the 1971-2010 period, including several Spanish observatories and the comparison is therefore highly reliable. Figure 3 shows the CI values of this study for Europe. It can be seen that the highest daily precipitation concentration on the continent is precisely on the east coast of the Iberian Peninsula, the south of France and other points of the western Mediterranean basin, in general over 0.68. This clearly contrasts with the British Islands, the Netherlands and Norway, which usually present a value of below 0.59. The extreme values are in Perpignan (France), at 0.72, and Kirkwall (United Kingdom), at 0.51. Indeed, an imaginary diagonal line could be drawn from northern Portugal to the Baltic Republics, to the northwest of which daily concentration is low, whereas to the south it is moderate or high.

Daily concentration of precipitation in Europe is well correlated with annual number of rainy days (Pearson's $r = -0.68$, $p < 0.01$), so that, the higher the number of rainy days, the lower the pluviometric concentration, but the daily concentration is not well correlated with the annual total (Pearson's r =-0,31).

In relation to other planetary environments, the daily concentration of precipitation on the eastern façade of the Iberian Peninsula can be considered to be high, clearly greater than that of the Malaysian Peninsula (Suhaila and Jemain, 2012), but lower than that of the Pearly River Basin in China (Zhang *et al.*, 2009), with sharp contrasts among amounts, likely due to the occurrence of typhoons.

5. CONCLUSIONS

1) The daily precipitation concentration index (CI), defined in a similar way as Gini's, based upon the distribution of daily amounts of rainfall into 1 mm long classes, but using exponential curves of the $y=axe^{bx}$ type (Martín-Vide, 2004), values the weight of the rainiest days in the annual total, thus reflecting the torrentiality of the precipitation.

2) In peninsular Spain, the area with highest CI values is the eastern façade, particularly from the mouth of the river Ebro to the north of the province of Alicante where, depending on the period analysed, 0.70 is reached in several points, which is about equivalent to 25% of the rainiest days contributing 80% of the annual total. The lowest values correspond to points in the northwest and inland on the peninsula, with a CI of 0.57 or somewhat lower.

3) The location of the highest CI values in Spain coincides with the area of highest daily and hourly precipitation intensity, i.e., between Valencia and northern Alicante.

4) The eastern façade of the Iberian Peninsula is, together with the south of France and other points in the western Mediterranean Basin, the zone presenting the highest daily rainfall concentration in Europe. The CI values on the eastern façade of the Iberian Peninsula are, compared with those of other planetary regions studied, high, although they are not the highest ones recorded.

REFERENCES

Alijani, B., O'Brien, J. and Yarnal, B. (2008): Spatial analysis of precipitation intensity and concentration in Iran. *Theoretical Applied Climatolology*, 94, 107–124.

Beguería, S., Vicente-Serrano, S.,López-Moreno, J.I. and García-Ruiz, J.M. (2009): Annual and seasonal mapping of peak intensity, magnitude and duration of extreme precipitation events across a climatic gradient, northeast Spain. *International Journal of Climatology*, 29, 1759–1779.

Benhamrouche, A. and Martín Vide, J.(2012) Avances metodológicos en el análisis de la concentración diaria de la precipitación en la España peninsular. *Anales de Geografía*, 32, 1, 11-27.

Brooks, C.E.P. and Carruthers, N. (1953): *Handbooks of statistical methods in Meteorology*. Londres, Meteorological Office.

Burgueño, A., Martínez, M., Serra, C. and Lana, X. (2010): Statistical distributions of daily rainfall regime in Europe for the period 1951–2000. *TheoreticalAppliedClimatolology*, 102, 213–226.

Elías Castillo, F. and Ruiz Bertrán (1979): *Precipitaciones máximas en España*. Servicio de publicacionesagrarias, Ministerio de Agricultura.

Gallego, M. C., García, J. A., Vaquero, J. M. and Mateos, V. L. (2006): Changes in frequency and intensity of daily precipitation over the Iberian Peninsula, *Journal of Geophysical Research*, 111, D24105, doi: 10.1029/2006JD007280.

González-Hidalgo, J. C.,Cortesi, N., and Brunetti, M. (2011): Monthly contribution of largest daily events of precipitation (1956–2005) across Mediterranean basin. *GeophysicalResearchAbstracts*, 13, EGU2011-4182.

Guilló, A.M. and Puigcerver, M. (1970): Sobre las contribuciones relativas de las precipitaciones local y generalizada a la precipitación total en Cataluña. *Revista de Geofísica*, XXIX, 3, 205-216.

Martín Vide , J. (1987): *Característiquesclimatològiques de la precipitació en la franja costera mediterrània de la Península Ibèrica*, Barcelona, InstitutCartogràfic de Catalunya.

Martin-Vide, J. (2004): Spatial distribution of daily precipitation concentration index in Peninsular Spain. *International Journal of Climatology*, 24, 959-971.

Martín Vide, J. (2011): Estructura temporal fina y patrones espaciales de la precipitación en la España peninsular. *Memorias de la Real Academia de Ciencias y Artes de Barcelona*, LXV, 3, 119-162.

Martín Vide, J. and Olcina, J. (2001): Climas y tiempos de España, Madrid, Alianza Editorial.

Rodrigo, F.S. (2010): Changes in the probability of extreme daily precipitation observed from 1951 to 2002 in the Iberian Peninsula. *International Journal of Climatology*, 30, 1512–1525.

Sánchez-Lorenzo and Martín-Vide, J. (2006): Distribución espacial de la concentración pluviométrica diaria en la Península Ibérica. *5ª AsambleaHispanoportuguesa de Geodesia y Geofísica*, Sevilla.

Zhang, Q., Xu, C.Y., Gemmer M., Chen Y.Q. and Liu C.L. (2009): Changing properties of precipitation concentration in the Pearl River basin, China. Stochastic *Environ. Res. Risk Assess*. 23, 377–385.

CHAPTER 11

HEAVY PRECIPITATION AND ATMOSPHERIC TELECONEXION PATTERNS OVER THE SOUTHERN IBERIAN PENINSULA

José Manuel HIDALGO MUÑOZ, Sonia Raquel GÁMIZ-FORTIS,

María Jesús ESTEBAN PARRA, Yolanda CASTRO-DÍEZ

Depto. de Física Aplicada. Facultad de Ciencias. Universidad de Granada
jhidalgo@ugr.es, srgamiz@ugr.es, esteban@ugr.es, ycastro@ugr.es

ABSTRACT

This work studies the atmospheric patterns associated with heavy precipitation events in the south of the , and the relationship between them and two of the main large-scale circulation indices affecting the precipitation over this area: the North Atlantic Oscillation (NAO) and the Western Mediterranean Oscillation (WeMO). The analysis has been made using 86 stations with daily precipitation records for the period 1955-2006. The main synoptic configurations at the surface level related to heavy rainfall days were found by using a Principal Component Analysis (PCA) in T-mode. Composites of Sea level Pressure and 500 hPa Geopotential Height associated with these main configurations have been analysed. In addition, the inter-annual and intra-annual distribution of the atmospheric patterns has been also analyzed and its variation in two subperiods (1955-1980 and 1981-2006) has been examined. The main results indicate a reduction in the number of occurrences of patterns bringing advection from the Atlantic Ocean, and an increase of a pattern carrying humid winds from the . In addition, it is shown that heavy rainfall days associated with these patterns tend to be grouped in autumn during 1981-2006 instead in winter (as happened in 1955-1980). Finally, most of the synoptic patterns were related to highly negative WeMO values, whereas only some of the patterns were linked with high negative values of NAO index.

Key words: extreme precipitation, atmospheric patterns, Iberian Peninsula, NAO, WeMO.

1. INTRODUCTION

The question of whether an intensified hydrological cycle may increase the frequency and intensity of extreme precipitation events has been specifically addressed in recent years, because of their impact on the economy, environment

and society, in terms of losses associated with their occurrence. In particular, understanding the atmospheric mechanisms controlling heavy rainfall is necessary for assessing natural hazard risk and for developing strategies of mitigation and response to these extreme events.

Addressing the atmospheric mechanisms related to extreme precipitation events over different areas of the Iberian Peninsula (IP) has claimed the attention of several researches (Lana *et al*., 2001; Fragoso and Gomes, 2008; Penarrocha *et al*., 2002; Romero *et al*., 1999; Hidalgo-Muñoz *et al*., 2011). In particular, this study focus on the south of IP, an interesting area because of its situation in a transition zone between different climate domains, the influence of two large water masses (the Mediterranean Sea and the Atlantic Ocean) and its complex topography (with mountain ranges reaching in Sierra Nevada), an interior depression (the Guadalquivir Valley) and steep elevation gradients with more than in), which favours the occurrence of heavy precipitation events. The North Atlantic Oscillation (NAO) is the dominant mode of winter climate variability in the North Atlantic region, which has important impacts on the weather and climate of this region and surrounding continents, especially . In particular, the NAO has been identified as the main large-scale phenomenon controlling winter precipitation over western and central of IP (Hurrell and VanLoon, 1997; Trigo *et al*., 2004). It is a large-scale seesaw in atmospheric mass between subtropical high and polar low. The positive phase of the NAO shows a deeper than normal Iceland Low pressure centre and a stronger than normal subtropical high is stronger than normal. Negative phase shows the opposite situation of pressure centres. On the positive (negative) phase, the increased (reduced) pressure difference results in more and stronger (fewer and weaker) winter storms crossing the Atlantic Ocean on a more northerly (west-east) track, producing warm (cold) and wet (dry) winters in Europe. Specifically for the IP, the negative (positive) phase of winter NAO is related to above (below) normal precipitation anomalies over central and western areas.

The nature of the precipitation on the east of the IP is mainly convective and the moist air is driven by easterly flows (Romero *et al*., 1999), and is poorly related to NAO phenomenon. In order to find an atmospheric index which presents a better relationship with precipitation on this area, Martín-Vide and López-Bustin (2006) defined the Western Mediterranean Oscillation (WeMO) index. This index is based on the pressure values in two locations, Padua, in the north of Italy, an area with relatively high barometric variability and San Fernando, in the Gulf of Cádiz (southwest of Spain), often subject to the influence of the Azores anticyclone.. This index has been widely applied in studies regarding rainfall in the IP, in particular on the eastern façade of the IP (Martín-Vide *et al*., 2008; López-Bustins *et al*., 2008; Vicente-Serrano *et al*. 2009; Hidalgo-Muñoz *et al.,* 2011).

This study is an attempt to improve the understanding of the dynamical mechanisms that produce these heavy rainfall episodes in the south of the IP, and also evaluate possible variations in its occurrence during the period 1955-2006. The relationship of the NAO and WeMO teleconnection indices with these heavy rainfall events and its associated synoptic patterns was been also addressed.

2. DATA

2.1 Precipitation data

The daily precipitation data used in this study has been compiled from the website (http://www.juntadeandalucia.es/medioambiente/servtc5/WebClima/) of the Government of Andalusia (*Subsistema de Climatología Ambiental, Consejería de Medio Ambiente, Junta de Andalucía*). Series with less than 10% of missing values for period 1955-2006 has been selected for this study. This period resulted from a balance between the number of almost complete (maximum of 10% of missing data) series and the length of the period. These data series overcame a quality control in order to detect inhomogeneities, which was based in identification of suspicious records, such as extremely high or negative values, and the application of a homogeneity test following the guidance provided by the joint CCI/CLIVAR/JCOMM Expert Team (TE) on Climate-Change Detection and Indices (ETCCDI) (http://etccdi.pacificclimate.org/indices.shtml). The software used for this purpose was the RHtestV2, which can be freely downloaded from this website, and it allows to detect, and adjust for multiple changepoints (shifts) that could exist in a data series with first order autoregressive errors. More details concerning the theoretical basis of this test can be found in Wang *et al*. (2007, 2008a, 2008b). This quality control was overcome by 86 daily rainfall series, which were acceptably distributed throughout the study area (see Figure 1), covering the period 1955-2006 and presenting less than 10% of missing values.

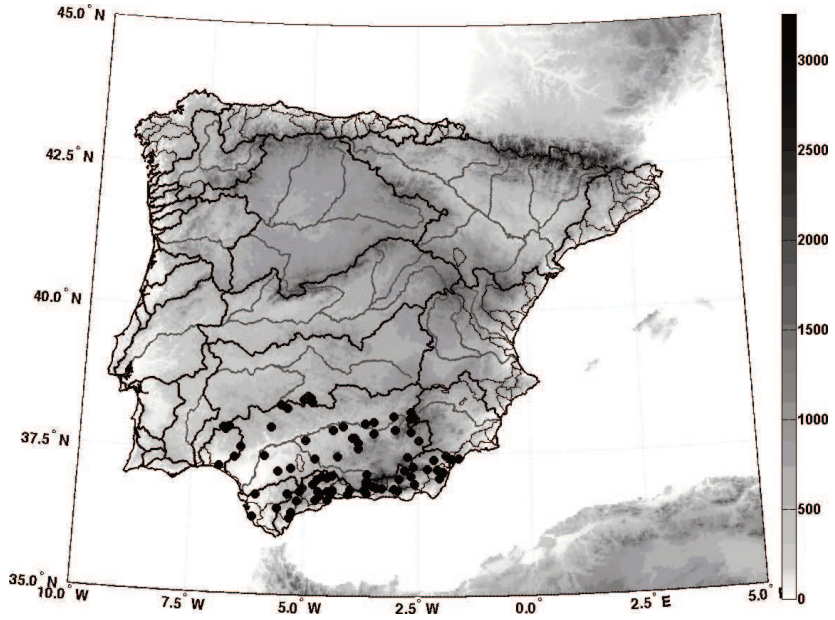

Figure 1. Location of the 86 daily rainfall series used in this study (circles) and topographic features of the IP. Grayscale indicates elevation in m.

2.2 Atmospheric Data

Daily averages for sea-level pressure (SLP) and geopotential height at 500 hPa (HGT500) have been used for the classification of synoptic patterns associated with heavy precipitation events. These data were provided by the NCEP-NCAR reanalysis dataset (Kalnay *et al*., 1996). This is a gridded dataset presenting a resolution of 2.5º latitude x 2.5º longitude for the entire globe, from 1948 until present. Data corresponding to a geographical window defined by 20°N-70°N and 40°W-20°E, and covering the period 1955-2006, have been used for this study.

The daily data series corresponding to the teleconnection indices, the North Atlantic Oscillation (NAO) and the Western Mediterranean Oscillation (WeMO), have been obtained from the Climate Prediction Centre (http://www.cpc.ncep.noaa.gov/) and the website http://www.ub.edu/gc/English/wemo.htm, respectively. Note that, because of daily records for WeMO index end in 2000, the daily WeMO values from 2000 to 2006 were completed using the monthly values.

3. METHODOLOGY

The choice of an appropriate threshold to define a heavy rainfall day is the first stage. Previous studies regarding circulation patterns associated with heavy rainfall days in the Iberian Peninsula (Fragoso and Gomes, 2008; Penarrocha *et al*., 2002; Romero *et al*., 1999; Hidalgo-Muñoz *et al*., 2011) have applied a threshold of around 40, 50 and even 100 mm/day for this purpose. In this study, heavy rainfall days are considered when precipitation records exceed in 4 or more stations (to reduce the importance of local thunderstorms) their respective 95th percentile. A threshold variable for each station has been used instead a fixed threshold because of the spatial variability of precipitation across the study area. For example, a rainfall value of 50 mm could be a rare event in some stations and a normal o moderate event in another ones. The values corresponding to the 95th percentile range between 19.5 mm and 89.4 mm, with an average of 37 mm for all stations. The 95th percentile has been calculated using days with precipitation records greater than 1 mm. Following this criteria, a total of 854 days were identified as heavy rainfall events in the study area for the period 1955-2008.

The second stage consisted in classifying the synoptic patterns related with these heavy rainfall days. For this regard a Principal Components Analysis (PCA) approach (Preisendorfer, 1988), in T-mode, has been applied to the SLP values corresponding to these heavy rainfall days. The PCA is a useful tool to reduce the dimensionality of the data, identifying dominant modes of variability. In this case, the PCA was used in order to distinguish and group days with similar SLP configurations. More details of this technique can be found in Wilks (2006).

Once the main modes of variability (more common SLP configurations in these heavy rainfall days) were identified and retained for further analysis, each day was grouped into the corresponding mode or principal component. It should be also noted that, for each principal component retained, two possible classes could result, the positive and negative phase, respectively (Huth, 1996). The days were sorted into their corresponding class using "the highest factorial loading", in absolute value. Note that the loading factors represent the correlations between the spatial

configuration of the mode and the configuration of the heavy rainfall day. In other words, they represent how similar a SLP configuration of a particular heavy rainfall day is to one of these main modes of variability. After days were grouped into the more representative class, composites of the SLP and HGT500 (using the groups of days identified in PCA) were generated for each ones.

4. RESULTS

The inter-annual and intra-annual variability of the 854 days considered as heavy-precipitation days is displayed in the Figure 2. As regards the inter-annual variability, the Figure 2 shows a slightly decrease in the number of annual events. The annual distribution of the heavy rainfall days reveals a predominance of these events during autumn and early winter, with a progressive decrease in spring to almost disappear in summer.

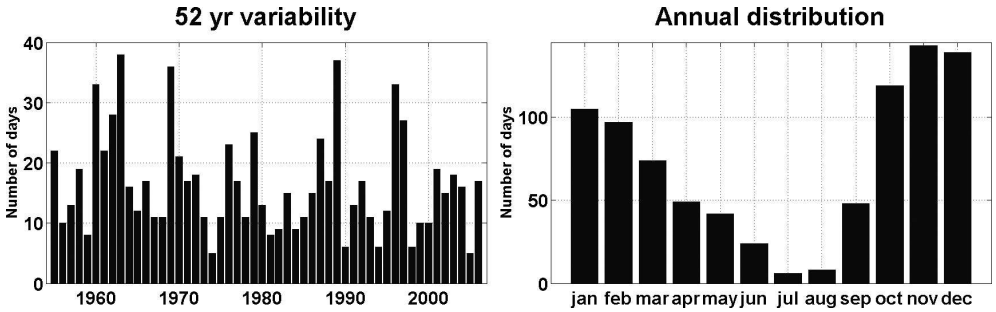

Figure 2. Inter-annual (left) and intra-annual (right) variability of the 854 days identified as heavy rainfall days.

From the PCA to the SLP gridded data corresponding to these 854 days, the first six components, representing variability modes, accounting for 87.29% of the total variance (29.17%, 24.05%, 15.82%, 7.07%, 6.61% and 4.56% respectively), have been retained for the study. Twice the number of retained components was considered as classes (according to their positive and negative phases, respectively). In order to give a general overview of the main patterns, classes with less than 30 days have been excluded from our analysis and their patterns have been not discussed. The composite charts of large-scale atmospheric circulation schemes (on the surface and 500 hPa level) for the selected positive and negative classes are displayed in Figures 3 and 4, respectively. Note that the classes are identified as CLi±, where "i" represents the number of the respective component and "+" or "– " the phase. Therefore, as a result of the dimensionality reduction from PCA, the 854 synoptic charts associated with each heavy rainfall day were reduced to 12 classes, and just 7 of them (classes that group more than 30 days) were analysed.

Additionally, the inter-annual variability of each class has been assessed in order to identify possible variations in the occurrence of this pattern through the study period. In addition, with the aim of evaluating possible changes in the intra-annual

variability of each class, two subperiods were defined, 1955-1980 and 1981-2006, and the annual distribution of days belonging each subperiod was compared for each pattern (Figures 5 and 6, for positive and negative classes, respectively).

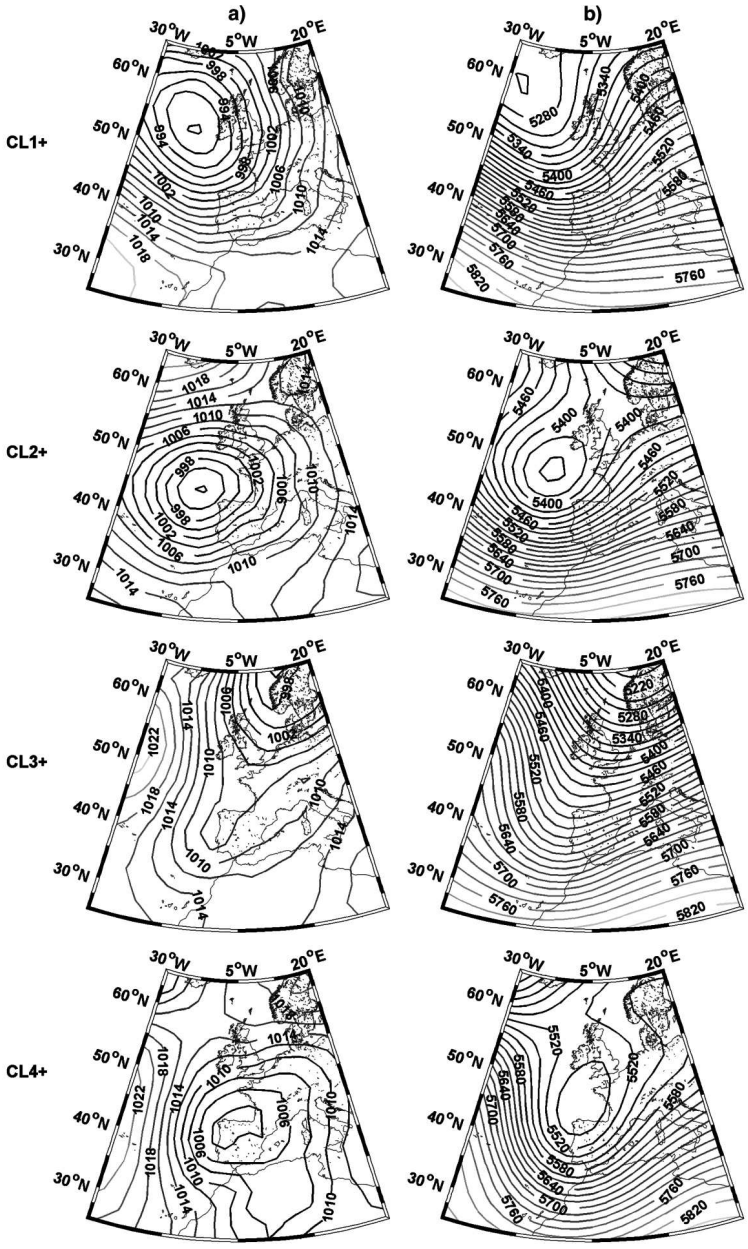

Figure 3. a) Composite charts on surface for the synoptic patterns representative of the positive classes. b) As a), but for 500 hPa level.

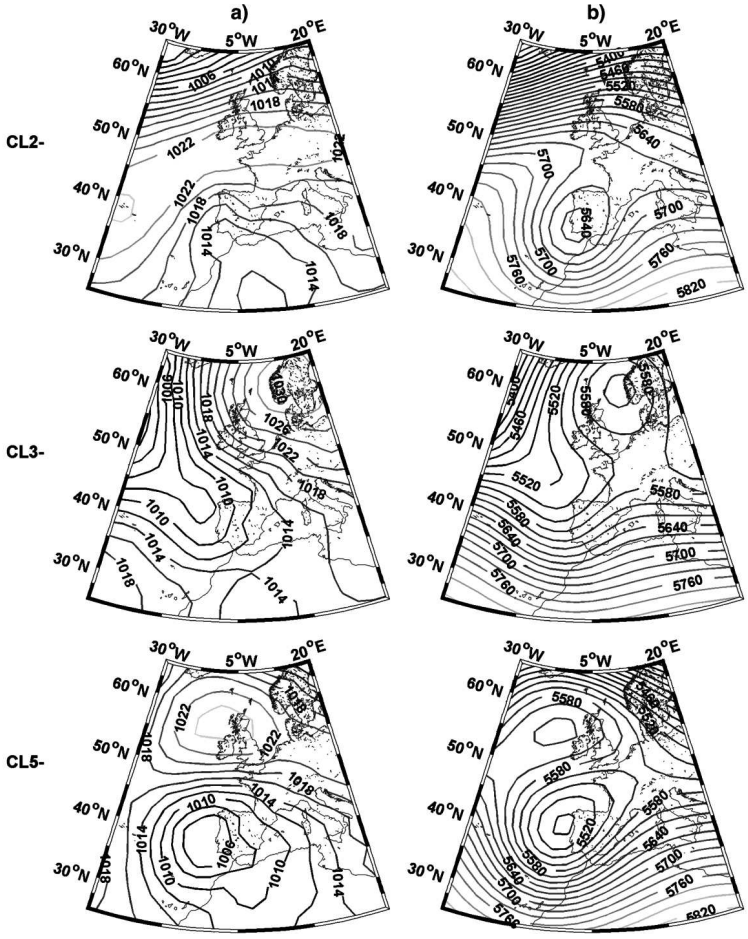

Figure 4. As Figure 3, but for negative classes.

The main features corresponding to each class as summarized as follow:

The CL1+ pattern is the most frequent mode associated with heavy rainfall days in the south of Spain (grouping 238 days from the 854 days defined as heavy rainfall days). The synoptic configuration of this pattern is shown in Figure 3. It is characterized by a deep low in surface, located near to the west coast of Ireland, producing strong western southwestern airflow over the IP. In upper level (500 hPa), the low is displaced northern, near Iceland with strong zonal flow over the IP. From Figure 5 it could be appreciated that this pattern predominates during autumn and winter, although, a decrease in its occurrence during the second half of the study period together with a more (less) frequency during autumn (winter) is also observed. The average NAO index related to the days associated to this pattern shows a slight negative value (-0.29), whereas the WeMO index shows a moderate negative average value (-0.61).

The synoptic configuration of CL2+ shows some similarities with respect the CL1+ pattern, although in this case, the low-pressure centre in surface is located in the northwest coast of the IP, bringing wet flow from south-western into the IP. At 500 hPa level, the configuration is similar to surface, but with stronger zonal wind. This pattern is representative of 110 heavy rainfall days and more frequent during early winter. Also, it presents (Figure 5) a significant reduction in its occurrence in the second half of the period of study (from 73 days before 1980 to 37 days after 1980). This reduction is particularly noticeable in winter months (from January to march), and, similarly to the case of CL1+, during the second half of the study period, it seems to be more frequent in late autumn than in winter (as happened for the 1955-1980 period). High negative averaged values of the NAO and WeMO indices (-1.19 and -1.36, respectively) are shown with this pattern.

The CL3+ pattern presents a weak trough in surface (which is not defined in upper level) with the axis in north-eastern direction over the north-western of the IP and the Gulf of Biscay, bringing south to south-westerly airflow to the IP. This pattern tends to be more frequent in later autumn and February. As for the CL2+ pattern, the number of occurrences of this pattern presents a significant reduction comparing events before 1980 (58 days) and after 1980 (34 days), which became more evident during winter (from January to March) months. NAO and WeMO indices in days associated with this synoptic configuration present moderate negative values (-0.63 and -0.72, respectively).

The CL4+ pattern shows a low-pressure centre in surface over the IP together with a deeper low in upper level over the Gulf of Biscay. This configuration carries westerly winds to the study region. This pattern tends to appear with less frequency than the previous ones (41 days) and mainly in spring. However, its occurrence has diminished in the period 1981-2006 with respect to 1955-1980 (31 days versus 10 days), being especially remarkable the decrease observed in spring months, when its occurrence has almost disappeared, whereas its occurrence in late summer and autumn has increased. The NAO average corresponding to the heavy rainfall days associated with this pattern is 0.15, while the WeMO average value is significantly negative (-1.18).

The CL3- is the second more frequent pattern related to heavy rainfall days (154 days). It shows a low-pressure system at 500 hPa level located in the south of the IP. On surface, the low-pressure centre is placed over the Sahara desert and warm and moist air from the Mediterranean Sea penetrates in the IP by the eastern coast. From the inter-annual variability it can be observed a tendency to more heavy rainfall days during this atmospheric configuration after 1980. This pattern is more frequent during autumn, although its occurrence has increased during winter. The average value of NAO and WeMO indices are contrary in sign, being particularly high in case of the WEMO (0.61 and -1.46, respectively).

The CL4- pattern is associated with the formation, in front of the north-west coast of the IP, of a weak trough in upper level with the axis in north-west direction from the Atlantic Ocean to the IP, which appears more defined in surface. This configuration brings south-westerly airflow to the south of the IP. This pattern, which is related to 59 heavy rainfall days, has moved its occurrence from March and October (before 1980) to late autumn and winter months (after 1980). Both, NAO and WeMO indices, show negative values in average during the days related to this pattern, but WeMO values are much more negative (-0.24 for NAO and -1.62 for WeMO).

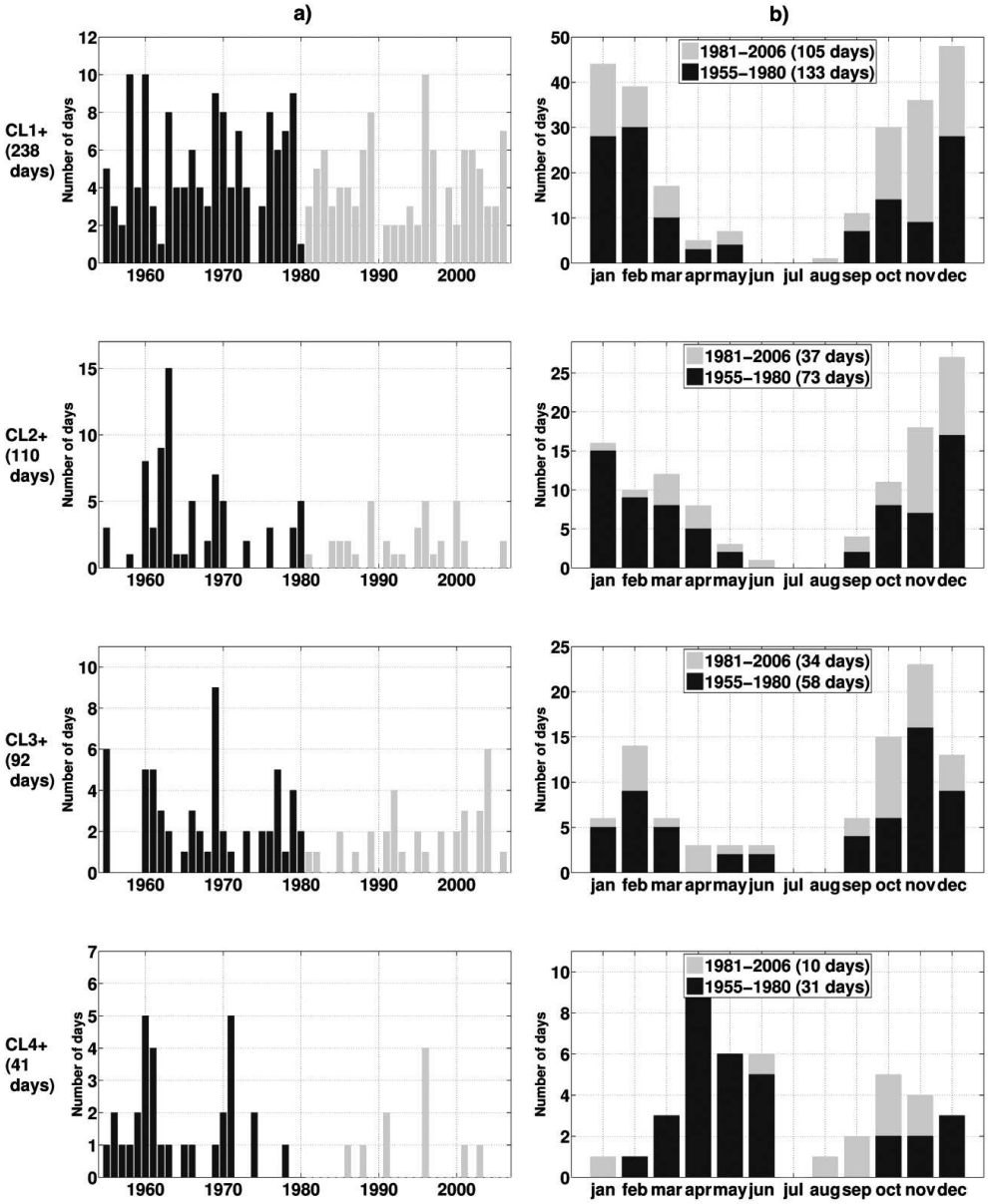

Figure 5. a) Inter-annual variability of heavy rainfall days associated to each pattern corresponding to positive classes. (b) Intra-annual variability of heavy rainfall days associated to each pattern corresponding to positive classes. The dark grey colour in bars corresponds to the period 1955-1980 and the light grey colour in bars corresponds to the period 1981-2006.

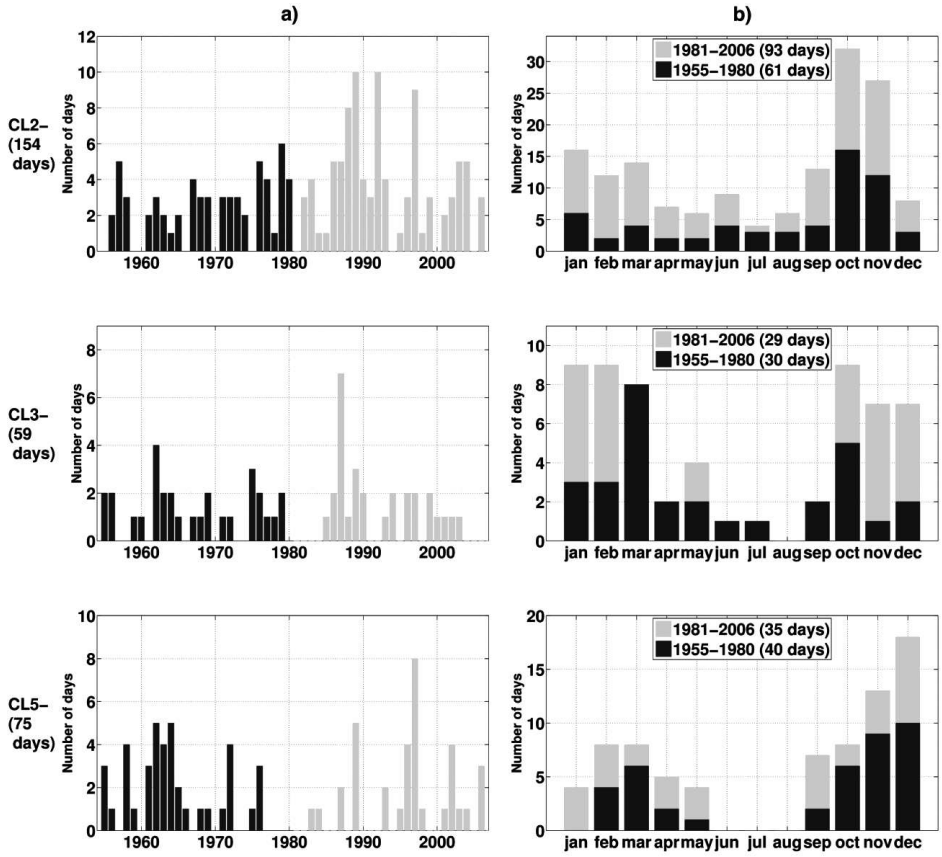

Figure 6. As figure 5 but for negative classes.

The CL5- pattern presents a dipole in surface, with low-pressure centre in front of the Portugal coast together with a high-pressure centre in British Isles. This configuration is also reproduced at 500 hPa. This pattern was found in 75 of the 854 heavy rainfall days identified, without a noticeable interannual tendency. A moderate negative NAO index and highly negative WeMO (-0.52 and -2.05, respectively) result when this pattern is related to heavy rainfall days.

5. CONCLUSIONS

The aim of this study has been to determine the atmospheric patterns associated with heavy rainfall events during the second half of the 20th century in the south of the Iberian Peninsula, and also to examine their inter/intra-annual variability. The main conclusions obtained from this study are summarized as follows.

The total number of heavy rainfall days, which appear more frequently in autumn and early winter and descend until summer, has shown a slight decrease through the entire period 1955-2006. In particular the synoptic patterns CL2+, CL3+ and

CL4+ have shown a significant decrease. On the contrary, the pattern CL3- shows an increase in the number of heavy rainfall days that are associated with its occurrence (especially during winter).

Regarding the intra-annual variability, a remarkable result is the change in the seasonality of some patterns. Particularly, the CL1+ and CL2+ patterns, two of the most frequent patterns found, changed the time of the maximum amount of appearances from winter (for 1955-1980) to autumn (for 1981-2006). The pattern CL4+, whose occurrence was focused on spring during 1955-1980, almost does not happen during 1980-2006 during this season. On the contrary, it increases its occurrence during autumn. The pattern CL4-, which used to appear in transient months as March and October, during the period 1955-1980, has turned to be more frequently found in winter.

Finally, in terms of the relationship between the heavy rainfall days grouped in the different synoptic configurations and the NAO and WeMO indices, a remarkable result is that, although some of these patterns are related with high negative values of NAO index (especially the CL2+ pattern), all patterns are related with moderate and even high negative values of the WeMO index, so this index shows a particular relevance in the heavy rainfall occurrence in the south of the IP.

ACKNOWLEDGMENTS

The Spanish Ministry of Science and Innovation, with the additional support from the European Community funds (FEDER), project CGL2010-21188/CLI, has financed this study.

REFERENCES

Fragoso, M. and Gomes, P.T. (2008). "Classification of daily abundant rainfall patterns and associated large-scale atmospheric circulation types in Southern Portugal". *International Journal of Climatology*, 28(4), 37-544.

Hidalgo-Muñoz, J.M., Argüeso, D., Gámiz-Fortis, S.R., Esteban-Parra, M.J. and Castro-Díez, Y. (2011). "Trends of extreme precipitation and associated synoptic patterns over the southern Iberian Peninsula". *Journal of Hydrology*, 409, 497-511.

Hurrell, J.W. and VanLoon, H. (1997). "Decadal variations in climate associated with the north Atlantic oscillation". *Climatic Change*, 36(3-4), 301-326.

Huth, R. (1996). "An intercomparison of computer-assisted circulation classification methods". *International Journal of Climatology*, 16(8), 893-922.

Kalnay, E., Kanamitsu, M., Kistler, R., Collins, W., Deaven, D., Gandin, L., Iredell, M., Saha, S., White, G., Woollen, J., Zhu, Y., Chelliah, M., Ebisuzaki, W., Higgins, W., Janowiak, J., Mo, K.C., Ropelewski, C., Wang, J., Leetmaa, A., Reynolds, R., Jenne, R. and Joseph, D. (1996). "The NCEP/NCAR 40-year reanalysis project". *Bulletin of the American Meteorological Society*, 77(3), 437-471.

Lana, A., Campins, J., Genovés, A. and Jansà, A. (2007). "Atmospheric patterns for heavy rain events in the Balearic Islands", *Advances in Geosciences.* 12, 27-32, doi:10.5194/adgeo-12-27-2007.

López-Bustins, J.A., Martín-Vide, J. and Sánchez-Lorenzo, A. (2008). "Iberia Winter rainfall trends based upon changes in teleconnection and circulation patterns". *Global and Planetary Change*, 63(2-3), 171-176.

Martín-Vide, J. and López-Bustins, J.A. (2006). "The western Mediterranean oscillation and rainfall in the Iberian Peninsula". *International Journal of Climatology*, 26(11), 1455-1475.

Martín-Vide, J., Sánchez-Lorenzo, A., López-Bustins, J.A., Cordobilla, M.J., García-Manuel, A. and Raso, J.M. (2008). "Torrential rainfall in northeast of the Iberian Peninsula: synoptic patterns and WeMO influence". *Advances in Science and Research*, 2, 99-105, doi:10.5194/asr-2-99-2008.

Penarrocha, D., Estrela, M.J. and Millán, M. (2002). "Classification of daily rainfall patterns in a Mediterranean area with extreme intensity levels: The Valencia region". *International Journal of Climatology*, 22(6), 677-695.

Preisendorfer, R.W. (1988). *Principal component analysis in meteorology and oceanography*. Elsevier, 425 pp.

Romero, R., Sumner, G., Ramis, C. and Genovés, A. (1999). "A classification of the atmospheric circulation patterns producing significant daily rainfall in the Spanish Mediterranean area". *International Journal of Climatology*, 19(7), 765-785.

Trigo, R.M., Pozo-Vázquez, D., Osborn, T.J., Castro-Díez, Y., Gámiz-Fortis, S. and Esteban-Parra, M.J. (2004). "North Atlantic Oscillation influence on precipitation, river flow and water resources in the Iberian Peninsula". *International Journal of Climatology*, 24(8), 925-944.

Vicente-Serrano, S. M., Beguería, S., López-Moreno, J.I., El Kenawy, A.M. and Angulo-Martínez, M. (2009). "Daily atmospheric circulation events and extreme precipitation risk in northeast Spain: Role of the North Atlantic Oscillation, the Western Mediterranean Oscillation, and the Mediterranean Oscillation". *Journal of Geophysical Research*, 114, D08106, doi:10.1029/2008JD011492.

Wang, L. and Yang, F. (2007). *RHtestV2 user manual*. Published online (http://cccma.seos.uvic.ca/ETCCDMI/software.shtml)

Wang, X.L. (2008a). "Accounting for autocorrelation in detecting mean shifts in climate data series using the penalized maximal t or F test". *Journal of Applied Meteorology and Climatology*, 47(9), 2423–2444

Wang, X.L. (2008b). "Penalized maximal F test for detecting undocumented mean shift without trend change". *Journal of Atmospheric and Oceanic Technology*, 25(3), 368–384

Wilks, D.S. (2006). *Statistical Methods in the Atmospheric Sciences.* Academic Press.

CHAPTER 12

ELECTRICAL DISCHARGES IN THE ATMOSPHERE

Francisco PÉREZ PUEBLA

Spanish State Meteorological Agency (AEMET)
fperezp@aemet.es

ABSTRACT

This chapter aims at presenting the necessary products to do a study of the risk through electrical natural discharges at a given place and time. The risk is usually specified in terms of time of day, month or season of the year and its assessment is wholly of a empirical nature. The products included here have been developed by the author and are based on operationally data recorded by the electrical detection network of the Spanish State Meteorological Agency (AEMET) which started operation in 1992. This network has gone through two clearly defined phases, the first one until 1999 when the phenomenon was tracked with an already obsolete technology in a rather incomplete way; then the latter one, which has provided the data for the products presented here, used GPS technology thereby achieving a degree of detail and resolution for the ground-hitting discharges considerably higher than before.

Key words: lightning, electrical discharge, cloud to ground stroke, electrical storm, stroke density, keraunic risk, direction finder, lightning sensor, lightning dead.

1. BRIEF DESCRIPTION

Following the definitions set by the World Meteorological Organization (Manual WMO Nº 407, 1993) concerning the term storm this refers to an electrical phenomenon by the presence of atmospheric electrical discharges, which appears through lighting effects (lightning) or sounds effects (thunder). This is worth remembering to avoid possible ambiguities caused by the abuse of the term storm, even in specialised contexts.

Figure 1. Engraving on the thunderstorms experiments with a kite by Franklin. "Natural Philosophy for Common and High Schools" 1881. Le Roy C. Cooley.

Since the experiments on atmospheric electricity with a kite performed by Benjamin Franklin in 1752, we know that most cumulonimbus, the typical storm clouds, have a negatively charged centre located just above the minus 10-15ºC. This negative nucleus, generally generated by the friction and fracture of small ice crystals entrained by convective currents, induces at surface level a redistribution of the positive electrical charges (telluric currents) that follows the cloud as it moves as its electric shadow.

The knowledge of the electrical phenomena that occur in the troposphere has progressed in step with the evolution of the electrical detection and communication

technologies. To get an idea of their complexity suffice it to describe the lightning according to the state of the art science and the international statistical assessments of more reputation. (Rakov *et al.,* 2003)

According to these assessments the more common sort of lightning (with negative polarity, carrying down electrons to earth) would comprise three or four strokes with an average duration of sixty millionths of a second. The separation between strokes would amount normally around thirty millionths of a second. These component strokes could connect the cloud with the ground at the same place (flickering or twinkling) or at several places, perhaps not too close (around ten kilometres), but some strokes could be several tenths of even hundreds of kilometres apart.

The simple stroke could come preceded by different phenomena such as the stepped descent of the charge from the negative nucleus in the cloud (stepped leader) with duration of a few tenths of milliseconds. The ground also plays an active part unleashing other preliminary discharges with opposite polarity (streamers) towards the cloud that make easier the intensification of the atmospheric electric fields and the ionisation of least electrical resistance. Through these travels the initial discharge (pilot streamer or stepped leader) or others to follow (dart leader) that make up the same lighting (flash lightning).

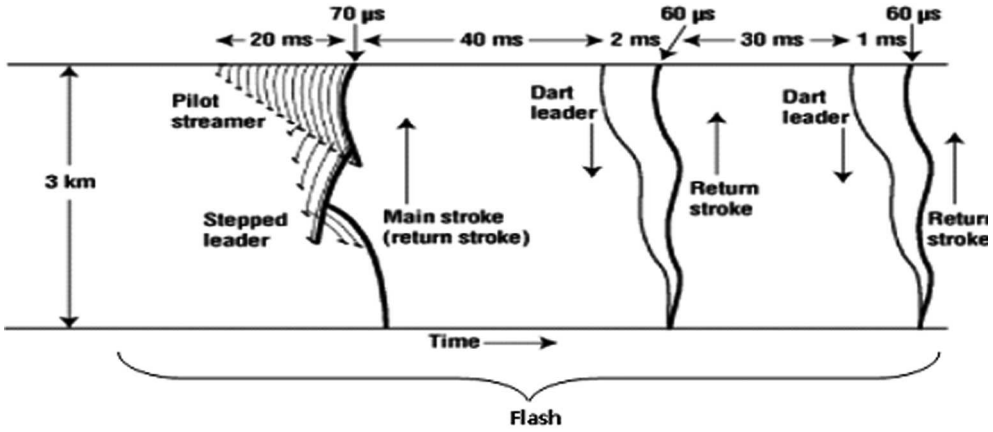

Figure 2. Sketch of a flash composed of three successive strokes. The pilot streamer, the stepped leader and the dart leader travel through the same channel towards the ground in a time of around 100 microseconds. Adapted from Rakov-Uman, 2003.

The discharges have maximum intensities of a few tens of kilo ampere and bring down negative charges of a few Coulombs though exceptionally they can exceed 100 Coulombs and several hundreds Ampere.

It follows that, in principle, given their important energetic transfer, the strokes can have grave consequences for human activities and may be able to seriously compromise the security and integrity of infrastructures and, obviously, be a danger for human life.

2. DETECTION AND TRACKING SYSTEMS FOR ATMOSPHERIC ELECTRICAL DISCHARGES

The sudden electric currents between ground and atmosphere can reach high intensities and generate powerful electromagnetic pulses whose radiation spectrum has a maximum energetic emission in the radiofrequencies bands of the electromagnetic spectrum, mainly the ELF/ LF/VLF (extremely low frequency, low frequency y very low frequency).

In former times the analogue radio emissions were contaminated by sound crackle that were put down to the so called "atmospheric parasites" or "atmospheric noise" in those emission bands. Nowadays this reviled noise is the main source of data for the radio detection systems used for the tracking down of electric storms. Its analysis allows the knowledge of the atmospheric discharge that generated it and the deduction of the characteristics of the storm.

During the XX century the detection and positioning of the radio frequency sources was based on trigonometry by means of "cohesors" and later with direction finders. In the last decade of the past century the use of reception antennae of the time signal coming from satellites of the Global Position System (GPS) made its appearance. This meant the start of a new tracking technology: the temporal technology.

So the technology for tracking electric discharges is relatively old (even more so than radars) since the triangulation methodology has been used since the beginnings of the aviation and applied also to navigation. However the capacity of dealing simultaneously with the information from several antennae far apart had to wait until the last quarter of the XX century by means of the concentration of the signal records in reliable communication systems that allow its processing. At the same time the increasing speed of concentration and computing systems has made possible the evaluation with complex algorithms the situation of tens or even hundreds of discharges simultaneously, revealing also their main characteristics with such a speed that the thunder could arrive after the position of the source has been showed by means of digital cartography on a monitor.

At present the most used technology to locate electrical discharges is based in the time of arrival of the pulse to different sensors of lightning network. The greater the numbers of sensors that provide information on the same signal and more accurate are measurement; the better will be the positioning of the pulse. During the first decade of this century several statistical assessment of the accuracy of some lightning networks has been carried out, the positioning errors of the events have decreased below 500 metres (Schulz *et al.,* 2012).

The precision of the arrival time of the signals recorded by the GPS sensors is about a tenth of microsecond after the correction of the different time delays due to the different conductivity of the soils that carried the signals in that way from the source to the sensor. This increased time accuracy will allow the positioning the electrical discharges with an accuracy between a few tenths an little more than one hundred meters in the coming years. This fact is a remarkable improvement over the precision of only few kilometres that could be reached with the techniques and algorithms based on magnetic direction finders networks of the eighties and

beginning of the nineties. This way the last decades have brought an increase in the accuracy of the positioning that has allowed a first method for the continual tracking of the phenomenon in the meteorological micro scale (instead of meso scale before) So multiple applications have appear for infrastructures and natural assess protection.

The state of the art of lightning detection in networks deployed on the earth surface has also made it possible to specify the location of each of the discharges belonging to one flash. The analysis of these discharges provides also other parameters, among which the maximum intensity of the strokes. It is also possible to determine the polarity of the signal which makes it easier the determination of the discharge typology.

As well as the accuracy, one of the performance measures that better characterize one lightning network is its real efficiency. This is to be understood as the percentage of the located discharged over the total that have occurred. We have algorithms that estimate this parameter easy. In order to verify this efficiency, observations surveys are carried out in a systematic way with recording measurement systems (video and electric field recordings) on small regions that serve as a representative sample of the entire lighting network. The real efficiency stays usually about 90% for flashes or first strokes, and above 80% for rest of strokes (Schulz *et al.,* 2012).

A lot of countries carry out measurements at instrumented towers which record on line the variables that characterize that impact on them. The data so gather by the instrumental tower are contrasted with the data from lightning network by the national meteorological services or other organizations. It has been verified that there is a high degree of concordance between remote sensing and direct measurements.

There are lightning networks whose detection technology is based on interferometry of VHF emissions that come from strokes. The range of these observation systems is confined practically to the inside of the polygon that envelopes the detection stations and a few tenths of kilometres around. However the range of the VLF/LF detection networks is much longer, out to a few hundred of kilometres from the network polygon envelop. The ionospheric refection carries the electromagnetic pulses over great distances, which has led some network owners to postulate in exaggerated way a global coverage, the spite the fact that the performance falls off drastically as we get far from the contour of the network.

Satellite based exploring systems are now being introduced (Pérez, 2011). The first experiments along this line counted with instrument lodged on satellite MicroLab and TRRM ("Tropical Rainfall Rate Mission"), both with a polar orbit around 1000 kilometres over the earth surface. The sensors are now based on the light flash emitted by the discharges. So they worked on visible band of spectrum in contrast with earth based systems. Notables results concerning global coverage were obtained but this coverage was not complete nor and interrupted in time.

The experience gained with the polar satellites has been transferred to the geostationary satellites that travel at a distance over 30,000 kilometres from the earth surface. The last GOES mission already has adequate instrument and the next

Meteosat (Meteosat Third Generation, MTG) will have also another similar instrument that will allow a 10 kilometre spatial and about a millisecond temporal resolution, which in practise will amount to a continual temporal tracking of the phenomenon.

Besides the very wide coverage, another strong point of the space-based lightning observation system is the homogeneity of the exploration method. This means a quality which is distributed reasonably uniformly across all the exploration area. But the greater precision and efficiency still corresponds to the ground-based networks, which are the reference against which the space-based observations have to be valuated.

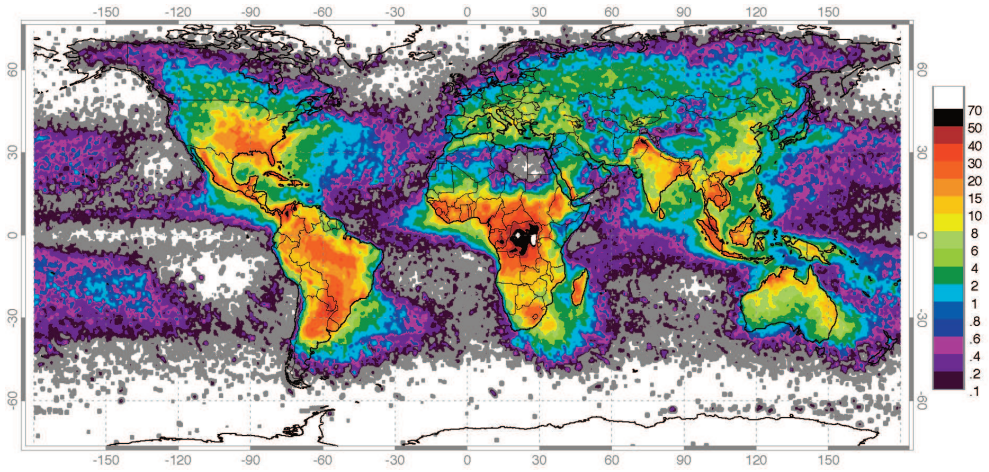

Figure 3. Mean annual distribution of lightning per square kilometre. Image obtained through the combination of data from missions TRRM and MicroLab. Period: from April 1995 to February 2003. Source: "Global Hidrology and Climate Center" (GHCC) NASA, Huntsville, Alabama.

3. IMPACT ON HUMAN LIFE LOSS

Recent statistical studies on lightning strike risk for persons (Holle, 2012) have been able to provide a detailed description of the damages and the conditions. To summarise practically all the casualties happened on opened spaces or more generally outdoors. One of main results is that the frequency of deaths by lightning is comparatively much smaller in urban and developed societies than in the ones more backwards and more primitive or rural economies were the number of victims can be several orders of magnitude greater than in the former.

For the protection of the human life, a rate of 0.1 lightning deaths per million inhabitants is considered a tolerable risk (IEC® standards, 2009) The lightning deaths rate depends obviously on the frequency of electrical storms, but it is even more dependent on the degree of development of the societies and their economies. Looking at Table 1 we can see that the lower death risk corresponds to those areas of the planet where the natural lightning frequency is low (coldest regions) and the degree of development is high.

Country (Region)	Average
China (Hong Kong)	**0.04**
Lithuania	**0.1**
Canada	**0.1**
Greece	**0.2**
USA	**0.2**
China (general)	**0.5**
Brasil (Sao Paulo)	**0.8**
Bangladesh	**0.9**
Vietnam (general)	**1.2**
Southafrica (urban)	**1.5**
Sri Lanka	**2.4**
India	**2.5**
Nepal	**2.7**
Malaysia	**3.4**
Vietnam (rural)	**8.8**
Southafrica (rural)	**8.8**
China (rural)	**10.6**
Zimbawe	**14.2**
Yemen	**71.4**
Malawi	**84. 0**

Table 1. Number of lightning related deaths per million inhabitants during the first decade of this century. Adapted from Ronald L. Holle.

The reduction of the number of lightning fatalities in Spain since the forties of the past century until now is to be attributed, in accordance with what has been said before, to the sociological and economical evolution of the country. This incidence has gone progressively from 2,5 lightning deaths per million inhabitants (Pérez, 2005) in the forties of XX century to the 0,6 in the seventies, reaching later even lower stable values according to Statistical Official Bureau of Spain (see Figure 4).

In the USA tornadoes have displaced lightning as the second cause of meteorological deaths in the last five years. According with some sources (Holle, 2012), the prevention campaigns carries out in the last years by the NOAA (National Oceanic and Atmospheric Administration) have been a key factor in the decrease in the number of lightning fatalities.

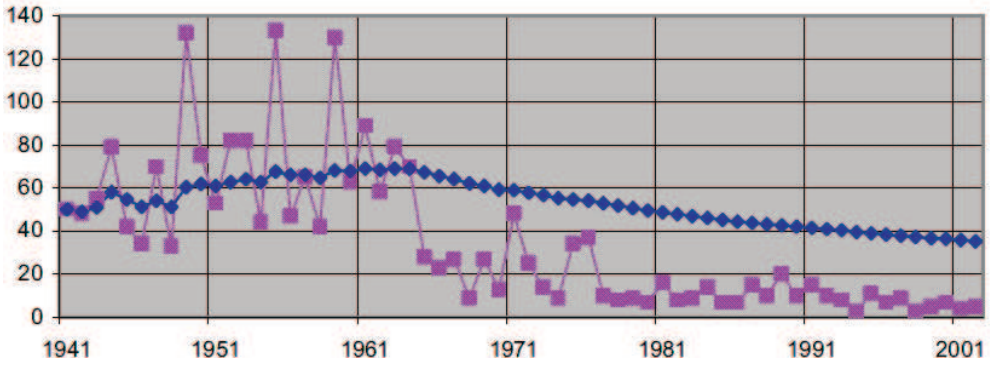

Figure 4. Temporal evolution of the five year moving average of lightning deaths (dark diamond shape) and their yearly evolution (clear square shape) for 2,186 lightning deaths in Spain from 1941 to 2002.

In USA the first cause of death by meteorological causes, leaving a side the cold and heat extreme events (Goklany, 2009), is still the flash floods according to the statistics of the last thirty years (NOAA, 2013). In general terms, in the more advanced societies, owing to the growth of the services sector and the technological innovations in protection measures, the increase of the information among the population has led to a progressive reduction in the number of lightning deaths that have became now tolerable even in urban areas with great storminess.

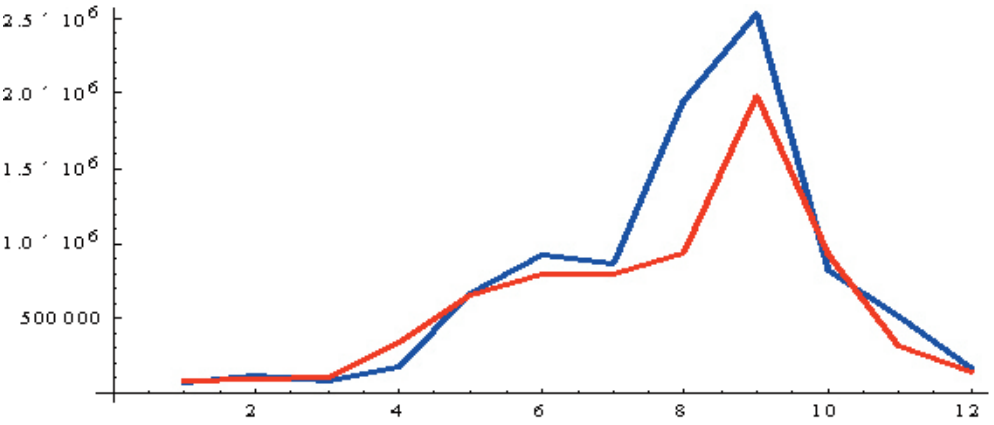

Figure 5. Comparison of the two annual cycles of the total number of the monthly discharges over the peninsula, the Balearic Islands and the adjoining maritime areas in two periods of six years. Maximum cycle: 2000-2005 and under: 2006-2011.

In Spain, the risk of lightning strike during the hottest months of the year (May – October) is around 90% of the yearly total taking to account the whole covered

area by Lightning Detection Networks in the Peninsula. This fact changes substantially when one considers only one autonomous region or province of less extension, owing to the variability in the climatology of storm frequency, which can even show two yearly maxima. Over the whole peninsula we can see that there is a unique marked maximum of activity just at the end of the summer (September), though if we take out the activity of the maritime areas the maximum shifts to August.

The risk for life is greatest for open air activities such as sport events, trekking, farming, etc. The risk depends of the time of day that regulates the human activities. Obviously there is a greater lightning vulnerability the greater the number of persons that are exposed during the daily maxima of electrical activity. In the same way the risk also increases due to the fact the maxima electrical stormy is closed to the maxima of opened air leisure activities. Consequently for a given place it is essential the knowledge of the mean yearly evolution of electrical activity as well as the mean daily evolution. This way we can assign a probability to the risk, depending on the time of the day, and the month of the year, based on empirical frequencies such as those shown in Figure 6.

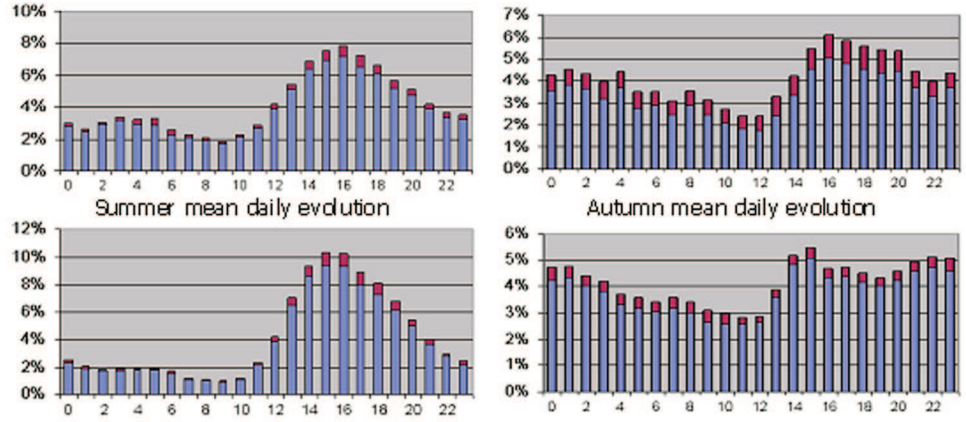

Figure 6. Seasonal mean daily evolution for the Iberian peninsula in 2002 – 2004. UTC time. On upper site of each bar positive discharges are dark. The negative discharges percentages are under the first ones.

4. KERAUNIC INDICES. SPATIAL AND TEMPORAL DISTRIBUTION

In order to study and research the empirical risk it is useful to analyze the parameters in terms of geographical distribution so as to highlight the areas with more risk. The most used parameters are the average number of storm days and the average number of strokes for a given period of time.

However in other cases other parameters are taken in account in order to give a more complete vision of the intensity, or the duration, or time of occurrence of the phenomenon. All these are called keraunic indices. We can mention, in addition to the two listed above, the following: the mean duration of daily storm time, the average number of discharges during the daily storm time, the time of the day

when the activity is maximum, the maximum number of hourly discharges, the average hour number of activity over a period o time, ….etc.

Concerning the geographical distribution an advantage of using administrative units (such as provinces) is that it makes easier the assessment of efforts directed to the adverse consequences of the phenomenon, not only with respect to socio-culture and industrial aspects but also the natural one (protection against forest fires). As an example, Figures 7 and 8 show the provinces where there is more electrical activity, be it, in number of storm days (Figure 7) or in number of hours with storm over the year (Figure 8).

This type of representation allows the ranking of territories according to the risk. One must however not forget that there is a great different in extension among the provinces, which is the main drawback of this representation.

In Figures 7 and 8, in addition to the colour scales, there is a number which reflects the ranking of the provinces among the total number of provinces, with one ranking for Portugal and another for Spain. According to Figures 7 and 8, Aragon and Catalonia have an average number of thunderstorm days close to ninety and their yearly number of hours with thunderstorm reaches 500. This is also reflected in their provincial ranking.

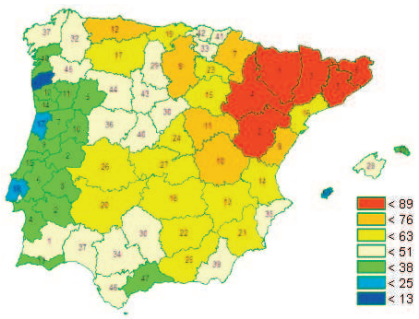

Figure 7. Average number of thunderstorm days per year in provinces according the scale and country ranking for provinces. Period 2000 – 2009.

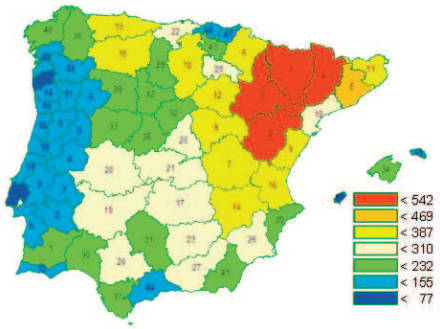

Figura 8. Average duration of hours with thunderstorm per year in provinces according the scale and country ranking for provinces. Period 2000 – 2009.

Provincias	Nºdías tormenta					Duración media					Actividad media horaria					Media del máximo horario					Hora máximo				
	AÑO MEDIO (00-09)					Horas					Descargas/hora					(descargas/hora)					horas (GMT.)				
	A	I	P	V	O	A	I	P	V	O	A	I	P	V	O	A	I	P	V	O	A	I	P	V	O
ANDALUCIA																									
Almería	44	5	15	15	9	4.1	3.3	3.8	4.6	4.0	22	15	14	30	24	81	68	51	97	102	14	12	14	14	15
Cádiz	38	10	10	5	13	5.2	5.0	4.9	5.4	5.5	15	7	12	41	11	48	20	44	114	41	12	13	12	13	13
Córdoba	48	8	19	11	10	4.6	3.7	4.9	5.1	4.3	31	10	28	53	26	94	43	84	153	70	14	15	14	14	13
Granada	51	7	19	16	10	4.6	3.6	4.7	5.2	4.4	24	5	24	28	25	64	14	63	73	74	14	13	14	14	15
Huelva	44	9	15	7	14	5.0	4.4	5.1	5.3	5.1	29	12	29	57	22	104	52	93	178	93	14	14	14	14	12
Jaén	53	7	22	15	9	4.7	3.2	5.1	5.2	4.1	31	13	28	41	31	103	53	98	120	109	15	15	14	15	15
Malaga	34	8	10	6	10	4.5	4.4	3.8	5.2	5.0	18	10	13	37	15	70	40	73	110	55	12	10	12	12	14
Sevilla	46	8	16	8	13	5.3	5.1	5.2	5.7	5.2	22	8	22	38	20	76	37	71	116	73	14	14	14	13	13

Table 2. Average keraunic indices for period 2000 – 2009 in the provinces of Andalucia (Spain).

We can also make a more detailed analysis using a tabular display. As an example, table 2 contains statistical description of the phenomenon for the Andalucian provinces for the period 2000- 2009. Though less intuitive, this sort of representation is more descriptive than the cartographic one.

In order to make the cartographic representation independent on the province extension it is necessary using a uniform gridding. The resolution in the description of the phenomenon depends on the dimensions of the cell. It has been usual in the last ten years to use a cell of 10 x 10 kilometres. If we want more detail we can reduce the size of the cell but it can not be so small in order to avoid lack of data than produces excessive noise.

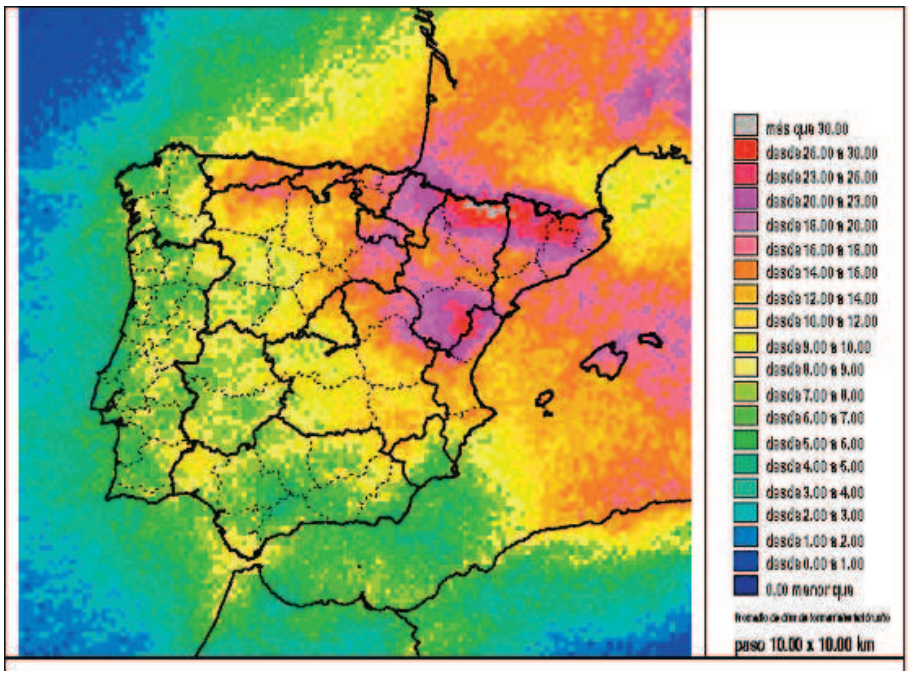

Figure 9. Average number of storm days registered in Lightning network of AEMET (Spain) during the period 2000-2009 with a resolution 10 km x 10 km.

An example of this approach is Figure 9 which gives the yearly average of days with thunderstorm over a ten-year period. We can see that the first decade of this century has been characterised by a maximum in the storminess over the Peninsula and adjoining seas located in the NE quarter with two nuclei of storm activity: the Aragon Pyrenees and the mountain ranges at the boundary between Teruel and Castellón, where the number of days with storm is about thirty. The activity in the maritime areas is greatest in the Mediterranean basin though it is also intense in the Biscay Gulf. By contrast the Atlantic maritime areas show much weaker storminess, the same as the SW Peninsula and Portugal.

A more detailed description of the storminess can be given by looking at the seasons of the year, or even down to the monthly evolution. An example of the seasonal average evolution is provided in Figure 10 which shows the seasonal (Jan-Mar, Apr-Jun, Jul-Sep and Oct-Dec) average storm days.

The storm activity is at a minimum in winter in the inside of the mini-continent formed by the Peninsula, but in the maritime periphery the activity is weak. Spring turns on the convective activity in the peninsular interior while it is still weak in the maritime areas, similar to winter. In summer we see an intensification of convection and instability in the NE of the Peninsula and close maritime areas, especially in the Mediterranean. Finally in fall the energy accumulated during the preceding months in the maritime Mediterranean areas and the arrival of the first frontal systems from the West produce an intensification of convection in these maritime areas, while in the interior of the Peninsula the convective activity falls sharply.

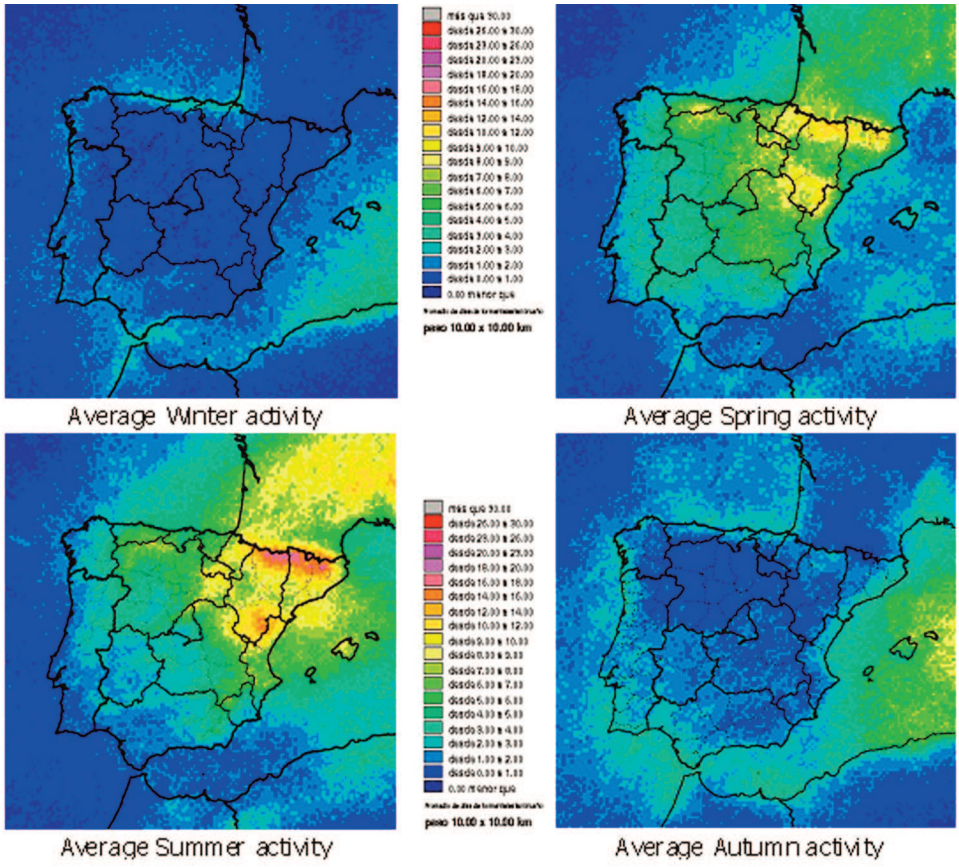

Figure 10. Average number of storm days on the year season registered in Lightning network of AEMET (Spain) during the period 2000-2009 with a resolution 10 km x 10 km.

More details are provided by the monthly evolution which is best suited to planning prevention campaigns aimed at the population in each territory. This type of cartography allows the selection of areas, seasons, months and moments of day more susceptible in lightning risk.

4.1 Homogeneity and trends in the electric activity series

As we have seen before the ten-year period statistics provide enough detail for the description of storminess in general, but in order to extract conclusions on the trends and possible unhomogeneities of the series, treating them as climatological series, this is a rather short time. For these purposes at least a whole 11-year solar cycle would be desirable.

This would be still far less than the 30-year period usual in climatology, which includes almost three complete solar cycles. In our case it has not been possible to work with homogenous periods longer than 10-12 years, despite having observational records of storm activity for 22 years. But during these 22 years there has been an instrument update that meant the substitution of the angular positioning technology applied in the first 10 years by the temporal one (GPS) in the last 12 years. Unfortunately no simultaneous observations with both systems were carried out, which would have allowed the prolongation of the older series with the new ones avoiding homogeneity cuts.

This notwithstanding we have carried out trend and homogeneity analysis of the last 12 years series, from 2000 to 2011 (López *et al.,* 2012). It has turned out that there are, as far as it is possible to discern with such short period, no important homogeneity issues with the data, and no clear trends either.

4.2 Characterization by parameters

A usual approach in climatological studies is to classify the data of a given period of time, such as year or month, according to its rank in the reference series of data for similar periods over a number of years. This way in Figure 11 we define six categories: 0 for extremely low storminess when the datum is below the minimum of the reference series, 1 for little storminess when the datum falls in the first quintile, and so on until the category 5 for datum falling in the highest quintile, and finally 6 for datum exceeding the maximum of the reference series.

A more uniform areal coverage is obtained by carrying out the preceding analysis on the basis of the data for each pixel, as was done at the provincial level. Figure 12, which follows this approach, represents the characterisation of the year 2011 against the period 2000-2010 in terms of the number of storms recorded in the year.

This type of representation offers a rapid and synthetic vision of the behaviour of the parameter of interest over the whole are of study in terms of its relative intensity over the reference period. From figure 12 we may conclude that the western half of the Peninsula has been very or extremely stormy in 2011, while the eastern half has had little or very little storminess, with only a few local exceptions.

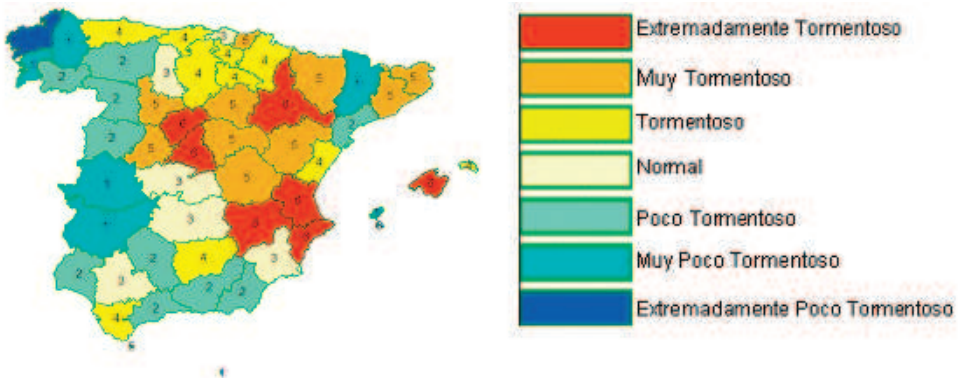

Figura 11. Year characterization of 2009 respects the behaviour of the period 2000-2008 in number of storm days by year for each Spain provinces.

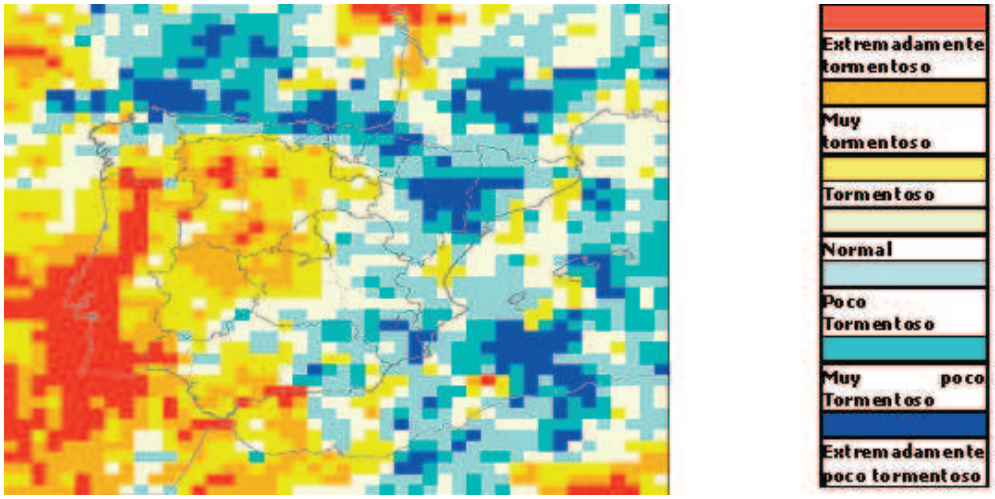

Figura 12. Year characterization of 2011 respects the behaviour of the period 2000-2010 in number of storm days by year. Resolution 20 km x 20 km.

If we were interested in the season or months of the year that contributed more to this result we would need the monthly or seasonal pixel-based series. This would allow the characterisation along the year or particular seasons, as well as the identification of regional and temporal anomalies.

5. CONCLUSION

As can be appreciated from the foregoing paragraphs the exploitation of the data recorded by the modern radio-detection networks allow to evaluate the impact of

cloud-ground electrical discharges with a spatial resolution of a few kilometres when series with around ten year length are available. This assessment requires the generation of the daily and monthly average time evolution of the phenomenon, the latter providing the evolution of the frequency along the year. An important application of this assessments is the design of the radio-electrical protections for some electrical or communication systems or pipelines and other civil infrastructure based on the local distribution of the maximum electric intensity recorded by the lightning network.

REFERENCES

Atlas internacional de nubes. Vol. I: Manual de observación de nubes y otros meteoros. ISBN: 92-63-30407-6. Ginebra, (1993)

Rakov, V. A. and Uman, M. A., (2003). Lightning: *Physics and Effects*. Cambridge University Press.

Schulz, W., Vergeiner, C., Pichler, H., Diendorfer, G., Cummins, K., (2012). Location accuracy evaluation of the Austrian lightning locations systems ALDIS.. 22nd International Lightning Detection Conference. *4th International Lightning Meteorology Conference*. Broomfield, Colorado, USA.

Schulz, W. *et al.,* (2012). Validation of the Austrian Lightning Location Systems ALDIS for negative flashes. *CIGRE C4 Colloquium on Power Quality and Lightning*. Sarajevo, Bosnia and Herzegovina.

Pérez Puebla, F. (2011). Observación sistemática de las tormentas eléctricas desde satélite. *Boletín de la Asociación Meteorológica Española*, 31.

Holle, R. L. (2012). Recent studies of lightning safety and demographics.. 22nd International Lightning Detection Conference and 4th International Lightning Meteorology Conference. Broomfield, Colorado, USA.

Lightning protection handbook. Designing to the IEC 62305 Series of Lightning Protection Standards. ERICO. www.erico.com. IEC® standards, (2009).

Pérez Puebla, F. (2005). El valor de la información sobre electricidad atmosférica. La evolución de la red de rayos de España. *Ambienta*. Revista del Ministerio de Medio Ambiente.

Goklany, I. M. (2009). Deaths and death rates from extreme weather events: 1900-2008. *Journal of American Physicians and Surgeons,* 14 (4).

Natural Hazard Statistics. http://www.nws.noaa.gov/om/hazstats.shtml NOAA National Weather Service. USA, (2013).

Pérez Puebla, F. y Zancajo Rodríguez, C. (2008). La frecuencia de las tormentas eléctricas en España. *Boletín de la Asociación Meteorológica Española*, 21.

López Díaz, J. A., Pérez Puebla, F. y Zancajo Rodríguez, C. (2012). Tendencias y homogeneidad en las series de descargas eléctricas del periodo 2000–2011. *Boletín de la Asociación Meteorológica Española*, 38.

CHAPTER 13

FOG AND ITS SOCIETAL IMPACTS

Joan CUXART

University of the Balearic Islands, Dpt. of Physics, Mallorca (Balearic Islands, Spain)
joan.cuxart@uib.es

ABSTRACT

Fog is a meteorological phenomenon that reduces visibility below 1000 m and is a threaten to all transportation sectors, especially road traffic, where it causes a significant number of casualties yearly. Massive affectation in take-off and landing operations takes place when fog is installed on an airport, and can also create icing problems on wings in winter. Collisions between boats can occur in dense marine fog, especially near harbors. Fog combined with pollutants may produce effects on health of living beings. Therefore, a good knowledge of fog is needed, both on the causes of formation and time-space evolution, as on the weather situations conducting to fog in specific target locations. This work briefly summarizes the current knowledge on fog physics, its monitoring and forecasting, and addresses the impact on societal issues and the strategies to minimize it.

Key words: fog physics, radiation fog, advection fog, road traffic, airport delays.

1. INTRODUCTION

Fog is the presence of microscopic water droplets reducing the visibility at the surface below 1000 m. For larger visibility, we call it mist. The separation is rather arbitrary, but it is widely accepted and used by National Weather Services, and it is approximately equivalent to have of the order of 0.1 g of liquid water per cubic meter (Duynkerke, 1991). Fog is said to be dense when the visibility is reduced below 200 m, a situation when related risks are high, especially in marine and road traffic as well as in parking and take-off and landing airport operations.

Research on fog understanding and development of proper monitoring and forecasting tools have been intense in the last decades. A good summary was published by Gultepe *et al.* (2007) and the report of the European COST Action 722 on its short range forecasting (Jacobs *et al.,* 2008) is an illustrative compendium of the current efforts on fog research and development. A special issue on fog and

dew appeared in 2012, which updates references for the last years (Gultepe *et al.,* 2012). The reader is directed to these works for extensive referencing on the subject.

A fog layer is formed either when an air mass cools and the water vapor in it becomes saturating, or by addition of water vapor finally leading to condensation. These processes are a function of a variety of parameters, such as the aerosol charge of the air, or of the mechanisms causing the cooling or the evaporation. The evolution of fog depends on the characteristics of the area where it happens; it can be very local or cover tens of thousands of square kilometers, last for less than an hour or for several days.

Over land, areas prone to fog are essentially the terrain depressions in the bottom of the valleys, where calm air cools radiatively in clear nights, but also coastal areas where warm air may be advected over colder terrain and lead air to vapor saturation. Other areas include the mountain slopes when air is forced to ascent, or warm wet surfaces evaporating in cold air, like the river fog.

Coastal and valleys areas have very often high densities of population, with many infrastructures sensitive to the presence of fog, such as airports, harbors and highways. In flat inland areas radiation fog can be a persistent feature, and at the coast warm advection may last as long as the advection continues. They usually have a huge economic impact and, in the case of road traffic, cause casualties often.

Even if the basic mechanisms of the fog are essentially understood, their accurate forecast is still a challenge. False alarms and hit rates happen not uncommonly, despite the theoretically high predictability of the phenomenon. These failures are often related to slight differences between observations and forecasts of the wind, temperature and moisture near the surface, or to the lack of knowledge of the aerosol composition of the air. Monitoring for nowcasting is improving due to the increase of visibility sensors in sensitive areas as well as to the development of adequate diagnostics from satellite images.

Progresses in the forecast of the fog will be based on its good climatological knowledge, the improvement of the fast detection of an event using cameras or visibility sensors, the use of high spatial resolution and high frequency satellite images available in real-time and of numerical tools adapted to the characteristics of target locations and running in almost continuous mode. This should warning with enough anticipation the population and the concerned public and private operators.

2. THE BASIC PHYSICAL MECHANISMS

The condensation of water vapor in the air is described by the Clausius-Clapeyron formula adapted to the usual range of values in the atmosphere, and it is normally given for practical purposes as an empirical formulation that expresses the amount of vapor saturating the air increases exponentially with temperature.

Therefore, for a given air mass with a fixed contents of water vapor, a cooling will imply a decrease of the saturating water vapor pressure, meaning that the available water vapor vapor may become saturating if the temperature drops enough. Alternatively, for a fixed temperature of the air mass, increase of the water vapor contents through, for instance, evaporation from a wet surface, may lead the air to saturation.

These two ways (air cooling and evaporation) are the subjacent basic mechanisms of fog formation, air cooling being the most frequent one. Four are the methods of air cooling: i) by radiative cooling, usually at night; ii) through contact to a colder body, such as a cold soil or a snowed surface; iii) by mixing with a colder air mass and iv) through adiabatic expansion when the air mass is lifted.

Condensation of water near the ground can occur by direct contact with colder surface elements, leading to dew or frost, or within the air mass, producing fog. Surface elements may keep temperatures distant to the ones of the air due to the bad thermal conductivity of air, allowing each body to reach its own radiative temperature of equilibrium. Therefore, these elements have different saturating water vapor pressure that the surrounding air and may condensate first, eliminating part of the water from the air as dew is created on them, water that is no longer available for the creation of fog.

For the formation of the microscopic water drops, it is necessary to have a particle over which the water molecules can accumulate on, otherwise, pure water condensation would require saturations much larger, not reachable in ambient conditions in the atmosphere. The condensation nuclei provide bodies of larger radius and the surface tension is diminished over them, they take apart the molecules decreasing the effect of electric repulsion between them and, if they are hygroscopic, they allow the dissolution of water in their interior. Condensation nuclei are abundant over land and sea and they allow condensation to take place at humidities of 100% in air.

The hygroscopic condensation nuclei attract moisture into them, increasing their volume and diminishing visibility, creating mist, which would the initial phase of the establishment of fog. As the temperature will continue to fall, drops will continue to radiate cooling faster than the air and leading water to condensate over them like dew on the surface elements (Bott *et al.,* 1990). It is clear that the composition of the condensation nuclei is a key factor for the formation of fog. If they are too few or not hygroscopic enough, fog may not form.

To go from mist to fog, a certain amount of liquid water must be created and, due to the fact that the amount of water vapor diminishes as temperature decreases, there is less condensable water in initially cold air than in a temperate air. This explains why the creation of fog by cooling is usually found for initially temperate air bodies that may cool significantly and generate enough condensate water, such as for diurnal mild air cooling strongly radiatively during night.

3. KINDS OF FOG AND MECHANISMS OF FORMATION

Four main types of fog can be found, related to different processes leading to saturation of air near the ground: radiation, advection, mixing and evaporation and adiabatic expansion over slopes. Usually one specific kind dominates at a given location where fog is a common phenomenon, and each type has different time and space evolutions.

Radiation fog

For nights with weak winds and clear skies, the surface energy budget is dominated

by the strong radiative cooling by the surface and the air close to it. The other terms of the budget try to compensate this loss, namely the heat flux from the ground, the turbulent latent and sensible heat fluxes or small scale heat advections due to terrain heterogeneities. Usually the radiative cooling is not compensated by all the other terms leading to net cooling of the air close to the ground (Duynkerke, 1991; Zhou and Ferrier, 2008).

This cooling normally generates a thermal inversion close to the ground. When the wind is not too weak, air is mixed upwards and the inversion grows in height with time, allowing renewal of air close to the ground. Instead, for weak winds, these renewal of air is much smaller, the inversions are shallower and stronger, and the air can cool significantly close to the surface, making it easier to reach the saturation point.

This situation is normally taking place under anticyclonic conditions, with very weak pressure gradients and in locally flat areas, otherwise the cold air would flow downslope. It typically occurs inland, in wide and small basins and inside river valleys, between mid-autumn and the beginning of spring in mid-latitudes, when nights are relatively long and temperatures can become low enough during the night (Figure 1).

Condensation starts close to the ground and fog may be only of a few meters of depth, allowing solar radiation in the morning to heat the ground and dissipate it rapidly. However if the amount of condensed water is large, fog becomes dense and acts as separated thermodynamical body, the top of the layer emitting as a new ground upwards, cooling radiatively and mixing convectively downwards, generating a well mixed structure with a strong thermal inversion at its top.

In valleys and basins, interaction with the downslope flows flowing above them may enhance mixing across the inversion and make them grow further vertically (Cuxart and Jiménez, 2012). These dense layers are harder to dissipate and can last for days, since the solar radiation can hardly penetrate few meters, showing perhaps some lift in the central hours of the day, if solar radiation manages to reach the ground (Figures 2c and 2d).

Advection fog

When warm moist air is advected over a colder surface, the air layer closer to the surface can cool the incoming air mass and can generate fog if saturation conditions are met. In this case a well defined and relatively persistent wind is a necessary condition for its maintenance. These fog cases are not linked to the diurnal cycle, except for the particular case of early morning advection coastal fogs, when the marine air would flow over the cold land surface after the night cooling. Therefore they can appear anytime in the day when the conditions are met and last as long as the adequate conditions persist (Zhang *et al.,* 2009).

Wind acts as a mixing agent, generating turbulence by shear production, and making possible the exchange of heat between the surface and the advected air mass, allowing the fog layer to deepen as it progresses. Many times, to have warm air over a colder surface is enough to cause the formation of fog, even if the warm mass is not very moist, because the necessary moisture can come from the soil or the sea surface. However, if the wind is too strong, turbulence will mix very efficiently upwards and will not allow the fog formation. Advection fog is usually

deeper, wider and homogeneous than radiation fog due to the fact that the latter needs specific local conditions.

Evaporation and mixing fog

When a surface of water or a land area with water on it is below an air layer colder than it, evaporation is very intense into the air, even if the air is saturated, since the surface is warmer. Once this vapor enters the saturated air, it condensates immediately, sometimes called steam fog, as it is generated in cold seasons from rivers and lakes (Figures 1d and 1e). This is also favored by the accumulation of cold air in the bottom of the valley by katabatic drainage. The presence of a temperature inversion in the area is necessary to avoid dispersion upwards by convective turbulent mixing. Over the sea, it usually happens over areas of open water surrounding by marine ice. A similar effect is produced when very cold air blows over a warm surface, as it might happen with polar winds over adjacent waters.

Sometimes fog is formed under the clouds in an area where precipitation is occurring. As the rain drops cross an air layer colder than them and unsaturated, evaporation may occur, which will in turn cool further the layer. This may lead to local saturating conditions. This phenomenon is normally related to the passage of warm fronts, when rain falls through the colder air below it and it is called a pre-frontal fog.

A special case of fog generated by mixing from above is related to warm marine advection over a layer of cold air, such as a warm front over cold anticyclonic air over the continents in winter. At the interface mixing occurs in form of Kelvin-Helmholtz billows, which incorporates moist air in the bottom cold layer and generates a cloud propagating downwards and reaching the surface. These fogs can form very rapidly whenever there is an inversion at few hectometers over the land and warm moist air is blowing above, especially in the early morning hours.

Fog over slopes by adiabatic expansion

The case of fog over the slopes of the mountains as the air progresses upwards is equivalent to the case of formation of clouds by adiabatic expansion and consequent cooling, provided that this ascending saturated air stays in contact with the surface (Figure 1c).

4. INLAND, COASTAL AND MARINE FOGS

As we focus on the impact of fog in society, we must describe its peculiarities in the areas of major impact for human activities, that is over land, typically in valleys, where road and air traffic are heavily affected, over the coastal areas, where affectation to harbor activities must be added, and over the sea, where marine transport is concerned.

Flatlands, basins and valleys

Over land all kinds of fog can take place, oftentimes combining different causes of formation. A critical issue, especially for radiation fog, is the availability of water in the surface, which may be determining for fog formation and its duration and deepening in time. If water is available at the surface or in the upper layers of the

soil, saturation near the ground is easier to reach, turbulent mixing helping to expand the saturated layer upwards. Sometimes saturation is reached only in the late night hours and shallow fog layers are seen at dawn, shortly after destroyed by solar irradiation.

Figure 1: (a) Top left: Measuring the radiation fog in Raimat (Ebro Valley, February 2011); (b) Top right: Radiation fog bands in the airport of Munich (April 2011); (c) Middle left: slope fog in the northern coast of Tenerife (August 2011), (d) Middle right: contained valley evaporation and radiation fog in the Tremp basin (Pre-Pyrenees, December 2012); (e) Bottom: valley fog lifting over the Noguera Ribagorçana river (Pre-Pyrenees, December 2012). Pictures by the author.

Inland water bodies, like moors, lakes or rivers, may act contrarily to the surrounding land areas. Evaporation fog may be formed only over water when the surface becomes warmer than the air, cooled by the land surrounding it, typically in the early morning hours. On the other hand, it may well be that the land areas generate a wide radiation fog, which would only be broken over the water bodies, that have much less radiative cooling.

Over wide flat areas, with minor topographic accidents, no limits other than the extension of the anticyclone and the water availability exist (Haeffelin *et al.,* 2010). Very weak winds can advect fog locally, but the establishment of a general synoptic wind will probably mix and eliminate the fog layer. Instead, the areas that are topographically well delimited, like valleys or larger basins surrounded by mountains, the evolution of the fog layer is determined by the shape of the valley or basin (Figures 2a and 2b).

Narrow mountain valleys generate very often fog due to the availability of water in the rivers, that after evaporating is contained within the valley, and to the fact that a narrow valley cools faster than a flat area, because there is proportionally more surface cooling at night and the cold air accumulates at the bottom. If the valley has a general slope, fog will be transported down-valley at night and up-valley in the day.

Wide basins combine some characteristics of the flatlands and some of the narrow valleys. They contain usually a wide flat area in their center where radiation fog is formed when the proper conditions are met. Once a large fog layer is formed in the basin, downslope flows blow over the fog top and enhance mixing with the clear above, a mechanism that may help to deepen the fog layer (Cuxart and Jiménez, 2012) or may dissipate it, depending very much on the strength of the inversion at the top of the fog and the characteristics of the air above.

Often winter anticyclones over midlatitudes generate persistent fog layers, that in the case of basins stay contained by the topography, with some pulsation over the slopes since they are eroded by the solar radiation in the daytime and recover in the nighttime (Gurka, 1978 and Figure 2d). This kind of topographically contained fog usually stays in place until a change of air mass takes place.

General advection fog over a region is related to the entrance of warm moist air over a cold ground, and it is usually related to a marine air intrusion in the cold season. Wind may be moderate and enhances mixing, generating deep fog layers, usually independently of the diurnal cycle, that will last as long as the situation persists. Sometimes radiation fog is combined with marine advection in well defined valleys (Fitzjarrald and Lala, 1989). More details are given in the discussion on the coastal fog.

Cities generate an urban heat island, that depends on their size and the compactness of the urbanization, being of the order of 3 to 7 degrees higher than its rural surroundings. Obviously radiation fog will be much more difficult to generate over them, also because the availability of soil from the ground is restricted by the surface materials. However, if a large river crosses them, or if the urbanization is not too compact, fog can also cover a cite provided that the temperature is low enough. They also may disrupt an advection fog if they are warmer than the incoming air.

Sea and large lakes

Over the sea -or other large water masses, like lakes or wide rivers-, radiation fog cannot be formed, because of the large heat capacity of water and also because cold water falls into deeper layers and warmer water rises to the surface, preventing the rapid formation of a cold surface at the top of the water body.

The main mechanism of fog formation over the sea is advection (Zhang *et al.,* 2009). At the daily time scale, the surface temperature can be taken as constant and, even if advection of warm air over it may slowly increase the sea surface temperature, this is a very shallow layer staying at the top of the water and losing this heat by conduction downwards into the water, thus maintaining essentially its temperature lower than the one of the advected air mass.

Advection fog is a typical situation with lower latitude advections over colder seas, like in advance of the warm fronts, leading to mist or fog, depending on the characteristics of the arriving air mass. A surface inversion develops as the mass advances and the fog usually occupies its lower layer, the clear-air inversion above disconnecting the fog layer from the shear production of turbulence at the top of the inversion. The depth of the inversion and of the fog layer increases with the distance travelled over the cold surface, starting as a very shallow fog and deepening to several hundreds of meters later on.

Warm advection over seas can also be produced when warm continental air flows over cold sea, which is summer marine fog (as opposed to winter coastal and inland fog, when warm marine air enters land), but also when the air blows from above a warm area or current to a colder one, such as flows blowing first over the warm Gulf current and afterwards over the cold Labrador current, a situation frequent in summer.

Mixing fog generated at the interface of a cold layer over the sea with a warmer layer above and progressing downwards can happen over cold sea waters, especially for warm fronts in winter, as described in the previous section. Also, as mentioned before, mixing and evaporation fog may take place over polar waters under very cold advections.

Coastal

In the coastal areas, there are specific phenomena combining the characteristics of the marine fog and the valley fog. Being a discontinuity area between land and sea, often fog takes place sharply, responding to the abrupt changes of the surface conditions.

The main mechanism related to synoptic conditions is the advection of warm moist air over the colder land surface, usually in the cold season. The fog layer is created at the coast line and it deepens as it progresses from there. This phenomenon can then take place for tens or hundreds of kilometers inland, depending on the conditions found. Usually ascents in land, due to turbulent convection or forced motion uphills will disrupt the fog layer and may lead it to dissipation. This implies that fog inland can be restricted to some preferred passes along valleys, when the surface is moist and convection is very weak or non existent, conditions usually found in winter.

Regarding offshore fog, an important mechanism is related to a warm continental air outbreak over a colder sea. For instance, a synoptic advection pushing warm continental air to the sea, which can happen in the warm season, when the water is usually colder than the land most of the day. Stabilization of the air takes some distance offshore to happen, leading to the formation of fog in front of the coast.

More subtle is the formation of fog due to the existence of land breezes or downslope flows onto the sea. If the sea is warmer than the air, shallow convection disrupts the flow and an area of temperate air is located between the warm sea offshore and the cold land, where evaporation fog could take place in front of the coast and eventually enter some hectometers inland by wind meandering in the early morning. If the sea is colder (by sea upwelling, a cold current or a particular time in spring), air will stratify and generate a shallow advection fog layer that will not progress much further offshore. A third possibility is when land breeze may push inland radiation fog over the coast.

The lowering of a stratus layer to the surface can also happen, especially in areas like offshore California, where the stratus are formed at the trade wind inversion layer and grow downward by turbulent mixing sometimes reaching the ground (Pilié *et al.,* 1979).

Large cities at the coast are able to generate a significant urban heat island. Therefore they may not allow warm marine advection fog be generated over them, but only downwind. They also may disrupt offshore flows, warming them compared to the surrounding areas.

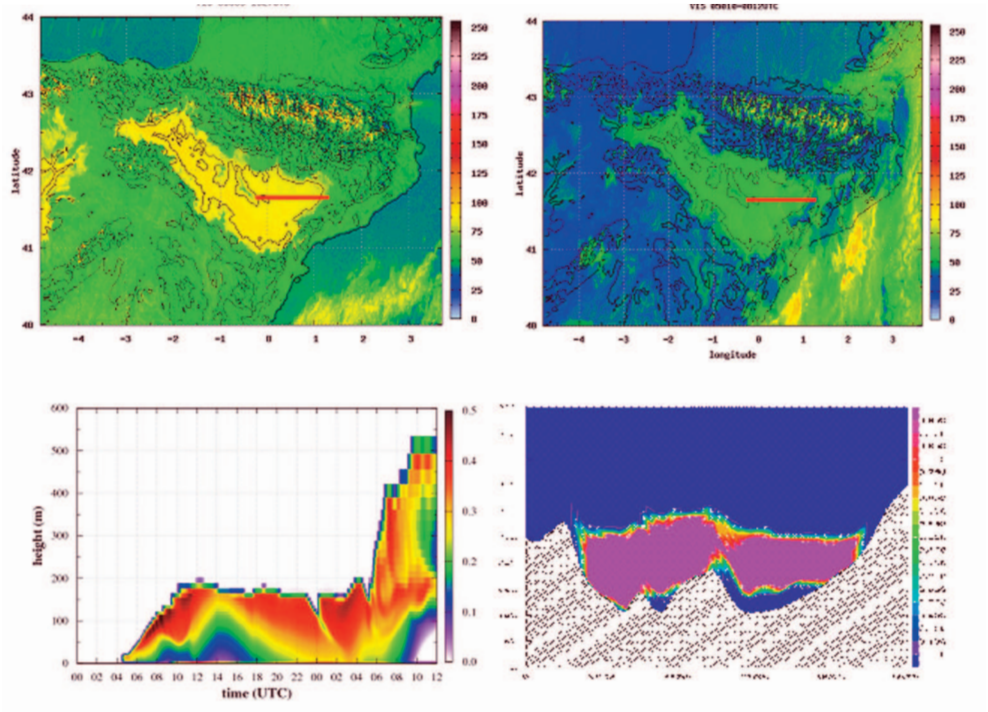

Figure 2: Horizontal coverage of a persistent fog case in The Ebro valley in December 2005. On the upper left (a), extension at noon as seen by the Meteosat visible channel, on the upper right (b) the same for the image after sunrise. Differences only happen in the edges of the cloud layer over the slopes. On the bottom left (c), cloud water evolution (in g/kg), in a mesoscale simulation of the same case, for the Raimat station in the center of the Ebro valley, showing erosion at the bottom at noon. At bottom right (d), for the same simulation, fog layer over the basin at noon (in g/kg, vertical cross-section E-W), indicating erosion of the layer at the bottom and at the edges.

5. MONITORING AND FORECASTING FOG

Due to the very large societal impact of fog events, its adequate monitoring and forecasting is a necessity. New tools of monitoring have been developed in the last decades based on direct sensing of fog along roads or in airports, and also new diagnostics have been built from satellite observations. Forecasting is always difficult because of the subtleties in fog formation, especially related to the lack of knowledge on the aerosol composition of air or the errors in the forecast of the near-the surface temperatures and humidities.

Climatological knowledge

In every part of the world, areas prone to fog are well known by the inhabitants as are the most likely times of the year when they can occur. To make this knowledge quantifiable is attained by statistical analysis of the available data (Tardif and Rasmussen, 2007). These studies can be made with point observational data from visual observations by human observers, recently by visibility observations in specific locations, or by the analysis of satellite fields revealing fog (Bendix, 2002). They allow for planning and anticipating action, establishing the areas and times of risk.

Direct measurement of fog

Until very recently, a fog event was declared in the records when a human observer notified that the visibility was below 1 km. This implies that historical records usually only contain if the event occurred or not in one particular day, without much information on timing within that day. Currently methods that measure the decay of a signal between an emitter and a receiver based on different principles allow to estimate continuously the visibility, are common is most of the main commercial airports, and are becoming widely used in road parts that experience fog often, allowing warning to drivers and authorities in almost real time. This data allows for finer temporal statistical study.

Determining the presence of fog from satellites

Satellites with several spectral channels can be used for the determination of areas covered by low clouds and fog, using the difference between channels in the infrared spectrum (Cermak *et al.,* 2009). Developments continue to distinguish low clouds from fog, sometimes using also available surface information. Monitoring the satellite images allows to characterize the time evolution at the regional scale of the fog layer. The second generation of Meteosat has now enough temporal, spatial and spectral resolution to be used for almost real-time monitoring of large areas of fog.

Numerical and experimental studies for fog-prone regions

For areas where fog is recurring problem, specific studies are a good approximation to characterize the more typical cases (Fitzjarrald and Lala, 1989; Van de Velde *et al.,* 2010; Cuxart and Jiménez, 2012; Cuxart *et al.,* 2012). A possible approach is combining experimental data, usually vertical profiles and information near the surface -including satellites-, with high resolution modeling that resolves properly

the topographical features and has good vertical resolution to describe properly the fog layer. If model results are well supported by the available experimental data, they allow a deep exploration of the physical processes taking place, such as the exploration of energy, momentum. water or turbulence budgets and to seek for the most relevant processes for each particular case.

Direct forecasting methods using local data

Local forecasters are usually well trained to predict radiation fog looking at the conditions at the evening, if very weak or calm winds are expected, if they know the usual cooling rate in their point of interest, they may anticipate the time when fog will be formed following a number of standard methods to determine the saturation temperature (Castejón and García-Legaz, 1985). However, this forecast may fail depending on the magnitude of water and heat fluxes to the surface. If the ground is able to supply heat at good pace, surface may not cool enough to reach the air saturation point. Deposition of water at the surface may go against cloud formation close to the ground. The amount of water vapor above the surface layer may determine if there is enough moisture supply to maintain the fog layer formation. A forecast based on local data would require soil information and a profile of temperature, moisture and wind for some tens of meters of air. The forecast, anyway, could fail, if the aerosol contents of the air is not known or if the wind is not well predicted.

Operational mesoscale simulations

Currently numerical forecasts at high horizontal resolution (few kilometers) are common. These simulations are able to generate fog and describe the time and spatial evolution with detail, similarly to what is made for the specific numerical studies described above (Bergot *et al.,* 2007). Usually operational numerical forecasts have a moderate rate of success in predicting accurately the timing of fog (especially formation and dissipation), especially in coastal areas. This is most likely linked to an inaccurate forecast of nighttime values of the surface layer values of wind, temperature and wind and, for models with a suitable microphysics scheme, also to the lack of information on the aerosol charge of the air. Recent studies shows that sometimes, empirical methods perform better than sophisticated high resolution simulations in terms of forecasting fog occurrence (Holtslag *et al.,* 2010).

Forced one-dimensional models

An alternative approach, implemented in some airports, is to apply one-dimensional versions of the numerical models forced with local observations and locally estimated advections (Terradellas and Cano, 2007). Running these models locally and often allow the forecasters to update their information and to overcome partially the limitations of the inaccurate forecasts of the surface layer meteorological variables.

6. SOCIETAL IMPACTS OF FOG

Effects on human health

On industrialized areas, pollutants can be inside fog droplets, either as condensation nuclei or simply dissolved into them (Kokkola *et al.,* 2003). These droplets can

become acidic. The effects of breathing air containing such droplets is a subject of active medical research. The term "smog" originated in London for episodes combining fog and industrial pollution. Lately it has also been extended to dry pollution episodes involving tropospheric ozone, which is not the subject of interest here. The 1952 event in London reported great impact on the population leading to significant increase of mortality and morbidity for some weeks. The effects are mostly cardiovascular and respiratory (Wichmann *et al.,* 1989). Cleaner air policies have lowered the impact in many parts of the world but it is still an important issue in fast developing countries.

Agricultural impact

Fog can harm cultures in two main ways. Firstly, increasing the time that the leaves of a plant are wet, which is the main factor leading to fungus infection and loss of production if treatment is not timely provided and in the proper amount (Carroll and Wilcox, 2003). Secondly, frequent fog in the growing season may also affect productivity by diminishing the amount of insolation on the leaves and retarding the plant growth. On the other hand, on arid climates with frequent fog formation, such as on slopes where marine air is pushed upward and condensates, fog water may allow plants to survive and the use of artificial devices to capture this water may be used for agricultural purposes as well (Marzol, 2002).

Road traffic

Areas prone to fog suffer an important affectation on road traffic. Besides the obvious speed reduction that dense fog implies, low visibility is linked with an increase of collisions between vehicles. According to a report of the USA Federal Highway Administration (FHWA, 2012), fog affects the drivers capabilities and behavior and implies action on road treatment strategy, access control to highways and adjusting the speed limits and controlling them. Weather-related crashes are mostly due to heavy rain and snow conditions, only 3% being related to fog in the USA between 1995 and 2008. However the fog-related crashes amount 8% of the total casualties of weather-related crashes, that usually involve many vehicles in one single accident. ADAC informs that in 2011, 1% of the total number of traffic casualties in Germany were related to fog (ADAC, 2013).

Airport operation

Fog affects very heavily airport operation (Allan *et al.,* 2001). It is one of the weather events provoking more flight delays and cancellations (Robinson, 1989). Many airports are located in areas where fog can take place, in the flat bottoms of basins or near the coast. Typically 1% of the time fog may affect an airport. According to the USA Bureau of Transportation (2013), weather related delays are about one-half of the total delays. Statistics for individual airports report foggy conditions as one of the major disrupting events for their ordinary operation. Only few airports can operate in dense fog and not many aircraft are equipped to do so. In consequence, fog implies cancellation or severe delay of flights, also because the security delay imposed between takeoff and landing operations. Another issue, important at high latitudes in winter, is freezing fog, that deposits ice on the wings and implies de-icing, an operation causing significant delay, especially in busy airports.

Maritime transport

Fog severely limits mobility of the large vessels inside harbors and generates conditions for incidents or collisions between vessels. For the Rotterdam harbor, visibility is less than 1500 m 1.4% of the time. On the other hand, large maritime areas may be covered by persistent advection fog, as in the China seas or the English Channel, and risk of collision is high. The Marine Accident Inquire Agency of Japan reported (2007) that 4% of the marine accidents in the Japan area occurred in fog, about 30 per year. Failure in adequately following the safety protocols in fog (involving acoustic signals, use of fog lights and radar monitoring) is reported as the main cause of accident. Most collisions happen close to harbors, where traffic density is maximal.

7. STRATEGIES TO MINIMIZE THE IMPACT

In the past, efforts have been devoted to artificially modify clouds, either to increase the probability of precipitation in arid areas, to avoid hail or to dissipate fog. In a restricted range of the relevant meteorological parameters, some tries have been successful. Nevertheless, it is now commonly accepted that the performance of these methods, that aim to modify the microphysical composition of the cloud or its thermal state, is generally very low and that they present numerous drawbacks.

Fog dispersion methods include aerosol contents modification that, if used regularly, generates concerns about accumulation of the used material in the ecosystems once it falls on the ground. Another approach is the warming of the layer, which either implies combustion of material or mixing with warmer air above. Both methods are very energy consuming, the first leading often to pollution problems, the second necessitating fanning by wind mills or helicopters. Nevertheless, the essential limitation of all these methods is that they act very locally and are not suited to address large areas. Besides, weak wind meandering will import over the place surrounding air continuously. A method that works in many occasions and has relatively low cost and impact is the seeding of supercooled radiation fog with ice condensation nuclei, which promotes the growth of ice crystals, eliminating droplets and finally falling to the ground.

Current general practice is to know well the phenomenon locally, to analyze well the fog climatology before choosing the location of a new installation, and to improve as much as possible its forecast for places prone to fog, which is a task for atmospheric scientists. On the other hand. methods must be developed continuously to improve the "sense and avoid" strategy of the concerned transport methods, especially for road and marine transportation. Direct detection onboard scanning the surroundings, using optical devices, and remotely controlling the position of other vehicles, using GPS or similar tools, are currently in development. Use of cameras in real time broadcasted through the internet is also an option for road traffic. For aircraft transportation, installation of technology for landing operations onboard and in airports is a clear way to proceed.

Finally, avoiding smog is a matter of public health policy and it must be regulated with the appropriate local, national and supranational regulations. In what refers

the affectation of fog on crops, very sensitive species should not be cultivated in fog-prone areas, such as the bottom of valleys, but on elevated slopes, where the occurrence of fog is much less frequent.

8. SUMMARY

The occurrence of fog affects many aspects of the daily life, especially transportation. In midlatitudes it is essentially a winter and spring phenomenon over land and in the coast, linked to high-pressure systems for the radiation fog and to warm advections over cold surfaces in the case of advection fog. Both types of fog can be very persistent and affect normal operations for several days. Cities may suffer less fog than their surroundings because they are usually warmer.

The amount of time that one specific location, such as an airport or a harbor, can be affected by fog is around 1 % of the time. However its impact in terms of economic losses or road traffic casualties is high. Artificial dispersion of fog is not very efficient, except for the case of supercooled fog, and prevention, monitoring and good forecasting are the available tools to treat the challenge that a fog event poses to a transport infrastructure.

ACKNOWLEDGMENTS

Part of the information exposed is fruit of research funded by the Spanish Ministry of Economy and Innovation, through grant CGL2009-12797-C03-01, co-funded by European FEDER funds. Maria Antònia Jiménez (IMEDEA, UIB-CSIC) has contributed in the making of Figure 2.

REFERENCES

Allan, S. S., S. G. Gaddy, and J. E. Evans. Delay causality and reduction at the New York City airports using terminal weather information systems. No. ATC-291. Lincoln Laboratory, Massachusetts Institute of Technology, 2001.

Bott, A., U. Sievers, and W. Zdunkowski. "A radiation fog model with a detailed treatment of the interaction between radiative transfer and fog microphysics." *Journal of the Atmospheric Sciences* 47,18 (1990): 2153-2166.

Carroll, J. E., and W. F. Wilcox. "Effects of humidity on the development of grapevine powdery mildew." *Phytopathology* 93.9 (2003): 1137-1144.

Castejón, F. and García-Legaz, C. (1985). "Predicción de nieblas. Aplicación particular al aeropuerto de Madrid Barajas", Instituto Nacional de Meteorología, Publicación A-112, 89 pp., Madrid (Spain).

Cermak, Jan, *et al.* "European climatology of fog and low stratus based on geostationary satellite observations." *Quarterly Journal of the Royal Meteorological Society* 135.645 (2009): 2125-2130.

Cuxart, J., and M. A. Jiménez. "Deep radiation fog in a wide closed valley: Study by numerical modeling and remote sensing." *Pure and Applied Geophysics* 169.5 (2012): 911-926.

Duynkerke, Peter G. "Radiation fog: A comparison of model simulation with detailed observations." *Monthly Weather Review* 119.2 (1991): 324-341.

Fitzjarrald, David R., and G. Garland Lala. "Hudson Valley fog environments." *Journal of Applied Meteorology* 28.12 (1989): 1303-1328.

Gultepe, I., *et al*. "Fog research: A review of past achievements and future perspectives." *Fog and Boundary Layer Clouds: Fog Visibility and Forecasting* (2007): 1121-1159.

Gultepe, I. "Fog and Dew Observations and Modeling: Introduction." *Pure and Applied Geophysics* (2012): 1-2.

Gurka, James J. "The role of inward mixing in the dissipation of fog and stratus." *Monthly Weather Review* 106 (1978): 1633.

Haeffelin, M., *et al*. "PARISFOG: Shedding New Light on Fog Physical Processes." *Bulletin of the American Meteorological Society* 91.6 (2010): 767-783.

Holtslag, M. C., G. J. Steeneveld, and A. A. M. Holtslag. "Fog forecasting:"old fashioned" semi-empirical methods from radio sounding observations versus "modern" numerical models." *5th International Conference on Fog, Fog Collection and Dew*. 2010.

Jacobs, W., Nietosvaara, V., Bott, A., Bendix, J., Cermak, J., Michaelides, S., & Gultepe, I. (2008). Short range forecasting methods of fog, visibility and low clouds. In *COST Action* (Vol. 722).

Kokkola, H., S. Romakkaniemi, and A. Laaksonen. "On the formation of radiation fogs under heavily polluted conditions." *Atmospheric Chemistry and Physics* 3.3 (2003): 581-589.

Pilié, R. J., Mack, E. J., Rogers, C. W., Katz, U., & Kocmond, W. C. (1979). The formation of marine fog and the development of fog-stratus systems along the California coast. *Journal of Applied Meteorology*, *18*(10), 1275-1286.

Robinson, Peter J. "The influence of weather on flight operations at the Atlanta Hartsfield International Airport." *Weather and Forecasting* 4.4 (1989): 461-468.

Tardif, Robert, and Roy M. Rasmussen. "Event-based climatology and typology of fog in the New York City region." *Journal of Applied Meteorology and Climatology* 46.8 (2007): 1141-1168.

Van der Velde, I. R., Steeneveld, G.J., Wichers Schreur, B.G.J. and Holtslag, A.A.M. "Modeling and forecasting the onset and duration of severe radiation fog under frost conditions." *Monthly Weather Review* 138.11 (2010): 4237-4253.

Wichmann, H. E., *et al.*, "Health effects during a smog episode in West Germany in 1985." *Environmental health perspectives* 79 (1989): 89.

Zhang, S. P., Xie, S. P., Liu, Q. Y., Yang, Y. Q., Wang, X. G., & Ren, Z. P. (2009). Seasonal Variations of Yellow Sea Fog: Observations and Mechanisms. *Journal of Climate*, *22*(24), 6758-6772

Zhou, Binbin, and Brad S. Ferrier. "Asymptotic analysis of equilibrium in radiation fog." *Journal of Applied Meteorology and Climatology* 47.6 (2008): 1704-1722.

I. ADVERSE PHENOMENA

B) MIXED

CHAPTER 14

A HOLISTIC APPROACH TO KNOWLEDGE OF FLOODS

María del Carmen LLASAT BOTIJA

Department of Astronomy and Meteorology. University of Barcelona
carmell@am.ub.es

ABSTRACT

According to the International Strategy for Disaster Reduction of the United Nations (UNISDR, 2009), floods are among the so-called hydro-meteorological hazards. Meteorological and climatic factors, drainage basin factors, drainage network and channel morphometrics and human factors play a major role, and for this reason they can be considered as a paradigmatic example of complex hydro-meteorological hazards. The first objective of this chapter is to present floods from a holistic approach, useful for the greater part of natural risks, ranging from prevention to subsequent recovery. The second focuses on providing some notions on the classification of floods with a view to their multidisciplinary treatment, as well as their temporal and spatial distribution in the Mediterranean area, and particularly in Catalonia. Finally, trends and future scenarios launch a reflection on their potential increase, as well as proposals for action.

Key words: floods, heavy rainfalls, natural risk, vulnerability, hazard, risk awareness.

1. INTRODUCTION

Floods constitute the main natural hazard in the world. A comparison made by the United Nations, relating to the frequency and spatial distribution of natural disasters in the world, shows that on average 284 disasters produced by floods or storms (including hurricanes and tornadoes) are recorded annually, as against 31 associated with earthquakes and 6 with volcanoes, most of them affecting Asia, with Europe in second place. Again as an average, the number of people affected annually by floods exceeds one hundred and five million, compared with the forty-one million who might be affected by storms, tornadoes and hurricanes (UNISDR, 2009). In Spain, floods constitute the main natural hazard. Thus, between 1971 and 2002, floods accounted for the Consorcio of Compensation of Seguros for over 75% of the compensation payments made, while between 1995 and 2004 they were responsible for 31% of the fatalities produced by natural hazards.

According to the European Directive on Floods (DIRECTIVE 2007/60/CE), "flooding" is deemed to be the temporary submerging of land that is not normally covered by water. That includes floods caused by rivers, swollen mountain streams, intermittent water courses, and the Mediterranean floods caused by the sea in coastal zones. The Directive does not contemplate flooding of drainage networks, which constitutes the basis of what are termed "urban floods". In the light of that definition, floods can be treated as a natural hazard in which there converge causes of a very diverse nature, starting with the strictly meteorological, whether they be heavy rainfalls or storms at sea. However, and given that other chapters in this book deal with both themes, this chapter centres its attention on floods per se, and their treatment from an integrating perspective. The work is completed by drawing up a climatology of floods and their distribution in the Mediterranean area.

2. A MULTIDISCIPLINARY TREATMENT OF THE RISK OF FLOODING

Given the complexity of the processes involved in floods, they constitute one of the natural hazards most in need of treatment from a holistic and interdisciplinary perspective. Accordingly, the first difficulty arises from the need to use a common language among the various actors involved, or at least for there to exist a mutual comprehension that encourages the communication process and work between different scientific disciplines and sectors. Words such as "storm", for example, are not associated with the same meaning in a setting of hydrological modelling as in the meteorological sphere. Indeed, not even the classification of the types of hazards or of the content that includes the terms "vulnerability" and "hazardousness" can be considered to be standardised for a common use. It is for that reason that this chapter will be governed by the definitions given by the United Nations within its International Strategy for Disaster Reduction (UNISDR, 2009).

2.1 Anatomy of the risk of flooding

In essence, the UNISDR classifies risks into those which derive from a hydrometeorological, a geological or a biological hazard or threat. A hydrometeorological threat would thus be seen as a "Process or phenomenon of atmospheric, hydrological or oceanographic nature that may cause loss of life, injury or other health impacts, property damage, loss of livelihoods and services, social and economic disruption, or environmental damage". They would include, for example, forest fires, droughts and floods. For the last of these, and in view of the notable interweaving of sociological aspects in them, the nomenclature of "socio-natural" hazards is also used in referring to them.

To continue with the above discourse, natural hazards, and therefore the hazard of floods, call for a prior knowledge of some basic concepts. Firstly, it should be noted that the expression "natural risk" is used as against "technological risk", but does not imply that the risk is the consequence of an exclusively natural hazard or that human beings had not intervened or might intervene in unleashing or mitigating it. This is an aspect inherent to the study of floods, since actions such as channelling, construction of channelling structures, reservoirs and dams, alterations and diversions of water courses and, in general, most hydraulic works, involve a certain amount of risk. Then, on the other hand, human beings can also intervene in processes of mitigation.

In order to be able to calculate the risk and create a cartography of it, risk is usually considered as the product of "dangerousness/hazardousness" by "vulnerability". The former is known in English as "hazard" and in French as "aléa", and refers to the probability of a certain natural phenomenon, of a certain extension, intensity and duration, with negative consequences, arising. According to the type of phenomenon, man may have an influence on that probability (for example, work carried out on hydrographic basins may alter the dangerousness of floods). The analysis of return periods or the representation of maps of frequency is the object of this first part. Vulnerability refers to the impact of the phenomenon on society and on ecosystems, and it is precisely an increase in vulnerability that is leading to a greater increase in natural hazards (IPCC, 2011). The concept of vulnerability is very broad, ranging from the use that is made of the territory through to the structure of buildings and constructions, and depends heavily on the response of the population in the face of the risk (Brilly and Polic, 2005). Aspects such as the existence of emergency plans and the perception and education of the population vis-à-vis the risks are nowadays considered to be included here, although they do not enter into a quantification of the risk. "Exposure" refers to the exposed goods liable to be affected by a risk, such as people, buildings, vehicles, etc. In some scientific settings this is included within vulnerability, while in others it is considered as a third factor in the product.

One cannot speak of the risk of floods without bearing in mind mitigation and adaptation measures, which in essence include prevention, prediction, emergency management and resilience. There thus exist four clearly identifiable spheres of action:

• *Prevention by means of intervention in the territory and the establishment of forecasting and announcement mechanisms.* This is in general a matter of measures implemented over the long term, which can be of a structural (e.g. dams) or non-structural (e.g., regulations on the occupation of floodable zones, action plans and procedures) nature. This sphere also includes research and study of the factors involved in risk of floods.

• P*rediction, which refers to anticipating a phenomenon a varying amount of time ahead of its occurrence.* Prediction is limited by the existing techniques and instruments, and in the case of floods depends heavily on the characteristics of the associated processes. Episodes such as the floods that affected the basins of the Danube and the Rhine in the summer of 2002 (James *et al.,* 2004) called above all for working with propagation hydrological models, while in the case of the flash floods that occurred in September of that same year in the basin of the River Gard (Delrieu e*t al.,* 2004) in southeast France, prediction required the utilisation of mesoscale meteorological models and meteorological radar, as is also usual for the floods recorded in the Spanish Mediterranean (Atienza *et al.,* 2011). A notable emphasis has been placed in recent years on early warning systems, referring to the overall capacities needed to generate and disseminate alerts in an appropriate and efficient manner in order to prepare sufficiently in advance to reduce the possibility of losses and damage arising. Meteorological and hydrological services lie fully within this sphere, though the role of research in improving prediction tools should not be forgotten.

• *Management of emergencies.* Usually laid on by Civil Protection teams and mainly concentrated on the time interval between the alert issued by the pertinent media and the end of the necessary coordination and salvaging work. Management implies the existence of action procedures laid down in advance, and fitting in with the two preceding aspects.

• *Recovery.* This refers to the capacity to return to normality following a flood, and to the public and private measures of assistance and repair of the damage caused by the disaster. Included under this are compensation for damage (insurance) and decrees or extraordinary measures focusing on aid to help the affected zones to recover (such as the establishment of tax allowances). Strictly speaking, resilience also refers to that capacity for recovery, but given that such capacity also depends on the preceding spheres, the usual practice is to evaluate the greater or lesser resilience of a city or region in the light of all four spheres.

This section should not be brought to a close without mentioning the importance of legislation, which lies behind procedures, definition of floodable zones, action measures and actors involved, or processes laid down as a consequence of catastrophic flooding episodes or ones with loss of human lives. Finally, and although already mentioned above, stress should be laid on the importance of communication in processes centring on mitigation of flood damage. Informing the population of the flooding risk to which the zone is exposed, about how to act in the face of a river overflowing its banks, would prevent many of the deaths that still occur worldwide as a result of floods.

2.2 A diagnosis of the present situation

There exists nowadays an international consensus concerning the need to tackle floods from a holistic perspective in order to increase adaptation and resilience, as well as reduce the negative impacts. That approach is set out in the latest report from the IPCC on climatic extremes and climate change (IPCC, 2011), and in the proposals from the United Nations encompassed within the Hyogo Framework for Action 2001-2015, on increasing the resilience of nations and communities in the face of disasters. One example of the latter would be the initiative "Making Cities Resilient. My City is Getting Ready!", which deals in particular with floods in the case of the Mediterranean cities. All these initiatives contemplate all the aspects outlined above, and most particularly, the ones connected with vulnerability. Factorial breakdown of the causes and consequences of a flood, and particularly of vulnerability, still remains a challenge today.

Within this context, and at European level, the present situation is governed by the European Directive on Floods (DIRECTIVE 2007/60/CE, European Parliament, 2007) which looks at flood risk management plans focusing on prevention, protection and preparation, taking account of the fact that many European basins are shared between different countries or autonomous regions within countries, thereby bringing into play the solidarity principle. The Directive looks at five consecutive phases: 1) preliminary evaluation of the flood risk; 2) maps of hazardousness due to floods, and maps of flood risk; 3) flood risk management plans; 4) coordination with the Framework Directive on Water (Directive 2000/60/CE, European

Parliament, 2000), public information and consultation; 5) execution measures and amendments. The first two phases have to be concluded by the end of 2013, a task on which all the Hydrographic Confederations are currently working.

3. CLASSIFICATION OF FLOODS

There is no single or commonly accepted classification for floods. If we look at those caused by overflowings, within many contexts the term "floods" refers to swellings of large river courses, usually basins larger than 10,000 km^2, while the term "flash floods" would be used for the ones affecting small basins and having a response time of only a few hours, though even here no objective criterion exists. We will nevertheless remain with the definition already introduced, considering both types to be floods.

3.a Taking account of the causes

This is basically the approach taken by Civil Protection personnel. In it, floods are floods distinguished by:

- Floods due to "in situ" precipitations.
- Floods due to freshets or overflowings of rivers, streams or gulleys, lakes or marshes caused or boosted by precipitations, thawing, obstruction of river beds or the action of tides and winds.
- Floods due to breakage or improper operation of hydraulic infrastructure works.

3.b Taking account of the impacts

When the aim is to work with flood series the main problem lies in a lack of information about levels and flows. And the problem becomes insurmountable in the case of non-instrumentalised basins, as is the cases of most of the Mediterranean streams. That is why recourse is usually had to documentary sources such as municipal or ecclesiastical archives, which are fundamental where the aim is to work on historical floods (Barriendos *et al.,* 2003; Barnolas and Llasat, 2007a), or press reports, technical reports and eye witnesses for the relatively more recent episodes (Llasat *et al.,* 2009a).

Many scientific studies indeed use the press as a basis for the identifying events and damage, for drawing up a cartography of zones at risk from flooding, or for studies on perception and communication (Petrucci and Polemio, 2003; Guzzetti and Tonelli, 2004). By way of example, Figure 1 shows the distribution of the number of news items published by *La Vanguardia* newspaper about floods, in comparison with the INUNGAMA database (Barnolas and Llasat, 2007b). Although a certain correlation can be observed from the outset, that correlation increases when referring to the number of episodes of floods, in which case it is 0.5, with a significance level of 95%, a value that is surpassed if restricted to the news items published in the first month following the floods (Llasat *et al.,* 2009b). For information purposes, the number of headlines per flood event is around five on average.

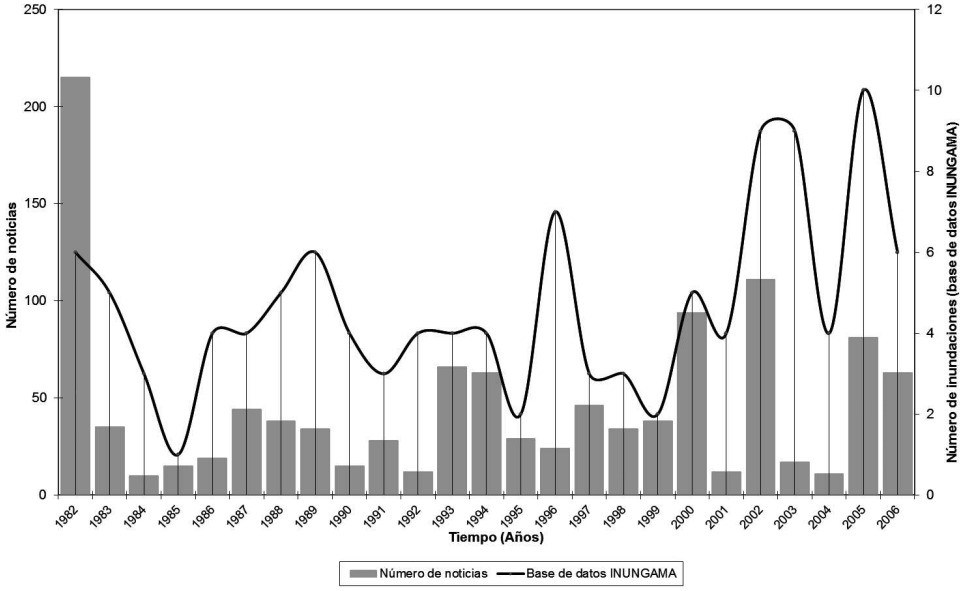

Figure 1. Comparison between the number of news items about flood episodes occurring in Catalonia (source: La Vanguardia) and the number of episodes according to the INUNGAMA database, for the period 1982-2006). (Adapted from Llasat *et al.,* 2009).

Accordingly, one of the most frequently used is based essentially on the impacts of the event and its description. A distinction could thus be drawn between *catastrophic extraordinary and ordinary floods.* In the literature, particularly that which focuses on treatment and comparison of flood series (Barriendos *et al.,* 2003; Llasat *et al.,* 2005; Barrera *et al.,* 2006), that terminology refers to the damage caused in a particular place or basin. *Catastrophic* thus involves overflowings with serious damage to or total destruction of one or more infrastructures or buildings; *extraordinary* also involves overflowings, but with less damage; *ordinary* floods refers to rises in level that could carry away temporary infrastructures on the river, or (nowadays) vehicles. Losses of life may occur in any of them, though in the last case it is usually due to lack of prudence.

The concept of catastrophic varies, however, when used in other types of cataloguing. For example, in the database created by the Catholic University of Louvain and known as EM-DAT (Emergency Events Database), a condition is set that a state of emergency must have been declared or that more than 10 people must have died, among other criteria (for a comparison of criteria, the reader may consult Llasat *et al.,* 2013). It is for that reason that one of the current lines of research of projects such as HYMEX (Hydrological I MEditerranean EXperiment) centres on the creation of a database of flood impacts and a proposal for homogeneous criteria.

3.c Taking account of the physical characteristics

This type of classification refers essentially to precipitation and to the response of the river or water course, although it also considers aspects of prediction,

management and impacts (Llasat, 2009). Given that the characteristics of the basins will play a decisive role, we will take the view that, broadly speaking (and especially for the Mediterranean zone), that they can be grouped together into three types: A) basins larger than 2000 km^2, with rivers having permanent flow with a greater or lesser snow-melt contribution, usually arising in high-mountain areas; B) intermediate basins (50–2000 km^2), with permanent flow, but with markedly seasonal regime; C) small basins (less than 50 km^2) with steep gradients and torrential flows, for which a distinction can be made between those situated at the head of rivers of types A and B, and the littoral watercourses commonly known as streams or gulleys. We could also include in this last section some urban basins.

If the intensity and duration of the pluviometric episode responsible for the freshets, the degree of convection of the precipitating system, the hydrological response, the possibility of prediction and management, and the potential impacts are taken as indicators, it is possible to point to the following classification:

Type 1. Flash floods produced by very heavy and localised rainfall

These are the sudden floods ("flash-floods") that occur in type-C water courses as a consequence of highly convective rainfall episodes with very high peak intensities (it is not unusual to encounter intensities per minute in excess of 3 mm/min), of short duration (about one hour or less) and with accumulated quantities of less than 100 mm. They are usually caused by the development of local unicellular or convective systems in a meteorological setting characterised by a strong instability at low levels, although they do not require a high degree of organisation. They typically occur in summer and may seriously affect densely populated zones or ones with considerable tourist activity. Predicting them calls for the application of mesoscalar meteorological models and the use of meteorological radar, and can be improved using "blending" techniques (Atenzia e*t al.,* 2010). The application of hydrological models is difficult in that they are usually non-gauged basins. The response time is practically nil, so that prevention through warnings and signalling, and adopting prudent behaviour, is of fundamental importance. The damage mainly centres on the sweeping away of vehicles, cutting of communication ways and, if there is electrical storm activity there may also be local power cuts. In general they can be classified as lying between ordinary and extraordinary floods.

Type 2. Floods due to very heavy and continuous rainfall

These are episodes associated with rainfalls of strong or moderate intensity, but which can accumulate more than 200 mm in less than seventy-two hours. They normally occur in autumn, since they require the formation of more organised convective systems, but cases have also been recorded in summer (e.g., the floods of August 1983 in the Basque Country), or in the spring (such as the floods of June 2000 in Catalonia). In the light of their duration and extension it is possible to distinguish between two subtypes.

Type 2a includes the flash floods that can affect basins of types B and C, produced by very abundant precipitations within a time interval that ranges from 2 to 6 hours, and which are usually associated with stationary multicellular systems, convective trains or Mesoscalar Convective Systems (MCS) (Rigo and Llasat, 2004). If they

affect populated torrential basins they produce catastrophic damage and usually loss of human lives, since the response times for the salvage teams is very short. The models already permit an "early warning" to be given, but uncertainties regarding how much and when and where remain high, also calling for the use of meteorological radar. One example would be that of Biescas (Aragón) in August 1996, or those in the Vallès region of Barcelona province in September 1962.

Type 2b floods correspond to larger basins, with response times of one to two days, associated with more continuous and extensive precipitations, which are moderately convective, with a duration of two to four days though with high intensity peaks, in which it is not unusual for the overall rainfall to exceed 300 mm, while it can even reach 1000 mm. They are associated with stationary synoptic configurations, as in the case of the floods in October (Valencia) and November 1982 (Catalonia). The radar generally shows the Mesoscalar Convective Systems or multicellular storms developing in a setting of extensive but low-intensity precipitation. They may also cause catastrophic damage, particularly due to material losses, while any victims are usually the result of imprudence, accidents or of being left trapped in buildings without possibility of evacuation.

Type 3. Floods due to continuous rains

Produced by long-duration, weakly convective rainfall, but with peaks of high intensity, associated with convection absorbed into stratiform precipitation (Rigo and Llasat, 2004). This can give rise to floods in basins of type A, such as the River Ebro or the River Tajo, an example being the floods of August 2002 in Central Europe. In this case the response time for management of the emergency does allow measures to be taken, such as the construction of temporary dykes, or lamination by means of reservoirs. In very large basins the prediction of flow is based on hydrological models of propagation. It should also be noted that if the peaks of some intensity affect small sub-basins they can give rise to freshets of the foregoing types. If they occur in spring they can be swollen by snow-melt. The type of damage they produce is usually estimated as extraordinary, though in some cases — owing to cultural and personal goods remaining underwater for several days, or losses of crops — they can be catastrophic (e.g., the floods of 2002).

Type 4. Floods due to snow-melt

These are not common in Spain, and in general occur in spring. One case would be freshets of the rivers that rise in the high mountains when early snow-melts occur (winter) as a result of an unusual increase in temperature.

4. FLOODS IN THE MEDITERRANEAN AREA

Figure 2 shows the distribution of floods in the Mediterranean for the period 1990-2006 (Llasat *et al.,* 2010), with a total of 185 episodes of flooding, some of which affected more than one basin, and even more than one country. In total, they caused 4,500 victims and damage exceeding 29,000 million euros, with Italy being the country that registered the greatest economic losses over that period. The data were obtained from various European projects and databases, and although they still suffer from certain gaps, given the disparity of criteria, they show how

significant they are, particularly in the Western Mediterranean. The months of September and November (the period when most of the type-2 floods are recorded) account for 55% of them; some 17% are recorded in the summer (generally type-1 floods), while 15% are recorded in the winter, mostly in the Eastern Mediterranean. The interannual analysis for the period shows a certain tendency to increase, but as has been shown in many studies that increase is more closely related with a rise in vulnerability and exposure (Barredo, 2009; IPCC, 2012). Indeed, between 1985 and 2006 the population in the countries on the Mediterranean coastline rose from 352 to 450 million people, most of them concentrated on the coast, and in many regions close to torrential watercourses.

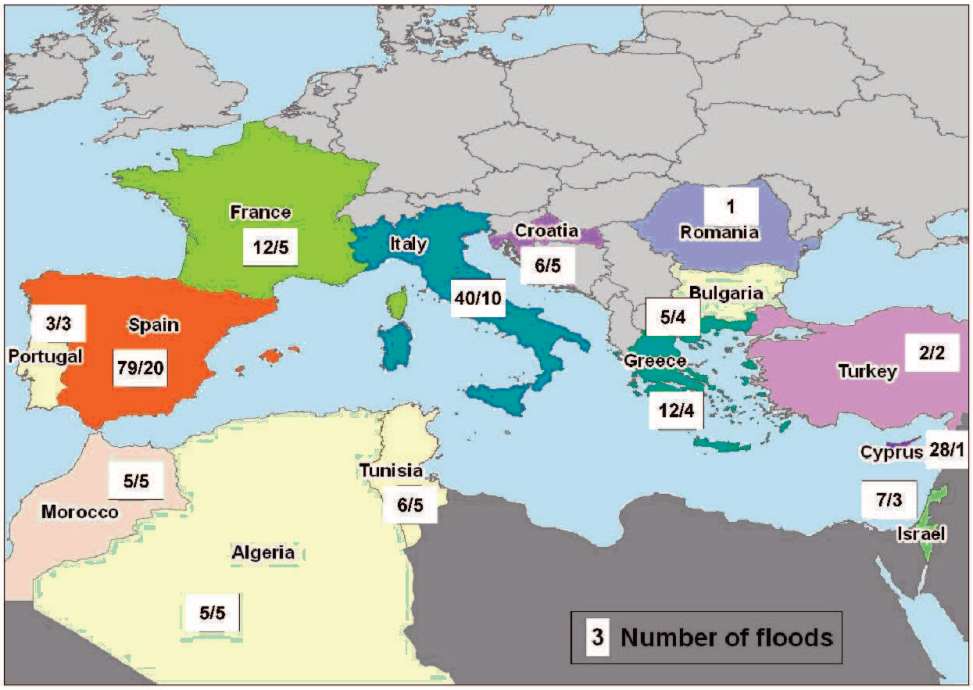

Figure 2. Number of episodes of floods recorded for the period 1990-2006 (left), and for the period 1996-2004 (right), according to the database of the MEDEX project (Llasat *et al.,* 2010).

A recent study (Llasat *et al.,* 2013) on flood episodes recorded between 1981 and 2010 in Catalonia and the Balearic Islands (Spain), Calabria (Italy) and SE France, showed a total of 385 episodes, of which 19% caused human casualties, while 61% may be considered catastrophic. Most of them were concentrated on the coast, as in the case of Catalonia (Figure 3), where of the 213 recorded episodes only 10.3% were catastrophic, while 53.5% had impacts of extraordinary character. The same study revealed the difficulty of creating homogeneous databases, as for France only 19 catastrophic episodes were recorded, with no information for the other types of events. For the Balearic Islands, whose basins are mostly of type C, with non-

permanent flow, of the 36 episodes recorded 77% were extraordinary. While in the preceding regions the type 1 and 2a episodes predominated, and the catastrophic episodes were usually of type 2b, the conditions in Calabria are very different, since a substantial proportion of the 107 were of type 3. An analysis of tendencies supports the conclusions set out above, with a significant tendency being observed only for catastrophic floods, and that disappears with the onset of the economic recession in 2007, a phenomenon which opens up future channels for study.

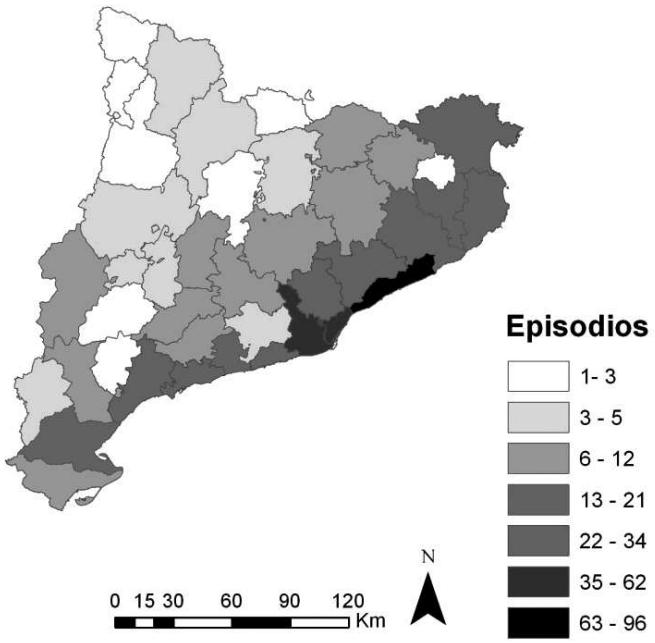

Figure 3. Number of floods per county in Catalonia, for the period 1981-2010 (Llasat *et al.*, 2012).

5. DISCUSSION AND CONCLUSIONS

All studies currently indicate that the increase in natural risks in the world is due to increased vulnerability, economic impact and perception, rather than increased hazardousness. More specifically, European Directive (DIRECTIVE 2007/60/CE, European Parliament, 2007) and the IPCC (2011), noted that an increase in human settlements and economic goods on alluvial plains, a reduction of the natural capacity of water retention by the soil as a consequence of changes in the use of land, and deforestation and impermeabilisation, along with climate change, are contributing to an increased potential for floods worldwide, as well as an increase in their negative impact.

It is for this reason that it is now necessary to approach the study of floods from a holistic perspective that also takes account of improved techniques in prevention, prediction, emergency management and recovery. That also depends on the

inherent characteristics of the flood, however, it being possible to distinguish between different types, ranging from the flash floods occurring as consequence of highly convective, short-duration, local and intense rainfall through to floods over large basins associated with long-duration, essentially statiform rainfall, with absorbed convection in some areas. A knowledge of the essential, physical characteristics of this type of events, as well as their spatial and temporal distribution in some zones, would be of great help in improving prevention. The application of different hydrological models fed into different meteorological outputs, whether they be feeds of rain taken from mesoscalar models or from radar data, can be discerned as a requirement for the future. For this purpose, the utilisation of GRID-type (networked computers, data and models) are emerging as a valuable tool.

ACKNOWLEDGEMENTS

This paper has been drawn up within the framework of the project Distributed Research Infrastructure for Hydro-Meteorology (DRIHM), under FP7-INFRASTRUCTURES-2011-2, as well as the HYMEX programme.

REFERENCES

Atencia, A., Rigo, T, Sairouni, A., Moré, J., Bech, J., Vilaclara, E., Cunillera, J., Llasat, M.C., Garrote, L. (2010). Improving QPF by blending techniques at the meteorological Service of Catalonia. *Nat. Hazards Earth Syst. Sci., 1*0, 1443–1455.

Atencia, A., Llasat, M.C., Garrote, L., Mediero, L. (2011). Effect of radar rainfall time resolution on the predictive capability of a distributed hydrologic model. *Hydrol. and Earth Syst. Sci Discussions,* 15, 3809–3827.

Barnolas, M. y Llasat, M.C. (2007a). *Metodología para el estudio de inundaciones históricas en España e implementación de un SIG en las cuencas de Ter, Segre y Llobregat,* Ministerio de Fomento, ISBN: 978-84-7790-449-0, NIPO: 163-07-016-0, 264 pp.

Barnolas, M. y Llasat, M.C. (2007b). A flood geodatabase and its climatological applications: the case of Catalonia for the last century, *Nat. Hazards Earth Syst. Sci.,* 7, 271–281.

Barredo, J. I. (2009). Normalised flood losses in Europe: 19702006, *Nat. Hazards Earth Syst. Sci.,* 9, 97–104.

Barrera, A., Llasat, M.C. y Barriendos, M. (2006). Estimation of the extreme flash flood evolution in Barcelona County from 1351 to 2005, *Nat. Hazards Earth Syst. Sci.,* 6, 505–518.

Barriendos, M., Coeur, D., Lang, M., Llasat, M.C., Naulet, R., Lemaitre, F. y Barrera A. (2003). Stationarity analysis of historical flood series in France and Spain (14th-20th centuries), *Nat. Hazards Earth Syst. Sci.,* 3, 583-592.

Brilly, M. y Polic, M. (2005). Public perception of flood risks, flood forecasting and mitigation, *Nat. Hazards Earth Syst. Sci.,* 5, 345-355, 2005.

Guzzetti, F. y Tonelli, G. (2004): SICI: an information system on historical landslides and floods in Italy, *Nat. Hazards Earth Syst. Sci.,* 4, 213–232.

Delrieu, G., Ducrocq, V., Gaume, E., Nicol, J., Payrastre, O., Yates, E., Andrieu, H.,

Ayral, P.-A., Bouvier, C., Creutin, J.-D., Livet, M., Anquetin, S., Lang, M., Neppel, L., Obled, C., du Châtelet, J. Parent., Saulnier, G.-M., Walpersdorf, A., Wobrock, W., (2004). The catastrophic flash-flood event of 8–9 september 2002 in the Gard region, France: a first case study for the Cévennes-Vivarais Mediterranean hydro-meteorological observatory. *J. of Hydrometeorology* 6, 34–52.

IPCC, 2007. *Climate Change 2007: Synthesis Report. Contribution of Working Groups I, II and III to the Fourth Assessment Report of the Intergovernmental Panel on Climate Change* [Core Writing Team, Pachauri, R.K and Reisinger, A. (eds.)]. IPCC, Geneva, Switzerland, 104 pp.

IPCC (C.B.; Barros, V.; Stocker , T.F et al. [eds.]) (2012). *Summary for Policymakers. A: Managing the Risks of Extreme Events and Disasters to Advance Climate Change Adaptation. A Special Report of Working Groups I and II of the Intergovernmental Panel on Climate Change*. Cambridge: Cambridge University Press, p. 1-19. http://www.ipcc.ch.

James, P., Stohl, A., Spichtinger, N., Eckhardt, S. y Forster, C., (2004). Climatological aspects of the extreme European rainfall of August 2002 and a trajectory method for estimating the associated evaporative source regions. *Nat. Hazards Earth Syst. Sci.,* 4, 733–746.

Llasat, M.C., Barriendos, M., Barrera, A. y Rigo T. (2005). Floods in Catalonia (NE of Spain) since the 14th Century. Climatological and meteorological aspects from historical documentary sources and old instrumental records, *Special Issue of Journal of Hydrology. Applications of palaeoflood hydrology and historical data in flood risk analysis,* 313, 32-47.

Llasat, M.C., 2009. Chapter 18: Storms and floods. I*n The Physical Geography of the Mediterranean basin.* Edited by Jamie Woodward. Published by Oxford University Press, ISBN: 978-0-19-926803-0,pp. 504-531.

Llasat, M.C., Llasat-Botija, M. and López, L. (2009 a). A press database on natural risks and its application in the study of floods in northeastern Spain. *Nat. Hazards Earth Syst. Sci.,* 9, 2049-2061.

Llasat, M.C., Llasat-Botija, M., Barnolas, M., López y L. Altava-Ortiz, V. (2009b). An analysis of the evolution of hydrometeorological extremes in newspapers: the case of Catalonia, 1982-2006, *Nat. Hazards Earth Syst. Sci.,* 9, 1201-1212.

Llasat, M.C., Llasat-Botija, M., Prat, M.A., Porcú, F., Price, C., Mugnai, A., Lagouvardos, K., Kotroni, V., Katsanos, D., Michaelides, S., Yair, Y., Savvidou, K., Nicolaides, K. (2010). High-impact floods and flash floods in mediterranean countries: the flash preliminary database. *Advances in Geosciences,* 23, 1-9.

Llasat, M.C., Llasat-Botija, M., Gilabert, J., Marcos, R., (2012). Treinta años de inundaciones en Cataluña: la importancia de lo cotidiano. 8º *Congreso Internacional de la Asociación Española de Climatología*: Extremos e impactos.

Salamanca, Septiembre 2012.

Llasat, M. C., Llasat-Botija, M., Petrucci, O., Pasqua, A. A., Rosselló, J., Vinet, F., Boissier, L. (2013). Towards a database on societal impact of Mediterranean floods in the framework of the HYMEX project. *Nat. Hazards Earth Syst. Sc*i., 13, 1–14. www.nat-hazards-earth-syst-sci.net/13/1/2013/ doi:10.5194/nhess-13-1-2013

Parlamento Europeo, 2000: *Directiva 2000/60/CE del Parlamento Europeo y del Consejo de 23 de octubre de 2000 por la que se establece un marco comunitario de actuación en el ámbito de la política de aguas.*

Parlamento Europeo (2007): *Directiva 2007/60/CE del Parlamento Europeo y del Consejo de 23 de octubre de 2007 relativa a la evaluación y gestión de los riesgos de inundación. Diario Oficial de la Unión Europea. L288/27-L288/34*.

Petrucci, O. y Polemio, M. (2003). The use of historical data for the characterisation of multiple damaging hydrogeological events, *Nat. Hazards Earth Syst.* Sci., 3, 17-30.

Rigo, T., Llasat, M.C., (2004). A methodology for the classification of convective structures using meteorological radar: application to heavy rainfall events on the Mediterranean coast of the Iberian Peninsula. *Nat. Hazards Earth Syst*. Sci. 4, 59-68

UNISDR (2009). *UNISDR Terminology on Disaster Risk Reduction.* Online: http://www.unisdr.org/eng/terminology/ terminology-2009-eng.html.

CHAPTER 15

DROUGTH MONITORING FROM SATELLITE ESTIMATES OF BIOPHYSICAL VARIABLES

F. Javier GARCÍA-HARO, M. Amparo GILABERT NAVARRO,
Joaquín MELIÁ MIRALLES

Departament de Física de la Tierra i Termodinàmica. Universitat de València
J.Garcia.Haro@uv.es, M.Amparo.Gilabert@uv.es, Joaquin.Melia@uv.es

ABSTRACT

Monitoring the vegetation activity over long time-scales is necessary to discern ecosystem responses. The use of remote sensing observations for monitoring and detecting drought is justified on the basis that vegetation vigor is closely related to moisture condition. We derive satellite estimates of biophysical variables such as fractional vegetation cover (FVC) from MODIS (2000-2010) time series. Derived maps offer a means for obtaining direct indicators of vegetation biomass, structure and condition. The potential of derived variables in the field of drought conditions monitoring is assessed. This study evaluates also the strength of temporal relationships between precipitation and vegetation condition at time-lag and cumulative rainfall intervals. From this analysis, we estimated that the climatic disturbances affected both the growing season and the total amount of vegetation. However, the impact of climate variability on the vegetation dynamics has shown not to be the same for every region. The relationships between vegetation anomaly and water stress are highly significant for the arid and semiarid areas. This implies that the anomaly of vegetation cover is a good indicator of moisture condition and can be an important data source when used for detecting and monitoring drought in Spain.

Key words: drought, vegetation cover, climate, SPI, remote sensing.

1. INTRODUCTION

The complex drought phenomenon is difficult to detect and monitor since it is not universally defined and its impact is nonstructural and often spreads over very large areas. Meteorological drought indices and satellite sensor data have been playing an increasingly important role in monitoring drought-related vegetation condition.

Precipitation and temperature control differences in the Earth's vegetation cover, affecting growth rate, plant reproduction, and frost damage. the productivity of a region is limited by water availability, the importance of the relationship between water availability and vegetation is widely recognised in the Mediterranean and Sahelian zones (Lobo and Maisongrande, 2006; Martínez *et al.,* 2011). In particular, rainfall variations often cause the vegetation to experience water shortage during the growing season.

Satellite remote sensing enables cost-effective and accurate monitoring at frequent time steps over large areas, which is necessary to discern ecosystem responses to climate variability. The use of remote sensing observations for monitoring and detecting drought is justified on the basis that vegetation vigor is closely related to moisture condition. A number of studies have indicated a strong relationship between satellite vegetation indices and precipitation (e.g. Wang *et al.*, 2003). The complexity of this relationship is primarily influenced by regional rainfall patterns, vegetation and soil types, growth stages of vegetation and spatial scale of the data (Paruelo and Lauenroth *et al.,* 1995; Ji and Peters, 2003; Vicente-Serrano, 2006). Furthermore, it may be also affected by other factors such as pest/disease infestation, wild fire, grazing and anthropic disturbances.

Although the majority of studies have focused in the impact of water availability on vegetation, the vegetation cover, far from being a passive component of the climate system, acts on climate regulating exchanges of energy, mass, and momentum between the surface and atmosphere. Recent studies also indicate that land surface vegetation can considerably feed back on climate, revealing significant local impact of the vegetation state on monthly mean rainfall anomalies. For example, Moreno *et al.* (2010) evidenced the potential of remotely sensed observations of vegetation activity to improve rainfall prediction over land in Spain. Similar studies have also suggested that vegetation could have much higher impacts on rainfall at seasonal and longer time scales (Liu *et al.,* 2006).

In this study, we derive satellite estimates of bio-physical variables such as fractional vegetation cover (FVC) from MODIS (2000-2010) time series and assess the potential of these variables in the field of drought conditions monitoring. The aim is to analyse the vulnerability of natural ecosystems against the effects of climate fluctuations like drought. The study assesses the strength of temporal relationships between precipitation and vegetation condition at time-lag and cumulative rainfall intervals. In order to analyze the response to rainfall of different vegetation types and climatic regions, a stratified analysis was performed considering the major regional climates and vegetation communities in Spain.

2. MONITORING THE VEGETATION FROM REMOTE SENSING

Since the early 1980s, the Advanced Very High Resolution Radiometer (AVHRR) on the National Oceanic and Atmospheric Administration (NOAA)'s polar-orbiting satellites (Tucker, 1996) have dominated the field of large-scale monitoring of vegetation due to the long time series available. The Normalized Difference Vegetation Index (NDVI) derived from AVHRR data has been widely used to monitor and evaluate terrestrial vegetation vigor (Pettorelli *et al.,* 2005).

However, NDVI is susceptible to the spectral influence of the soil and soil moisture in discontinuous canopies such as arid and semi-arid environments. The advent of modern satellites (e.g. MERIS, MODIS, VEGETATION) has improved the possibilities to retrieve vegetation properties thanks to a better radiometric, spectral and angular performance of imaging instruments. Biophysical variables such as the fractional vegetation cover (FVC) and leaf area index (LAI) have proven to be appropriate for modeling terrestrial ecosystems on the global, continental, and regional scales.

In this study, spatial and temporally consistent estimates of fractional vegetation cover (FVC) were obtained using a probabilistic spectral mixture analysis (SMA) method (García-Haro *et a*l., 2005), an adapted variants of the algorithm which is currently used operationally in the context of the EUMETSAT/LSA SAF mission (http://landsaf.meteo.pt). The method decomposes the soil/vegetation into a number of subclasses and then estimates FVC as a linear combination of single-model estimates. The aim is to characterize the variability of the soil/vegetation components using a large, robust training set. Both vegetation and non-vegetation classes are represented by a multi-modal distribution attributable to differences due to biophysical and biochemical composition.

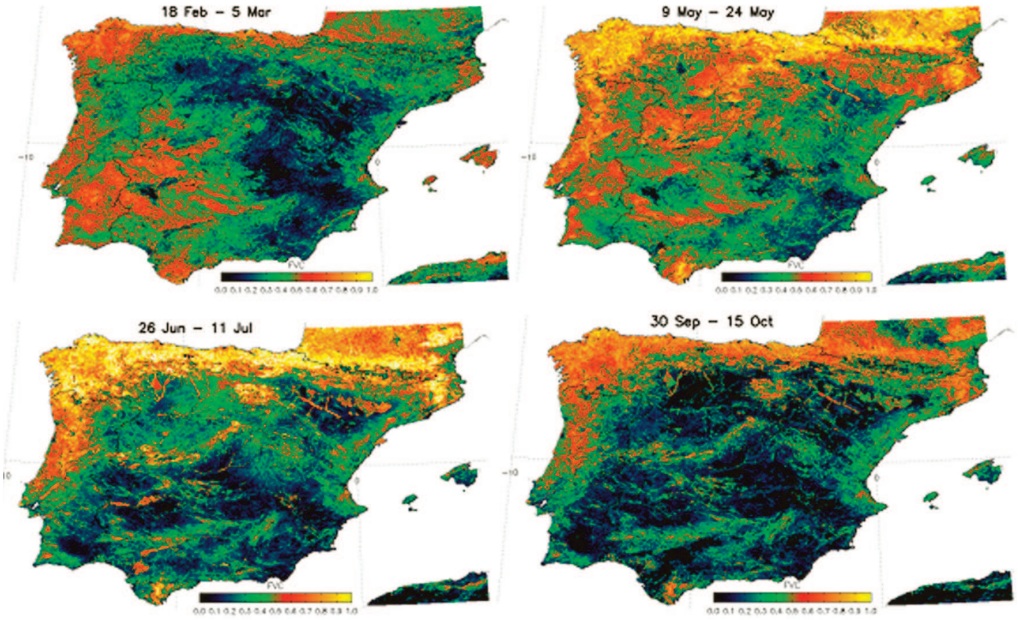

Figure 1. Monthly average (2000–2010) fractional vegetation cover (FVC) for the Iberian Peninsula at four different time periods.

The methodology was applied on time series of MODIS reflectance (MOD13A2). The considered data set covered a 11-year period (2000-2010), presenting a 1km spatial resolution over 16-day periods. Figure 2 shows several examples of derived FVC maps in the Iberian Peninsula at different time periods comprising the annual

cycle of vegetation. Geographically and ecologically coherent patterns that are consistent with the known phenological behavior in the study area can be observed. It is observed a strong north-south gradient shift in the timing of green-up onset. This complex spatio-temporal variation comes about not only through climatic variability but also through variations in community composition, soils and land management (e.g. irrigation practices). For example, the green-up in some north-eastern and southern areas at the end of the year is explained by agricultural practices (irrigation and cereal crops) (Peñuelas *et al.,* 2004).

3. THE PRECIPITATION AND ITS SPATIO-TEMPORAL VARIABILITY

In this study, monthly climatic maps of precipitation and temperature in Spain were derived during the 1950-2010 period at a 2-km spatial resolution using geostatistical approaches for interpolation (García-Haro *et al.,* 2008). The accurate estimation of the spatial distribution of precipitation requires a very dense network of measuring gaugement. The climatic data used in the study were obtained from the AEMET (Agencia Estatal de Meteorología). The recording stations of precipitation are evenly distributed although its number has significantly changed during this period, reaching a maximum (5136) in 1975. From the monthly maps, annual and monthly averages for the analyzed period were computed (see example in Figure 2).

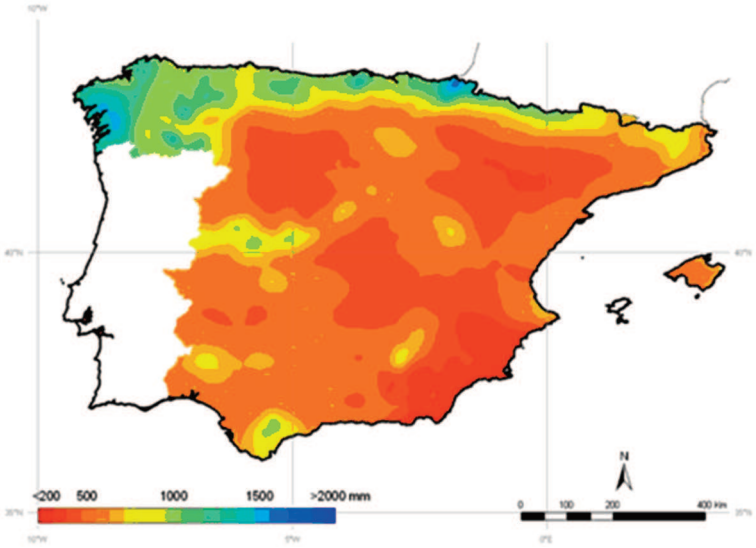

Figure 2. Average values (1950-2007) of annual precipitation.

The Standardised Precipitation Index (SPI) was calculated to quantify and monitor the precipitation deficit distributions at different time scales. The SPI calculation for any location is based on the long-term precipitation record for a desired period. The SPI expresses the number of standard deviations that the precipitation values –fitted to a Gamma probability distribution and transformed then to follow a normal

distribution- would deviate from the long-term mean (McKee *et al.* , 1993). The SPI was selected because of its flexibility to measure drought at different time scales. The precipitation total of the current month and previous i months (i=1, 3, 6, 12 and 24) was used to compute the i-month scale of the SPI. For example, the 3-month SPI of June uses the precipitation total of June, May and April, providing a seasonal estimation of precipitation. In this way we obtained images of the SPI at different time scales and a resolution of 2 km to drought conditions in Spain.

During the period 1950-2010, Spain has experienced several stern and extended episodes of drought, particularly during 1980-84, 1990-95 and the most recent 2004-2007 (Poquet *et al.,* 2008). Figure 3 shows the 12-month SPI of December 2005 in Spain. This is indicative of long-term precipitation patterns, reflecting the severe drought suffered by the Iberian Peninsula during 2004-05. This lead to devastating economic losses in many parts of Spain, particularly in the western areas and caused a considerable increase of summer fire season.

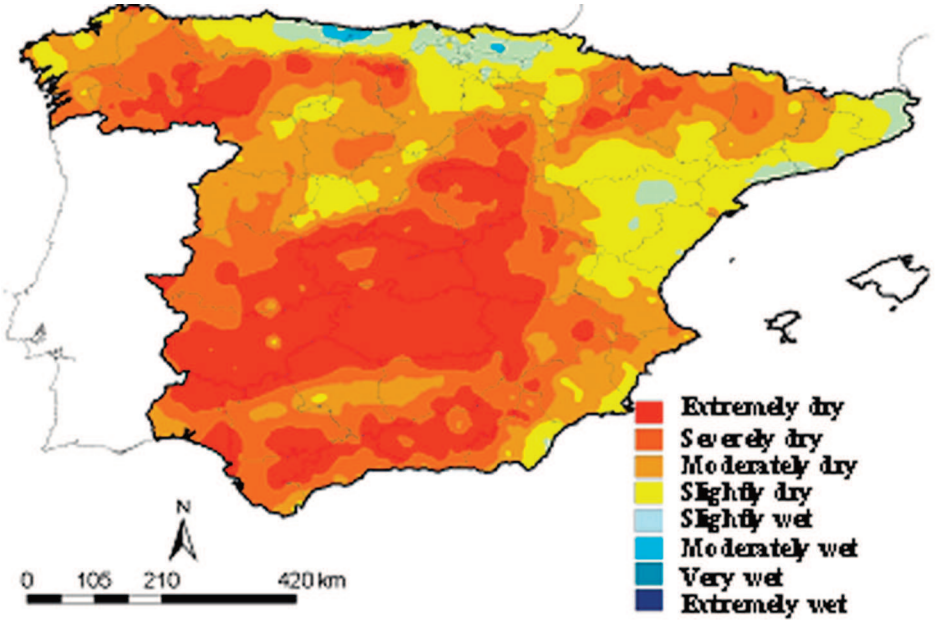

Figure 3. 12-month SPI values for Spain in December 2005 stratified into 8 intervals: extremely wet (>2.0), very wet (1.5 to 1.99), moderately wet (1.0 to 1.49), slightly wet (−0.99 to 0.0), slightly dry (0 to 0.99), moderately dry (−1.49 to 1.0), severely dry (−1.99 to 1.5), and extremely dry (<−2.0).

4. STRATIFICATION OF THE STUDY AREA

In order to analyze the response to rainfall of different vegetation types and climatic regions, a stratified analysis was performed considering the major regional climates and vegetation communities in Spain. The aim was to stratify the landscape into homogeneous zones presenting similar ecological structures and climatic conditions.

4.1 Vegetation classification

A classification method was applied to derive a land cover mapping of Spain from multitemporal MODIS data. The land cover classes were characterized by temporal trajectories of fractional vegetation cover (FVC), which have proven useful for improving classification accuracy, especially because of the differences in the growth cycle of vegetation. SIOSE *(Sistema de Información de Ocupación del Suelo en España)* database provided a spatially detailed (1:25.000) reference for determination of selection of training samples, and accuracy assessment. A method based on Artificial Neural networks (ANN) provided a reliable thematic map with a hierarchy level of 14 major classes (Figure 4). The overall accuracy was 80.0%, with balanced values of user's accuracy and producer's accuracy for individual classes. The classification was also assessed by comparing it with global and continental land cover mapping currently available, CORINE, GLC2000 and GLOBCOVER. The derived land cover presented closer agreement to reference data and an overall good consistency with existent products.

The area is dominated by non irrigated arable land (20%) which extend over the plain areas in the center and herbaceous cover (17%). The main forest areas are: coniferous (9%) in the Northeast regions, broad-leaved deciduous (4.5%) in the North and broad-leaved evergreen (4.8%) in the West and Southwest. Shrublands (12%) include transitional woodland-shrub and sclerophyllous mediterranean vegetation.

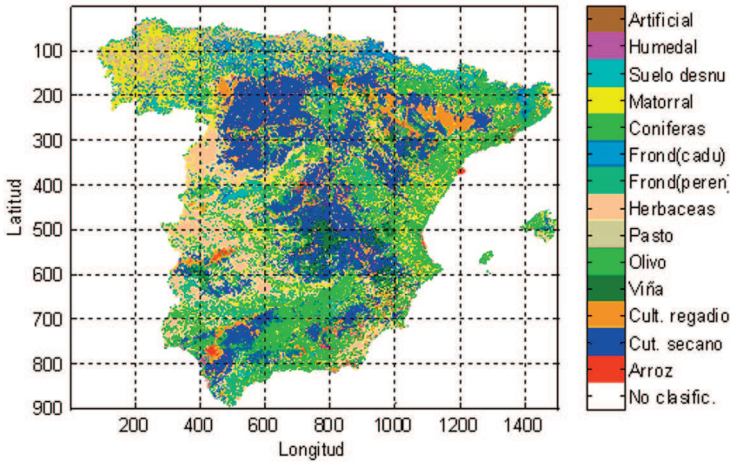

Figure 4. Derived land cover map with a hierarchy level of 14 major classes.

4.2 Climatic classification

We calculated potential evapotranspiration (PET) from the monthly temperature maps according Thornthwaite and Mather (1957). The Thornthwaite moisture index was then computed using the difference between monthly precipitation and evapotranspiration (P-PET). This climate index is a useful indicator of the supply of water in an area relative to the demand for water (P) under prevailing climatic

conditions (PET). It reflects the portion of total precipitation used to nourish vegetation over a certain area.

Using average values over a 61 year period (1950-2010) the moisture index was computed. By stratifying this map into 9 intervals Spain was classified into nine climatic regions was obtained (Figure 5a). It is observed a high contrast between humid and very humid regions in the North (moisture index values from 80 to 160) and the desertic South-eastern region (values below -40). A total of 15 percent of the Spain landmass is considered either arid of semi-arid (provinces of Almería and Murcia, the Ebro Basin and most of the La Mancha elevated plains of central Spain). One obvious limitation of this climatic classification is that it does not explicitly has into account the important influence of geographic conditions and orography(Poquet *et al.,* 2008).

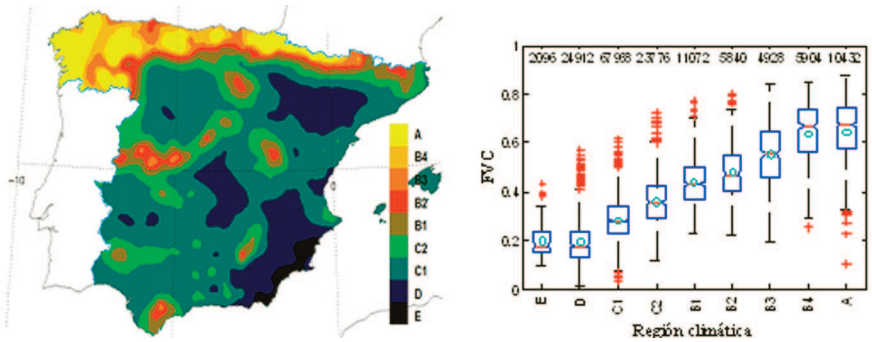

(a) (b)

Figure 5. Climatic classification based on the moisture index. It corresponds to average values of climatic parameters over a 61 year period (1950-2010): A, very humid (≥100); B, humid (20 to 100); C, subhumid (-20 to 20); D: semiarid (-40 to -20); E, arid (≤-40). (b) Boxplots of mean fractional vegetation cover for the main moisture regions. The central segment in each box marks the median. The upper and lower edges of the box plot are placed at the first and third quartile, whereas the lower and upper extremes correspond to the 0 and 100% percentiles, respectively. A cyan circle denotes the mean value. The number of valid pixels is printed on top of each box.

A strong linear trend was observed between the values of mean fractional vegetation cover and moisture index (Figure 5b), evidencing the importance of the relationships between water availability and vegetation coverage in Spain.

5. RESPONSE OF ECOSYSTEMS TO CLIMATE VARIABILITY

The spatial patterns and temporal dynamics of FVC and SPI enabled spatially explicit comparisons of vegetation condition in response to precipitation.

5.1 Impact of the 2004-2007 drougth

We focus on the severe drought in Spain during the 2004-2007 period. In order to analyse the differential responses of vegetation classes to climatic characteristics,

we differentiated among major forest and managed classes, making also a distinction between moist and dry climates. Figure 6 shows the course of FVC values during year 2005 averaged for vegetation types, for the . The long term (2000-2010) mean were used establish a reference level (average year). Time profiles indicate the intra-annual variation (average year) whereas error bars reflect the inter-annual variability (standard error) for each 16-day period.

In the moist regions (40.1% of the study area), vegetation did not show large deviations from the typical response, with the exception of herbaceous cover. However, in the dry regions (relative area of 59.9%), a severe disturbance in vegetation cover can be generally observed across for the majority of vegetation types (Figure 6). The disturbances are most noticeable during the period of greatest vegetation activity (e.g. middle of the growing-season), typically in spring, and drastically decrease during autumn. Anomalies are largely negative for herbaceous (natural vegetation or pastures), cultivated areas, broadleaved forest and shrub cover. The long episode of hydric stress seems also to alter the phenology of Broadleaved forest and shrublands, for which one-month delay in the maximum of vegetation cycle can be observed.

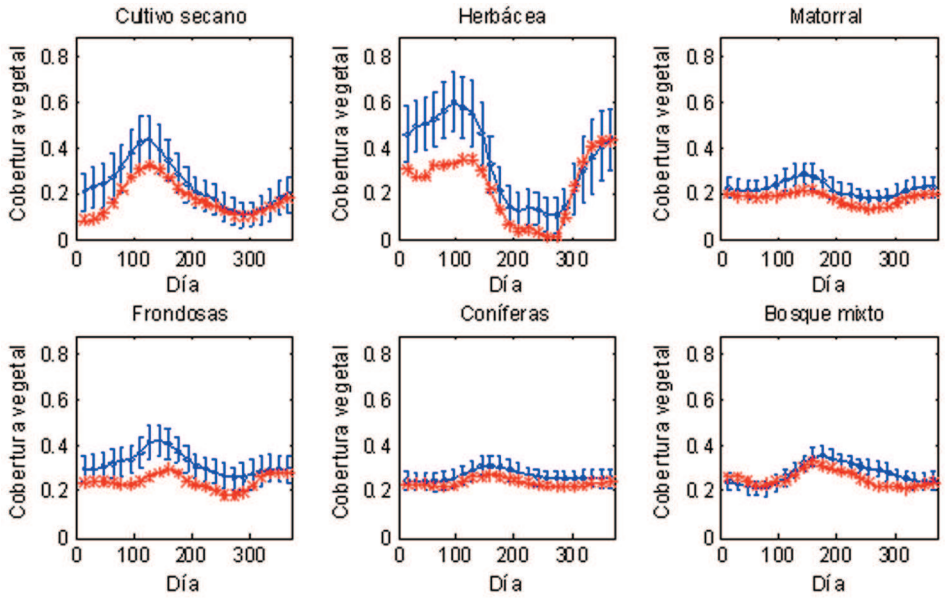

Figure 6. Annual courses of FVC, at a 16 day time step, for different vegetation classes. Blue, average period 2000-2010 (bars represent the standard deviation observed in the period); red, 2005. It corresponds to areas with negative values of the moisture index, ranging from dry sub-humid to arid occupying a relative area of 59.9%.

We develop particular attention to the relationship between the disturbance in vegetation cover during the growing season and the water deficits. Since the impact of water deficits on vegetation is cumulative, we considered the 1 month lagged SPI-3 (i.e. corresponding to the period February-April). Values of 3-month SPI (SPI-3) are grouped by intervals of summer FVC anomaly in a boxplot (Figure 7).

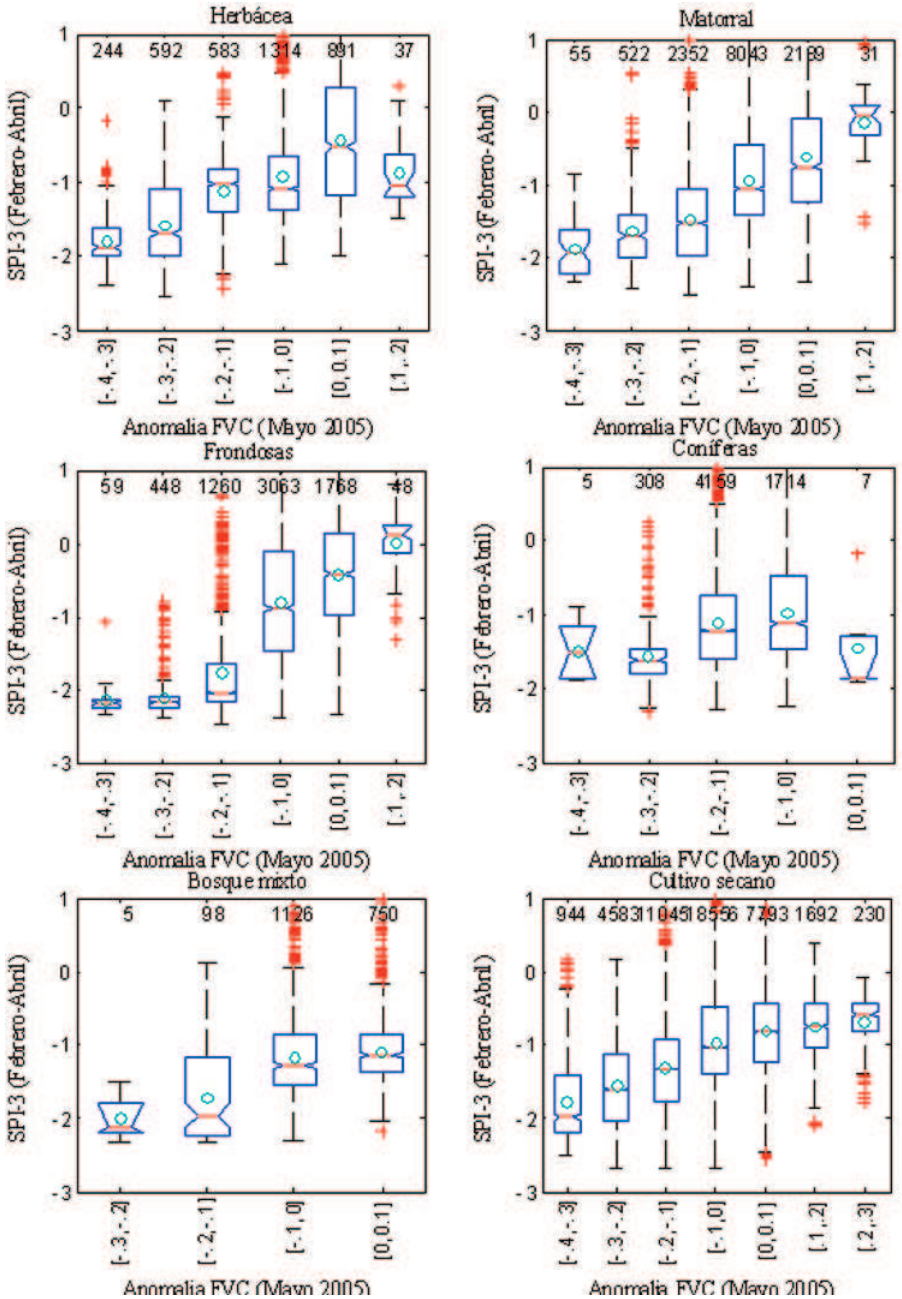

Figure 7. Boxplot of SPI-3, 1-month lagged (i.e. using the precipitation of February, March and April) as a function of the FVC anomaly (May 2005) for different vegetation classes. A cyan circle denotes the mean value. The number of valid pixels is printed on top of each box.

For the majority of vegetation formations, the medians show an increasing trend with SPI-3. This result suggests that vegetation cover anomalies are highly influenced by cumulative rainfall summed over the preceding three month period. Note that two given medians significantly differ if notches in the boxplot do not overlap. While herbaceous and sclerophyllous vegetation show a strong linear relationship, in woodland structures such as evergreen needle-leaved and mixed forests this relationship is not significant. Different studies suggest that these classes are non-sensitive to short droughts but the longest and most intense droughts can affect the physiological structure and thus take longer to recover their normal activity (Vicente-Serrano, 2006).

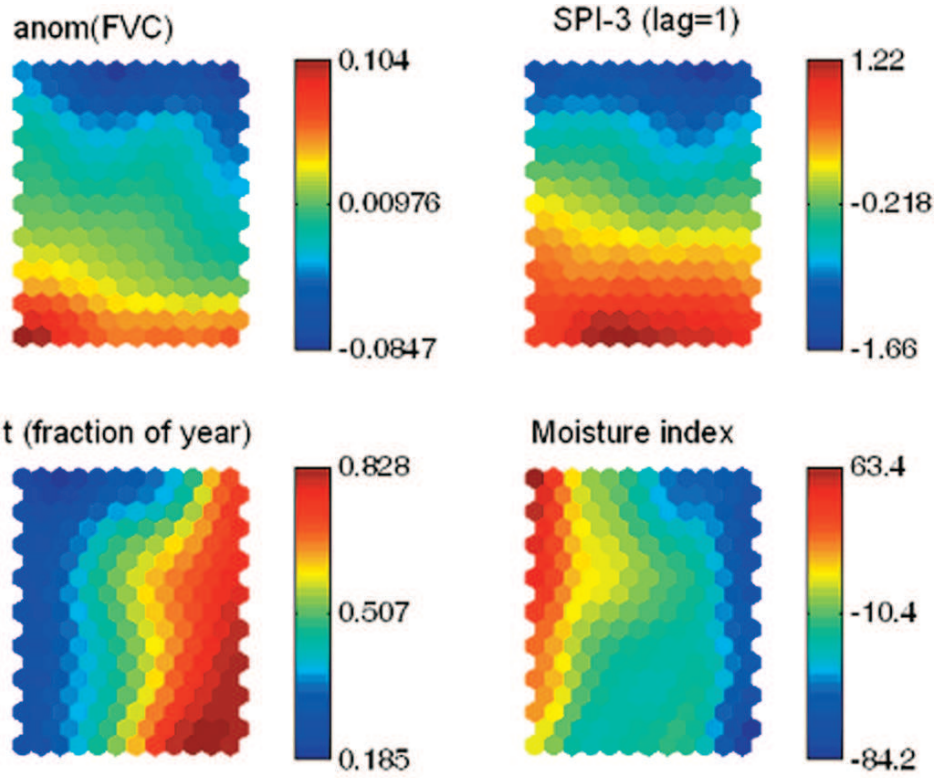

Figure 8. Visualization of the SOM trained from time series of vegetation and climatic data of the study area. The four Figures are linked by position: in each Figure, the hexagon in a certain position corresponds to the same map unit.

5.2 Association between vegetation and climatic variables

In order to gain a deep insight into the relationship between vegetation activity and rainfall in Spain, a Self-Organizing Map (SOM) has been built. The SOM is a nonlinear projection of the probability density function of the high-dimensional input data onto a 2-D codebook map of units or neurons (Kohonen *et al.,* 1996). The neurons are connected to adjacent neurons by a neighborhood relation, i.e. spectral classes that are close in spectral distance are mapped to adjacent or nearby nodes in the codebook.

Component planes (see Figure 8) allowed us to visualize the relationship between time series of vegetation and climatic data in Spain. The Figure reveals as anomaly of vegetation cover and SPI are very closely related to each other (e.g. a strong correlation between the planes associated to both variables). The dominance of intermediate moisture index values is in agreement with the mild conditions in most parts of Spain. The strongest negative anomalies of vegetation cover (< -0,06) are found around August (t ~ 0,7-0,8) in dry regions, and around early spring (t~0,3) in sub-humid areas. In both cases, they were coincidently to the anomalous dry period, in agreement with expectations.

5.3 Temporal relationships

Figure 9 shows several examples of long-term series of monthly drought indices (SPI) and anomalies of vegetation cover. Results suggest that herbaceous cover and sclerophyllous vegetation appear to be very sensitive to precipitation variability demonstrating the most rapid response to rainfall in these semiarid environments. In addition to the severe drought of 2004-2005, moderate droughts in years 2001 and 2003 appeared also to be related with disturbance in the growing cycle of vegetation. Multi-year drought affects these environments, influencing plant community composition, physiology, and growth (Weiss *et al.*, 2004). Drought has a less influencing effect on woodland structures such as coniferous forest.

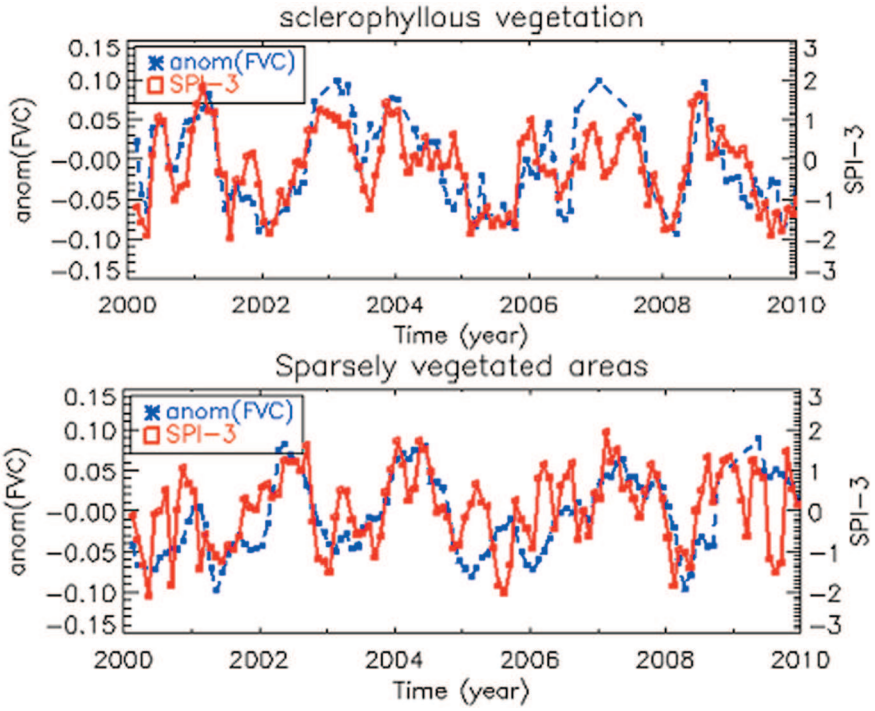

Figure 9. Temporal patterns of SPI and FVC anomaly over a 11-year period, at a 16 day time step, for two different vegetation types.

Both the soil moisture conditions and the vegetation activity respond to precipitation anomalies on a relatively short scale. However, seasonal timing of measurements is an important factor in the understanding of vegetation vigor and precipitation relationships, and should be taken into account. In order to take into account this seasonal effect, a regression model with seasonal dummy variables was used to build a relationship between vegetation cover (FVC) and 3-month SPI (SPI-3) at different time scales and time lags. In general, the 1-month lag SPI-3 was found to have the best correlation, indicating lag and cumulative effects of precipitation on vegetation. In order to simplify the regression model and evaluate the effect of seasonal timing, different temporal windows covering a 4 month period were considered. A stepwise multiple regression was required to determine a minimum number of regressors which explained the largest amount of variation in the anomaly of FVC. We began with an initial model with all possible dummy variables and then compared the explanatory power of incrementally smaller models. At each step, the p-value of an F-statistic is computed and the variable with maximum p-value (higher than 0.05) was removed from the model. Once the variables for a given pixel were selected, a multiple regression model was developed.

Figure 10 shows the spatial distribution of the coefficient of determination R2 between SPI-3 and anomaly of FVC, corresponding to the temporal window May-August. During this period, which covers the growing season in most of the area, statistically significant correlations have been found between SPI and satellite-derived anomalies of vegetation activity, although they are highly dependent on the regional climate and vegetation community. Such influences are further documented in Figure 11, which shows a negative linear trend of R^2 against moisture index level. The most important correlations (R^2=0.4-0.7) were noted in the arid (E) and semiarid (D) areas, which reveals the notorious impact of water availability on vegetation activity for the summer period in these environments. This implies that the anomaly of vegetation cover provides a meaningful description of moisture condition and can be an important data source when used for detecting and monitoring drought in these areas. By contrast, rain has a low impact on summer vegetation activity over humid regions, presenting moderate to weak correlations. These high correlations occurred only in the middle of the growing season, but are much lower during green-up and senescence, probably because plants are more sensitive to water availability in the reproductive growth stage.

6. CONCLUSIONS

Ecological and climate models require high-quality biophysical parameters as input. This study performs a joint analysis of time series of satellite observations of vegetation activity (e.g. FVC) and water drought indices (e.g. SPI) in Spain over the period 2000–2010. FVC has shown meaningful relationships with inter-annual climate variability. Significant positive correlations have been found between

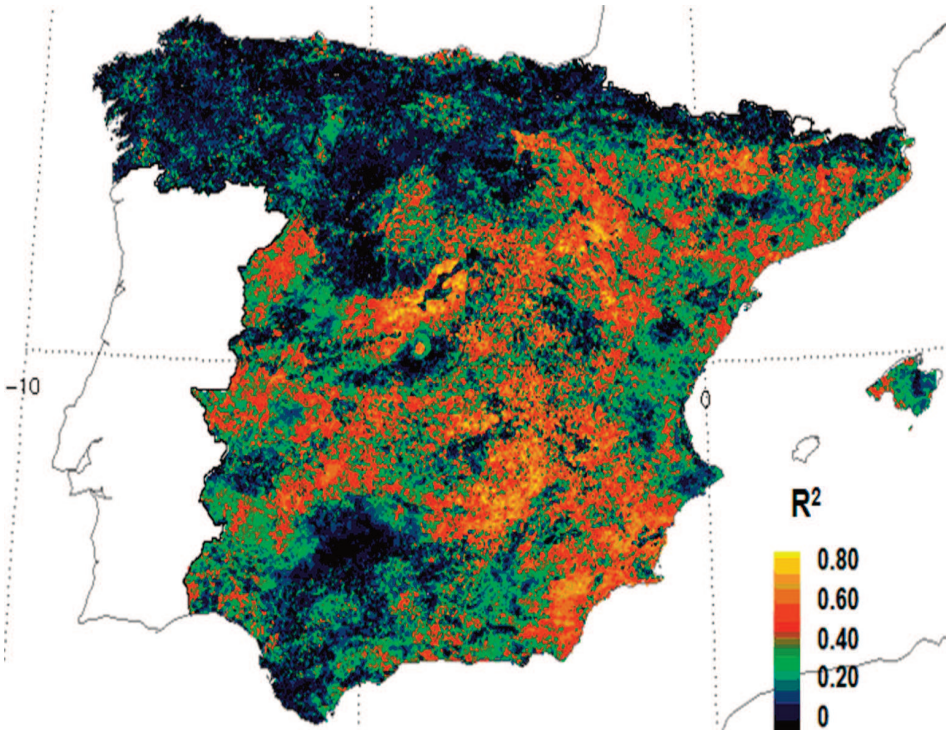

Figure 10. Coefficient of determination (R^2) of the regression model with seasonal dummy variables between SPI-3 (1 month lagged) and monthly values of FVC anomaly covering the period April-August.

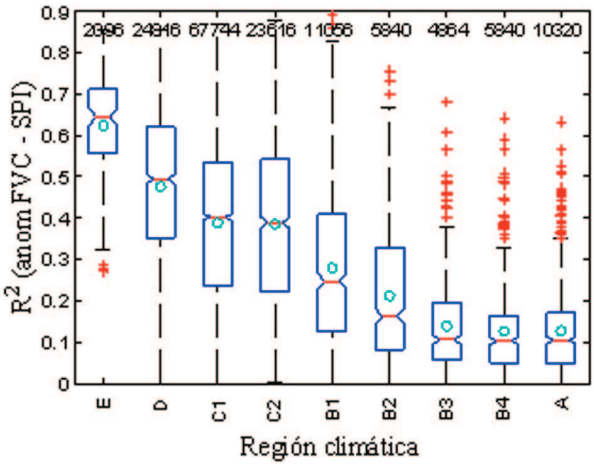

Figure 11. Boxplot of R^2 values displayed in Fig. 10 grouped for the main moisture classes.

anomalies of the FVC and SPI which employ cumulative rainfall summed over the preceding months. This implies that the anomaly of vegetation cover is a good indicator of moisture condition and can be an important data source when used for detecting and monitoring drought in Spain. This is not only because of the perceived response to drought, but also because vegetation is a relatively complete integrator of the physical variables that are affected by climatic conditions. Although the climatic disturbances affect both the growing season and the total amount of vegetation, these relationships are highly dependent on the regional climate and vegetation community. In general, they are more significant in arid and semiarid areas, since water availability most strongly limits vegetation growth in these environments.

ACKNOWLEDGEMENTS

This work has been supported by DULCINEA (CGL2005-04202), ARTEMIS (CGL2008-00381) and RESET CLIMATE (CGL2012–35831) projects. Special thanks are due to Fernando Belda (AEMET) for supplying the climatic data used in the study.

REFERENCES

Alessandri, A., A. Navarra (2008). On the coupling between vegetation and rainfall inter-annual anomalies: Possible contributions to seasonal rainfall predictability over land areas, *Geophys. Res. Lett.,* 35.

García-Haro, F.J., F. Belda and D. Poquet. (2008). Estimation of climatological variables in Spain during the 1950-2008 period using geostatistical techniques, 8*th Annual Meeting of the EMS / 7th ECAC EMS8/ECAC7, 5, EMS2008-A-00319.*

García-Haro, F.J, S. Sommer, T. Kemper (2005), Variable multiple endmember spectral mixture analysis (VMESMA), *International Journal of Remote Sensing, 26, 2135-2162.*

García-Haro, F.J., A. Pérez-Hoyos, (2010). Land cover classification in Spain from seasonal trajectories of MODIS data, Proceedings of the RAQRS2010. *3rd Symposium on Recent Advances in Quantitative Remote Sensing,* Torrent, Spain, 27 Sept-1 Oct. 2010, (Publ. Univ. Valencia: Valencia), Ed. J. Sobrino, 562-567.

Ji, L., Peters A.J. (2003). Assessing vegetation response to drought in the northern Great Plains using vegetation and drought indices. *Remote Sens. Environ.,* 87, 85-98.

Kohonen T., Hynninen J., Kangas J., Laaksonen J. SOM_PAK (1996)- The Self-Organizing Map Program Package, Technical Report A31, Helsinki University of Technology.

Liu, Z., Notaro, M., Kutzbach, J. (2006). Assessing global vegetation climate feedbacks from observations. *Journal of Climate,* 19, 787–814.

Lobo, A. and P. Maisongrande, (2006). Stratified analysis of satellite imagery of SW Europe during summer 2003: the differential response of vegetation classes to increased water deficit. *Hydrol. Earth Syst. Sci.,* 10:151–164.

McKee, T.B., N. J. Doesken, and J. Kliest, (1993). The relationship of drought frequency and duration to time scales. Pro*c. 8th Conference of Applied Climatology,* 17-22 January, Anaheim, CA. American Meterological Society, Boston, MA. 179-184.

Martínez, B., M.A. Gilabert, García-Haro, F.J. A. Faye, J. Meliá (2011). Land condition analysis in Ferlo, Senegal (2001-2009) using multi-temporal 1-km apparent green cover (AGC) SPOT VEGETATION data, *Global and Planetary Change,* 76, 152-165.

Moreno-Martínez, A., Soria-Olivas, E., García-Haro, F.J., Martín Guerrero, J.D., Magdalena, R. (2010). Neural models for rainfall prediction, Chapter 21 in "Soft Computing Methods for Practical Environmental Solutions: Techniques and Studies", 353-369. Information science reference, Hershey, New York (Gestal, M. and Rivero, D. Eds), 397 pp.

Paruelo, J. M. and Lauenroth, W.K. (1995). Regional Patterns of Normalized Difference Vegetation Index in North American Shrublands and Grasslands, Ecology, 76, 1888-1898.

Peñuelas, J., Filella, I., Zhang, X. Llorens, L., Ogaya, R. Lloret, F. Comas, P., Estiarte, M., Terradas, J., (2004). Complex spatiotemporal phenological shifts as a response to rainfall changes, *New Phytologist,* 161, 837–846.

Pettorelli, N., Vik J.O., Mysterud A., Gaillard J.M., Tucker C.J., Stenseth N.C. (2005). Using the Satellite-Derived NDVI to Assess Ecological Responses to Environmental Change. *Trends in Ecology and Evolution,* 20, 503-510.

Poquet, D. Belda, F. García-Haro, F.J. (2008). Regionalización de la sequía en la península ibérica desde 1950 hasta 2007 a partir del SPI y una modelización digital terreno, XXX *Jornadas Científicas de la Asociación Meteorológica Española* "Agua y Cambio Climático", IX Encuentro Hispano-Luso de Meteorología y XII Congreso Latinoamericano e Ibérico de Meteorología, Zaragoza (España), 5-7 de mayo.

Roujean J.L. and R. Lacaze, (2002). Global mapping of vegetation parameters from POLDER multiangular measurements for studies of surface-atmosphere interactions: A pragmatic method and its validation. *J. Geophysical Res.,* 107D, 10129-10145.

Vicente–Serrano, S. M., (2007). Evaluating the Impact of Drought Using Remote Sensing in a Mediterranean, Semi–arid Region. *Natural Hazards,* 40, 173-208.

Thornthwaite, C. W. and Mather, J. R, (1957). Instructions and tables for computing potential evapotranspiration and water balance, Drexel Institute of Technology, Laboratory of Climatology, *Publications in Climatology,* 17, 231–615.

Wang, J., Rich, P. M., & Price, K. P. (2003). Temporal response of NDVI to precipitation and temperature in the central Great Plains, USA. *International Journal of Remote Sensing*, 24, 2345–3364.

Weiss, J. L., Gutzler, D.S, Coonrod, J.E.A, and Dahm, C.N., (2004). Long-term vegetation monitoring with NDVI in a diverse semi-arid setting, central New Mexico, USA, *Journal of Arid Environments,* 58, 249–272

CHAPTER 16

SNOW AVALANCHES IN SPAIN: THE ROLE OF SPANISH STATE METEOROLOGICAL AGENCY

Gerardo SANZ ARAÚZ, Javier RODRÍGUEZ MARCOS, Samuel BUISÁN SANZ

Spanish State Meteorological Agency (AEMET), Aragon Regional Office
gsanza@aemet.es, frodriguezm@aemet.es, sbuisan@aemet.es

ABSTRACT

Snow avalanches are most likely the greatest danger in the mountains in winter. One way or the other, avalanches suppose a risk for anyone going through snowed areas when performing a recreational or professional activity. From the relatively harmless 'roof avalanches', to the large avalanches which can destroy entire buildings, the danger of avalanches is always present when there is a snowpack. This document describes the phenomena and gives an insight of the tools available to mitigate their risk.

Key words: avalanche, snow, forecast, observation, danger, risk.

1. THE RISK ASSOCIATED TO SNOW AVALANCHES

Every winter in Spain avalanches cause material losses on properties and infrastructures, as well as interruptions on road traffic. Unlike other countries, losses caused by avalanches are not covered by the Insurance Compensation Consortium, making it difficult to quantify them, yet in some occasions these have been significant: The Baños de Panticosa spa during the second decade of the 20th century, the Hospital of Benasque on several occasions, the Canfranc church on 2nd February 1986, the refuge of Respomuso on the 8th February 1996, the rack railway in Nuria, as well as losses of several consideration on ski resorts such as Boí-Tahull, Super Espot and Valter 2000. Among the claims, the one with the most expensive assessment so far with 30 million pesetas is the claim for the refuge of Respomuso, where an avalanche entered coming from the peak of Frondellas. Fortunately, its five occupants escaped unscathed. Regarding the roads, it is relatively frequent for roads like the A-2606 and A-139, both in Huesca, to be cut-off due to avalanches, and in some occasions they remain closed for up to several weeks.

Regardless of the material losses, the number of people involved in accidents in the snow has increased considerably in the last decades. The number of victims every year in the alpine region is estimated to be of one hundred; in the United States there were an estimate of 32 victims last winter 2011-2012. In Spain, which is a very mountainous country although with less areas with seasonal snowpack, according to estimates from the State Register of Avalanche Accidents, the victims in the past one hundred years exceed 300 by far, and most of half (191) were in the last 30 years. The majority of accidents (up to 90%) involve skiers trapped by avalanches triggered by themselves.

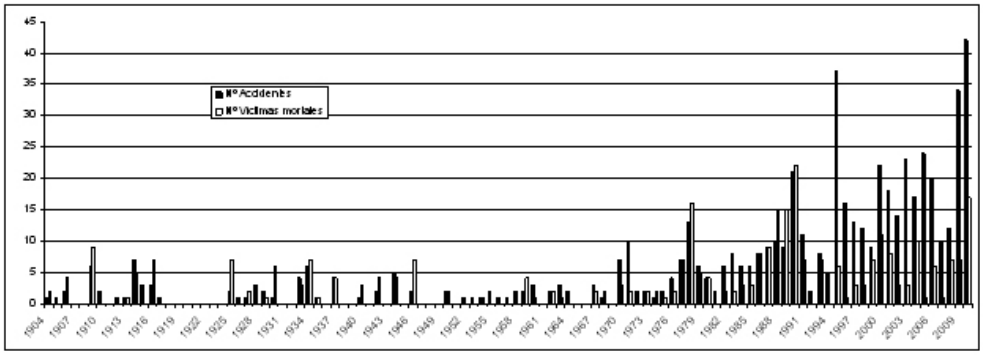

Figure 1. Accidents and victims of avalanches in Spain (by Rodés and Miranda, 2011).

Reducing the risks caused by avalanches requires for both spatial and temporal actions. The spatial management of the risk includes mapping the areas with avalanche risks, placing signs on-site and building infrastructures in the affected areas. Thus, canopies to protect stretches of road, meshes and retaining or deflection walls, supporting structures and other obstacles are fairly common to favour the selective accumulation of snow during snowstorms. In the temporal field, in order to be able to adopt the preventive measures it is necessary to assess the current avalanche danger and its evolution. Typically, if the exposure or the vulnerability are high, as in ski resorts or some stretches of road, preventive triggering is performed when the accumulated snow or the internal structure of the snowpack is considered dangerous.

2. THE SNOW IN THE SNOWPACK

Both when snow falls and when it settles on the surface it is far from being an inert material, as it experiences a set of transformations that will be determining when conferring characteristics to the snowpack, such as the resistance to sliding or to breakage, essential factors for the triggering of avalanches and their typology. Usually, snowpacks are stratified, with different types of grain in each layer.

The snow grains that stay on the surface when they fall are named *new snow* and the cohesion between them is weak. The effect of wind, the increase in temperature and weight cause for the snow to transform into *fragmented particles*, forming a

slightly more cohesive layer. Once in the snowpack, it is mainly the thermal gradient existing between the ground and the base of the snowpack that is the conducting agent in the evolution of the grain. Large gradients, normally associated to intense cold periods over thin snowpacks, cause transformations to angular side grains, *faceted crystals* and *depth hoar*, the main characteristic of which is the low or zero cohesion.

Either due to the effect of wind or to a weak temperature gradient, or due to a combination of the two- which is the most frequent-, the fragmented particles get progressively smaller and rounded, forming the so called *rounded grains*. The main characteristic of the layer formed by this type of grain is its high cohesion and resistance, as well as its capacity to propagate a possible fracture very far.

The characteristic grain type of wet snow is the so called *melt forms* or *wet rounded grains* and is the end-stage of all grain types. Its cohesion varies depending on its water content, from very low to very high. It becomes really strong when melt-freeze crusts form.

3. TYPES OF AVALANCHES

An avalanche is a mass of snow in swift movement down a mountain slope. Although the typology of avalanches is vast, with regard to the characteristics of the snow there are three types of avalanches: Loose snow avalanches, slab avalanches and wet snow avalanches. They can also be considered as natural or accidental depending on how they are triggered. Naturally triggered will be those avalanches in which there is no external intervention and the cause for the triggering is the actual structure of the snowpack. Accidentally triggered will be those avalanches in which there is an external intervention to the snowpack and we will only consider the cases in which the origin is an additional load on the slabs' structure. Considered as external agent are non-human causes (falling of cornice, animal, etc) or human causes (skier, snowmobile, etc.).

3.1 Loose snow avalanches

These are naturally triggered and occur mainly during and after snowfalls. They take place as a consequence of the accumulation of new snow and of the unbalancing of forces between the weight of the snow and its opposition to movement.

The main factors that influence their triggering, and therefore their size and number, are intensity and the amount of the snowfall. When the snow is very light, generally because it fell at very low temperatures and without wind, the avalanches are characterised by the associated aerosol and the shock wave caused in their displacement. These types of avalanches are also known as powder avalanches.

Although not all loose snow avalanches share this pattern, they do share similar characteristics. They are typically point released and can reach high speeds during their route, more than 100 km/h, and are capable of surrounding obstacles and reaching roads or buildings if triggered near them.

If it rains immediately after a heavy snowfall, the number of avalanches will usually be high. It is also normal to find sluffs due to humidification if the temperature rises considerably after a snowfall.

Figure 2. On the left, cleaning works during the days after a loose snow avalanche on the road of Llanos de Hospital, in Benasque, February 2009, photo: S. Buisán. On the right, loose snow avalanches humidified after exposure to sunlight. Valle de Estós, February 2010, photo: Refugio de Estós.

3.2 Wet snow Avalanches

Wet snow avalanches are triggered naturally and usually take place at the end of the season. This is the reason why they are also known as spring avalanches. These take place when the snowpack is at a temperature of 0 ºC and completely humidified, with a high liquid water content (around 10-12%) which impedes the cohesion between the wet rounded grains that form it. This humidification has its origin in the percolation from top to bottom, due to the melting of the superficial snow.

The displacement takes place over a less permeable layer, either the ground or a layer within the snowpack. When the entire depth moves, these avalanches are also known as 'glides' or 'ground wet snow avalanches'. They are usually point released and tend to channel through gullies and couloirs and therefore have known paths; they are also a great erosive agent. The speeds are slower than in the case of loose snow, between 20 and 60 km/h. In the debris zone, the snow takes the shape of snow balls joined to each other due to their high humidity content.

The factors that have an influence on this type of avalanches are the aspect of the slope, the lack of night melt-freeze cycle and rain. They can also occur in the winter, in episodes of high temperatures, with or without rain, and their size can vary from sluff to considerably large-size avalanches.

3.3 Slab Avalanches

This type of avalanches is the one that cause a major number of human casualties and are usually triggered accidentally. When the slabs are hard, the debris can be identified as it is formed by blocks of snow. These blocks have a 'slab structure' as shown in Figure 4, which is formed by two differentiated parts. One layer with weak cohesion, subject to give way when submitted to an effort such as that exerted by

the passing of a skier, and one top layer or slab which when it breaks usually in a thin upslope area, is capable of propagating the fracture linearly, causing for the detachment of a significant part of the snowpack.

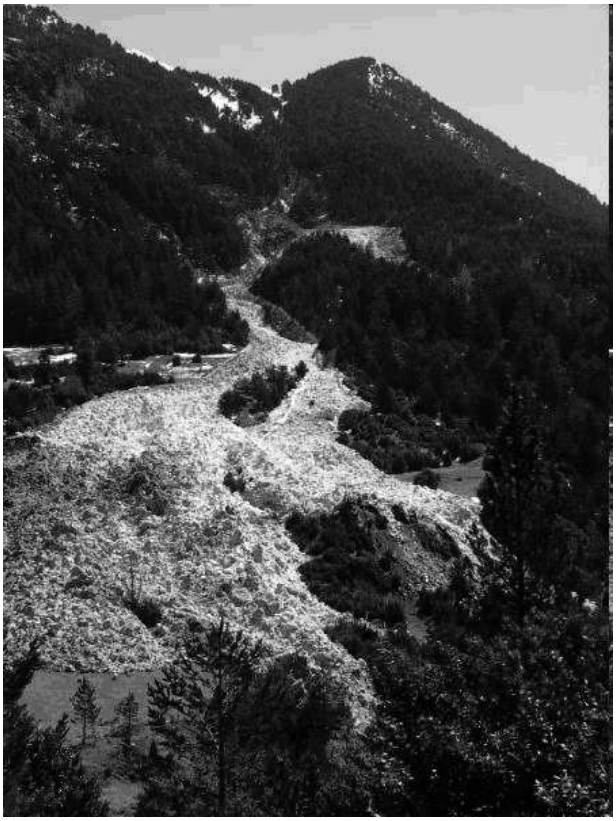

Figure 3. Wet snow avalanche, debris area. The avalanche reached the end of the valley channelled through a couloir. La Sarra, Sallent de Gállego, April 2008. Photo: M. Suárez (High Mountain Military Post).

The most typical process for the formation of this type of structure is a period of intense cold, which forms the type of grains characteristic of the layer with weak cohesion, and a subsequent period of snowfalls with moderate or strong wind. The wind crumbles the snow and transports it, accumulating it in the form of wind slabs. The cornices seen in mountain passes and crests are usually indicators of the wind's direction and of the areas of accumulation where it is easier to find the slabs: The leeward valley slopes of the predominant wind. The slab structures often persist in the snowpack, unless they break or their evolution make them disappear. They usually persist for longer on north slopes. An aggravating factor is the accumulation of new snow on this type of structures, as in the case an avalanche is triggered, the amount of snow moved is greater.

Figure 4. On the left, slab structure. In the centre, cornice and slab, Aragonese Pyrenees, March 2010, Photo: Samuel Buisán. On the right, soft slab by accumulation of precipitation, Ordesa and Monte Perdido National Park, February 2010, Photo: Ibán Urbieta Etxeberría, Góriz refuge.

The so called 'soft slab' avalanches are also very similar, although they are often framed within the category of 'loose snow avalanches'. In these types of avalanches the top layer is much softer, offering little resistance to the penetration of a probe, although their internal cohesion confers them slab properties and are capable of propagating the linear fractures in the snowpack. Although its ability to propagate the fracture is less than in the case of hard slabs, and so the avalanches they cause are usually smaller, the soft slab structures have the added danger of being unnoticed for the passer-by. It is easier to identify the slab structure as it does not offer a clear resistance to the superficial layer. In this case the detachment does not take place in blocks, but the material crumbles, and leaves an accumulation similar to that of loose snow avalanches. Its formation is similar to that of the hard slab structures, except that the action of moderate or strong wind in this case is not necessary.

4. FORECASTING AVALANCHE DANGER: THE ROLE OF THE AEMET

Estimating the danger that avalanches may suppose is not something immediate. It is carried out at different scales, ranging from local, which take place on one individual slope, to regional which include several mountain massifs. Estimates are made on a slope regarding the probability of a natural avalanche, or regarding the effort necessary to artificially trigger an avalanche. Therefore, physical and structural parameters of the snowpack are measured and conceptual models are applied as well as numerical simulations performed. On a greater scale, the approach to the problem with regard to a mountain massif or a region is different. Snow bulletins are made with overall information which serves as the framework on which to plan itineraries and activities, being also a tool to estimate the current local danger depending on the terrain and present factors.

4.1 The European Avalanche Danger Scale

The regional forecast of the danger of avalanches is structured around an international consensus element: The European Avalanche Danger Scale (Figure 5). It is the reference to refer to the possibility of the occurrence of snow avalanches in large areas, that is, within an area of at least 100 km^2. It defines five levels of danger depending on the probability of avalanche triggering, summarising the main

elements to take into consideration. The danger level on the scale is given by the number and size of the expected avalanches, whether these can take place in many or few slopes, the additional load needed to trigger them and the probability they have to occur naturally. The lower the number on the scale, the higher the stability of the snowpack is against extra efforts to which it can be submitted. These additional loads can be low, such as the passing of a skier, or high, such as the passing of a group of skiers without maintaining the safety distance, or the passing of a snowmobile.

Danger level	Icon	Snowpack stability	Avalanche triggering probability
5 - VERY HIGH		The snowpack is poorly bonded and largely unstable in general.	Numerous large-sized and often very large-sized natural avalanches can be expected, even in moderately steep terrain.
4 - HIGH		The snowpack is poorly bonded on most steep slopes*.	Triggering is likely even from low additional loads** on many steep slopes. In some cases, numerous medium-sized and often large-sized natural avalanches can be expected.
3 - CONSIDERABLE		The snowpack is moderately to poorly bonded on many steep slopes*.	Triggering is possible, even from low additional loads** particularly on the indicated steep slopes*. In some cases medium-sized, in isolated cases large-sized natural avalanches are possible.
2 - MODERATE		The snowpack is only moderately well bonded on some steep slopes*, otherwise well bonded in general.	Triggering is possible primarily from high additional loads**, particularly on the indicated steep slopes*. Large-sized natural avalanches are unlikely.
1 - LOW		The snowpack is well bonded and stable in general.	Triggering is generally possible only from high additional loads** in isolated areas of very steep, extreme terrain. Only sluffs and small-sized natural avalanches are possible.

Figure 5. European Avalanche Danger Scale.

4.2 The snow and weather observation network

AEMET has observation networks in several high mountain areas within Spain. The first snow and weather station was installed in 1981 in the refuge of Góriz, in the National Park of Ordesa y Monte Perdido, followed a few years later by the station at the refuge of Estós, in the Valley of Benasque. With several ups and downs regarding the number of observatories and their location, the installation and maintenance of observatories has been consolidating and systematising.

In this process AEMET has always had the support from regional and local bodies, as well as from private entities. In the case of the region of Aragón, it has the support especially from the Aragon Mountaineering Federation (FAM). In Spain there are also other networks of official bodies, with different characteristics. AEMET also collaborates with Météo-France exchanging information from its network of automatic stations and derived products.

The importance of the network of snow and weather observatories is that they are the only ones within the network of AEMET's collaborators which issue daily bulletins through the World Meteorological Communications System, coded according to the NIVOMET key by the World Meteorological Organization. The majority collect data 365 days a year, both instrumental data (temperature, humidity, etc.) as well as visual observation (type of snow, clouds, blizzard on altitudes, avalanches observed, etc.). Their contribution is of great help for many fields such as climatology, numerical simulations, meteorological and snow forecast, etc. Apart from preparing NIVOMET bulletins, many observatories, mainly those at a greater altitude, once per week carry out ram hardness profiles, snowpits, and stability tests of the snowpack.

Snow-meteorological Station	Province (m)	Altitude	Collaborating Body	Data	Penetro meter
Isaba-El Ferial Nordic ski resort	Navarra	1590	Gov. of Navarre	Annual	No
Linza refuge	Huesca	1340	City Council of Ansó	Annual	No
Lizara refuge	Huesca	1540	FAM	Annual	No
Candanchú ski resort	Huesca	1560	ARAMÓN - ETUKSA	Annual	Yes
Formigal-Furco ski resort	Huesca	1855	ARAMÓN	Annual	Yes
Formigal-Sextas ski resort	Huesca	1558	ARAMÓN	Annual	Yes
Respomuso refuge	Huesca	2200	FAM	Annual	Yes
Panticosa-Los Lagos ski resort	Huesca	1830	FAM	Annual	Yes
Panticosa-Casa de Piedra refuge	Huesca	1660	FAM	Annual	Yes
Ibones de Bachimaña refuge	Huesca	2190	FAM	Annual	Yes
Góriz refuge	Huesca	2215	FAM	Annual	Yes
Pineta refuge	Huesca	1240	FAM	Annual	No
Angel Orús-El Forcau refuge	Huesca	2150	FAM	Annual	Yes
Estós refuge	Huesca	1890	FAM	Annual	Yes
Cerler ski resort	Huesca	2020	ARAMON	Winter	Yes
La Renclusa refuge	Huesca	2140	FAM	Annual	Yes
Valdelinares ski resort	Teruel	1960	ARAMON	Annual	No
Rabadá y Navarro refuge	Teruel	1520	FAM	Winter	No
Navacerrada	Madrid	1894	AEMET	Annual	Yes
Port del Compte ski resort	Lleida	1750	Guimaru	Winter	No
Núria ski resort	Girona	1967	Gov. of Catalonia	Winter	No
Vallter 2000 ski resort	Girona	2160	Gov. of Catalonia	Winter	No

Table 1. Network of snow-meteorological observatories.

As a complement to the manual network, AEMET has deployed 7 high mountain automatic weather stations, three in the Aragonese Pyrenees, three in the Catalan Pyrenees and one in Sierra Nevada, which will provide hourly data of the temperature, wind and snow depth.

4.3 Snow information and avalanche danger bulletins

The information collected from the high mountain networks, together with the rest of the observational information and the weather forecasts, is used to prepare AEMET's avalanche bulletins.

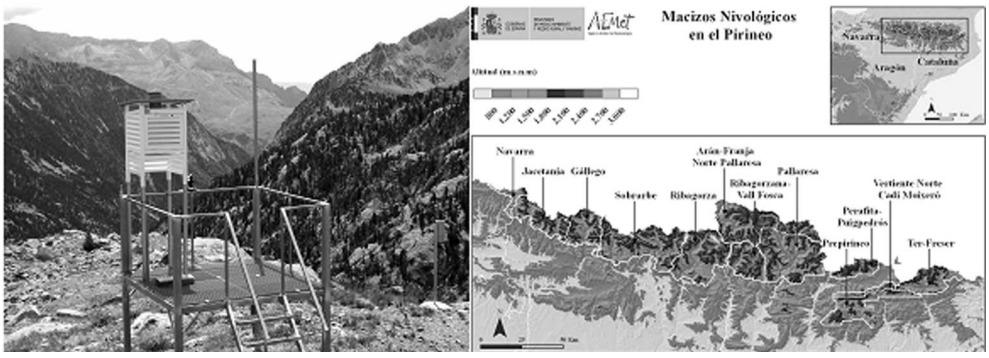

Figure 6. On the left, observation platform at Los Ibones – Bachimaña refuge. On the right, map of the massifs for avalanche danger forecast in the Pyrenees.

The bulletins inform on the state of the snowpack, its level of stability and the type of avalanches to be expected. An estimate is provided on the possibility of a natural or accidental avalanche triggering, depending on the weather and snow conditions present and forecasted, and a danger level is provided according to the European Avalanche Danger Scale.

Their contents is valid in the areas in which the snowpack has not been artificially altered, that is, outside managed areas, such as the ski resorts ones. Avalanche bulletins are issued as from 3 pm and refer basically to the following day, with an outlook also for the subsequent day. They can be consulted on the Internet (www.aemet.es) and are available in mountain refuges and ski resorts.

The spatial reference scale on avalanche bulletins is the mountain massif, a geographic area of a limited extension and with sufficiently homogeneous climatic characteristics. The bulletins are issued daily during the snow season for the Pyrenees and on a weekly basis for Guadarrama and Picos de Europa areas. In the case of the Pyrenees, one dozen massifs are taken into consideration for the snow forecast, one in the Navarre Pyrenees, four in the Aragonese Pyrenees and seven in the Catalan Pyrenees (Figure 6).

4.4 Avalanches as adverse phenomena in METEOALERT

When the conditions are objectively adverse, from level 4 on the European Scale, the State Meteorology Agency issues an alert according to the National Plan of Adverse Meteorological Phenomena, METEOALERT. The alerts are differentiated by colours depending on their level of danger:

- Yellow: Danger level 4 (high) with the avalanche starting point below 2100 meters or danger level 5 (very high) with starting point above 2100 meters.
- Orange: Danger level 5 with the avalanche starting point below 2100 meters.
- Red: Exceptional situation, orange level general risk affecting a vast area.

5. SNOW-WEATHER ANALYSIS OF TWO AVALANCHE EPISODES

This section analyses in detail the weather factors which favour the triggering of two avalanches which caused material damages to buildings or impacts on infrastructures, without causing human casualties. One slab avalanche in Astún, and the other a wet snow avalanche on the road of Llanos del Hospital.

5.1 Wind slab avalanche: Astún, 25th December 1993

The ski resort of Astún has its base at 1730 m, and is located in a valley without vegetation and prone to avalanches. Several defences have been built such as empty dams, supporting structures and reforestation. At that time, there were 87 supporting structures built on the slope of Torrullas and at the end of 1995 there were 118. The avalanche fell in the middle of the night, coming from the south slope of Peak Escalar (2297 m), on the slope of Torrullas, north of the station's base and outside its area of operation. It entered through the back of the Hotel Europa and of the apartment building Sarrios, built supported on the slope, at the level of the sixth floor. The snow descended through the stairway, causing material losses valued in 12 million pesetas.

5.1.1 Snow-weather Analysis:

Although there is no data from the ski resort of Astún in those days, there is information from Candanchú, at 1560 m and only 3 km SW away, and with very similar climatic conditions. Below is a summary of the most significant meteorological information from the days before the avalanche and its main consequences regarding the stability of the snowpack in the area and in the slope in question.

Until the 21st of December there was little snow on the Pyrenees, at least on low and medium altitudes, with bare ground in Candanchú and only 15 cm is the nearby resort of Formigal, less than 20 km away and at 1850 m altitude. On the 21st and 23rd of December it snowed weakly, with WNW flow. As a result, on the 23rd Candanchú and Formigal had 10 and 28 cm total snow depth of the snowpack, respectively. This previous snowfall, although weak, was key for the subsequent snow to fall on a more uniform and smooth surface, thereby configuring a slope more prone to trigger avalanches of a significant size if the future conditions were to be suitable. Another important factor was that the temperatures were relatively low on the 22nd and 23rd, with minimum temperatures of -6.5 and -7.5 ºC and maximum temperatures only slightly above zero (Figure 7), with cloudy skies in general. The greater the height, in the area of Astún, the temperatures were probably lower, given the type of weather situation. These temperatures, and especially the very thin snowpack (5 and 10 cm in Candanchú the mornings of the 22nd and 23rd of December) favoured strong temperature gradients inside the snowpack and the formation of faceted forms (faceted crystals and depth hoar), representing a persistent weak layer.

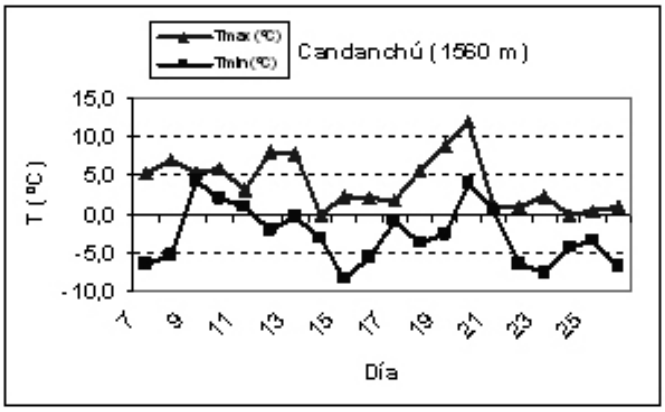

Figure 7. Maximum and minimum temperature in Candanchú (1560 m), 7th - 26th December 1993.

On the 24th of December, with an intense NW flow practically on all levels, the snowfalls were significant. Between 20 and 40 mm in La Jacetania, with a relatively low snow level, of around 800 m. In Candanchú, although the snowfall was of 38 mm, due to the blizzard, the accumulation of snow only reached 5 cm. Larger amounts probably fell at higher altitudes, although due to the blizzard its distribution would be very irregular, accumulating preferably on S and W slopes. The wind, of around 90 and 120 km/h at 850 and 700 hPa respectively, played a very important role in this episode.

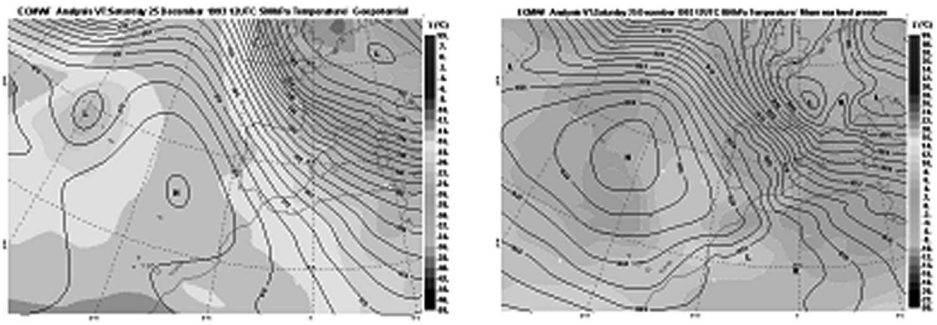

Figure 8. On the left, Era-Interim (ECMWF) temperature and geopotential reanalysis at 500 hPa. On the right, pressure at sea level and temperature at 850 hPa. Both at 12 UTC on 25th December 1993.

On Saturday 25th the situation intensified slightly, with a low pressure that moved throughout the day from the British Isles to the Gulf of Genoa, passing close to the area of interest favouring the strong flow from the NW, with 140 km/h at 700 hPa (Figure 8). The snowfalls in the area were more abundant, between 40 and 70

mm. In Candanchú they measured 24 cm new snow, not recording blizzard in the bulletin, although they did record it in nearby observatories such as in Formigal and Respomuso, which indicates the blizzard was greater at medium and high altitudes than in low altitudes, forming new slabs of wind over the one that had already formed the previous day.

Therefore, all the propitious circumstances led to the formation of slab structures on the slope of Torrullas, which can be summarised as follows:

- Slope already snowed prior to the severe episode.
- Temperatures relatively low the days 22nd and 23rd with a very thin snowpack (it didn't exceed 30-40 cm in the area in which the avalanche triggered), a favourable situation for the forming of faceted forms, creating a persistent weak layer on the surface.
- Up to 100 mm snowfall in the area during the 48 h prior to the avalanche.
- Strong NW blizzards during the 24th and 25th of December with the corresponding transport and destructive transformation of the snow, which would form well-joined rounded grain slabs in E and S directions. These slabs, which were possibly hard, formed on top of the pre-existing weak layer, giving rise to slab structures.
- Finally, the continuous increase of additional load on the weak layer, originated by the snowfall and the blizzard of the 25th of December, was what probably caused for the weak layer to break and thus the avalanche to trigger.

5.2 Wet snow Avalanche: Llanos del Hospital, 19th January 2013

The road A-139, mainly in SW-NE direction between Benasque and Llanos, usually presents problems related to the danger of avalanches that reach the road following the couloirs with the same name. In this case, the avalanche occurred during the afternoon-evening, channelling through the Las Fites couloir and cutting-off the road at km 67.5, approximately 7 km NE from the town of Benasque. On this occasion, the road was closed to traffic on the 15th of January due to the heavy snow that fell on the 14th and 15th of January, and was not opened again until the 27th, for which the guests and staff of the high mountain hotel of Llanos del Hospital were isolated.

The couloir through which the avalanche shifted starts at approximately 2150 m altitude and reaches the road at 1450 m, and has an approximate length of 1.2 km. Its aspect is mainly SE and its inclination is of 40, 34, 33 and 31º (averages per 250 m horizontal stretches) from the highest to the lowest stretch (Figure 9).

5.2.1 Snow-weather Analysis:

The closest information we have of the avalanche is the snow-weather information collected at the refuges of Estós (1890 m) and La Renclusa (2140 m), the information of this latter being more representative on the days of N flow.

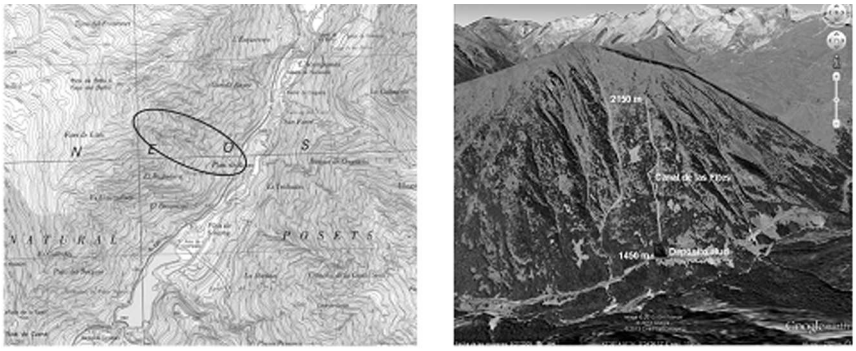

Figure 9. On the left, detail of the area from the National topographical map of Spain 1:25000 (IGN). On the right, view of the Las Fites couloir from Google Earth.

On the 12th of January the ground in the area was almost bare at 1500 m altitude, and the snowpack was scarce and stable on the highest altitudes (18 and 65 cm total depth respectively in Estós and La Renclusa). However, weak snowfalls on the 12th and moderate and persistent snowfalls on the 13th left around 50 cm of new snow in the area, covering the ground on the lowest part of the couloir and homogenising even more the bed at the top areas which already had snow.

It continued to snow the following days in a more or less persistent way, with moderate intensity in general, although strong on the 14th and 15th, during which approximately 130-140 cm of snow accumulated since the snowfalls started on the afternoon of Saturday the 12th and up until Friday the 18th in the morning. (Figure 10). The wind was strong all those days, with strong blizzards from the 14th up until the 17th. In general it came from the North although it varied: Initially from the NW, it turned to West on the 16th to go back again to being from NW and finally NE. In line with the oscillations in the flow's direction, the temperature changed also. The potential snow level varied between 200 and 750 m on the 14th and 15th, it went up from 500 to 1400 m on the afternoon of the 16th, to go down from 900 m to 0 m on the 17th passing to a synoptic situation of advection of cold continental air. (Figure 10).

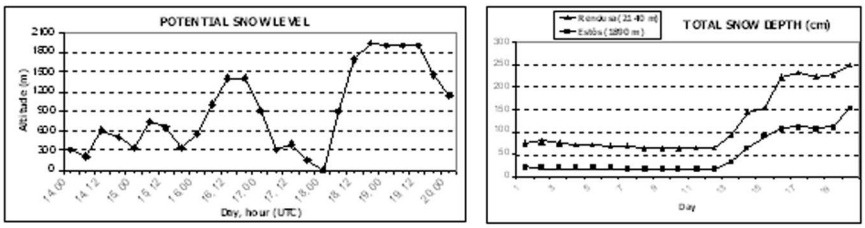

Figure 10. On the left, snow altitude estimated by the analysis HIRLAM 0.16º at the Las Fites couloir, 14th - 19th January 2013. On the right, total snow depth at the refuges of La Renclusa (2140 m) and Estós (1890 m) 1st-20th January 2013. The measurement was taken at 8 UTC, 9 AM local time.

On the 18th a brusque N to S change of the flow occurred on low levels, rapidly elevating the potential snow level for the first half of the day, from 0 to 1700 m, reaching 1950 m in the afternoon. Weak although fairly persistent snowfalls continued, and so did the strong blizzards, passing from NW to WSW. It already rained in the first hours of the morning in the refuge of Estós at 1890 m, for which it was likely for the snow level to go up faster than that estimated by the model. On the refuge's snowpit, performed at 10.15 am on the 18th, a moist snowpack appeared, practically isothermal throughout the vertical, with mainly rounded grains and fragmented particles, resulting from the blizzards and from the relatively warm snow that fell on the afternoon of the 16th, with a more moist layer on the surface.

Thus, during the day of the 18th, the snowpack below 1900 m in the area of the Las Fites couloir was humidified both due to the brusque temperature increase (8 ºC at 850 hPa, from -4 to +4 ºC) and to the rain. The most superficial part of the layer was probably the most affected as the rounded grains usually act as a sponge, absorbing a large amount of snow water, which would make them lose cohesion and transform to melt forms, giving place to moist superficial sluffs on steep slopes. Due to the rain that fell almost all day, the grains were growing in size forming percolation channels which would allow the snow water to penetrate even deeper.

The precipitation was moderate and persistent on the 19th in the area of the avalanche, still with a very high snow level (1700-1900 m) until midday, becoming more intense upon the passing of a low pressure in the afternoon, with the corresponding associated cold front which passed through the area of interest between 12 and 18 UTC (Figure 11). At 18 UTC the estimate snow snow level was 1450 m and at 24 UTC on Sunday 20th it was 1150 m. Therefore, for at least 24 h the precipitations were in the form of rain below 1700-1900 m, and then went on to be solid although moist below this altitude.

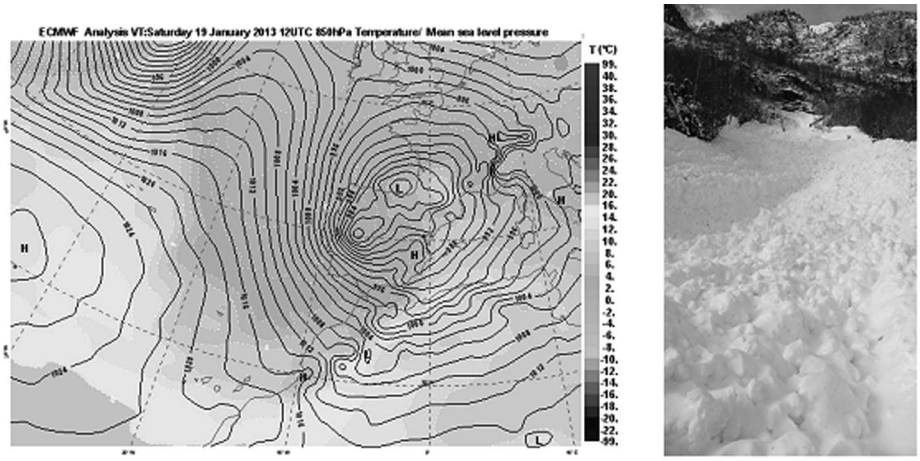

Figure 11. On the left, Era-Interim (ECMWF) reanalysis of pressure at sea level and temperature at 850 hPa at 12 UTC on the 19th. On the right, avalanche debris zone, where we can see the channelling in the lower stretch of Las Fites couloir. Photo: Javier Rodríguez.

Between 8 UTC on Friday 18th and 8 UTC on Sunday 20th 49 mm (36 cm) of snow were collected in Estós and 21 mm (60 cm) in La Renclusa. Also in the area, in the refuge of Ángel Orús, which is usually more affected in South situations, 100 mm were collected. Therefore, taking into consideration the information from the Ebro Water Confederation, at least between 30 and 50 mm can be estimated in the area of the avalanche between the morning of the 18th and the afternoon-evening of the 19th. It is very likely that during the morning of the 19th the water percolated until the ground or until a relatively non-permeable layer, a weak interface that would cause the sliding of the snowpack over a sufficiently smooth surface. This type of surface, a melt-freeze crust, appears on the profile of Estós on the 18th, originated at the beginning of January in a period with melt-freeze cycles. All these conditions, together with the greater inclination of the couloir on its highest part (around 34º at 1900 m) and the fact that witnesses from the area ruled out the possible breakage of a dry slab on high altitudes, where all the precipitations were in the form of snow, point towards the most probable area for the starting point of the avalanche an altitude between 1700 and 1900 m. According to this, it would be a middle-size wet snow avalanche, a glide or an avalanche involving most of the snowpack. As seen on the photograph (Figure 11), both the channelling and the type of debris correspond to a wet snow avalanche.

Paradoxically, the avalanche occurred in the afternoon-evening, time in which the temperature was going down (Figure 10), after the passing of the front and probably when the precipitation was solid, although still quite moist, throughout the path of the avalanche. However, it seems coherent as it was during the second half of the day when the precipitation was more intense, what would produce a greater additional load, and the snow level would still be relatively high and therefore the recently moist snow would continue to add liquid water. Moreover, according to the bibliography, ground wet snow avalanches (glides) have a certain preference to occur during a descent of the temperatures after a long period of snow melting, in this case accelerated by the abundant rain.

To summarise, the weather ingredients for the sliding of the wet snow avalanche through the couloir of Las Fites, were the following:

- Major accumulation of new snow prior to the melting episode.
- Notable rise in the temperature during the 18th. The high temperatures prevailed until midday on the 19th.
- Weak-moderate, although fairly persistent, rain for 24-30 h below 1700-1900 m, between the morning of the 18th and the midday of the 19th, with accumulations from 30 to 50 mm. These two last factors caused a fast development of an isothermal moist snowpack, with mainly melt forms, increasing in size as the hours passed favouring the forming of large percolation channels.
- Moderate, even strong, moist snowfall in the afternoon of the 19th. Favoured a greater additional load and the continuation of the humidity contribution.
- Drop in temperature in the afternoon of the 19th, which favours the final triggering of ground wet snow avalanches (glides).

ACKNOWLEDGMENTS

The collaborators of AEMET snow-weather network, the GREIM of Benasque, managers of the road A-139, José Antonio Vada Manzanal (AEMET), José Voces Aboy (AEMET).

REFERENCES

Keiler y Sailer, (2006). Avalanche risk assessment – a multi-temporal approach, results from Galtür, Austria*. Nat. Hazards Earth Syst. Sci*., 6, 637–651.

Fierz *et al*., (2009). The International Classification for Seasonal Snow on the Ground*. IHP-VII Technical Documents in Hydrology*, N°83, IACS Contribution N°1, UNESCO-IHP, París.

Rodés y Miranda, (2011). Breve aproximación histórica a la nieve y a los aludes de nieve en España*. Asamblea ACNA*, Camprodón. Disponible en Internet: http://www.acna.cat/noticies/111112_Assemblea_General/PRodes_EVOLUCIO_ALLAUS.pdf

Ayora, (2012). Seguridad y responsabilidad en accidentes por aludes de nieve*. Acciones e investigaciones sociales*, 31, 7-38. ISSN: 1132-192X.

Leo y Cuchí, 2004. *Los aludes en el Alto Aragón*. Lucas Mallada: Revista de Ciencias, ISSN 0214-8315, Nº. 11, págs. 135-162.

McClung and Schaerer, (1996). Manual de Avalanchas. Ed. Desnivel, 1ª Edición.

Tremper, (2008). Staying Alive in Avalanche Terrain. Mountaineers Books, 2nd Edition.

Baggi y Schweizer, (2009). Characteristics of wet-snow avalanche activity: 20 years of observations from a high alpine valley (Dischma, Switzerland). *Natural Hazards*, 50, 97-108.

Marienthal *et al*., (2012). Depth hoar, avalanches, and wet slabs: A case study of the historic March, 2012 wet slab avalanche cycle at Bridger Bowl, Montana. *Proceedings of the International Snow Science Workshop*, 17-21, Anchorage, Alaska.

Vada *et al.*, (2013) [en prensa]. Análisis del alud del 8 de mayo de 2012 en los Llanos del Tornu, Macizo Central de los Picos de Europa. *Revista de la ACNA*.

Sanz *et al*., (2013). Guía para la Observación Nivometeorológica*.* MAGRAMA-AEMET. NIPO: 281-13-006-4. Disponible en Internet: http://www.aemet.es/documentos/es/conocermas/publicaciones/Guia_nivometeorologica/guia_nivometeorologica.pdf

Buisán *et al*., (2010). Aludes: sus tipos y causas*. Boletín de la AME*, nº 29.

CHAPTER 17

FOREST FIRES IN SPAIN

Antonio MESTRE BARCELÓ

Spanish State Meteorological Agency (AEMET)
amestreb@aemet.es

ABSTRACT

Currently forest fires represent one of the most critical environmental concerns that Spain has to face up. Wildfires not only devastate the current vegetation, but also produce mean and long-term impacts that can be irreversible, leading to a decrease of the capacity amble of life of the soil. Despite of majority of forest fires in Spain are caused by human activity (intentionally caused or due to negligence), the meteorological and climatic factors play an important role in both the probability of occurrence and in his later development. This highlights the importance of having a meteorological support specifically aimed at fire prevention and firefighting activities, particularly concerning the early warning of extreme fire risk conditions. Several aspects of the relationship between meteorology and forest fires are considered and detailed in this work. The support that national meteorological services can provide to the Agencies with competence in the field of fire-fighting and fire-prevention, as a base for the setup of forest fires early-warning systems it is also considered. Finally the current operational activities in AEMET, aimed at providing meteorological support to the forestry services for fire prevention purposes, will be addressed.

Key words: forest fire; fire danger rating; fire behaviour.

1. INTRODUCTION

Wildfires have always been a part of natural cycles in the ecosystems of the Mediterranean part of Europe, where the dominant vegetation species are adapted to specific climate conditions marked by a long dry and hot summer with a clearly defined fire-season. Natural wildfires have played a role of selection on the evolutionary patterns of Mediterranean ecosystems.

Nevertheless, the number and the extension of these fires have been increasing more and more since the 60´s and consequently, the wildfires (most of them

intentionally caused) have become one of the most critical environmental issues that Spain has to face up nowadays. These forest fires not only devastate the current vegetation, but also produce mean and long-term impacts that can be irreversible leading to a decrease of soil's ability to support life.

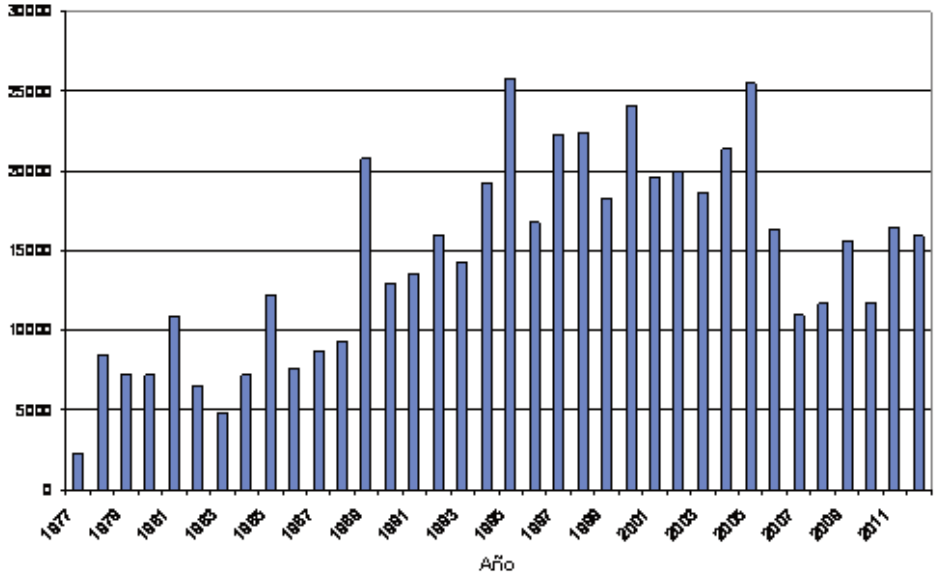

Figure 1. Annual number of forest fires in Spain since 1997. (Source: MAGRAMA data, with author´s elaboration).

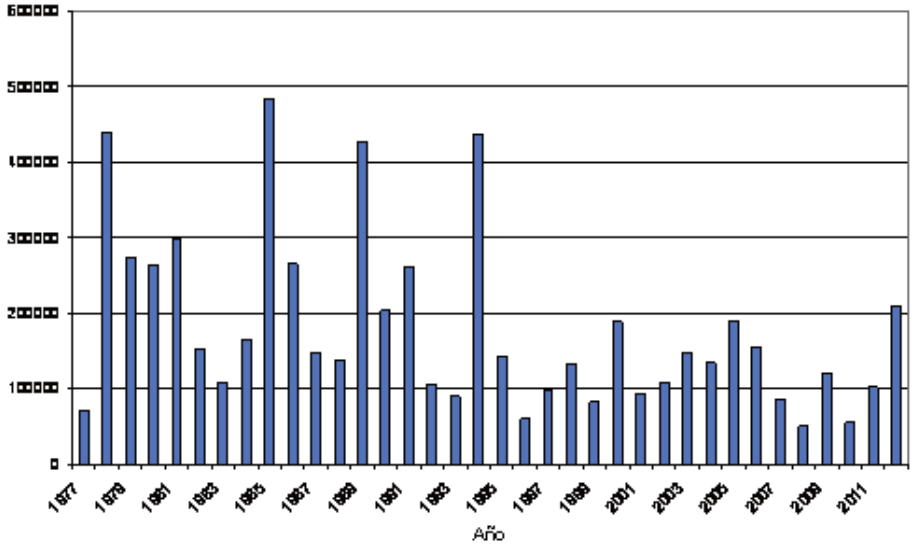

Figure 2. Evolution of total burned surface by forest fires in Spain from 1977 to 2012. (Source: MAGRAMA data, with author´s elaboration)

In Figures 1 and 2, total number of forest fires in Spain and total burned surface are respectively represented. Both graphics have been generated making use of the data provided by the Spanish National Forestry Service, the historical data (period: 1961-2012, being provisional the data from 2011 and 2012) of both them. It can be observed from these time series that the number of fires have been gradually increasing, whereas the annual burned surface has experienced big variations from one year to the other, being these abrupt changes strongly dependent on the prevailing climate conditions in spring and summer seasons. The whole burned surface over Spain reached very pronounced peak values in the years 1978, 1985, 1989 and 1994, when the burned surface exceeded 400000 Ha.

From the data in Figures 1 and 2 it emerges that the mean extension of the forest fires in Spain has gradually decreased to a mean value of 7-8 Ha by fire in recent years, although with a sharp increase in last year 2012.

The Mega fires (those in which burned surface exceeds of 500 Ha) is one of the most critical issues of the problem of forest fires in Spain. The occurrence of these Mega fires is closely linked to the presence of very specific weather conditions, characterized by strong winds blowing from land perpendicularly to a mountain chain, and reaching the coastal areas located leeward in very dry and hot conditions. It is a fact to be mentioned that, since 1970 until now, the surface burned in these big fires has represented more than 36 % of the total burned surface in Spain (Chuvieco and Martin, 2004). In the first decade of this century this percentage was about a 37,5% . In some years this percentage reached values above 70% (76,6% in 1994 and 75,9% in 2012).

Figure 3 shows the evolution of the annual number of Mega fires. It can be that it reached a maximum in the 80s and early 90s to be followed by a drastic decrease around 1996, and a further increase with sudden changes up to 2012.

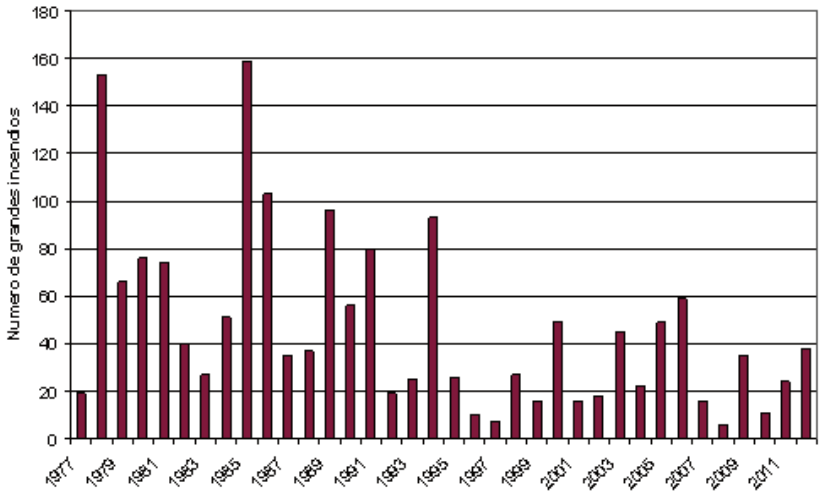

Figure 3. Annual number of big forest fires (burned surface above 500 hPa) in Spain (1977-2012). (Source: MAGRAMA data, with author´s elaboration).

Concerning the causes of the forest fires, in Spain as in the rest of the Mediterranean part of Europe, most of these fires are of human origin, being an important percentage of them (48%) intentionally produced, another 24% are due to negligence, whereas only a 7% have a natural origin, mainly light strokes (Vélez, 2000). There are around a 17 % of fires with unknown origin. This quite significant percentage has been gradually decreasing in the last years, due to the improvement of in-situ investigation techniques (Porrero, 2001).

Analyzing the forest fires spatial distribution, a very unequal distribution of the frequency of occurrence of forest fires it is observed. Forest fires are mainly concentrated in the northwest part of Spain (Galicia, northwest of Castilla y León, Asturias and Cantabria) as well as in the north of Extremadura, west part of the Central Mountainous System, the Mediterranean coastal area that extends from Catalonia to the north of the province of Alicante and some areas of Murcia and Andalucía.

As regards to the seasonal distribution of wildfires, in most of Spain these fires occur mainly in the summer season (from July to September). However in areas of the Pyrenees and the Cantabrian mountains, more than half of the wildfires occur at the end of the winter and early spring, a clearly marked secondary fire season. This fact can be explained in the frequency of adverse meteorological situations, with dry and cool winds blowing from the Central Plateau, aggravated by the large number of fires of grasslands fires the shepherds and farmers make in those dates in the north of Spain.

2. METEOROLOGICAL AND CLIMATOLOGICAL FACTORS RELATED TO FOREST FIRES

The basic factors in determining the fire behaviour features are: topography, meteorology, and fuels. Of these three fundamental factors, the meteorological factors experience significant changes in short term, and they can be forecasted, at least in the short and medium term. This underlines the importance of the meteorological support in forest fire prevention and control, especially in relation to the early warning of critical situations with fire risk conditions. The various aspects of this broad and complex relationship between meteorology and wild fires are listed below.

2.1 Weather phenomena as causal agents in forest fires

Thunderstorms, particularly those that are accompanied by scarce precipitation, are actually the only meteorological phenomenon which is direct cause of occurrence of forest fires. Besides this, these thunderstorms (that accounts for much of the summer season precipitation in the Mediterranean climate countries), come often accompanied by strong winds gusts of rapidly changing direction, which increases the potential severity of fires caused by strikes. Strikes act as sources of ignition under conditions in which the dead plant fuel humidity is low due to the marked seasonality of rainfall and temperature that characterizes these Mediterranean areas.

Unlike countries with extensive forested areas and very sparsely inhabited, such as Canada and the United States, where the percentage of fires caused by lightning reaches values close to 50 %, in Spain only around 4 % - 5% of the forest fires are started by lightning (MAGRAMA, 2012). However, in certain mountainous areas of central and north Spain, especially in the Iberian.

Mountain, the number of fires caused by lightning reaches values that are close to 40% of the total number of fires. This is because in this area the storms are quite frequent (around 30 days of storm by year), 80% of these days are concentrated in the period from June to September. On the other hand, many of these thunderstorms are characterised by a high number of strikes but with a very low amount of precipitation, what increases the risk that the sparks ignite the dry vegetation.

Whereas the number of fires caused by lightning is relatively small in Spain, the mean surface burned in these fires is on average much higher than that produced by other causes. Among the factors that explain this fact, the following can be quoted: preferential location of thunderstorms in summer in mountain areas, the access to the wildfires is more difficult when occurring in less populated areas of irregular land and, finally the timing of greatest probability of storm occurrence in summer, which is late in the morning or afternoon.

During the period 1986-95 the strikes caused a 4,2 % of the forest fires that took place in Spain, although it represented a 14,0 % of the burned wooded entire surface and a 6,4 % of not wooded burned surface. In 1994, a year in which an extraordinary wave of forest fires affected all the Mediterranean regions during the first days of July, the fires started by lightning accounted for only 2.7% of the total, but they fires burned the 27.7 % of the forested area that was affected that year.

Due to the fact that the electric discharges of the thunderstorms generate enormous quantities of radiant energy in a in a broad spectrum of frequencies, it is possible to determine the point where the lightning has struck by means of special sensors measuring the azimuth angle. If the lightning is recorded simultaneously by several sensors, its location can be established with high spatial accuracy when it struck, using methods of triangulation. Based on these principles, the networks for lightning detection determine instantly and with an error that ranges from hundreds of meters to a few kilometers, the position in which they have struck and the moment with precision of milliseconds, its polarity, the total number of discharges and the total energy released. The possibility of having access in real-time to this information, as well as to other climatological products that can be obtained from the strike database, certainly constitutes a valuable contribution to fire prevention activities. The information proceeding from these sensors can also be combined with the probability of ignition in order to estimate the lightening–caused fires probability (Latham, 1983).

2.2 The effect of meteorological and climatological factors in the short-term

2.2.a *Effect of meteorological and climatological factors on the ignition probability*

Weather conditions, both the instantaneous as well as the averaged values on a given time interval, exert a decisive influence on the probability of occurrence of forest fires. Weather conditions determine the moisture content of fuels and, consequently, their level of flammability. The temporal variability in the short-term (daily scale) of the risk of forest fires is mostly explained by the combined effect of the instantaneous values of a set of meteorological variables on the humidity and temperature of dead fine fuels, which quickly adapt to the current weather conditions.

The moisture content of these fine fuels is directly related to the probability of ignition or likelihood of an ignition point when there is a heat source, such as a spark. The meteorological variables that define this moisture content are, in descending order of direct relevance, precipitation, relative humidity, temperature and wind

The separate effects for each of these variables, as well as the meteorological situations that give rise to the worst combination of these factors are described below:

a) *Effect of the precipitation:* From a minimal threshold of intensity (which can be very low: 0,5 mm / hour), the precipitation maintains, while it takes place and from a minimal threshold of intensity, which can be very low (), low values of the moisture of the thin fuel and consequently, low values of the probability of ignition. Nevertheless, its effect is very transitory in the conditions of strong evaporation that prevail along the summer periods in areas with dry and hot seasons, as it is case of the areas of the Iberian Peninsula with Mediterranean climate. In those areas, in which the average number of days of precipitation along the fire season is very small, precipitation will play a role relatively limited on the temporary evolution of the risk of fires along the Campaign. Nevertheless it can be important in the case of a abnormally humid summer season.

b) *Effect of the relative humidity:* Relative humidity is an essential meteorological variable in the determination of the short-term variability of ignition probability during wildfire high risk period. For a temperature of around 25° C and, under equal conditions for the rest of meteorological and topographical variables, a decrease in relative humidity from 60% to 30% will lead to an increase of the probability of ignition from 40% to 70% (Pouliot, 1991). For all these reasons, the values of the various meteorological forest fires risk indexes are, in general, very sensitive to this variable, which is characterized by its strong temporal and spatial variability. Temporal variability in the short term may be associated with changes of predominant air mass or with the diurnal cycle of temperature, especially in the summer time, when a sharp decrease in the values of the relative humidity at noon is associated with the strong daytime heating, although the air mass be the same and so, with total mass of atmospheric water vapour significantly constant.

c) *Effect of the temperature:* The direct effect of the temperature on the probability of ignition is similar to the previously indicated for the relative moisture, although this effect is of opposite sense and of many less intensity. Nevertheless, upon to the direct effect of high temperatures, (due to the highest temperatures that reach the fuels, especially the fine ones and to the higher drying rate), it is necessary to add an indirect effect based on the fact that, for an air mass that remains over an area without changing its water vapor content, the higher the temperature, the lower is the relative humidity. Therefore, the effects of the temperature and the relative moisture on the ignition probability are added.

d) *Effect of wind:* Being constant the rest of the weather variables, the direct influence of the wind speed on the fuel moisture is in general of little significance. This effect is related to the greater or lesser speed of drying depending on the wind, so it only acquires quantitative significance in cases when the fine fuel moisture content is high, something that occurs infrequently in climatic zones characterized by a long warm and dry season. However, and regardless of the above-mentioned direct influence, the overall effect of the wind on the probability of ignition can be of great importance, due to the fact that the direction and speed of the wind is often a decisive factor in the determination of the characteristics of the air mass that affects a specific area. Therefore, the wind fields tend to be strongly correlated with fields of temperature and relative humidity. For this reason, the effects of these important variables are added to the direct wind effect.

e) *Extreme risk conditions:* There is a meteorological situation in which the effects of wind, temperature and relative humidity add one to the other, creating especially favourable conditions for forest fires occurrence. It happens when a wind flow crosses perpendicular to a mountain range, and reaches areas located leeward. This results in a warming of the mass of air downwind the mountain, accompanied by a pronounced drying and heating of the descending air mass, due to the retention of cloudiness and moisture to windward of the mountainous range. This is the so-called "foehn effect" , that lead to high temperatures and strong gusty winds conditions in the leeward side, that jointly with the scarcity of clouds, high direct irradiation values and high rates of evaporation (that usually accompanies such situations), produces an intense drying of the fuel giving rise to a rapid increase of the ignition probability.

2.2.b *Effect of meteorological and climatological variables on forest fire spreading*

Once a forest fire starts, the wind is the main driver of its development and the regulator of the supply of oxygen. Wind direction and speed as well as wind gustiness are the factors that determine the fire spreading process parameters: speed and direction of propagation and the energy release rate. However, as regards the role of the wind in the propagation of wildfires, it should be taken into account the complex interaction of wind with topographic factors, as well as the significant disruption introduced in the field of winds by the great amount of heat generated by the fire itself.

The degree of atmospheric stability plays too a very important role in the fire propagation characteristics because a high instability of the air column leads to a greater oxygen supply and to more favourable conditions for a rapid fire spreading. Therefore, in different meteorological danger rating schemes the atmospheric stability indexes are taken into account. The amount, size distribution, and dead plant fuel humidity as well as the characteristics and water content of the living vegetation have also a direct influence on the fire spreading rate. These parameters are largely determined by both the current values of temperature, relative humidity,

precipitation and radiation and the accumulated effect of these variables over different time scales (ranging from days to months) on the living vegetation water content and on the plant development process throughout its different phenological stages.

2.3 Effect of climatological variables (medium and long term)

The structure of the natural vegetation and its flammability level strongly depends on the climatic factors. It is particularly important the influence of both the thermal and rainfall regimes (including the annual precipitation value and the timing and inter-annual variability of rainfall), as well as the intensity and timing of the received amount of radiant energy. The rhythm of development of the plants through its different phenological stages is also determined by some accumulative climatic parameters, in particular by the evolution of the temperatures in reference to the average values.

In climate regions characterized by the existence of a long dry season with high temperatures, strong evaporation rates and low relative humidity conditions, it is possible to define a well marked "fire season", in which the dead vegetation and, to some extent also the living one, reach very high flammability levels. Such is the case of the of the Iberian Peninsula regions with a climate of Mediterranean type, in which the period with climatic conditions favouring a high forest fires risk is clearly delimited between the beginning of June and the end of that of September. Figure 4 shows the surface affected by the fires in the period 1971-2012 in Spain versus the summer season precipitation averaged at national level. It could be observed the important percentage of the inter-annual variability of total burned area explained by the summer precipitation, even considering an average at national level.

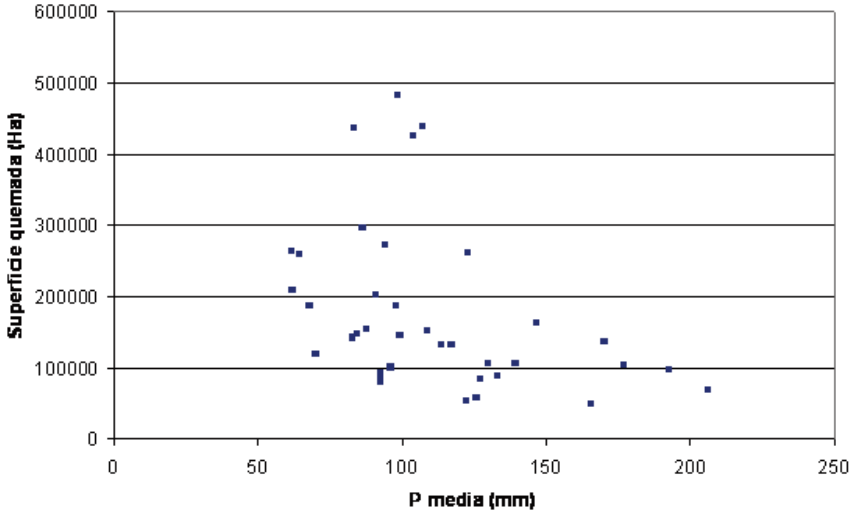

Figure 4. Annual total burned surface in Spain versus average rainfall in summer season.

2.4 Quantifying the integrated effect of meteorological variables: meteorological indexes for forest fire risk

For all types of preventive actions, as well as for planning, distribution, mobilization and allocation of resources for fire-fighting, it is essential to have a magnitude that quantifies the effect of the integrated meteorological variables on the risk of fire ignition and spreading. Indices are useful to define the risk class level and specific actions can be adopted depending on the current or expected risk class.

This quantification of the forest fire danger levels is made by the use of the fire meteorological risk indexes. The development of systems for the analysis and prediction of forest fire risk based on the use of a numeric index began in the United States during the 1920s. A parallel system was set up in Canada in the next decade. At present there are in operation many national systems for the assessment of the risk of initiation or propagation of the fire. Other experiences based on indices applied at the regional level have also been developed.

If follows a brief description of a set of fire risk assessment systems which have been used or are being currently used in different countries:

1. The Canadian Fire Weather Index, (Van Wagner, 1987; Van Wagner y Pickett TL, 1987), is a meteorological forest fire danger rating system that was developed by the Canadian Forestry Service. This index is based on the modelling of dead fuel flammability present in the soil and the subsoil, which strongly depends on its moisture content. The FWI contains several sub-components that reflect the effect of the weather conditions on the fine fuel moisture content (Fine Fuel Moisture Code-FFMC), the moisture content of fuels of medium size and the low density organic matter (Duff Moisture Code-DMC), the combined effect of the wind and the fine fuel moisture (Initial Spreading Index), as well as the so-called accumulation rate (Built Up Index-BUI) that integrates the effect of meteorological variables on fuels with higher size and compacted layers of organic detritus.
2. The National Fire Danger Rate System (NFDRS) is the fire risk assessment method used in the United States. Its very complex structure is classified in hierarchical levels that incorporate the ignition components, based on a model called the BEHAVE for estimation of the fine fuel moisture (Rothermel *et al.,* 1984), as well as the spreading components. Meteorological parameters involved are: relative humidity, 2m-temperature, cloud cover and the speed and direction of 10m-wind as well as the risk of lightning, the duration of the precipitation and the daily extreme values of temperature and relative humidity of the previous day.
3. The system for the evaluation of the fire danger in Australian forests is based on the calculation of the fine fuel moisture content based on the values of temperature, relative humidity and a drought component that integrates rainfall and temperature conditions of the antecedent period. The risk is quantified through a combination of the previous indices with a factor depending on wind conditions (McArthur, 1967).

4. The so-called Fire Potential Index (FPI) was developed in the late 90s as a new way to assess fire risk index. This index, plus the meteorological component or dynamic variable in the short term, integrates a structural component that considers both the short-term weather information for the estimation of the dead fine fuel moisture content and the living vegetation water status, that is obtained through the use of satellite remote sensing data. This index was developed in the United States (Burgan *et al.,* 1998) and has been successfully validated in California.
5. An index based on a simplified adaptation of the model called BEHAVE was operationally used in Spain, until his subsequent replacement in 2011 by the FWI. That index estimated the probability of ignition from the instantaneous values of the relative humidity and the temperature, together with other non-meteorological variables related to topography, time of the year and degree of shading (Velez, 1988). The final risk index value, which was classified in four classes, integrated the components of ignition and propagation and was obtained by a combination of the probability of ignition with the wind speed. The final risk class value was increased in the specific case of foehn winds. Other indices have been developed by AEMET to be applied at regional level, in particular in the cases of the Autonomous Communities of Valencia and Aragon.

3. THE ROLE OF NATIONAL METEOROLOGICAL SERVICES ON FOREST FIRES EARLY WARNING AND FIGHTING

The important collaboration that the national meteorological services can provide to the Agencies with competence in fire prevention and fire fighting relies on its ability to generate real-time estimations and predictions at different time-ranges of the numerical values of fire ignition and fire spreading indexes that are useful to evaluate certain parameters of fire (Mestre, 1996). To generate these estimates, the NMS makes use of real-time data coming from its observation networks, remote-sensed data, outputs from numerical weather models and subjective predictions.

On the other hand, once the forest fire has started, the support of the NMS is essential to estimate the fire spread speed. Especially critical is to provide predictions of the direction and intensity of the winds. These predictions should be made in the adequate spatial and temporal resolution for the scale of the forest fire. The predictions of the probability of precipitation are also needed.

From a wider point of view, a classification of the meteorological support provided, depending on the achieved level of integration, has been developed (Reyfsnaider, 1994). This classification includes three categories ranging from a basic level (level 1), in which the weather service issue predictions and specific warnings for fire-fighting with a format agreed with operational forestry services, up to an advanced level (level 3) that requires that the weather service setup a forestry meteorology specialized department, with the capacity, to move to the forest fire area to provide in-situ support. This unit, equipped with highly specialized staff, as well as mobile units of observation and prediction to work in the field and in permanent contact with Central forecasting services, is responsible for evaluating the foreseen effects of meteorological conditions on fire evolution.

In addition to the aforementioned aspect, the increasing development of products based on remote sensing data opens up a much broader range of collaboration of the Meteorological Services, due to their capacity to develop operationally a set of products (biomass estimation, evaluation of the water status of the vegetation and its flammability level, monitoring of large fires, etc.) and processing a huge amount of data coming from different sources. The great advantage of using remote sensing data comes from its low cost and its high spatial and temporal resolution as well as its capacity to completely covers the territory, making possible to estimate parameters of structure of the vegetation cover in cases when it is very difficult or expensive to make "in situ" measurements. However these techniques should always be validated with terrestrial data before its operational use.

4. SUPPORT PROVIDED BY AEMET ON FOREST FIRES EARLY WARNING AND FIGHTING

AEMET currently provides meteorological support services aimed at prevention and fire fighting to all the forestry services of the Autonomous Communities as well in the General Direction of the Natural Environment and Forestry Policy, to the Civil Protection Directorate and, in general to the set of autonomous agencies with expertise in the field of Civil Protection. This collaboration is provided in the framework defined by the basic guideline for Planning of Civil Protection of forest fire emergencies. This framework sets the general characteristics that must be met by the meteorological information system of the National Plan for Civil Protection in case of emergency by forest fires.

Special bulletins of prediction for fire-fighting purposes were daily generated from 1993 to 2010 for each Spanish Autonomous Communities. These forecasts were made by the corresponding groups of prediction and monitoring of the Delegations of AEMET. This support remained active during the campaign periods established by each community. The bulletins contained a set of predictions for the next day, referred to different weather variables that integrate the risk index for a set of previously defined zones in which each autonomous community has been subdivided. The bulletin also included a prediction of the daily maximum ignition probability. The methodology used for the calculation of this parameter was developed by the former Directorate General of Nature Conservation. The final value of the index of risk, classified in 4 levels (low, moderate, high and extreme) was obtained by the combination of the ignition probability with the wind. A map incorporating the values of the indices provided for each of the areas was also generated daily (Mestre and Cadenas, 1998).

In 2007 AEMET developed a specific project aimed at the improvement of the meteorological fire risk prediction system, and seeking for both an improvement in the index of the system and a further automation of the process. A comparative analysis among the FWI and the previous risk index was carried out using a 10-years data sample of meteorological variables and fire occurrence, over a set of testing areas. The results of this research showed that the risk assessment method based on the FWI index was more appropriate than that used in the previous scheme of calculation, because of the better correlation found between risk index values versus number of fires and total area affected by fires, (Manta, 2003). It

was also proved that the FWI provided a higher economic value as it used as the decisive element in a decision-making scheme (Manta et al, 2006). Another factor that was considered to take the decision to replace the former meteorological risk index by the FWI was the fact that the FWI had been gradually becoming a worldwide reference, being currently used in many countries of our geographical environment. For the operational implementation of the FWI a local celebration of the index was undertaken; thus allowed to attribute, for each geographical area, a class of risk depending on the numerical value of the index (Mestre *et al.,* 2008).

At present, in the framework of the new meteorological support system in the field of forest fires, operating from the fire campaign of 2011 in mainland Spain and the Balearic Islands and in pre-operating state in the Canary Islands, the observed values at 12UTC of the FWI index and that of all its components (FFMC, DCM, DC, ISI, BUI) are generated automatically on a daily basis and throughout the year at the all points of a grid (resolution 0.05º; area /-9.5W/4.3E/35.5S/44.0N) covering the Spanish territory. FWI forecasts on the same grid up to 72 hours in advance are also available. All the variables above mentioned are mapped, being these maps routinely generated and delivered to interested users. The values of the fire classes; classified into five risk strata (low, moderate, high, very high and extreme) are also generated on the same grid already described and the corresponding maps are produced as shown in the example of Figure 5.

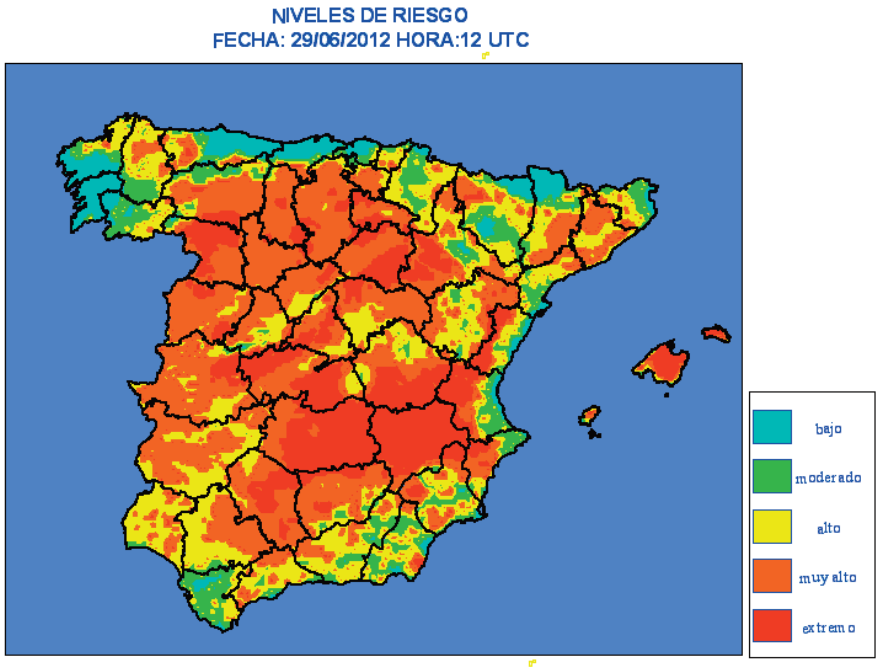

Figure 5. Example of meteorological forest fire risk class analysis based on FWI issued by AEMET.

The index calculations are routinely made at 12 UTC (that is the time of the day with highest risk conditions). Maps of FWI, risk level and of all the meteorological variables involved in the calculations (temperature and relative humidity at 2 m, wind speed at 10 m and daily rainfall) are also issued. The fields of temperature and relative humidity at 2-m and 10-m wind speed, come from the surface analysis at 12 UTC of the short-term numerical prediction weather model HIRLAM 0.05 °, which is currently running at AEMET. The precipitation analysis is made from all the precipitation data available at the automatic weather station network of AEMET. The forecasted values for temperature, relative humidity, wind and precipitation for D+1, comes from the outputs of the high resolution HIRLAM (resolution 0.05 °) numerical weather model, whereas for the forecasts for the D+ 2 and D+3, the outputs of the operational HIRLAM (0.16 ° resolution) are used.

REFERENCES

Burgan, R.E., Klaver, R.W., Klaver, J.M. (1998). Fuel Models and Fire Potential from Satellite and Surface Observations, *International Journal of Wildland Fire,* 8(3), 159-170.

Chuvieco y Martín, eds., (2004). "Nuevas Tecnologías para la estimación del riesgo de incendios forestales". CSIC. Madrid 2004, 187 pp.

Dirección General de Desarrollo Rural y Política Forestal del Ministerio de Agricultura, Alimentación y Medio Ambiente. Los incendios forestales en España en el año 2012 (avance). Madrid. Publicación anual.

Latham, (1983). LLAFS – A lightning-locating and fire-forecasting system. USDA Forest Service, Research Paper INT-315.

Manta, M. (2003). Estudio de la estructura y funcionamiento de dos índices de peligro meteorológico de incendios forestales. Aplicación a tres zonas climáticas de España peninsular, Tesis Ph. D. Escuela Técnica Superior de Ingenieros de Montes. Universidad Politécnica de Madrid. Madrid, España, 329 pp.

Manta, M., Mestre, A. and Viegas, D.X., (2006). Economical value of two meteorological wildfire risk indexes in Spain, *V International Conference on Forest Fire Research D. X*. Viegas (Ed.).

McArthur, (1967). Fire behaviour in eucalyptus forests, *Australia Forestry and Timber Bureau*. Leaflet N 107, 36 pp.

Mestre, A., (1996). El papel de los Servicios Meteorológicos en la prevención de incendios: Influencia decisiva de los factores climáticos. *Revista de Protección Civil*, Núm. 27.

Mestre, A. and Cadenas, I., (1998). "Meteorological support activities in fighting against forest fires in Spain", *Proceedings of the International Symposium on Applied Agrometeorology and Agroclimatology*. European Comission- COST 77, 79 and 710. Ed by N. Dalezios. Luxembourg, 541-548 pp.

Mestre, A., Allúe, M., Peral, C., Santamaría, R. and Lazcano, M., (2008). Operational Fire Danger System in Spain. Operational Fire Danger Rating System in Spain, *International Workshop on Advances in Operational Weather Systems for Fire*

Danger Rating. GOFC-GOLD/WMO. Edmonton (Canada), 14-16 July 2008.

Porrero, M. A., (2001). Incendios forestales. Investigación de causas. Madrid. Ediciones Mundi-Prensa.

Pouliot, L., (1991). Forecasting Fire Weather Indices. Environment Canada, April 1991. Tech. Doc.

Reyfsnaider, W., (1994). Systems for evaluating and predicting the effects of weather and climate of wildlands fires. World Meteorological Organisation. *Special Environment Report Nº 11*. OMM, Ginebra.

Rothermel, R. C., Wilson, R. A., Morris, G. A., Sackett, S. S., (1986). Modelling moisture content of fine dead wildland fuels: input to BEHAVE fire prediction system. USDA Forest Service, *Research Paper INT-359*, Intermountain Research Station, Odgen, Utah, 61 pp..

Van Wagner, C. E., (1987). Development and structure of the Canadian Forest Fire Weather Index System. Canadian Forestry Service, *Technical Report 35*, 37 pp.

Van Wagner, C. E., Pickett, T. L., (1987). Equations and Fortran program for the Canadian Forest Fire Weather Index System. Canadian Forestry Service, *Forestry Technical Report 33*, Ottawa.

Vélez, R., (2000). La defensa contra incendios forestales. Fundamentos y experiencias. Madrid, McGraw-Hill/ Interamericana de España S.A.U.

Vélez, R., (1988). Experimentación de un nuevo sistema para determinar el peligro de incendios de bosques derivado de los combustibles. ICONA. Ministerio de Agricultura, Madrid.

II. RELATED CLIMATOLOGIES

CHAPTER 18

TRENDS OF PRECIPITATION IN SPAIN (1945-2005)

J. Carlos GONZÁLEZ-HIDALGO 1-2 (*), Nicola CORTESI 1-2, Estela NADAL 1-2, Michele BRUNETTI 3, Pter STEPANEK 4, Martín DE LUIS 1-2

(1) Departamento de Geografía, Universidad de Zaragoza. 50009, España (2) IUCA, Universidad de Zaragoza, España (3) Instituto di Scienze dell´Atmosfera e del Clima ISAC-CNR, Bologna, Italia. (4) Hydrometeorological Service, Brno Division, República Checa
(*) e-mail: jcgh@posta.unizar.es

ABSTRACT

The analyses of monthly precipitation trends during 1946-2005 in the conterminous Spain show that monthly trend, except in March and June (negative signal) and October (positive), is not significant. At seasonal scale it is detected a decrease in the spring precipitation percentage and increase in the autumn ones; as a consequence we detected an extended seasonal rainfall change, and total annual precipitation depens more on the beginning of wet period (autumn).

Key words: precipitation; trends, Spain, seasonal rainfall regime.

1. INTRODUCTION

The Mediterranean basin is located in the subtropical transition zone and is characterized by extraordinary natural climate variability (Lionello et al. 2006). The various studies concerning the evolution of precipitation around the Mediterranean basin did not identify any global pattern of its tendencies during the second half of the XX century, although a negative signal was detected, even if without a clear statistical significance (Norrant y Douguédroit, 2006). A small increase during the last years of the past century was discovered by Xoplaki *et al.* (2004), along with changes in the seasonal regimen in the western sector (de Luis *et al*., 2010). Previsions of last IPCC report (AR4) for this area suggest a generalized decrease of mean values in the XXI century and an increase of its variability (Christiansen *et al.* 2007, pp. 874-877).

The uncertainty of these previsions is very high since precipitation is one of the climate variables with the greater spatial and temporal variability and its changes can be detected only using high-density networks with an appropriate temporal coverage (New *et al.*, 2001; Mitchell y Jones, 2005; Auer et al., 2005; Valero *et al.,* 2009). This is particularly true for zones with convective rainfall regimes or with precipitation concentrated in time and/or space, in which case the values recorded in one rain gauge site are representative of a greatly reduced area (Mosmann *et al.,* 2004; del Río *et al.*, 2005). For these reasons, the AR4 report recommends to keep developing datasets with the highest spatial and temporal density for the purpose of the analysis of precipitation at subregional scale (Trenberth *et al.*, 2007).

In the Mediterranean area, the impacts of precipitation changes could have serious consequences in part because of its irregularity, but especially because of its strong demand. Iberian Peninsula could be one of the regions where this situation could be taken to the extreme because of the unrestrained growth of the demand and its spatial concentration. From this perspective, it is not difficult to understand why precipitation has been described as the "most important climate element of Spain, both from a climatic point of view, both because of its availability, given its moderate quantity in the most part of the territory and its high spatial and temporal variability" (de Castro *et al.,* 2006, p. 9).

As already mentioned, the various studies realized on rainfall in peninsular Spain didn't detected any global significant trends at annual, seasonal or monthly time scale (see review in González-Hidalgo *et al.,* 2011). Its extreme variability combined with the high frequency of rainfall anomalies measured since 1984 questioned if the origin of the oscillations was natural or caused by human activity. The lack of evidence of significant tendencies could also be due to differences between methods in conjunction with the lack of a global dataset with an appropriate spatial density and temporal coverage.

In the current work, we present the global conclusions of a research started in 2000 concerning precipitation tendencies in peninsular Spain. Such study was conducted using a dataset with a high spatial resolution, developed by means of an exhaustive analysis of the entire Spanish Agency of Meteorology (AEMET) documentation; in most cases the results presented here, and their most relevant methodological aspects, have been published previously and presented in scientific meetings, so the reader can refer to these quotations for the details.

2. MONTHLY PRECIPITATION DATABASE OF SPAIN. MOPREDAS

AEMET archives stores a huge amount of climatic data, which is part of our common heritage. In the case of precipitation, such funds include information of more than 10000 rain gauges whose level of spatial coverage, except for mountainous areas, is extraordinary. In the Peninsula, the total count is well above 9000; to this number it should be added the stations of the Comunidades Autónomas (Regional Governs) networks, more recent and not always with the expected quality. This information is very variable: time series have different length, gaps, missing data, repetitions, duplications, and metadata are rarely available. Up to now, there are only a few

studies that massively employed this data source (see Cano y Gutiérrez, 2004; Luna y Almarza, 2004; Hernández *et al.,* 1999; Ninyerola *et al.,* 2007; Herrera *et al.,* 2010).

The monthly precipitation database MOPREDAS (MOnthly PREcipitation DAta of Spain) was created applying quality controls followed by the creation of reference series in an iterative way. The quality control consisted in the identification of repeated data within the same station, the identification of repeated series, the identification of anomalous data and inhomogeneous series. The final series were reconstructed with reference series created using nearby series at a distance of 10, 25 and more than 25 km. Finally, the analyzed series during 1946-2005 period were selected as a function of the percentage of original data and reconstructed at different distances; these series were used to create a high resolution grid at 0.1º x 0.1º resolution, considering that the mean distance between the 2670 reconstructed observatories is roughly of 12 km. A detailed explanation of the process can be found in González-Hidalgo *et al.* (2009, 2011).

Trends were analyzed by means of the Mann-Kendall non-parametric test performed on the monthly series, seasonal series and annual ones, and also on the series of the seasonal contribution (in %) to total annual precipitation.

3. RESULTS

During period 1946-2005, MOPREDAS can count on 2670 reconstructed monthly series, free of suspicious data and homogeneous. The series are composed for 69.2% of original data and for 21.7% of data from surrounding stations at a distance less than 10 km; the remainder data (9.1%) belongs to neighbourhood series at a distance greater than 10 km. During period 1931-2005, the total number of reconstructed series drops to 900 and during 1916-2005 to 400. Actually, we are working on the data not still digitalized from the Books of Annual Summaries to fill the gaps in the central and western area before 1946.

MOPREDAS global density during 1946-2005 is of one observatory each 185 km2. Density is approximately constant in each elevation interval up to 1500 m. Finally, a feature that was not usually considered in the most part of the previous studies is that MOPREDAS includes also series in mountain areas. For example, from the total number of Spanish observatories listed by Aupí (2005) for the Peninsula, only 6 are localized above 1000 m, and only 14 above 750 m, although the 57% of Spanish territory is above 600 m and 19% is above 1000 m. MOPREDAS includes data in the 1000-1500 m elevation interval, up to now not well studied and of great interest because of the effect of the Iberian Peninsula on precipitation. Over, although some reconstructions are available in altitude over 1500 m, they have to be considered as simple local info, due to the strong disparity of their distribution.

3.1 Monthly Trends

The analysis of the monthly trends for period 1946-2005 didn't found a global signal or trend in none of the twelve months. Table 1 shows the percentage of land according to the trend signal, and for three different p-values ($p<0.10$, $p<0.05$ y $p<0.01$). If we exclude momentarily the magnitude of the significance, January, February, March, June, August and December present a predominance of the

negative sign; in May and July, roughly half of the territory is affected by the positive sign and half by the negative sign; and in September, October and November the positive sign is predominant (Figure 1). If we consider values of p<0.10, only three months have a significant spatial signal: March and June (negative sign) and October (positive sign).

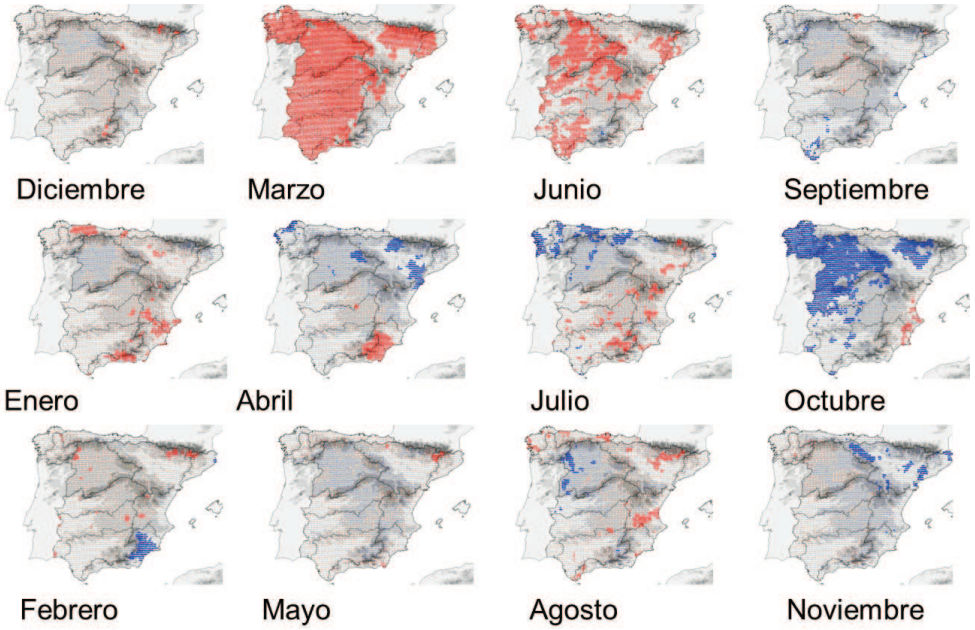

Figure 1. Spatial distribution of onthly precipitation trends. Blue and red color positive and negative trends. Dot size correspond to different probability levels (p<0.01, y p< 0.05, p<0.10, y p>0.10), from González-Hidalgo *et al.* (2011).

MOPREDAS shows that the negative March signal is evident not only in the central and south-westerly sector, but also along some sectors of the Mediterranean coast, as we already highlighted in the previously years (González-Hidalgo *et al.* 2009). Significance in these areas is small except along the left fringe of the Ebro Basin and north-eastern areas, but the pattern is quite clear. This tendency was also

detected for different time periods in Castilla (del Río *et al.,* 2005), western Andalucía (Aguilar *et al.* 2006), Mediterranean coast and Ebro Valley (González-Hidalgo *et al.*, 2009), Portugal and central and southwestern areas (López-Bustins, 2006; Paredes *et al.,* 2006; Trigo y Da Camara, 2000; Norrant y Douguedroit 2005) during different periods between 1920 and 2000, and also for the whole Peninsula between 1921 and 1995 (Serrano *et al.,* 1999b). Moreover, the spring precipitation decrease, although not significant, of part of inland plateau "Meseta" (Galán et al., 1999), Duero basin (del Río *et al.,* 2005) and northeast (Saladié *et al.,* 2002, 2004), can be related to with the March decrease, that seems to be the only clear signal at seasonal scale (de Castro *et al.,* 2006), even if del Río *et al.* (2011) shifts such a

decrease in February, interpreted by Blade and Castro (2010) as an example of how the selection of the period or the number of series can change the results. March precipitation decrease is connected to the observed storm displacement towards north (Paredes *et al.,* 2006) and according to MOPREDAS affects 68% of the territory. Furthermore, it is consistent with the positive insolation trend and with the anticyclonic conditions observed by Sánchez-Lorenzo *et al.* (2007).

Table 1. Precipitation monthly trends. Percentage of land accordingly signal and probability

Trend	p	Jan	Feb	Mar	Ap	May	Jun	Jul	Ag	Sep	Oct	Nov	Dec
Positive	< 0.01	0	0.3	0	0.1	0	0	0.2	0	0	4.4	0	
	< 0.05	0	1.6	0	1.7	0	0	2.2	0.4	0.2	21.4	1.2	0
	< 0.10	0	2.4	0	5	0	0.1	6.1	1.6	1.3	33.7	3.3	0
	+	14.8	17.6	4.4	69.7	44.1	4.3	40.6	34.1	67.9	84.9	68	14.4
Negative	-	85.2	82.4	95.6	30.3	55.9	95.7	59.4	65.9	32.1	15.1	32	85.6
	< 0.10	6.1	1.9	68.9	3.6	0.6	31.8	6.2	5.1	0.3	1.4	0	0.8
	< 0.05	1.9	0.4	57.0	2.8	0.2	16.2	2.2	1.4	0.1	0.1	0	0.2
	< 0.01	0	0.1	23.6	0.9	0	2.0	0.3	0	0	0	0	0

During June the areas with significant tendencies ($p<0.10$) are circumscribed to the interior basins of the Meseta, especially the Duero Basin, the south-eastern part and the left margin of the Ebro Basin to the northeast, but with a lesser spatial continuity than in March. In the same month the affected surface drops to 31.8%, in agreement with the areas signalled between 1961-1990 by Mosmann *et al.* (2004) and del Río *et al.* (2005) during 1961-1997 in the inner of the peninsula and in the south-West. Again, the increase of the anticyclonic condition detected in the interior during 1957-1996 by Fernández and Martín Vide (2004), could justify the global negative tendency found for precipitations during this month, in this case without a clear relationship with the observed insolation (Sánchez-Lorenzo *et al*., 2007).

October situation is opposite to March or June: the positive trend prevails affecting 33% of land ($p<0.10$). Signal is stronger in the north-western quadrant (in agreement with del Río *et al.,* 2005) and central Pyrenees. These positive tendencies have been briefly pointed out by Paredes *et al.* (2006), during 1941-1997 for the whole peninsula, while Norrant and Douguedroit (2006) found Mediterranean areas with positive tendencies between 1951-2000 that we didn't detected. On the other hand, this positive signal agrees with the negative insolation trend (Sánchez-Lorenzo *et al.,* 2007).

In many circumstances, the delimitation of the areas with a homogeneous tendency (significant or not), follow the alignment of the main mountain chains. The mountain chain from the Cantabric range, the Iberian System and the Bethic System, isolate the northern side from the interior, and create a transition from the northern coast up to the Mediterranean coast along the Ebro basin. This transitional characteristic was detected for the first time by Serrano *et al.* (1999a) and more recently by Muñoz

Díaz and Rodrigo (2004), which suggested that the rainfall in the Ebro basin has a typical Mediterranean component, although Mills (1995) linked Ebro Valley with the Duero and Tajo basin, especially during autumn, opinion supported also by Morata *et al.,* (2006). The area to the west of the mountain chain is usually identified as the area under NAO influence (Rodríguez-Puebla *et al.* 1998). The regularity of the entrance of Atlantic weather fronts, along with the relief disposition mainly in the west-east direction (Paredes *et al.,* 2006), suggests that such mountain arch represent a true climatic barrier from the point of view of precipitations trends. Such effect of orography on rainfall tendencies is an agreement with the conclusions of Dünkeloh and Jacobeit (2003) for the Mediterranean basin, and of Sotillo *et al.* (2003) about the spatial distribution of precipitation in the Peninsula. Finally, MOPREDAS allows detecting sectors at sub-regional scale with significant and homogeneous trends in which also the relief seems to be a factor affecting its spatial delimitation.

In conclusion, the spatial distribution of the monthly precipitation trends sometimes depends clearly from the main mountain alignments which divide in space the easily identified sectors. This suggests that the distribution in space of the rainfall trends in the Iberian Peninsula depends both on global factors (such as atmospheric patterns), both on local factors (topography).

3.2 Seasonal Trends

The main results of the analysis of seasonal tendencies are shown in Table 2 and Figure 2 expressed as percentage of land affected. In general term, the signal is negative in winter, spring and summer, and positive in autumn, even if the area with negative trend is small, except during spring season.

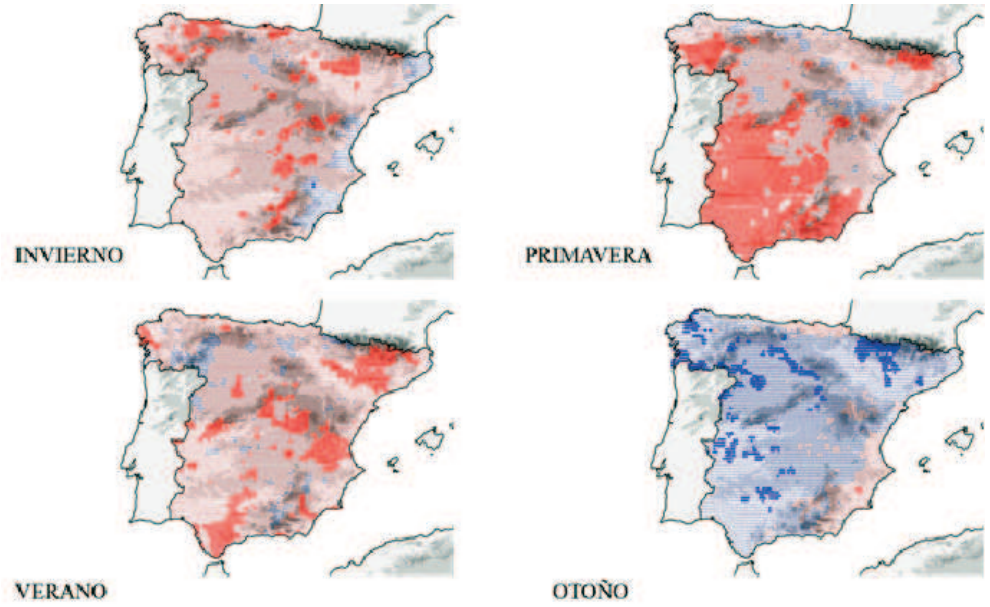

Figure 2. Spatial distribution of seasonal precipitation trends (mm).Legend as Figure 1, from de Luis *et al.* (2010).

Winter precipitation decreased in the peninsular Spain, except along the Mediterranean coast and along some isolated areas in the northern plateau, where signal is positive. Significant negative tendencies ($p<0.10$) affect 10.4% of territory. Spring signal is clearer, almost 40% of land is affected by a negative significant tendency ($p<0.10$). Areas where such a signal is more evident are localized in the south-western quadrant, west of the mountain chain already mentioned. A similar distribution was detected for summer tendencies, although its significant level is lower, and only 17% of territory is affected by negative tendencies ($p<0.10$). In a different way, autumn precipitation trends are mainly positive and significant in approximately 10% of territory, especially the north-western quadrant.

Table 2. Precipitation seasonal trends (A, in mm) and trends of seasonal contribution (B)

		Winter		Spring		Summer		Autumn	
Trend		A	B	A	B	A	B	A	B
Positive	<1%	0.0	0.0	0.0	0.0	0.0	0.0	0.1	6.5
	<5%	0.0	0.0	0.0	0.0	0.0	0.0	3.0	36.0
	<10%	0.1	0.2	0.0	0.0	0.0	0.1	10.0	60.2
	+	8.3	12.8	9.8	18.3	8.1	12.0	88.8	97.4
Negative-	91.7	87.2	90.2	81.7	91.9	88.0	11.2	2.6	
	<10%	10.4	2.7	37.7	17.5	17.4	9.1	0.1	0.0
	<5%	3.1	0.5	25.9	7.9	8.0	3.6	0.0	0.0
	<1%	0.1	0.0	9.6	0.5	1.3	0.7	0.0	0.0

As a consequence, the trends in the yearly percentage of its seasonal contribution have changed (Table 2). In Figure 3 is shown its spatial distribution, being the most noTable observation the decrease of the percent rainfall contribution to total annual precipitation during spring season (in a 17.4% of territory), and to a lesser extend during winter and summer. On the contrary, autumn precipitation raised its percentage over the yearly total, affecting 60.2% of territory, except along the northern coast and the Mediterranean coast. The most clear signal of the increase of such contribution was found in the Ebro basin, Pyrenees, both inland plateaus and in the north-eastern corner. The spring decrease affects especially the south-western quadrant, while the winter decrease is localized in the northern coast, central Pyrenees and along the Iberian and Bethic chains.

The final result during the analyze period has been the decrease, mainly not significant, of the yearly precipitation, affecting less than 10% of peninsular Spain (Figure 4). The most affected areas are localized in the Bethic system, in the first part of Guadiana and Tajo basin, along sectors of the Central System, and sites of the northern fringe, however there isn't a continuous pattern, and the overlapping with areas with weak positive signal is common, especially in the northern peninsular half.

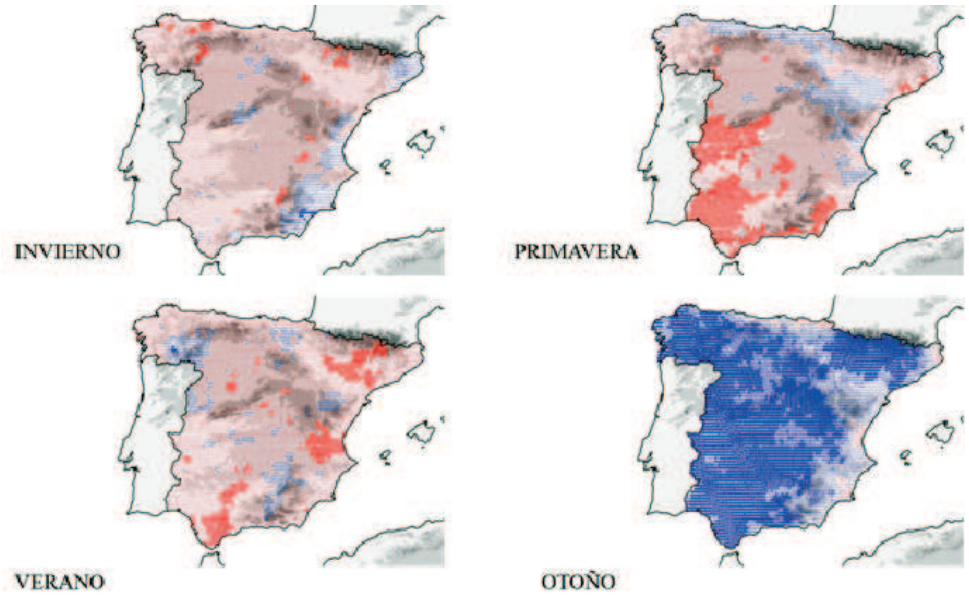

Figure 3. Seasonal contribution trends.Legend as Figure 1, from de Luis *et al.* (2010).

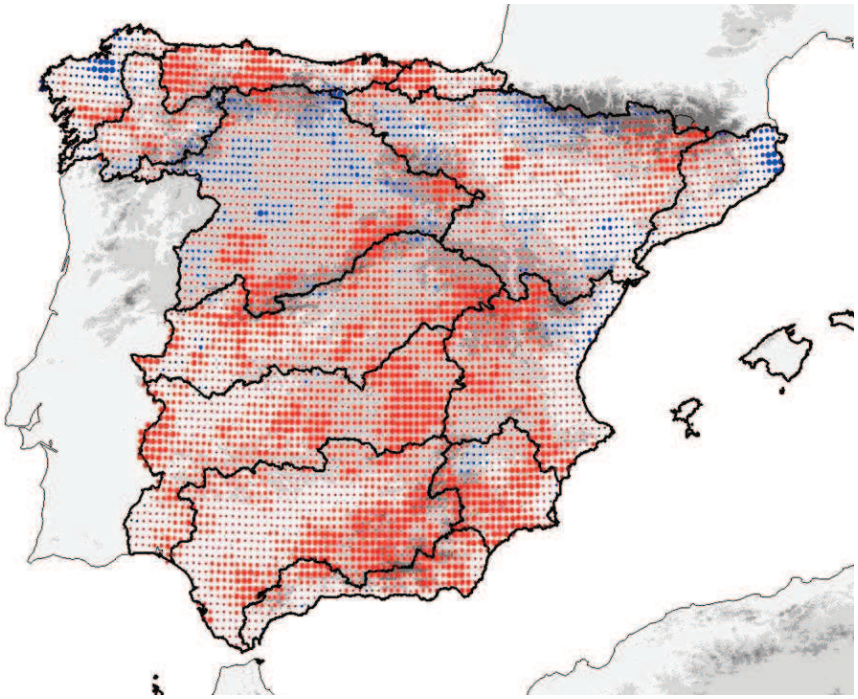

Figure 4. Annual precipitation trends. Legend as in Figure 1.

3.3 Precipitation Regimen

One of the consequences of the observed precipitation behaviour in peninsular Spain has been the change of the seasonal rainfall regimen. This analysis was done comparing the average values for two different 30-years periods included in MOPREDAS.

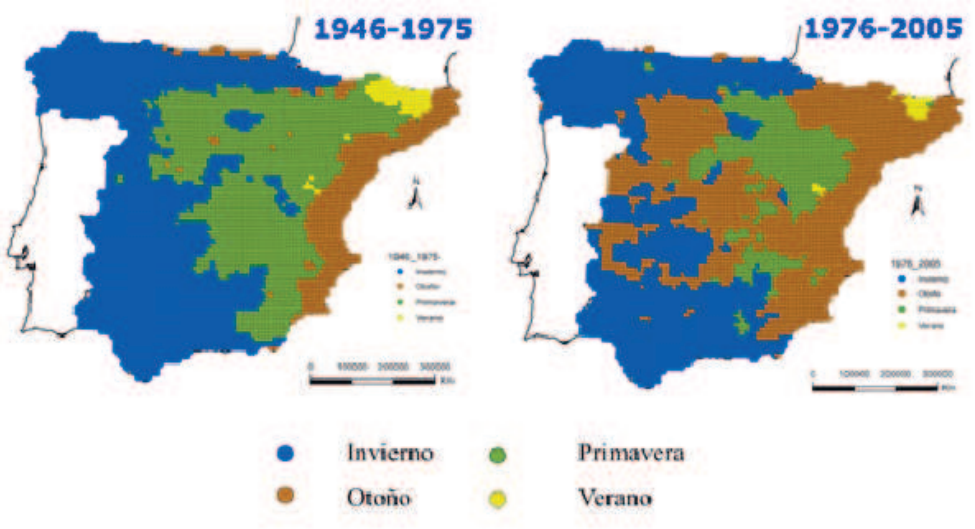

Figure 5. Seasonal precipitation regimes changes between 1946-1975 and 1976-2005, from de Luis *et al.* (2010)

In Figure 5 it is shown the distribution of the seasonal regimen, (season with the maximum), during two periods (1946-1975 and 1976-2005). During the first period, there is predominance in the northern fringe of the winter regimes, in the western sector winter/autumn regimes, and in the eastern sector winter/spring regimes (not shown in Figure). Towards east, spring maximum regimen is typical of large areas surrounding the Ebro Basin, Iberian system and western sectors of the two plateau, with transitions from spring to winter and spring to autumn in the direction W-E. Finally, autumn regimen is localized along the Mediterranean coast, while summer regime dominates along two small sectors of Teruel and eastern Pyrenees.

During the second period (1976-2005), substantial changes were detected that affect not only the dominant season, but also its variation to the regimen (Figure 5). The most interesting alteration is the extension to the west of the autumn regimen and the reduction of the areas with spring regimen. Along with them, we detected also a decrease in the Pyrenees of the area affected by summer regimen and a change from the winter-spring regimen to the winter-autumn regimen towards the western peninsular part of Spain. Lastly, the winter-autumn regimen of the Cantabric Cordillery changed to winter-spring.

Consequently, the surface under a winter regimen decreased from 51.1% to 42.7% in the two periods. The areas with a spring regimen, affecting 36.1% during 1946-

1975, dropped to 15%, which was replaced by the autumn regimen. Finally, the area linked to the autumn regimen raised from a 10.8% of territory, limited to the Mediterranean coast and southern Ebro basin, to 41.4%, expanding in the great extension of the interior, mostly under a spring regimen areas in the first period. The changes in the areas affected by the dominant regimes are shown in Table 3.

Table 3. Variation (in %) of land under seasonal rainfall regimes 1946-1975 (rows) and 1976-2005 (columns)

	Winter	Spring	Summer	Autum
Winter	41.1	0.7	0.0	9.3
Spring	1.2	13.9	0.1	20.8
Summer	0.0	0.1	0.7	1.1
Autumn	0.4	0.3	0.0	10.1

4. GLOBAL CONSIDERATIONS

The analysis of the highest density available up to the present monthly precipitation database for the Peninsular Spain allowed us to detect that during the second half of the XX century, precipitation trends show a global and statistical significant signal only in three months: March and June, with a negative signal, and October, with a positive signal. Moreover, the inspection of the cartographies allows identifying homogeneous areas at sub-regional scale with clear and significant signals that weren't detected until now. Given that the seasonal rainfall values were calculated by aggregation, the tendency is mostly negative during spring, winter and summer, and also at annual scale, while in autumn is mostly positive. Nevertheless, we have to stress that the significance is very low in all seasons except spring and that the areas with significant tendencies are strictly localized in space. Finally, significant tendencies of the seasonal rainfall percentage contribution were detected, affecting wide areas during spring and autumn, as a consequence of the of the spring precipitation decrease, especially in March, and not because of a real increase of the rainfall amount during autumn months.

The distribution of the monthly tendencies is quite complex and cannot be explained only by a single mechanism, given that they seem to mirror the concatenation of global atmospheric factors and local spatially varying effects. Some of the observed tendencies (especially in March) might be related with the NAO behaviour and the changes in the entry direction of Atlantic storms which affect the majority of the south-western Peninsula (Paredes *et al*., 2006); in some other occasions they could be related with the increase of the frequency of cyclonic condition in western Mediterranean during spring and autumn, and with its decrease in spring and winter (Trigo *et al*., 2000; Bartholy *et al*., 2009), or also with the insolation (Sánchez-Lorenzo *et al.,* 2007). On the other hand, the observed distribution of the trend signs clearly reveals that the relief pick out the central-western part of the Peninsula, with a clear Atlantic influence, from the Cantabric litoral areas, Ebro Valley and

Mediterranean eastern coast. As a matter of fact, the latter area is mainly affected by the Mediterranean cyclonic activity with a low persistence, localized in the western Mediterranean sector (Jansá. 2001), which didn't show any changes in the last fifty years (Bartholy *et al.,* 2009). These results globally agree with the recent study of Cortesi et al. (2013) about the relationship between circulation weather types and monthly precipitation, which pointed out that more than 60% of total rainfall amount between October and May over all the central-western peninsula Spain depends on more than 4 weather types, while on the Mediterranean fringe and for the majority of Ebro basin, it usually depends only from one weather type, although greatly varying from month to month and also spatially. The most influent weather types are the South-westerly, Westerly and North-Westerly; their tendencies might be a cause of the abovementioned trends. It is also interesting to highlight how this author points out that not only the Mediterranean fringe and Ebro Valley are far away from the typical Atlantic circulation, but also the Cantabric litoral areas.

The month of October is particularly interesting and up to now hasn't been studied in detail. Generally, the affected area corresponds with the same area highlighted by Serrano *et al.* (1999 a) affected by atmospheric configuration consisting in a low pressure area and centered over the Britannic Isles and characterized by frontal precipitations. Lorenzo *et al.* (2008) suggested that the positive October tendency is correlated with the South-westerly and Westerly weather types, the former being linked to low pressure areas to the west of Ireland and an anticyclonic field over Iberian Peninsula, and the latter characterized by a low pressure area over the north Atlantic and the north Europe and a high pressure area over the Azores, both situations being highly correlated with the East Atlantic Patron, which during the last ten years showed a positive tendency (Lorenzo *et al.,* 2008).

Results show that during the second half of the XX century precipitation in peninsular Spain, instead of change the total rainfall amount, underwent changes in its temporal distribution and in its seasonal regimen, whose effects need still to be analyzed in detail. In general terms, the wet season shortened and the total annual rainfall amount is increasingly affected mostly by the precipitation at the beginning of the wet period. The effects that such alteration to the seasonal regimen could produce are numerous because the seasonal distribution of precipitations has a critical importance on different ecological, economical and social processes (Caramelo y Manso, 2007; Ceballos *et al.,* 2004), for example water resources available for plants during summer (Ceballos *et al.,* 2004), soil erosion caused by the decrease of the vegetal cover for lack of spring water (Thornes 1985; Kirkby and Neale, 1986), the modification of the calendars and the increase of the period of fire risk (Reinhard *et al.,* 2005; Pausas 2004; Carvalho *et al.,* 2008), the modification of the hydrological regimen, river discharge and water availability (Aguado *et al.,* 1992; Paredes *et al.,* 2006; López-Moreno e*t al.,* 2009), of hydroelectric production, (Paredes *et al.*, 2006), etc.

5. CONCLUSIONS

- ✓ The AEMET archives permitted the creation of a high resolution monthly precipitation database during period 1946-2005.

- ✓ At monthly level, precipitation trends exhibits very high variability. The only months with clear and significant spatial patterns are March and June (negative sign) and October (positive sign).
- ✓ The analysis of the seasonal tendencies shows that spring is the only season where the negative signal is clear and significant in broad areas, especially towards the south-western quadrant.
- ✓ Annual tendencies don't show a significant signal, although the negative sign is predominant during the study period. The only areas where the signal is significant are aligned on the mountain arch where the station density is very low, therefore any conclusion must be taken with caution.
- ✓ The main mountain alignments turn into borders in the spatial distribution of monthly precipitation trends.
- ✓ The seasonal precipitation regimen changed too, and in the widespread areas of the central-east the highest percent rainfall contributions in the second half of the XX century have been during autumn, but without increasing in magnitude. Such seasonal change has been caused principally by a spring decrease, mainly due to the March reduction. As a consequence, the duration of the rain period also decreased during 1946-2005, and the dependency from the yearly rainfall amount (in relative terms) from the start of the rain period has increased.

ACKNOWLEDGEMENTS

This research was carried out with the support of the Government of Spain and Feder (projects CGL2011-27574-C02-01, CGL2008-05112-C02-01/CLI, CGL2007-65315-C0301/CLI, CGL2005-04270, REN2003-07453, REN2002-01023-CLI, CLI99-0957), and the regional Government of Aragón and Feder (project P003/2001). Nicola Cortesi has a fellowship of the FPI programme and Estela Nadal is a researcher of the Juan de la Cierva programme, both funded by the Spanish Government. The original data were obtained from the AEMET documental files.

REFERENCES

Aguado E, Cayan D, Riddle L, Roos M (1992). Climatic fluctuations and the timing of West-Coast streamflow. *Journal of Climate,* 5, 1468-1483.

Aguilar M, Sánchez-Rodríguez E, Pita MF (2006). Tendencia de las precipitaciones de marzo en el sur de la Península Ibérica. En Cuadrat JM et al (eds.) *Clima Sociedad y Medio Ambiente.* Publ. AEC, Ser A, 4, 41–51.

Auer I, Böhm R, Jurkovic A, *et al.* (2005). A new instrumental precipitation dataset for greater Alpine region for the period 1800-2002. *International Journal of Climatology*, 25, 139-166.

Aupí V (2005). Guía del clima de España. Omega, Barcelona.

Bartholy J, Pongracz R, Pattanyús-Abraham M (2009). Analyzing the genesis, intensity and tracks of western Mediterranean cyclones. *Theoretical and Applied Climatology,* 96, 133-144.

Bladé I, Castro Y (2010). Tendencias atmosféricas en la península Ibérica durante el periodo instrumental en el contexto de la variabilidad natural. En Pérez F y Boscolo R (eds.) *Clima en España: pasado presente y futuro,* 25-42.

Cano R, Gutiérrez JM (2004). Relleno de lagunas y homogeneización de series de precipitación en redes densas a escala diaria. En J.C. García Cordón et al. (eds.) *El Clima entre el mar y la montaña*. Publ AEC, Serie A, 4, 431-440.

Caramelo L, Manso-Orgaz MD (2007). A study of precipitation variability in the Duero Basin (Iberian Peninsula). I*nternational Journal of Climatology*, 27, 327-339.

Carvalho A, Flannigan MD, Logan K, Miranda AI, Borrego C (2008). Fire activity in Portugal and its relationships to weather and the Canadian Fire Weather Index System. *International Journal of Wildland* Fire, 17, 328-338.

Ceballos A, Martínez J, Luengo MA (2004). Analysis of rainfall trends and dry periods on a pluviometric gradient representative of Mediterranean climate in the Duero Basin, Spain. *Journal of Arid Environment* , 58, 214-232.

Christensen JH, Hewitson B, Busuioc A, *et al.* (2007a). Regional Climate Projections. In Solomon S et al. eds.) *Climate Change (2007) The Physical Science Basi*s. Contribution of Working Group I to the Fourth Assessment Report of the Intergovernmental Panel on Climate Change Cambridge University Press.

Cortesi N, Trigo R, González-Hidalgo JC, Ramos A (2013). High resolution reconstruction of monthly precipitation of Iberian Peninsula using circulation weather types. *Hydrol. Earth Syst. Sci. Discuss*., 9, 1–43. doi:10.5194/hessd-9-1-2012.

De Castro M, Martín-Vide J, Alonso S (2006). El clima de España: pasado, presente y escenarios de clima para el siglo XXI. En: *Impactos del cambio climático en España.* Ministerio Medio Ambiente, Madrid, 64 pág.

de Luis M, Brunetti M, González-Hidalgo JC, Longares LA, Martín-Vide J (2010). Changes in seasonal precipitation in the Iberian Peninsula during 1946-2005. *Global Planetary Changes*, 74, 27-33. doi:10.1016/j.gloplacha.2010.06.006

del Río S, Penas A, Fraile R (2005). Analysis of recent climatic variations in Castile and Leon (Spain). *Atmospheric Research,* 73, 69-85.

del Río S, Herrero L, Fraile R *et al.* (2011). Spatial distribution of recent trends in Spain (1961-2008). *International Journal of Climatology*, 31, 656-667.

Dünkeloh A, Jacobeit J (2003). Circulation dynamics of Mediterranean precipitation variability 1948–1998. *International Journal of Climatology,* 23, 1843-1866.

Fernández AJ, Martín-Vide J (2004). Tendencias de los patrones de circulación estivales en Europa en la segunda mitad del siglo XX. Precipitaciones asociadas en la Península Ibérica. En J.C. García Cordón et al. (eds.) El Clima entre el mar y la montaña, Publ. AEC, Serie A, 273-282.

Galán E, Cañada R, Rasilla D, Fernández F, Cervera B (1999). Evolución de las precipitaciones anuales en la Meseta Meridional durante el siglo XX. En JM Raso y J Martín-Vide (eds.) *La climatología en España en los albores del siglo XXI*. Publ. AEC, Ser A, 169-180.

González-Hidalgo JC, López-Bustins JA, Stepanek P, Martín-Vide J, de Luis M (2009). Monthly precipitation trends on the Mediterranean fringe of the Iberian Peninsula during the second-half of the twentieth century (1951-2000). *International Journal of Climatology*, 29, 1415-1429.

González-Hidalgo JC, Brunetti M, de Luis M (2011). A new tool for monthly precipitation analysis in Spain: MOPREDAS database (Monthly precipitation trends December 1945- November 2005). *International Journal of Climatology,* 31, 715–731.

Hernández A, Quesada V, Valero F (1999). Mapas de autosimilaridad de la precipitación en España en baja frecuencia. En JM Raso y J Martín-Vide (eds.) *La climatología en España en los albores del siglo XXI,* Publ. AEC, Serie A, 1, 253-258.

Herrera S, Gutiérrez JM, Ancell R *et al.* (2012) Development and analysis of a 50-year high resolution daily gridded precipitation dataset over Spain (Spain02). *International Journal of Climatology,* 32, 74-85. DOI 10.1002/joc.2256.

Jansá A, Genovés A, Picornell MA *et al.* (2001). Western Mediterranean cyclones and heavy rain. Part 2: Statistical Approach. *Meteorological. Appl.,* 319, 43-56.

Kirkby MJ, Neale RH (1986). A soil erosion model incorporating seasonal factors. En V Gardiner (ed.) *International Geomorphology* II, 189-210.

Lionello P, Boscoso R, Malanotte-Rizzoli P (2006) (eds.). *Mediterranean Climate Variability.* Elsevier.

López-Bustins JA (2006). Temperatura de la estratosfera polar y precipitación de la Península Ibérica en marzo (1958–2004). En Cuadrat JM et al. (eds.) *Clima Sociedad y Medio Ambiente*. Asociación Española de Climatología, 175–189.

López-Moreno JI, Vicente S, Gimeno L, Nieto R (2009). Stability of the seasonal distribution of precipitation in the Mediterranean region: observations since 1950 and projections for the 21st century. *Geophysical Research Letter,* 36, L10703. doi:10.1029/2009GL037956.

Lorenzo MN, Taboada JJ, Gieno L (2008). Links between circulation weather types and teleconnection patterns and their influence on precipitation patterns on Galicia (NE Spain). *International Journal of Climatology*, 28, 1493-1505.

Luna MY, Almarza C (2004). Interpolation of 1961-2002 daily climatic data in Spain. En *Proceedings of International Meeting on Spatial Interpolation in Climatology and Meteorology,* Budapest, Hungry 2004.

Mills GF (1995). Principal Component Analysis of Precipitation and Rainfall Regionalization in Spain. *Theoretical and Applied Climatology,* 50, 169-183.

Mitchell TD, Jones PD (2005). An improved method of constructing a database of monthly climate observations and associated high-resolution grids. *International Journal of Climatology*, 25, 693-712.

Morata A, Martin ML, Luna MY, *et al.* (2006). Self-similarity patterns of precipitation in the Iberian Peninsula. *Theoretical and Applied Climatology*, 85, 41-59.

Mosmann V, Castro A, Fraile R e*t al.* (2004). Detection of statistically significant trends in the summer precipitation of mainland Spain. *Atmospheric Research*, 70, 43-53.

Muñoz-Díaz D, Rodrigo, FS (2004). Spatio-temporal patterns of seasonal rainfall in Spain (1912-2000) using cluster and principal component analysis: comparison. *Annales Geophysicae*, 22, 1435-1448.

New M, Todd M, Hulme M, Jones P (2001). Precipitation measurements and trends in the twentieth century. *International Journal of Climatology,* 21, 1899-1922.

Ninyerola M, Pons X, Roure UJM (2007). Monthly precipitation mapping of the Iberian Peninsula using spatial interpolation tools implemented in Geographical Information System. *Theoretical and Applied Climatology,* 89, 195-209.

Norrant C, Douguédroit A (2006). Monthly and daily precipitation trends in the Mediterranean (1950–2000). *Theoretical and Applied Climatology*, 83, 89–106.

Paredes D, Trigo RM, Garcia-Herrera R *et al.* (2006). Understanding precipitation changes in Iberia in early spring: Weather typing and storm-tracking approaches. *Journal of Hydrometeorology,* 7, 101-113.

Pausas JG (2004). Changes in fire and climate in the eastern Iberian Peninsula (Mediterranean basin). *Climatic Change,* 63, 337-350.

Reinhard M, Rebetez M, Schlaepfer R (2005). Recent climate change: Re thinking drought in the context of Forest Fire Research in Ticino, South of Switzerland. *Theoretical and Applied Climatology,* 82, 17-25.

Rodríguez-Puebla C, Encinas AH, Nieto S, Garmendia J (1998). Spatial and temporal patterns of annual precipitation variability over the Iberian Peninsula. *International Journal of Climatology,* 18, 299-316.

Saladié O, Brunet M, Aguilar E, Sigró J, López D (2002). Evolución de la precipitación en el sector suroriental de la depresión del Ebro durante la segunda mitad del siglo XX. En J.A. Guijarro et al., *El Agua y el clima,* Publ. AEC, Ser A, 3, 335-346.

Saladié O, Brunet M, Aguilar E, Sigró J, López D (2004). Variaciones y tendencia secular de la precipitación en el sistema Mediterráneo catalán (1901-2000). En JC García Cordón et al. (eds.) *El Clima, entre el mar y la montaña,* Publ. AEC, Ser A, 4, 399-408.

Sánchez-Lorenzo A, Brunetti M, Calbó J, Martín-Vide J (2007). Recent spatial and temporal variability and trends of sunshine duration over the Iberian Peninsula from homogeneized data set. *Journal of Geophysical Research*, 12, D20115, DOI: 10.1029/2007/JD008677.

Serrano A, García JA, Mateos VL *et al.* (1999a). Monthly modes of variation of precipitation over the Iberian peninsula*. Journal of Climate*, 12, 2894-2919.

Serrano A, Mateos VL, García JA (1999b). Trend analysis of monthly precipitation over the Iberian Peninsula for the period 1921-1995. *Physics and Chemistry of the Earth Part B-Hydrology Oceans and Atmosphere*, 24, 85-90.

Sotillo MG, Ramis C, Romero R, Alonso S, Homar V (2003). Role of orography in the spatial distribution of the precipitation over the Spanish Mediterranean zone. *Climate Research* ,23, 247-261.

Thornes JB (1985). The ecology of erosion. *Geography*, 70, 222-235.

Trenberth KE, Jones PD, Ambenje P *et al.* (2007). Observations: Surface and Atmospheric Climate Change. In Solomon S, Qin D, Manning M et al. (eds) *Climate Change 2007: The Physical Science Basis. Contribution of Working Group I to the Fourth Assessment Report of the Intergovernmental Panel on Climate Change*. Cambridge University Press.

Trigo IF, Davies TD, Biggs GR (2000). Decline in Mediterranean rainfall caused by weakening of Mediterranean cyclones. *Geophysical Research Letters,* 27, 2913-2916.

Trigo RM, Da Camara C (2000). Circulation weather types and their influence on the precipitation regime in Portugal. *International* J*ournal of Climatology* ,20, 1559–1581.

Valero F, Martín ML, Sotillo MG *et al.* (2009). Characterization of the autumn Iberian precipitation from long-term datasets: comparison between observed and hindcasted data. *International Journal of Climatology*, 29, 527-541.

Xoplaki E, González-Rouco F, Luterbacher J, Wanner H (2004). Wet season Mediterranean precipitation variability: influence of large scale dynamics and trends. *Climate Dynamics,* 23, 63–78.

CHAPTER 19

SPATIAL AND TEMPORAL EVOLUTION OF PRECIPITATION DROUGHTS IN SPAIN IN THE LAST CENTURY

Sergio M. VICENTE-SERRANO
Instituto Pirenaico de Ecología, Consejo Superior de Investigaciones Científicas (IPE-CSIC), Avda Montañana 1005, 50059 Zaragoza, Spain
svicen@ipe.csic.es

ABSTRACT

This study analyses the evolution of precipitation droughts in Spain considering a long time period (1910-2011). Drought severity has been quantified by means of the Standardized Precipitation Index and drought events identified by means of a threshold approach. The results stress the strong spatial variability of droughts in Spain identifying six regions in which drought evolution has been independent from the other regions. Some regions are showing a decrease of the precipitation drought severity (e.g., Galicia and the Southeast) whereas other regions are showing increased severity (e.g., Southwest, Catalonia and the central Ebro basin). Thus, Southern Spain has shown a large increase of the duration and magnitude of the drought events, which has clearly increased the climate dryness of the region.

Key words: drought, precipitation, Standardized Precipitation Index, spatial variability, climate change.

1. INTRODUCTION

Drought is among the most complex climatic phenomena affecting society and the environment (Wilhite 1993). The root of this complexity is related to the difficulty of quantifying drought severity since we identify a drought by its effects or impacts on different types of systems (agriculture, water resources, ecology, forestry, economy, etc.), but there is not a physical variable we can measure to quantify droughts. Thus, droughts are difficult to pinpoint in time and space since it is very complex to identify the moment when a drought starts and ends and also to quantify its duration, magnitude, and spatial extent (Burton *et al.,* 1978; Wilhite, 2000). Moreover, the effects of a drought can persist many years after it has finished (Changnon and Easterling, 1989; McKee *et al.*, 2002).

Drought is one of the main climatic hazards affecting Mediterranean regions. In Spain, it is a frequent phenomenon due to the high spatial and temporal variability of precipitation. Several studies have identified dry periods that have affected Spain in different centuries (Martín-Vide and Barriendos, 1995; Vicente-Serrano and Cuadrat, 2007; Domínguez-Castro *et al.,* 2012). Droughts have been also frequently recorded in Spain during the period when instruments have been used (Pérez-Cueva, 1983; Pita, 1989; Vicente-Serrano, 2006a).

Usually, the spatial patterns of droughts are very complex in Spain (Vicente-Serrano *et al.,* 2006b). It is very common for one area to suffer dry conditions whilst other, often proximal, areas experience normal or even humid conditions. Such variation is often attributable to complex atmospheric pressure patterns affecting drought in Spain (e.g., Vicente-Serrano, 2005; Vicente-Serrano and López-Moreno, 2006), complicated by the fact that droughts cannot be associated with a single type of atmospheric condition. Together, this makes it difficult to determine areas over which drought histories may be homogeneous.

In Spain, droughts generate important losses in non-irrigated agriculture, and crop yields are severely reduced during dry years (Austin et al., 1998; Iglesias et al., 2003). Moreover, the frequent and severe droughts that affect the semi-arid areas of Spain represent an important factor in environmental degradation (Vicente-Serrano *et al.,* 2012) and also forest growth decrease (Pasho *et al.,* 2011; Martín-Benito et al., 2013). Further, drought reduces the availability of water for vegetation and thereby increases the risk of fires. Furthermore, the increase of irrigated land and urban and tourist growth has produced an important increase in water demands and greater social and economic vulnerability to drought (Morales *et al.,* 2000; Ruiz-Sinoga and Gross, 2013).

This chapter updates and improves previous studies (Vicente-Serrano, 2006a and 2006b) on drought spatial and temporal variability in Spain, using the Standardized Precipitation Index to analyse droughts between 1910 and 2011. The objective is to show the evolution of droughts, to identify important episodes, and to segregate regions according to their drought variability.

2. DATA AND METHODS

2.1 Data

For drought analysis, 42 precipitation series covering the period between 1910 and 2011 were used, obtained from the Spanish Meteorological Agency (Agencia Estatal de Meteorología). Some series were created by combining data from different observatories within the same locality. This was necessary due to the frequent location changes of Spanish, observatories during the 20th century. Data was checked by means of a quality control process which identified anomalous records (ANCLIM program, Stepanek, 2003). To guarantee the final quality of the precipitation series, the homogeneity of each one was checked (Peterson et al., 1998) against an independent reference series generated by selecting the five series whose difference series correlated best with difference series in question (Peterson and Easterling, 1994). The Standard Normal Homogeneity Test was used (SNHT,

Alexandersson, 1986). The few non-homogeneous series identified were corrected and temporal gaps were completed using linear regressions with respective reference series. The spatial distribution of the series is shown in Figure 1, in which the homogeneous spatial distribution over Spain can be observed.

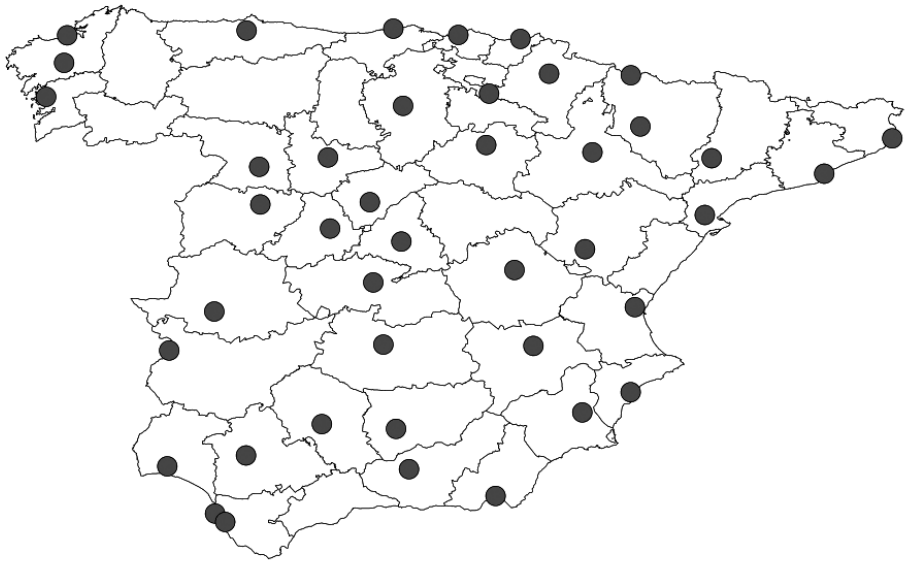

Figure 1. Spatial distribution of the precipitation series used in Spain (1910-2011).

2.2 Drought quantification

Droughts are apparent after a long period without precipitation, but it is difficult to determine their onset, extent and end. Thus, it is very difficult to objectively quantify their characteristics in terms of intensity, magnitude, duration and spatial extent. For this reason, much effort has been devoted to developing techniques for drought analysis and monitoring. Different indices have been developed for the analysis and monitoring of drought (Heim, 2002).

It is commonly accepted that drought is a multi-scalar phenomenon (McKee *et al.,* 1993). Thus, the time scale over which water deficits accumulate becomes extremely important, and functionally separates hydrological, environmental, agricultural and other droughts. For this reason, drought indices must be associated with a specific timescale to be useful for monitoring and management different usable water resources. This explains the wide acceptance of the Standardized Precipitation Index (SPI), which is comparable in time and space, and can be calculated at different time scales to monitor droughts with respect to different usable water resources. Recently, the SPI has been accepted by the World Meteorological Organization as the reference drought index. In the "Lincoln Declaration on Drought Indices," 54 experts from all regions of the world agreed

on the use of a universal meteorological drought index for more effective drought monitoring and climate risk management. They made the significant consensus agreement that the Standardized Precipitation Index (SPI) should be used by national meteorological and hydrological services worldwide to characterize meteorological droughts (Hayes *et al.,* 2011).

The SPI was developed by McKee e*t al.* (1993 and 1995) to identify non-normal dry and humid periods. The SPI is based on the conversion of the precipitation data to probabilities based on long-term precipitation records computed on different time scales. Probabilities are transformed to standardized series with an average of 0 and a standard deviation of 1. The main advantage of the SPI as compared with the Palmer indices is that the former allows analyzing drought impacts at different temporal scales while the latter does not. McKee *et al.* (1993) used the Gamma distribution to transform precipitation series to standardized units. Nevertheless, the frequency distributions of the precipitation series show significant changes that depended on the time scale (Vicente-Serrano 2006b). Among the different evaluated models, the Pearson III shows enhanced adaptability to precipitation series at different time scales (Guttman 1999; Vicente-Serrano 2006b; Quiring 2009). Therefore, here we use the algorithm described by Vicente-Serrano (2006b) to calculate SPI values based on the Pearson III distribution and the L-moments approach to obtain the distribution parameters. As a general measure of the drought conditions, the 12-month SPI time-scale has been calculated in each one of the 42 precipitation observatories between 1910 and 2011.

2.3 Analysis

Previous studies describe a highly diverse spatial precipitation pattern in the Iberian Peninsula: several regions with markedly distinct pluviometric regimes (e.g., Rodríguez-Puebla *et al.,* 1998). For this reason, a spatio-temporal analysis was applied to the 12-month SPI series in order to retain the general temporal and spatial patterns of drought. The analysis was based on a principal component analysis (PCA). PCA has been widely used to determine the general temporal and spatial patterns of climatic variables. It allows common features to be identified and specific local characteristics to be determined. We have used a S-mode PCA to obtain the general temporal patterns of drought in Spain. Since the SPI corresponds to a standardized variable, the obtained PCA series can be associated to the SPI variability of a region. The areas represented by each mode (component) were identified by mapping the factorial loadings. The number of components was selected in accordance with the criteria of an eigenvalue larger than 1, and the components were rotated (Varimax) to redistribute the final explained variance and to obtain more stable, physically robust patterns (Richman, 1986).

The changes in precipitation drought during the long 1911-2011 period have been assessed by means of two different procedures. On the one hand, the magnitude of the SPI changes have been quantified by means of regression analysis between the series of time (independent variable) and the SPI series (dependent variable). The slope of the regression models indicated the change (SPI change per year), with greater slope values coinciding with greater change. The change has been analyzed in three different periods: 1911-2011, 1940-2011 and 1970-2011 to

determine a possible accentuation or decrease in the drought severity. On the other hand, we have focused on independent drought events by means of a threshold level that does not vary in time and space. The threshold level was set up at the 10% of cumulative probability (SPI <−1.28, given the standardized characteristic of the variable), and a drought event was thus registered when the monthly SPI fell below that level (van Loon *et al.,* 2010). Based on this threshold, precipitation droughts were characterized using drought duration and drought magnitude. The duration of a given drought event was defined as the consecutive and uninterrupted time steps (one or more months) with an observed SPI below –1.28. Drought is the accumulated deficit volume defined as the sum of the deficit volumes generated during an uninterrupted number of months, delimiting a drought event expressed as accumulated deficits of the SPI.

3. RESULTS

Table 1 shows the results of the PCA applied to the 12-month SPI series of Spain. The first component represents the main percentage of the total variance (24%). The components 2 to 6 represents very similar percentages (between 7.3 and 10.3%), showing an abrupt decrease between the component 6 and 7, which only represents the 2.8% of the total variance. Therefore, for further analysis we have selected the first six components, which represent a 68.8% of the total temporal variability of the 12-month SPI series across Spain.

Component	Total	% of the variance	Cummulative %
C. 1	10.454	24.891	24.891
C. 2	4.352	10.363	35.253
C. 3	3.828	9.115	44.368
C. 4	3.714	8.843	53.211
C. 5	3.491	8.311	61.522
C. 6	3.081	7.336	68.858
C. 7	1.187	2.826	71.684

Table 1. Results of the principal component analysis applied to the SPI series of Spain.

Figure 2 shows the temporal variability of the six components and Figure 3 shows the spatial distribution of the PCA loadings, which inform on the regions represented by each component. The pattern is very robust spatially. Component 1 represents the main percentage of Spain, covering the Southwest and central areas. Component 2 represents the observatories closed to the Bay of Biscay. Component 3 represents the extreme Northwest of Spain. The component 4 shows high loadings in some observatories of the Northern plateau. Components 5 and 6 represent the Northern and southern Mediterranean areas. The regionalization according to the variability of precipitation droughts stresses the

strong spatial variability of droughts in Spain and the very different temporal variability observed in each area.

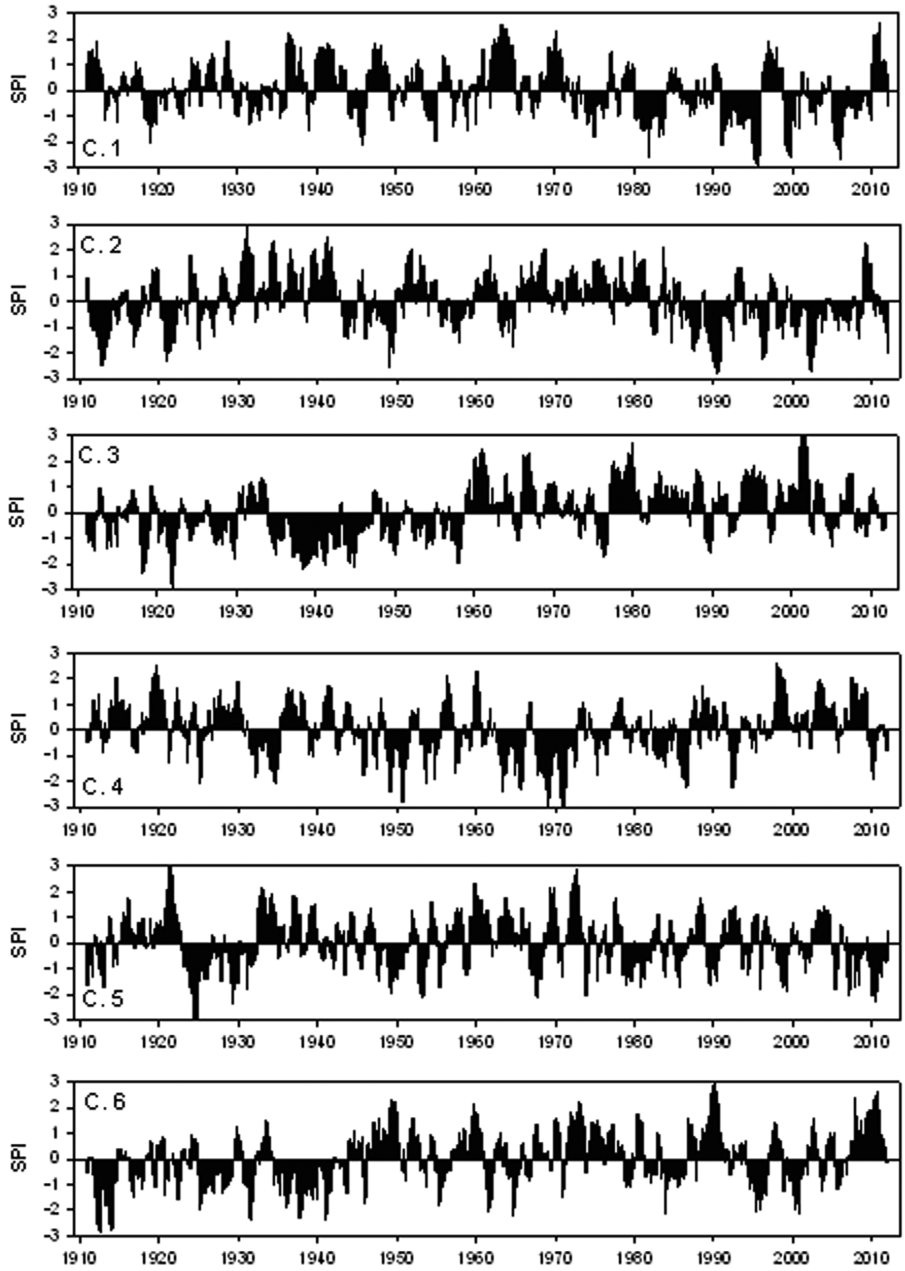

Figure 2. Temporal evolution of the SPI series corresponding to the six extracted components.

Areas represented by component 1 show the main drought episodes recorded since the decade of 1970. Thus, the two main droughts were recorded in the last two decades (1991-1995 and 2005-2009). Component 2 shows strong droughts in the decades of 1910, 1920, 1940 and also from 1980 to the present. The two main droughts were recorded in 1990 and 2002. Component 3 shows very different pattern. The areas of Galicia represented by this component show dominant drought periods between 1910 and 1960, whereas humid conditions are the dominant between 1960 and 2011. Areas represented by Component 4 (Northern plateau) also diverge noticeably with previous patterns since the main drought episodes were recorded around 1950 and between 1965 and 1972. In opposition to the neighbor areas represented by component 1, decades of 1990 and 2000 have been dominantly humid. Component 5 (main part Catalonia and the central Ebro basin) show the strongest drought episodes in the decade of 1920 and 2000, and the last years (2006-2011) were affected by severe drought conditions. Finally, component 6 shows a pattern that mostly resembles Component 3 since the main drought episodes are identified in the first two decades of the twentieth century and, with the exception of some periods of the 1900's and 2000's, the period between 1960 and 2011 has been dominated by humid conditions.

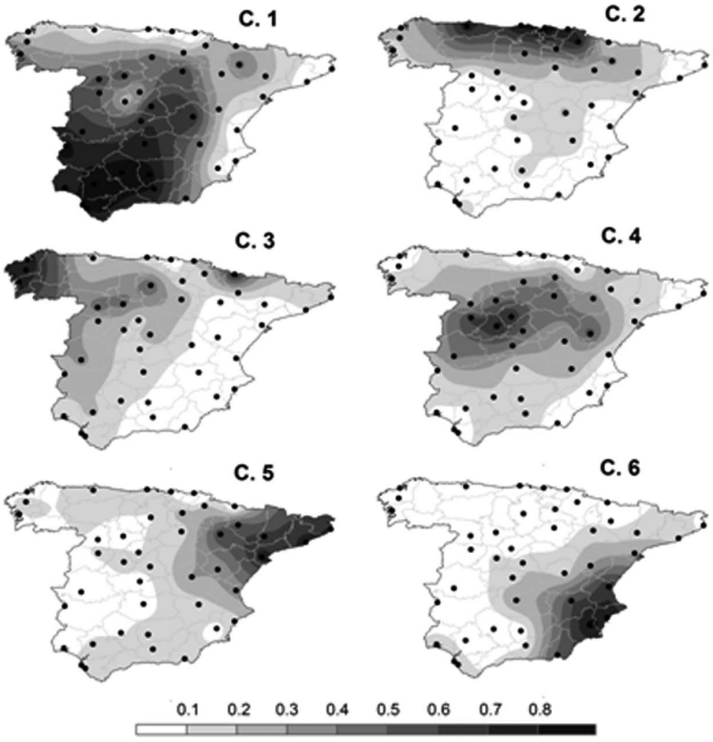

Figure 3. Spatial distribution of Principal Component loadings for the six principal components.

The analysis of the SPI changes observed in the last decades also stresses the strong spatial variability observed with the PCA. The magnitude of the changes in the SPI observed in each one of the 42 available observatories is shown for three different periods (Figure 4). Between 1910 and 2011 the changes are in general small (between -0.1 and 0.09 SPI units decade-1). The observatory showing the strongest increase is Santiago de Compostela and the strongest decrease is Jaén. In any case, considering the complete period of records, there is strong spatial variability, even some neighbor observatories are showing opposite changes (positive or negative). In any case, the majority of observatories located in Andalucía are showing negative changes (intensification of drought severity), whereas observatories located in Northwest and southeast are showing a dominant positive pattern. The behavior identified for the 1940-2011 period shows dominant negative SPI changes over most Spain. A strong decrease (<-0.15 decade-1) is observed in Jaén, Cuenca, San Fernando, Huesca and Bilbao. With the exception of the Valencia observatory, all the observatories located in the South and eastern areas show negative SPI changes. In the Northwestern half of Spain the pattern is also showing observatories with positive changes, some of them very strong (Ávila, Canfranc and Santiago de Compostela). Therefore, although showing some spatial differences, the dominant pattern since 1940 is reinforcing drought conditions in most Spain. In some of these areas, the strongest SPI changes have been recorded between 1970 and 2011, mainly in northeast (e.g., Barcelona, Huesca, Pamplona).

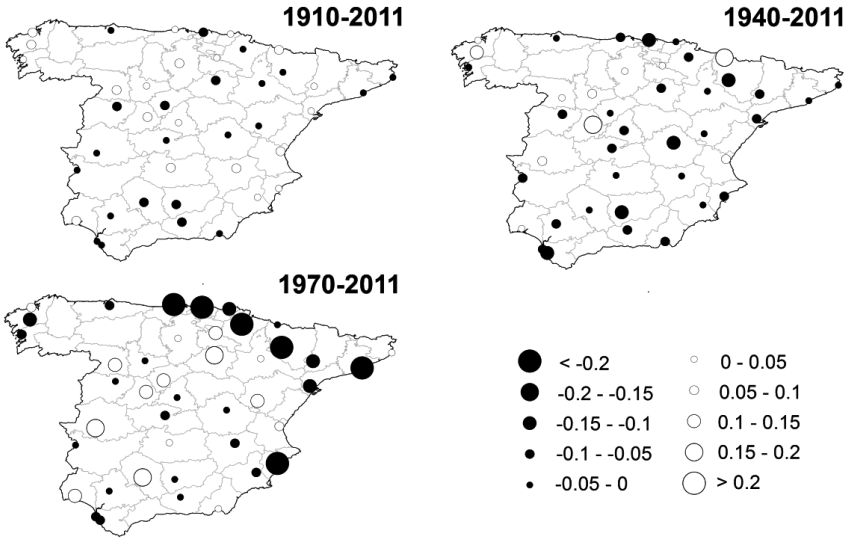

Figure 4. Spatial distribution of the magnitude of change of SPI values (in SPI units decade-1) between three different periods (1910-2011, 1940-2011 and 1970-2011).

The variability of the independent drought episodes has been analysed by means of the series of the six Principal Components obtained previously. Figure 5 shows the average drought duration (in months) and magnitude (in SPI units) observed

in the regions represented by each one of the six principal components in three different periods (1910-1940, 1940-1970 and 1970-2011). Areas represented by component 1 have showed higher frequency of drought episodes for 1970-2011 (18) in relation to previous decades: 4 and 6 for 1910-1940 and 1940-1970, respectively. In addition, the average duration and magnitude and the occurrence of extreme drought episodes have been much stronger between 1970 and 2011 than in previous periods. Component 2 also shows higher frequency of drought events between 1970 and 2011. Nevertheless, the average magnitude and duration is closer to that observed between 1910 and 1940. In this region (North Spain), decades between 1970 and 2011 showed drought episodes characterized by lower duration and magnitude. Component 3 shows that although the number of drought events was similar in the periods of 1910-1940 and 1940-1970 the average drought duration and magnitude, and the occurrence of extreme drought events was much stronger between 1940 and 1970. Between 1970 and 2011 only three drought episodes were recorded, with low average duration and magnitude. In areas represented by Component 4 (Northern plateau) there are few differences in the average drought duration and magnitude between the three analysed periods, although the highest frequency and the most extreme events were recorded between 1940 and 1970. In Catalonia and the central Ebro basin (Component 5), there are very few differences in the average duration and magnitude of the drought events between the three analysed periods. Nevertheless, there is a clear reinforcement in the frequency of the drought episodes during the last decades (24 between 1970 and 2011), although the most extreme drought event, both in duration and magnitude, was recorded between 1910 and 1940. Southeast of Spain (Component 6) also shows few differences in the average duration and magnitude of the drought events between 1910 and 2011, but much higher frequency of events was recorded between 1910 and 1940, and this period also showed the most extreme drought events.

4. DISCUSION AND CONCLUSIONS

The results of this chapter have stressed the strong spatial variability of precipitation droughts in Spain recorded between 1910 and 2011. Thus, a drought episode can be restricted to concrete areas without the whole of Spain being affected. We frequently observed humid or normal conditions in one region whilst another suffered drought over the same period. Examples highlighting individual droughts demonstrated they are sometimes local phenomena and, with the exception of the most intense episodes, are usually regional. Moreover, even the most important drought episodes did not affect the entirety of Spain.

Six different patterns of drought evolution have been isolated using Principal Component Analysis. Each pattern applied to a distinct area, showing internal homogeneity and with well-defined boundaries (southwest, north, northwest, North plateau, northeast and southeast). Among these regions, transition areas can be identified on the borders between the areas. This introduces a higher spatial diversity and complexity in drought behaviour and also a higher uncertainty in drought evolution in these areas than in well-defined sectors.

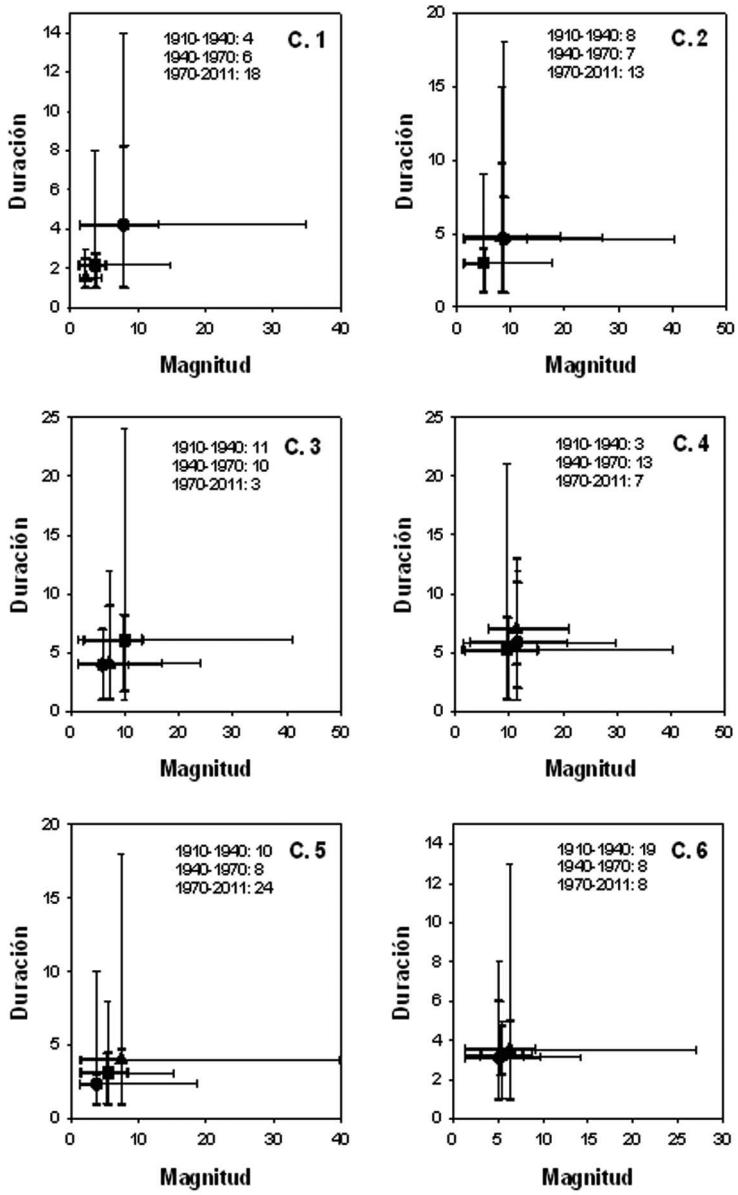

Figure 5. Drought duration and magnitude in three different periods (1910-1940, 1940-1970 and 1970-2011) for each one of the six Principal Components. Triangles: 1910-1940, Squares: 1940-1970, Circles: 1970-2011. The symbols represent the average duration and magnitude for each one of the three periods. Bold lines represent the 25th and 75th percentiles and thin lines the maximum and minimum values. The drought events recorded in each period are showed by numbers.

This study has showed how drought frequency, duration and magnitude have increased in the last decades in large parts of Spain based only on precipitation records. The series of the SPI have dominantly declined in large areas of Spain (Northeast, South and central areas) showing more severe drought events in the last three decades characterized by longer duration and magnitude than in previous decades. These areas correspond to major surface area in Spain, which indicate that precipitation drought severity may be increasing in average, although some regions are showing lower drought severity. Moreover, there is another factor, not analyzed in this study, which may affect the increased drought severity in Spain since the SPI does not consider other variables that can influence droughts, mainly the evaporative demand by the atmosphere.

The role of warming-induced drought stress is evident in recent studies that have analysed drought impacts on net primary production and tree mortality (e.g., Anderegg *et al.,* 2012). The strong role of temperatures on the drought severity was evident in the devasting 2003 central European heat wave, in which extreme high temperatures dramatically increased evapotranspiration and exacerbated summer drought stress, drastically reducing Aboveground Net Primary Production (ANPP) (Ciais *et al.,* 2005). Thus, to illustrate how warming processes are reinforcing drought stress and related ecological impacts worldwide, Breshears *et al.* (2005) enunciated the term global-change-type drought to refer to drought reinforcement under global warming conditions. Under this scenario the increased potential evpotranspiration in Spain (Vicente-Serrano *et al.,* 2013) may increase climate aridity since the soil water availability cannot supply the increased atmospheric demand. For these reasons other more robust drought indices may be used in the future to analyse drought evolution in Spain, mainly the recently developed Standardized Precipitation Evapotranspiration Index (SPEI) (Vicente-Serrano *et al.*, 2010), which includes the role of temperature on drought severity by means of its influence on the atmospheric evaporative demand, hence improving the performance of previous drought indices based on precipitation data alone when determining the drought impacts on different hydrological and ecological systems at the global scale (Vicente-Serrano *et al.*, 2011 and 2012b).

ACKNOWLEDGEMENTS

We would like to thank the Spanish State Meteorological Agency (AEMET) for providing the database used in this study. This work has been supported by the research projects CGL2011-27574-CO2-02 and CGL2011-27536 financed by the Spanish Commission of Science and Technology and FEDER, "Efecto de los escenarios de cambio climático sobre la hidrología superficial y la gestión de embalses del Pirineo Aragonés" financed by "Obra Social La Caixa" and the Aragón Government and Influencia del cambio climático en el turismo de nieve, CTTP01/10, Financed by the Comisión de Trabajo de los Pirineos.

REFERENCES

Alexandersson, H., (1986). A homogeneity test applied to precipitation data, *Journal of Climatology,* 6, 661-675.

Anderegg W.R.L. *et al.,* (2012). The roles of hydraulic and carbon stress in a widespread climate-induced forest die-off, *Proc Natl Acad* Sci USA, 109, 233–237.

Austin, R. B., Cantero-Martínez, C., Arrúe, J. L., Playán, E., y Cano-Marcellán, P., (1998). Yield–rainfall relationships in cereal cropping systems in the Ebro River valley of Spain, European *Journal of Agronomy,* 8, 239–248.

Breshears, D.D., *et al.* (2005). "Regional vegetation die-off in response to global-change type drought", *Proceedings of the Natural Academy of Sciences of the USA,* 102, 15144–15148.

Burton, I., Kates, R.W. and White, G.F. (1978). The Environment as Hazard. Oxford University Press, 240 pp.

Changnon, S. A. y Easterling, W. E. (1989). Measuring drought impacts: the Illinois case, *Water Resources Bulletin*, 25, 27–42.

Ciais Ph, et al. (2005) Europe-wide reduction in primary productivity caused by the heat and drought in 2003, *Nature,* 437, 529–533.

Domínguez-Castro, F., Ribera, P., García-Herrera, R., Vaquero, J.M., Barriendos, M., Cuadrat, J.M. and Moreno, J.M., (2012). Assessing extreme droughts in Spain during 1750-1850 from rogation ceremonies, *Climate of the Past*, 8, 705-722.

Guttman, N.B. (1999). Accepting the standardized precipitation index: A calculation algorithm, *J. Amer. Water Resour*., Assoc., 35, 311–322.

Hayes, M., Svoboda, M., Wall, N. and Widhalm, M. (2011). The Lincoln declaration on drought indices: Universal meteorological drought index recommended, B*ull. Amer. Meteor*. Soc., 92, 485–488.

Heim, R. R., (2002). A review of twentieth-century drought indices used in the United States, *Bull. Amer. Meteor.* Soc., 83, 1149–1165.

Iglesias, E., Garrido, A. y Gomez-Ramos, A., (2003). Evaluation of drought management in irrigated areas, *Agricultural Economics,* 29, 211–229.

Martin-Benito, D., Beeckman, H., and Cañellas, I. (2013). Influence of drought on tree rings and tracheid features of Pinus nigra and Pinus sylvestris in a mesic Mediterranean forest, European *Journal of Forest Research*, 132, 33-45.

Martín-Vide, J. and Barriendos, M., (1995). The use of rogation ceremony records in climatic reconstruction: a case study from Catalonia (Spain), C*limatic Change*, 30, 201–221

McKee, T. B. N., Doesken, J. and Kleist, J. (1993). "The relationship of drought frequency and duration to time scales", Proc. Eight Conf. on Applied Climatology, Anaheim, CA, Amer. Meteor. Soc. 179–184.

Morales, A., Olcina, J. y Rico, A. M., (2000). Diferentes percepciones de la sequía en España: adaptación, catastrofismo e intentos de corrección, *Investigaciones Geográficas*, 23, 5–46.

Pasho, E., Camarero, J.J., de Luis, M. and Vicente-Serrano, S.M. (2011). Impacts of drought at different time scales on forest growth across a wide climatic gradient in north-eastern Spain, *Agricultural and Forest Meteorology*, 151, 1800-1811.

Pérez-Cueva, A. (1983). La sequía de 1978–1982, ¿excepcionalidad o inadaptación?, *Agricultura y Sociedad,* 27, 225–245.

Peterson, T.C., and Easterling, D.R., (1994). Creation of homogeneous composite climatological reference series, *International Journal of Climatology,* 14, 671-679.

Peterson, T.C., Easterling, D.R., Karl, T.R. *et al.,* (1998). Homogeneity adjustments of in situ atmospheric climate data: a review, *International Journal of Climatology*, 18, 1493-1517.

Pita, M.F., (1989). La sequía como desastre natural. Su incidencia en el ámbito español, *Norba,* 6–7, 31-61.

Quiring, S. M. (2009). Developing objective operational definitions for monitoring drought, *J. Appl. Meteor. Climatol.,* 48, 1217–1229.

Richman, M. B. (1986), Rotation of principal components, J*. Climato*l., 6, pp. 29– 35.

Rodríguez-Puebla, C., Encinas, A.H., Nieto, S. y Garmendia, J. (1998). Spatial and temporal patterns of annual precipitation variability over the Iberian Peninsula, *International Journal of Climatology*, 18, 299–316.

Ruiz Sinoga, J.D. y León Gross, T. (2013). Droughts and their social perception in the mass media (southern Spain), *International Journal of Climatology*, 33, 709-724.

Stepánek, P., (2004). AnClim – Software for Time Series Analysis (for Windows), Dept. of Geography, Fac. of Natural Sciences, MU, Brno. 1.47 MB.

van Loon, A. F., van Lanen, H. A. J., Hisdal, H., Tallaksen, L.M., Fendekov´a, M., Oosterwijk, J., Horvát, O., y Machlica, A. (2010). Understanding hydrological winter drought in Europe, IAHS Publ., 340, Wallingford, UK.

Vicente-Serrano, S.M., (2005). El Niño and La Niña influence on drought conditions at different time scales in the Iberian Peninsula, *Water Resources Research*, 41, W12415, doi:10.1029/2004WR003908.

Vicente-Serrano, S.M., (2006a). Spatial and temporal analysis of droughts in the Iberian Peninsula (1910-2000), *Hydrological Sciences Journal*, 51, 83-97.

Vicente-Serrano, S.M., (2006b). Differences in spatial patterns of drought on different time scales: an analysis of the Iberian Peninsula, *Water Resources Management,* 20, 37-60.

Vicente Serrano, S.M. y López-Moreno, J.I., (2006). The influence of atmospheric circulation at different spatial scales on winter drought variability through a semiarid climatic gradient in north east Spain, *International Journal of Climatology*, 26, 1427-1456.

Vicente-Serrano, S.M. y Cuadrat, J.M., (2007). North Atlantic Oscillation control of droughts in Northeast of Spain: evaluation since A.D. 1600, *Climatic Change,* 85, 357-379.

Vicente-Serrano S.M., Beguería, S. y López-Moreno, J.I., (2010). A Multi-scalar drought index sensitive to global warming: The Standardized Precipitation Evapotranspiration Index – SPEI, *Journal of Climate,* 23, 1696-1718.

Vicente-Serrano, S.M., Beguería, S. y López-Moreno, J.I., (2011). Comment on "Characteristics and trends in various forms of the Palmer Drought Severity Index (PDSI) during 1900-2008" by A. Dai, *Journal of Geophysical Research-Atmosphere,* 116, D19112, doi:10.1029/2011JD016410

Vicente-Serrano, S.M., Zouber, A., Lasanta, T. y Pueyo, Y., (2012). Dryness is accelerating degradation of vulnerable shrublands in semiarid Mediterranean environments, *Ecological Monographs,* 82, 407-428.

Vicente-Serrano, S.M. *et al.,* (2012). Performance of drought índices for ecological, agricultural and hydrological applications, *Earth Interactions*, 16, 1–27.

Vicente-Serrano, S.M. *et al.,* (2013). Reference evapotranspiration variability and trends in Spain (1961-2011). Under review.

Wilhite, D.A., (1993). Drought Assessment, Management and Planning: Theory and Case Studies. Kluwer, 293 pp.

Wilhite, D.A., (2000). "Drought as a natural hazard: Concepts and definitions." in Drought: A Global Assessment, D. Wilhite, Ed., Vol. 1, Taylor and Francis, 3–18.

CHAPTER 20

TEMPERATURE TRENDS

José Antonio GUIJARRO

Spanish State Meteorological Agency (AEMET), Balearic Islands Office, Spain
jguijarrop@aemet.es

ABSTRACT

Mean maximum and minimum monthly temperatures have been collected for all stations of Spain with at least 10 years of observations during the period 1951-2012. 2856 series were compiled in total, which were homogenized with the R package "Climatol". Trends of the homogenized series were computed by linear regression with time, whose greater positive values were obtained in summer and spring, but with differing patterns in the main hydrological basins. Maximum temperature trends were negative in the Canary Islands only. Geographical distribution of trends and dependence with altitude have been studied, the higher trends corresponding to the eastern third of the Iberian peninsula and Tajo river basin.

Key words: homogenization, Spanish temperature series, trends, DTR.

1. INTRODUCTION

Temperature is the most studied variable in the current concern about the outcomes of the continuous rise of CO_2 in the atmosphere, since a higher concentration of a gas transparent to short wave radiation but absorbing important portions in long wave bands implies an increment of the energy retained by the atmosphere (greenhouse effect) that must end in an increase of the mean temperature of our planet, although this heating can vary significantly depending on the geographical areas.

The Spanish thermometric series have already been studied by different authors, either on the whole country (Brunet *et al.,* 2007; Moratiel *et al.,* 2010; del Río *et al.,* 2011 y 2012) or focusing on specific areas (Piñol *et al.,* 1998; Serra *et al.,* 2001; Morales *et al.,* 2005; del Río *et al.,* 2005 y 2007; Martínez *et al.,* 2010; Homar *et al.,* 2010; Moratiel *et al.,* 2011; Martín *et al.,* 2012). But the heterogeneity of these studies is not limited to the application area, since they differ in the density of stations and the period covering the series as well as in the quality control and

homogeneity applied to them, making it difficult to compare their results. for this reason, and because in any case the series are getting longer over the years, the approach chosen here is to update the study of Spanish thermometric series, covering a common period and comprising a large number of observing stations. The methodology used and the results obtained will be presented and discussed in the following sections.

2. METHODOLOGY

In order to have a wide spatial representation, the study involved all series of monthly average maximum and minimum temperature that had a minimum of 10 years of observation during the period 1951-2012. 2856 series met this condition, whose distribution by major watersheds can be seen in Table 1, while their locations are displayed on the map in Figure 1. The total number of monthly maximum and minimum mean temperatures amounted to 934,615 and 934,615 respectively, although fewer than 500 data were available each month at the beginning of the studied period (Figure 2), to increase progressively until about 1500 around 1975-78 and, after a slight decrease, continue to climb up to some 1800 monthly observations around 1995. Afterward there is a sharp decline, until around 1,000 observations per month by the end of the period.

The "Climatol" R package V. 2.2 (Guijarro, 2013) has been used for quality control, gap filling and homogenization (correction of abrupt jumps in the average due to changes of instrumentation or observing conditions) of the series, applied independently to each hydrological basin. This program is designed to take advantage of all available climatological information throughout the study area, even that from short series, and that is why series with up to only 10 years of observation have been included. They obviously can not be used directly for representative trend calculation, but they can act as reference for the longer series. Table 1 shows the number of outliers rejected and cuts made in the series to correct the detected jumps in the average, accounted by basins. In relative terms, 0.20% of average maximum and 0.19% of minimum temperatures were rejected, while the average number of jump corrections has been 2.23 and 2.31 per series respectively.

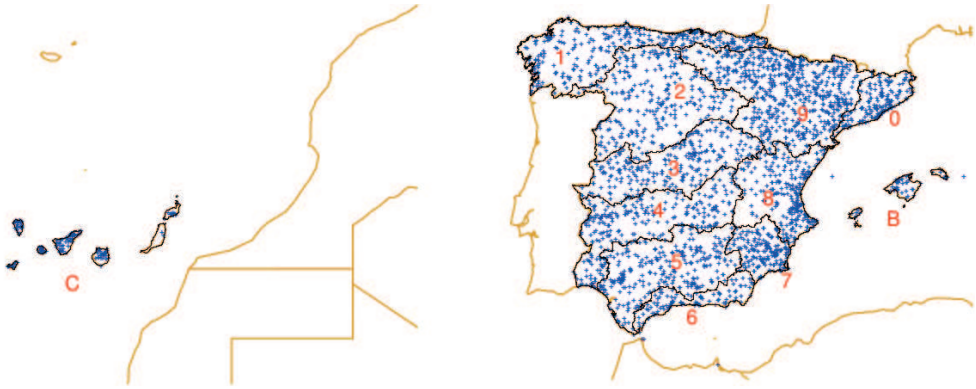

Figure 1. Location of stations used from Canary Islands (left), and from Balearic Islands and mainland watersheds (right).

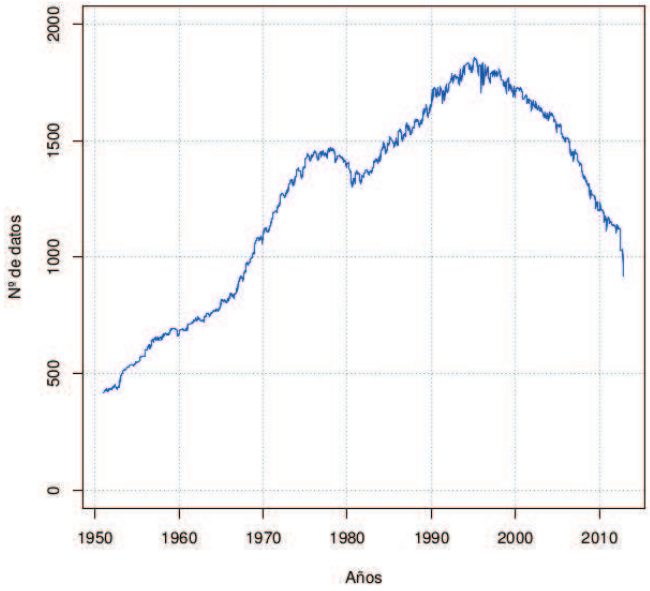

Figure 2. Number of available monthly data over the study period. (Valid both for maximum and minimum temperatures).

			Maximum temp.		Minimum temp.	
	Watersheds	**Nr. of stations**	**Rejected outliers**	**Nr. of jumps**	**Rejected outliers**	**Nr. of jumps**
1	Norte	323	150	602	145	603
2	Duero	279	250	727	224	667
3	Tajo	232	146	552	131	513
4	Guadiana	271	225	658	184	645
5	Guadalquivir	264	221	548	209	556
6	Sur	104	55	214	82	262
7	Sureste	175	149	504	165	549
8	Levante	255	120	723	119	705
9	Ebro	588	414	1237	328	1323
0	Pirineo Oriental	174	109	284	140	378
B	Baleares	48	13	84	26	100
C	Canarias	143	45	248	62	307
	TOTAL	2856	1897	6381	1815	6608

Table 1. Number of stations, rejected outliers and corrected jumps in the series, by watershed.

3. RESULTS AND DISCUSION

3.1 Variations of the average annual temperature

In the first place we are going to examine the evolution of temperatures over time, averaging by basin the annual mean temperatures computed form the completed and homogenized series, and smoothed by applying a five year moving average. Figure 3a shows that the maximum temperature variability has been quite similar over the different basins, with an increasing trend whose main exception is the cooling period that occurs approximately in the decade 1965-1974. The Canary archipelago, because of its location away from the rest of Spain and subject to a distinct climate, displays the most discrepant behavior, since it has an overall negative trend, and the common decline period is accompanied there by another descent around 1980-90. Minimum temperatures, on the other hand, appear more regular, both over time and space, the Canary Islands now following the general trend (Figure 3b).

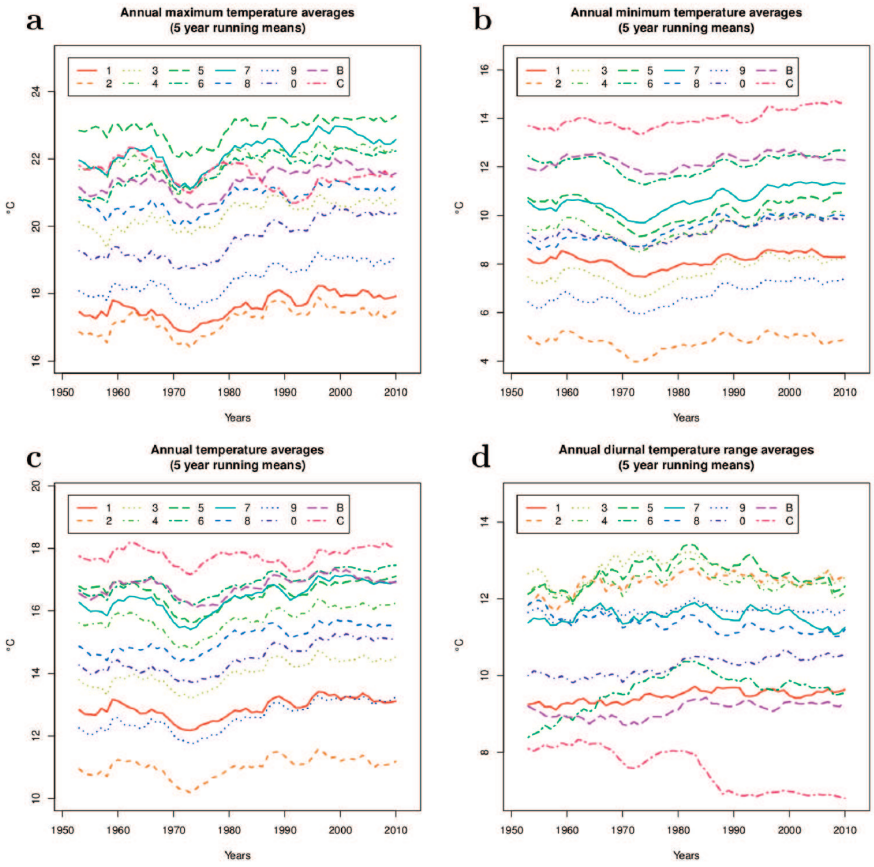

Figure 3. Time variations of the average annual maximum temperature (a), minimum (b), mean (c) and DTR (d) in each watershed.

Figure 3c shows the variations of the average temperature, which obviously are intermediate between those of maximum and minimum since they are calculated as their half-sum, while their difference yields the average daily temperature range, DTR (Figure 3d). Its evolution is the most varied between basins, since it shows a sharp decline between 1983 and 1988 in the Canary Islands (basin C) reflected only in some other basins, but much weaker. Moreover, it presents a sustained increase in basin 4 (Guadiana) since the beginning of study period until 1982 that is not in the others, whose behaviors show very different trends, both positive and negative. These DTR spatial variations deserve further studies to evaluate its possible causes, among which you can find variations of cloudiness, relative humidity, wind and urbanization of the station surroundings (Karl *et al.,* 1993).

The variability of temperature series over time makes trends dependent on the years used for their computation, since they can match ascent or descent phases of long period oscillations that would skew the results. In the 62 years studied here we may find both the descent thermometric phase and the subsequent increase that may be associated with the dimming and brightening observed in the series of incident solar radiation (Sánchez-Lorenzo *et al.,* 2007), although the temperature series have a delay lag of around a decade. In any case, as both phases of descent and ascent are included in the period 1951-2012, this 62 years seem suitable for the computation of trends, that presumably will be less biased than if any other sub-period were taken for their calculation.

3.2 Temperature trends over the last 62 years

Monthly and annual temperature trends have been obtained through ordinary least squares linear regression with time from the homogenized series, using a post-processing function included in the Climatol package. Figure 4 shows the monthly trends for the period 1951-2012 averaged by watershed and expressed in °C per 100 years. The most outstanding feature in mean maximum temperatures (Figure 4a) is the Canary Islands graph, which is the only one displaying negative values in all months except in December. The more negative trends, lower than -2°C/100yr, happen in September and October, followed by May.

The rest of the basins show trends almost always positive, except for some not significant values in September, November and December, while maximum trends occur in summer and spring, especially in the months of June and August (more than 4°C/100yr in some basins), followed by March, February and July. In the Atlantic basins (5-Guadalquivir, 3-Tajo, 2-Duero and 4-Guadiana) trends in April and May are almost as low as those of the months between September and January, while in the other basins they are similar to the February and March trends.

As to the minimum temperature trends (Figure 4b), patterns are somehow similar to those of the maximum, with a majority of positive trends, peaks in June and August, and insignificant values in September, November and December, but these patterns are more different between basins than they were in the case of maximum temperatures. The Canary Islands graph is very similar to that of its maximum counterpart, only shifted around 3°C/100yr higher, and therefore all monthly values have now positive trends. Eastern basins, mainly Levante (8) and Sureste (7), have

higher trends in the summer months, while in December and January they drop to insignificant values. In other basins, however, there is much difference between the trends in summer and in the rest of the year.

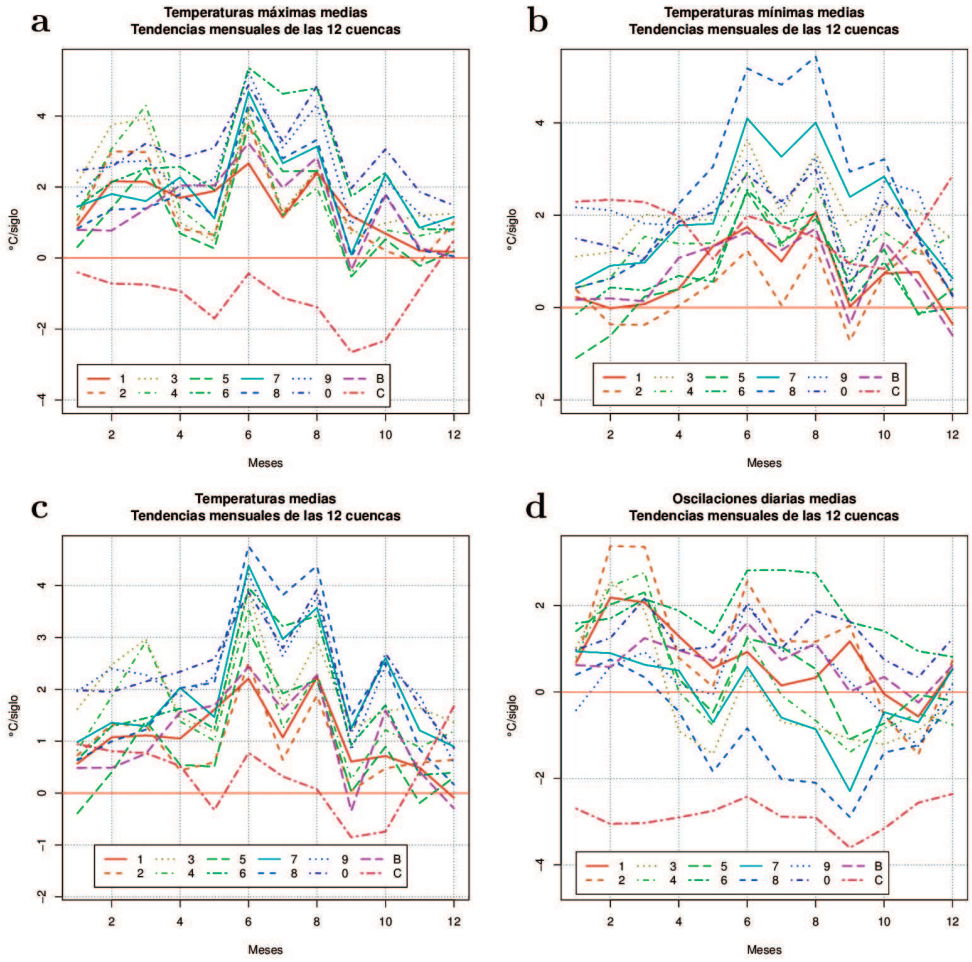

Figure 4. Monthly trends of maximum temperature (a), minimum (b), mean (c) and DTR (d) in each watershed during 1951-2012.

Being intermediate between those of maximum and minimum, it is unnecessary again to discuss the trends in mean temperatures (Figure 4c), so we will focus on the DTR trends (Figure 4d), which generally appear positive in February, March and June. In the Canary Islands they are negative all year, by far when compared to other basins, and without showing large variations between months. DTR trends in the other basins are quite similar from November to January, while between June and September they are more diverse, with positive peaks in the Sur (6), Pirineo Oriental (0) and Duero (2) basins, and minimum (mostly negative, especially in September) in the Levante (8), Sureste (7) and Tajo (3) watersheds.

Martin *et al.* (2012) also found a decreasing DTR trend on the Tenerife Island, calculated over a period of 67 years (1944-2010), while in the higher elevations that trend was not significant. Table 2 shows the trends in annual maximum and minimum temperatures averaged per basin and their dependence with altitude. All annual trends are positive except those of maximum temperatures in the Canary Islands. Moreover, all maximum temperature trends are more significant than $\alpha=0.01$, while the significance of minimum temperatures trends is more varied, from highly significant in seven watersheds to non-significant in those of Duero and Guadalquivir. It is in the Canary Islands where the correlation of these trends with altitude is higher, and with opposite signs for maximum (which decrease with height) and minimum temperatures (that increase with altitude), resulting in an increase of the DTR trend with height (contrary to what Martin *et al.,* 2012 obtained in the Tenerife Island). However the Canary Islands location away from the Iberian Peninsula is unique, and in most other basins the maximum temperature trends increase with altitude (except in Duero and Ebro), while minimum temperature trends exhibit a varied dependence with altitude, with an equal number of positive and negative correlations.

It is noteworthy that annual trends of all annual maximum and minimum temperature series are positive in the Iberian Peninsula and Balearic Islands, as well as all the annual maximum temperature trends in the Canary Islands, where here annual minimum temperature trends are, on the contrary, negative, also in all Canary observatories. Their spatial distribution is shown in Figure 5, with circles representing positive trends and negative values appearing as inverted triangles, with sizes proportional to the absolute trend values. In the Canaries the maximum temperature trends are more negative in the western islands, where those of the minimum temperatures are also more positive. In both cases it is also evident the effect of altitude on the increase of the absolute value of trends, as discussed above.

Trends in the Iberian Peninsula, both for maximum and minimum temperatures, are higher in the eastern third and the Tajo basin. Maximum temperature trends are also high in the Sur watershed, but in the Balearic islands trend values are small in both cases. However, the strong trend discontinuities in some basin divides (more visible in the minimum temperatures) seem difficult to explain just by the barrier effect of the mountain ridges, and therefore in future work it will be advisable to perform the homogenization and gap filling for the entire Peninsula instead of on a per basin basis.

4. CONCLUSIONS

The temperature evolution of the last 62 years shows an upward trend, although for a period of about 10 years around 1970 there was a cooling phase. Overall maximum temperatures all have positive trends except in the Canary Islands, where they are negative. The minimum temperature trends are all positive, without exception, although in some basins their values are not significant.

Trends in average maximum temperatures are particularly high in summer and

spring, exceeding in some basins 4°C/100yr in June and August. But in the Canaries they are negative in most months.

	Altitude (m)			Maximum temperature				Minimum temperature			
Cu	Min.	Max.	Dif.	Trend	Sig.	r	Sig.	Trend	Sig.	r	Sig
1	1	1500	1499	1.44	***	0.53	***	0.67	*	0.04	-
2	116	1890	1774	1.49	**	-0.17	**	0.37	-	-0.08	-
3	220	1500	1280	1.94	***	0.50	***	2.06	***	-0.14	*
4	2	1020	1018	1.65	***	0.66	***	1.46	***	0.47	***
5	1	1592	1591	1.15	**	0.17	**	0.63	-	0.52	***
6	2	1800	1798	2.59	***	0.69	***	0.77	*	0.45	***
7	0	1350	1350	1.94	***	0.33	***	2.06	***	-0.61	***
8	2	1730	1728	1.60	***	0.64	***	2.56	***	0.14	*
9	4	2263	2259	2.42	***	-0.12	**	2.10	***	-0.55	***
0	0	1967	1967	2.96	***	0.23	**	1.70	***	-0.34	***
B	2	1030	1028	1.39	***	0.34	*	0.71	*	-0.26	+
C	3	2367	2364	-1.07	**	-0.81	***	1.80	***	0.81	***

Table 2. Station altitudes in each basin, trends in maximum and minimum temperatures annual averages (°C/100yr), and correlation coefficients (r) with altitude. Significance levels: 0 '*' 0,001 '**' 0,01 '*' 0,05 '+' 0,1 '-' 1.**

Minimum temperatures, with notable variations between basins, also have significant positive trends especially in June and August. They are positive throughout the year in the Canary Islands, with the highest values concentrated from December to March.

The seasonal pattern of Daily Temperature Range trends is very diverse in the studied basins, the most outstanding feature being the negative values in the Canaries throughout the year.

Trends in annual mean maximum are positively correlated with altitude in all basins except in the Canaries, Duero and Ebro, where the relationship is reversed. The dependence of the minimum trends on altitude is much more varied, with a majority of positive correlations in the Atlantic basins and negative in the Mediterranean watersheds.

In future works it will be advisable to homogenize all series together rather than basin by basin, to smooth the strong discontinuities observed in their divides.

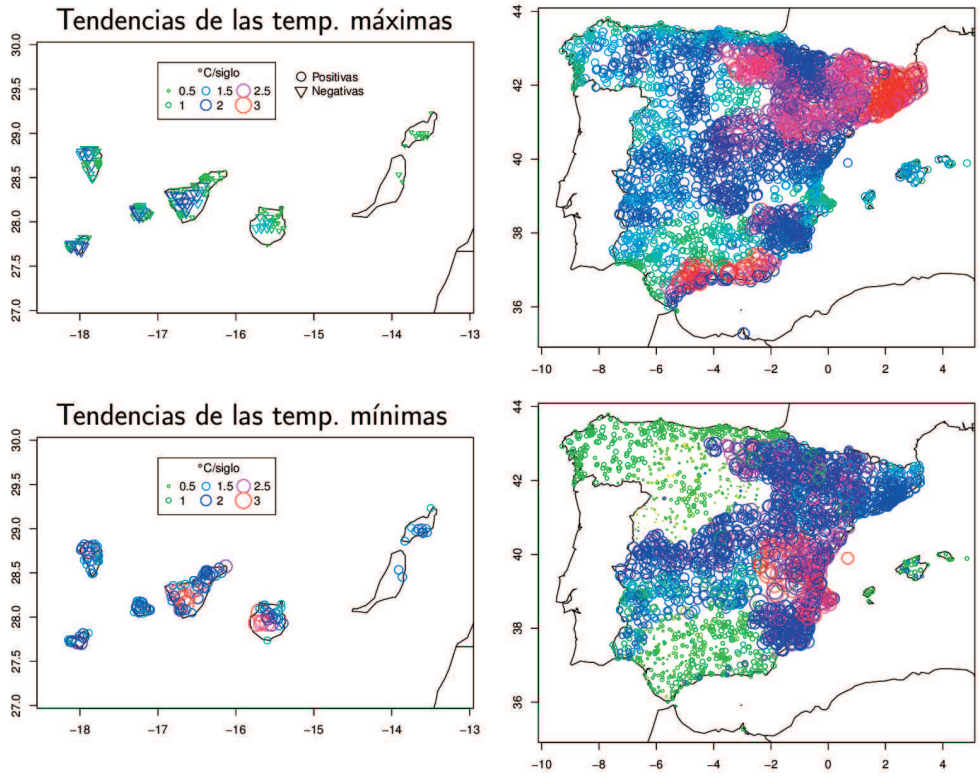

Figure 5. Annual trends in average maximum (top) and minimum (bottom) temperatures during the period 1951-2012, in °C/100yr.

REFERENCES

Brunet, M., Jones, P.D., Sigró, J., Saladié, O., Aguilar, E., Moberg, A., Della-Marta, P.M., Lister, D., Walther, A. and López, D. (2007). "Temporal and spatial temperature variability and change over Spain during 1850-2005". *J. Geophys. Res.*, 112, D12117, doi: 10.1029/2006JD008249.

Del Río, S., Penas, A. and Fraile, R. (2005). "Analysis of recent climatic variations in Castile and León (Spain)". *Atm. Res.*, 73, 69-85.

Del Río, S., Fraile, R., Herrero, L. and Penas, A. (2007). "Analysis of recent trends in mean maximum and minimum temperatures in a region of the NW of Spain (Castilla y León)". *Theor. A Climatol.*, 90, 1-12.

Del Río, S., Herrero, L., Pinto-Gomes, C. and Penas, A. (2011). "Spatial analysis of mean temperature trends in Spain over the period 1961-2006". *Glob. Planet. Change*, 78, 65-75.

Del Río, S., Cano-Ortiz, A., Herrero, L. and Penas, A. (2012). "Recent trends in mean

maximum and minimum air temperatures over Spain (1921-2006)". *Theor. Appl. Climatol*, DOI: 10.1007/s00704-012-0593-2.

Guijarro, J.A. (2013). User's guide to climatol. An R contributed package for homogenization of climatological series. Disponible en http://www.climatol.eu/climatol-guide.pdf

Homar, V., Ramis, C., Romero, R. and Alonso, S. (2010). "Recent trends in temperature and precipitation over the Balearic Islands (Spain)". *Clim. Change*, 98, 199-211.

Karl, T.R., Jones, P.D., Knight, R.W., Kukla, G., Plummer, N., Razuvayev, V., Gallo, K.P., Lindseay, J., Charlson, R.J. and Peterson, T.C. (1993). "Asymmetric Trends of Daily Maximum and Minimum Temperature". *Bull. Am. Meteor. Soc*., 74, 1007-1023.

Martín, J.L., Bethencourt, J. and Cuevas-Agulló, E. (2012). "Assessment of global warming on the island of Tenerife, Canary Islands (Spain). Trends in minimum, maximum and mean temperatures since 1944". *Climatic Change*, 114, 343-355.

Martínez, M.D., Serra, C., Burgueño, A. and Lana, X. (2010). "Time trends of daily maximum and minimum temperatures in Catalonia (ne Spain) for the period 19752004". *Int. J. Climatol*., 30, 267290.

Morales, C.G., Ortega, M.T., Labajo, J.L. and Piorno, A. (2005). "Recent trends and temporal behavior of thermal variables in the region of Castilla-León (Spain)". *Atmósfera*, 18, 71-90.

Moratiel, R., Snyder, R.L., Durán, J.M. and Tarquis, A.M. (2011). "Trends in climatic variables and future reference evapotranspiration in Duero Valley (Spain)". *Nat. Hazards Earth Syst. Sci*., 11, 1-11.

Piñol, J., Terradas, J. and Lloret, F. (1998). "Climate warming, wildfire hazard and wildfire occurence in coastal Eastern Spain". *Clim. Change*, 38, 345-357.

Sánchez-Lorenzo A, Brunetti M, Calbó J and Martin-Vide J. (2007). "Recent spatial and temporal variability and trends of sunshine duration over the Iberian Peninsula from a homogenized data set". *J. Geophys. Res*., 112, D20115, 18

Serra, C., Burgueño, A. and Lana, X. (2001). "Analysis of maximum and minimum daily temperatures recorded at Fabra Observatory (Barcelona, NE Spain) in the period 1917-1998". *Int. J. Climatol*., 21(5), 617-636.

CHAPTER 21

HEAT AND COLD WAVES IN SPAIN

José M. CUADRAT PRATS, Roberto SERRANO NOTIVOLI,

Ernesto TEJEDOR VARGAS

Instituto Universitario de Ciencias Ambientales (IUCA). Universidad de Zaragoza
jmcuadrat@unizar.es, rsnotivoli@gmail.com, etejedor@unizar.es

ABSTRACT

This paper describes the temperature extremes recorded in Spain since 1900 and analyzes the main episodes of heat and cold weather. It details also synoptic patterns that cause heat waves and cold waves, with direct consequences. Finally, the study describes a trend analysis from the annual frequency of extremely hot days (EHD) and extremely cold days (ECD). An EHD has been defined as one in which the maximum temperature exceeds the threshold of 95% of the distribution of daily maximum temperatures; an ECD is defined as a day whose minimum temperature is within the lowest 5% of the daily temperature series for each observatory.

Key words: temperature extremes, cold waves, heat waves, trends in Spain.

1. INTRODUCTION

Heat and cold waves are weather events that cause a sporadic alteration of the normal heat rate, with very negative effects on public health, socio-economic activities or the natural environment with different frequency. In Spain, it is well known indeed that the threshold of 40° C exceeds almost every year in many observatories in the southern peninsular, where some days become exceptionally hot. For instance, the town of Écija, popularly known as "the frying pan of Andalusia", has recorded at various times 47° C; Seville, Córdoba and Jaén have reached 46° C; therefore, it is probably that a temperature of 50° C has been reached somewhere in the Guadalquivir basin. The sweltering heat of these 40° C is not exclusive of Andalusia, even though its occurrence is minor, is not rare that we achieve and exceed the 40° C threshold in Extremadura, Murcia and large areas of the Meseta or the Ebro Valley. Even the temperature maximum absolute of Bilbao or Santander has exceeded this value under the South weather situations.

Likewise, cold waves are another constant of the Spanish climate. The tourist vision from central Europe or Northern differs significantly from reality, and the mild winters are only certain in the peninsular coastline or archipelagos; on the contrary, continentality and altitude of the inland favor the existence of rigorous records. In the Northern Meseta some observatories have recorded temperatures below -20° C, and even more: -22° C in Burgos; -20.4° C in Ávila. But the Peninsula is likely to suffer intensely cold days, as they prove the -24° C reported in Albacete; -21° C in Vitoria; or -28.2° C in Molina de Aragón (Guadalajara); -30° C in Calamocha (Teruel). And probably, in the highest peaks of the Pyrenees have grazed once up to -40° C. Fortunately they are not common values, but neither they are extraordinary.

These extreme events are causing considerable material damage and above all have an immediate impact on human beings. Recent studies in the United States have indicated that the mortality associated with episodes of high or low temperatures may be greater than that caused by floods, tornadoes, or hurricanes (Kunkel *et al.,* 1999). For example, the heat wave that struck Europe in summer 2003 caused, only in France, more than 14,000 deaths, according to l´Institut National de la Santé (INSERM, 2003). In Spain the situation was less alarming, but temperatures are one of the main causes of deaths related to adverse weather phenomena, as they stressed, among others, Linares and Díaz (2008) and García Herrera *et al.* (2005). In the case of cold waves, consequences can be still more severe, although it is not easy to establish the relationship of cause and effect due to delayed and prolonged period in the impact of the cold weather (Díaz *et al.,* 2005).

In the context of the current global warming, the scientific effort to know the characteristics and evolution of the climate extremes has been increased. At European level, Cony *et al*. (2008 and 2010) analyzed 7 Spanish temperature stations between 135 used in Europe and observed a decrease in the days of extreme cold since the year 1955 and an increase in the number of days and warm nights. The results coincide largely with previous studies of Klein Tank *et al.* (2002) in the framework of the project ECA & D, and with works of Moberg *et al.* (2006) within the project EMULATE. Identical results were obtained for the Iberian peninsula Miró *et al.* (2006), Brunet *et al.* (2007), Rodriguez Puebla *et al.* (2008), and more recently Sigró *et al.* (2012), based on time series and different observatories. In all of them, the upward trend is clear in the case of heat waves, but the descent of cold waves is less evident, and looks as if there is a rise of cold waves in recent years, according to Yagüe *et al.* (2006).

In this work an exhibition of the absolute extremes of temperature in Spain since 1900 is made, describing the main waves of heat and cold and the trends followed by these events are evaluated from an examination of the annual frequency of days of extreme heat and cold. First of all, these atmospheric episodes are studied as well as their characteristics and synoptic conditions; then, its evolution and trend will be discussed; finally, some conclusions are presented.

2. DATA AND METHODOLOGY

Records of maximum and minimum daily temperature of the Spanish provincial capitals available have been used, based on climatological data of the Spanish State Agency of Meteorology (AEMET) from the year 1900, when they began to normalize

the observations. Previous to this date different weather stations were also measured, but its reliability is uncertain because it is not known with accuracy if the observations took place under appropriate conditions; for this reason, it was decided to do without them. Subsequently, some stations whose information seemed uncertain data have also been rejected. The result is a very broad and representative database of the Spanish territory. However, the length of the series is not homogeneous: for example, Zaragoza series starts in 1900, while that of San Sebastian has worked since 1930; for this reason, an episode record of heat or cold may not be registered in all the observatories.

OBSERVATORIES	T°C min	Date	T°C max	Date
Albacete (Los Llanos)	-24.0	03/01/1971	45.5	31/08/1903
Alicante (Ciudad Jardín)	-4.6	12/02/1956	41.4	04/07/1994
Almería Aeropuerto	0.1	27/01/2005	41.2	30/07/1981
Ávila	-20.4	17/01/1945	37.6	24/07/1995
Badajoz Aeropuerto	-7.2	28/01/2005	44.8	01/08/2003
Barcelona (Fabra)	-10.0	11/02/1956	39.8	07/07/1982
Bilbao Aeropuerto	-8.6	03/02/1963	42.0	26/07/1947
Burgos	-22.0	03/01/1971	41.8	13/08/1987
Cádiz	-1.0	11/02/1956	43.0	19/08/1982
Castellón de la Plana	-7.3	11/02/1956	40.6	23/07/2009
Ceuta (Monte Hacho)	-0.4	05/01/1941	40.2	30/07/2009
Ciudad Real	-13.8	03/01/1971	44.2	23/07/1945
Córdoba Aeropuerto	-8.2	28/01/2005	46.6	23/07/1995
Cuenca	-17.8	03/01/1971	39.7	10/08/2012
Gerona Aeropuerto	-13.0	09/01/1985	41.2	13/08/2003
Gran Canaria Aeropuerto	6.5	27/03/1954	44.2	13/07/1952
Granada Aeropuerto	-14.2	16/01/1987	42.6	22/07/1995
Guadalajara (El Serranillo)	-12.5	28/01/2009	43.5	10/08/2012
Huelva	-3.2	28/01/2005	43.8	25/07/2004
Huesca (Monflorite)	-13.2	12/02/1956	42.6	07/07/1982
Jaén	-8.0	11/02/1956	46.0	08/07/1939
León Aeropuerto	-17.4	13/01/1945	38.2	13/08/1987
Lleida	-16.0	31/01/1947	42.8	07/07/1982
Logroño	-16.0	30/12/1917	42.8	07/07/1982
Madrid Aeropuerto	-15.2	16/01/1945	42.2	24/07/1995
Málaga Aeropuerto	-3.8	04/02/1954	44.2	18/07/1978
Melilla	0.4	27/01/2005	41.8	06/07/1994
Murcia (Base Aérea)	-6.0	21/12/1941	46.1	04/07/1994

OBSERVATORIES	T°C min	Date	T°C max	Date
Ourense (Diputación)	-8.6	25/12/2001	42.6	20/07/1990
Oviedo (La Cadellada)	-10.0	17/01/1946	42.0	17/08/1943
Palencia	-14.8	04/01/1971	40.0	19/07/1990
Palma de Mallorca	-10.0	12/02/1956	41.4	25/07/2001
Pamplona Aeropuerto	-16.2	12/01/1985	41.4	10/08/2012
Pontevedra	-6.5	26/01/1919	40.0	14/06/1981
Salamanca Aeropuerto	-20.0	05/02/1963	41.0	10/08/2012
San Sebastián	-12.1	03/02/1956	38.6	04/08/2003
Santa Cruz de Tenerife	8.1	22/02/1926	42.6	12/07/1952
Santander	-5.4	21/01/1957	40.2	17/08/1943
Santiago de Compostela	-9.0	22/02/1948	39.4	20/07/1990
Segovia	-17.0	06/01/1938	38,6	24/07/1995
Sevilla	-5.5	12/02/1956	46.6	23/07/1995
Soria	-15.0	17/12/1963	38.0	28/07/1951
Teruel	-22.0	17/01/1945	40.2	10/08/2012
Toledo	-14.4	18/01/1945	43.2	10/08/2012
Valencia	-7.2	11/02/1956	43.0	27/08/2010
Valladolid	-18.8	03/01/1971	40.2	19/07/1995
Vitoria Aeródromo	-21.0	25/12/1962	39.8	26/07/1947
Zamora	-13.4	16/01/1945	41.0	24/07/1995
Zaragoza	-11.4	05/02/1963	43.1	22/07/2009

Table 1. Maximum temperatures and absolute minimum recorded in the main cities of Spain since 1900. (Data from the State Meteorological Agency).

Regarding to the concept of heat wave and cold wave, with its thermic extremes, there are no uniform criteria for its definition and differs according to authors and studies. Frequently relies on consideration of thermal period above or below a certain threshold (Prieto *et al.,* 2004; Díaz *et al.,* 2005; Cony *et al.,* 2008 and 2010), and this has also been the approach that we have followed. An Extremely Hot Day (EHD) has been defined as one in which the maximum temperature exceed the threshold of 95% of the distribution of daily maximum temperatures for each observatory from June to August; and Extremely Cold Day (ECD) is defined as a day whose minimum temperature is within the lowest 5th centile of the daily temperature series for each observatory from December to February. These values have a severe impact on health and on the environment hence are considered as indicators of the tendency of the climate. In this analysis, daily maximum and minimum temperature records have been used, limited to the period 1950-2010 due to the greater continuity of measures. We have selected four observatories that permit a reasonable representation of the thermic behaviour of the Iberian

Peninsula: Santander, Madrid, Seville and Barcelona. The data have been subjected to a quality control and homogeneity using Standard Normal Homogeneity Test (Alexandersson and Moberg, 1997) Toreti *et al.,* 2011) and the process was developed with the support of the ProClim DB (www.climahom.eu/software-solution/proclimdb) software.

3. HEAT WAVES

Heat waves are phenomena of sudden intense rise in temperatures caused by the invasion of a mass of warm air that affects more or less extensive surfaces for several days. In the Iberian Peninsula, they have their origin in the arrival of tropical, warm and dry air from the Sahara desert, which is why it is frequent the expression "Saharan invasion" to refer to the days of stifling heat affecting southern Europe. As Ayala and Olcina (2002) point out, its duration is short, since they usually do not exceed 3-5 days, affects a broad territory and high temperatures are accompanied by a sharp decrease in relative humidity.

Intense advections of North African air may occur at any time of the year; however, July and August are the months where the risk is increased. June and September are common as well, however in both cases its effects are not the same because the surface of the Sahara and the mass of air in contact with it are less hot and temperatures have a lower rise. When they appear in mid-summer, daily maximum temperatures usually exceed 35° C and reach much higher records; at the same time, minimum temperatures rarely go down 18-20° C, which contributes to increase the stifling environment. During these days, since middle morning heat is strong; since noon, sultry; at night it takes too long to cool; and only in the morning, the temperatures are pleasant.

When situations of continental tropical air are dominating, heat is felt with strength in the peninsular interior, but notably in the Valley of the Guadalquivir, where at different times have exceeded 45° C; as shown by the 47.1° C recorded in Montoro (Córdoba) on 1 August 2003; or the 47.0° C measured at Beas de Segura (Jaén), on July 15, 1978; as well as Hornachuelos (Córdoba) during the warm period of July 1995. Such values, but with a lower frequency, can be seen also in Extremadura, Castilla - La Mancha or Murcia, and sometimes on Levantine land, inside the basin of the Ebro or some places in Galicia. There are plenty of examples: 47.0 ° C have been recorded in Bohonal de Ibor, Cáceres (24 July 1995); 47.0° C at Vianos, Albacete (16 July 1978); 46,0° C in Xàtiva, Valencia (27 July 2003); 45,0° C in Puigverd, Lleida (6 July 1982).

Although the more general heat wave atmospheric situation is originated by the Sahara Air, in Levantine lands and in the southeast of Spain the so-called "ponentadas" or much overheated West winds, affected by a foëhn process, can cause during some hours or a day sudden records of temperature in the East Coast. The same process occurs in the Basque coast with southern winds and in the Pontevedra coast with Eastern Air advections. In the case of the Canary Islands situations of strong heat are known by the popular name of "Southern weather"

(by his antagonism to the prevailing winds from the NE), whose origin is, in fact, the arrival of winds from the East or Southeast that favor invasion of Saharan air to the archipelago, altering the usual Canary softness of the regime of the trade winds. This situation causes an emerging widespread temperature, top times at 40° C, an increase in the hours of sunshine in sectors usually covered by the sea of clouds and the visibility reduction by Saharan dust in suspension in the atmosphere. These are stifling days, feeling overwhelmed by the thick haze, whose duration average in summer are round the five days.

Depending on their intensity and permanence, the effects of these extremes of heat can be catastrophic. Some agricultural lands, such as fruit trees and vineyard productions, which do not withstand high temperatures and prolonged dehydration, suffer considerable losses. Crops do not reach to extract soil water that is needed to restore the losses by evapotranspiration, and due to their high water content, fruits are literally burned; and if they are flowering, physiological trauma prevents adequate pollination and fruiting. Like crops, livestock or forestry suffer from irreparable losses. The forest is weakened and is more vulnerable to diseases and insect attacks. Lack of water also favors forest fires that happen to be particularly violent, with severe consequences for ecosystems. The economic damage resulting from the phenomenon can be very high. For instance, in the heat wave of 2003, according to the Confederation of cooperatives agricultural of the Union European, COPA-COGECA, the damage to agriculture and forests in Spain that year was 810 million euros.

In the human body effects of the heat wave are varied and diverse. The most important effects are the hyperthermias and dehydration, which can cause death if not treated in time. It is true that the climate-death relationship varies depending on the geographic location (there is a daily maximum temperature from which an accused of the mortality increase is observed: in the case of Madrid, for example, the threshold temperature of 36.5° C; 41° C for Seville) and the impact is also determined by demographic and socio-cultural factors that may expand or minimize their consequences; but the damage of the high temperatures in health, especially in temperate regions, where the organism should force their thermoregulatory ability. In the case of the catastrophic heat wave that hit Europe the summer of 2003, the consequences were terrible, especially for the older population. In Spain caused 5.440 deaths (García Palomares and Alberdi, 2005); in Madrid there were 1,273 killed more than in 2002; in Barcelona deaths grew 60% between July 1 and August 15, and in Seville 100% between 8 and 18 August compared to the previous year (Trejo *et al.,* 2005).

3.1 Extraordinary heat waves

Since systematic observations are made, Spain has registered a great number of heat waves, some of them of exceptional intensity and impact. In the 19th century there are annotations of very high temperatures whose reliability is doubtful; from 1900, with more normalized data and progressive increase of observatories there is evidence of notable warm episodes in 1933, 1935, 1943, 1947, 1957, 1982, 1995, 2003, 2009 and 2012. Several of which some comments are made.

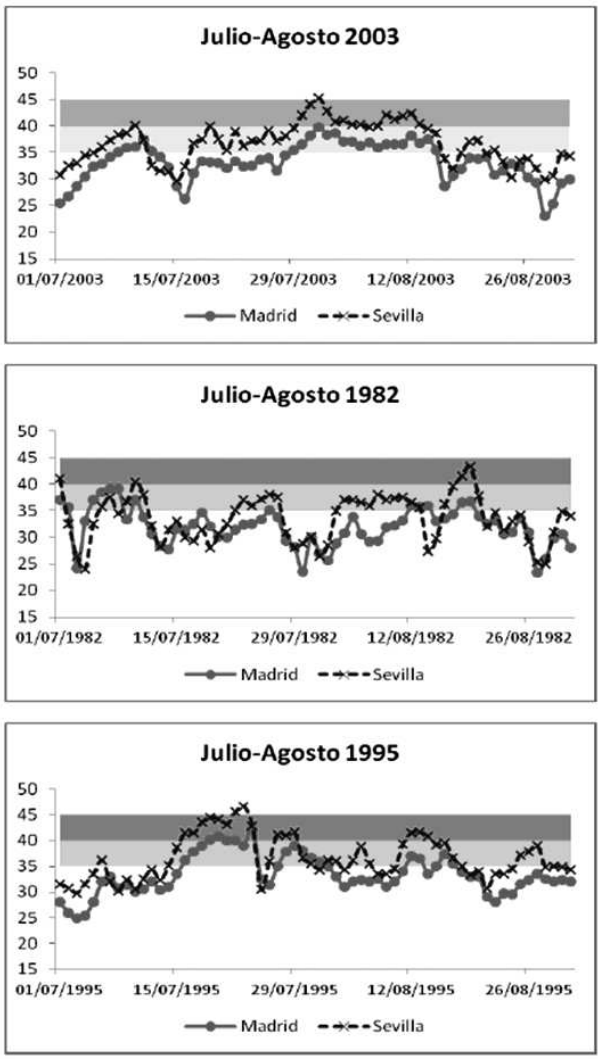

Figure 1. Daily maximum temperature during three heat waves events in Madrid and Seville.

3.1.a Warm episode of 1982

In July and August of this year the arrival of warm African Air caused strong thermal ascents, with several moments of oppressive heat that were especially intense in the North of Spain. During days 6, 7, 8 and 9 of July in the Ebro valley, Northern Meseta and Mediterranean area temperature records exceeded 40° C in a good number of observatories: 42° C en Logroño; 41° C in Zaragoza; 39.8° C in Barcelona. The stifling heat, with maximum temperature records, many of them still in force, was the remarkable note of the summer.

3.1.b Warm episode from 1995

The heat wave was concentrated from the 18 to the 25 of July and affected much of the Peninsula and the Canary Islands. In inner Andalusia, South of Castilla-La Mancha and Extremadura reached 45° C at many observatories (46.6° C in Seville; 44.6° C in Badajoz and 42.2° C in Madrid). On the Mediterranean coast these values were not reached, but the atmosphere was also blazing by the situation of sweltering and minimum temperatures above 20° C (the so-called "tropical nights").

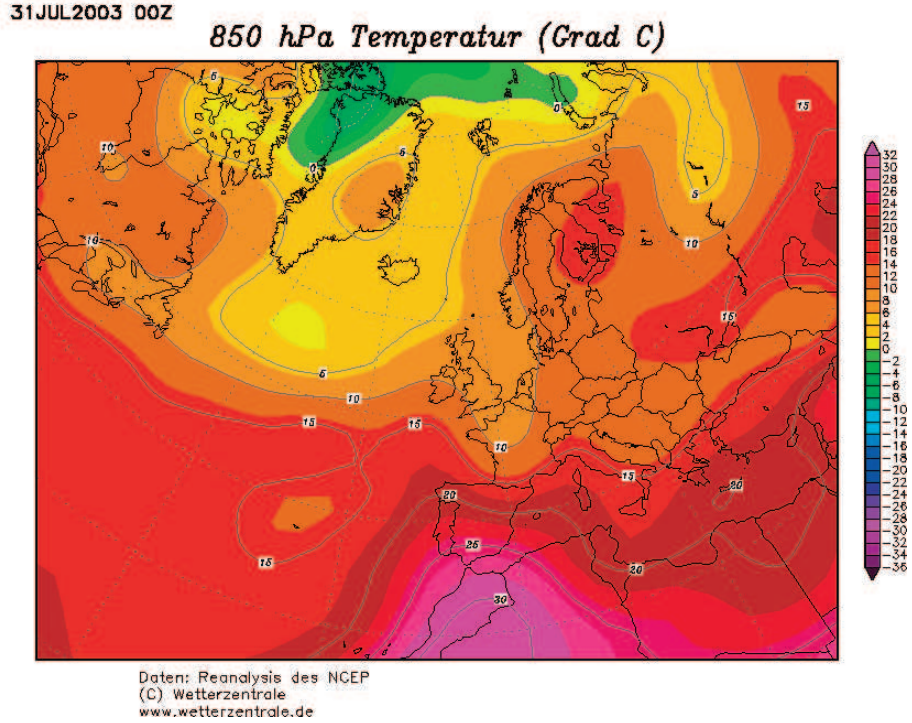

Figure 2. Temperature (ºC) at 850 hPa level for 00Z 1 August 2003. (NCEP/NCAR reanalysis).

3.1.c Warm episode from 2003

The summer 2003 heat wave was one of the warmest and driest summers from the climatic records ever. It widely affected Spain and much of Europe, where its negative impact has been considered one of the ten worst natural disasters of the last hundred years. The heat was exceptional not only because it was higher than average, both maximum and minimum temperatures, but also by their persistence, practically without interruption since early June to late August.

Almost since may, a powerful dorsal of the anticyclone of the Azores moved northward and a mass of warm and dry air, both in area and height, occupied much

of Europe and the Mediterranean. The persistent anticyclonic situation made that daytime maximum temperatures reached records unprecedented in European historical series (43° C recorded Lisbon; 39.3° C Paris; 37.2° C Vienna), the minimum night reached unexpected values (27.6° C in Weinbiet, Germany), dry conditions fostered wildfires and hospitals revenues soared sick population.

In Spain, the most intense heat period occurred between July 27 and August 14, in which the average maximum temperature was maintained between 35 and 36° C. 47.1° C were measured in Montoro (Córdoba) and above 45° C is reached in a number of locations. The consequences are known: it was the fall of the most important agricultural production since the Ministry has reliable statistics and, above all, affect the health of people increasing significantly mortality.

4. COLD WAVES

Definition of the World Meteorological Organization, the cold wave is a strong cooling air (irradiation frost) or an invasion of very cold air (cold advection), frequently accompanied by abundant snowfall, which extends over a vast territory.

Accompanying the low winter temperatures, many years, mainly from December to February, are presented with greater or lesser intensity several waves of cold air from the Arctic and Polar Regions that make the thermometer descend well below 0° C. These invasions have a deep importance for life and economic activities. These invasions are associated with the large dry and cold anticyclones of the Northern Europe. Furthermore, these invasions are associated as well to the presence of low pressure in the Western Mediterranean that turn air masses icy toward our Peninsula from different nature and properties according to the relative position of these anticyclones.

The rigorous cold leading to such events affects almost the entire Peninsula and Balearic Islands with similar characteristics, but above all, the continental inland and mountain areas are the most susceptible of suffering heavily freezing days. In the Northern Meseta, where the altitude also plays an important role, many observatories have registered temperatures of -15° C and up to more than -20° C, as indicated by the Burgos -22° C or -20.4° C of Ávila. But the crudeness of these figures is not very different from where it can be found in the Southern Meseta (Albacete -24° C), in the Intrabaetic Basin (Granada -14.2° C), in the Ebro valley (Vitoria -21° C) or in the environment of the high Jiloca river and head of the Tajo, qualified as the "pole of cold of Spain", where the town of Calamocha recorded -30° C the year 1963 considered the record of our country, except the -32° of the Estany Gento Lake, 2140 m, in the Pyrenees.

After the invasion of a very cold air mass, temperatures may remain for several days when installed in the Peninsula winter anticyclones, which create conditions of strong frosts of nocturnal radiation and intense and persistent fogs. With these conditions the temperatures maintain negative values for several days, heat stroke is very weak, and daily maximum temperatures just above 0° C. Thus, cold waves are not only rigorous by its effects, but also by its duration; and this last might be the cause of the harshness of the cold to acquire its maximum value.

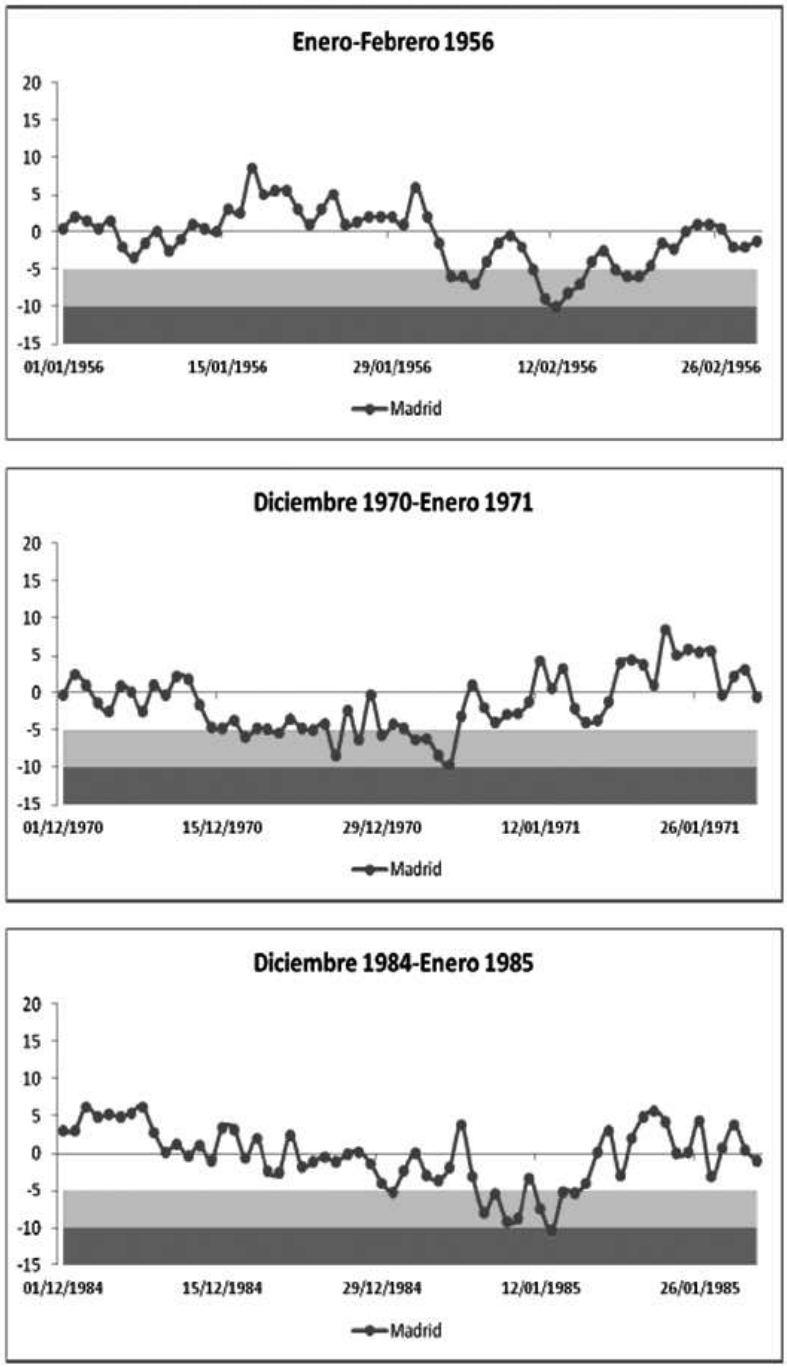

Figure 3. Daily minimum temperature during three cold wave events in Madrid.

The cold waves have deep negative impact on broad sectors, exceeding the impacts that generate heat waves: consequences such as: problems in infrastructure, increased urban pollution, strong energy consumption, development of specific diseases or losses in the agricultural sector. In agriculture, damage varies depending on the time of year and the seeded crop. In thermophile cultivation regions, such as Levantine land and the Spanish South, the invasion of these masses of cold air becomes disastrous. The fruit freeze on large areas. Horticultural crops out of season, are lost; and even more resistant, such as almond and olive trees, suffer severe damage. Apart from not giving fruit that year, strong frosts cause the death of the tree or severe wounds that heal very slowly. The shock is general and the economic losses are remarkable.

Last but not least, cold effects concerning health are more severe than those caused by excess heat, but less immediate. The impact of low temperatures on the human organism is less intense but longer in time, so it is more complicated to establish cause-effect relationship. Similarly to the threshold of heat, there is a daily maximum temperature below which the mortality soars, according to Díaz *et al.* (2005), ranges from 2.7° C in Ávila to 15° C in Alicante.

4.1 Extraordinary cold waves

From all cold invasions, the most rigorous and fearsome are the Arctic air and continental polar air, especially when they are delayed in their rush and come at the end of winter, a fact that is not common but if likely. The cold advections of maritime polar air constitute a fact quite normal hence with fewer consequences. Since 1900 there is evidence of notable cold in 1901, 1914, 1917, 1926, 1937, 1945, 1956, 1963, 1971, 1985, 2001 and 2005; some of them, which we discuss in the following lines, very stringent.

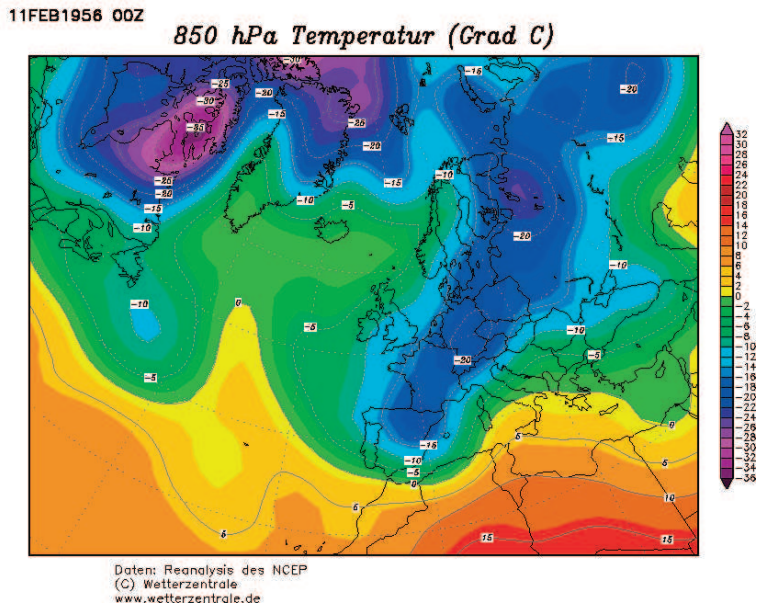

Figure 4. Temperature (ºC) at 850 hPa Level for 00Z 11 February 1956. (NCEP/NCAR reanalysis).

4.1.a Cold episode of 1985

It took place between 5 and January 16 due to the presence of an anticyclone of blockade on the British Islands and a low pressure in the Western Mediterranean that favoured the arrival of Siberian winds in the Peninsula. In the roughest days, the maxims of many observatories of the North of Spain were kept below 0° C and minima were below -10° C in several provincial capitals: -16.2° C in Pamplona; -13° C in Soria; -16° C in Ávila.

4.1.b Cold episode of 1970-1971

The winter of 1970-1971 was very long and cold and abundant in terms of snowfalls. During the second fortnight of the month of December 1970 records began to be beaten at many observatories of Spain; low temperatures continued in January 1971 and returned in March, after a truce in February. The coldest moment focused on middle Christmas. During those days the maximum temperatures overcame with difficulty the 0° C and the minimum widely surpassed the -15° C in the interior and Northern Peninsula: -24° C in Albacete; -18.8° C in Valladolid; -19° C in Viella (Lleida). In the days that lasted the invasion of continental polar air cold acquired a rigor never known; not in vain this wave was then considered by its intensity as "the cold of the century"; appreciation which is still valid today.

4.1.c Cold episode of 1956

February of 1965 was an exceptional month, mainly, for the minimum temperatures that were recorded, the amount of snowfall and the duration of the intense cold, unprecedented since the measured temperatures at the observatories. Earlier this month a powerful anticyclone located in the North of Scotland dragged frigid air from the Arctic regions to southern Europe; the air mass overflowed the Pyrenees and abruptly entered the Peninsula where temperatures decreased to unsuspected limits: -12.1° C measured San Sebastian; -10° C, Barcelona; -10° C, Madrid; -7.2° C Valencia; -5.5° C Seville. The only capitals that did not freeze, apart from the Canary Islands, were Málaga (1° C) and Almería (1.2° C). The importance of this episode was its persistence and its recidivism during the entire month, with icy consecutive and serious snowfall that hindered communications and crops were seriously affected. In Catalonia would be remembered as "L'any que el fred va matar les oliveres" (the cold year that killed olive trees).

5. TREND OF HEAT AND COLD WAVES

The global warming projections indicate that in southern Europe heat waves are becoming more frequent and severe, while cold waves will tend to go down. This is the trend that has followed the climate in Europe during the 20th century (Cony *et al.,* 2010), and the same evolution seems observed in Spain, with some particular characteristics. Data from four observatories of maximum temperature and daily minimum temperature since 1950 have been used. These data allow a reasonable representation of the thermal behaviour of the Iberian Peninsula: Santander, Madrid, Seville and Barcelona.

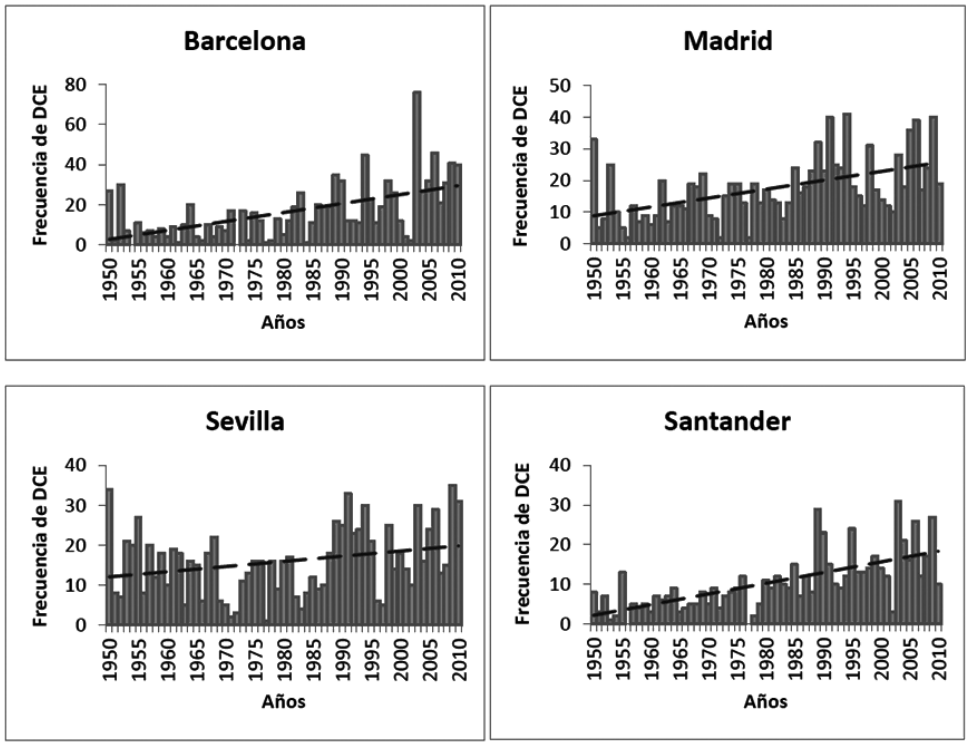

Figure 5. Annual frequency of extreme heat days (EHD) in the observatories of Barcelona, Madrid, Valencia and Seville.

In the case of heat waves, the criterion for its definition has been to establish a threshold temperature to identify the hottest days, the so-called extreme heat days (EHD). In this case EHD defined as one in which the maximum temperature exceeds the threshold of 95% of the distribution of daily maximum temperatures for the months of June, July and August of each observatory. The results obtained highlight several facts: the first is the high variability in the annual frequency of extremely hot days, with values ranging between 40 and EHD per year and their virtual absence of some years. And the second is the rising trend in recent years, being especially numerous waves of heat in the 1990s and in recent years. This is a fact which matches the majority of published studies and reinforces the idea of the increase of temperatures that is experiencing the Mediterranean region. As for what might happen in the future, in a recent work by Fischer and Schar (2010), the weather for the Iberian Peninsula projections estimate that the days of heat waves will increase an average of two in the period 1961-1990 to an average of 13 days from 2021 to 2050, and up to 40 days if the scenario is 2071-2100; and add heat episodes will have longer duration.

In the case of cold waves the criterion used has been also set a threshold temperature to identify the coldest days, so-called extreme cold days (ECD). In this case, ECD is defined by the 5% percentile of the series of daily minimum temperatures for each observatory of the months of December, January and

February. The results also show marked variability in the annual frequency of very cold days, but the trend shows significant regional differences: in Barcelona and Seville the trend is downward, but has the opposite in Madrid and Santander. These territorial differences coincide largely with works by Sánchez *et al*. (2004) and Cony *et al.* (2008) for the European regions. In both cases, it is concluded that cold waves will decrease in the peninsular Northeast, but will increase on the Meseta and North of Spain. Regarding the climate modeling these authors, indicate a certain decline of the cold waves but with very little significant statistical trends.

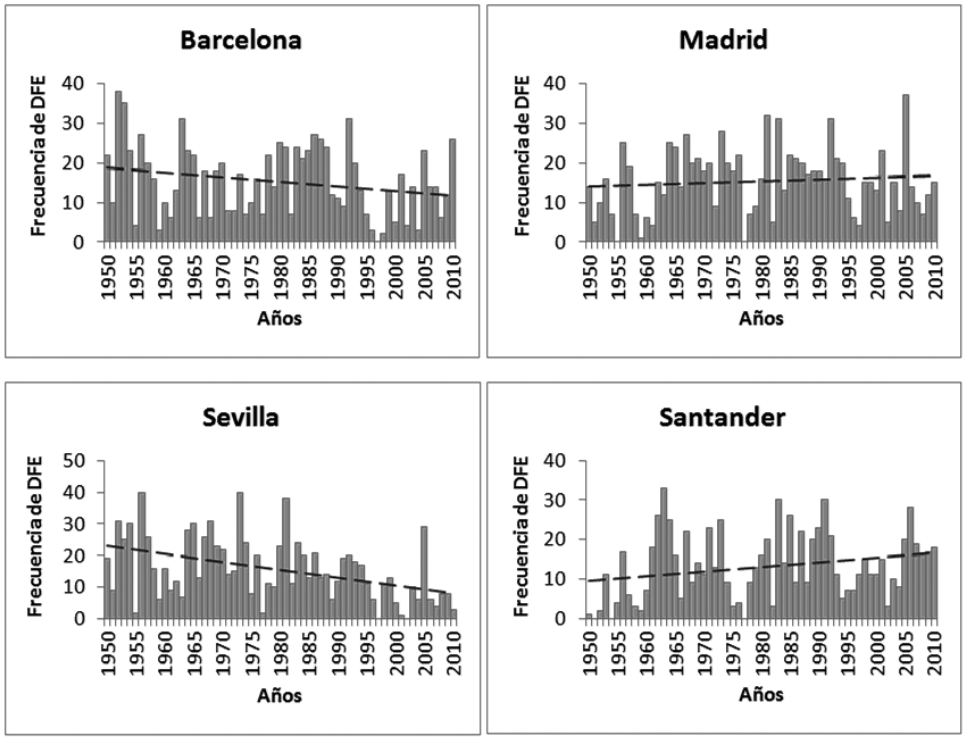

Figure 6. Annual frequency of extreme cold days (ECD) in the observatories of Barcelona, Madrid, Valencia and Seville.

6. FINAL COMMENTS

In Spain heat waves and cold waves are usual and frequent meteorological risks, which have occasionally very negative consequences. There is every year the possibility that during several days hot air masses coming from the Sahara desert, or cold perturbances arriving from polar areas generate exceptional thermal events of serious repercussion for health, the economy or the natural environment. In summer time, the threshold of the 40° C is almost every year exceeded in the South of the peninsula and in winter time the harshness of the cold can be felt with temperatures below -20° C in of the lands of Centre and North Spain. In the last

years, besides, there is a widespread increase of heat waves, and they will keep on rising, as for the predictions of the climatic models. Cold waves seem to decrease, but they do not show such a significant trend. In this context, and due to the risks involved, it would be necessary to analyse in detail their evolution as well as possible future scenarios.

ACKNOWLEDGEMENTS

This work has been supported by the projects: CGL2011-28255, financed by the Apanish Commission of Science and Technology and FEDER; and "Programa de Grupos de Investigación Consolidados" financed by the Aragon Government and European Social Fund.

REFERENCES

Alexanderson, H., and Moberg, A. (1997). "Homogeneization of swedish temperatura data. Part 1: homogenety test for linear trends". *International Journal of Climatology,* 17, 25-34.

Ayala, F. y Olcina, J. (2002). *Riesgos naturales*. Edit Ariel.

Brunet, M.; Jones, P.; Sigró, J.; Saladié, O.; Aguilar, E.; Moberg, A.; Della-Marta, P.; Lister, D.; Walter, A. and López, D. (2007). "Temporal and spatial temperature variability and change over Spain during 1850-2005". *Journal of Geophysical Research Atmospheres*, 112, D12117, doi: 10.1029/2006JD008249.

Cony, M.; Hernández, E. and Del Teso, T. (2008). "Influence of synoptic scale in the generation of extremely cold days in Europe". *Atmósfera*, 21, 389-401.

Cony, M.; Martín, L.; Hernández, E. and Del Teso, T. (2010). "Synoptic patterns that contribute to extremely hot days in Europe". *Atmósfera*, 23, 295-306.

Díaz, J.; García, R.; Prieto, L.; Linares, C.; López, C. (2005). "Mortality impact of extreme Winter temperaturas". *International Journal of Biometeorology*, 49, 178-183.

Fischer, E.M. and C. Schär, C. (2010). "Consistent geographical patterns of changes in high-impact European heatwaves". *Nature Geoscience,* 3, 398-403

Flores Herráez, C. y López Díaz, J.A., (2010). "Extremos de temperatura". *Calendario Meteorológico 2010*, 266-278.

García Herrera, R.; Díaz, J.; Trigo, R.M. y Hernández, E. (2005). "Extreme summer temperatures in Iberia: health impacts and associated synoptic conditions". *Annales Geophysicae*, 23, 239-51.

García Palomares, J.C. y Alberdi, J.C. (2005). "Mortalidad en la ciudad de Madrid durante la ola de calor del verano de 2003". *GeoFocus*, 5, 19-39.

INSERM (2003). "Surmortalité liée à la canicule de l´été 2003". AP September 25.

Klein Tank, A.; Wijngaard, J. and Van Engelen, A. (2002). "Climate of Europe. Assessment of observed daily temperatura and precipitation extremes". *European Climate Assessment & Dataset project ECA¬D, KNMI*, DeBilt, Netherlands.

Kunkel, K.; Pielke, R.; Changnon, S.A. (1999). "Temporal fluctuations in weather and climate extremes that cause economic and human impacts". *Bulletin of the American Meteorological Society*, 80, 1077-1098

Linares, C. y Díaz, J. (2008). "Temperaturas extremadamente elevadas y su impacto sobre la mortalidad diaria según diferentes grupos de edad". *Gaceta Sanitaria*, 22, 115-119

Miró, J.; Estrela, M.J. and Millán, M. (2006). "Summer temperature trends in Mediterranean area (Valencia región)". *International Journal of Climatology*, 26, 1051-1073.

Moberg, A.; Jones, P.; Lister, D.; Walther, A.; Brunet, M.; Jacobeit, J.; Alexander, L.; Della-Marta, P.; Luterbacher, J.; Yiou, P.; Chen, D.; Tank, A.; Saladie, O.; Sigró, J. and Aguilar, E. (2006). "Indices for daily temperature and precipitation extremes in Europe analysed for the period 1901-2000". *Journal of Geophysical Research Atmospheres,* 111, D22106.

Prieto, L.; García Herrera, R.; Díaz, J.; Hernández, E. and Del Teso, T. (2004). "Minimum extreme temperatures over Peninsular Spain". *Global and Planetary Change*, 44, 59-71.

Rodríguez Puebla, C.; Encinas, A. and García Casado, L. (2008). "Trend of warm days and cold nights in the Iberian Peninsula". *Asamblea Hispano-Portuguesa de Geodesia y Geofísica.*

Sigró, J.; Brunet, M. y Aguilar, E. (2012). "Los extremos térmicos en el litoral mediterráneo: evolución y factores de forzamiento". *Territoris*, 8, 265-281.

Toreti, A.; Kuglitsch, F.G.; Xoplaki, E.; Della-Marta, P.M.; Aguilar, E.; Prohom, M.; Luterbacher, J. (2011). "A note on the use of the Standard Normal Homogeneity Test to detect inhomogeneities in climatic time series". *International Journal of Climatology*, 31, 630-632.

Trejo, O.; Miró, O.; de la Red, G.; Collvinent, B.; Bragulat, E.; Asenjo, M.; Salmerón, J. y Sánchez, M. (2005). "Impacto de la ola de calor del verano de 2003 en la actividad de un servicio de urgencias hospitalario". *Medicina Clínica*, 125 (6), 205-209.

Yagüe, C.; Martija, M.; Torres, J.; Maldonado, A. y Zurita, E. (2006). "Análisis estadístico de las olas de calor y frío en España". *XXIX Jornadas Científicas de la AME*, 20-26.

III. BIOMETEOROLOGICAL APPROACH

CHAPTER 22

METEOROLOGICAL CONDITIONS AND HUMAN HEALTH

Pablo FERNÁNDEZ DE ARRÓYABE HERNÁEZ
Department of Geography, Urbanism and Territorial Planning
Vice-president of the International Society of Biometeorology
University of Cantabria
fernandhp@unican.es

ABSTRACT

The first section of this chapter is focused on describing the relation between atmospheric variables and human health. Secondly, a brief review on the main theoretical concepts traditionally used by researchers for the development of biometeorological studies is presented. Thirdly, some examples of active Biometeorological Warning Systems (BWS) are given to finally conclude with a list of recommendations for future design and development of this kind of climatic services.

Key words: BMS, Climatic Services, eustress, distress, ions.

1. INTRODUCTION

It is important, even if this is clear for researchers, to start this document insisting on the differences between two concepts such as climate and weather. While the first one relates to the average state of the atmosphere in a specific geographic area for a given period of 30-40 years (WMO), the second one refers to the atmospheric conditions in one place today or in a few days. In this sense, it is relevant to point out that this article is focused on how weather can affects human health not considering here other very interesting issues related to climate change and emerging diseases. There are many proverbs that tell us about the relation between weather and health. These sayings represent the accumulated experience by many individuals through time (Fdez-Arróyabe, 1999) and they, even not being scientific truths, incorporate an important empirical background. Meteorological conditions are substantial in the natural cycles and affect to numerous biological, physical and chemical processes activating and making them faster or slowing and stopping them. The main aim of this article is to show how the interaction between

atmospheric conditions and human beings can become a risk for their physical and psychological welfare and how new climate services can be and are being developed to help us manage and minimize the risks

2. ATMOSPHERIC VARIABLES AND HEALTH

2.1 Temperature

It is perhaps, with the rainfall, the most mentioned meteorological variable by citizens. The higher the temperature is, the higher the sweating and the heart rate related to peripheral blood vessels are and a loose of heating is generated by irradiation. On contrast, a decrease on environmental temperature means an increase of muscular fibrillation to produce more heat and a vasoconstriction to minimize the loose of internal heat through the skin (Cámara, 2006).

Extreme temperatures become a clear risk for some people´s health. When the temperature is very or extremely high problematic situations, from a sanitary point of view, can happen. Heat stroke is one of them. It is an increment of corporal temperatura over 40º C. This usually produces multi organic dysfunctions which can provoke the death of the person. It affects to young people practicing sports in very hot conditions and to old people with chronic diseases that are exposed to very intensive heat (Piñeiro *et al*., 2004). Heat waves have similar relevance, in this case because of the number of people who can be affected by them. They are understood as a series of consecutive days in which temperatures (minimum and maximum) are remarkably high. Extreme temperatures vary according to the climatic characteristics of each region or country. There have been many studies on this topic after 2003, being considered specifically in another chapter of this publication.

Heat syncope can also be a minor result of a long exposure to high temperatures. It is normally associated to dehydration and can produce loss of consciousness. The effects can be severe if proper intervention is not applied. *Exhaustion by heat* is also another minor disease, being weakness and sicknesses its main symptoms. In conclusion, irregular events as heat stroke or heat waves imply a higher risk for people´s health than other more generalized happenings linked to high temperatures such as burns, dermatitis, muscle cramps… whose risk for health is far from having tragic results.

Extreme cold produces hypothermia, frostbite and an increase in the number of broken bones because of the ice on the streets. Cold produces a thermic stress that indirectly affects the respiratory and circulatory systems in human bodies. Intense cold reduces the blood vessels section and changes the blood composition what implies a bigger effort for heart and can promote the formation of blood clots. Low temperature is linked to colds, laryngitis, bronchitis and the spreading of some viruses and bacteria associated to infectious diseases such as influenza or pneumonias.

Daily low anomalous temperature in urban areas of and has been connected with a higher risk of suffering a myocardial attack (Bhaskaran *et al*., 2010) being the most vulnerable persons those who are ancient and suffer some chronic diseases. Some authors have demonstrated that there is a higher number of heart attacks in

the East of USA after big snowing periods. These extra episodes have been explained by the extraordinary physical effort done by old sedentary people to clean the street and the entrance to their houses from snow. This is also an example of how meteorological conditions can indirectly become a risk for human health.

Being known the effect of heat on mortality and morbidity, it is also important to point out that cold seasons are much more impacting in these aspects than summer periods.

2.2 Atmospheric humidity

The amount of water vapor in the air is crucial to understand many diseases evolution. A good example of this statement is the relation between air humidity and respiratory diseases and allergies. Allergic asthma produced by mites, and rhinitis occur in in autumn, normally. According to the Spanish Society of Allergies and Immunology, meteorological optimal conditions for the spreading of mites are those with temperature between and , and a relative humidity of 75%. When relative humidity decreases to 65% the mites do not progress so easily and below 45% they disappear. Being air humidity a key factor, these diseases will have a bigger incidence in coastal areas than in the interior regions.

On contrast, allergies to gramineous pollens have a spatially opposed distribution in the Iberian Peninsula, being registered the highest levels of pollen grains in the inner areas and the lowest by the sea. In this case air humidity plays an important role because steam can make the pollen grains weightier and this will make their dispersion much more difficult. These kinds of allergies depend on the pollination periods of trees, plants and bushes. Winter rainfall can be used as a biometeorological indicator of the future impact of pollen allergens in our health.

2.3 Atmospheric pressure

Atmospheric pressure sudden changes have traditionally been associated to cephaleus, migraines and headaches by people. Jehle and Moscati (1994) carried out a research in which 257,000 men between 25 and 64 years were studied and they detected a V shape function between atmospheric pressure and the rate of coronary episodes. Landers *et al.* (1997) found also a clear association between the starting of symptoms indicating an intracranial aneurism and change in the average pressure bigger than 10 hPa in the previous day to symptoms. A different study (Scott *et al.*, 1989) based on the analysis of five years of hospitalized people by spontaneous pneumothorax, it was found that 72% of them had been exposed to, at least, one unusual change of air pressure in the four day before the beginning of the symptoms. Moreover, it is well known that some winds, generated by pressure differences, have the ability to alter the central nervous system of meteo-sensitive persons in many different parts of the world for instance, Foehn in Austria, Sirocco in Sahara and some Mediterranean countries, Mistral in France, Santa Ana in California, Chinook in USA and Canada, Zonda in Argentina, Sharav in Israel y Middle East (Sulman *et al.,* 1974). Some countries such as Switzerland have legally recognized the wind as a mitigating factor in some cases in court.

2.4 Sun radiation

Sun radiation has a key role in the development of live in the Earth. The visible range of the electromagnetic specter has an impact, through the eyes, in brain neurotransmitters which control our attention, behavior and mood. Niels Ryberg Finsen received the Nobel Award by his treatment of lupus using light therapies being considered today as the founder of Phototherapy. Life style in cities and the discovering of electricity have altered the natural day-night cycle. The lack of sunlight is linked to different pathologies such the Stationary Affective Disorder (SAD) that happens in temperate and cold climates in autumn and winter seasons.

In the last decades, indoors architectures has reported how our offices, schools and houses are lighted with intensities between 300 and 500 lux far from the 10,000 lux there is in a cloudy day or the 15,000 lux in a sunny day.

Light therapies in some temperate and cold climates have become a must. They consist of the exposure of the person to a light source of 2,500 lux for some hours in order to regulate melatonin segregation.

On the other hand, too much light or the lack of darkness can alter circadian rhythms and affect physiological processes (Chepesiuk, 2009) as the brainwaves patterns, hormones production by the pineal gland and other biological procedures whose alteration can contribute to the development of insomnia, depression and other cardiovascular diseases.

Ultraviolet radiation (UVR) is also another type of electromagnetic radiation. Its wavelength ranges from 315-400 nm (type A), 280-135 nm (type B) and 100-280 (type C), being most harmful for health types A and B. These limits can change depending on the scientific discipline we work. Geographical location (Outer *et al.,* 2010) and meteorological conditions are relevant in relation to the amount of UVR that is received by people. Clouds and atmospheric ozone are normally considered protection factors from UVR (Bais *et al*., 2011). Measurements of UVR developed during last decades have allowed the definition of world ultraviolet index (UVI).

According to the World Health Organization (WHO), a very reduce exposure to UVR can be negative for human beings because it supposes a risk for human health. A low exposure promotes the development of several diseases related to the skeleton (rickets, and osteoporosis) because 90% of vitamin D that our organism produces endogenously requires the action of UVR on our skin (Lucas and Ponsonby, 2002), (Hughes *et al*., 2011). Nevertheless, an overexposure to UVR increases the risk of the development of some types of skin cancer and different ocular diseases such as cataracts.

2.5 Atmospheric electricity

The proper ionization of the atmosphere affects our physical and mental equilibrium mainly to those people who are meteo-sensitive.

Atmosphere is charged positively through many physical processes such as land irradiation, by air masses friction in the previous days to storms or in the full moon periods because of having ionosphere closer to the Earth. This natural positive balance can be reinforced by artificial sources, for instance TV sets and computers

and any other electric and electronic devices that are located in not ventilated rooms or even by some synthetic clothes. Having an excessive level of positive ions can produce tiredness and weakness provoking insomnia and promote depressive disorders. A very high positive electric charge in the atmosphere is also scientifically linked to headache and generalized malaise.

Atmospheric ions affect to biological processes. Albert Krueger and Tchijewsky with other researchers demonstrated that a high concentration of negative ions was able to stop the growth of some common bacteria (Krueger *et al.*, 1958; 1975; 1985). They indicated that an excess of positive ions in the atmosphere affected also the chemical process in the body of human beings. This statement was based on the experimentation they carried out with mice which were infected by different bacteria and viruses in order to expose them to tree different atmospheric environments: two positively and negatively ionized and one neutral. 35% and 59% of mice exposed to neutral and positive ionized environments died. From those exposed to negative ionized environment 19 % died. The given explanation was that the filter function of the trachea worked more efficiently under an atmosphere ionized negatively.

A second finding (Krueger *et al.*, 1968), (Danon and Sulman, 1969), (Yuliwer *et al.*, 1970), (Tal *et al*., 1976) was that positive ions were able to increase levels of serotonin in blood and environments charged negatively were able to reduce its level. This hormone is a powerful constrictor of the blood vessels and it plays an important role in the transmission of chemical signs in the brain and in the regulation of the mood of people.

Air with negative ions is given multiple favorable advantages for health such as cleaning the atmosphere from pollution particles, a bacteria killer effect, to generate a fresh sensation and well-being, clearing the mind and improving several digestive and respiratory functions in our bodies.

2.6 Other atmospheric variables

There are many other atmospheric variables playing an important role in the human beings life. Rainfall, snow avalanches, hail, lighting and extreme storms events are very dangerous for citizens and their properties being their direct and indirect consequences catastrophic in many cases. It is important to mention how relevant the combined effect of meteorological variables can be on human health. Thermic sensation does not only dependent on temperature because it varies enormously when wind and air humidity and clothing are also considered. A high relative humidity in a cold environment can increase symptoms of diseases such as arthritis, arthrosis, rheumatism, and fibromyalgia or increase the infectious processes in the respiratory tracts. By contrast, a dry environment with a low relative humidity (bellow 20 %) implies a mayor risk for the outbreak of viral or bacterial infections for example meningitis.

3. BIOMETEOROLOGICAL CONCEPT OF HEALTH

3.1 Biometeorology

Biometeorology is a scientific discipline that studies the interactions between the atmosphere and living organisms attending to three different research lines:

animals, plants and human beings. Human Biometeorology has defined its own concept of health in order to develop multiple studies. This concept of health is based on the aptitude of human beings to conciliate their vital functions with climatic and meteorological variability and change, without compromising people´s well-being (Fdez-Arróyabe, 2012). This matching is constantly taking place throughout any persons live. When the required effort for the conciliation is minimum or moderate, health crisis that are taking place are solve autonomously by different processes that are mentioned bellow. When the demanding effort is extreme and the body answers do not cover the required needs, a severe health crisis happens. Mechanisms that human beings have developed to conciliate atmospheric conditions and health are:

- Thermoregulation, as a process associated to the hypothalamus functions and to homeostatic processes that affect human body at a microbiological level and takes places in short periods of time.
- Acclimatization, as a group of compensative changes that occur in the organism due to multiple natural deviations of our environment because of seasonality or geographical reasons. It is a gradual answered, in a short/medium period of time, that starts when one person is continuously exposed to a new environmental context.
- Adaptation as a biological procedure, understood as the result of a natural selection process that takes place in a long period of time in order to increase the survival changes of species.
- Adaptation as a cultural, infrastructural and technological process (Burton *et al.*, 2009). It is here where the development and complexity of social systems represents a new challenge for the scientific study of the interactions between natural and artificial atmospheric conditions and human health. .

Last type of adaptation has opened the door for the development of a wide variety of mitigation strategies (Figure 1) by human beings that range from wearing a heat to the development of Early Warning Systems (EWS) or Biometeorological Warning Systems (BWS) as new climate services.

3.2 Atmospheric comfort

Comfort and discomfort sensations are generated and controlled by our hypothalamus which acts in a homeostatic way in our organisms. Comfort thresholds are relative for each person because they depend on many factors such as geographic latitude, degree of pigmentation of the skin, genetics, the biometeorological history, physiological constitution, emotional state and others.

Thermic comfort is defined as a state of the mind that expresses satisfaction in relation to the environment temperature (Parsons, 2003). Climatic comfort has been studied by numerous scientists (Steadman, 1979), (Fiala *et al.*, 1999), (Jendritzky, 2000), (Jendritzky *et al.,* 2008), (Höppe, 1999), (Blazejczyk, 1994), (Matzarakis *et al.*, 2010), (Lindberg *et al.*, 2008) who have developed many indexes (McGregor, 2011) considering one atmospheric variable or combining many in order to create complex mathematical models that explain energy balance between the atmosphere and human body.

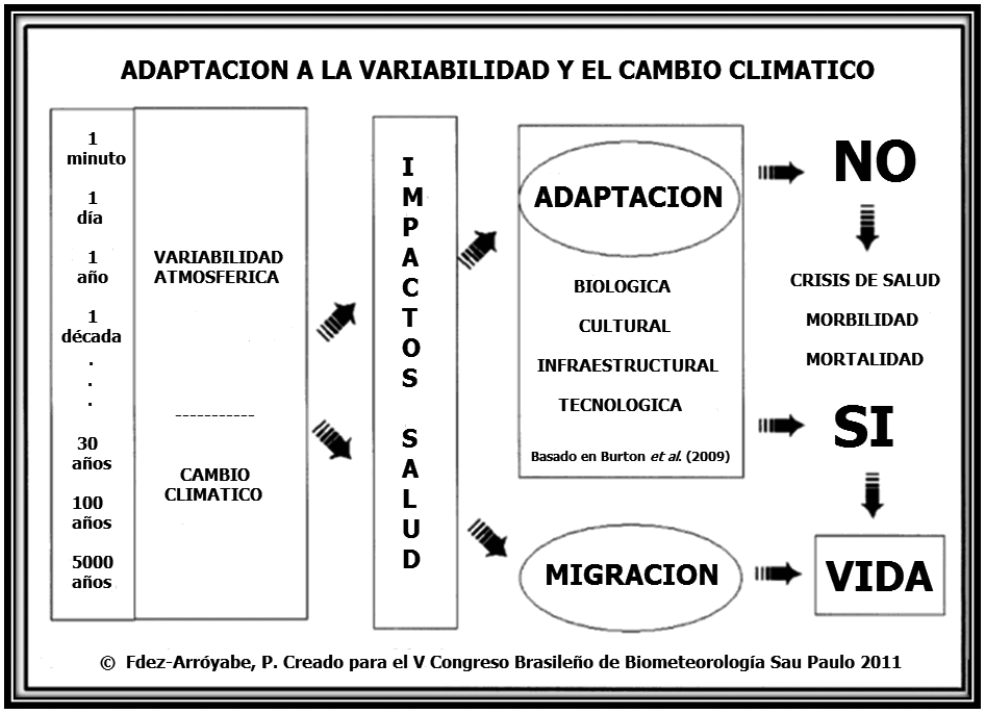

Figure 1. Human adaption to climate variability and change (Burton *et al.,* 2009).

Professor Tromp S.W. (1963) defined the climatic or biometeorological stress as an excess of tension imposed on different nervous, neuroendocrine or psychological systems by intensive and prolonged stimuli due to an exaggerated demand, alteration or aggressiveness of the atmospheric environment that it is able to try out homeostatic mechanisms for adaptation.

Relations meteorology-health do not attend to lineal processes but to V,U,W shaped-functions or more complex mathematical models. When meteorological conditions correspond to a comfortable environment (Zone E), biometeorological eustress happens and as far as we leave the Zone E, human organism moves towards a biometeorological Distress (Zones D1 and D2) in Figure 2.

Sanitary risk increases according to the level of biometeorological distress being the magnitude of the increment subjected to factors such as the place towards the displacements occurs (D1 cold versus D2 hot), the atmospheric variable considered, the age, gender and socio-cultural profile of the person or the disease that is studied.

A simulated scenario with a multiple biometeorological distress in a demographically old population, with high levels of air pollution and atmospheric stability can generate an extreme risk situation in which impacts on morbidity and mortality can be catastrophic.

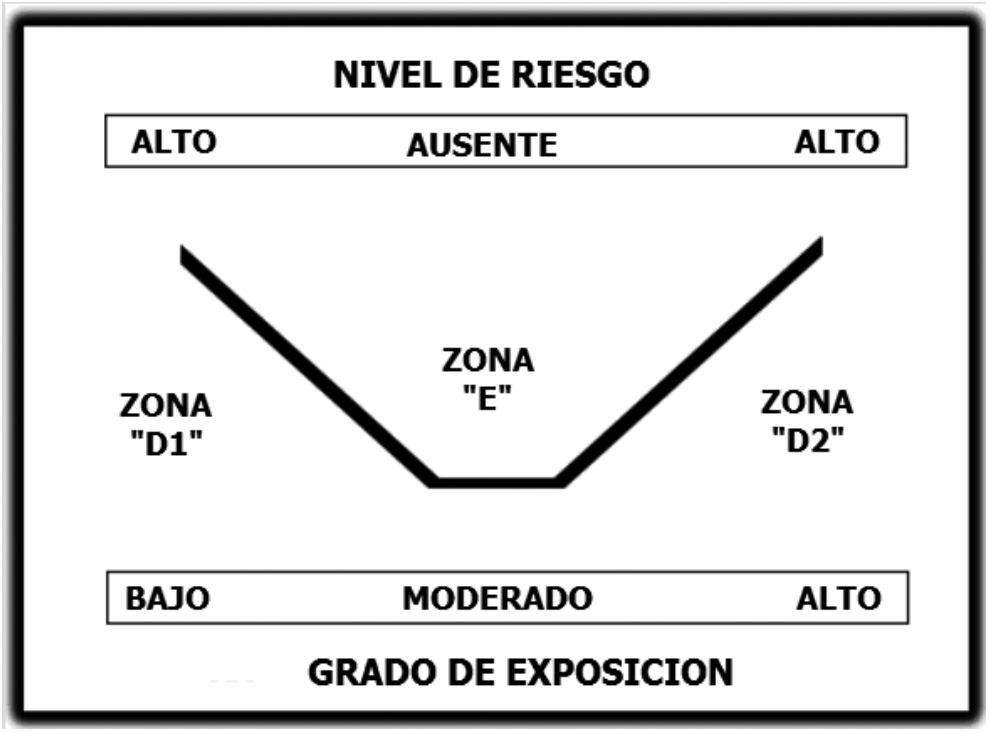

Figure 2. Degree of exposure to meteorological variables and risk level for health

Biometeorological distress can occur:

- By exhaustion: in those situations in which atmospheric conditions are extreme and persistent.
- By contrast: in those situations of extreme variability take place in relation to the normal biometeorological thresholds experienced by each person.

3.3 Biometeorological history and profiles

Meteo-sensitivity is a key element in order to define sanitary risks. An important percentage of people are meteo-sensitive what means they are able to anticipate through their body, consciously or unconsciously, atmospheric changes.

According to Sulman (1966) classification, (Moreno, 2002), there are five different hormonal typologies that generate five different biometeorological profiles (BP):

- Vagotonic profile is very sensitive to the weather variability because the vagus nerve reacts with high intensity to the meteorological changes due to an hyper function of the parasympathetic system
- Sympathicotonic profile which is the opposite to vagotonic profile. It is

characterized by a high level of secretion of adrenaline and noradrenaline when meteorological conditions change.

- Serotonic profile whose answers to extreme environmental and meteorological variability is the production of serotonin.
- Thyroid profile does not like extreme temperatures and reacts to cold and hot fronts with a hyper sensitivity of the thyroid gland.
- Balanced profile is for those people who are not meteo-sensitive, so atmospheric changes and variability do not affect them seriously.

4. CLIMATE SERVICES AND BIOMETEOROLOGICAL WARNING SYSTEMS

World Meteorological Organization (WMO), through the Global Framework for Climate Services (GFGS), has define one of its main goals for the future decades as the achievement of a better management of the atmospheric risks associated to climate variability and change including adaptation to climate change. In order to do this, WHO proposes the development and incorporation in the planning policies, of climatic information and scientific-based forecasting to a global regional and national scale.

Early Warning Systems (EWS) are a group of instruments, data, procedures and knowledge that, based on the observation and monitoring of specific phenomena allow us to anticipate levels of risk for people and for their properties being its function to warn and to activate actuation protocols and emergency plans in order to avoid or minimize the risks. Design and implementation of EWS is habitual in relation with fires, earthquakes, drought, hill slopes, hurricanes… Nevertheless, the existence of BWS that anticipate and manage the impact on morbidity or mortality of some specific meteorological conditions is much less frequent.

As it happens with many other warning systems, the risk management requires of a previous scientific knowledge of the interaction atmosphere-disease that allows us the development of BWS. The relevance of these warning systems lies in its capacity to forecast in advance different types of threats for human health and to delimit geographic places according to expected levels of the risk.

An example of a BWS based on the study of extreme heat and human mortality has been created by Prof. L. Kalkstein for some of the main cities in the USA (Kalkstein, 1996; 1997; 2004; 2005; 2008). The know-how has also been applied to other cities in Italy (Kirchmayer *et al*., 2004) or in other continents (Jianguo *et al*., 2003) being nowadays active in most of them.

The basic fundaments of the developed systems consist on the definition of a statistical classification of air masses that affect to each city and a study of the risk that each has in relation to anomalous mortality rates.

A different BWS is the one developed by researcher Prof. Luis Lecha Estela (1981, 1999, 2007, 2008) and his team of collaborators in the Center for Environmental Studies in Villa Clara (Cuba) and the Meteorological Service of Villa Clara http://www.cmp.vcl.cu/area/000001 where daily biometeorological forecasting are generated for Cuba and the Caribbean region and North America.

This BWS has been inspired in the theoretical background of the Ovcharova´s research about the physiological impact of oxygen variation in mice´s health. The Pronbiomet Warning System was created according to her experimentations outcomes, among others studies. In this sense, it is estimated the DOA index, which represent the daily variation of the partial density of the oxygen in the atmosphere being defined hyperoxia and hypoxia conditions that are linked to specific pathologies in the groups of circulatory and respiratory diseases. Risk is defined cartographically using a grey scale to express oxygen variation in en g/m^3. In the map, dark tones correspond to areas in risk of suffering atmospheric hyperoxia conditions and white tones to areas in risk of being affecting by hypoxia ones.

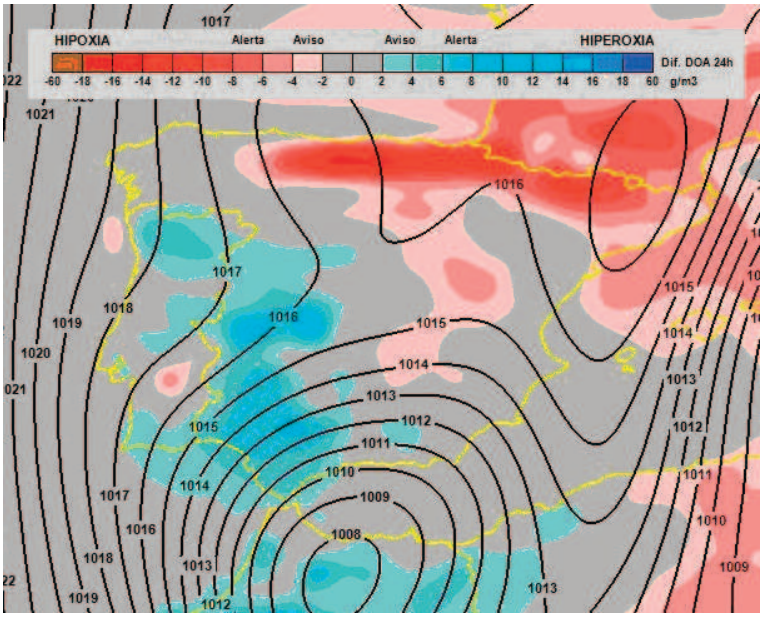

Fiure 3. DOA index Health Warning System. Forecasting for the Iberian Peninsula © Created by L. Lecha and A. Estrada.

Some results of this process of validation carried out in Spain has already been published (Fdez-Arróyabe, P. y Lecha, L., 2008), (Olcina, J. y Martín, D., 2012) with relevant conclusions. The DOA index forecasting will be published shortly for Europe and specifically for the Iberian Peninsula at the http://www.geobiomet.es in the section of biometeorological forecasting.

The third example of Biometeorological Index is being developed and its theoretical background shares the previous biometeorological concepts plus the outcomes of advanced research on influenza microbiology (Lowen *et al.,* 2008). It is called the Meteorological Contrast Index (ICM) and it is has a meso-scale dimension and a local one (Fdez-Arróyabe y Rasilla D., 2012), (Fdez-Arróyabe, P., 2012). It has been recently applied to the study of influenza in Spain and France. The system tries to determine levels of risk that specific atmospheric conditions have on the existence of outbreaks of influenza and on the speed of their expansion in a specific region.

In this case, working with an infectious disease such as influenza introduces a mayor complexity in the development of the theoretical modeling which is going to be discuss at the Abdus Salam International Center for Theoretical Physic (ICTP) in the near future by a group of international researchers.

5. CONCLUSIONS

There are many researchers working on the development of EWS, BWS or Health Warning Systems (HWS) or Climate Services in relation to human health. Thus, some recommendations are given in order to facilitate their future development and successful implementation:

- Development of indexes and methodologies should be initially simple to make possible that the process of validation of the BWS could be easily joined by as many researcher as possible around the world.

- BWS must be designed based on the basic operative systems of the Meteorological Services. In this way, they can be easily implemented if they become success in their task of analyzing the risk for human health and become active warning systems.

- Medical information should be easily accessible to be able to developed alarm systems. The access to medical data is one of the biggest inconvenient for the development of BWS today because of the privacy of the datasets.

- Actuation protocols must clearly defined and agreed with the authorities who will have the responsibility of activating security protocols once the alarm has been given in the same way it happened in other kind of warning systems. This means managing emergency services and medical staff.

For instance, heat waves in Europe are now a public health problem that has received little attention (Sari and Ebi, 2006). An efficient intervention would require integrating medical and meteorological data and warning protocols into the public services and administration (Sheridan and Kalkstein, 2004) in order to make similar decisions than other warning systems such as hazards, fires, earthquakes…

Biometeorological Warnings Systems organization must be based on a very serious information management protocols in order not to influence people nor generate panic situations among citizens that suffer some of the diseases that are consider in the system.

In some circumstances, warnings can be public and in others should be kept and manage internally. The way to procedure should be include in the warning systems. For instance, anticipate an unusual morbidity increase can be very useful in the management of sanitary resources and emergency rooms.

Any BWS should be surrender to a cycle of supervision constantly (Figure 4) though a process of design and creation, implementation, assessment, validation and improvement.

Figure 4. Cycle of quality assessment for Biometeorological Warning Systems.

The creation of custom built BWS is the main aim for the future activities in any field related to atmosphere and human health. Its implementation requires interdisciplinary groups of researchers working together, sharing information and knowledge from different disciplines, to make possible to transform scientific understanding in applicable and useful health warning systems based on macro and micro atmospheric forecasting. Accuracy and liability are factors to be considered in the assessing process and constant improvement based on scientific feedbacks from the use of the systems must be applied.

REFERENCES

Bais, A.F.; Tourpali, K.; Kazantzidis, A.; Akiyoshi, H.; Bekki, S.: Braesicke, P.; Blazejczyk, K. (1994). New climatological and physiological model of the human heat balance outdoor and its application in bioclimatological studies in different scales. In *Bioclimatic Research of the Human Heat Balance* 28, p. 27-28.

Bhaskaran, K.; Hajat, S.; Haines, A.; Herrett, E.; Wilkinson, P.; Smeeth, L. (2010). Short term effects of temperature on risk of myocardial infarction in England and Wales: time series regression analysis of the Myocardial Ischaemia National Audi Project Registry. *British Medical Journal* – BMJ 10, 341:c3823.

Burton, I. (2009). Biometeorology for adaptation to climate variability and change. In Ebi, K.L., Burton, I. and McGregor, G. (Eds). Springer, VIII, 284 pág. ISBN 978-1-4020-8921-3

Cámara, E. (2006) Variables meteorológicas y salud. Documentos de Sanidad Ambiental. Comunidad de Madrid.

Chepesiuk, R. (2009). Missing the dark: health effects of light pollution. *Environ Health Perspect*., 117 (1), 20–A27. PMC2627884

Danon, A. and Sulman, F.G. (1969). Ionizing effect of winds of ill repute on serotonin metabolism. *Biometeorology* 4. (Suppl. to Int. J. Biometeor.) 4 - Part II 135-136.

Burton, I. (2009). Biometeorology for adaptation to climate variability and change. In Ebi, K.L., Burton, I. and McGregor, G. (Eds). Springer.

Fiala D.; Lomas, K.J.; Stohrer, M. (1999). A computer model of human thermo-regulation for a wide range of environmental conditions: The passive system. *Journal of Applied Physiology*, 87 (5), 1957-1972

Fdez-Arróyabe, P. (1999). Evaluación del valor científico de los refranes como fuentes indirectas de información climática. LURRALDE, 22, 323-338

Fdez-Arróyabe, P. (2002). The develop and application of dibreakib method in order to study the relationship between atmospheric dynamic and flu rate in the city of Vitoria in the expansion period of the virus. *Int. Conf. Biomet*., 2002. AMS, 31-33.

Fdez-Arróyabe, P. y Estela, L. (2008). Validación en el norte de España de dos sistemas de alerta sanitarios basados en la idea del contraste meteorológico extremo. Publicaciones AEC, Serie A, Nº 6, 781-791.

Fdez-Arróyabe, P. y Rasilla, D. (2012). Impacto sanitario de la variabilidad climática asociada al desarrollo de epidemias gripales en la Península Ibérica durante el periodo 2000-09. Publicaciones de la AEC, Serie A, Nº 8, Salamanca,

Fdez-Arróyabe, P. (2012). Inluenza epidemics and Spanish climatic domains. HEALTH Vol.4, Special Issue, 941-945. SciRes. doi:10.4236/health.2012.430144

Höppe, P. (1999). The physiological equivalent temperature: a universal index for the biometeorological assessment of the thermal environment. *Int. Journal of Biometeorology*, 43, 71-75.

Hughes A.M.; Lucas R.M.; Ponsonby A.L.; Chapman, C.; Coulthard, A.; Dear, K.; Dwyer, T.; Kilpatrick, T.J.; McMichael, A.J.; Pender, M.P.; Taylor, B.V.; Valery, P.; Van der Mei, I.A.; Williams, D. (2011). The role of latitude, ultraviolet radiation exposure and vitamin D in childhood asthma and hay fever: an Australian multicenter study. *Pediatric Allergy and Immunology,* 22 (3), 327-333. DOI: 10.1111/j.1399-3038.2010.01099.x Blackwell Publishing Ltd.

Jehle D. and Moscati R. (1994) The incident of spontaneous subarachnoid haemorrhage with change in barometric pressure. *American Journal of Emergency Medicine*, 12 (1), 90-101.

Jendritzky G. (2000). The Universal Thermal Climate Index for the Thermo-physiologically Significant Assessment of the Atmospheric Environment. 3rd *Symposium Urban Climatology* 9–13 October 2000 (ed. W. Kuttler), Essen, 43 – 44.

Jendritzky G. and DeDear, R. (2008). Adaptation and the Thermal Environment. In: Ebi KL, Burton I, McGregor G (eds.) Biometeorology for Adaptation to Climate

Variability and Change: Research Frontiers and Perspectives. Springer, Heidelberg.

Jianguo, T.; Kalkstein, L.S.; Huang, J.; Songbai, L.; Yin, H.; Shao, D. (2004). An operational heat/health warning system in Shanghai. *Int. Journal of Biometeorology*, 48, 157–162, doi: 10.1007/s00484-003-0193-z

Kalkstein, L.S.; Jamason, P.F.; Greene, J.S.; Libby, J.; Robinson, L. (1996). The Philadelphia hot weather–health watch/warning system: development and application, Summer 1995, *Bull. Am. Meteorol. Soc*., 77, 1519–1528.

Kalkstein L.S.; Greene J.S. (1997). An evaluation of climate/mortality relationships in large U.S. cities and the possible impacts of a climate change. *Environ. Health Perspect*., 105(1), 84–93.

Kalkstein, L.; Sheridan, S. (2004). A bioclimatological analysis of heat health: progress in heat match warning systems technology. El clima entre el Mar y la montaña. IV Congreso de la AEC.B-4 (Conferencias invitadas).

Kalkstein, L.S. (2005). The 2003 European Heat Wave and Analog Studies for U.S. Cities. IN: Harvard Medical School, UNDP, SwissRE, Climate Change Futures: Health, Ecological, and Economic Dimensions, 53-58.

Kalkstein, L.S.; Greene, J.S.; Mills, D. and Perrin, A. (2008). The Development of Analog European Heat Waves for U.S. Cities to Analyze Impacts on Heat-Related Mortality. *Bulletin of the American Meteorological Society*, 89, 75-86.

Kirchmayer, U.; Michelozzi, P.; de Donato, F.; Kalkstein, L.S.; Perucci, C.A. (2004). A national system for the prevention of health effects of heat in Italy. Epidemiology, 15(4), 100-101.

Krueger, A.P. and Smith R.F. (1958). Parameters of gaseous ion effects on the mammalian trachea. *Journal of General Physiology,* 42 (5), 959-969.

Krueger, A. P.; Andriese, P.C.; Kotala, S. (1968). Small air ions: their effects on blood levels of serotonin in terms of modern physical theory. *International Journal of Biometeorology*, 12, 225-239.

Krueger, A.P.; Reed, E.J.; Brook, K.B.; Day, M. B. (1975). Air ion action on bacteria. *Int. Journal of Biometeorology*, 19, 65-71. DOI: 10.1007/BF01459843

Krueger, A. P. (1985). The biological effects of air ions. *International Journal of Biometeorology*, 29(3), 205-206, 1985 DOI: 10.1007/BF02189651

Landers A.T. and Narotam, P.K. (1997). The effect of changes in barometric pressure on the risk of rupture of intracranial aneurysms. *British Journal of Neurosurgery,* 11(3), 191-195.

Lecha, L. and Méndez, T. (1981): Relación entre la ocurrencia de infartos agudos de miocardio y una selección de parámetros meteorológicos en Santa Clara. 1er Congreso de Cardiología y Cirugía Cardiovascular, Cienfuegos, Cuba; 15 pp.

Lecha, L. (1999). Effects of climate variability on the health of the Cuban population. *Bulletin of the World Meteorological Organization*, 48(1), 18-22.

Lecha, L. (2007). Pronósticos para la mitigación de los impactos del tiempo sobre la salud humana. Simposio Cambio Climático y Salud. VI Congreso Nacional de Epidemiología e Higiene. La Habana, Cuba.

Lecha. L. B.; Ciómina de Carvajal, E.; Estrada, A.; Gómez, E .C. (2008). Pronósticos biometeorológicos: vía para reducir la ocurrencia de crisis de salud. Caso de Sagua La Grande. *Rev. cub. salud pública*,34(1), La Habana.

Lindberg, F.; Holmer, B. and Thorsson (2008). Solweig 1.0 modelling spatial variations of 3D radiant fluxes and mean radiant temperature in complex urban settings. *International Journal of Biometeorology*, 52, 679-713.

Lucas , R. and Ponsonby A.L. (2002). Ultraviolet radiation and health: friend and foe. *The Medical Journal of Australia* (MJA), 177, 594-598.

McGregor, G. 2011. Human Biometeorology. *Progress in Physical Geography*, 1-17

Matzarakis A.; Rutz, F. and Mayer, H. (2010). Modelling radiation fluxes in simple and complex environments: Basics of the RayMan model. *Int. Journal of Biometeorology,* 54, 131-139.

Michelozzi P. and De Sario, M. (2010). Temperature changes and the risk of cardiac events. PMID: *BMJ*2010; 341: c3720 Doi: 10.1136/bmj.c3720

Moreno i Oliver F. X. (2002). Meteoropedagogía. Revista de Psicología Universitas Tarraconensis, *Revista de ciències de l'educació*, ISSN 0211-3368, 1, 93-102.

Ovcharova, V.F. (1987). A new prognostic approach to meteoropathologic responses. *Rev Fisiotherapy, Climotheraphy and Physical Culture*, 5 49-53.

Olcina, J. and Martín, D. (2012): Variaciones en la densidad del oxígeno en el aire y su influencia sobre la salud humana. *Boletín AGE*, 58, 7-32.

Parson, K. C. (2003). Human Thermal Environment, the effects of hot moderate and cold environments on human health, comfort and performance. ISBN 978-0-415-23792-5. Ed.Taylor & Francis, London. Doi: 10.1201/9781420025248.bmatt1

Piñeiro Sande, N.; Martínez J. L.; Alemparte, E. and Rodríguez García, J. C. (2004). Golpe de calor. *Emergencias*, 16, 116-125.

Requejo C. M. (2010). Iluminación interior, salud del habitat y rendimiento laboral. Domobiotik. *Arte y técnica para la casa sana.* http://domobiotik.blogspot.com.es/

Sari Kovats, R. and Ebi K. L. (2006). Heat waves and Public Health in Europe. Oxford University Press. *European J. Public Health*, 6, 592-599.

Sheridan, S. C. and Kalkstein, L. S. (2004). Progress in Heat Watch-Warning System Technology. *Bulletin of the American Meteorological Society*, 85, 1931-1941.

Steadman, R. G. (1979). The assessment of sultriness. Part I: a temperature-humidity index based on human physiology and clothing science. *J. Appl. Meteor.*, 18, 861–873.

Sulman F. G. (1966) Influencia de las hormonas sobre la personalidad y el comportamiento. MENG, H. Ed. Endocrinología psicosomática. Madrid, Morata, 363-416 (trad. española de la obra publicada en alemán en 1960).

Sulman, F. G.; Levy, D.; Lewy, P.; Feifer, Y.; Superstine, E. and Tal, E. (1974). Air ionmetry of hot, dry desert winds (sharav) and treatment with air ions of weather sensitive subjects. *Int. J. Biometeor.*, 18, 313-318.

Scott G. C.; Berger, R. and McKean H. E. (1989). The role of atmospheric pressure variation in the development of spontaneous pneumothoraxes. *American Review of Respiratory Diseases,* 139, 659-62.

Tal, E.; Pfeifer, Y. and Sulman, F. G. (1976). Effect of air ionization on blood serotonin in vitro. *Experienta* (Basel), 32, 326-327.

Tromp, S. W. (1963). Medical Biometeorology. Ed. by S. W. Tromp. Amsterdam (Elsevier). 1st Ed. 1963. Pp. Xxvii, 991; 101 Figures; 44 Tables. *Q.J.R. Meteorol. Soc.*, 90, 368. doi: 10.1002/qj.49709038528

WMO (2006). Public Health and the Environment. Lucas, R.; McMichael, T.; Smith, W.; Armstrong, B. (2006). Solar Ultraviolet Radiation: Global burden of disease from global ultraviolet radiation. Environmental Burden of Disease Series. Nº 13. Editors: Annette Prüss-Üstün, Hajo Zeeb, Colin Mathers, Michael Repacholi. Geneva.

WMO (2003). Scientific Assessment of Ozone Depletion: 2002, World Meteorological Organisation, Geneva, Global Ozone Research and Monitoring Project, Report No. 47, 498.

IV. INSURANCE COVERAGE APPROACH

CHAPTER 23

THE CONSORCIO DE COMPENSACIÓN DE SEGUROS AND COVER FOR ADVERSE WEATHER RISKS

Carmen GARCÍA CANALES, Alfonso NÁJERA IBÁÑEZ

Consorcio de Compensación de Seguros
cgarciac@consorseguros.es, anajera@consorseguros.es

ABSTRACT

Weather phenomena are nothing new, although the level of economic and social loss they have recently caused is –as a result of increased vulnerability and development– clearly on the rise. Insurance constitutes a mechanism for the financing of losses. The behaviour of natural hazards takes on special characteristics which must be considered in relation to their treatment for insurance because they are relatively infrequent compared to other ordinary risks covered by insurance, but when they do occur they can cause vast amounts of damage, simultaneously affecting a very large number of insureds. The high (and rising) potential for loss from natural hazards and the need to make a more generalised insurance cover viable has led many countries to involve the State in specific cover schemes, collaborating to varying degrees with the private market. Spain's disaster insurance system, managed by the Consorcio de Compensación de Seguros or CCS (Insurance Compensation Consortium), is highly developed, consolidated and stable.

Key words: natural disasters, storm, flood, damage, insurance, Consorcio de Compensación de Seguros.

1. INTRODUCTION

In addition to the physical factors comprehensively dealt with in this publication, weather events have social, economic, financial and indeed political repercussions. Seen from a global perspective, the economic consequences of certain meteorological hazards have done nothing but increase in recent decades because of growing population, the concentration of assets and the social and economic development. On the other hand, as a result of climate change, the experts are forecasting a significant increase in the frequency and intensity of extreme climatic phenomena.

Increasing trends in the damage from adverse weather events is a cause of increasing concern for governments and international organisations, and represent a real challenge in the search for mechanisms to finance losses arising from these occurrences.

Insurance is a good tool for financing losses from unforeseeable developments. An insurance policy transfers one individual's risk to a large community of individuals so that, in the case of an event which causes damage to one of them, the financial charge is distributed among all of them. The advantage of insurance is that it eliminates uncertainty as to the financial burden to be met by the policyholders.

However, the low frequency and high intensity which are a feature of natural disasters makes their treatment from an insurance standpoint difficult. Flood for example has traditionally been a non-insurable risk in many countries, due not just to the potential for damage but also to the scant information available and the resulting impossibility of evaluating the risk, namely the maximum level of loss which, for given return periods, flooding or any other natural phenomenon may reach. Although new technologies have made it possible in the last two decades to gather very detailed topographic and climatic data, the information available continues to be uneven, and the uncertainty relative to frequency and intensity persist, in the belief that climate change may be altering weather patterns.

While the insurance and reinsurance markets have adapted, innovating to offer insurance solutions accessible to the insured, exposure to large potential losses has led some countries to examine formulas for public-private collaboration. In addition to States' regulatory function, they may involve themselves in various ways in the development of insurance solutions against natural risks: introducing compulsory assurance and application of the principle of national solidarity, use of State-guaranteed insurance and reinsurance formulas, creating resource-accumulation financial mechanisms, fomenting an understanding of risk, etc.

Spain has a specific disaster insurance system adjusted to the special financial and management features of this risk category, the central component being the *Consorcio de Compensación de Seguros* or CCS (Insurance Compensation Consortium), established as a "public business institution" attached to the Ministry of the Economy and Competitiveness, with its own legal capacity and its own assets, independent from those of the State.

2. INSURANCE COVER FOR CLIMATIC RISKS IN SPAIN

2.1 Risks covered

The system insuring catastrophic risks managed by the CCS goes under the name of *extraordinary risk insurance* and takes in both natural risks and those of a political-social character (such as terrorism and civil commotion). The risks included in the CCS's cover have varied as it has developed over time. Climatic risks like hurricane, hail, snow and rain were covered in the past. However, given the CCS's status, subsidiary and complementary to the private sector, the inclusion or exclusion of certain risks has been determined by the actual dynamic of the Spanish insurance market. At this time, the natural risks covered by the system are

earthquakes and seaquakes, extraordinary flooding, volcanic eruptions, atypical cyclonic storms or A.C.S. (including tornadoes) and falling of sidereal bodies or meteorites.

In connection with meteorological risks, since 1987 extraordinary risk insurance has included the phenomenon known as the "atypical cyclonic storm". This concept has shifted over time and in 2004 was substantially enlarged to take in damage caused solely by wind. At present, under the "atypical cyclonic storm" event, the CCS covers damage caused by violent tropical and extratropical cyclones, cold squalls, tornadoes and winds exceeding 120 km/h, as defined in the Extraordinary Risks Regulations[i].

The other risk covered by the CCS and related to weather events is flooding caused by the direct action of rain, thawing, river overflow or the impact of the sea on the coasts.

2.2 Basic aspects of cover

Sums the CCS pays those affected by an extraordinary event which is covered by the system are not in the form of aid or subsidies but of insurance indemnifications offered to policyholders who had prior to a catastrophic event taken a policy to protect persons and property located in Spain in one of the following branches of insurance (or combined categories thereof):

- For property insurance: policies for land vehicles[ii], rail vehicles, fire and natural events, other property damage (robbery, glass breakage, damage to machinery, electronic equipment and computers) and various pecuniary losses.
- For personal insurance: life and accident policies.

When contracting an insurance policy in one of these branches, the policyholder must pay a surcharge to the CCS which will meet losses arising from extraordinary events when not specifically assumed by the company covering the ordinary risks. In other words, the CCS does not issue a policy of its own but rather takes on the extraordinary risk cover in the terms of the policy concluded with the insurer for the ordinary risks, protecting the same property and persons, with the same sums insured and the same optional arrangements (first risk insurance, at new value, automatic revaluation of capital, etc.) as under the policy.

That surcharge, collected by the insurer together with its premiums, furnishes the resources the CCS uses to meet its compensatory obligations.

Unlike other systems operating around the world, Spanish cover is automatic and qualitative in relation to claims for indemnification. Should an extraordinary event occur in Spanish territory affecting persons and properties situated in the country and covered by policies in the categories referred to, the indemnification mechanism comes into operation automatically: no consultative or decision-making body need rule on the matter, nor is a declaration of a "disaster zone" by the authorities relevant. Entitlement to indemnification does not take account of the number of claims nor the geographical area affected, or the total damage arising in the claim, because the priority is the qualitative criterion according to the specificity, nature and potential of the damage from the events covered. As these are legally defined,

the only requisites for entitlement to indemnification from the CCS are: 1) to have an insurance policy in one of the aforementioned branches with a private company; 2) to be up to date in payment of the CCS surcharge, and 3) cover of the extraordinary risk causing the damage is not explicitly assumed by the private insurer in the policy.

As well as compensating direct damage to insured persons and properties, the CCS has also been able since 2004 to indemnify business interruption caused by alteration of the production process as a consequence of direct damage to insured property.

2.3 The claim record

While extreme climatic phenomena have not been seen to be as destructive as in other countries, they are the cause of the largest-scale damage. Specifically floods -conditioned by geological factors- and arising in a high proportion from torrential precipitation (flash floods) have, historically, been the most frequent event of disastrous consequences. The episodes retained in the historical memory extend practically throughout the country, albeit with different frequencies and intensities.

Flooding accounts for the largest percentage of indemnifications paid for all extraordinary risks covered by the CCS. Taking by way of illustration the compensation for property damage between 1987 and 2011, the claim rate for flooding accounts for 67.9%.

Flood	67.9%
Earthquake	8.3%
A.C.S.	16.5%
Sidereal bodies and meteorites	0.0%
Terrorism	6.0%
Riot	0.0%
Civil commotion	1.3%
Armed Forces events	0.0%
Various	0.0%
TOTAL	**100%**

Table 1. Percentage of each cause in indemnification for property damage.

The historical floods which occurred in the Basque Country on 26 August 1983 hold the record for insured losses indemnified by the CCS for a single event, amounting to 813 million (in 2011 values). This flooding was caused by a downpour which caused the River Nervión to break its banks, with huge material damage and several dozen deaths, affecting virtually all the province of Bizkaia, part of the province of Gipuzkoa and the localities of Llodio and Amurrio in Álava.

Intense hurricane-force phenomena have, as already pointed out, been covered by the CCS since 2004. The huge losses following the violent storm Klaus on 23, 24 or 25 January 2009 set a standard in the CCS's compensatory record, making it the costliest natural event of the last 25 years.

ATYPICAL CYCLONIC STORM (A.C.S.)

Sums in updated euros to 31-12-11

YEAR	No. of Files	Indemnifications	Average Costs
1987 - 1991	-	-	-
1992	904	2,668,367	2,952
1993 - 1996	-	-	-
1997	930	2,836,202	3,050
1998	-	-	-
1999	20	1,949,819	97,491
2000	-	-	-
2001	6,891	32,735,834	4,751
2002	-	-	-
2003	3,829	16,191,996	4,229
2004	6,195	19,100,056	3,083
2005	16,024	88,742,282	5,538
2006	3,332	15,113,435	4,536
2007	10,133	56,811,245	5,607
2008	3,312	15,543,605	4,693
2009	272,970	551,928,514	2,022
2010	89,500	133,625,866	1,493
2011	2,675	4,420,275	1,652
TOTAL	**416,715**	**941,667,495**	**2,260**

Table 2. Indemnification paid for property damage caused by atypical cyclonic storm.

In atmospheric terms, this was a process known to meteorologists as explosive cyclogenesis. Klaus moved from West to East from the Azores to the Gulf of Genoa, crossing the Bay of Biscay and generating winds of up to 190 km/h and waves more than 20 metres high, affecting particularly northern Spain and southern France.

The storm led to an unprecedented number of claims, nearly 270,000 and, at 533.6 million euros, remains the CCS's second largest natural event by volume of losses.

Of similar atmospheric characteristics as Klaus, although less severe in terms of management and cost for the CCS, were the cyclones Floora and Xynthia, unleashed in January and February 2010.

Floora arose in the middle of the Atlantic Ocean on 11 January 2010 as a very deep squall, moving over the provinces of Cantabrian coast from West to East and noted in a large part of the peninsula, affecting mainly Galicia and the Mediterranean coast. The wind gusts, well above 120 km/h at some points, caused a great deal of material damage.

For its part, depression Xynthia affected the Canary Islands and part of the peninsula, especially the northern third, associated with hurricane-type gusts of more than 120 km/h in many parts of Spain and reaching 180 km/h in Segovia province. Across France, it caused several dozen deaths.

EVENTS INDEMNIFIED WITH SUMS EXCEEDING €50,000,000 + A.C.S. FLOORA

Sums in updated euros to 31-12-11

Order No.	Month and Year	Place	Cause of Loss	No.of claims	Indemnification
1	August 1983	Basque Country, Cantabria, Navarre	Flooding	25,664	813,538,204
2	**January 2009**	**Various (Klaus)**	**A.C.S.**	**268,046**	**533,610,416**
3	May 2011	Murcia (Lorca)	Earthquake	27,962	452,843,543
4	November 1987	Valencia Region, Murcia	Flooding	18,800	282,119,857
5	October 1982	Valencia	Flooding	9,136	220,113,070
6	November 1989	Andalusia, Valencia Region	Flooding	7,548	158,734,835
7	June 1997	Basque Country	Flooding	5,701	107,124,809
8	October 2000	Valencia Region, Murcia	Flooding	8,939	98,171,878
9	November 2005	Canary Islands	Flooding and A.C.S.	15,482	95,847,708
10	October 2007	Valencia Region	Flooding	10,782	92,943,990
11	October 1994	Catalonia	Flooding	4,631	76,284,712

Order No.	Month and Year	Place	Cause of Loss	No.of claims	Indemnification
12	September 2006	Catalonia	Flooding	3,872	64,549,480
13	September 1989	Valencia Region, Murcia, Balearic Islands, Eastern Andalusia	Flooding	5,999	63,544,52
14	June 2008	Basque Country	Flooding	5,832	63,413,283
15	June 1977	Basque Country	Flooding	3,889	59,520,597
16	November 1982	Catalonia	Flooding	1,587	58,118,201
17	**February 2010**	**Various**	**A.C.S. (Xynthia)**	**39,463**	**57,842,168**
18	September 1997	Valencia Region	Flooding	7,489	55,967,205
19	April 1982	Madrid Region	Terrorism	46	54,740,888
20	December 2010	Western Andalusia	Flooding	3,439	54,324,121
21	November 1983	Catalonia, Valencia Region	Flooding	6,846	52,918,762
22	September 2009	Valencia Region	Flooding	10,419	52,505,023
23	July 1988	Basque Country	Flooding	2,322	51,445,220
24	November 2011	Basque Country	Flooding	4,121	51,436,780
25	October 2005	Catalonia	Flooding and A.C.S.	5,328	50,662,230
28	**January 2010**	**Various**	**A.C.S. (Floora)**	**39,472**	**47,641,712**

Table 3. Events indemnified with sums exceeding € 50,000,000 + A.C.S. Floora.

The great quantitative and qualitative impact of those storms, Klaus, Floora and Xynthia on the insurance sector made it advisable to review not just the scope of CCS cover, but also the procedures to be followed to define when such cover would be effective. As a result, in 2011 the speed of extraordinary winds covered was reduced from 135 to 120 km/h.

3. CLIMATE RISK INSURANCE SYSTEMS IN OTHER COUNTRIES

The high potential loss from natural hazards explains why in many countries the insurance market does not have the capacity to cover them. Just some markets in the most developed countries offer some form of insurance solution for one or more of these hazards, e.g. Germany, the United Kingdom, Canada, Australia… However, also in many of those countries, the market does not have the financial capacity to cover certain risks to which they are more vulnerable, and they are excluded from covers or their premiums are very high and difficult for a policyholder to take on: flooding in the Netherlands, earthquake in Japan (except household cover), earthquake and volcanic eruption in Italy, etc. Natural disaster cover in countries where it is available on the private market is voluntary except in some cases such as Norway for example.

Clearly, management of the insurance for this high potential loss requires specific mechanisms which, among other things, allow sufficient financial capacity and efficient handling of what may be a very high volume of claims. In response to that, many countries have designed insurance schemes in line with their particular circumstances (more threatening hazards, level of development, the structure of the insurance market, the culture of insurance, etc.) and with varying degrees of public backing and involvement. The heterogeneity seen in the configuration and operation of those specific cover systems is a consequence precisely of that diversity of conditions. They do share the aim of offering universal cover at accessible prices and with guarantees of financial solvency. Most of these systems are based on close collaboration between public bodies and the insurance market.

Direct public participation in the systems for disaster cover adopts varied forms, defining whether the system takes the shape of a direct cover regime as in Spain through the CCS or via reinsurance as in France through the Caisse Centrale de Réassurance (Central Reinsurance Agency). A fundamental pillar of some more-recently created systems involves the assignment of risks to the capital market using disaster bonds, as in the case of the California Earthquake Authority.

Unlike what happens in private insurer schemes, where there is public participation the cover is in most cases compulsory for the risks included in the system but which, as will be seen, does not include all the risks. That compulsory nature is what makes the cover provided by the systems viable, generalizable and affordable, and which would otherwise cease to function as a consequence of anti-selection, that is because only policyholders whose interests are most exposed would be inclined to acquire cover.

That obligatory nature may be linked to possession of a property, generally a building. Thus the owners, merely as such, must secure cover against fire, to which that for natural risks is linked, as happens for example in Switzerland, Iceland,

Rumania or Turkey. The obligation may however also be linked to the contracting, in this case voluntarily, of a policy for property damage (usually fire) as in the systems in Spain, France, Belgium, Denmark, New Zealand, Taiwan… In these cases and save in exceptional circumstances where the systems issue their own policy (Turkey and the US flood program) the base for natural risk cover is an ordinary risk policy issued by a private insurer.

As already indicated, these specific assurance systems do not cover all natural risks, across a range with, at one extreme, the most inclusive as in France and Spain and, at the other, those covering just a single risk such as Denmark (marine flooding), Japan, Turkey and Taiwan (earthquake in homes), United States (flooding), etc

These systems also differ in the type of loss they cover, some including just direct material damage in the guarantee (the US, Iceland, New Zealand, Japan, Turkey …); others add business interruption to that damage (France, Norway, Denmark), and finally there is the exceptional case of the Spanish system which, in addition to all the above, covers personal damages. Moreover, many systems cover damage only when affecting homes (Japan, New Zealand, Rumania, Turkey).

To provide sufficient financial capacity, many of the systems are authorised or even obliged by their legislation to constitute equalization reserves (Spain, France, Norway, Turkey, Japan, Belgium …). These are disaster funds designed to accumulate resources for high claim rates and which enjoy favourable fiscal treatment within certain quantitative and temporal limits. Should the accumulated damage exceed those resources, some systems benefit from guarantee by the State concerned, whether limited (Denmark, USA, Taiwan, Japan, Belgium …) or unlimited (France, Spain, New Zealand …).

The large international organisations (United Nations, World Bank, G-20, OECD) are concerned about the effect of natural disasters in development of countries, particularly those less favoured, and the manner of managing those risks in an integrated way (knowledge, mitigation, financing) with a view to reducing losses of lives and property (World Bank, OECD, G-20, 2012). The World Bank is particularly active in cooperating with developing countries to design mechanisms to finance losses from natural disasters.

[i] The full definition given in the Extraordinary Risks Regulations is: *"extremely adverse and rigorous atmospheric conditions produced by:*

1.- Violent tropical cyclones identified by the presence and simultaneity of wind speeds exceeding 96 kilometres per hour over a mean of 10 minute intervals, representing a movement in excess of 16,000 metres in this interval, and precipitation of intensity exceeding 40 litres of water per square meter and hour.

2.- Intense cold squalls with the advection of Arctic air, identified by the presence and simultaneity of wind speeds exceeding 84 kilometres per hour, also over a mean of 10 minute intervals, representing a movement in excess of 14,000 metres in this interval, with potential temperatures below 6ºC below zero referred to sea level pressure at the nearest coastal point.

3.- Tornados, defined as extratropical squalls of cyclonic origin which generate revolving tempests produced as a consequence of an extremely violent storm in

the form of a narrow cloud column projected from the base of a cumulonimbus cloud toward the ground.

4.- Extraordinary winds, defined as those with gusts of more than 120 kilometres per hour. A gust is understood to be the highest wind speed value sustained over an interval of three seconds".

[ii] Vehicle damage, not civil liability arising from its movement.

REFERENCES

AEMET (2010). *Análisis preliminar de la situación del 25-28 de febrero de 2010 sobre la profundización violenta de una borrasca-Ciclogénesis explosiva asociada*. En: http://www.aemet.es/documentos/es/noticias/2010/03/Ciclognesisexplosiva2528-02-2010(3).pdf.

Consorcio de Compensación de Seguros (2008). *La cobertura aseguradora de las catástrofes naturales. Diversidad de sistemas*. CCS, Madrid.

Consorcio de Compensación de Seguros (2012). *La cobertura de los riegos extraordinarios en España*. CCS, Madrid.

Consorcio de Compensación de Seguros (2012). *Estadística riesgos extraordinarios. Serie 1971-2011*. CCS, Madrid.

Consorcio de Compensación de Seguros (2010). *Memoria de responsabilidad social 2009*. CCS, Madrid.

Consorcio de Compensación de Seguros (2012). *Recopilación Legislativa*. CCS, Madrid.

García-Legaz, C. and Valero, F. (Eds.) (2003). *Riesgos climáticos e impacto ambiental*. Editorial Complutense, Madrid.

González, J.L. (Ed.) (2007). *Implicaciones económicas y sociales de los riesgos naturales*. Ilustre Colegio Oficial de Geólogos, Madrid.

Insurance Europe (2012). *How Insurance Works*. Bruselas. En:

http://www.insuranceeurope.eu/uploads/Modules/Publications/how-insurance-works.pdf

OECD/G-20 (2012). *Disaster Risk Assessment and Risk Financing. A G-20/OECD Methodological Framework.* En:

http://www.oecd.org/gov/risk/G20disasterriskmanagement.pdf

Swiss Re (2012). *Flood – An underestimated risk*. Zurich. En:

http://media.swissre.com/documents/Flood.pdf

World Bank/G-20 (2012). *Improving the assessment of Disaster Risks to Strengthen Financial Resilience*. En:

http://www.gfdrr.org/sites/gfdrr.org/files/GFDRR_G20_Low_June13.pdf